IMPLEMENTATION OF ELECTROLYSERS IN THE POWER SYSTEM AS A LOAD MANAGEMENT MECHANISM

Enrique Troncoso

Submitted for the qualification of Doctorate of Philosophy

Heriot Watt University

Energy Academy, School of Engineering and Physical Sciences

January 2008

ABSTRACT

A future power system with a large installed capacity of intermittent renewable power sources (RE) relative to its maximum system demand, also requires large capacities of controllable thermal power plant to cover periods of low RE generation. The most prominent example of intermittency is wind power, where natural fluctuations are challenging to achieve high penetrations, especially in islanded power systems. If high wind penetrations are to be realised, two carbon emissions problems associated with managing intermittency need to be addressed. Firstly, the requirement for flexible operation of back-up fossil-fuelled power plant increases with wind penetration in order to balance the intermittent supply with the time-varying demand. This results in a carbon penalty that increases with wind penetration. Secondly, if at any time wind power plant generation exceeds that which can be safely absorbed by the power system, some of the available RE input needs to be curtailed. The curtailment of wind generation inhibits the production of low-carbon electricity and penalizes efforts to achieve high wind penetrations. The value of wind penetration at which such measures need to be taken depends on the characteristics of the specific power system, but an islanded power system without significant interconnections is the most challenging to manage.

Solutions are therefore required for regions of high wind resource to facilitate the achievement of high wind penetrations. The solution presented in this thesis is to deploy water electrolysers as controllable loads for load management exclusively in case of "valley filling". In combination with hydrogen storage systems, electrolysers can thus be used for hydrogen production both in the case of a fluctuating excess supply (e.g. during prolonged and rising RE generation) and during periods of low electricity demand. The supply of electricity becomes effectively decoupled from the demand in such a way that the operation of power plant depends less on consumer demand.

An analysis is carried out to assess the mass implementation and operation of a stock of electrolysers in combination with wind power plant (WPP) and zero-carbon thermal power plant (ZPP, e.g. nuclear, CO_2-sequestered). Three electrolyser implementation cases were simulated for increasing WPP and ZPP penetrations and periods of different

wind availability. The key objectives are: (i) increasing the penetrations of RE in the power system (by reducing wind energy curtailment); (ii) maximizing the efficiency of utilization of FPP (by maximizing the load factor of the aggregate FPP load profile, LF_{TH}); and (iii) creating a source of zero/low-carbon hydrogen. A generic simulation tool, namely the AELM model, has been developed for implementing and controlling a large stock of electrolysers for an islanded power system. From power plant availability, demand and RE forecast profiles, the AELM model generates utilization strategies for the electrolyser stock, ZPP, WPP and FPP. Preferred capacity levels are obtained for the required stock of electrolysers as a function of the penetration of WPP and ZPP in the power system. Other general outputs are energy balances, hydrogen yields and carbon intensities for electricity and hydrogen for the time period analyzed. Results are presented for an isolated power system based on wind generation and demand data for Eastern Denmark.

It is found that load management via electrolysers is an attractive option with the view of optimizing the operation of the power system. LF_{TH} of up to 100% can be achieved (a virtually flat FPP load profile) at wind penetrations $\geq$ 50% of system maximum demand (SMD). For high wind penetrations the electrolyser stock must include implementations close to WPP if wind curtailment is to be avoided. Results also indicate that the deployment of ZPP in addition to WPP is a considerable benefit. In particular much greater hydrogen yields and electrolyser utilization factors can be obtained especially on days of low wind availability, thus solving the main drawbacks of a pure wind-hydrogen (or more generally renewables-hydrogen) implementation. The key parameters of the analysis presented are system-specific, and the outcomes for different energy/power systems will be different. The intention is to establish a generic methodology and the boundary conditions for the deployment of a large electrolyser stock in any given power system. The approach presented could be a valuable tool in the decision-making processes towards more sustainable energy systems and eventually towards a prospective hydrogen economy.

ACKNOWLEDGEMENTS

I would like to acknowledge several companies and organizations for providing information about electrolyser systems including the US National Renewable Laboratory (thanks to Kevin Harrison), Proton Energy Systems, Norsk Hydro and ITM Power. My thanks go also to Andrew Peacock for fruitful discussions and cooperation throughout this investigation.

On a personal level I am deeply grateful to my family for their constant love and support. Thanks also go to Charo, Paloma, Carmen, Hugo, Neruda and Helio for the chats, support and coffee breaks. I specially want to thank my girlfriend Ada for her unconditional love and care, for being supportive and understanding through heavy times of thesis writing. You are my shining light.

My deepest gratitude goes to my supervisor Professor Marcus Newborough for guiding me through this study and helping me pushing the boundaries of my thinking. He has helped me in every aspect I needed and I always found his support. Thanks Marcus.

ACADEMIC REGISTRY
Research Thesis Submission

Name:	ENRIQUE TRONCOSO		
School/PGI:	SCHOOL OF ENGINEERING AND PHYSICAL SCIENCES / MECHANICAL ENGINERING		
Version: *(i.e. First, Resubmission, Final)*	FINAL	Degree Sought:	PhD

Declaration

In accordance with the appropriate regulations I hereby submit my thesis and I declare that:

1) the thesis embodies the results of my own work and has been composed by myself
2) where appropriate, I have made acknowledgement of the work of others and have made reference to work carried out in collaboration with other persons
3) the thesis is the correct version of the thesis for submission*.
4) my thesis for the award referred to, deposited in the Heriot-Watt University Library, should be made available for loan or photocopying, subject to such conditions as the Librarian may require
5) I understand that as a student of the University I am required to abide by the Regulations of the University and to conform to its discipline.

* *Please note that it is the responsibility of the candidate to ensure that the correct version of the thesis is submitted.*

Signature of Candidate:	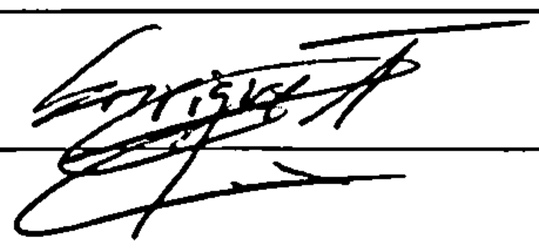	Date:	25/01/08

Submission

Submitted By *(name in capitals):*	ENRIQUE TRONCOSO
Signature of Individual Submitting:	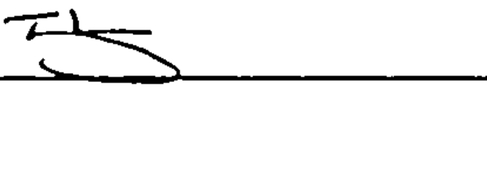
Date Submitted:	25/01/08

For Completion in Academic Registry

Received in the Academic Registry by *(name in capitals):*	J. TOUGH		
Method of Submission *(Handed in to Academic Registry; posted through internal/external mail):*	HANDED IN		
Signature:	J. T	Date:	25·1·08

CONTENTS

NOMENCLATURE

CI_e	Carbon intensity of electricity (kg CO_2 / kWh_e)
CI_H	Carbon intensity of hydrogen (kg CO_2 / kg H_2)
E^{rev}	Reversible electrochemical potential
F	Faraday constant (96500 A·s/mol)
IC_E	Installed capacity of electrolysers (MW)
kWh_e	Kilowatt-hour of electricity
LF_{TH}	Daily load factor of the aggregate thermal load profile, i.e. the ratio of average to peak load across 24h (%)
NGC	Net generating Capacity (MW)
P_C	Aggregate consumer electrical load (MWh)
P_E	Aggregate electrical load of the electrolyser stock (MWh)
P_{DSE}	Aggregate electrical load of the demand-side electrolyser stock (MWh)
P_{FPDE}	Aggregate grid electricity supplied to electrolysers (MWh)
P_{FPP}	Aggregate electrical load of thermal power plant (MWh)
P_G	Aggregate grid load (MWh)
P_W	Aggregate electrical output of wind power plant (MWh)
P_{WD}	Aggregate electrical output of wind power plant which is curtailed (MWh)
P_{WDE}	Aggregate wind generation exported to demand-side electrolysers (MWh)

P_{WSE}	Aggregate wind generation exported to supply-side electrolysers (MWh)
P_{WG}	Aggregate wind generation exported to the main grid (MWh)
P_{WC}	Aggregate wind generation exported to consumers (MWh)
P_{WE}	Aggregate wind generation exported to electrolysers (MWh)
P_{ZPP}	Aggregate electrical load of zero-carbon thermal power plant (MWh)
P_{ZPSE}	Aggregate zero-carbon thermal generation exported to supply-side electrolysers (MWh)
P_{ZPG}	Aggregate zero-carbon thermal generation exported to the main grid (MWh)
P_{ZPC}	Aggregate zero-carbon thermal generation exported to consumers (MWh)
P_{ZPSE}	Aggregate zero-carbon thermal generation exported to demand-side electrolysers (MWh)
R	Ideal gas constant (8.314472 J / mol · K)
SMD	System Maximum Demand (MW)
T	Temperature
TC	Total CO_2 emissions from electricity generation (t)
Y_H	Net daily hydrogen yield (t)
UF_E	Average utilization factor of the electrolyser stock, i.e. the ratio of actual utilization to the installed capacity across the time period considered (%)
WC	Wind curtailment (% of wind generation)

Φ_W	Wind Power Penetration, i.e. the ratio of the installed capacity of wind power plant to the maximum system demand (%)
Φ_{ZPP}	Zero-carbon thermal Penetration, i.e. the ratio of the installed capacity of ZPP to the maximum system demand (%).
β_E	Installed Capacity Ratio, i.e. the minimum required installed capacity of electrolyser plant to achieve a given installed capacity of wind power plant, expressed as a proportion (%)
ΔG	Gibbs free energy
μ	Chemical potential
η_{ELS}	Electrolysers' efficiency (kWh_e / kg H_2)

ABBREVIATIONS

AE	Alkaline electrolyser
CCGT	Combined cycle gas turbine
CF	Capacity factor
DG	Zero-carbon distributed generation (e.g. micro-wind and building-integrated photovoltaics)
DSE	Demand-side electrolyser
ELS	Electrolysers
FC	Fuel cell
FPP	Fossil-fuelled power plant (coal, gas, oil-fired power plant)
HHV	Higher heating value (3.54 kWh/Nm^3 for hydrogen)
HV	High Voltage (> 33 kV in the GB power system)
ICE	Internal combustion engine

LHV	Lower heating value (2.99 kWh/Nm^3 for hydrogen)
LV	Low Voltage (< 11 kV in the GB power system)
NG	Natural Gas
OCGT	Open Cycle gas turbine
O&M	Operation and maintenance costs
PEME	Polymer electrolyte membrane electrolyser
RE	Intermittent renewable power sources
SOE	Solid oxide electrolyser
SSE	Supply-side electrolyser
T&D	Transmission and Distribution electricity system
TSO	Transmission system operator
WPP	Wind power plant
ZPP	Zero-carbon Thermal Power Plant (e.g. nuclear, CO_2-sequestered power plant)
ZCPP	Zero-carbon Power Plant (includes ZPP and RE)

GLOSSARY

Back-up capacity/generation	Fossil-fuelled power plant which is used for supply/demand matching on a short-term basis (less than 4h).
Capacity factor	The ratio of the actual electrical output over a designated period to the maximum output that it could have produced under continuous operation at rated capacity during that period. It applies to individual wind turbines, wind power plants or national/regional aggregate of wind power plant.

Carbon intensity of hydrogen	Mass of carbon dioxide emitted per unit mass of hydrogen generated.
Carbon intensity of grid electricity	Mass of carbon dioxide emitted per kWh of electricity generated.
Intermittent renewables	Those power sources inherently unable to sustain a steady and consistent output (e.g. solar, wind, wave and tidal generation), their output being a function of the natural availability of the energy resource.
Low-carbon hydrogen	Hydrogen generated in a manner which results in it having significantly lower (e.g. less than half) carbon intensity than that made by conventional methane reformation.
Low-load limit	Penetration limit imposed on the aggregate wind power input that can be admitted by the power system due to the minimum loading levels of thermal power plant and the need to maintain dynamic stability of the system.
FPP load profile	The transient variation in the aggregate load placed on thermal power plant.
Utilization factor of thermal power plant	The ratio of the electrical output of thermal power plant over a designated period to the maximum output that it could have produced under continuous operation at rated capacity during that period.
Utilization factor of electrolyser stock	Ratio of the hydrogen output of a water electrolyser over a designated period to the maximum output that it could have produced under continuous operation at maximum output during that period.
Wind curtailment	Wind power that is available but must be discarded because of the low-load limits of the power system.

Zero-carbon hydrogen	Hydrogen generated in a manner which causes no significant CO_2 emissions.
Zero-carbon power sources	Power plant whose carbon emissions are very low or zero. This includes generators that are independent of hydrocarbon fuels (e.g. wind, solar, marine, nuclear) or hydrocarbon–based but with CO_2 capture/sequestration.

DISSEMINATION OF RESEARCH

Four public domain outputs have so far arisen from this thesis:

'Active Electrolysers Load Management for High Penetrations of Wind Power', US National Hydrogen Association Conference, Long Beach March 2006

'Electrolyser Load Management for High Penetrations of Wind Power in Island Power Systems, Seminar: Hydrogen Applications in Stationary Power Generation, Lanzarote September 2006.

'Implementation and Control of Electrolysers in Combination with Wind and Zero-carbon Thermal Power Plant', US National Hydrogen Association Conference, San Antonio March 2007

'Implementation and Control of Electrolysers to Achieve High Penetrations of Renewable Power', International Journal of hydrogen Energy (2007), http://dx.doi.org/10.1016/j.ijhydene.2007.02.034

CHAPTER 1 - INTRODUCTION

1.1 OVERVIEW: LOAD MANAGEMENT WITH ELECTROLYSERS

At present, the penetration of renewable power sources within the electricity system (as generated by wind, solar, wave and tidal power sources) is serving to displace fossil-derived electricity. However, a power system with a large installed capacity of RE power plant relative to its peak demand also requires a large installed capacity of controllable fossil-fuelled power plant (FPP). The most prominent example of intermittency is wind power. As the installed capacity of intermittent wind power rises there are inevitably periods of low availability when conventional capacity must be called upon to cover a shortfall in wind generation [1], [2]. This 'covering' of wind power plant by fossil plant results in carbon emissions for no useful electrical output. Conversely, if wind power production exceeds the amount that can be safely absorbed by the electricity system while still maintaining adequate reserves and dynamic control of the system, some of the available wind power has to be curtailed [3], [4]. This 'curtailment' inhibits the production of low carbon electricity despite the availability of sufficient wind power plant (WPP) within the power system, presents an economic penalty for WPP operators and ultimately discourages investment in new WPP.

Therefore there is a need to implement solutions to facilitate the absorption of very high penetrations of wind power by electricity networks, particularly in those so-called island power systems that are weakly interconnected to neighbouring systems. Essentially, until such technologies are developed, the security of electricity supplies will depend on having back-up capacity available on a substantial scale, so that they can be used as and when needed to meet shortfalls in the supply of electricity from intermittent renewable sources, with the environmental implications described herein.

If there were some way that large amounts of intermittent RE loads such as solar, wind and wave power sources could be time-managed on a large scale, the contribution of these technologies to supplying energy demand could be much greater than thought today. Load management via water electrolysers is one option. Instead of adapting power generation in an electricity system with a high penetration of wind power to the time varying demand profile, there is a role for improving the way power systems are operated today. In combination with hydrogen storage systems, water electrolysers can be used for load management in the same way as a variable electricity consumer, while producing clean hydrogen and by-product oxygen valuable for other energy uses (e.g. transport, heating and industrial purposes). By including electrolysers in the system as additional controllable loads, the load placed on FPP can increase or decrease through their operation in time phase with the zero-carbon power inputs to the electrical grid.

In combination with zero-carbon power sources like wind, solar, nuclear and CO_2-sequesered power plant electrolysers can be used as variable loads in the electric grid to support the increasing demands made on regulating capacity. Electrolysis is considered to be the preferred option here because it produces a premium value fuel or chemical feedstock for other energy sectors, whereas other electricity storage methods (e.g. pumped hydro storage, CAES, flywheels or flow batteries) provide only "electricity-in, electricity-out" possibilities [5], [6]. Few technologies can facilitate carbon abatement across all energy sectors, but water electrolysers can transform any zero-carbon electricity source to a zero-carbon energy carrier, hydrogen, suitable for a wide variety of end-use applications, including transportation, power generation and portable power systems, industrial heaters, chemical feedstock in the petrochemical, electronics and food industries as well as ammonia and methanol manufacturing processes.

Rather than using hydrogen to be recovered as electrical output via fuel cells or hydrogen engine gensets to the grid, a more efficient approach is to use hydrogen as an energy carrier for industrial, domestic or transport applications. Omitting the

converting of energy back to electricity could represent a preferable starting point. Zero-carbon power sources (large scale centralised or demand-located) can then operate as a combined hydrogen/electricity production unit with high control flexibility, and electrolysers (large scale centralised and/or demand-side located) can be used for hydrogen and oxygen production both in the case of fluctuating excess supply (e.g. during prolonged, rising renewable electricity production) and in the case of demand deficiencies on the consumer side during low-load periods.

In addition to renewable power sources, a large deployment of electrolysers (ELS) within the power system invites a wide deployment of zero-carbon thermal power plant (ZPP) like nuclear and CO_2–sequestered power plant. Using ZPP to make hydrogen could help improve plant efficiencies, electrolyser utilization and hydrogen yields, improving the economic case for a large deployment of ELS in the power system. In the approach considered here ZPP would be running continuously at full capacity, with perhaps most of the output being supplied to the grid at peak periods, and any surplus not needed to meet consumer electrical demand would be used to make H_2. This would enable a far better operational efficiency for the zero-carbon thermal power plant.

In the short and medium term the electricity sector is likely to rely on FPP to supply consumer electrical demand. Thus the approach proposed here, while maximizing the penetration of zero-carbon power plant (ZCPP), also aims to maximize the efficiency of utilization of FPP. It is expected that load management through ELS can lead to a higher efficiency of utilization rate for FPP (since gencrating capacities must be reserved to a minor extent for regulating tasks) by increasing the LF_{TH} of the aggregate FPP load profile beyond those levels applying today. It is also anticipated that deploying ELS in the system as controllable loads can give smoothing opportunities for wind power delivered to the grid, while at the same time enables a larger penetration of wind energy and other intermittent renewables (PV, wave, tidal) into the electricity system. Active load management with electrolysers could then be applied to:

- Minimise RE curtailment
- Maximise the LF_{TH} and mean efficiency of fossil power plant (FPP) and ZCPP.
- Provide a supply of zero- or low-carbon hydrogen and oxygen.

In summary, ELS integrated within the electricity system and properly managed in time-phase with the zero-carbon power inputs to the grid are proposed herein as a load management mechanism to overcome problems derived from the stochastic nature of wind power and other RE. A large electrolyser stock could be used to manage large intermittent loads in a power system relying heavily on zero-carbon power inputs. ZPP could complement large-scale RE generation, using electrolysers as controllable loads by reducing or increasing their power input at short notice when they are required. This would reduce the need for back-up FPP and carbon dioxide emissions associated, creating a more efficient and flexible power system capable of delivering two valuable products: electricity and hydrogen, with the further possibility of exploiting the by-product oxygen.

1.2 THESIS OBJECTIVES & CONTRIBUTIONS

Clearly island power systems without significant interconnections are the most challenging in terms of integrating large amounts of RE generation. A proposed solution is presented here for the case of the integration of large amounts of wind power plant (as an example for intermittent renewable sources in general) and zero-carbon thermal power plant into an isolated or island power system.

The main objective of the thesis is to create a systematic approach for the implementation of ELS as a load management mechanism in combination with ZCPP and FPP. The intention is to identify the boundary conditions for implementing a large electrolyser stock into a generic island power system, to analyse the carbon and energy implications, and to explore the influence of key parameters (e.g. electrolyser

stock size, utilization factor, hydrogen yield, carbon intensity of electricity and hydrogen delivered to consumers, etc) in the final attractiveness of such implementation. This can provide a helpful tool in the decision-making processes towards a more sustainable energy system and as a first step towards an anticipated hydrogen economy.

The concept of a wide scale implementation of electrolysers within the electricity system is examined from an energy point of view, not an economic one. However it outlines the framework for conducting an economic analysis based on the results presented here. The approach is set out to:

1. Maximize the efficiency of the system by increasing the load factor of the aggregate FPP load profile.

2. Increase the capture of intermittent RE sources by reducing wind power curtailment.

3. Generate a valuable clean fuel (alternatively a clean energy vector) for other energy sectors.

Consider a generic power system that consists of only two types of power plant on the supply side, namely fossil power plant, FPP, and zero-carbon power plant, ZCPP (e.g. renewable, nuclear or CO_2-sequestred power plants); and one independent load (consumer demand) on the demand side. The power system under consideration has no significant interconnections with neighbouring power systems (i.e. islanded system). Such power system is then modified to accept an electrolyser stock, but no other energy storage technologies or load management mechanisms (such as peak demand reduction) are considered. Hence three independent loads are now included: equivalent electricity consumer, equivalent embedded "demand-side ELS" (additional electricity demand in the T&D system) and equivalent "supply-side ELS" as shown in **Figure 1.1**

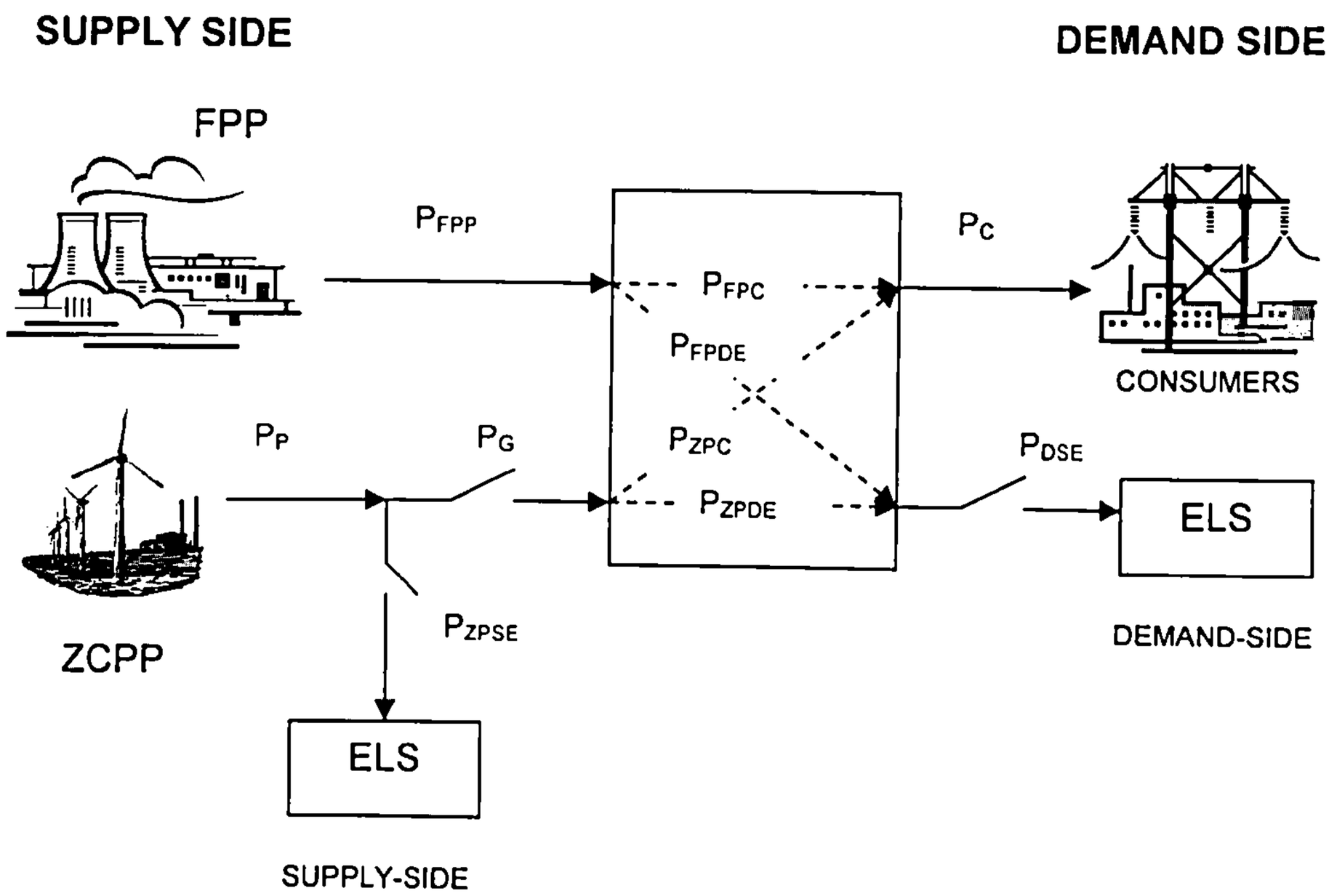

Figure 1.1 Schematic of a power system with active ELS demand management

In summary FPP and ZCPP are connected to the electrical grid on the supply side, which now feeds electricity to consumers and also to a fleet of electrolysers. The study deals with the optimization of medium-large scale power plant (MW scale) and does not include the use of dispersed generation on the demand side.

To optimize the operation of a power system with a high penetration of zero-carbon power sources and a large stock of electrolysers, it is necessary to develop a control strategy that takes into account:

- wind power availability
- the demand for electricity from consumers (excluding electrolysers)
- the interaction of these two with other (thermal) power generators

A heuristic approach **(namely AELM model)** has been developed for the implementation and operation of a large electrolyser stock into a generic power system, where several operational strategies are examined. Based on spreadsheets an input/output model has been developed based on power and energy flows **(namely AELM model)** which generates a utilization strategy for the electrolyser stock, FPP and ZCPP from forecast profiles of demand and wind availability which are the primary input data. Main outputs are daily energy balances, load profiles, hydrogen yields and carbon intensities for electricity and hydrogen as well as average power values for the period studied.

An analysis has been carried out based on wind generation and historical demand data for Eastern Denmark to investigate the capabilities of the AELM model. This is applied to an island power system because this is the most challenging type in which to integrate a large proportion of RE.

Three implementation cases have been simulated for the electrolyser stock, namely a supply-side implementation, demand-side implementation and a combination of both. For each implementation case several operational strategies are investigated which include: (i) deploying ELS in combination with WPP; (ii) deploying ELS in combination with ZPP; deployment in combination with both WPP and ZPP. In each case preferred capacity levels are identified for the electrolyser stock for increasing penetrations of WPP ($0 \leq \Phi_W \leq 100\%$) and/or ZPP ($0 \leq \Phi_{ZPP} \leq 35\%$) in the power system. Other general outputs are aggregate load profiles of FPP, WPP, ZPP and electrolyser stock, hydrogen yields, utilization factors and carbon intensities for electricity and hydrogen. Results are presented for daily and weekly periods on a time interval of one hour.

1.3 THESIS STRUCTURE

This chapter presents the main objectives of the work and contributions to the field. The rest of the thesis is structured as follows:

Chapter 2 gives a more detailed background for the motivations of the work, and examines the problems that arise when aiming for large penetrations of intermittent renewable sources, focusing on wind power. The chapter discusses integration issues and problems imposed on the system when integrating large amounts of wind power.

Chapter 3 outlines the concept of load management via electrolysers and defines the boundaries of the study. It describes the approach and the spreadsheet model developed for the implementation and control of electrolysers in a generic island power system.

Chapter 4 presents an application of the methodology described in Chapter 3 for the implementation and operation of a stock of electrolysers in combination with large penetrations of wind power within a generic power system. Three implementation cases are analysed, operational strategies are suggested and results are presented for 24h periods based on wind generation and demand data for Eastern Denmark.

Chapter 5 extends the analysis presented in **Chapter 4** to consider a power system which includes a deployment of zero-carbon thermal power plant. The spreadsheet model is applied to daily and weekly load profiles for studying the implementation and control of ELS in the power system and to identify likely variations in the principal parameters across periods longer than 24h. The same three implementation cases for the electrolyser stock are considered and three different operational strategies are suggested for each implementation case.

Chapter 6 deals with the practical and operational issues arising from the implementation of a large electrolyser stock. It gives an overview of electrolyser technology and explores the regulatory, economic and technical implications that may arise when implementing and operating a large electrolyser stock as a load management mechanism.

Chapter 7 provides a final overview, extracts the main conclusions from the analysis presented in previous chapters and gives final recommendations and suggestions for further research.

Appendix A extends the analyses in **Chapters 4 and 5** by applying the spreadsheet model using a different demand profile to those of Eastern Denmark.

Appendix B shows a sensitivity analysis of the assumption regarding the maximum penetration of wind power acceptable in the power system, namely the low-load limit assumption.

Appendix C presents an overview of existing and prospective end-use applications of electrolytic hydrogen.

CHAPTER 2 - ILLUSTRATING THE PROBLEMS DERIVED FROM HIGH PENETRATIONS OF INTERMITTENT RENEWABLE POWER SOURCES

2.1 INTRODUCTION

Renewable energy sources can be divided into two categories in terms of availability: (i) those which are constant and continuous, processing an innate storage capacity; (ii) those which are variable or intermittent, lacking any such capacity. The former category includes resources such as bio-fuels, biomass, hydro, geothermal and ocean-thermal. The latter category can be subdivided into those resources which vary periodically or cyclically, such as solar and tidal, and those which vary rather randomly, such as wind and wave. Deployment of indigenous intermittent renewable power sources (RE) like wind power is growing significantly in all regions as environmental concerns require cleaner electricity production and more efficient energy use, and issues related to security of energy supply become predominant. Wind power is by far the fastest growing among RE and also the most challenging when it comes to its integration into the power system. It will be the focus of the discussion presented in this chapter.

Intermittency is probably the most prominent feature of wind generation, and should not be confused with predictability. Intermittency within the context of RE basically means that the generation obeys weather patterns and therefore is not controlled, leading to frequent variations in the level of power produced. It also implies that periods of low/high generation do not necessarily coincide with low/high system demand. This inability is due to the intermittent availability of the primary energy source employed by the renewable generator and is distinctively characteristic of renewable energy sources such as solar, wind, wave, and tidal generation. Predictability on the other hand refers to the ability to forecast wind conditions and can be controlled or improved to a certain extent by developing more sophisticated wind forecast techniques.

Most wind turbines start generating electricity at wind speeds of around 3-4 metres per second (m/s), generate maximum rated power at around 15 m/s and shut down to prevent storm damage at 25 m/s or above (**Figure 2.1**).

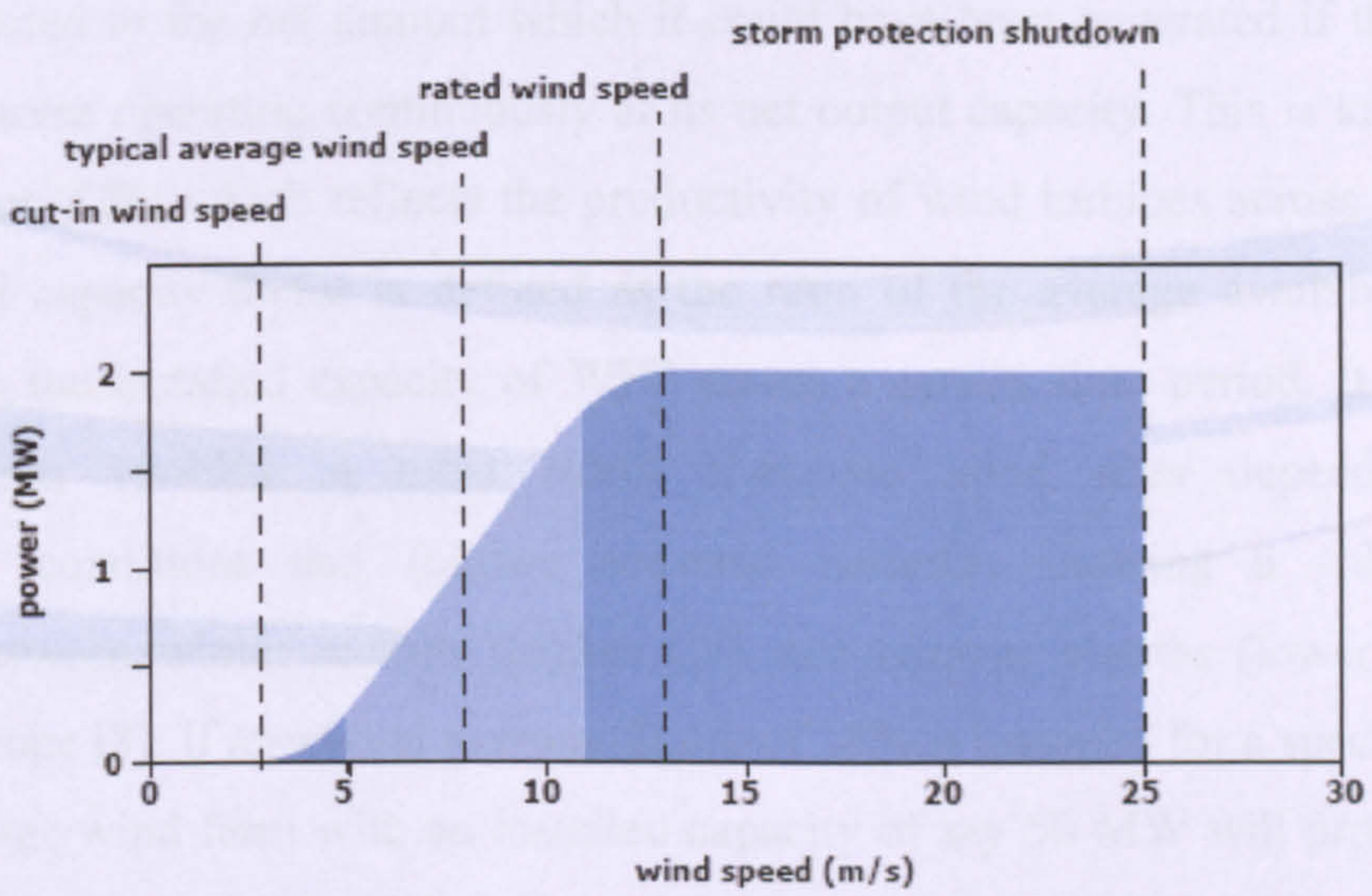

Figure 2.1. Typical wind turbine power curve [7]

The theoretical power extracted from wind is a cubic function of wind speed:

$$P = 0.5 \times \rho \times v^3 \times A \qquad (2.1)$$

Where

ρ = air density (about 1.2 kg / m^3 at 293K and sea level)

v = air velocity

A = swept area by wind turbine

This makes wind power very sensitive to speed and therefore very variable. To illustrate, doubling wind speed from 5m/sec to 10m/sec in **Figure 2.1** increases the theoretical power extracted from 6% to 72% of the rated 2 MW output (i.e. from 0.12 MW to 1.44 MW), a 12 fold increase. This illustrates why wind turbine output can vary enormously within short time-periods.

The average wind speed at the site will determine the net amount of electricity generated related to the net amount which it could have been generated if the wind power plant were operating continuously at its net output capacity. This is known as capacity factor (CF), which reflects the productivity of wind turbines across a stated period. Wind capacity factor is defined as the ratio of the average available wind generation to the installed capacity of WPP across a certain time period. It usually varies between 15-40% in most North European wind sites depending on geographical conditions and follows seasonal patterns, showing a substantial difference between winter months (higher CF) and summer months (lower CF) in Northern Europe [8]. If an annual average figure of 30% is assumed for a specific site, then an average wind farm with an installed capacity of say 50 MW will produce an annual energy output of $50 \times 8760 \times 0.3 = 131{,}400$ MWh_c, i.e. 30% of what it would produce if it were operating continuously (8760 h / year) at maximum rated output. It is axiomatic that a high CF will result in higher energy output from a WPP and a low CF needs a larger installed capacity to deliver a certain amount of electricity.

The concept of "dispersed wind generation" can be defined as the statistical compensation of the aggregate generation of a set of wind power plants (WPP) subject to partially or totally uncorrelated wind conditions. This means that, even though half of the time a particular WPP may not produce more that 15% of its rated power, having wind farms dispersed across the country usually places average national production at between 15% and 40% of the total installed capacity. Depending on the geographical situation and the extension of the region/country under consideration, wind conditions can be almost entirely de-correlated between WPP sites, thereby reducing the effects of intermittency e.g. in Spain [9] or highly

correlated like in Denmark [10], and therefore wind generation facilities are not always able to compensate one another at times when there are poor wind conditions.

Natural variability in wind speeds causes the level of wind generation to vary both on a local and a national scale. For instance examination of aggregate wind generation data from Spain of about 5,000 MW total capacity shows sudden changes in wind generation of the order of 500 MW, or 10% of the installed capacity across a time interval of 3 minutes (18/04/04) and up to 700 MW across 6 minutes (17/03/04) [11]. Also E.ON in Germany experienced a 59% fall in wind output (3,640 MW) over 6 hours, at an average of 10 MW per minute on 19/11/03 [12] as shown in **Figure 2.2**.

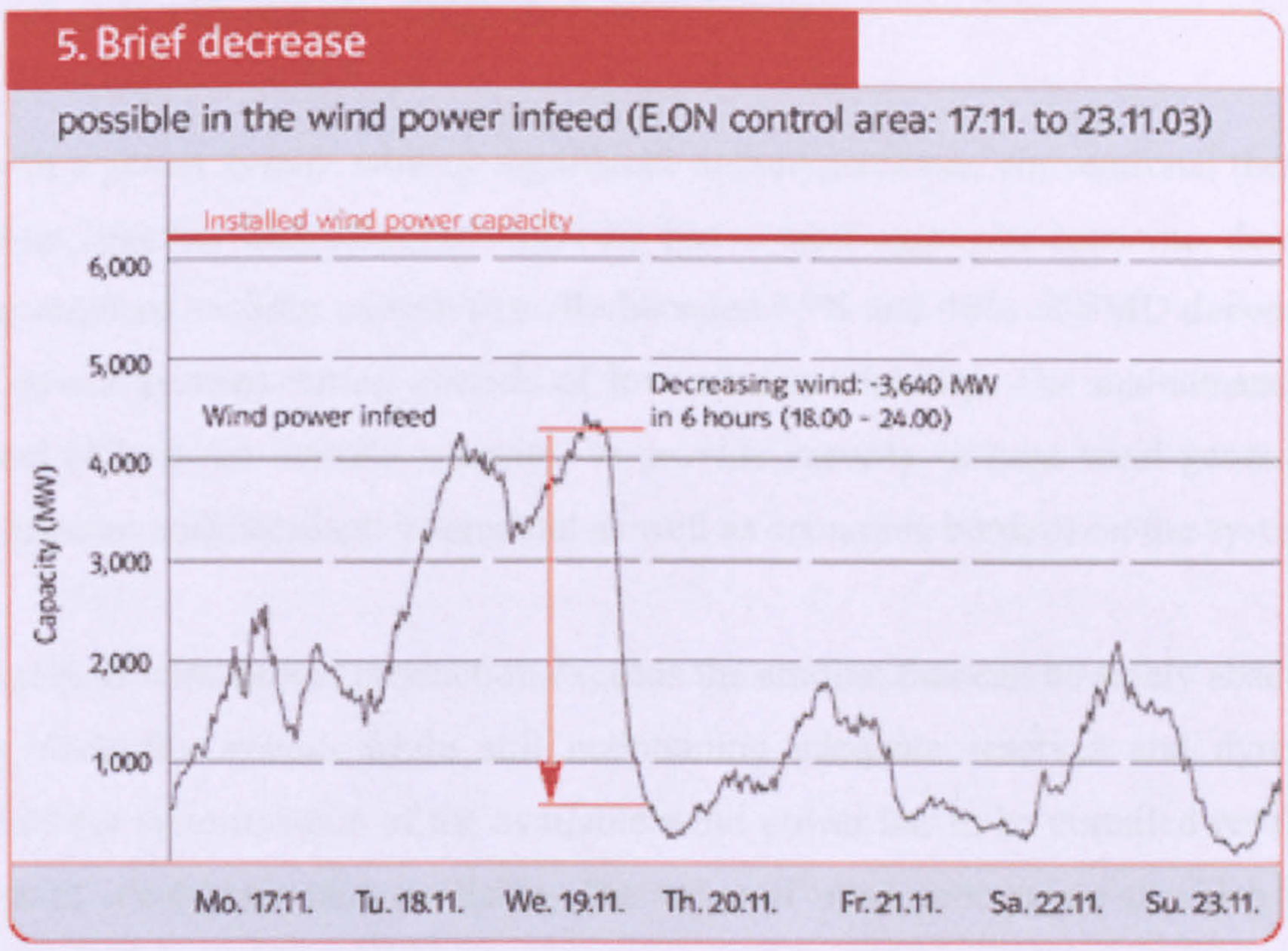

Figure 2.2. Variability of wind power generation across a weekly period in the EON control area in Germany (6,250 MW of wind installed capacity at the end of 2003) [12].

A number of authors ([13], [14]) have suggested that conditions of the coincidence of very high system demand and little or no wind may be possible and could even occur regularly. In contrast, other authors [15], [16] express uncertainty about the possibility of such events. They maintain that the combined output variations of intermittent generation geographically scattered in the system would be reasonably smooth, because every wind generator could not be disturbed at one single time; thus the amount of additional reserve required to manage unscheduled wind generation would not be on a "MW for MW" basis. There does not seem to be consensus so far regarding this matter in the literature consulted. Examination of actual wind generation data from countries with high wind penetrations like Denmark [17], and Spain [11] seems to corroborate that such wind calm events indeed exist, and they can in fact coincide with periods of high electricity demand.

Clearly in a power system with no significant interconnections, conventional thermal generation, together with other non-wind RE has to meet aggregate consumer demand plus the required security margin (usually between 15% and 40% of SMD depending on the power system) during periods of low wind availability. The maintenance of this level of back-up thermal capacity, to provide security in case wind generation drops, imposes additional environmental as well as economic burdens on the system.

Conversely, if wind power production exceeds the amount that can be safely absorbed by the electricity system while still maintaining adequate reserves and dynamic control of the system, some of the available wind power has to be curtailed resulting in a loss of wind generation available. The value of wind penetration at which such measures need to be taken depends on the exact stock of thermal power plant and the design of the specific power system [18], [19], but clearly an islanded power system without significant interconnections is the most challenging to manage. The curtailment of wind farms during periods of high availability but low consumer demand inhibits the production of low-carbon electricity and thus penalize efforts to achieve high wind penetrations.

Besides this the system must balance generation by all power plants (including wind power plants) with the aggregate demand at all times. Utility operators and automatic controls perform this task routinely, based on the known operating characteristics of conventional power plants, sophisticated decision-support algorithms and a great deal of operational experience. However, when a substantial amount of wind power is introduced into the system, measures must be taken to ensure that the additional uncertainties in meeting the supply/demand balance derived from sudden wind fluctuations are mitigated by appropriate measures (such as the provision of additional reserve and/or load levelling mechanisms).

Although highly dependent on the power system under consideration, it is commonly agreed that when wind penetration exceeds around 15%-20% (ratio of wind installed capacity over system maximum demand), system operation begins to become more difficult [3], [4]. Yet this threshold applies to interconnected power systems like Denmark or Germany which can make use of large-capacity electrical interconnections with neighbouring countries (to export electricity as required in response to surplus power during high wind conditions or import during windless periods). The wind power installed capacity that a specific power system can effectively integrate depends on several factors like power system size, generation capacity mix, power market regulations and procedures, geographical dispersion of WPP and importantly the degree of interconnection to neighbouring systems (see **Appendix C**). Those called "island" power systems lacking of significant interconnections, such as the British electricity system, are forced to manage the balance between generation and demand within their own domain and will possibly start experiencing problems at a threshold below 15% of wind penetration. Above this limit, the case for building new wind plant diminishes in terms of economics and carbon savings, because the fluctuations in output cannot be accommodated by the network within normal operating strategies. Several technical responses are needed, inevitably with environmental and cost implications.

On a system-wide level, operational constraints imposed by wind power at high penetrations relates to impacts that affect the behaviour of the system as a whole. These impacts have an effect on power system stability, in terms of:

- Frequency stability
- Voltage stability and Reactive power
- Reserve requirements

In the UK and in most of the electricity markets, the term 'Ancillary Services' is widely used to describe all the activities required to maintain the stability of the transmission system. In most of today's liberalized energy markets, the Transmission System Operators (TSOs) must regulate the correct operation of the electricity system to ensure all the customers have access to a reliable stable supply of electricity, and procure such ancillary services from conventional fossil-fuelled generators, although there is increasing scope for demand response. TSOs procured ancillary services include frequency response, voltage regulation, reactive power and reserve requirements.

With respect to frequency regulation, at all times the power output of the connected generation facilities to the power system must equal the total power load in the system. Frequency falls when total system load is greater than generation and rises when generation is greater than system load. In order to manage frequency effectively, generation reserves are made available to maintain the power balance in the event of a loss of connected generation (e.g. due to a fault in a generator or in a transmission line).

The impact of wind power on frequency control becomes more severe the higher the wind power penetration level is, caused by the fact that the prime mover of wind power is not controllable. Then the variability of the wind tends to complicate the load following with the conventional units that remain in the system, as the load profile to be matched by these units (which equals the system load minus wind power

generation) is less smooth than would be the case without wind power. At high wind penetrations this affects greatly the requirements on the ramping capabilities of conventional generators in order to match the remaining load profile and to keep the fluctuations of the system's frequency, caused by unbalances between generation and load, within regulatory limits (± 0.5 Hz in the UK [20]).

Voltage stability refers to the ability of a power system to maintain steady acceptable voltages at all buses in the system under normal operation conditions and after being subject to a disturbance. The main factor causing voltage instability is the inability of the power system to meet the demands for reactive power in the system in order to keep desired voltages (specified nominal voltage ± 10% as regulated in EU [21]). The impact of wind power on reactive power generation and voltage stability originates mainly from the fact that not all wind turbines are capable of varying their reactive power output. Also, wind power generation can not be very flexibly located when compared to conventional generation, as it must be erected at locations with good wind resources, locations that are not necessarily favourable from the perspective of grid voltage control.

In every power system various types of reserve plant are available for balancing supply and demand in the form of (i) synchronized regulating reserve (sometimes also named "spinning" reserve or response reserve), consisting mainly of coal and CCGT plants running continuously part-loaded at less than 100% output and able to change output within seconds according to TSO requirements; (ii) fast reserve, capable of delivering power output in less than 5 minutes, usually large oil-fired generators, or even pumped storage; and (iii) standing reserve (also called static reserve), which comprises non-synchronized thermal plants that can be started-up and synchronized at grid frequency within 15-20 minutes, typically OCGT plants and reciprocating ICEs) [22].

Pumped storage schemes use water power (potential to kinetic energy) to generate electricity and they operate in a cycle: low-cost electricity generated (e.g. during the

night) is used to pump water up to a reservoir, and electricity is then generated when desired by releasing the water through turbines to a lower reservoir. The time needed to bring this generation into operation is of the order of 15 seconds [23], but the operation of pumped storage reservoirs involves energy losses: three-quarters of the power needed for pumping is recovered [23]. In addition, this method of storing electricity requires construction of large dams and reservoirs. Feasible geographical locations are limited especially because of the associated environmental impacts.

The allocation of reserve between regulating, fast and standing reserve is usually an economic trade off between the cost of efficiency losses of part-loaded synchronized plant (plant with relatively low marginal costs but running at all times) and the cost of operating less efficient standing reserve plant (with relatively high marginal costs but running only occasionally). Given the increasing use of gas-fired generation across Europe, in the future the provision of synchronized and standing reserve using OCGT and CCGT plant is likely to increase at the expense of coal plant. However, as wind power penetration increases, there is a predictable requirement to provide extra back-up generation capacity[1] (both synchronized and standing reserve) so that the system can respond to larger reductions in the output from installed wind generation.

To maintain constant frequency of supply and stability of the system, the balance between supply and demand is achieved by having generating capacity in reserve on a continuous basis or also by having demand customers able and willing to reduce demand at short notice. This is known as demand response or more generally Demand Side Management (DSM) and refers to the ability to buy back capacity from customers with discretionary demand so that others with high and consistent demand levels can continue to be served during critical high demand periods. DSM programs are used to reduce the use of electricity within short timescales by large flexible consumers during times of peak demand and provide economic incentives to curtail electricity demand and reduce load during peak periods in response to system

[1] Throughout this document, the term back-up capacity will refer to this additional reserve above and beyond that reserve capacity currently available in any power system to deal with unforeseen changes in demand or a generator breakdown over a 4 h horizon.

frequency excursions or market conditions. These programs involve customer load reduction through either curtailment or reduction in electricity use or the use of distributed generation in response to price signals or directions from system operators. In exchange, customers are economically compensated for reducing their power usage when it is most needed.

For instance in the US, where concerns about security of power supply have become particularly critical in the past few years, peak load is reduced regularly in the New York area by 800 MW during reserve shortages through more than 2,300 commercial and industrial facilities, which get paid for curtailing their electric load during high-demand periods [24]. A study in 2002 showed that New York's electricity market along with its grid operator and large electric utility companies has the potential to reduce demand for electricity by at least 1,300 MW through Demand Side Management techniques, which is enough to supply power to 1.3 million homes [25]. Another example is the Spanish power system; where over 200 consumers are subject to flexible supply contracts totalling 2,000 MW of interruptible load or around 5% of annual System Maximum Demand (SMD). The power interruption offered by the subscriber to the service interruption service must not be less than 5 MW, and the system operator, namely Red Electrica, has to state, at least 2h in advance, a 6h or 12h interruption profile depending on the type of contract arranged [26]. In the UK, a Demand-Side aggregator, Gaz de France, is currently offering an instantaneous load reduction of 110MW for frequency control purposes, aggregated across thirteen cement production sites [27]. The crushing and milling processes at cement works are ideal for frequency response, consuming large, predictable and steady loads, which can be easily interrupted and restarted. Finally in Eastern Denmark the TSO (Elkraft) also allows consumers to "sell" DSM services as they are offered a capacity payment when called upon. Elkraft currently has 18 interruptible load contracts of in total 34 MW, although the total potential for flexible demand in Eastern Denmark has been estimated at 155 MW or nearly 20% of SMD [28].

2.2 INCREASED CYCLING OF THERMAL PLANT

In an electricity system with a high penetration of wind power plant, variations in output will force conventional power plants to provide compensating variations to maintain system balance between supply and demand, thus causing them to deviate from optimal operating points that are chosen to maximize efficiency of operation of the power system. The overall effect of increased cycling duties (caused by variability in the demand and/or the RE input) is to decrease the average efficiency of operation of thermal power plant because of increasing operation at part load and increased number of start-ups. This leads to an increase in the specific carbon emissions per unit of electricity generated.

Power systems operation covers several time scales, ranging from seconds to days (**Figure 2.3**). Generators must respond to changing loading conditions in different ways, depending on the time scale and operational practices. Although temporal wind fluctuations occur on timescales down to a second or so, they are of relatively small size and tend to be smoothed by wind turbine rotors. It is the fluctuations in timescales ranging from minutes to a few hours that influence the absorption of wind energy within electricity systems [28]. Hence there are typically three time scales of interest, which correspond to the operation of the utility system and the structure of the electricity market:

Regulation: during minute-to-minute load fluctuations, an automatic generating control (AGC) computer sends signals to one or more generators (instantaneous reserve) to cause an increase or decrease in output to match the unpredictable changes in load and/or generation. This service occurs at a time scale ranging from approximately several seconds to 10 minutes. To meet these fast fluctuations, sufficient instantaneous reserve must be online so that there is enough flexibility to respond.

The next time scale is known as **load –following,** covering approximately 10 minutes to several hours. In this time scale, dispatch decisions are made in response to the trend in demand. For example, during the early morning period, an increase in demand usually occurs from 6:00 AM to around 9:00 AM. The system operator is responsible for scheduling adequate operating reserve capacity to ramp unit up and down to follow the load shape.

Unit-commitment: some generators require several hours to be started and synchronized to the grid (e.g. coal-fired power stations). That means that the generation available during the morning peak, for example, must have been started hours in advance, in anticipation of the peak. In many cases, the shut-down process is also lengthy, and units may require several hours of cooling prior to restarting. The decision to utilize this type of unit often involves a period of several days that the unit must run prior to shutting down in order to be economic. This time scale is called unit-commitment, and it can range from several hours to several days, depending on specific generator characteristics and operational practice.

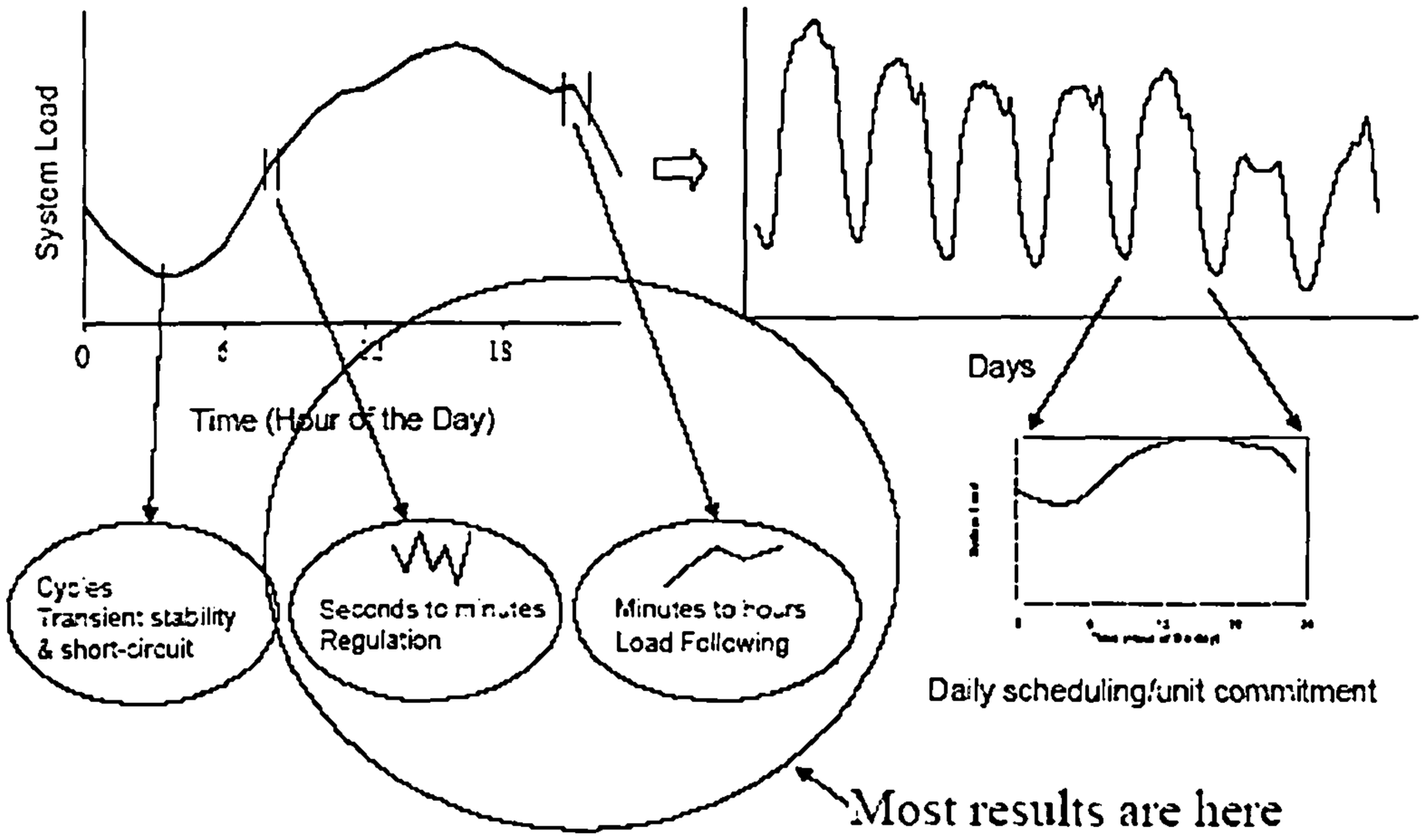

Figure 2.3. Time scales for power systems operation [28]

When significant wind penetration is added to the power supply, the impacts on system security derived from wind intermittency can extend across each of these time scales. As wind powered generation increases, it imposes extra demand fluctuations on thermal power plant, decreases base load, and thus raises CO_2 emissions per kWh_e generated. This loose of efficiency is due to the adverse impact of wind power on their operations, mainly increased number of start-ups and ramping duty:

- **Start-ups:** A large amount of energy is required to start-up large thermally powered units. For example a large oil fired unit can consume around 830 MWh of energy during the startup process [2]. The start-up process is also a quite onerous on the mechanical integrity of the unit. Even for peaking units such as OCGTs it is quite common to determine the allowable period between maintenance outages by specifying a maximum permissible number of start-ups.

- **Ramping duty.** The ability to pick up or reduce load on a generation unit is limited by the thermal and mechanical stresses imposed on the unit during the process of changing load levels. Ramp-up rates in the range of 1 to 10 MW per minute and ramp-down rates in the range from 1 to 15 MW per minute are typical performance levels for thermal units [2]. As there are limits to the ramp rate on individual units, a number of units must act in unison in order to maintain the demand supply balance during periods when either the demand or supply of electricity is changing rapidly. The impact of increasing wind power penetrations on the ramping duty of units can be quantified by determining the 'Average Hourly MW Change' for a unit over a period of one year. The higher the Average Hourly MW Change the larger the amount of energy (as fossil fuel input) required, and hence the higher the emission factor (carbon value emitted per unit of electricity generated).

The adverse impacts of wind power intermittency on the operating performance of conventional power plant can be analysed by examining their load profiles. **Figures 2.4 - 2.6** show an interesting example of the impact of wind on a single CCGT unit, applied to a power system with a wind power penetration of 24% (1,500 MW of installed capacity). The actual wind power profile is shown in **Figure 2.5**. As can be seen from the figures the effect is to invoke a much more irregular operating schedule in thermal units usually designed and scheduled to operate as base-load units. The utilization factor of the CCGT unit shown in the Figures is reduced in this case from 70% to 58%.

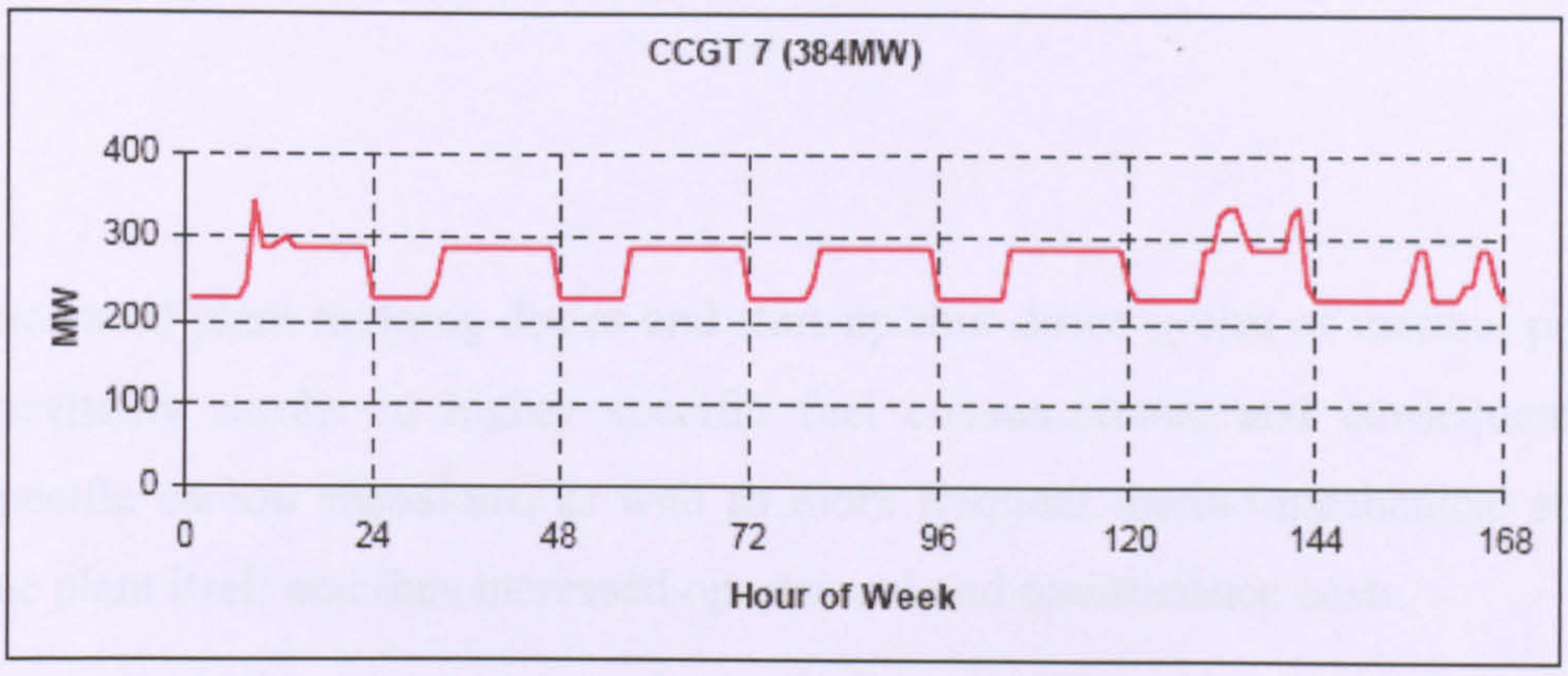

Figure 2.4 Typical operation profile of a 384 MW CCGT unit for a week. No wind capacity on the system [2].

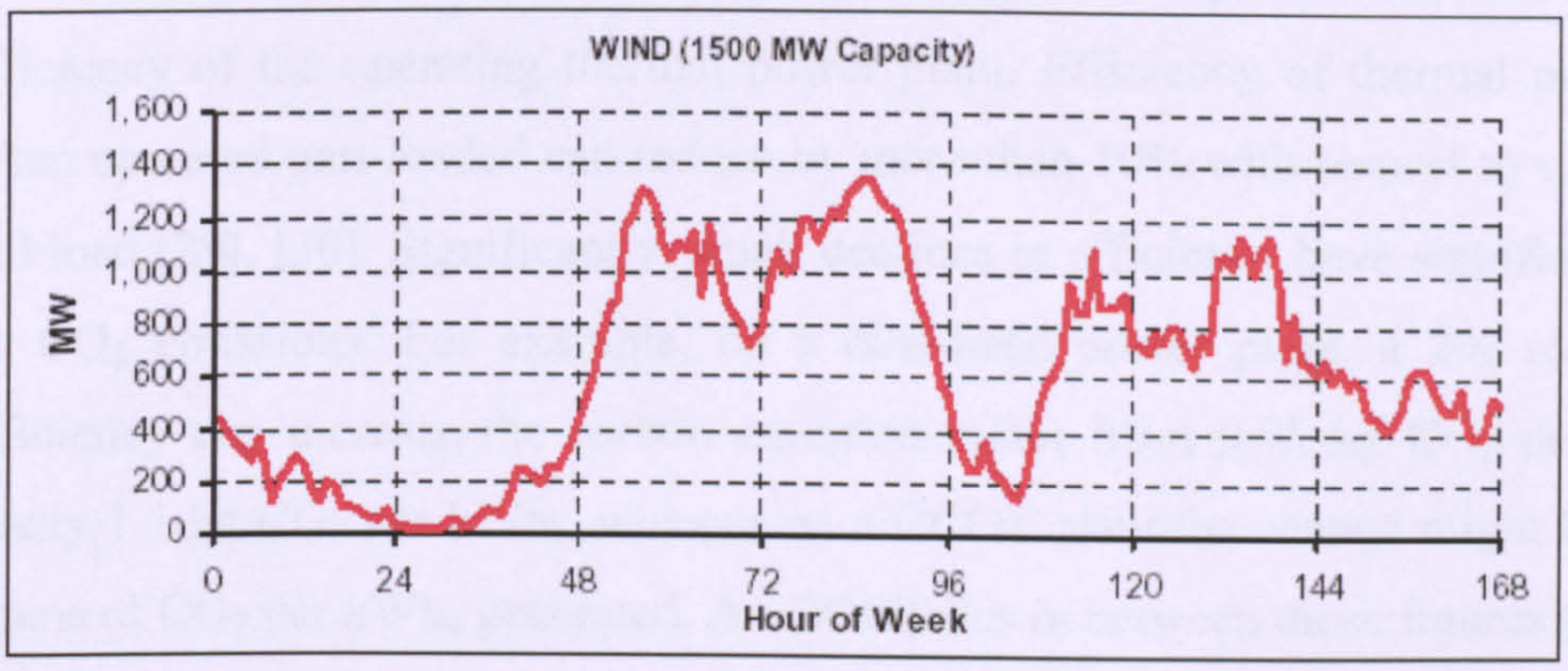

Figure 2.5 Wind power profile for the same week. 1,500 MW of wind installed capacity in the system [2].

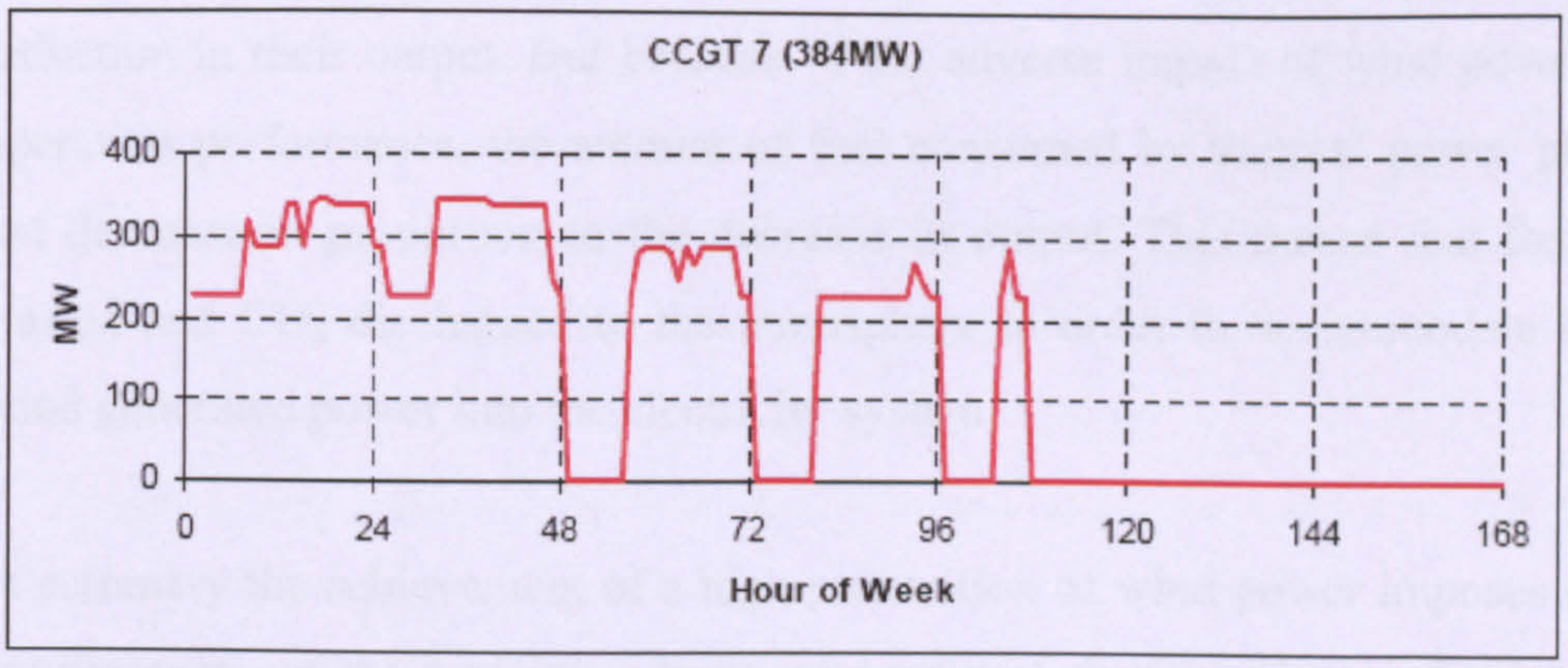

Figure 2.6 Simulation of the operational profile for the same 384 MW CCGT unit when including 24% penetration of wind power (1,500 MW) in the Irish power system [2]

Increased plant ramping duties and start-up/shut-down cycles of thermal power plant inevitably results in higher specific fuel consumptions, and consequently higher specific carbon emissions, as well as more frequent thermo-mechanical stressing of the plant itself and thus increased operational and maintenance costs.

Emissions from conventional power stations are usually minimized by reducing demand fluctuations and maximizing the base load, this allowing the cleanest power system to predominate. However, as wind powered generation increases, it imposes extra demand fluctuations on power stations, and ultimately results in a lower average efficiency of the operating thermal power plant. Efficiency of thermal power plant when operated part-loaded can reduce by more than 10% with respect to operation at full load [29], [30]. Significantly, small declines in efficiency have significant effects on CO_2 emissions. For example, on a coal-fired power plant, a 2% reduction in efficiency can increase the carbon emission factor from 0.95 kg CO_2 per kWh_e to nearly 1.1 kg CO_2 per kWh_e, whereas on a CCGT plant the change might be 30 – 50 grams of CO_2 per kWh_e generated. An OCGT lies in between those figures [31].

The energy output from WPP replaces an equivalent amount of electricity otherwise derived from thermal plants. Thus in theory it might be expected that this would reduce the amount of fossil fuel consumed at thermal plants in proportion to the reduction in their output. But because of the adverse impact of wind power on their operation performance, the amount of fuel consumed by thermal power plants does not decrease in proportion to the decrease in output. This means that fossil fuel is wasted and CO_2 discharged to the atmosphere in order to accommodate increasing wind generated power into the electricity system.

In summary the achievement of a high penetration of wind power imposes additional requirements on the remaining large conventional thermal plant and raises specific carbon emissions because the remaining power plant are forced to operate following more variable cycles thus reducing their operational efficiency. These factors drive

the need for new technologies and solutions (e.g. integration of electrolysers within the power system) to deliver both the capacity and flexibility necessary to maintain the continuous balance between demand and generation. Potential solutions are:

1. To deploy more flexible and efficient power plant able to operate under increased cycling duties.
2. To implement electricity storage systems for wind and RE in general.
3. To deploy electrolysers as a load management mechanism in the power system

Optimization of power plant to operate in combination with WPP is already underway [32], [33]; and the use of electricity storage methods (e.g. batteries, CAES, etc) has also been assessed by other authors [34], [35]. The focus of this study is then on the latter.

2.3 GREATER REQUIREMENTS FOR RESERVE GENERATION AND ASSOCIATED CO_2 EMISSIONS

It is commonly agreed that power systems will require an increasing thermal capacity to be kept as synchronized regulating reserve (coal and CCGT plant running part-loaded) as wind penetration increases. In addition more thermal plant will also be required as fast and standing reserve to start-up on short notice output[2], mainly OCGT plant.

Neither nuclear power nor gas Combined Heat & Power (CHP) plants are suitable as back-up reserve to provide rapid increase or decrease in load in response to a change in system demand. Hence the choice of back-up generation normally becomes restricted to gas (both CCGT and OCGT plant) and coal generators (at present oil

[2] OCGTs kept "warm" in a standby mode typically consume 25% that of fuel consumed when operating at full load with no electrical output being delivered [36]

generators also make a small contribution although trends are to eliminate the use of oil to produce electricity). **Figure 2.6** shows how different types of power stations are presently deployed to meet demand in England and Wells on a typical high demand winter day.

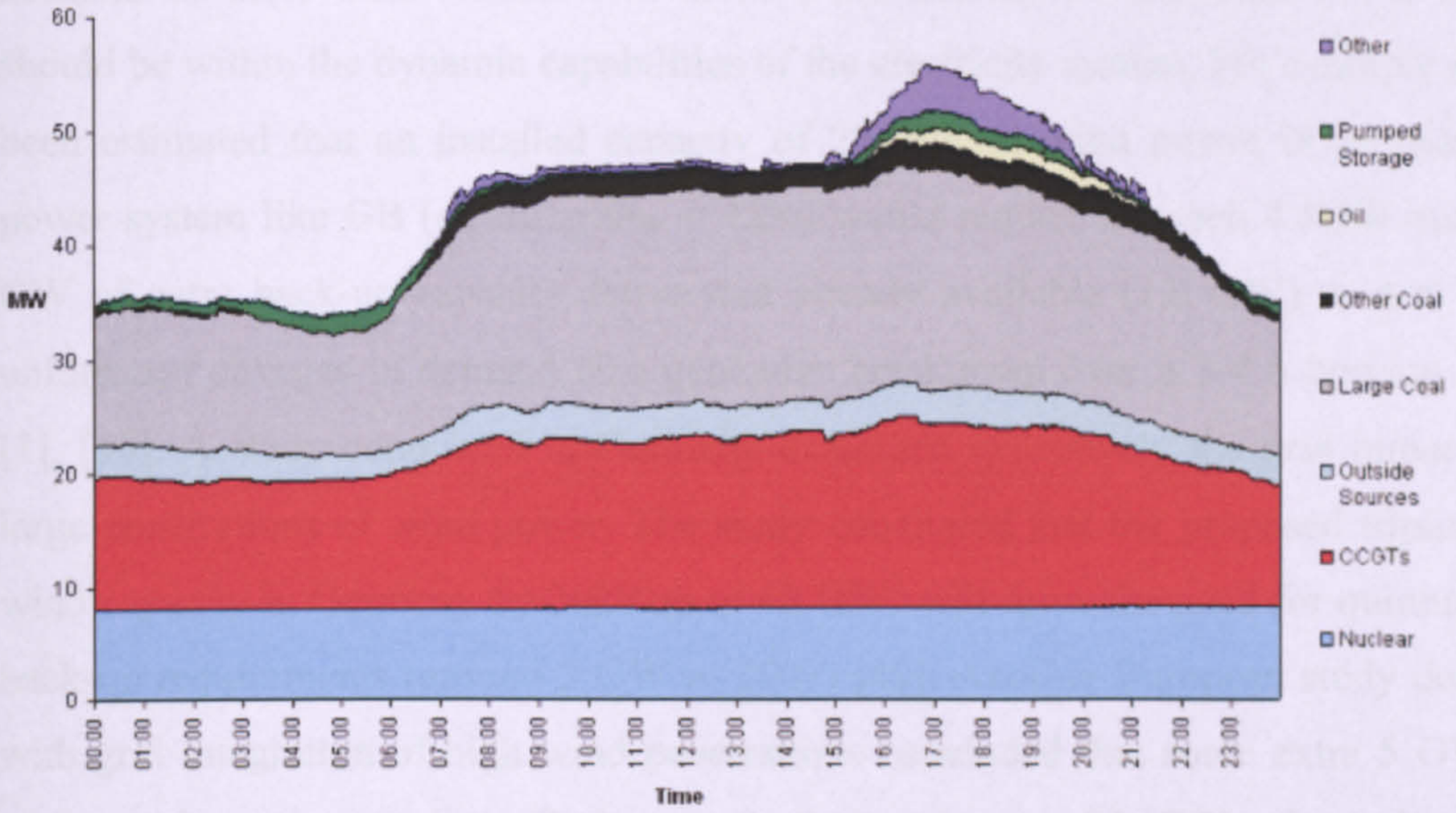

Figure 2.6. Generation-demand matching in the GB power system, 10th Dec 2002 [37]

From **Figure 2.6** baseload is met mainly by nuclear power stations and CCGTs, with some contribution from large coal-fired stations and electricity imported from France through the 2 GW HV DC link; when demand raises, more use is made of large coal-fired stations, and other types of plants are also brought into use. The total capacity of plant available to supply the grid needs to exceed the predicted maximum demand in order to cope with breakdowns and other unexpected eventualities, e.g. a sudden drop in the output of intermittent renewable sources; this is known as plant margin.

Some studies [38-41] have tried to estimate the amount of extra back-up capacity required to maintain balance between generation and demand when including a considerable amount of intermittent power in the electricity system. The extra requirement for reserve (synchronized and standing) in these studies is assumed to be driven by the overall system fluctuations of demand and generation (including wind power plants) over a 4 hour time horizon. This is driven by the assumption that time horizons of more than 4 hours will involve the start-up of additional units, which should be within the dynamic capabilities of the electricity system. For example it has been estimated that an installed capacity of 25 GW of wind power in an islanded power system like GB (equaling $\Phi_W = 42\%$) would require between 4.5GW and 5.5 GW of extra back-up capacity above that already available (1.2 GW) to deal with unforeseen changes in demand or a generator breakdown over a 3-4 h horizon [38], [1], [39]. A study conducted in Germany examined extensively the grid impacts of large penetrations of wind power. The study concluded that the proposed tripling of wind capacity in Germany by 2020 up to 48 GW[3] will drive the need for quintupling back-up requirements (around 2 GW in 2003) [40]. Another European study dealing with grid integration of high wind penetrations concluded that some extra 5 GW of back-up thermal capacity will be required to integrate 36 GW of wind power predicted in Germany by 2015, along with heavy network reinforcements and modification of Grid Codes at the high voltage level [41].

More importantly the use of extra back-up generation for supply/demand balancing purposes has negative carbon emissions implications. The CO_2 emissions avoidance from RE in an island power system must be assessed including the impact that the accommodation of intermittent power sources into the grid have on the whole power system. Ahead of a predicted decline or increase in RE input, additional OCGT plant and part-loaded CCGT and coal plant must be available in case RE availability is not as predicted, which in practice means fossil-fired capacity operating in parallel with RE to accommodate production into the grid. The actual level of back-up derived CO_2

[3] Wind Capacity in Germany was 16.6 GW at the time of conclusion of [40]. Installed Capacity as of March 2007 approached 21 GW, above 26% of SMD [42].

emissions will depend on the fuel mix of fossil-fuelled capacity being operated to match the output of RE power outputs. **Table 2.1** below summarizes response times and average carbon emission factors of power plant currently used as back-up generation.

Power Plant	**Response time**	**Carbon emission factor (kg CO_2/kWh$_e$)**
Pumped Storage	15-20 s	0.57
Standing Reserve (OCGT)	5-10 min	0.47-0.55
Spinning Reserve (Part-loaded CCGT)	5-20 min	0.35-0.42
Spinning Reserve (Part-loaded coal)	5-20 min	0.95-1.1

Table 2.1. Back-up generation, performance parameters[4]

Some studies have tried to estimate the increased in fuel consumption of back-up plant (and hence reduction in carbon savings derived from wind power) as wind penetration in the power system increases. [31] estimates the increase in CO_2 emissions of back-up coal and gas-fired plant at 10-15% due to increased operation at part load which decreases the average efficiency of operation. [2] concluded that in an isolated power system like Ireland the average CO_2 emission savings reduce by 20% (tonnes of CO_2 avoided per MWh$_e$ of wind electricity produced) when wind penetration increases from 10% to 30% due to the growing inefficiency of operation

[4]CCGT and coal plant are assumed to run at 50-70% of full load. If 50% loaded time response can approach 30 minutes [43], [2]. The higher values correspond to older plant and part-load (i.e. low efficiency) operation. Efficiency of pumped hydro is 75% [41] and grid carbon intensity factor is taken at 0.43 kg CO_2/kWh$_e$, the estimated value for the GB power system [31], giving an estimated carbon intensity of 0.43 / 0.75 = 0.57 kg CO_2/kWh$_e$.

of conventional power plant acting as back-up generation. [45] estimates that in North Germany (E-ON transmission grid, wind penetration of ca. 30%), around 118 GWh of additional fossil fuel (coal and gas-fired back-up plant) was used to accommodate 150 GWh of wind energy (around 0.8 GWh of fuel per GWh of wind energy) across a weekly period during which wind generation supplied 15% of the total system demand.

Although not always openly discussed, it seems clear that the use of back-up capacity is essential for RE power integration and that the CO_2 emissions from back-up capacity are not insignificant. Therefore, beyond modest penetration levels, the deployment of RE plant as a means of carbon abatement appears to be compromised by the inherent intermittency of most renewable energy supplies. Beyond a certain limit, this may eliminate a significant proportion of the carbon emission reductions associated with RE implementation. Accordingly, an increase in the installed capacity of RE plant in a power system does not result in a proportional decrease in the system's carbon emissions. In summary, the specific CO_2 saving credentials of wind power diminish with increasing wind penetrations.

2.4. CURTAILMENT OF WIND GENERATION

The ability of the grid to accommodate wind power production is limited by the power plants within the fuel mix that cannot reasonably be regulated (e.g. nuclear plant, where load changes affect reactor safety), or have preference over wind energy (usually hydropower), or are insufficiently flexible, namely large thermal plant at minimum load factor. For instance, coal-fired steam generation can load follow only over the range 40-100%[5], limited by unstable flame at low load [48], and CCGTs can

[5] Strictly speaking coal-fired power plant can turndown to 15-25% (depending on design, with plant modifications) limited by combustion stability, but at the expense of increasing thermal stresses in the boiler significantly [46], [47] and therefore plant operators tend to avoid operation at such low loads unless absolutely necessary.

load follow over 50-100%[6] (limited by ineffective low NOX burners at low load) [49].

Besides the minimum loading levels inherent to thermal power plant, to counter for the possibility of a sudden large drop in wind generation (this can be produced by a sudden loss in wind resource or by a network fault that exceeds the ride-through capability of the wind generators), a dynamic penetration limit is also enforced in power systems with significant wind power installed capacity, which effectively limits the amount of wind power that can be directed to the electrical grid.

These constraints result in an overall penetration limit characteristic for a specific power system which ultimately depends on: (i) the size and interconnections of the power system; (ii) type and size of conventional units in operation; (iii) dispersion of the wind generators within the system; and (iv) power market regulation and practice. Typical penetration limits applied for wind power in island power systems vary between 15% and 50%, meaning that wind power will be discarded at any time when the equivalent aggregate wind power output exceeds the penetration limit [52], [53].

As wind power penetration (Φ_W) increases, situations of imbalance arise, particularly at periods of low system demand and high wind availability, to the extent that in certain regions of the network not all the wind generation available can be accepted into the grid and some is in fact rejected. In practice the TSO has to instruct some wind power plant (WPP) to curtail some (if possible) or all of their wind generation output during a certain period to avoid surpassing the penetration limit established. This has been a recurrent situation in Germany [53] and Spain [54] in the last years, when low system load clashing with high wind conditions have induced a fraction of wind energy to be discarded by shutting down some wind plants to maintain system security levels and to avoid operating thermal power plants below their minimum load limits.

---

[6] The last generation of CCGT plant have a technical minimum operating point of around 40% limited by ineffective low NO_X burners (located in the combustion chamber) and thus subject to legislation applicable as well as flame instability at low-load. However turning down below 50% of load will increase wear & tear of the heat recovery steam generator considerably (thermal stresses), reducing the operating life of the plant and thus is not common practice [50], [51].

The degree of interconnection of the power system is probably the most critical factor affecting wind curtailment. The availability of transfer capacity to neighbouring power systems constitutes a significant tool for managing the intermittency of wind generation because it allows exports of surplus power in high wind conditions and imports during windless periods, increasing the dynamic penetration limit and thus reducing the need for wind curtailment. By definition island power systems lacking significant interconnections (e.g. Spain, UK or Ireland) must balance generation and demand internally. Hence they will have a more restricted capacity to absorb wind power, incurring wind curtailment at lower Φ_W, and will have wind penetration limits significantly lower that those of well interconnected systems (e.g. Denmark and Germany). To illustrate this, no significant wind curtailment has been reported in West Denmark even though wind penetration exceeds 60%, due to the availability of interconnections to Norway, Sweden and Germany, totaling a transfer capacity of 2,830 MW, in excess of its 2,400 MW of wind capacity installed[7] [55]. As **Figure2.7** shows, most wind power production in Denmark coincides with large power flows to neighbouring power systems. In other words, excess wind power is exported and the interconnections act as "relief valves" to discharge excess wind generation from the Danish power system. In contrast, curtailment of wind power has been recurrent in Spain since 2004, where total interconnector capacity is currently just 3% of total generating capacity and significantly lower than the country's wind generating capacity.[8] As a result wind curtailment reaches 12% of annual output in certain areas [54].

[7] Stranded wind power production has been a frequent event in Denmark in the past 3 years, but wind surges have been accommodated by exporting and importing power via the interconnectors (especially with Norway, which has large hydro resources that can respond at short notice). It is becoming more difficult for Denmark to export wind power to Germany, because of the large concentrations of wind turbines on both sides of their shared border. Therefore, although electricity trading with neighbouring countries has been a significant tool for managing the intermittency of wind generation in Denmark, it has become increasingly difficult to manage wind as more capacity is also integrated into the neighboring power systems. Accordingly the Danish government has decreased its subsidies for wind projects [55], [56] and the current regulatory uncertainty has put a halt to further new developments, to the extent that just 9 MW of new wind capacity were installed during the period 2004-2006 compared with a total of 1,600 MW installed in the period 1999-2003 [57].

[8] Installed Capacity in Spain as of March 2007 exceeded 11 GW, above 26% of SMD [42]

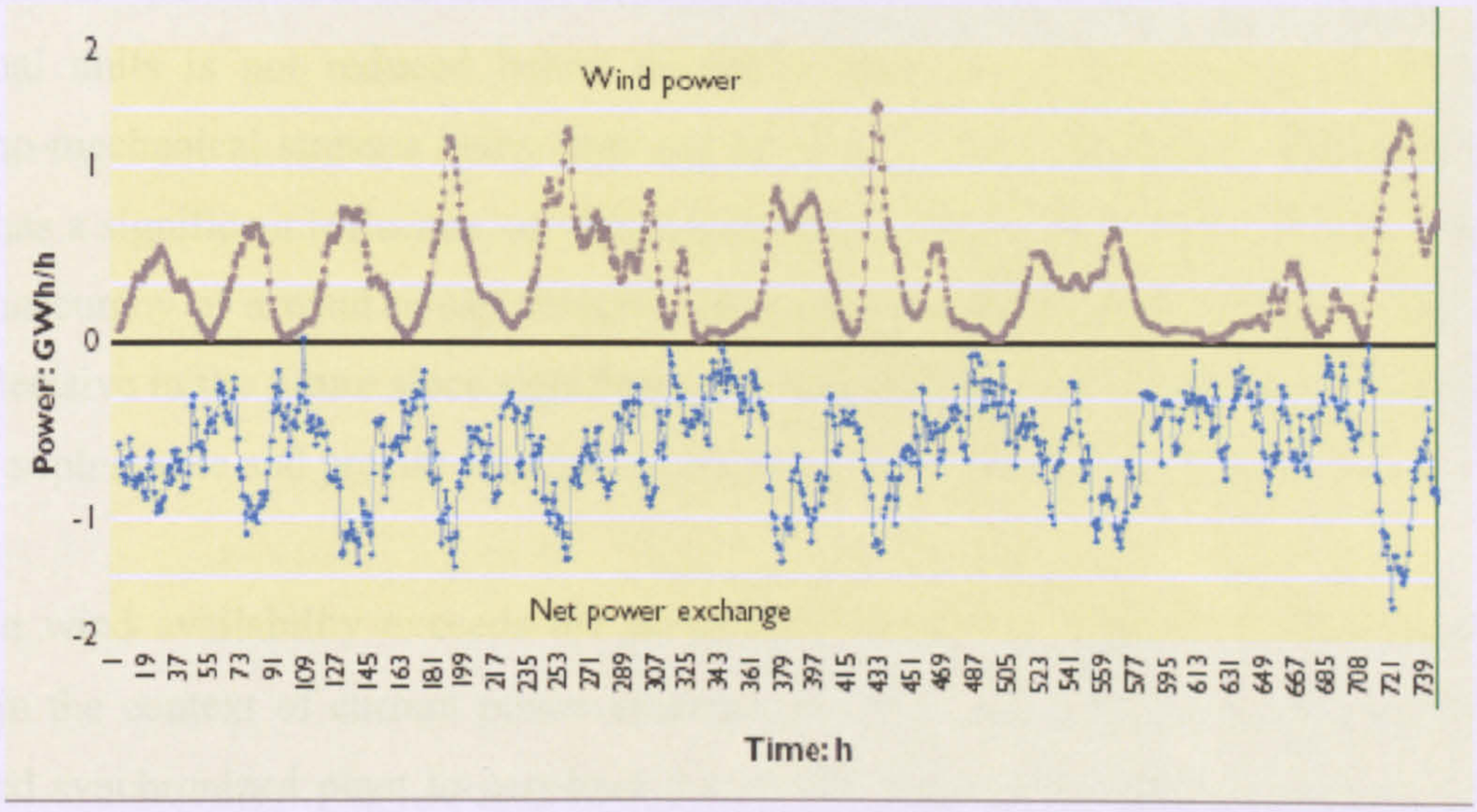

Figure 2.7. Wind power and net power exchange in West Denmark in January 2004 [53].

The flexibility of the generators within the power system is another key factor leading to wind curtailment. For instance, nuclear power plants are considered inflexible in this context because they are not designed to be turned down for short periods (as wind generation increases), whereas hydro power plants are highly flexible and they can be easily and rapidly regulated. Also, balance between synchronized and standing reserve is another key driver. Flexible standing reserve supplied by OCGTs can displace part-loaded synchronized reserve as back-up generation, increasing the amount of wind power that can be absorbed as fewer generating units are scheduled to operate, leaving more room in the system for wind and hence reducing the amount of wind generation that has to be rejected. However the allocation of back-up reserve between synchronized and standing units in practice is likely to be a trade-off between the costs of maintaining synchronized reserve and the costs of operating less efficient standing plants with high fuel costs.

In addition, for every thermal generation unit it is normal for manufacturers to specify a maximum permissible number of start-ups per year [58], so the operational life of thermal units is not reduced below desirable limits as a consequence of greater thermo-mechanical stresses being imposed on them. Lastly, quality of wind forecast also has a significant influence, as wind curtailment tends to be highly correlated with the inaccuracy of a wind power forecast. However, it is likely that this factor will be less decisive in the future since significant research is been carried out on this area and more sophisticate and precise forecasting methods are being developed [59], [60].

When wind availability exceeds the penetration limit, the common order of action within the context of current power systems would be to (i) reduce output of fully-loaded synchronized plant to part-load (ii) charge pumped storage installations with surplus wind, (iii) curtail some wind plants [61], [52]. Even though switching thermal plant from part load to off would seem a better alternative to (iii) in carbon terms, current operation of power systems worldwide is driven by costs and security criteria, not environmental criteria, and switching off part-loaded plants when there is an increase in wind generation from that forecasted is considered too perilous as to become an option under current operational procedures[9].

In principle, if no energy storage is available, the higher the wind penetration, the larger the amount of wind power that has to be discarded particularly in island power systems with no significant interconnections. For small penetrations of wind power in isolated systems, nearly no wind energy has to be discarded, while at higher penetrations the percentage of curtailed wind energy rises strongly. [62], [52] estimates total wind curtailment for an island power system with a wind penetration of 40% at 32% of total wind generation available. Wind curtailment and its impact on CO_2 emission savings from wind power is discussed further in **Chapter 4.3.2** including estimations of wind generation curtailed for different levels of wind penetration and wind availability for an island power system.

[9] CCGT units take between 1 and 3 hours to start-up depending on the duration of the shutdown, whereas coal units can take up to 8 hours [63], [64].

2.5 SUMMARY

When wind power production exceeds the amount that can be safely absorbed by the electricity system while still maintaining adequate reserves and dynamic control of the system, some of the available wind power has to be curtailed. This is becoming common practice in systems with high penetrations of wind power (e.g. Germany and Spain) and inevitably leads to loss of available RE resource. The value of Φ_W at which such measures are taken depend on a number of factors which are location specific, like the degree of interconnection with neighbouring systems, the flexibility of the rest of power plant available and the operational strategy of the power system, but undoubtedly the amount of wind generation curtailed increases with Φ_W in the system. This 'curtailment' inhibits the production of low carbon electricity despite the high installed capacity of wind power plant within the power system.

Solutions are therefore required for regions of high wind resource to facilitate the achievement of high wind penetrations. One solution, which may be applied for RE sources in general, is to deploy water electrolysers as controllable loads for load management. In combination with hydrogen storage systems, electrolysers can be used to enable the load placed on thermal power plant to be increased or decreased in time phase with the availability of RE inputs to the power system. Electrolysers can thus be used for hydrogen production both in the case of a fluctuating excess supply (e.g. during prolonged and rising RE generation) and during periods of low electricity demand. The supply of electricity becomes effectively decoupled from the demand in such a way that the operation of thermal power plant depends less on consumer demand. In addition, this form of load management can lead to a higher average utilization rate for preferred low-carbon thermal power plant. Furthermore curtailment losses could be eliminated by allowing electrolysers to absorb the wind output otherwise curtailed. Hence it is certainly at high wind penetrations levels when the case for implementing electrolysers into the power system becomes meaningful. The use of electrolysers to capture otherwise curtailed wind energy provides a major

stepping stone to the hydrogen economy, which is synergistic with the needs of the power industry.

CHAPTER 3 - LOAD MANAGEMENT THROUGH ELECTROLYSERS: BOUNDARIES OF THE STUDY AND MODEL DESCRIPTION

3.1. LOAD MANAGEMENT THROUGH ELECTROLYSERS: BASIC CONCEPT

A future power system with a large installed capacity of intermittent renewable power sources (RE) like wind, solar and wave power relative to its maximum system demand also requires a large installed capacity of controllable fossil-fuelled power plant (FPP) to cover periods of low RE generation. The most prominent example of intermittency (and also the fastest growing among RE) is wind power, where the natural fluctuations have raised concerns about achieving high penetrations, especially in isolated power systems lacking significant interconnections.

Predictions for several European countries suggest that in future much higher RE penetrations will be required if carbon abatement targets are to be met, possibly in excess of 100% of the system maximum demand [65-67]. Accordingly, the operation of a power system with very high wind penetrations deserves research attention. However if high wind penetrations are to be realised, two carbon emissions problems associated with managing supply intermittency and supply/demand balancing first need to be addressed:

- Firstly, the requirement for more flexible operation of back-up FPP increases with wind penetration in order to balance the RE supplies with the time-varying demand. This increasingly RE-dependent operation of thermal power plant for supply/demand matching results in a carbon penalties that increases with wind penetration (see **Chapter 2**).

- Secondly, if at any time wind power plant (WPP) generation exceeds that which can be safely absorbed by the power system, some of the available RE inputs need to be curtailed. The curtailment of WPP during periods of high availability but low demand will inhibit the production of low-carbon electricity and thus penalize efforts to achieve high wind penetrations.

In the power generation sector, a **load profile** shows power (MW) supplied (on the vertical axis) plotted against time of occurrence (on the horizontal axis) to illustrate the variance in a load across a specified time period. Power producers and TSOs use this information to plan how much electricity the supply side needs to produce to match consumer demand at given times, usually across 24h periods. A **thermal load profile** is commonly referred to as the load profile of the aggregate FPP and illustrates the variation in aggregate power output across a specified time period.

When a significant amount of wind power is added to the system the operation of FPP and therefore the thermal load profile becomes affected since their operation is now a function of the WPP output available. Throughout this investigation the aggregate wind power output of all WPP in the power system is considered as a negative demand, so the residual demand to be met by FPP is found by adding this negative demand to the aggregate consumer electrical demand, as shown in **Figure 3.1**.

The **load factor of the thermal load profile (LF_{TH})** is defined as the ratio of average to peak load (%) across a certain time period. The load factor of the net thermal load profile acts as an indicator of the carbon performance of the FPP portfolio. The greater the load factor, the flatter the load profile faced by thermal power plant, the more efficient its operation and therefore the lower the carbon intensity of the electricity generated [68], [2]. Comparing thermal load profiles with no wind and 30% wind penetration[10] based on actual data from East Denmark [17] in **Figure 3.1** we can observe clearly a huge increase in the variability of thermal load when a

[10] Throught this report the term wind penetration is referred to as percentage of wind power installed capacity over system peak demand, some 2,665 MW in East Denmark in 2003 [17].

significant amount of variable wind power is introduced into the power system. In particular, for the case shown the load factor of the thermal load curve (average profile value / peak value) drops from 83% (thermal load if no wind) to 71% (thermal load if 30% wind), increasing the variability of the thermal load profile.

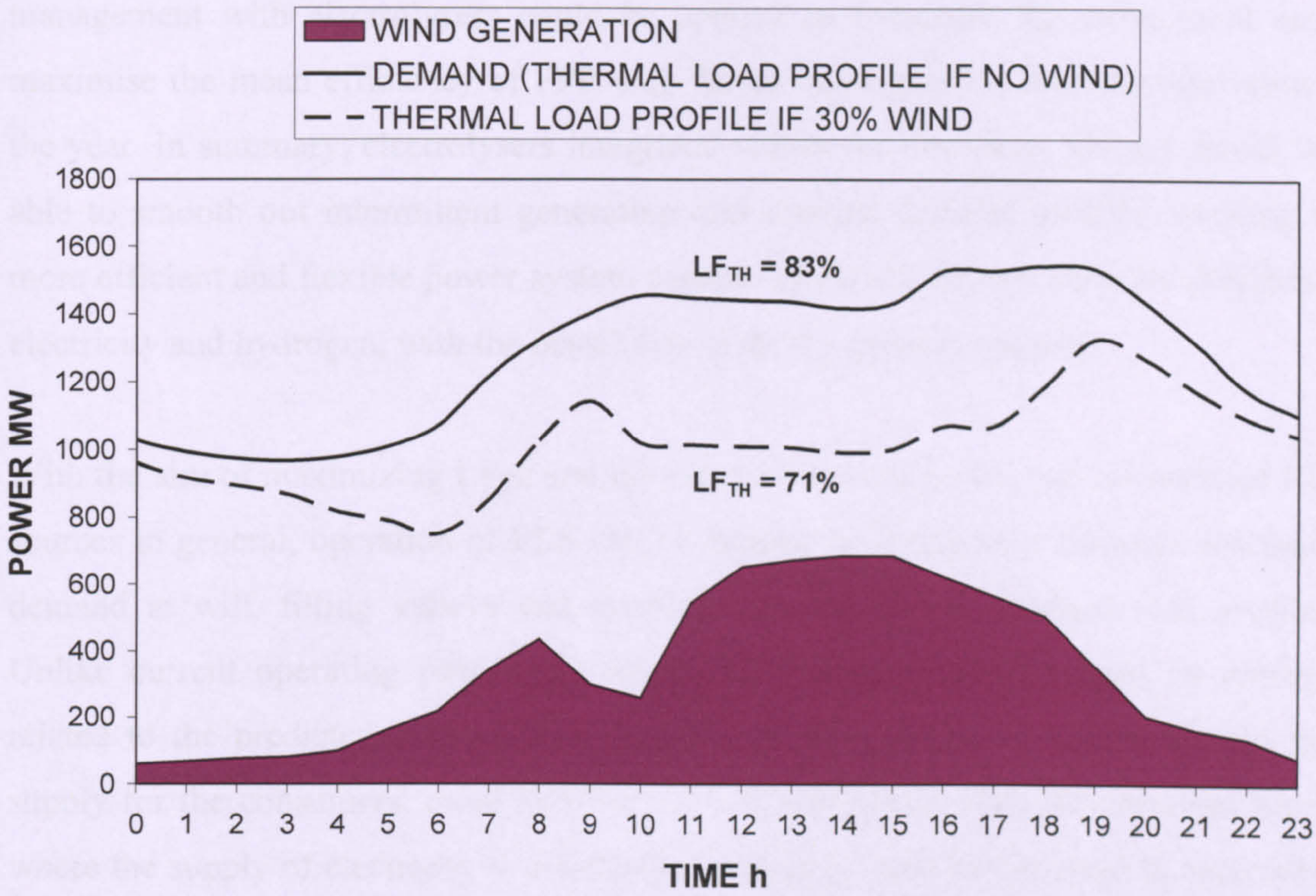

Figure 3.1. Demand, wind power input profile and thermal load profile based on actual data from [17]

In order to achieve large wind penetrations load management and energy storage solutions are required. A widescale deployment of water electrolysers (ELS) within the power system is suggested here to facilitate the achievement of very high wind penetrations beyond those limits considered feasible today. Instead of adapting power generation in an electricity system with a high penetration of wind power to the time varying demand profile, it is proposed that the demand profile could be arranged to suit the availability of wind power in a manner which increases (rather than

decreases) the load factor of the aggregate load profile placed on FPP. This partial decoupling of demand from supply would be achieved by electrolysers, where surplus electricity is used for hydrogen production. Active load management with electrolysers has the potential to be used as a central mechanism for controlling the load profiles placed on FPP in order to improve their carbon footprint. Load management with electrolysers could be applied to minimise RE curtailment and maximise the mean efficiency of FPP with fewer cycling duties and start-ups across the year. In summary, electrolysers integrated within the electricity system would be able to smooth out intermittent generation and thermal demand profiles, creating a more efficient and flexible power system capable of delivering two valuable products: electricity and hydrogen, with the possibility of the by-product oxygen.

With the aim of maximizing LF_{TH} and the capture of wind power and intermittent RE sources in general, operation of ELS can be adapted to increase or decrease the total demand at will, filling valleys and creating plateaus on the thermal load profile. Unlike current operating procedures where the operation of FPP must be always related to the predicted demand and wind generation profiles to ensure security of supply for the consumers, more flexible and efficient approaches are proposed here, where the supply of electricity is effectively decoupled from the demand in such way that the operation of FPP becomes decoupled from the instantaneous electricity demand. In combination with a hydrogen storage system, electrolysers can be used for load management in the same way as a variable electricity consumer.

By deploying electrolysers in the system and operating them as additional controllable loads, switching them on and off as required, the load placed on FPP can be increased or decreased through the operation of electrolysers in time-phase with the power inputs to the electrical grid (wind and thermal-derived). For instance, every time there is an excess of electrical power supply over and above that required to cover the consumers demand D_c, the surplus power is then used for electrolytic hydrogen production, thus raising the valleys in the thermal load profile and hence enabling a

less "demand dependent" operation of thermal power plants, maximising their efficiency and by implication minimizing carbon emissions per kWh_e delivered.

In order to operate prospective high wind power systems in combination with a large electrolyser stock, it is necessary to develop suitable electrolyser control strategies that take into account:

- wind power availability
- the demand for electricity from consumers (excluding electrolysers)
- the interaction of these two factors upon supply/demand matching of the other (thermal) power generators

A methodology has been developed to assess the implementation and operation of a large stock of electrolysers in conjunction with WPP and other zero-carbon power plant within a generic power system, so that very high load factors can be achieved on the FPP load profile during periods of different wind availability and consumer demand. Thereby preferred capacity levels and operational strategies were identified for the required stock of electrolysers. Results are presented here for an islanded power system based on wind generation and demand data for Eastern Denmark.

3.2. STUDY CONTEXT AND BOUNDARIES

In the absence of energy storage methods, island power systems lacking significant interconnections with neighboring systems present a number of unique characteristics and special challenges when it comes to the integration of large amounts of intermittent RE sources and in particular wind power. The isolated nature of such systems results in limitations to the amount of wind generation that can be absorbed, leading to wind power curtailments, and poses significant burdens on the thermal power plant operating in the system. Examples of these are Spain, UK and Ireland. Other systems with large transfer capacities (in relation to their SMD), e.g Denmark,

France or Germany, are capable of absorbing much higher wind penetrations before requiring wind curtailment and energy storage solutions. Therefore island power systems constitute the toughest challenge in which to integrate a large proportion of RE and are the objective of this investigation.

Consider a generic power system that consists of only two types of power plant, FPP and zero-carbon power plant, ZCPP (e.g. renewable, nuclear or CO_2-sequestred power plants), one independent load (consumer demand), no interconnections with neighbouring power systems (i.e. islanded system) and no energy storage technologies.

This is referred to here as the **Base Case**; it is employed to illustrate the diminishing returns associated with increasing Φ_W when no load management method is applied. The power system is then modified to accept an electrolyser stock, but no other energy storage technologies or load management mechanisms (such as peak demand reduction) are considered. Hence three independent loads are now included: equivalent electricity consumer, equivalent embedded "demand-side ELS" (additional electricity demand in the T&D system) and equivalent "supply-side ELS" as shown in **Figure 3.2**. In summary FPP and ZCPP are connected to the electrical grid, which now feeds electricity to consumers and also to a fleet of electrolysers.

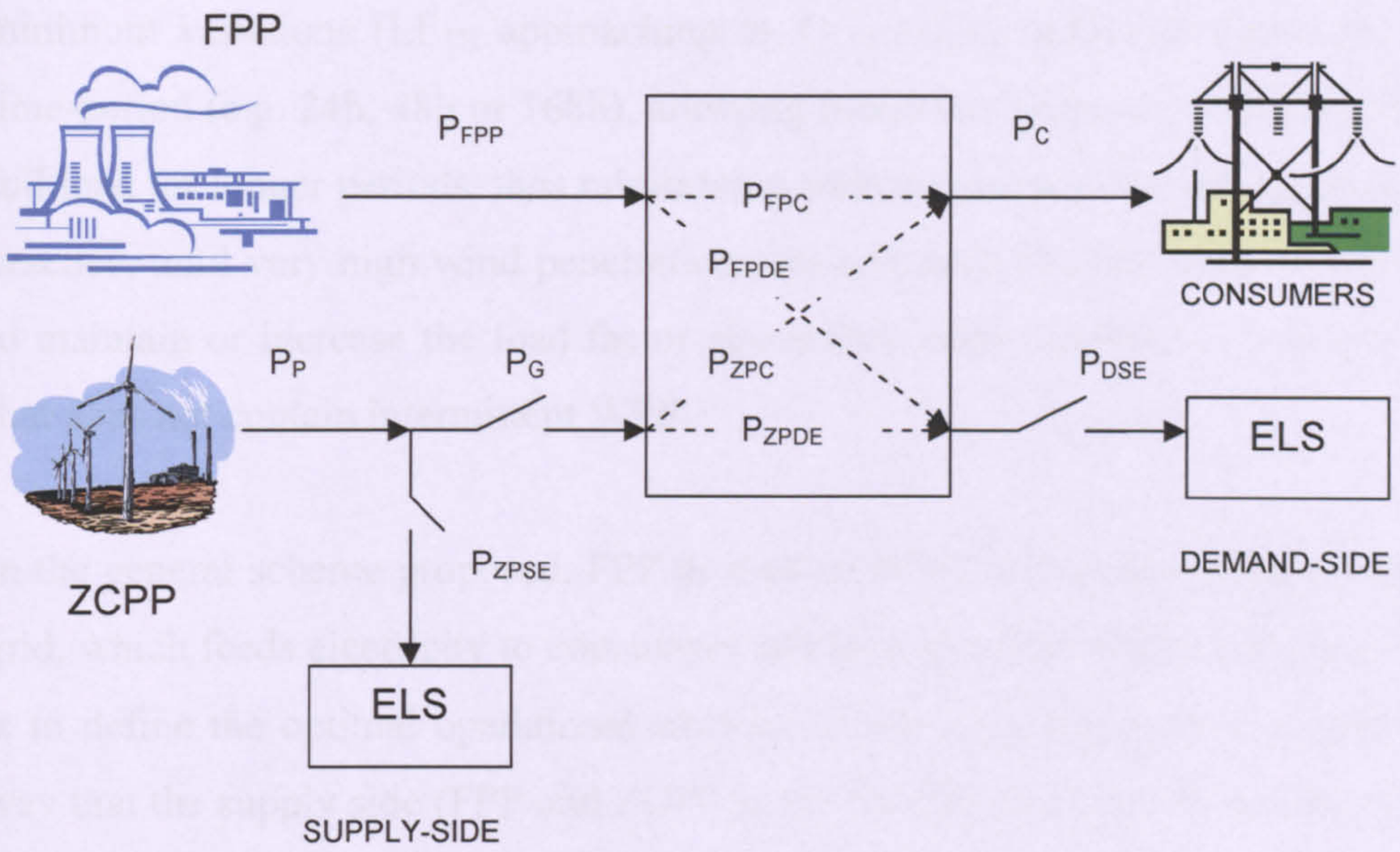

Figure 3.2. Schematic of a power system with active ELS demand management

If a low-carbon (as opposed to zero-carbon) supply of hydrogen is to be produced it is important that the associated carbon intensity value is maintained significantly below that of the conventional hydrocarbon reformation methods that typically yield 6-11 kg CO_2 / kg H_2 [67]. Only the production of zero-carbon hydrogen and low-carbon hydrogen of carbon intensity 3 kg CO_2 / kg H_2 is considered in this analysis. The latter value is chosen at half the carbon intensity of H_2 produced via hydrocarbon reformation methods to allow electrolysers to operate in a more flexible manner taking also some thermal power (P_{FPDE} in **Figure 3.2**).

An idealised 'power logic' approach is studied here: it is assumed that ideally, at every instant electrical power will be provided to the electrolysers stock (ELS) in relation to the renewable power coming into the grid, and that the electrolysers' operation is time-controlled in relation to the aggregated electricity demand, FPP load (i.e. demand to be met by fossil power plant) and wind power availability. For the purpose of this analysis it is also assumed that ELS would respond instantaneously to

a step-up or step-down in power input. Ideally, a continuous flat FPP load profile with minimum variations (LF_{TH} approaching to 1) could be achieved across an specific time-period (e.g. 24h, 48h or 168h), allowing fossil-fuelled power plants to operate at full load for longer periods, thus minimizing carbon emissions per kWh_c generated. In practice, until very high wind penetrations are achieved, the challenge will simply be to maintain or increase the load factor above that value applying to a power system that does not contain intermittent WPP.

In the general scheme proposed, FPP as well as ZCPP are connected to the electrical grid, which feeds electricity to consumers and also to a fleet of electrolysers. The aim is to define the optimal operational strategy of the integrated power system in such way that the supply side (FPP and ZCPP in the model) must always be able to supply electricity to the demand side (consumers and electrolysers).

The analysis presented here is based on daily and weekly load profiles and is intended to optimize the operational performance of FPP by raising the early morning and night-time valleys, and creating a day-time plateau that is much broader than the conventional peak (e.g. a plateau from 09:00 to 18:00). The higher the LF_{TH} the flatter the load profile faced by FPP and the more efficient its operation, minimizing carbon emissions emitted per kWh_c generated [19], [6] and [48].

As far as the analysis presented in this thesis is concerned, it is assumed that ample storage capacity exists to absorb all the hydrogen generated. In addition, an existent demand for the hydrogen produced is assumed to be in place as to absorb the totality of the hydrogen generated for all the implementation cases presented (see modelling assumptions below).

Implicit in this approach is that electrolysers are used mainly to produce hydrogen and oxygen as dictated by requirements external to the electricity sector. For the purpose of this analysis it is considered that the production of hydrogen is adequate to match an existent hydrogen demand, and the sizing of the electrolyser system is determined

by the availability of wind and thermal power inputs. In practice the electrolyser stock size would be dependent on the existent demand for hydrogen e.g. transport fuel demand, industrial and domestic heating demand, chemical industrial processes, etc. Practical considerations related to hydrogen storage and demand are discussed in **Chapter 6**.

It would be possible to reconvert the hydrogen produced from ELS (via fuel cells, H2 gensets or H_2 turbines) back to electricity for example at peak-price times for further supply-demand balancing. Controllable zero-carbon power generators could then be attained. Unfortunately the round-trip efficiency of these systems is rather poor, with examples of current technology being around 15-30% [69], [70]. Hence it is more energy-efficient to use the zero/low carbon hydrogen directly for transport, heating or industrial uses than to reconvert it back to electricity and use it as a mere electricity storage mechanism. Not only there are more efficient means of storing electricity like pumped storage, batteries, CAES, flywheels, etc but the potential and versatility of H_2 lies well beyond the electricity sector.

This study looks at the use of ELS as a load management tool, as an alternative "sink" for surplus wind electricity and as a primary source of a zero/low-carbon hydrogen fuel. It is suggested here that electrolytic hydrogen should not be used to store and reconvert to electricity except in specific conditions (e.g. emergency back-up generation or remote and off-grid applications) and if possible in CHP applications to maximize overall efficiency. Apart from providing controllable loads to help balance supply and demand in the power system, large-scale implementation of electrolysers in conjunction with ZCPP must be envisaged within the much larger context of the energy system which comprises not only electricity, but also transport, industrial, domestic and commercial sectors where the benefits of H_2 can also be fully exploited. Consequently the load management approach devised here implies the use of electrolysers exclusively to raise valleys in the FPP load profile and it does not consider looping peaks by reconverting H_2 back to electricity via fuel cells or H_2-fuelled engines.

It is also implicit that at all times the electrolyser stock is operated in such way that the combined load represented by consumers' demand and electrolysers, P_G, never exceeds the current system maximum demand (SMD), as expressed in **equation (3.1)**, so that the T&D capacity of the existing electricity system does not need to be enhanced.

$$P_G = P_C + P_{DSE} \leq SMD \tag{3.1}$$

Other authors [71] have suggested that the capacity of the power system could be substantially enhanced to include a very large electrolyser stock to facilitate the absorption of vast amounts of zero-carbon power sources beyond the existing SMD. This option, although valuable, implies radical changes and heavy upgrading of existing electricity systems if safety capacity margins are to be maintained and it is not considered herein. Instead the electrolyser stock is deployed here within the capacity limits of the existing electricity network. Depending on when the "new load" is operated, any existing T&D system has enough capacity to meet increased loads while maintaining safety capacity margins provided they do not occur at peak times since they are designed to handle SMD at any time and they . The operation of electrolysers then needs to be controlled in relation to consumers' electricity demand.

In terms of the specific configuration of the power system when integrating electrolysers, several options can be considered from the general scheme depicted in **Figure 3.2** taking into account the specific physical location and control strategy of electrolyser applications [67]. Such options include the following:

A. Deployment of electrolysers close to ZCPP (e.g. large renewable, nuclear or CO_2-sequestered power plants), or alternatively close to the nodes where electricity from large renewable power sites enters the onshore transmission network. This option implies large and medium scale electrolysers controlled to take some of the electricity output and so minimise the T&D reinforcement otherwise associated with

integrating these zero-carbon energy inputs. Rather than a widespread implementation strategy, this option could be regarded as a specific on-site fix for de-bottlenecking network capacity constraints resulting from increased levels of zero-carbon electricity sources connected to the existing network. It also allows a complete eradication of the curtailment issue associated with periods of low demand and high renewable output. However, the sitting of ELS away from the points of hydrogen use will require a significant hydrogen distribution infrastructure; unless a local demand for hydrogen as a heating, transport and/or industrial fuel can be identified.

B. Distributed embedded electrolysers (of small, medium and large scale) located at or near the points of hydrogen demand, with minimal hydrogen infrastructure requirements. On the other hand, ELS deployment would then be constrained by the potential need of an upstream reinforcement of the T&D system in relation to the sitting of ZCPP. Thus a careful and detailed analysis of both the transmission and distribution network is a pre-requirement for this configuration, including power flow constraints, possible bottlenecking at higher voltage levels, upgrading of low-voltage transformers, etc.

C. Electrolysers in off-grid or micro-grid configurations utilizing dedicated renewable, nuclear or CO_2-sequestred power plants (or some combination thereof). Even though this implies virtually zero impact on the existing power system, it also involves operation of ELS at the capacity factor of the power source, limited by the availability of the natural resource in the case of renewable power plants (e.g. around 25-30% yearly average for onshore wind power plants in the UK depending on location, compared to 80% for a nuclear power plant). This alternative also exhibit a substantial infrastructural requirement for the hydrogen generated solely by zero-carbon power sources, as well as electrolysers being capable of handling an intermittent and variable input.

Clearly if deployed to excess within a given area of the network (options A and/or B) they could significantly increase energy flows and some nodes might become

overloaded. Then additional upgrading of the system would be required to avoid load bottlenecks. Specific deployment configurations and therefore physical locations of electrolysers and network modelling issues are not considered any further here. A detailed network modelling to determine the most suitable location of ELS is beyond the scope of this thesis, but it would be a valuable topic for further analysis. Instead, a more simple approach is taken, according to the scheme shown in **Figure 3.2**. The focus here is on illustrating how the implementation of electrolysers within the power system can help to:

1. Maximize the efficiency of the system by increasing the load factor of the aggregate FPP load profile.

2. Increase the capture of intermittent RE sources by reducing wind power curtailment.

3. Generate a valuable clean fuel (alternatively a clean energy vector) for other energy sectors.

Following on the general scheme depicted in **Figure 3.2**, several possibilities for the implementation of electrolysers within the electricity system are considered, and an evaluation of these alternatives is carried out. Three implementation cases are described, preceded by a **Base Case**, included to illustrate the diminishing returns associated with a high penetration of intermittent wind power within the power system when no load management method is applied. These three cases are referred to here as:

- **Case 1** - Electrolysers on the supply side, located at or near the primary zero-carbon power plant in a manner which avoids having to transfer all of the generation to the grid. A proportion of ZCPP production P_{ZPSE} (0 to 100%) is sent to the SSE

stock, with no contribution whatsoever from grid electricity. Consequently only zero-carbon hydrogen is generated. No embedded electrolysers are implemented.

- **Case 2** – All electrolysers on the demand-side, embedded within the grid and located at or near the points of hydrogen demand. They are operated in such a manner that at every instant their aggregate electrical input P_{DSE} is always less than the total amount of zero-carbon power delivered to the grid P_G. Consequently only zero-carbon hydrogen is generated.

- **Case 3** – A combination of Cases 1 and 2. Electrolysers deployed both on the supply side and demand side. The production of low-carbon hydrogen with an average carbon intensity of 3 kg CO_2 / kg H_2 (kilograms of CO_2 emitted per kilogram of H_2 generated) is now considered and analysed against the production of zero-carbon hydrogen.

	IMPLEMENTATION CASE
Base Case	All wind power production is directed to the grid. Electrolysers are not applied to manage the renewable input in relation to the electricity demand.
Case 1	Supply-side electrolysers are deployed at or near ZCPP and exclusively fed by zero-carbon electricity, producing zero-carbon hydrogen. A maximized proportion of ZCPP production is directed to the grid to satisfy consumer demand.
Case 2	Demand-side electrolysers, distributed within the grid and located close to the points of hydrogen demand, are operated so that at any instant the aggregate load on FPP, is not allowed to exceed the consumer demand and no fossil-derived electricity is used to operate electrolysers. Therefore only zero-carbon hydrogen is generated.
Case 3	Cases 1 and 2 are combined by implementing both supply-side and demand-side electrolysers and permitting a hydrogen carbon intensity of 3 kg CO_2 / kg H_2

Table 3.1. Electrolyser Implementation cases

A heuristic procedure and a spreadsheet model, named **AELM model (Active Electrolyser Demand Management)**, has been developed for implementing and controlling a large stock of electrolysers in conjunction with high penetrations of ZCPP (e.g. wind, nuclear or CO_2-sequestered power plant) for an island power system, so that very high LF_{TH} can be achieved on the FPP load profile during periods

of different wind availability and consumer demand. Preferred capacity levels and operational strategies are identified for the required stock of electrolysers as a function of the penetration of zero-carbon power sources in the power system.

The three aforementioned implementation cases have been simulated and operational strategies investigated by using daily time series for the electricity demand and wind generation from the Eastern Denmark power system. Although the Eastern Denmark power system has in practice substantial interconnections with Sweden (1.9 GW) and Germany (0.6 GW) the analysis assumed an islanded power system, because this is the most challenging type in which to integrate a large proportion of intermittent wind power (see **Chapter 2**). The fuel mix for the Base Case is also required as input data. The general outputs are daily energy balances, load profiles, hydrogen yields and carbon intensities for electricity and hydrogen as well as average power values for the period studied.

3.3 APPROACH AND SPREADSHEET MODEL

3.3.1 Description of approach and spreadsheet model

The purpose of this section is to describe the approach followed for the implementation and control of large electrolyser capacities within a generic power system. A rule-based heuristic approach has been followed for the implementation of a "fleet" of electrolysers into the power system, to obtain:

- Aggregate capacity of electrolysers required

- Systematic control strategy for a national stock of electrolysers

The approach includes the analysis of different implementation cases, corresponding to Base Case and Cases 1, 2 and 3 in **Table 3.1**. The main focus is on optimising the load factor of the aggregate FPP load profile (LF_{TH}) thus reducing the cycling duties

of FPP and allowing them to operate more efficiently, consequently reducing their carbon dioxide emissions per kWh_e generated. This is achieved by filling valleys in the FPP load profile and creating a plateau at the level of peak FPP load through the operation of electrolysers. Analysis of the degree of smoothness of the FPP load profile is made through computation of the daily/weekly load factor. Modelling is based on a time interval of one hour.

The operation of electrolysers is time-controlled in relation to the aggregate electricity demand, thermal load (i.e. demand to be met by thermal power plants) and wind power availability. The AELM model has been developed using spreadsheets as an input/output model based on power and energy flows. The model can generate utilization strategies for the electrolyser stock, FPP and ZCPP from forecast profiles of demand and wind availability which are the primary input data. Other general outputs are energy balances, import/exports, resulting daily hydrogen productions and carbon emissions associated, as well as average power values for the time-interval appointed. These are summarised in **Figure 3.3**.

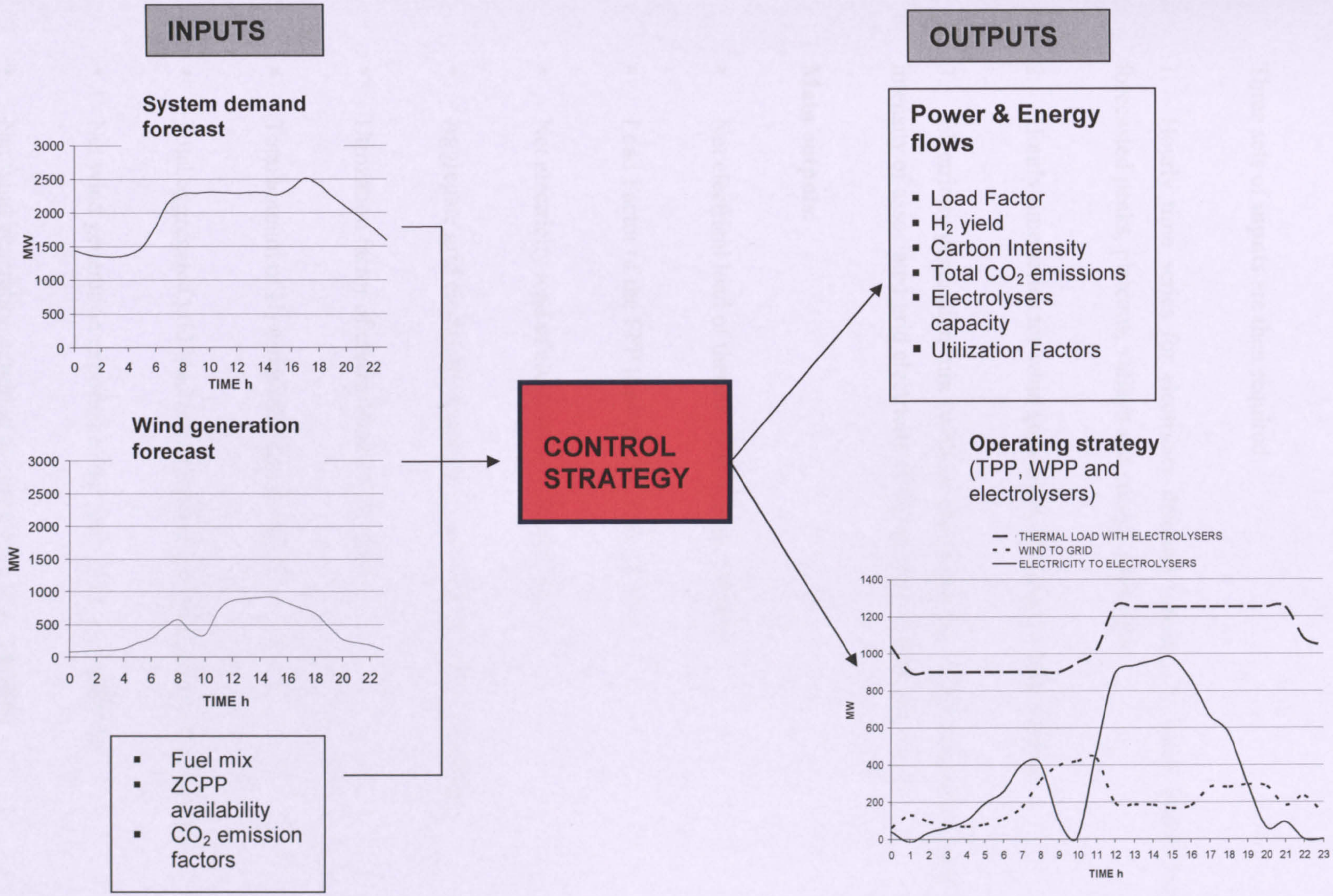

Figure 3.3. Description of the Active Electrolyser Demand Management (AELM) spreadsheet model

Three sets of **inputs** are then required:

1. Hourly time series for electricity demand forecast 24 hours ahead (including forecasted peaks, plateaus, valleys and energy demanded).

2. Hourly time series for wind generation forecast 24 hours ahead.

3. Electricity generation mix (without electrolysers), ZCPP availability and carbon intensity of associated grid electricity (CO_2 emitted / kWh_e delivered).

Main outputs:

- Net electrical load of thermal plants, $\mathbf{P_{FPP}}$ **(MWh)**
- Load Factor of the FPP load profile, $\mathbf{LF_{TH}}$ **(%)**
- Net electricity load of electrolysers, $\mathbf{P_E}$ **(MWh)**
- Aggregate grid electricity supplied to electrolysers, $\mathbf{P_{FPDE}}$ **(MWh)**
- Utilization factor of electrolysers, $\mathbf{UF_E}$ **(%)**
- Total amount of H_2 produced, $\mathbf{Y_H}$ **(t / day)**
- Total aggregated grid load (electrolysers and consumers), $\mathbf{P_G}$ **(MWh)**
- Net wind generation exported to the main grid, $\mathbf{P_{WG}}$ **(MWh)**
- Net wind generation exported to consumers, $\mathbf{P_{WC}}$ **(MWh)**
- Net wind generation exported to electrolysers, $\mathbf{P_{WE}}$ **(MWh)**

- Percentage of wind generation curtailed, **WC (%)**

- Carbon intensity of hydrogen generated, **CI_H (kg CO_2 / kg H_2)**

- Carbon intensity of electricity delivered to consumers, **CI_e (kg CO_2 / kWh_e)**

- Total carbon emissions derived from electricity generation, **TC (t CO_2 $\times 10^3$/day)**

- Installed capacity of ELS required, **IC_E (%)**

- Net plant generating capacity, including FPP, ZCPP and ELS, **NGC (MW)**

- Ratio of Installed capacity of ELS required to net plant generating capacity, **β_E (%)**

A different operational strategy has been investigated for each implementation case proposed, for where in each case the set-up variable is the LF_{TH}. Alternative set-up variables can be introduced (e.g. CI_H, CI_e, UF_E) in order to increase the flexibility of the model and allow its operation under different operational strategies. An operational strategy for the electrolyser stock is then derived with the main objectives of maximising the LF_{TH} value, increasing the capture of intermittent RE sources by reducing wind power curtailment and maximize the production of zero/low carbon hydrogen.

From a predicted daily system demand profile a forecasted wind profile can be subtracted to obtain the aggregate thermal load profile of the system (i.e. the residual demand to be met by thermal power plants) as shown in **Figure 3.1**. The spreadsheet

model is then used to simulate the daily/weekly scheduling operation of the electrolysers, which would then govern their switching following the scheduling plan.

For the three operational strategies each day at a specified time (e.g. 23:00 or t = -1), the operator of the system would access forecasts of consumer demand and wind power availability for the next 24h[11] on a certain time-interval). Based on this information, a scheduling plan for the next day's operation of the system can be devised as shown in **Figure 3.4**. For every hour in the next day, all the operational strategies take into account the electricity demand, ZCPP availability and LF_{TH} targeted in order to find the optimal operation of thermal plants and electrolysers as follows:

1. Based on the desired LF_{TH}, computation of the FPP load profile is obtained by raising early morning and night-time valleys for every hour (average hourly power output); creating a late morning-afternoon plateau of much greater duration than applies for the conventional profile.

2. Once a 24 h thermal load profile is defined, an hourly operational strategy for the electrolyser stock is calculated, primarily in relation to the proportion of hourly consumers' demand related to ZCPP availability and also subject to the FPP load appointed, this being the predictive part of the model. A dynamic output can later be obtained by updating the predicted FPP load on a real-time basis (say every 15-30 minutes depending on the information available) with updated wind and demand forecasts.

3. After this, subject to the restriction imposed by the maximum amount of intermittent wind power that the grid can accept (LLL = 30%, see modelling

[11] Given the inaccuracy inherent to wind and demand forecasting over a 24 h period, this schedule would be continuously updated (for instance across 15 min intervals) according to real-time information on average available wind generation (MW) and system demand (MW) across that time interval in order to get as close as possible to the desired thermal load previously scheduled (MW). The updated operation strategy would then govern the switching of the electrolyser stock on a continuous basis following the scheduling plan.

assumptions below) and the LF_{TH} selected, an hourly operation strategy is defined primarily for DSEs and/or for SSEs.

4. Finally, the hourly aggregated grid demand (electrolysers and consumers) is calculated to ensure that the total system demand (electrolysers and consumers) does not exceed SMD.

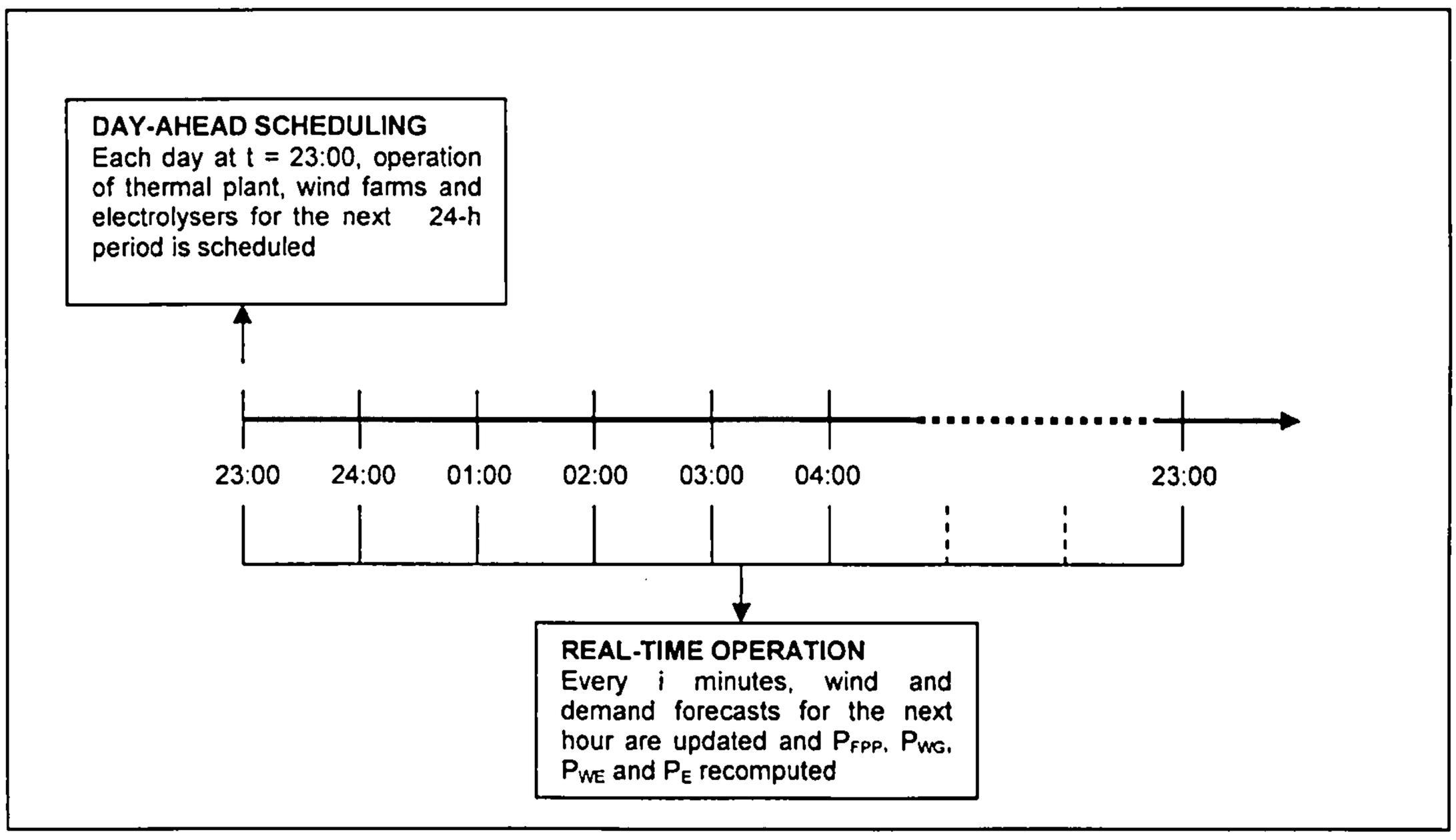

Figure 3.4. Illustration of the scheduled operational strategy

Details of the operational strategies devised for every implementation case are given in **Chapters 4 and 5**.

In practice, results achieved in terms of the operational strategy of electrolysers and thermal power plant will differ from those obtained here in relation to (i) accuracy of demand forecast; (ii) accuracy of wind forecast; and (iii) controllability and responsiveness of electrolysers. Clearly if the accuracy of wind and demand forecasts

is high then the scheduled and actual operation of ELS and power plant will be very similar. However by definition no forecasting method has 100% accuracy and accuracy drops as forecasts age[12]. Therefore the approach suggested here must also include a dynamic element obtained by updating the scheduling plan on a real time basis (e.g. every 5min) according to real-time information on wind generation and system demand to allow for unpredicted changes in system demand as well as the deviation of actual wind generation output from the forecast. Practical implementation issues related to the actual performance of ELS are reviewed in **Chapter 6**.

Although the analysis presented in this thesis is based on a time interval of one hour and results are displayed for daily and weekly periods, the methodology deployed here can be applied to any appropriate time-base (15 min, 30 min, 1 hour, etc) and for any period of time (0-24h, 48h, 7 days, etc) provided the required inputs are available on such time-base.

Even though the results presented and analysed here are derived from a calculation example based on data from Eastern Denmark, the methodology presented is well suited to study the benefits and impacts of the implementation of electrolysers as an active-load management mechanism within any generic power system, provided aggregate system demand and wind generation profiles are available. The AELM model has been designed to allow for different electricity generation mixes to be introduced as inputs.

3.3.2 Modeling set-up

Although it is possible to envisage an enhanced power system with very large penetrations of RE electricity sources beyond the existing maximum demand placed on the grid, clearly the feasibility of achieving such high levels of wind power and other intermittent RE will depend on the availability of low-carbon solutions to the problems posed by the intermittency of wind power. For the purpose of this

[12] State-of-the-art wind forecast models show forecast errors in excess of 10% of rated power beyond 6h [72], [73].

investigation wind power penetration is restricted to the domain $20 \leq \Phi_W \leq 100$, whereas penetrations of other ZCPP falls between 10 and 35% of SMD. The upper limit corresponds to minimum summer demand in Eastern Denmark, which is normally considered as a threshold for the deployment of baseload generating capacity in islanded power systems with no significant interconnections. Wind penetration and ZCPP penetration are both referred herein as installed capacity relative to maximum system demand in 2003, namely 2,665 MW.

A) Description of wind scenarios

Although most previous studies on wind power intermittency have been based on wind speed data converted into anticipated generation by using manufacturers' power curves, some authors [13], [66] have appropriately pointed out that the use of wind speed data might overestimate generation and underestimate intermittency. Consequently, the analysis carried out here utilises only actual metered wind generation data at one-hour resolution from more than 100 wind farms as declared by Elkraft [17]. The average capacity factor of wind generation for 2003 was 24%. The analyses presented in Chapters 4 and 5 are based on 24h profiles. To account for the variability of wind, three 24h profiles of wind power output for 2003 were selected to define three types of day: a relatively steady and high wind day (January 15th); a variable wind day (September 21st); and a low wind day (January 29th). **Figure 3.5** shows daily profiles for the three wind scenarios selected. These are thought to be representative of the variation likely to be experienced in a power system from a high wind availability period to a low one. Later in Section 5.4 the analyses were extended to weekly load profiles.

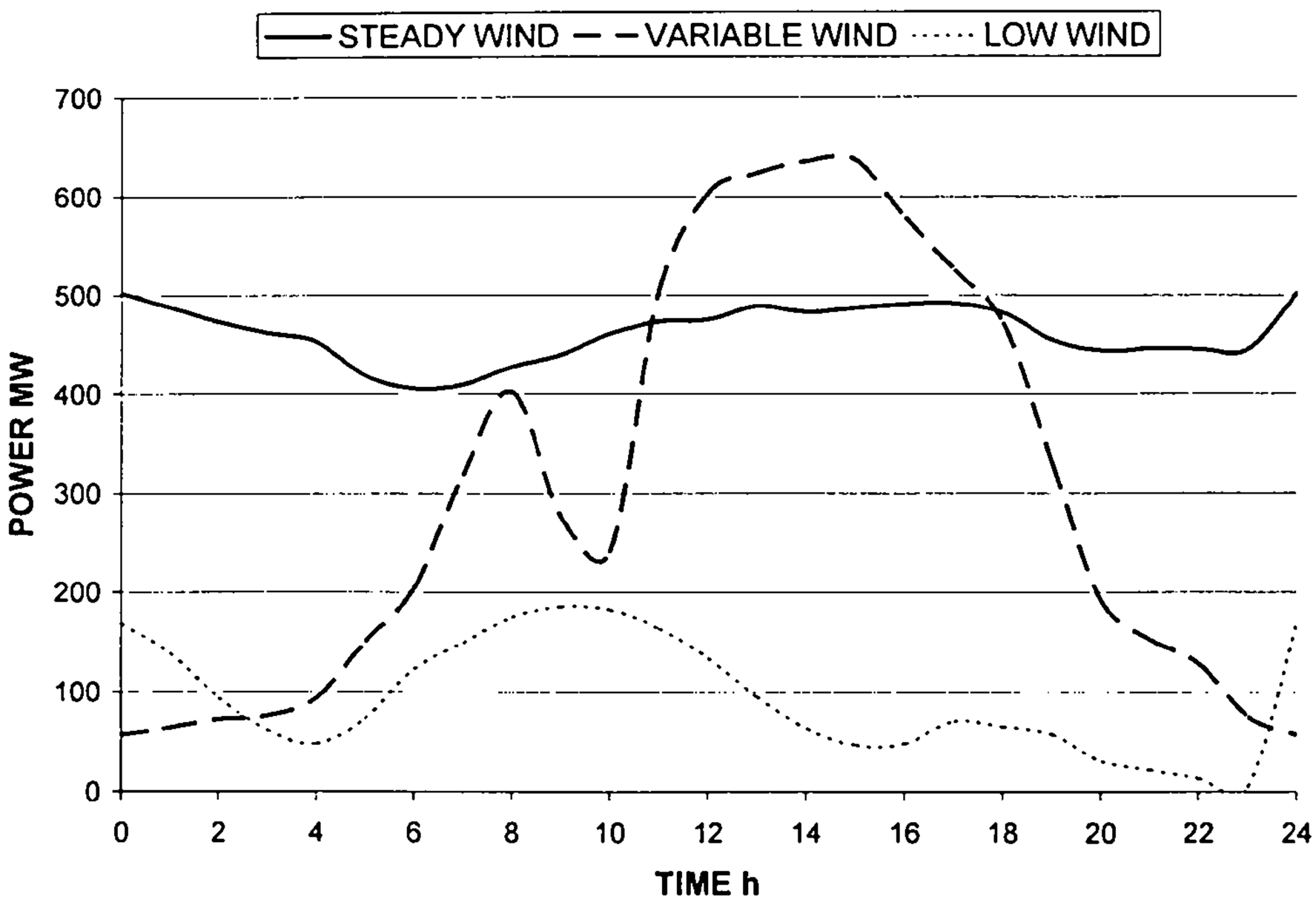

Figure 3.5. Daily wind scenarios selected from the East Denmark power system, 2003

The capacity factor of wind generation on the steady, variable and low wind days was 80%, 42% and 16% respectively. The installed capacity of wind generation in Eastern Denmark in January 2003 (573 MW) was the datum for the steady and low wind scenarios (wind penetration, Φ_W = 21%), while for the variable wind scenario the installed capacity at the end of 2003 (743MW) was employed (Φ_W = 28%) [17]. A statistical description of the daily profiles corresponding to the three selected wind scenarios is summarized in **Table 3.2**.

WIND SCENARIO	LOAD FACTOR (%)	COEFFIC VARIATION (%)	STANDARD DEVIATION (MW)	CAPACITY FACTOR (%)
Steady Wind	92	6	27	80
Variable Wind	48	69	213	42
Low Wind	50	62	57	16

Table 3.2. Statistical description of baseline steady wind scenario selected

In addition a weekly analysis is carrying out in **Section 5.4** based on two weekly profiles of wind power output for 2003 were selected from [17]. The average weekly capacity factor of wind profiles for the year 2003 lies between 3 and 51%, whereas daily capacity factors are in the range 0-80%. To account for the variability of wind across the year, a relative variable but high wind winter week (28/01/03 to 3/02/03) and a high wind summer week (19/06/03 to 25/06/03) were selected. The capacity factor of the winter week is 36% and the capacity factor of the summer week is 44%. The winter week is selected to assess the variability of wind across a weekly period and its implications on the operation and management of a large ELS stock. The summer week is selected as the week of maximum capacity factor over the summer period in order to further evaluate the benefits of a wide deployment of ELS in terms of eliminating wind curtailment at periods of low demand and high wind availability. An annual assessment lies beyond the scope of this thesis.

At high wind penetrations (Φ_W), the variability of the aggregate wind generation in a region or country will depend on several factors: (i) the geographical spread of wind farms; (ii) the size of the region; (iii) the number and capacities of individual wind farms; and (iv) the specific wind regimes. Estimates of aggregate wind generation profiles for future high Φ_W systems can be made by extrapolating from existing data. In this study of $20\% \leq \Phi_W \leq 100\%$, hourly wind generation data from Elkraft was upscaled by factors ranging from 1.4 to 4.7 for the steady and low wind scenarios, and

from 1.1 to 3.6 for the variable wind scenario. Across all wind scenarios the same number of individual windfarms, but of increased capacity, was assumed and specific penetration levels of 20%, 30%, 40%, 50%, 70% and 100% were assessed.

It is acknowledged that the adopted scaling method tends to overestimate variability in the aggregate profile due to the benefits usually derived in practice from the increased geographical diversity of constructing an increasing number of wind farms. Nevertheless, the total generation will be more variable if the correlation between wind sites is high, which is the case in Eastern Denmark because the maximum distance between metering sites is only about 200 km North-South and 100 km West-East [10]. Furthermore in Denmark, given the land resource limitations, the present trend is to replace existing wind turbines with larger ones [74]. Therefore this analysis provides a generic study (with all wind power implementations on the supply side), which is based on upscaled wind generation profiles for Eastern Denmark, rather than a specific analysis of a future power system for Eastern Denmark.

B) Description of demand scenarios

The winter demand profiles exhibit a typical North-European daily cycle, with an evening peak between 17:00 and 18:00, higher on weekdays (between 2,500 and 2,600 MW) than weekends (2,300-2400 MW). During the summer the demand profiles also exhibit a morning peak between 10:00 and 12:00, to the extent that sometimes this exceeds the evening peak value. On winter days system peak demand exceeds 2500 MW, while during the summer it is 1400-1800 MW. The peak demand on summer weekdays is around 1800-1900 MW and around 1,400-1,500 MW during the weekends. The system maximum demand across 2003 was 2,665 MW. Daily load factors generally exceed 75%[13] and the value of system maximum demand in 2003 was 2,665 MW.

[2] For comparison, LF in Great Britain on a typical winter day (10/12/2002), as calculated from hourly demand data available in [75], was 77%.

Although in practice it may take several years to achieve the high values of ZCPP penetration considered here, the investigation assumed that the consumer demand for electricity remained at the 2003 level. The daily and weekly system demand profile corresponding to each of the wind scenarios considered was employed. The daily electricity consumption, P_C, was 47,603 MWh (January 15th, steady wind day); 30,750 MWh (September 21st, variable wind day); and 47,276 MWh (January 29th, low wind day [17]. The electricity consumption was 327 GWh and 238 GWh on the winter and summer week respectively. Weekly demand and wind generation profiles analysed are shown in **Figures 3.6 and 3.7** for a wind penetration of 50%.

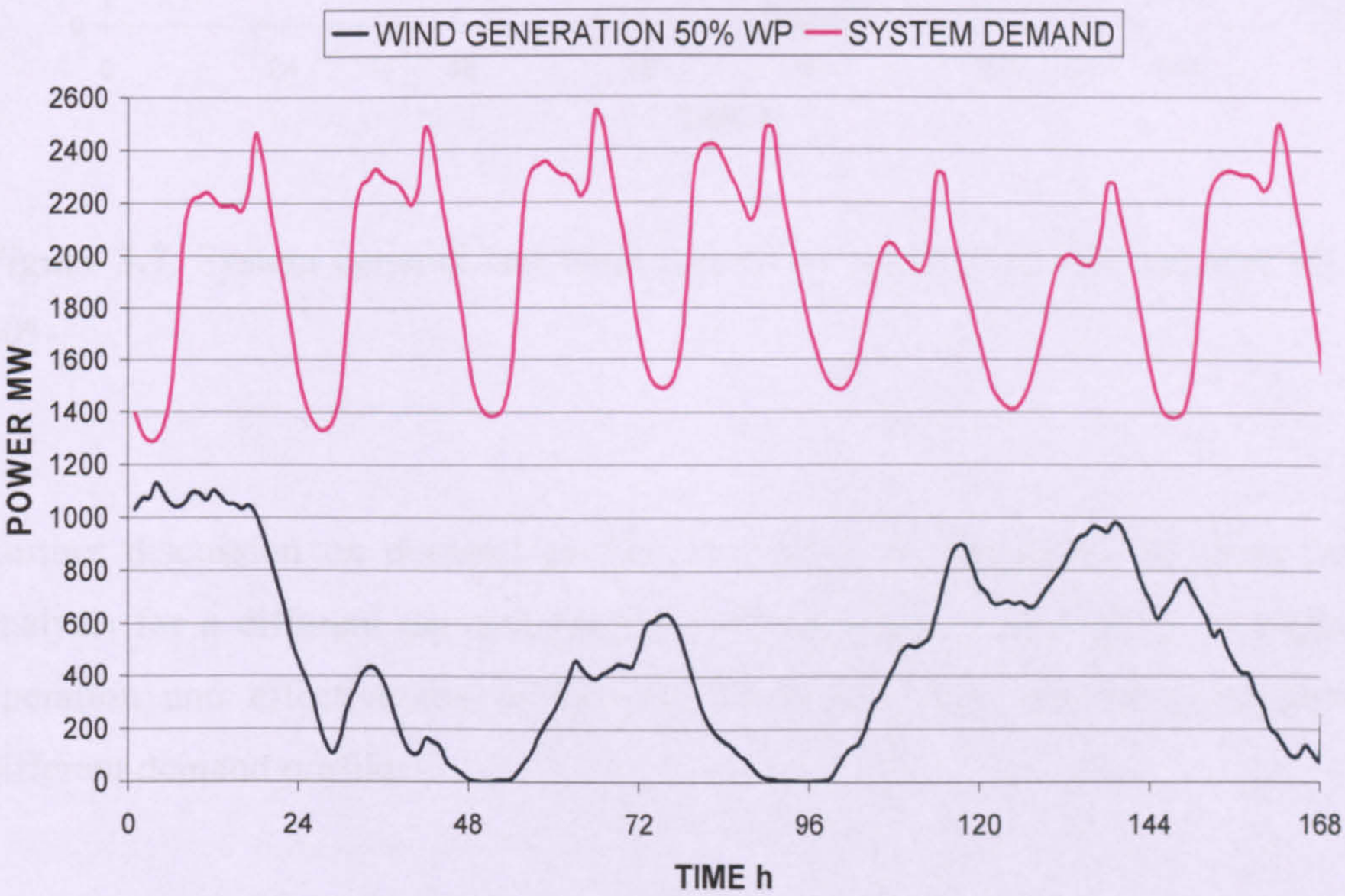

Figure 3.6. System demand and wind generation winter weekly profiles for Φ_W = 50%.

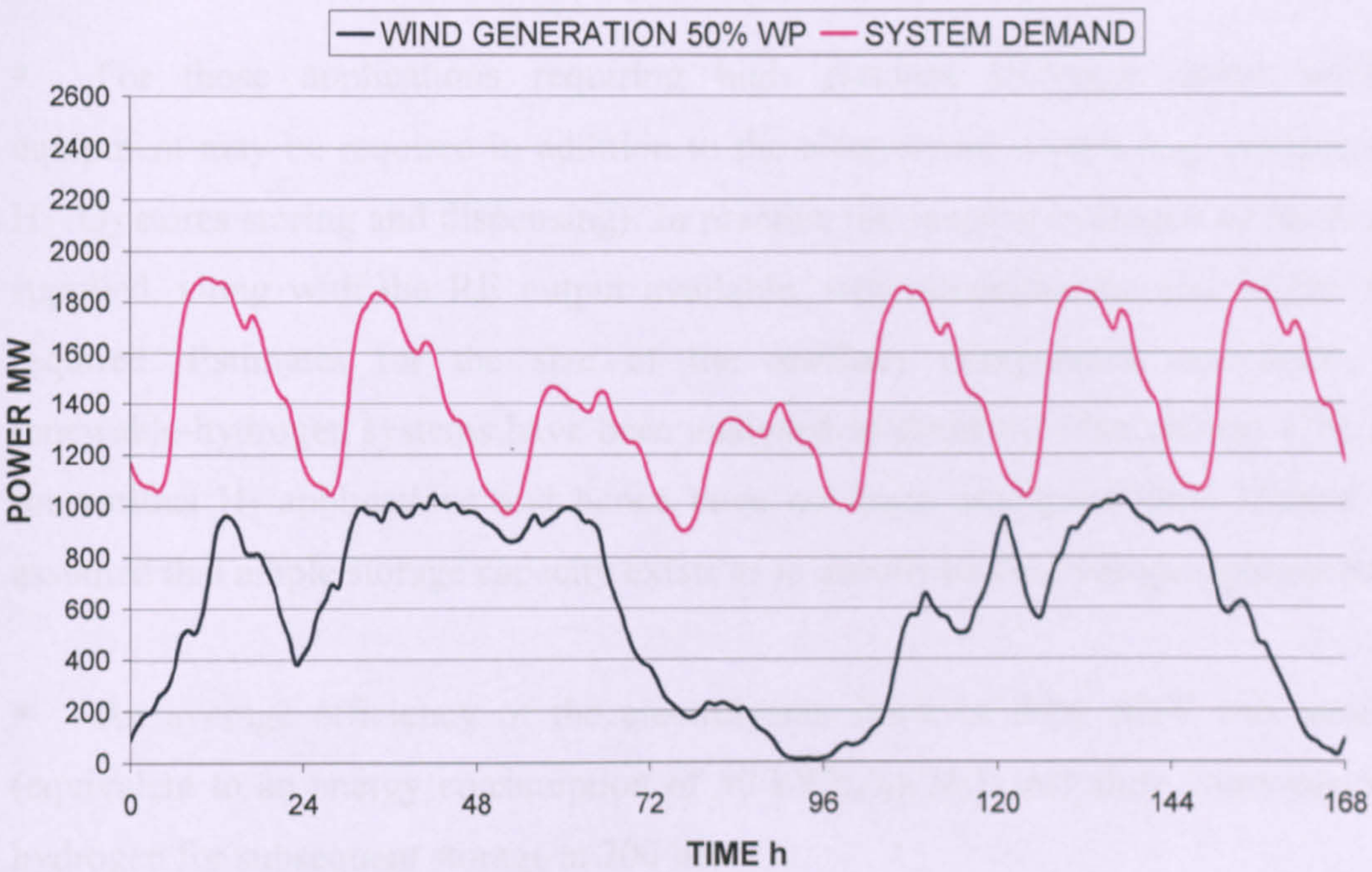

Figure 3.7. System demand and wind generation summer weekly profiles for Φ_W = 50%.

Further discussion on demand profiles is offered in **Appendix B**, along with an analysis for a different demand profile to those obtained from [17], to explore the operation and effectiveness of the AELM model when applied to regions with different demand profiles.

3.3.3 Main assumptions

- Even though in reality the electrolyser stock size would be dependent on the existent demand for hydrogen (e.g. transport fuel demand, heating demand, industrial processes), for the purpose of this analysis it is considered that the demand for hydrogen exceeds that generated in each case studied (i.e. there is no demand-side limit to electrolyser operation), and the sizing of the electrolyser system is determined by the availability of ZCPP and FPP inputs.

- For those applications requiring high pressure hydrogen some ancillary equipment may be required in addition to the electrolyser system (e.g. compressors, H_2 /O_2 stores storing and dispensing). In practice the specific hydrogen demand to be supplied, along with the RE output available, will determine the size of the store required. Estimates for the size of the ancillary components associated with renewable-hydrogen systems have been analysed in detail by other authors [76], [77] for various H_2 applications and hence have not been attempted here. Instead it is assumed that ample storage capacity exists as to absorb all the hydrogen generated.

- An average efficiency of the electrolysers stock of 80% HHV was assumed (equivalent to an energy consumption of 50 kWh_e/kg H_2), including compression of hydrogen for subsequent storage at 200 bar.

- It is assumed that the electrolysers are able to take a variable and/or intermittent power input, meaning that they can be switched on/off and down at will, that they will respond instantaneously to a step up/down in power input, and that the control decisions can be made on a real-time basis. However, in practice the transient response characteristics and ability to absorb fluctuating input currents will be less than perfect. This is discussed further in **Chapter 6**. Time-response would also depend on demand-side and storage considerations. For example for those applications where H_2 stores are required, the operation of the electrolyser would be affected by the state of charge of the store. If the store is full the electrolyser can not be switched on until the store starts discharging to supply the specific H_2 demand. Demand-side practical implementation issues are considered further in **Chapter 6.**

- The generic power system upon which the preliminary analysis is based lacks of significant interconnections with neighboring power systems (i.e. islanded system) and has no other energy storage technologies available apart from chemical storage in the form of hydrogen. In addition the power system is able to cover its maximum demand at any time without the need of an upstream reinforcement of the T&D

system in relation to the sitting of RE and thermal power plants. The analysis excludes consideration of T&D losses when the electrolyser stock is embedded within the grid and located on the demand side (Case 2).

- Besides the minimum loading levels inherent to thermal power plant, to counter for the possibility of a sudden large drop in wind generation (this can be produced by a sudden loss in wind resource or by a network fault that exceeds the ride-through capability of the wind generators), a dynamic penetration limit is also enforced which effectively limits the amount of wind power that can be directed to the grid, P_{WG}. These constraints result in an overall low load limit (LLL) characteristic for a specific power system which ultimately depends on: (i) the size and interconnections of the power system; (ii) type and size distribution of the conventional power plant in operation; (iii) dispersion of the wind generators within the system; and (iv) power market regulation and practice. Typical values are around 30% [4], [52] although conservative LLL values as low as 20%-25% are applied in large isolated power systems [54]. A low-load limit of 30% was assumed in this study. This means that wind power will be discarded at any time when the equivalent aggregate wind power output exceeds 30% of the total system demand P_G (consumers and demand-side electrolysers) as expressed in equation 3.2. It is acknowledged that the LLL changes as a function of the power plant mix in use and system demand on a particular day (e.g. LLL tends to be lower in summer when system demand is lower). Also in future power systems, more wind generation can be integrated if more flexible thermal plant is included in the power system. A sensitivity analysis is carried out in **Appendix C** by varying such 30% figure.

$$P_{WG}(t) \leq 0.3\, P_G(t) \qquad (3.2)$$

- Gradients of the aggregate FPP load profile when deploying the ELS stock (wherever located) are always maintained equal or below the gradients of the original FPP profile when no ELS are included in the power system.

- For every ZCPP penetration the SSE stock is sized to capture all wind (eliminate 100% of wind curtailment) subject to the LF_{TH} target, which implies sizing for the day of maximum wind availability in the year. The DSE is sized subject to LF_{TH} and the restrictions imposed by equations 3.1 and 3.2. In practice the size of the electrolyser stock would be also influenced by economic decisions and demand-side considerations which are discussed in **Chapter 6**.

- The carbon intensity of the electricity delivered to consumers and the carbon intensity of the hydrogen produced are both outputs from the model and are discussed in **Chapters 4 and 5**. However the trade-offs between the penalties imposed on the carbon intensity of electricity, CI_e, and the carbon benefits derived from achieving greater LF_{TH} values (e.g. carbon savings from reducing the usage of back-up power generation and the displacement of fossil fuels by zero-carbon H_2) are considered an area for further research and have not been quantified here.

3.3.4Description of main outputs

Definitions of all the variables corresponding to the main outputs obtained from the model are given below:

- Minimum ELS installed capacity required (IC_E) :

The minimum required installed capacity of electrolysers for each implementation case has been calculated as the maximum hourly electrical load required by the electrolyser stock on the day of maximum wind availability (CF = 80%) or steady wind day (see description of wind scenarios). The installed capacity of the ELS stock is then a function of the primary set-up variable (LF_{TH} in the results presented here), subject to the restrictions imposed by equations (3.1) and (3.2). This installed capacity is the basis for the calculation of the average utilisation factor (UF_E) of the electrolyser stock.

- Wind curtailment (WC):

The penetration limit at which wind curtailment takes place is characteristic for a specific power system (**Chapter 2.4**). Based on the 30% LLL assumed (equation 3.2), at any time wind power will be discarded if the equivalent aggregate WPP output exceeds 30% of total system demand, unless an electrolyser stock is available at the WPP to absorb the surplus WPP output that can not be integrated in the grid.

- Carbon intensity of electricity delivered to consumers (CI_e) :

The fuel mix used for electricity generation is assumed to change as wind penetration increases. The trends are to increase the use of natural gas and renewables (essentially wind power in East Denmark) at the expense of coal and oil. Different fuel mixes are assumed for every wind scenario, on the basis that different proportions of oil and gas peaking plants must be called upon depending on wind availability to cover the shortfall in wind-generated electricity. They reflect different hypothetical electricity supply choices for Eastern Denmark[14]. These are shown in **Figure 3.8**. Each is taken as the datum for calculating the carbon intensity of electricity delivered to consumers. No nuclear power has been assumed, as currently applies for the Eastern Denmark electricity mix [79], but the impact of including nuclear within the fuel mix would be to reduce the CI_e values in each line shown in **Figure 3.8** without modifying the trend.

Note that a 30% LLL has been set-up for the amount of wind power that can be integrated into the grid. This is the reason why there is no significant increase in the demand share covered by wind beyond 30% wind penetration for the steady and variable wind scenario even though the installed capacity of wind power increases with wind penetration.

---

[14] Investigations of future trends, whatever the subject area, are fraught with uncertainty, particularly over a timeframe of 20 years or more. This is no less true for the electricity sector, which is subject to a range of economic, social and political drivers, which could evolve in different ways. Consequently the fuel mix scenarios depicted here are just illustrative, and designed only to highlight the nature of the potential choices available for Eastern Denmark. They differ in one main respect: the assumed use of primary energy sources to cover the electricity demand. To create these scenarios, a review of the literature was carried out concerning historic electricity supply and demand data and projections for future electricity supply choices in Eastern Denmark [78], [79], [80].

The emission factor is the system average value based on projected fuel mix. Values have been taken for the emission factor derived from every primary source. Gas is assumed to be used in CCGT plants with an emission factor of 0.39 kg CO_2/kWh_e produced (see assumptions below); coal power stations emission factor is taken at 0.92 kg CO_2/kWh_e, and oil-fired power stations at 0.80 kg CO_2/kWh_e. Nuclear and renewable power stations are assumed to have negligible CO_2 emissions.

$$\% \text{ wind} = \frac{P_{WC}}{P_G} \qquad (3.3)$$

Example:

Considering $\Phi_W = 30\%$ for the Base Case, steady wind day:

$CI)_e$ = (% wind × 0) + (% oil × 0.80) + (% coal × 0.92 kg CO2 / kWh) + (% NG × 0.39)

$CI)_e = (0.29 \times 0) + (0.03 \times 0.800) + (0.41 \times 0.92) + (0.27 \times 0.39) =$

$= 0.50$ kg CO_2 / kWh

a)

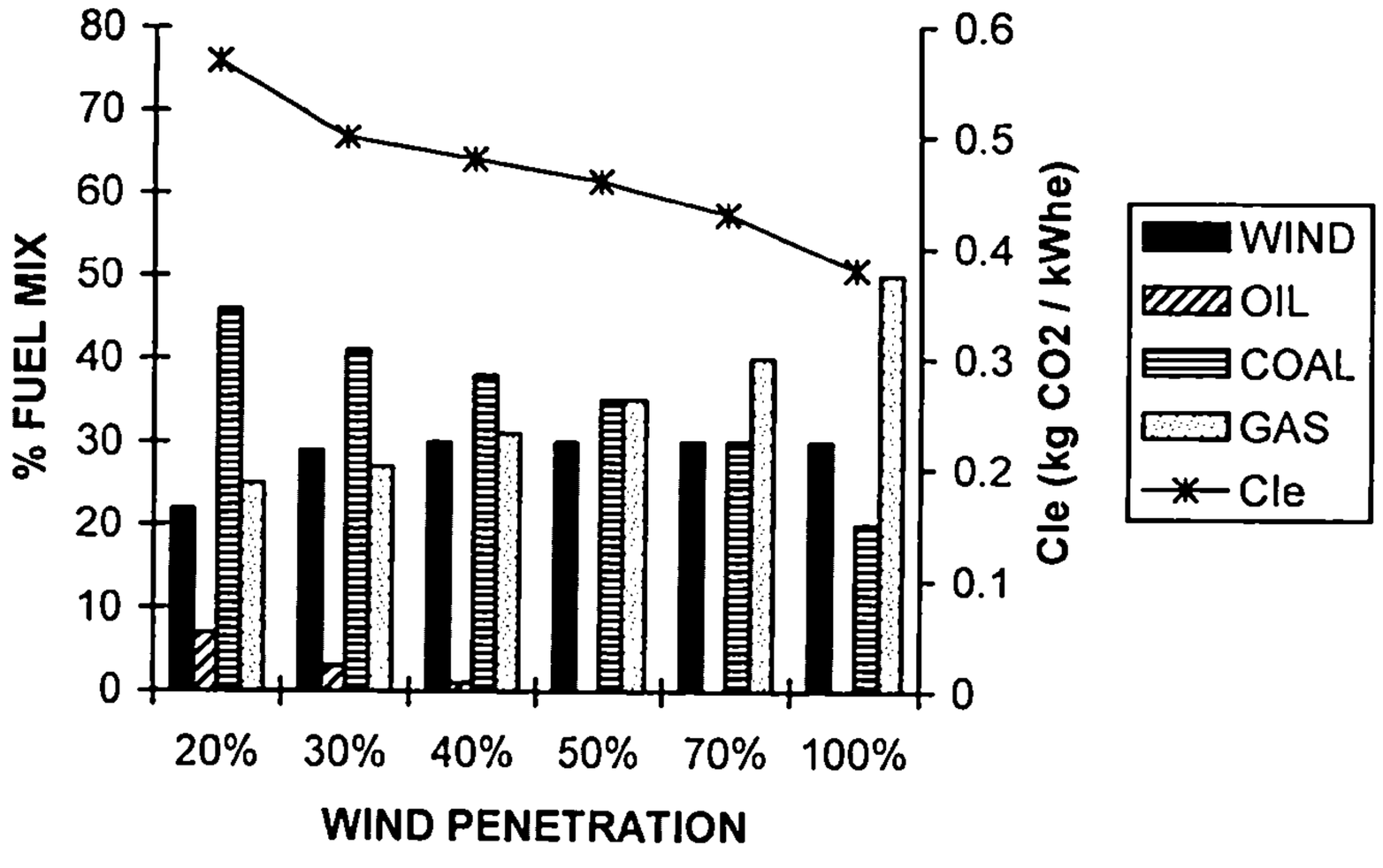

b)

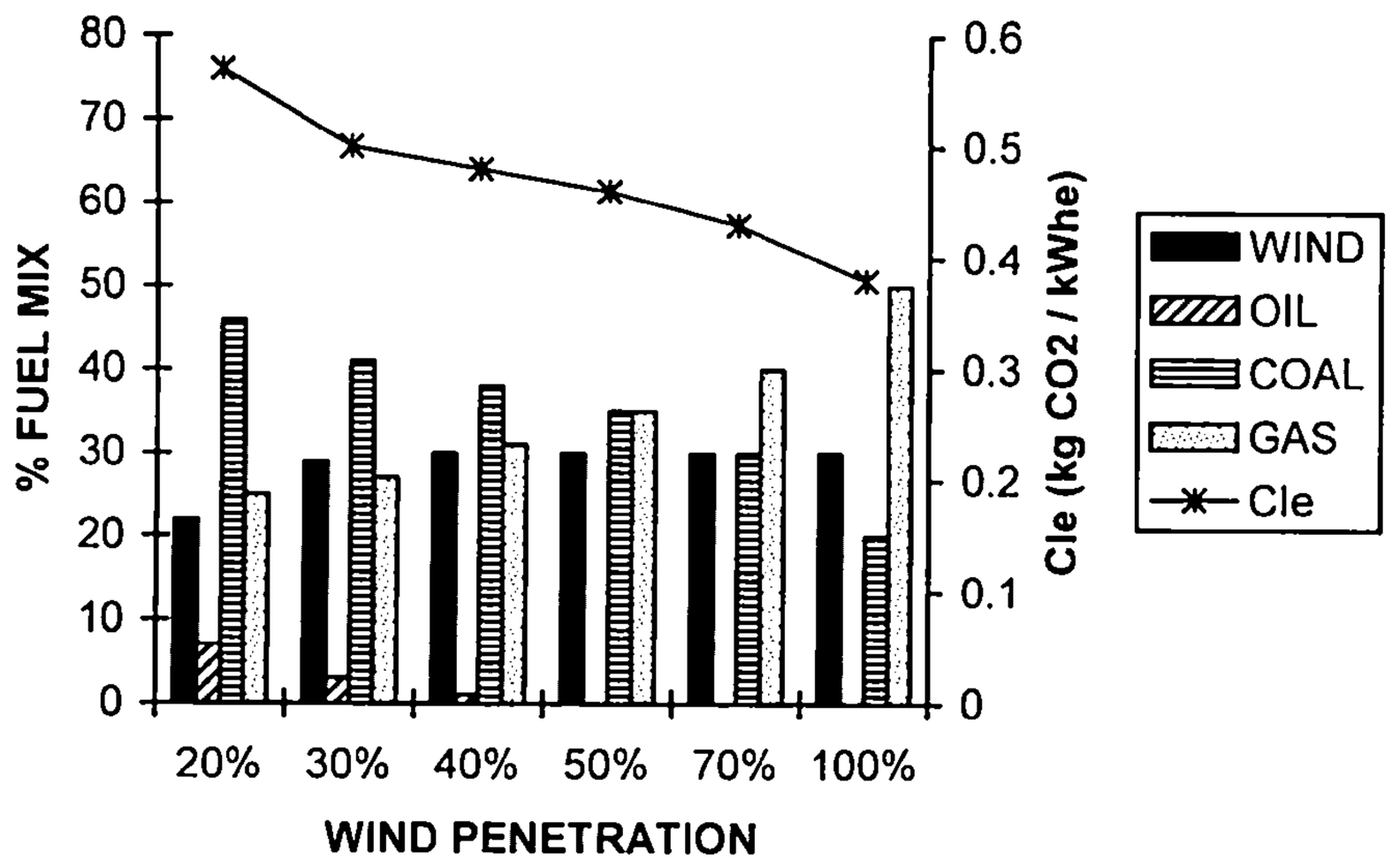

c)

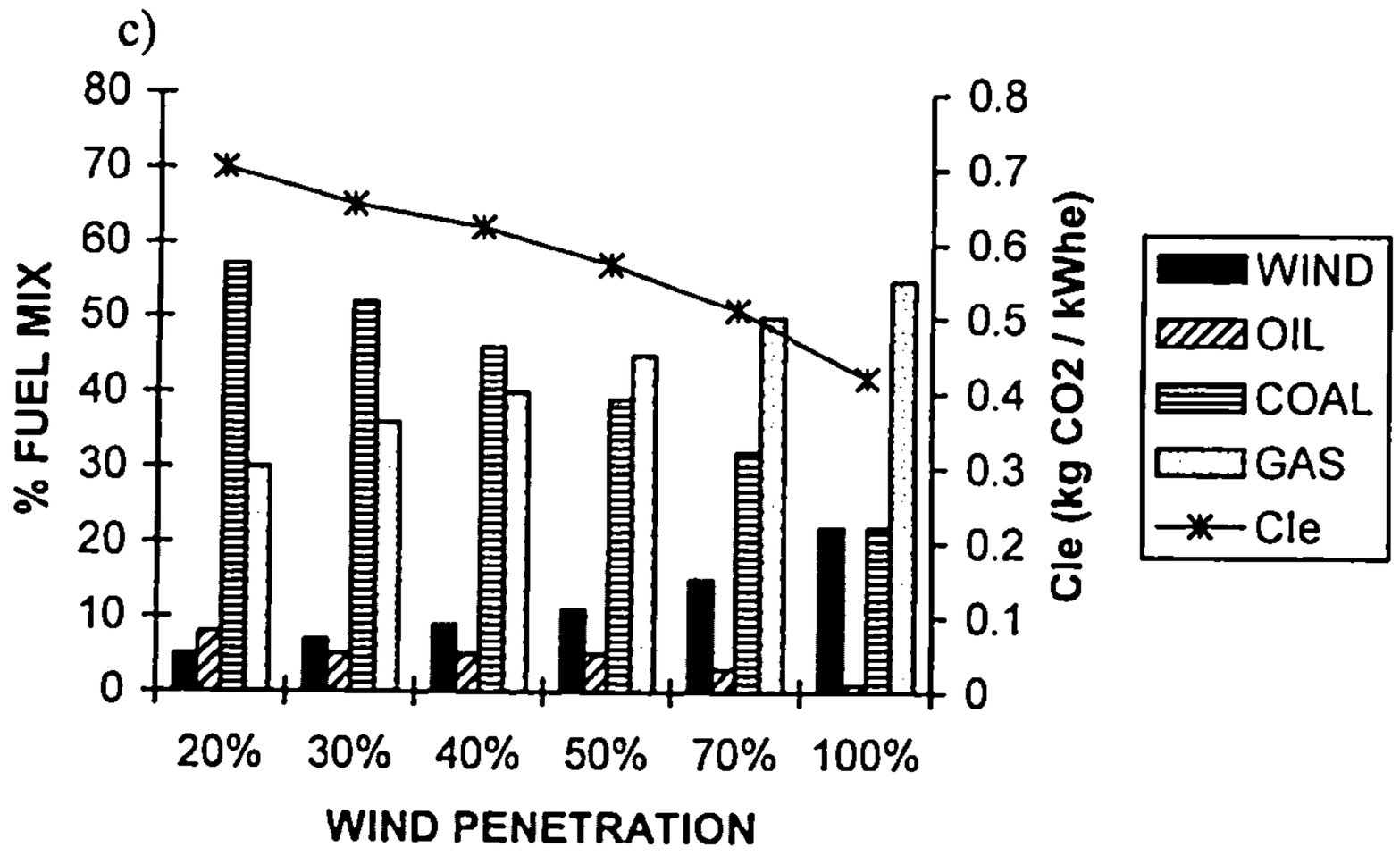

Figure 3.8. Fuel mix assumptions for the calculation of the carbon intensity

a) Steady wind day

b) Variable wind day

c) Low wind day

- Total carbon emissions derived from electricity generation (TC):

Multiplying the carbon intensity of electricity obtained by total consumers demand without ELS P_C, total carbon emissions derived only from electricity generation are obtained.

Example:

Considering Φ_W = 30% and implementation CASE 3, the total consumers demand P_C = 47603 MWh

$TC = 47603\ MWh \times 0.59\ tCO2 / MWh = 28.2 \times 10^3\ t\ CO_2$

- Carbon intensity of hydrogen generated (CI_H) :

Electrolysers' electrical demand is assumed to be covered exclusively by wind-derived electricity except for the implementation Case 3, where CI_H=3 kg CO_2 / kg H_2 is also considered and then ELS' demand is covered firstly by ZCPP-derived electricity and secondly by surplus FPP output (P_{ZPDE}) over and above that required to cover consumers' electricity demand P_C. A more detailed description of the different operational strategies proposed is given in **Chapters 4 and 5**.

As far as electrolysers' performance is concerned, efficiency figures for current technology are reported in the range of 45%-85% (including BoP but not compression requirements). For the purposes of this investigation, an average efficiency of 79% HHV was assumed (equivalent to an energy consumption of 50 kWh_c/kg H_2), including compression of hydrogen for subsequent storage at 200 bar. The carbon intensity of the hydrogen produced is then given by:

$$CI_H = \left(\frac{P_{FPDE}}{P_E} \right) \times 100 \times \mu_{ELS} \times CI)_e \qquad (3.4)$$

$$CI_H = \left(\frac{P_{FPDE}}{P_E} \right) \times 50\ kWh_e / kg\ H_2 \times CI)_e\ (kg\ CO_2 / kWh_e)$$

Example:

Taking on the same the example above (Case 3, 30% wind penetration), out of the total 7843 MWh of electricity demanded by ELS, P_E = 791 MWh, are provided by surplus FPP output P_{FPDE}. Hence the average carbon intensity of the H_2 generated is as follows:

$$CI)_H = (791 / 7843) \times (50\ kWh / kg\ H_2) \times 0.594\ kgCO_2 / kWh = 3\ kg\ CO_2 / kg\ H_2$$

Note for the implementation Cases 1 and 2 where no surplus FPP output is sent to ELS at any moment across the day $P_{FPDE} = 0$, and then the average carbon intensity of the H_2 generated results zero.

- Net daily hydrogen production (Y_H):

Net daily hydrogen production is obtained by dividing the total electricity input to ELS P_E by the electricity consumption required to produce one unit of hydrogen from electrolysis.

Example:

$$Y_H = (7843 \times 10^3\ kWh) / (50\ kWh / kg\ H_2) = 156{,}860\ kg\ H_2$$

- Utilization factor of ELS (UF_E):

Unless otherwise specified UF_E is defined as the ratio between the net daily hydrogen output and the maximum theoretical hydrogen output that could have been obtained assuming ELS operating at all times across the day at their maximum rated capacity (IC_E), expressed as a percentage.

Example:

Again for a 30% wind penetration level and CASE 3, net daily hydrogen production Y_H equals 156,860 kg H_2. An electrolysers' installed capacity of 840 MW is required (maximum hourly electrical load required).

Y_H = 156,860 kg

Max theoretical hydrogen output = (840 × 10^3 kW × 24h) / (50 kWh / kg H_2) = = 403,200 kg

UF_E = (156,860) / (403,200) × 100 = 39%

CHAPTER 4 - IMPLEMENTATION OF ELECTROLYSERS IN COMBINATION WITH WIND POWER PLANT

4.1. INTRODUCTION

At present, the penetration of intermittent renewable sources (RE) within the electricity system (as generated by wind, solar, wave and tidal power sources) is serving to displace fossil-derived electricity. However, a power system with a large installed capacity of RE power plant requires also large capacities of controllable FPP. The most prominent example of intermittency is wind power, where the natural fluctuations have received a great deal of attention in recent years and raise concerns about wind integration. Denmark, Germany and Spain, where wind penetrations have become significant, have become "case studies" for the integration of RE in general and wind power in particular.

Instead of adapting power generation in an electricity system with a high penetration of wind power to the time varying demand profile, it is suggested that the demand profile could be arranged to suit the availability of wind power in a manner which increases (rather than decreases) the load factor of the aggregate load profile placed on FPP. This partial decoupling of demand from supply would be achieved by water electrolysers, where surplus electricity is used for hydrogen production. Active load management with electrolysers has the potential to be used as a central mechanism for controlling the load profiles placed on FPP in order to improve their carbon footprint as well as managing large RE inputs in the power system.

A proposed solution is presented in this chapter for the integration of large amounts of wind power into electricity grids, using water electrolysers as a load management mechanism, as an example for intermittent renewable energies in general. The AELM model is applied to assess the implementation and operation of a stock of electrolysers in combination with large penetrations of wind power within a generic power system.

Results are presented in this chapter for an island power system based on wind generation and demand data for Eastern Denmark.

4.2. METHODOLOGY

4.2.1 Description of the approach

The aggregate WPP output of all wind farms in the system is considered as a negative demand, so the residual demand to be met by FPP is found by adding this negative demand to the system demand (see **Figure 3.1**). The load factor of this net thermal load profile (LF_{TH}) acts as an indicator of the operational performance of the conventional (thermal) power plant portfolio. The higher LF_{TH}, the flatter the load profile faccd by thermal plant and the more efficient its operation. With the aim of increasing the LF_{TH} and maximizing the capture of intermittent RE sources in general, operation of electrolysers can be adapted to increase or decrease the total demand at will, filling valleys and creating plateaus on the FPP load profile.

A methodology was developed for implementing and controlling a large stock of electrolysers in conjunction with high penetrations of wind power, so that very high load factors can be achieved on the FPP load profile on days of different wind availability and consumer demand. Preferred capacity levels and operational strategies were identified for the required stock of electrolysers as a function of wind power penetration in the electricity system. The main objectives are:

- Maximising the daily LF_{TH} value.

- Increasing the capture of intermittent RE sources by reducing wind power curtailment.

- Maximize the production of low/zero-carbon hydrogen via electrolysers.

The three implementation cases and the Base case described in **Chapter 3** have been simulated and operational strategies investigated by using daily time series for the electricity demand and wind generation from the Eastern Denmark power system.
The implementation cases are referred to here as:

- Case 1 - electrolysers on the supply side, at or near the primary WPP.

- Case 2 - electrolysers on the demand-side, at or near the points of hydrogen demand.

- Case 3 - some combination of Cases 1 and 2.

Figure 4.1 shows the different approaches for the implementation of electrolysers in the power system.

Although the Eastern Denmark power system has interconnections with Sweden and Germany the analysis assumed an islanded power system. The fuel mix for the Base Case is also required as input data. The main outputs obtained are daily energy balances, load profiles, hydrogen yields and carbon intensities for electricity and hydrogen as well as average power values for the period studied (see **Chapter 3).**

The approach adopted seeks to increase the daily load factor, LF_{TH}, by "valley filling" and creating a day-time plateau that is much broader than the conventional peak. Results are presented for 24h periods on a time interval of one hour based on historical data from [17], [79]. Three 24h profiles of wind power output for 2003 were selected to define three types of day: a high wind day, a variable wind day and a low wind day; and daily system demand profiles corresponding to each of the considered days was employed. Wind penetration levels of 20%, 30%, 40%, 50%, 70% and 100% are assessed. Wind and demand scenarios examined are described in **Chapter 3.2.**

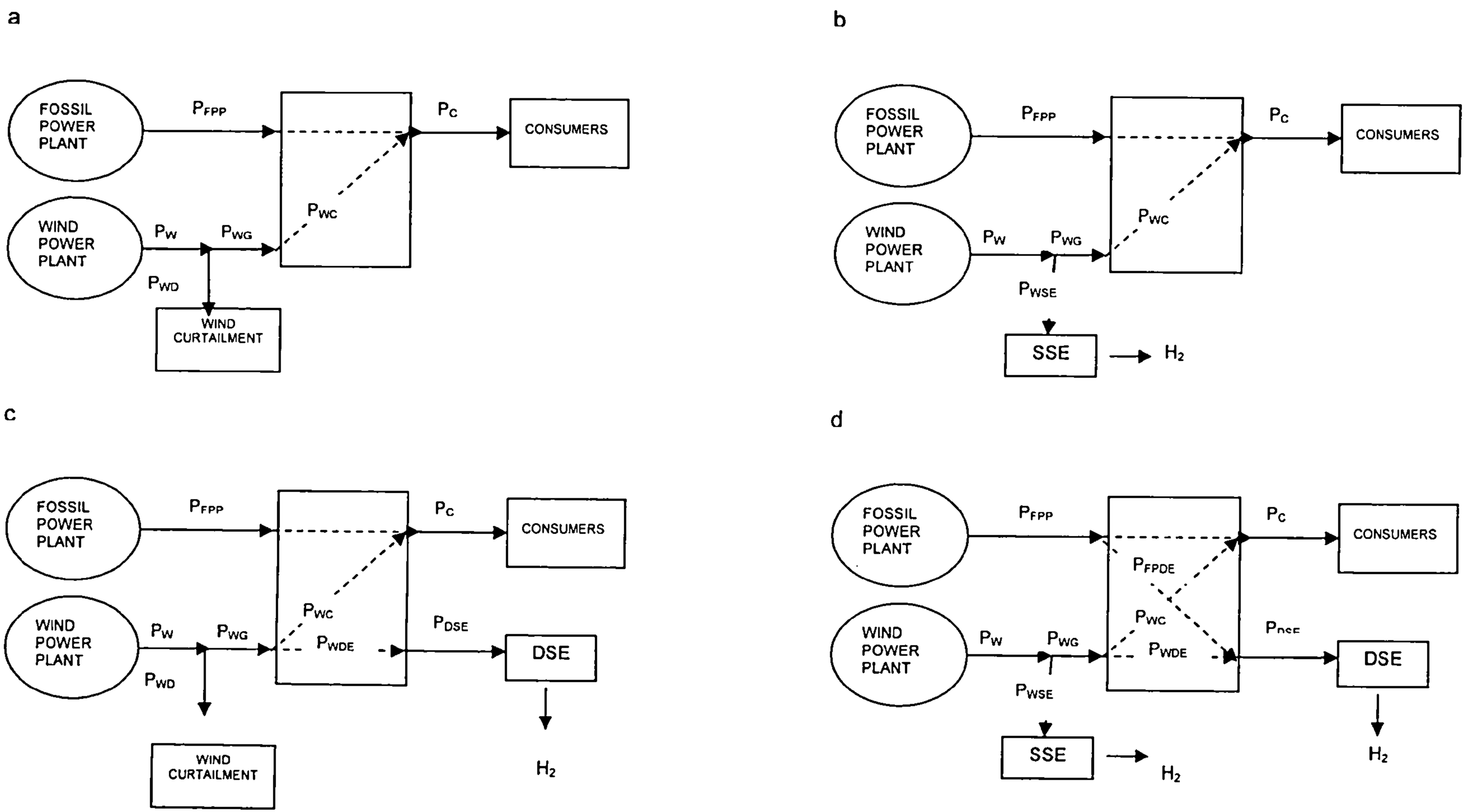

Figure 4.1. Alternative approaches for implementing electrolysers in the power system.

a) Base Case
b) Case 1
c) Case 2
d) Case 3

4.2.2 Description of Operational Strategies

Following a heuristic approach three different operational strategies have been investigated for the three implementation cases identified in **Section 2.1,** for where in each case the set-up variable is the LF_{TH}. Alternative variables can also be chosen as the set-up variable (e.g. Y_H, CI_H, CI_c). Thus emphasis was placed here on maximizing the smoothness of the aggregate FPP load profile.

For the three operational strategies each day at a specified time (e.g. 23:00 or t = -1), the operator of the system would access forecasts of consumer demand and wind power availability for the next 24h[15] on a certain time-interval. Based on this information and taking into account the LF_{TH} targeted, a preferred daily scheduling operation of FPP, WPP and electrolysers for each time-interval is devised as follows:

A) CASE 1:

The forecasted wind generation profile, P_W, is subtracted from the predicted consumer demand profile, P_C, to obtain the residual demand to be met by thermal power plant. Based on this information and taking into account the LF_{TH} desired, the FPP load profile P_{TH} is obtained by filling the early morning and night-time valleys to create a late morning-afternoon plateau at the level of the maximum load appointed to FPP, but of much greater duration than applies for the conventional FPP profile.

Subject to the low load limit,

$$P_{WC}(t) \leq 0.3\ P_C(t) \qquad (4.1)$$

The wind power output is directed to the grid and the electrolyser stock:

$$P_{WC}(t) = P_C(t) - P_{FPP}(t) \qquad (4.2)$$

$$P_{WSE}(t) = P_W(t) - P_{WC}(t) \qquad (4.3)$$

---

[15] Given the inaccuracy inherent to wind and demand forecasting over a 24 h period, this schedule would be continuously updated (for instance in 15 min intervals) according to real-time information on wind generation (MW) and system demand (MW) in order to get as close as possible to the desired thermal load previously scheduled (MW). The updated operation strategy would then govern the switching of the electrolyser stock on a continuous basis following the scheduling plan.

Because zero-carbon hydrogen is required ($CI_{II} = 0$),

$$P_{FPSE}(t) = 0 \tag{4.4}$$

In this way the operational strategy for the SSE stock, $P_{WSE}(t)$, can be defined and the net electrical energy exchanges obtained across a specific time period. For example, in the case of the load placed on thermal power plant:

$$E_{FPP} = \sum P_{FPPi}(t) \times \Delta t \qquad i = 1,\ldots,n \tag{4.5}$$

Where $P_{FPPi}(t)$ = average power output at i

Once the energy flows have been obtained, the main output variables (such as UF_{FPP}, UF_{EL}, CI_c, CI_{II}) can be computed.

B) CASE 2:

As in Case 1, from P_W and P_C, and taking into account the LF_{TII} desired, P_{FPP} is obtained by filling valleys and creating a plateau greater than applies to the conventional FPP profile.

Subject to the low-load limit,

$$P_{WC}(t) + P_{WDE}(t) \leq 0.3\ [P_C(t) + P_{DSE}(t)] \tag{4.6}$$

The wind power output is directed to the grid:

$$P_{WC}(t) = P_C(t) - P_{FPP}(t) \tag{4.7}$$

$$P_{WDE}(t) = P_W(t) - P_{WC}(t) \tag{4.8}$$

Because zero-carbon hydrogen is required ($CI_H = 0$),

$$P_{FPDE}(t) = 0 \tag{4.9}$$

The operational strategy for the DSE stock, $P_{DSE}(t) = P_{WDE}(t)$, is then defined subject to $P_C(t) + P_{DSE}(t) \leq SMD$ (4.10)

The net electrical energy exchanges obtained for a specific time period.

Once the energy flows have been obtained, the main output variables can be computed.

C) CASE 3:

As previously, P_{TH} is obtained by filling valleys and creating a plateau greater than applies to the conventional FPP profile, taking into account the LF_{TH} desired.

Subject to the carbon intensity of hydrogen appointed (e.g. $CI_H = 3$), the wind power output is directed to the grid, and the aggregate thermal load P_{FPP} is allowed to exceed the consumer demand P_C by an amount P_{FPDE} which is directed to the DSE stock where:

If $CI_H = 0$ then $P_{WC}(t) = P_C(t) - P_{FPP}(t)$ (4.11)

and $P_{FPDE}(t) = 0$ (4.12)

If $CI_H > 0$ then $P_{WC}(t) = 0$ (4.13)

and $P_{FPDE}(t) = P_{FPP}(t) - P_C(t)$ (4.14)

Subject to the low load limit,

$P_{WC}(t) + P_{WDE}(t) \leq 0.3\ [P_C(t) + P_{DSE}(t)]$ (4.15)

The wind power output is directed to the grid, and the DSE stock

$P_{WC}(t) = P_C(t) - P_{FPP}(t)$ (4.16)

$P_{WDE}(t) = P_W(t) - P_{WC}(t)$ (4.17)

The operational strategy for the DSE stock, $P_{DSE}(t)$, is then defined subject to the restriction:

$$P_C(t) + P_{DSE}(t) \leq SMD \quad (4.18)$$

$$P_{DSE}(t) = P_{FPDE}(t) + P_{WDE}(t) \quad (4.19)$$

The remainder wind power output, if any, is then sent to the SSE stock and the operational strategy for the SSE stock, $P_{WSEL}(t)$, is defined:

$$P_{WSE}(t) = P_W(t) - [P_{WC}(t) + P_{WDE}(t)] \quad (4.20)$$

$$P_{WSEL}(t) = [P_W(t) - P_{WC}(t)] - P_{WEL}(t) \quad (4.21)$$

The net electrical energy exchanges are obtained for a specific time period. Once the energy flows have been obtained, the main output variables can be computed.

Note the analysis presented in this chapter is based on a time interval of one hour and results are displayed for a 24h period (daily load profiles). However the methodology presented can be applied to any appropriate time-base (15 min, 30 min, 1 hour, etc) and for any period (0-24h, 48h, 7 days, etc) provided the required input data are available. Also different electricity generation mixes can be introduced as inputs.

4.3. RESULTS

4.3.1 Base Case

Following current trends, the effects of an increasing proportion of wind generation within the East Denmark power system are shown in **tables 4.2, 4.3 and 4.4** for the steady, variable and low wind scenarios respectively. Results for 20% wind penetration correspond approximately to the current situation in East Denmark.

Φ_W (%)	20	30	40	50	70	100
IC_W (MW)	**554**	**800**	**1066**	**1340**	**1866**	**2665**
LF_{TH} (%)	76	77	79	79	79	79
P_{FPP} (GWh/d)	37.3	35.2	33.3	33.3	33.3	33.3
CI_e ($kgCO_2/kWh_e$)	0.57	0.50	0.48	0.46	0.43	0.38
TC ($tCO_2 \times 10^3/d$)	27.3	23.9	22.6	21.7	20.4	17.9
WC (%)	2	11	30	44	60	72

Table 4.1. Results for the Base Case – Steady Wind Day Scenario

Φ_W (%)	20	30	40	50	70	100
IC_W (MW)	**554**	**800**	**1066**	**1340**	**1866**	**2665**
LF_{TH} (%)	76	76	78	81	86	84
P_{FPP} (GWh/d)	25.3	24.3	23.6	23.1	22.4	21.9
CI_e ($kgCO_2/kWh_e$)	0.61	0.56	0.51	0.48	0.43	0.39
TC ($tCO_2 \times 10^3/d$)	18.7	17.0	15.8	14.6	13.3	12.0
WC (%)	3	19	32	42	55	67

Table 4.2. Results for Base Case – Variable Wind Day Scenario

Φ_W (%)	20	30	40	50	70	100
IC_W (MW)	**554**	**800**	**1066**	**1340**	**1866**	**2665**
LF_{TH} (%)	78	77	77	76	74	74
P_{FPP} (GWh/d)	45.1	44.2	43.2	42.1	40.2	38.2
CI_e ($kgCO_2/kWh_e$)	0.70	0.65	0.62	0.57	0.51	0.42
TC ($tCO_2 \times 10^3/d$)	33.1	30.9	29.1	26.9	24.1	19.9
WC (%)	0	0	0	0	2	12

Table 4.3. Results for Base Case – Low Wind Day Scenario

For the steady and variable wind scenario the integration of larger penetrations of wind energy in the system does not penalise the aggregate load placed on FPP, P_{FPP}, and LF_{TH} even increases slightly due to the smoothing effect caused by the curtailment restriction imposed (wind power is discarded when the equivalent aggregate WPP output exceeds 30% of total system demand) which effectively reduces the peaks of the aggregate wind power profile, thus smoothing the load placed on FPP.

The load factors applying in 2003 were 78%, 76%, and 76% for the low, variable and steady wind day respectively; these are typical for North European countries. As a result of aiming for high penetrations of wind power in a system without energy storage, LF_{TH} can actually be increased up to 86% for $\Phi_W = 70\%$ on the variable wind day, but always at the expense of increasing the amount of wind generation discarded. The maximum LF_{TH} does not occur at $\Phi_W = 100\%$ for the variable and low wind days as might be expected, because at wind penetrations > 50% wind generation is curtailed even during peak demand periods, and the value of peak thermal load thus remains constant. Accordingly there is no case for implementing WPP beyond $\Phi_W = 70\%$.

With increasing wind penetration the proportion of available resource that has to be curtailed increase dramatically. For example, more than 30% of the resource is wasted for $\Phi_W = 50\%$, with LF_{TH} being 79% and 81% for the steady and variable wind days respectively. The significant scale of wind curtailment can be observed in the load profiles shown in **Figure 4.2**, where results for the steady wind scenario are displayed for $20\% \leq \Phi_W \leq 50\%$. It is clear that on this type of day, wind power is first discarded at times of low demand (the early morning and late evening periods). This is so due to the limited ability (or inability) of the electrical grid to accommodate wind power production when the power system lacks a method of storing the renewable output, leading to a substantial fraction of the resource being wasted. For wind penetrations above 30%, wind energy is wasted across the entire day, but more than 60% of the

curtailment occurs during low demand periods (00:00 to 05:00 and 20:00 to 24:00). From **Table 4.1**, if fully directed to the grid, more than 70% of the wind resource available is curtailed at Φ_w =100%.

a) $\Phi_W = 20\%$

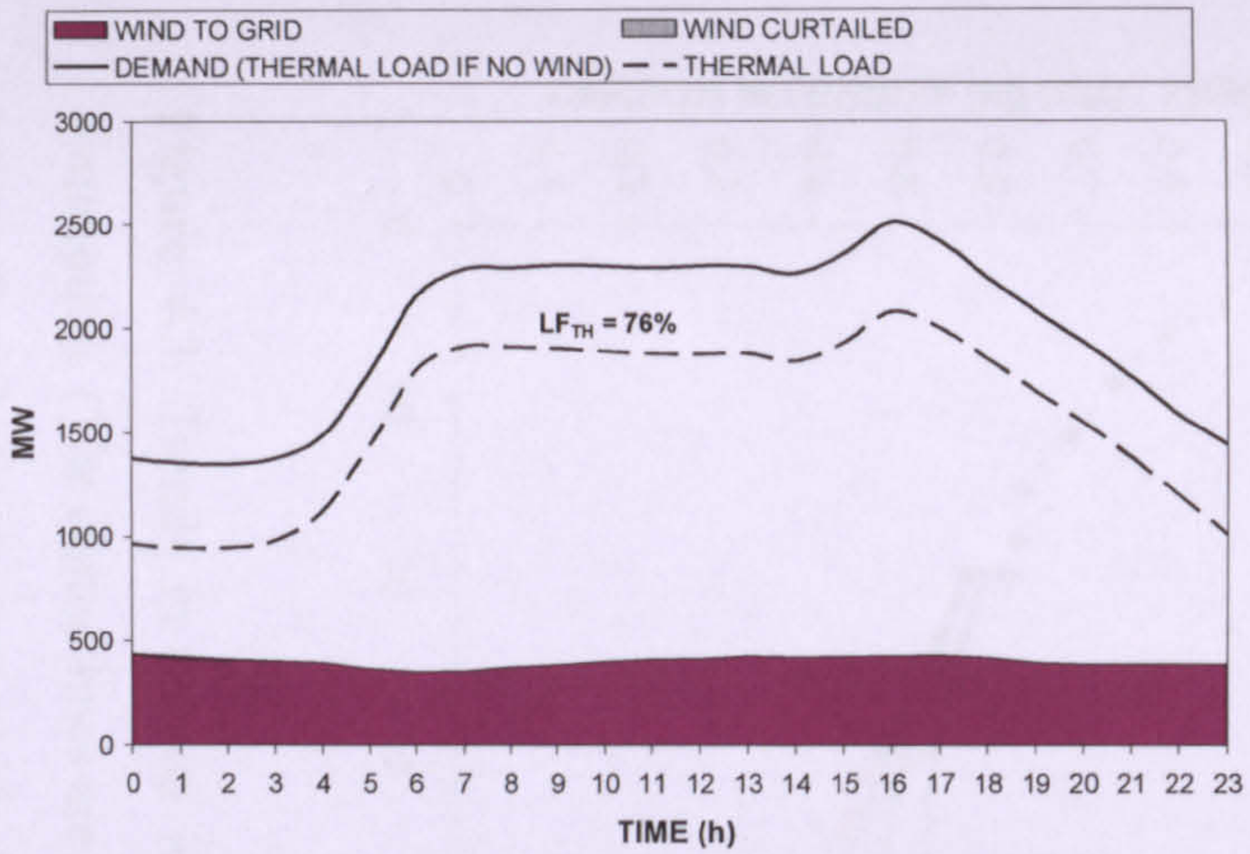

b) $\Phi_W = 30\%$

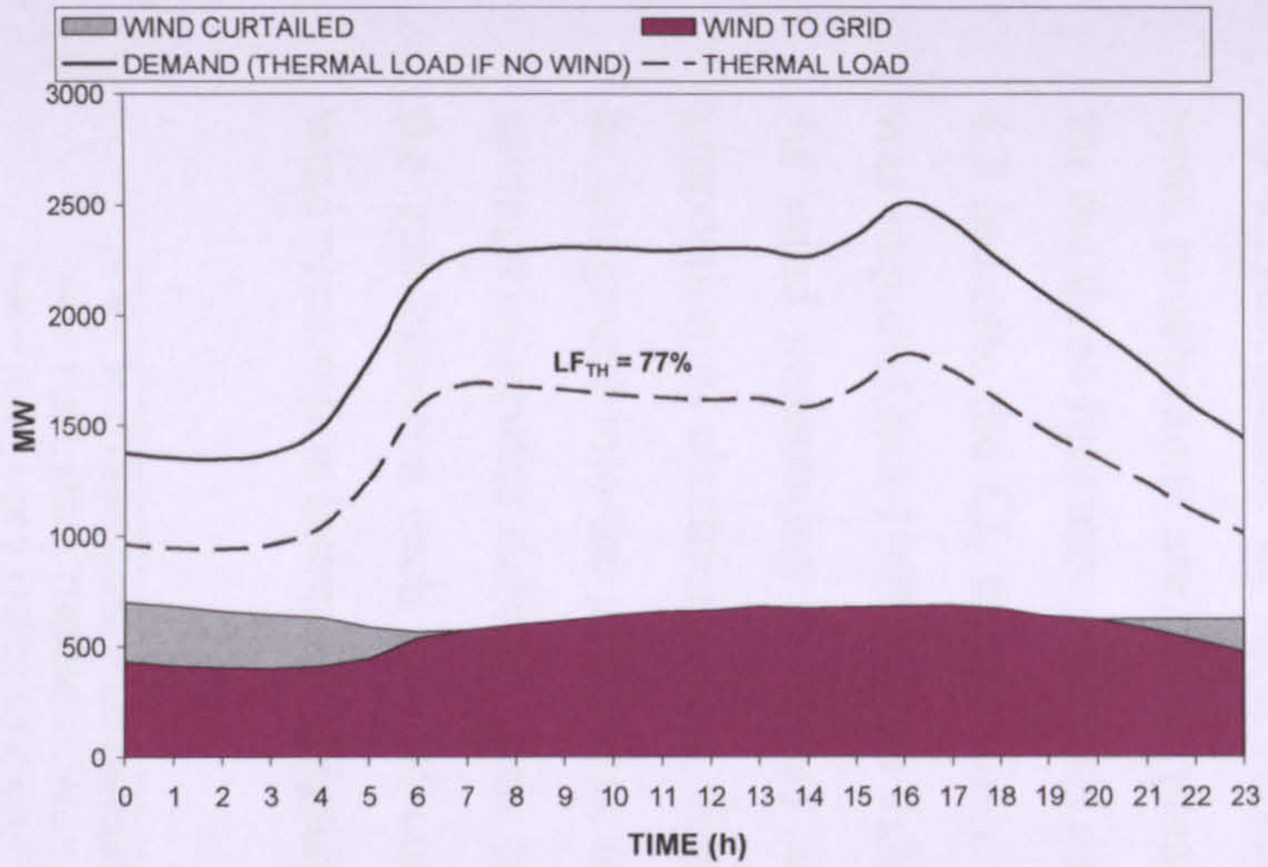

c) $\Phi_W = 40\%$

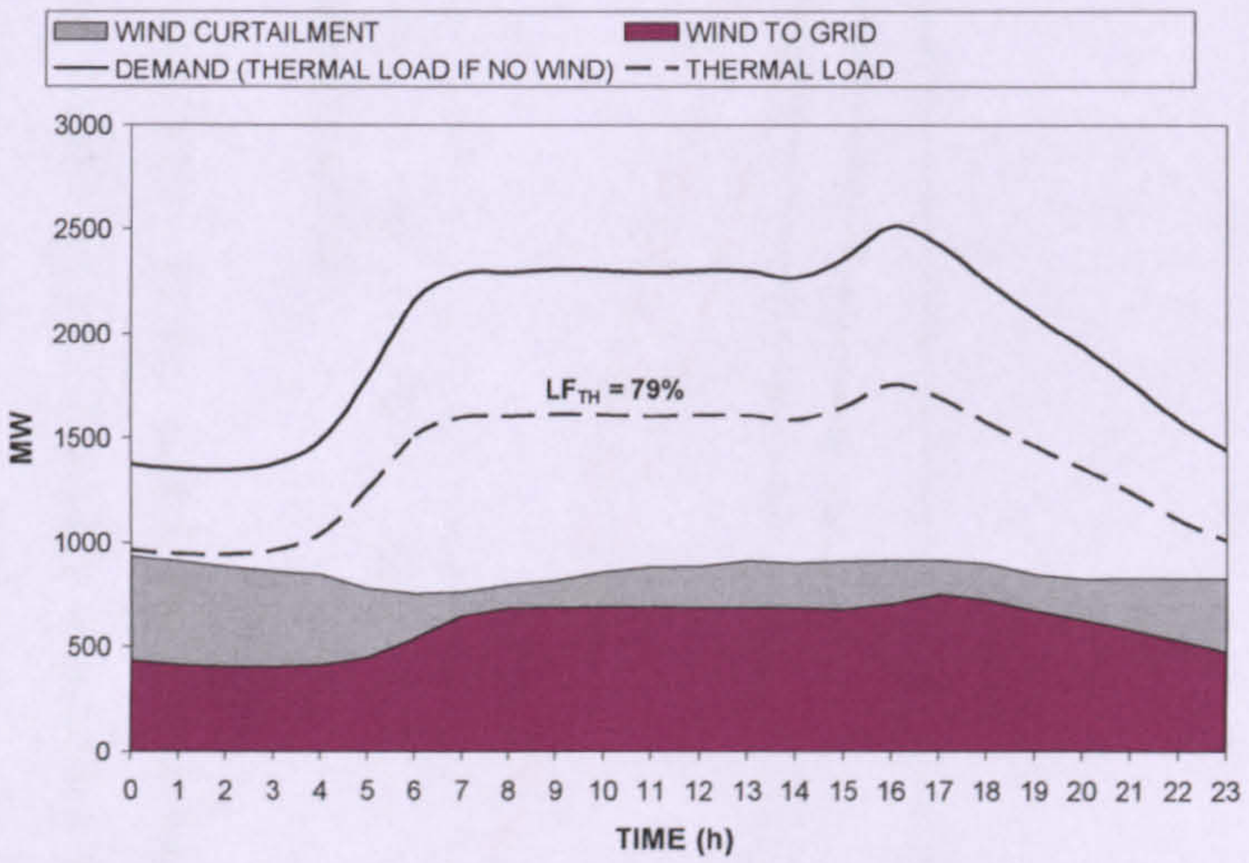

d) $\Phi_W = 50\%$

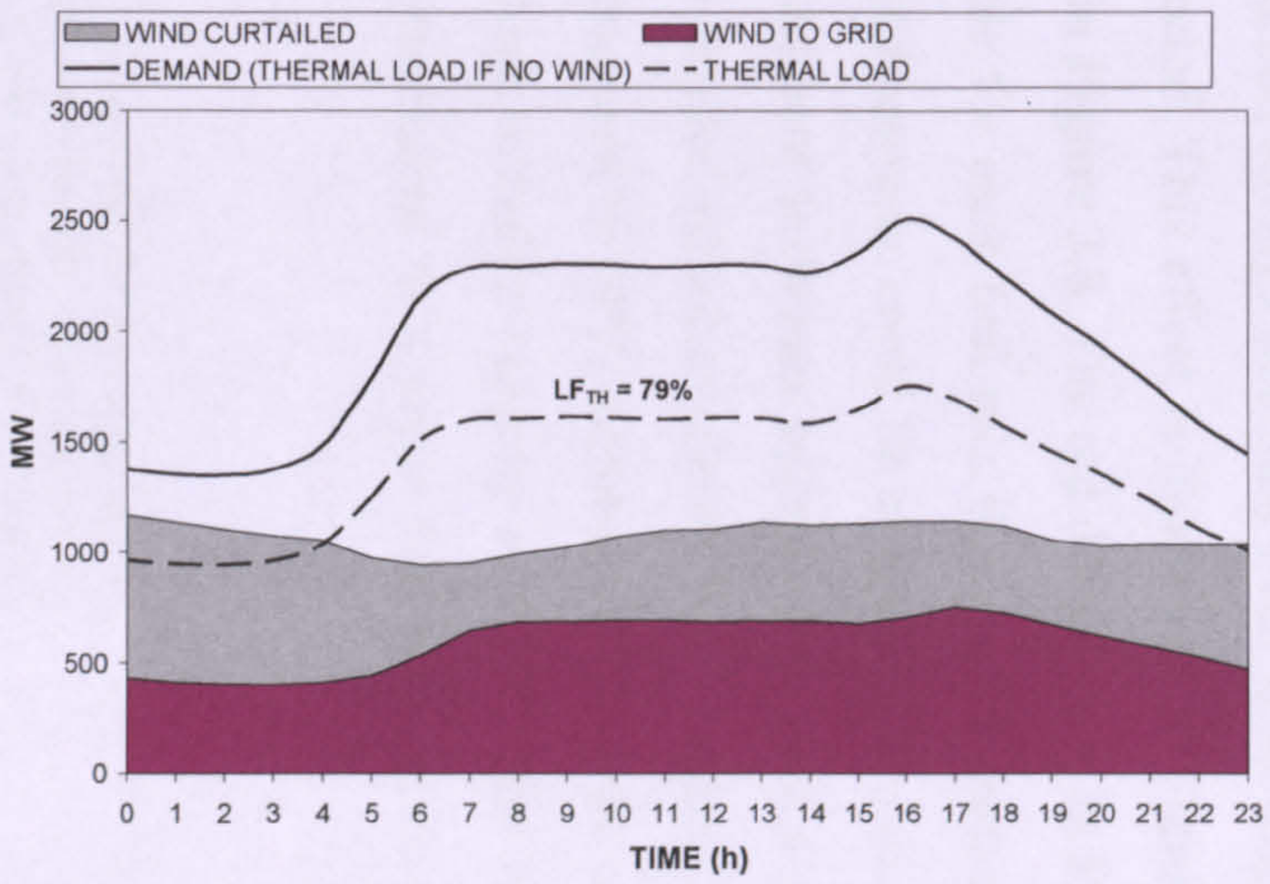

Figure 4.2. Base Case: effects of increasing wind penetration upon the FPP load profile and wind curtailment for the steady wind day

As a consequence of wind curtailment, carbon savings obtained from achieving high wind penetrations are not as great as expected. This effect is illustrated in **Figure 4.3** for the three fuel mix scenarios described in **Figure 3.8**. The red dotted lines in **Figure 4.3** indicate the CI_e theoretically achievable for each fuel mix if no wind curtailment was required and 100% of the available wind resource could be integrated into the grid. As wind penetration increases wind curtailment increases appreciably, and a larger proportion of electricity than theoretically needed (if all available WPP outputs could be integrated into the grid) must now be generated by FPP, thereby reducing the carbon savings otherwise derived from having a high installed capacity of WPP. This is why the gap between each pair of curves corresponding to a given fuel mix increases as wind penetration increases (**Figure 4.3)**.

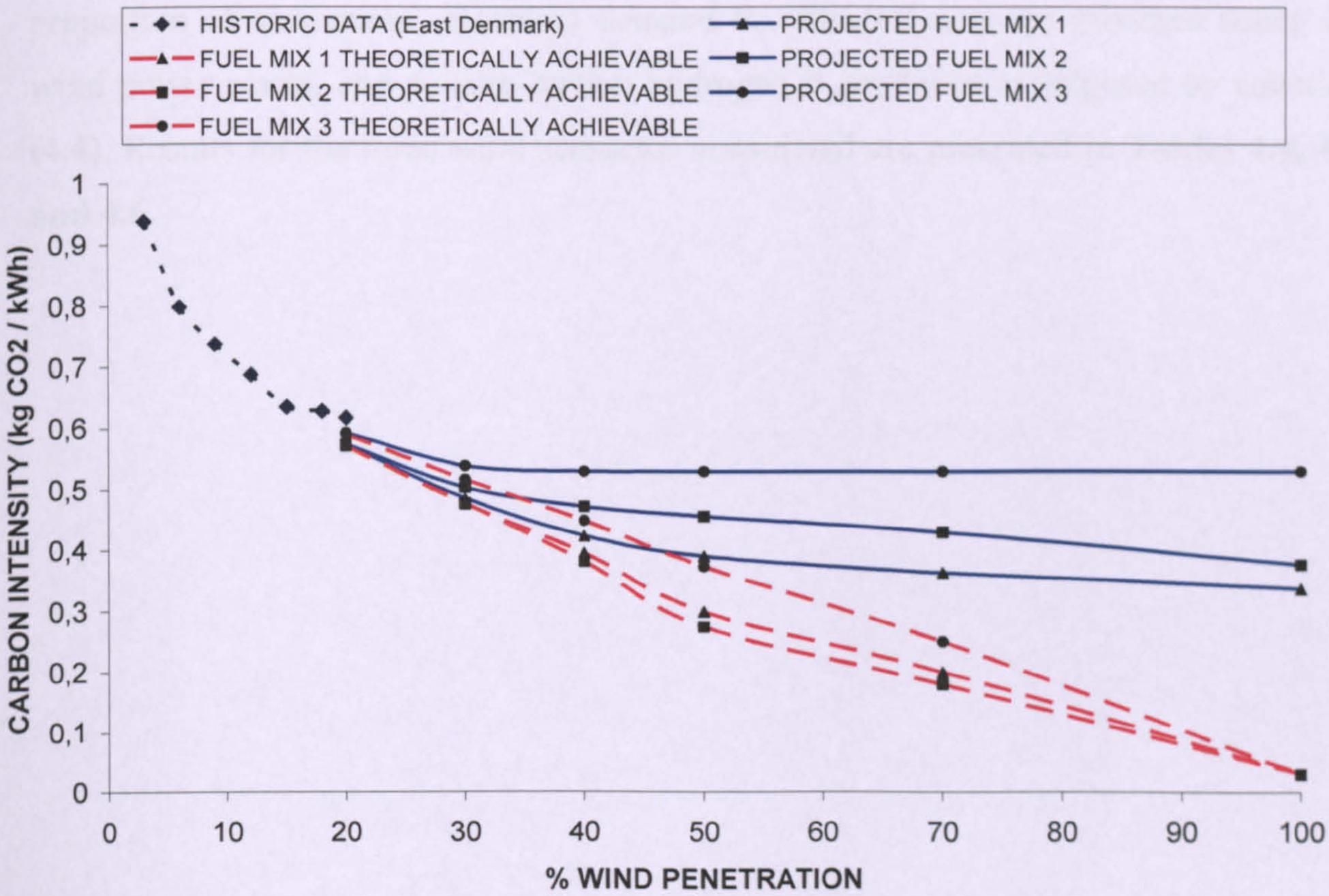

Figure 4.3. Trends in carbon intensity with wind power penetration and fuel mix assumption. (The dotted lines are theoretical – they are unachievable in practice at high penetrations but represent an ideal target and are shown for completeness).

In summary, when all wind-generated electricity can only be directed to the grid, the justification (in economic and carbon terms) for achieving high wind penetrations follows the law of diminishing returns. Alternatives are required which will reduce the gap in **Figure 4.3** between the red dotted lines of theoretically achievable minimum CI_e and that associated with a given fuel mix. Rather than simply increase uncontrollably the amount of wind power introduced into the grid, leading to a large proportion of the renewable resource being wasted, some alternatives are suggested here (see Cases 1, 2 and 3). All of them require a large deployment of electrolyser systems as controllable loads within the power system.

4.3.2 CASE 1

Case 1 includes "supply-side electrolysers" (SSE) deployed adjacent to wind power plants. Some wind generated electricity P_{WG} is also directed to the grid to cover a proportion of consumers' electrical demand P_C. Electrolysers are powered solely by wind power plants, and so zero-carbon hydrogen is produced as imposed by equation (4.4). Results for the three wind scenarios considered are presented in **Tables 4.4, 4.5 and 4.6**.

Φ_W %	20	30	40	50	70	100
IC_W (MW)	533	800	1,066	1,333	1,866	2,665
LF_{TH} (%)	85	85	85	85	85	85
CI_e ($kgCO_2/kWh_e$)	0.63	0.55	0.51	0.49	0.48	0.48
TC ($tCO_2 \times 10^3/d$)	29.9	26.1	24.3	23.3	22.9	22.9
P_{FPP} (GWh/d)	41.2	37.2	36.2	36.2	36.2	36.2
WC (%)	0	0	0	0	0	0
Y_H (t)	86	101	176	279	484	788
CI_H ($kgCO_2/kg\ H_2$)	0	0	0	0	0	0
UF_E (%)	39	38	49	60	73	78
IC_E (MW)	453	554	746	978	1381	2105

Table 4.4. Results for CASE 1. Steady Wind Scenario

Φ_W %	20	30	40	50	70	100
IC_W (MW)	533	800	1,066	1,333	1,866	2,665
LF_{TH} (%)	87	87	87	87	87	87
CI_e ($kgCO_2/kWh_e$)	0.68	0.63	0.57	0.52	0.49	0.46
TC ($tCO_2 \times 10^3/d$)	21.0	19.2	17.6	15.8	15.1	14.2
P_{FPP} (GWh/d)	28.7	27.8	26.6	25.0	25.0	25.0
WC (%)	0	0	0	0	0	0
Y_H (t)	71	100	128	151	259	418
CI_H ($kg\ CO_2/kg\ H_2$)	0	0	0	0	0	0
UF_E (%)	33	38	37	32	39	41
IC_E (MW)	453	554	746	978	1381	2105

Table 4.5. Results for CASE 1. Variable Wind Scenario

Φ_W %	20	30	40	50	70	100
IC_W (MW)	533	800	1,066	1,333	1,866	2,665
LF_{TH} (%)	80	80	80	80	80	80
CI_e ($kgCO_2/kWh_e$)	0.71	0.67	0.64	0.60	0.55	0.49
TC ($tCO_2 \times 10^3/d$)	33.5	31.9	30.3	28.5	26.0	23.2
P_{FPP} (GWh/d)	45.8	45.5	45.0	44.5	43.3	43.3
WC (%)	0	0	0	0	0	0
Y_H (t)	14	26	37	48	64	126
CI_H (kg CO_2/kg H_2)	0	0	0	0	0	0
UF_E (%)	6	10	10	10	10	12
IC_E (MW)	453	554	746	978	1381	2105

Table 4.6. Results for CASE 1. Low Wind Scenario

The utilization factor of the electrolyser sock, UF_E, increases with Φ_W except for the variable wind scenario and the hydrogen yield peaks at 788 tH_2 and UF_E =78% for Φ_W = 100% on the steady wind day. The electrolyser installed capacity lies in the range 453 MW to 2,150 MW, with the upper limit corresponding to Φ_W = 100%, and the ratio of electrolyser installed capacity to wind power capacity lies in the range 0.69 to 0.79, with the upper limit corresponding to Φ = 100%. To achieve a LF_{TH} of 87% at Φ = 100% would require installed wind and electrolyser capacities of 2,665 and 2,150 MW respectively.

One characteristic of this implementation strategy is that for every wind penetration and depending on wind availability there is an upper limit for the LF_{TH} achievable, above which there would be some surplus of thermal-generated electricity above that otherwise required to cover consumers demand ($P_{FPP} - P_C > 0$) that would be wasted. This is expressed by equation (4.4) in Section 2.2. The maximum achievable LF_{TH} values for the low, variable and steady wind days are 82, 90 and 88% respectively. These constitute significant improvements relative to the Base Case. For the sake of clarity in the results presented in **Tables 4.4, 4.5 and 4.6** the value of LF_{TH} is the maximum LF_{TH} achievable at $\Phi_W = 20\%$ and is fixed as Φ_W increases.

Through time-controlled operation of ELS wind curtailment is completely eliminated across the three wind scenarios. This becomes particularly important for high wind penetrations above 30% on a steady and variable wind day, where a large part of the resource is wasted when no electrolysers are implemented (see Base Case). For Φ_W = 50% on a day of 80% capacity factor, it is found that 44% of the available wind power would have to be curtailed, but that this can be eradicated if SSEs electrolysers are deployed. This harnessing of otherwise discarded wind power to produce zero-carbon hydrogen increases the utilization of the SSE stock.

At high wind penetrations, a much greater yield of hydrogen is observed for the steady wind scenario compared with the variable and low wind days **(Figure 4.4)**. This is simply the result of a larger availability of wind-derived electricity for the SSE stock on this day, which would otherwise have to be discarded. Taking the variable wind day as an example, at Φ_W = 50% 128 tonnes of zero-carbon H_2 are produced daily which would cover approximately 8% of the daily road transport energy demand in East Denmark.[16]

[16] The average daily road transport energy demand in Eastern Denmark is 55 GWh, equivalent to 1,652 tonnes of H_2 (LHV basis) [81].

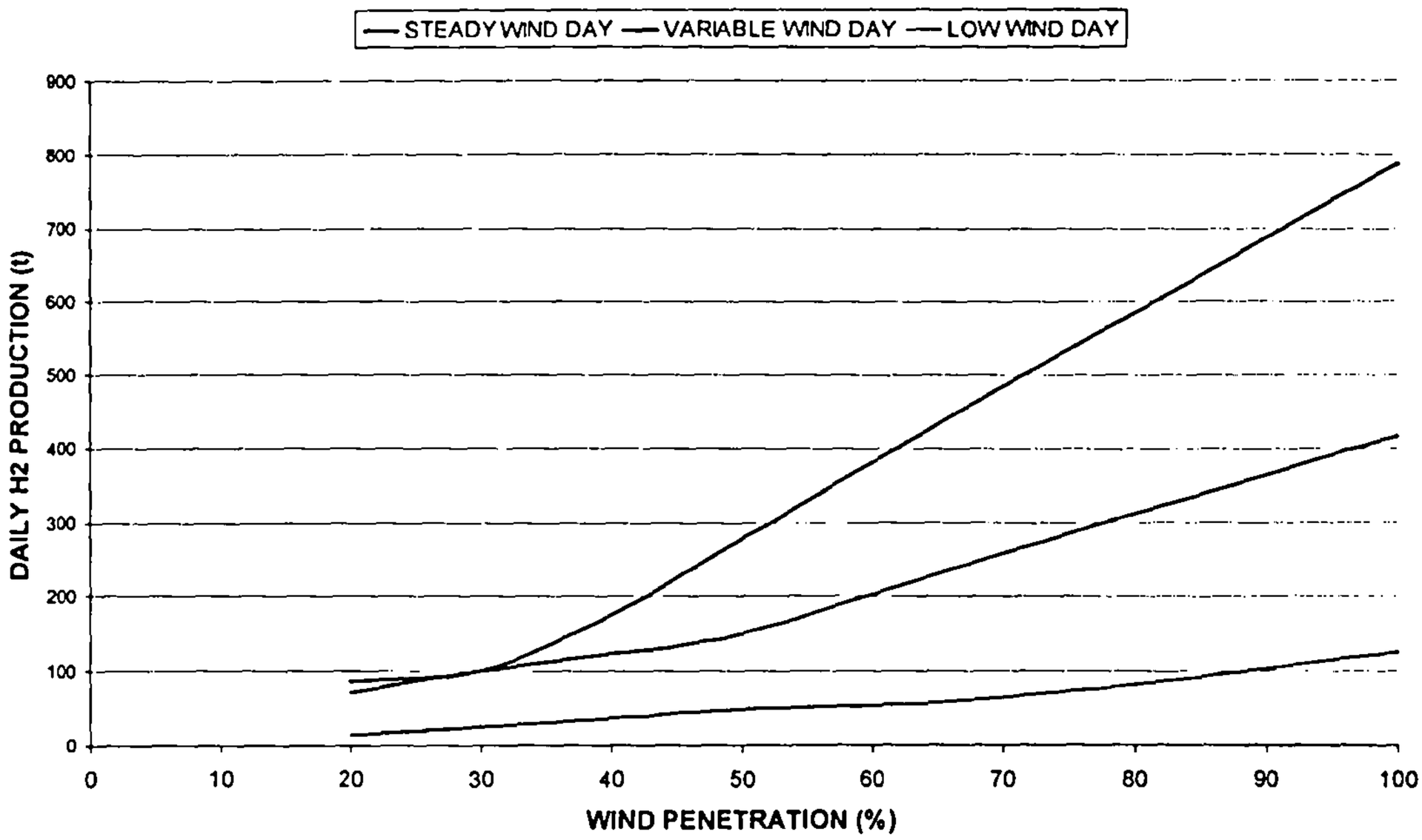

Figure 4.4. Case 1: daily hydrogen yield for the steady, variable and low wind days

It is also interesting to investigate the relationship between the carbon intensity of electricity CI_e and the wind penetration φ_W. This is plotted in **Figure 4.5**.

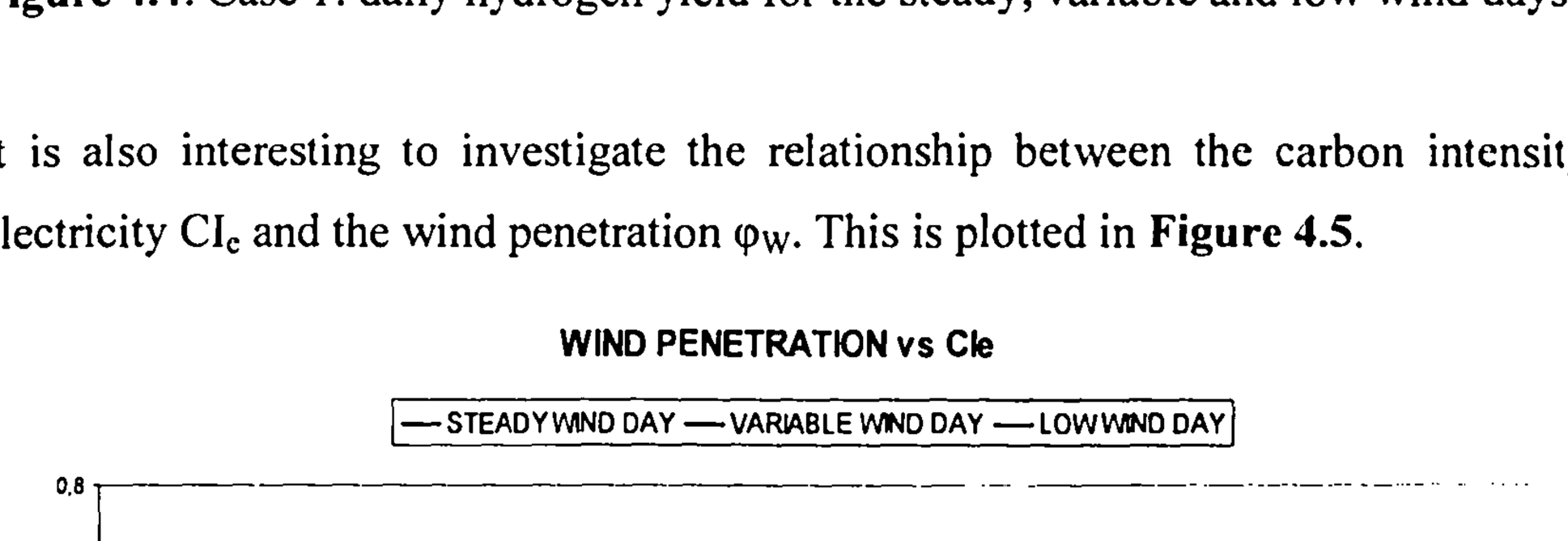

Figure 4.5. CASE 1. Average daily carbon intensity of electricity CI_e versus wind power penetration for steady, variable and low wind scenario.

As observed in **Figure 4.5**, for the variable and low wind scenarios, the reduction of CI_e is approximately proportional to wind power penetration, whereas for the steady wind scenario the decrease is not as marked as expected for wind penetrations above 30% and CI_e remains constant at $\Phi_W > 60\%$. This is due to the curtailment limit imposed on which in turn determines the load imposed on FPP P_{FPP}, and then by implication the daily average carbon intensity of the electricity generated. It is found that on a high wind day (steady wind scenario) at high wind penetrations P_{WG} is strongly limited by the curtailment limit, and the carbon abatement potential of wind energy reduces as Φ_W increases. For the variable wind scenario however the curtailment of wind does not influence the level of peak FPP load (curtailment of wind energy mainly occurs in the afternoon period before the peak thermal load is achieved, see **Figures 4.2a-d**) which can decrease steadily as Φ_W increases and then CI_e reduces gradually. As expected it is also clear in the figure that the higher the wind availability the lower the carbon intensity of electricity on that day.

Carbon emissions for electricity increase by 7-11% over those values of the Base Case. Because the amount of wind electricity delivered to consumers is reduced by the presence of the SSE stock. Note that the trade-offs between the penalties imposed on CI_e and the carbon benefits derived from achieving greater LF_{TH} values have not been quantified here. Further discussion on this topic is offered in **Section 4.4.4** below.

In summary, the implementation of an SSE capacity which is approximately 80% of the installed capacity of wind power plant will facilitate a power system with a very high wind penetrations, an improved LF_{TH} relative to the Base Case, and an utilization factor of the SSE stock that increases with wind penetration reaching values close to 80% for $\Phi_W = 100\%$. As a by product, it will provide the energy system with a major supply of zero-carbon hydrogen. Unfortunately these benefits will be acquired at the expense of CI_e. In order to lessen the penalties imposed on CI_e while at the same time aiming for improved LF_{TH} with respect to the Base Case, other implementation alternatives were considered.

Figures 4.6 and 4.7 show simulations of a 24h operational strategy for the steady and variable wind day respectively when applying the operational strategy described in Section 2.2 when 85% (**Figure 4.6**, steady wind) and 87% LF_{TH} (**Figure 4.7**, variable wind) are sought. Values of LF_{TH} are kept constant with φ_W and correspond to the upper limits achievable at φ = 20% under this implementation case. By operating ELS at will aggregated thermal load profiles clearly becomes more regular than those of a system without implementation of electrolysers (compare with results for the Base case in **Figure 4.2**). Time-controlled operation of ELS now allows FPP to operate at full load for longer periods, increasing their utilization and minimizing carbon emissions per kWh_e of electricity generated. Also the higher the wind penetration, the higher the zero-carbon electrical input to ELS and the higher the hydrogen production.

a)

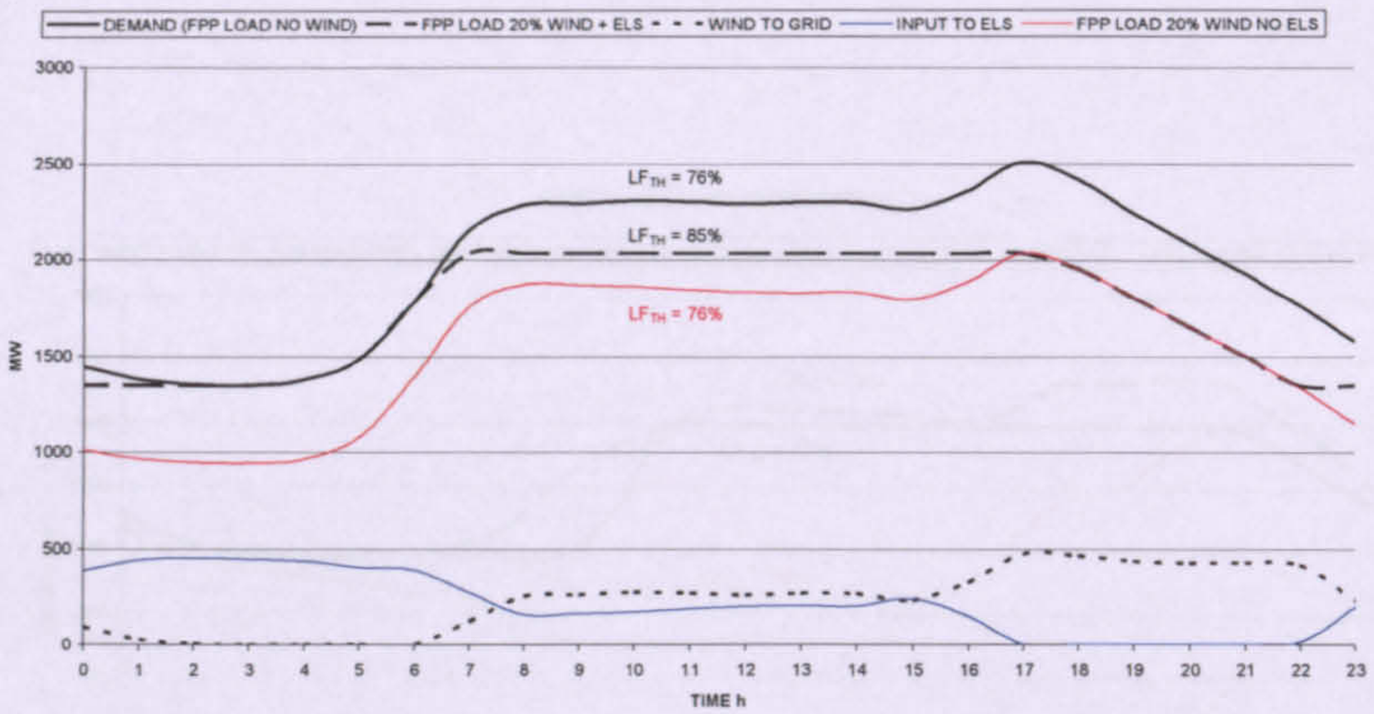

b)

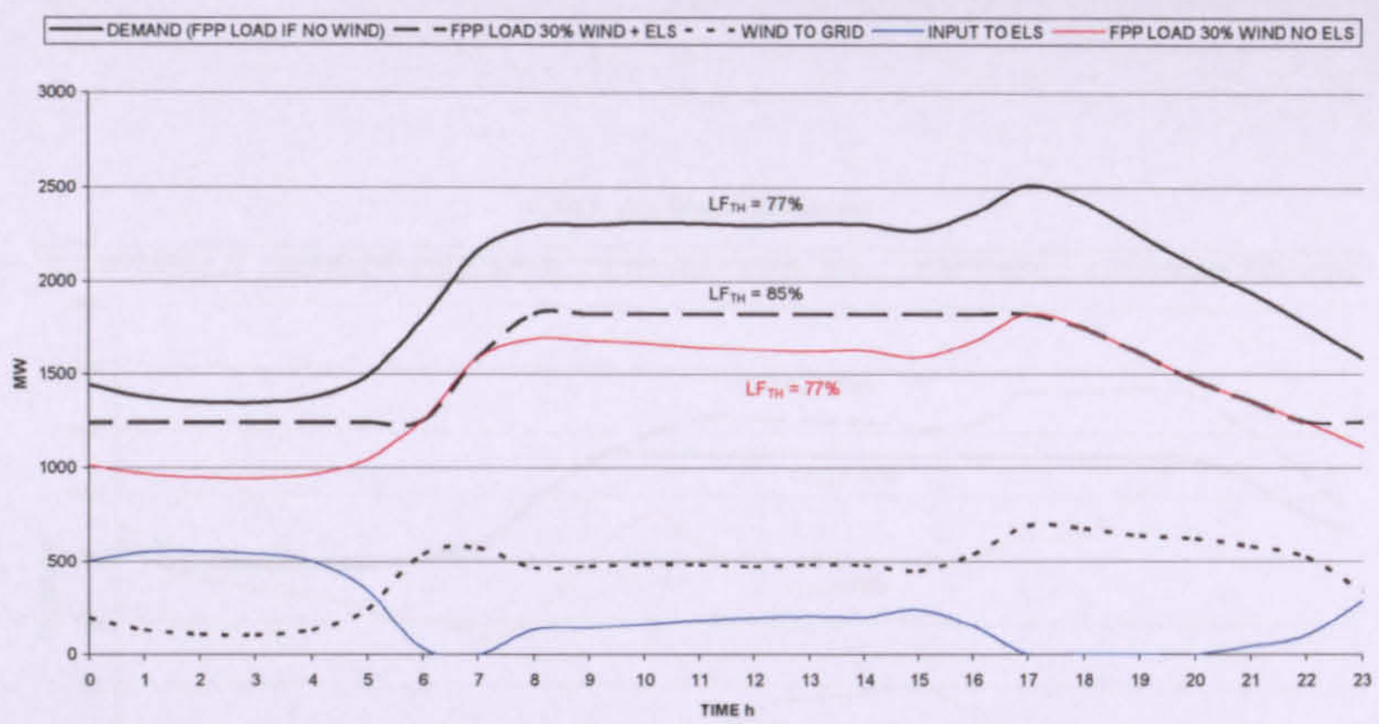

c)

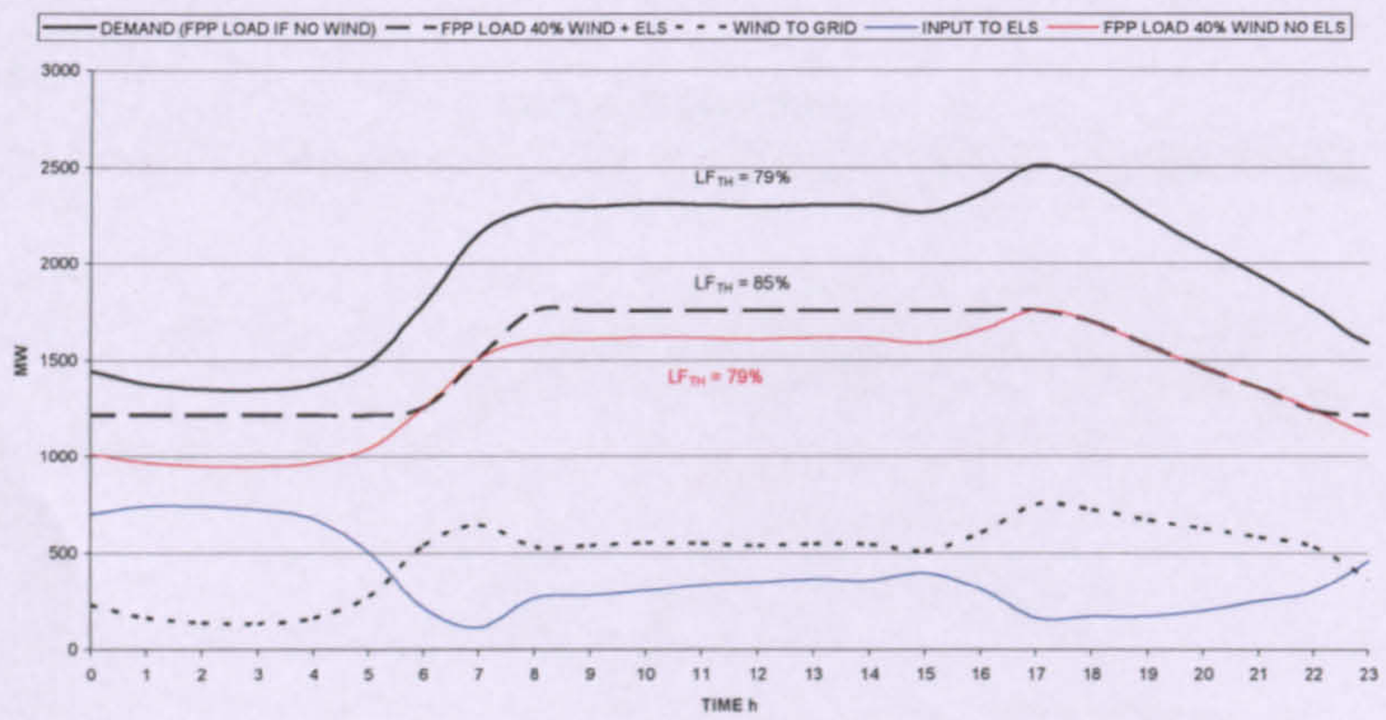

d)

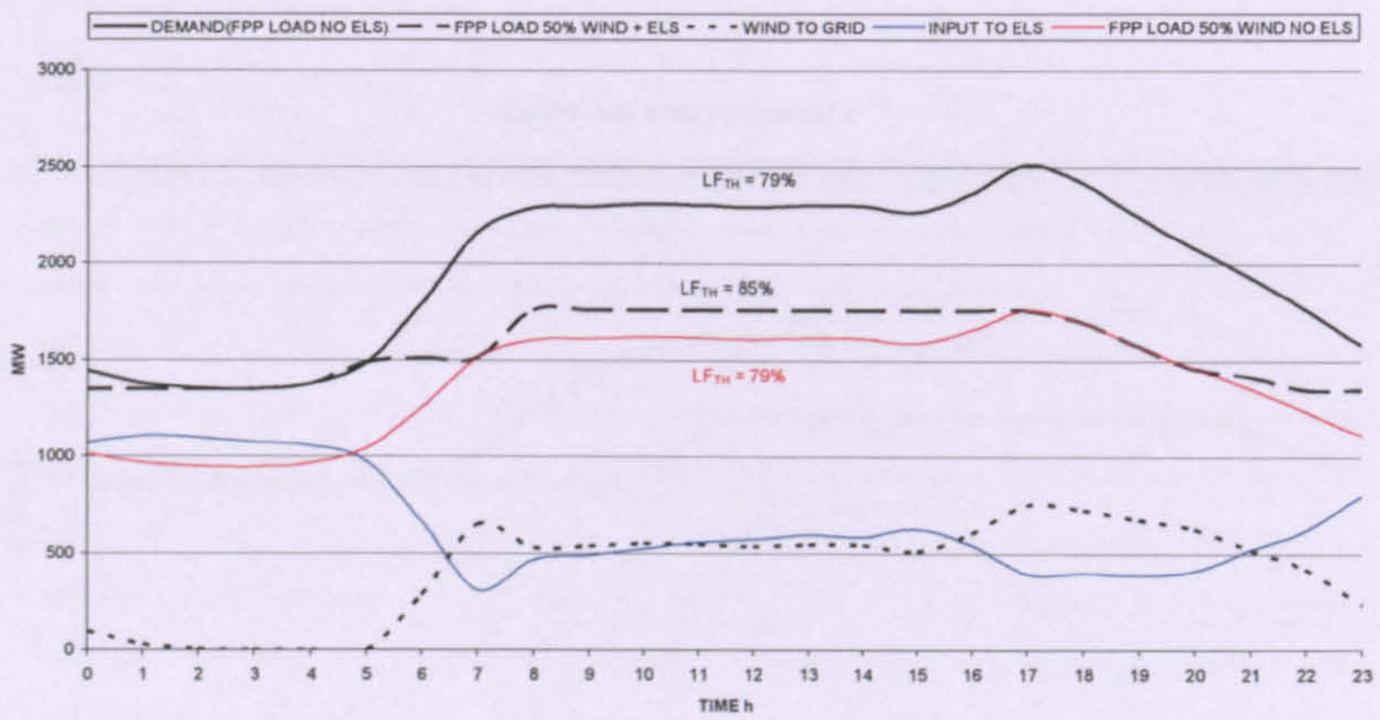

Figure 4.6. Results for CASE 1. Steady wind day. Effects of increasing penetrations of wind power upon the FPP load profile, the profile of wind power delivered to grid and the input profile to the electrolyser stock.

a)

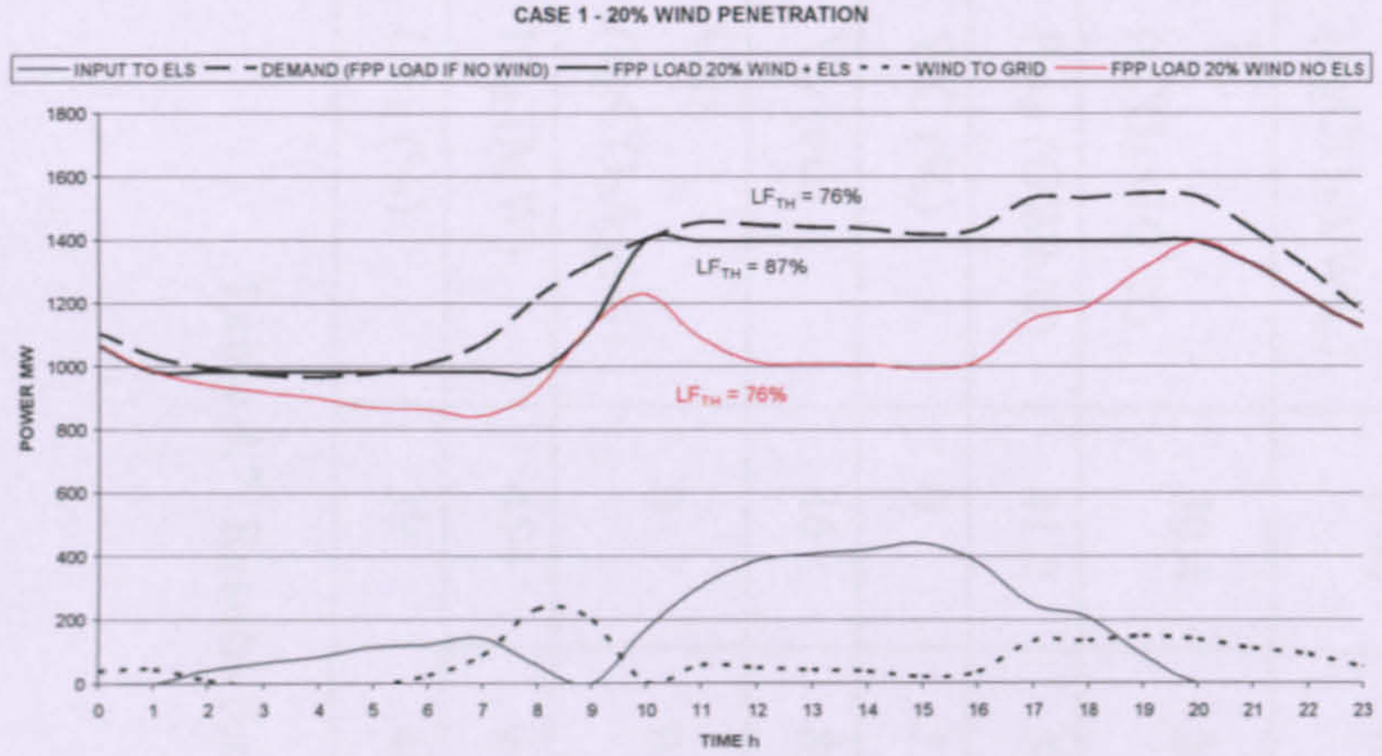

b)

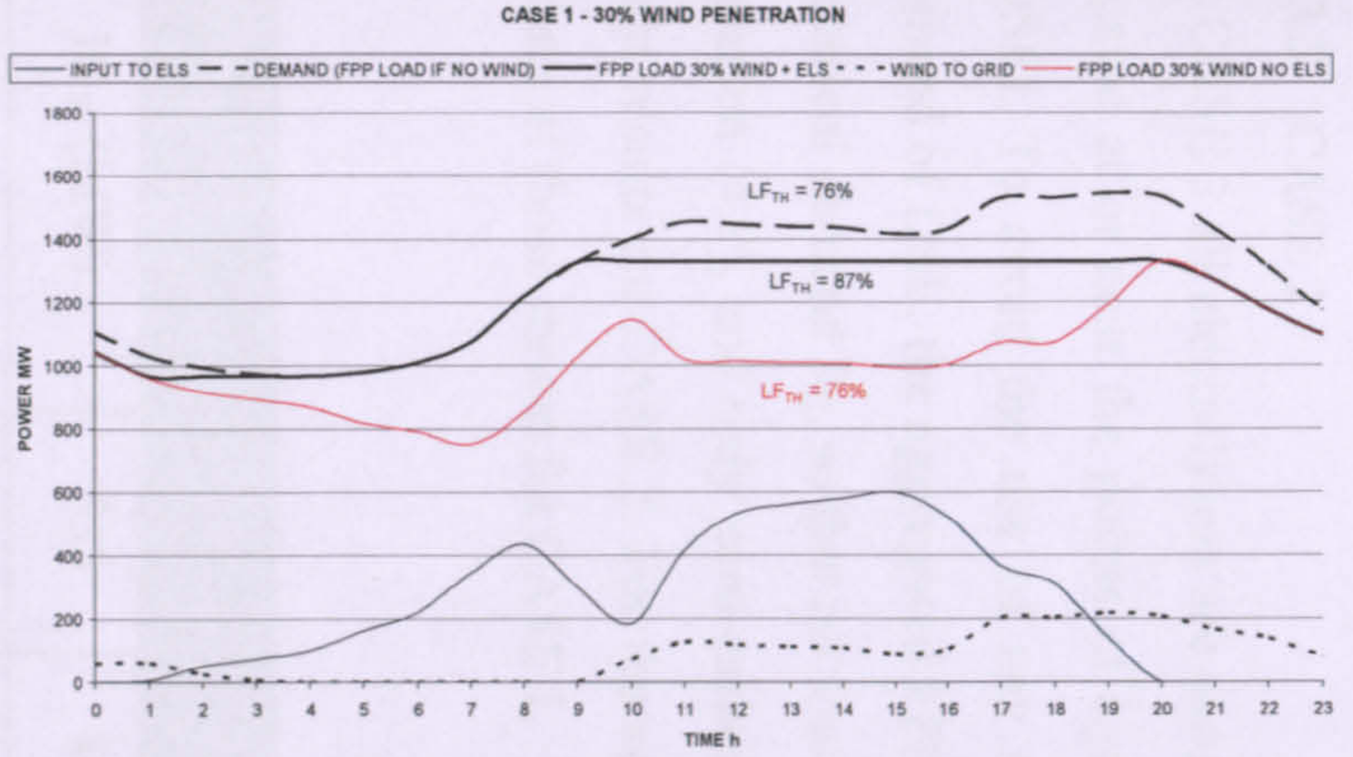

c)

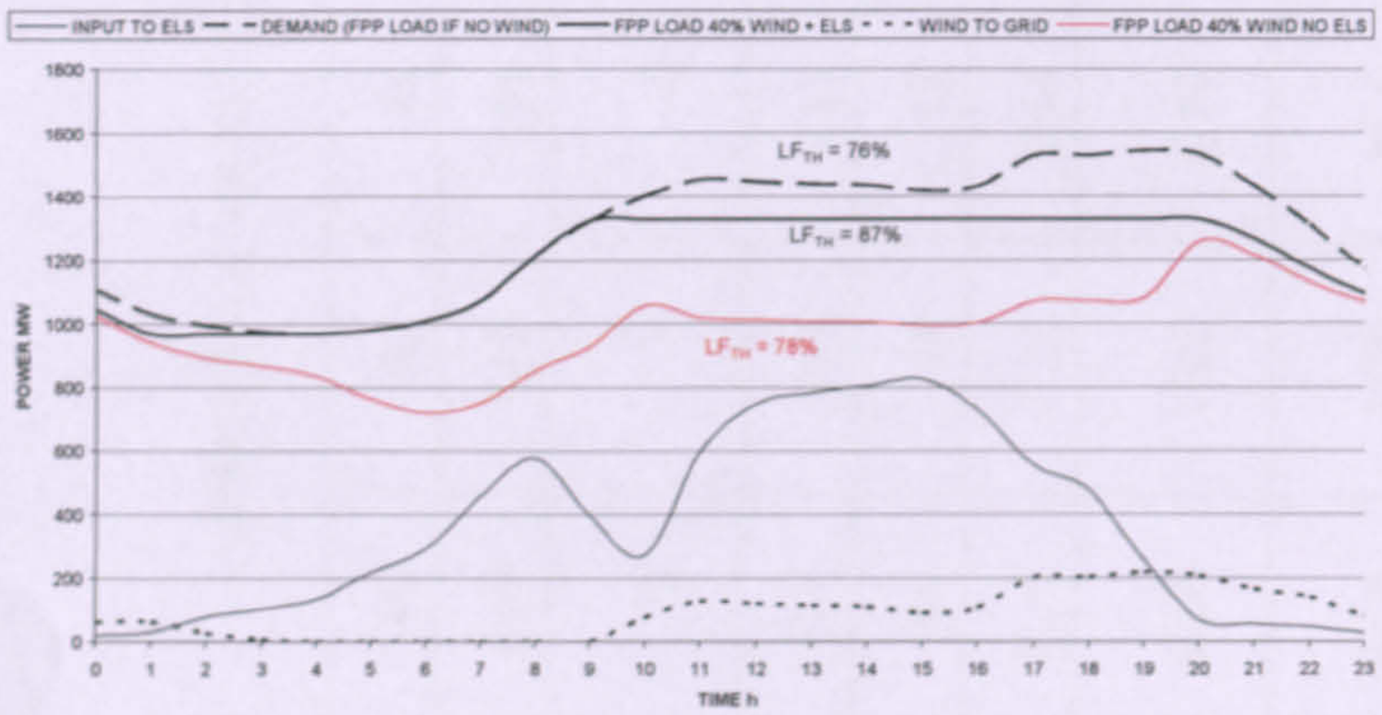

d)

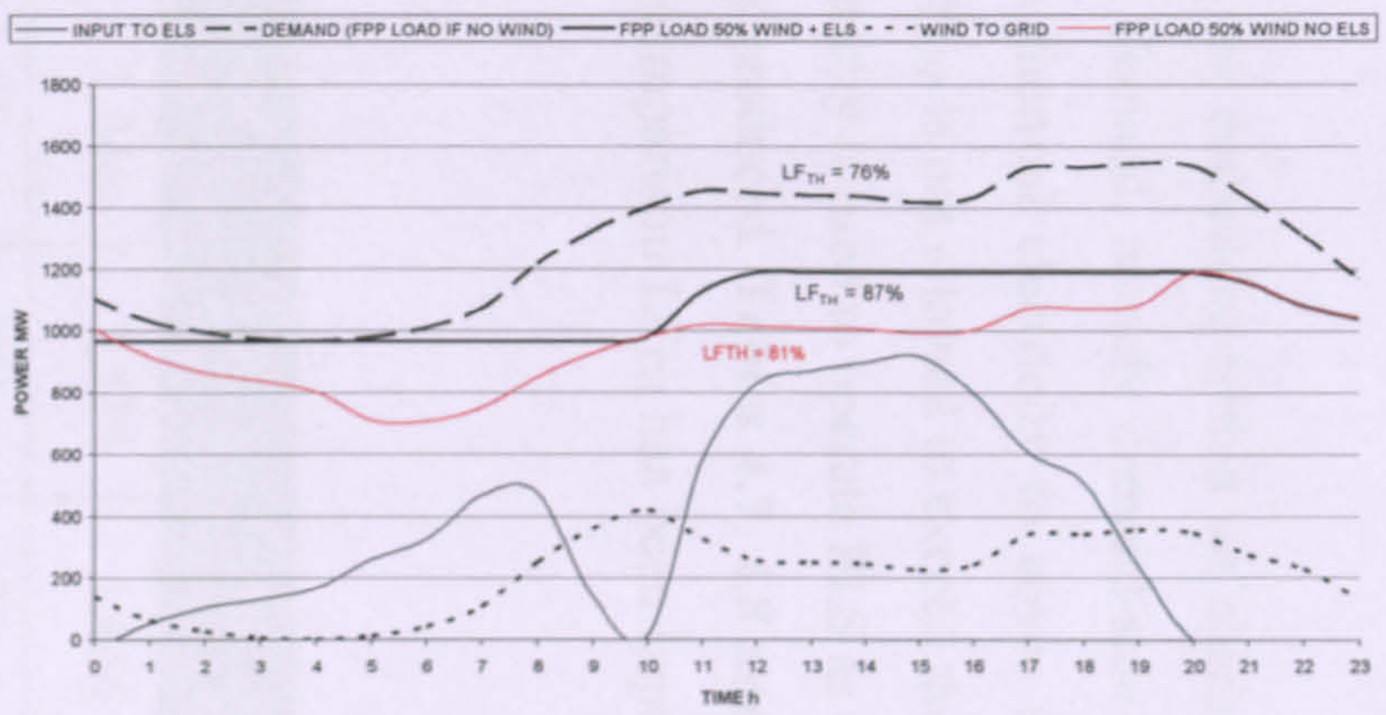

Figure 4.7. Results for CASE 1. Variable wind day. Effects of increasing penetrations of wind power upon the FPP load profile, the profile of wind power delivered to grid and the input profile to the electrolyser stock.

4.3.3 CASE 2

In CASE 3 all electrolysers are assumed to be embedded within the electrical grid and located at or near the points of hydrogen demand, namely demand-side-electrolysers (DSE). To avoid the use of any surplus thermal electricity to cover the electrical demand of DSE, the aggregated FPP load P_{FPP} is not allowed to exceed the consumers' electrical demand P_C, so that no fossil electricity is used to operate ELS as expressed by equation (4.9), and only zero-carbon H_2 is produced. **Tables 4.7, 4.8 and 4.9** display main results for CASE 2. For the sake of comparison LF_{TH} has been kept at the same values of those shown for CASE 1.

Φ_W %	20	30	40	50	70	100
IC_W (MW)	533	800	1,066	1,333	1,866	2,665
LF_{TH} (%)	85	85	85	85	85	85
CI_e ($kgCO_2/kWh_e$)	0.64	0.56	0.54	0.51	0.48	0.43
TC ($tCO_2\times10^3/d$)	30.4	26.8	24.8	24.3	22.9	20.5
P_{FPP} (GWh/d)	41.2	37.2	37.2	37.2	37.2	37.2
WC (%)	0	5	25	40	56	70
Y_H (t/d)	86	84	113	113	113	113
CI_H ($kgCO_2/kgH_2$)	0	0	0	0	0	0
IC_E (MW)	454	440	440	440	440	440
UF_E (%)	39	40	54	54	54	54

Table 4.7. Results for CASE 2. Steady Wind Scenario

Φ_W %	20	30	40	50	70	100
IC_W (MW)	533	800	1,066	1,333	1,866	2,665
LF_{TH} (%)	87	87	87	87	87	87
CI_e ($kgCO_2/kWh$)	0.68	0.63	0.57	0.52	0.45	0.42
TC ($tCO_2 \times 10^3/d$)	20.9	19.4	17.4	16.0	13.5	12.9
P_{FPP} (GWh/d)	29.0	27.9	26.3	25.1	23.4	23.4
WC (%)	0	6	24	37	54	65
Y_H (t/d)	73	93	74	54	23	24
CI_H ($kg\ CO_2/kg\ H_2$)	0	0	0	0	0	0
IC_E (MW)	454	440	440	440	440	440
UF_E (%)	34	44	35	26	11	11

Table 4.8. Results for CASE 2. Variable Wind Scenario

Φ_W %	20	30	40	50	70	100
IC_W (MW)	533	800	1,066	1,333	1,866	2,665
LF_{TH} (%)	80	80	80	80	80	80
CI_c ($kgCO_2/kWh$)	0.71	0.66	0.62	0.58	0.53	0.46
TC ($tCO_2 \times 10^3/d$)	33.6	31.2	29.3	27.4	25.1	21.8
P_{FPP} (GWh/d)	45.8	45.5	45.0	44.5	43.3	41.4
WC (%)	0	0	0	0	0	5
Y_H (t/d)	14	26	37	48	64	78
CI_H ($kg\ CO_2/kg\ H_2$)	0	0	0	0	0	0
IC_E (MW)	454	440	440	440	440	440
UF_E (%)	6	12	18	23	30	37

Table 4.9. Results for CASE 2. Low Wind Scenario

The maximum achievable LF_{TH} is a function of the restrictions imposed by equation (4.4), and so the same values as in Case 1 are obtained for the low, variable and steady wind days, namely 82, 90 and 88% respectively. As the electrolyser stock is embedded within the grid and located near the points of hydrogen demand, the elimination of wind curtailment cannot always be achieved because the low-load limit does not allow all available wind generation to come into the grid (see Base Case). For example, at Φ = 50%, between 35 and 40% of the wind resource is still wasted on the high and variable wind days.

Carbon intensities and emissions show fairly similar values to those obtained for CASE 1. For the steady and variable wind scenarios, elimination of wind curtailment is not achieved by implementation of DSE. Values for the ratio IC_E are lower for high wind penetrations, indicating that a lower installed capacity of electrolysers are now required to reach same LF_{TH} as those obtained in CASE 1. Consequently, lower utilization factors than previously are obtained on the steady and variable wind day at $\Phi_W > 30\%$ (e.g. only 11% for the variable wind day at $\Phi = 100\%$), but for the low wind scenario UF_E increases with wind penetration. The maximum utilization factors achieved are 37%, 44% and 54% on the low, variable and high wind day respectively.

Note that the steady wind day dictates the ELS installed capacity (see description of main outputs in **Chapter 3**), and the actual utilization factor UF_E will be a function of IC_E on this day, for any day of the year. The electrolyser stock is embedded within the grid and the amount of wind electricity that can be directed to DSE is limited by equation (4.6). This is why IC_E remains constant at $\Phi_W > 30\%$ and then the ratio of electrolyser capacity to wind installed capacity decreases significantly; and also explains why the daily hydrogen yield appears to be rather poor across all wind scenarios especially for high penetrations of wind power, with values for Y_H being only 25% to 50% of those obtained for Case 1. For example, for the variable wind scenario with $\Phi = 50\%$, $Y_H = 54$ tH_2 for Case 2 versus 151 tH_2 for Case 1.

Again the relationship between the carbon intensity of electricity CI_e and the wind penetration φ was investigated. This is plotted in **Figure 4.8**.

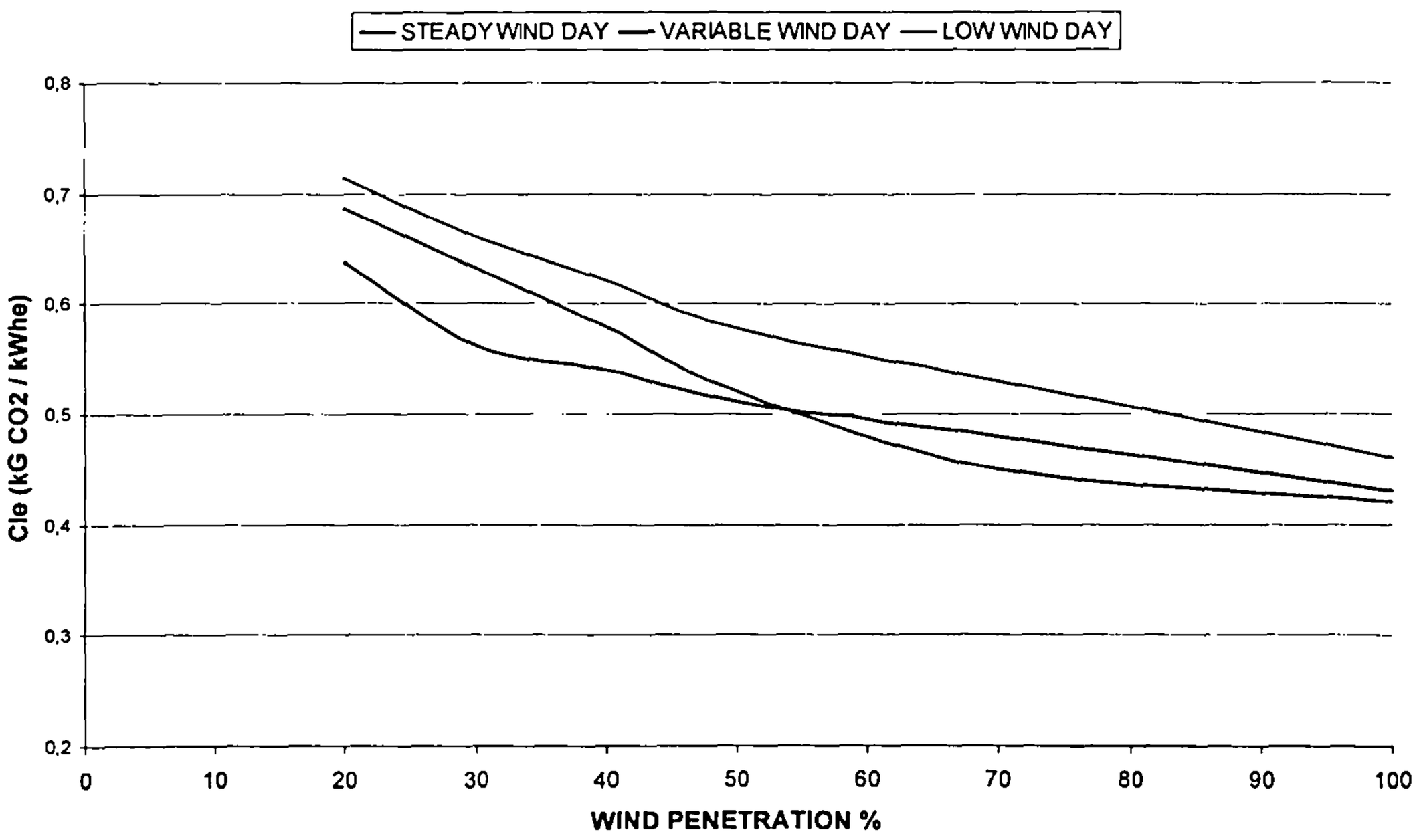

Figure 4.8. CASE 2. Average daily carbon intensity of electricity CI_e versus wind power penetration for steady, variable and low wind scenario.

Similar observations than those of CASE 1 can be extracted. From **Figure 4.8**, for the variable and low wind scenarios, the reduction of CI_e is approximately proportional to wind power penetration for $\Phi_W < 40\%$ for the same reasons as those aforementioned for CASE 1. For the steady wind scenario the decrease of CI_e is not as marked as expected for wind penetrations above 30%, due to the curtailment limit imposed (equation 4.6), and it is clear how the carbon abatement benefits of wind power diminish as Φ_W increases when all WPP output is directed to the grid and no SSE stock is deployed. In general the values of CI_e are fairly similar to those of Case 1 and 8-12% greater than those of the Base Case.

The relationship between Φ_W and the daily production of hydrogen Y_H is shown in **Figure 4.9**.

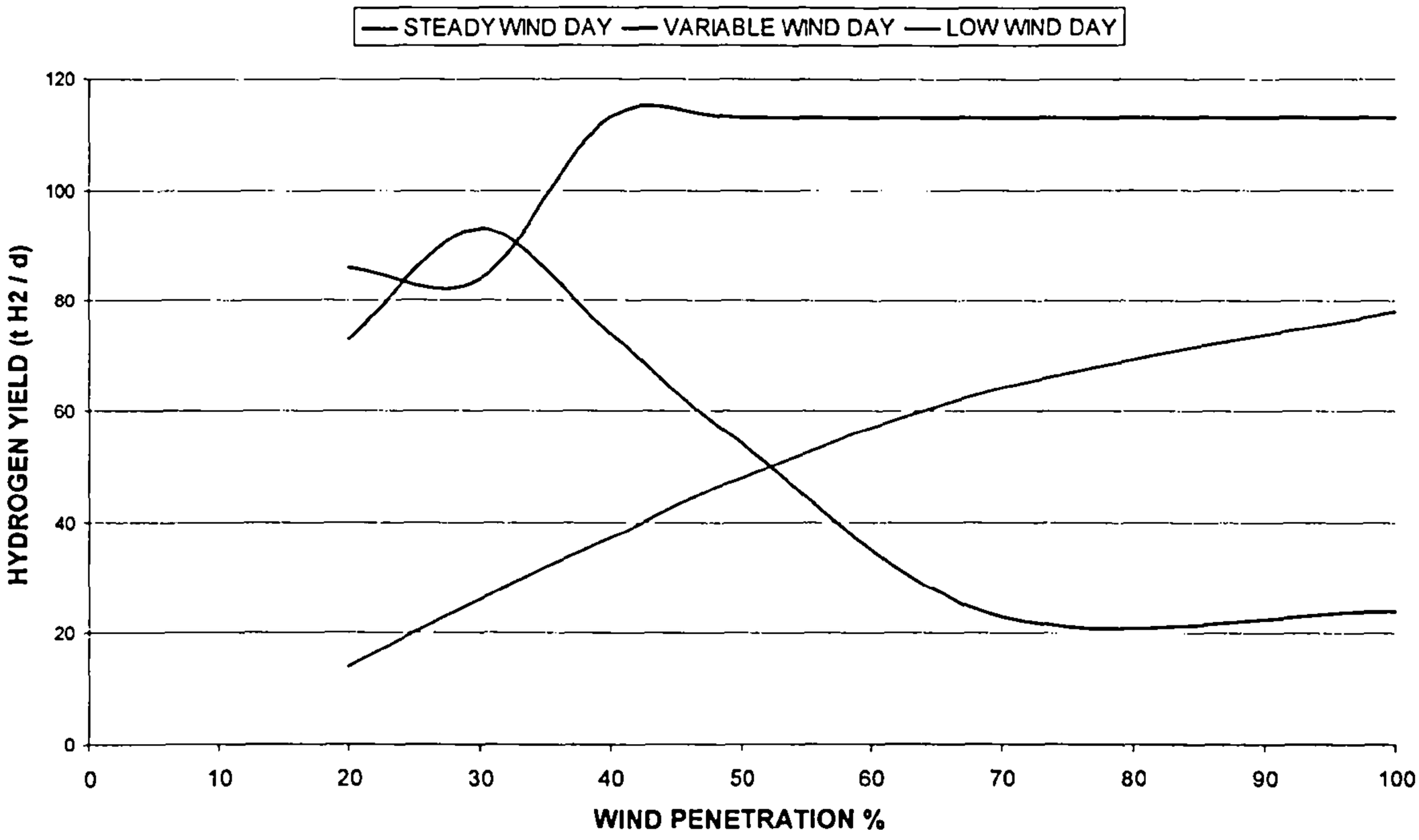

Figure 4.9. CASE 2. Daily hydrogen production versus wind power penetration for steady, variable and low wind scenario.

In this implementation, since the electrolyser stock is embedded in the grid, their electrical input P_{DSE} is determined by the amount of wind power that can be directed to the grid. In the steady wind scenario for wind penetrations below 40% P_{WC} increases at the expense of P_{WDE} subject to the wind curtailment restriction, then reducing the hydrogen output which remains constant at Φ_W >40%. At penetrations above 40% P_{WG} reaches its limit; then P_{WC} stops increasing and P_{WDE} ceases decreasing. For the variable wind scenario, the curtailment of wind does not have an influence at penetrations below 30% (on the variable wind day curtailment of wind energy mainly occurs in the afternoon period before the peak thermal load is achieved), and only above this level P_{WDE} reduces significantly and by implication the hydrogen output. The limit above which wind curtailment starts (30% of SMD) is not reached for $\Phi_W \leq$ 50% on the variable wind day, and hence P_{WC} keeps increasing at the expense of P_{WDE}.

On a low wind day the curtailment limit is never reached and the hydrogen yield always rises as Φ_W increases.

An interesting question is how increasing the load factor of the FPP load profile above the limits imposed by equation (4.4), thus "relaxing" the CI_H, influences the rest of the outputs of the system. Note that the higher LF_{TH} the more stable and efficient the operation of fossil power plant (less start-ups and ramping duties imposed) and then the lower the carbon emissions per kWh_c generated. Results for a 90% LF_{TH} for the steady wind scenario for $20\% \leq \Phi_W \leq 50\%$ are summarized in **Table 4.10.**

Φ_W (%)	20	30	40	50
LF_{TH} (%)	90	90	90	90
CI_e ($kgCO_2/kWh_e$)	0.65	0.59	0.55	0.53
TC ($tCO_2 \times 10^3/d$)	31.0	28.0	26.3	25.3
WC (%)	0	2	21	37
Y_H (t / d)	142	137	131	131
CI_H ($kgCO_2/kg\ H_2$)	7.6	1.9	0.8	0.8
IC_E (MW)	725	715	650	640
UF_E (%)	39	40	42	42

Table 4.10. Results for CASE 2. Steady Wind Scenario – 90% Load factor targeted

Comparing results in **Tables 4.7 and 4.10**, the benefits of increasing the load factor up to 90% are not very clear. More hydrogen is produced now (50 -70% more), but at the expense of higher carbon intensities for both electricity and hydrogen. In addition the minimum ELS' installed capacities required to achieve LF_{TH} = 90% increase by between 45-60%. Furthermore, curtailment is not reduced significantly. Only for Φ_W = 30% it would appear sensible to consider this option, offering a hydrogen yield much higher than in the previous case with relatively low carbon penalties. Similar conclusions are obtained when increasing the LF_{TH} above 87 and 80% (also relaxing the carbon intensity of the hydrogen produced) for the variable and low wind scenarios respectively. In summary, higher LF_{TH} can be obtained only at the expense of higher CI_H, also yielding higher hydrogen outputs.

Figure 4.10 shows daily profiles for the variable wind scenario obtained following the operational strategy devised for CASE 2. Again time-controlled operation of ELS allows fossil-fuelled power plants to operate more steadily and increase their utilization factor and efficiency, thus reducing carbon emissions emitted per kWh_e produced. When comparing to **Figure 4.7**, it can be observed how the operational strategy for CASE 2 is also effective for arranging a steadier wind power profile into the grid, especially at wind penetrations beyond 30%. Electrolysers in this case act purely as a demand-side management mechanism, modifying the total aggregate grid demand P_G in order to maximise the utilization of the existing generating capacity, with the subsequent benefits for the management of the power system (see **Chapter 2**).

a)

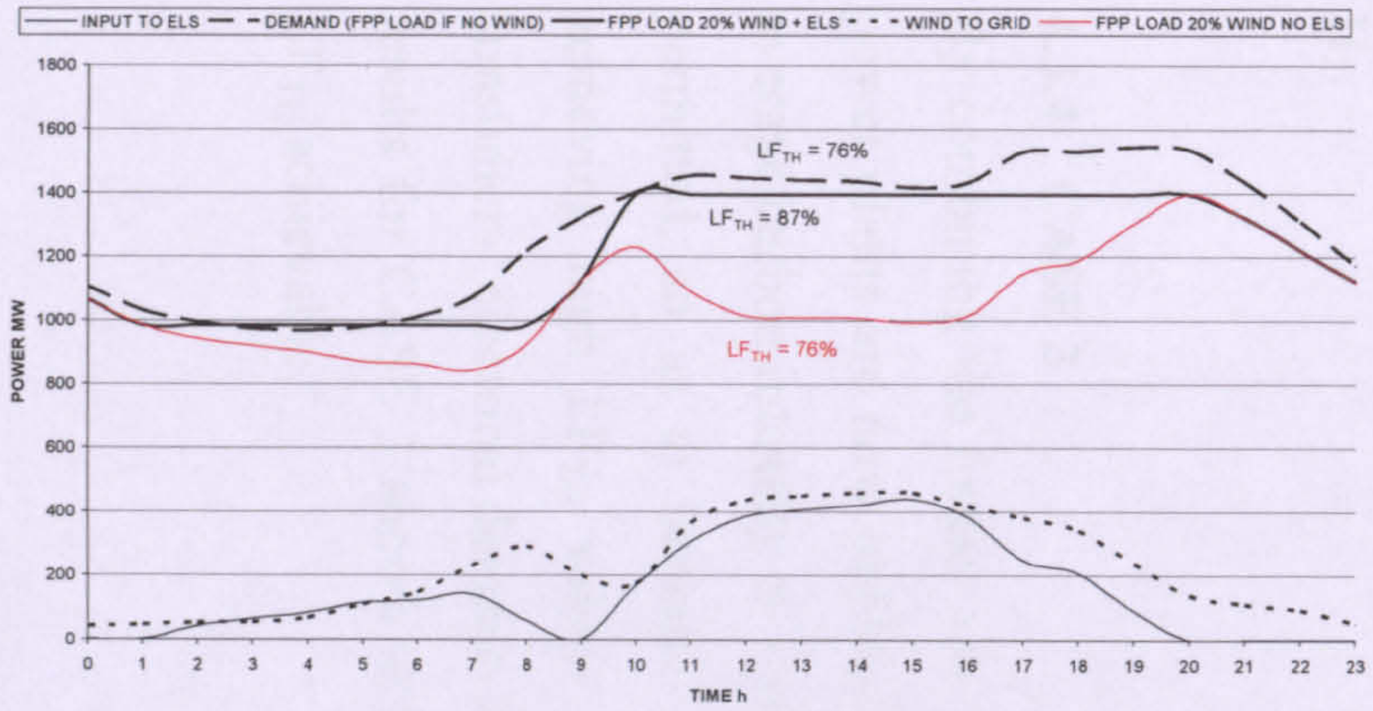

b)

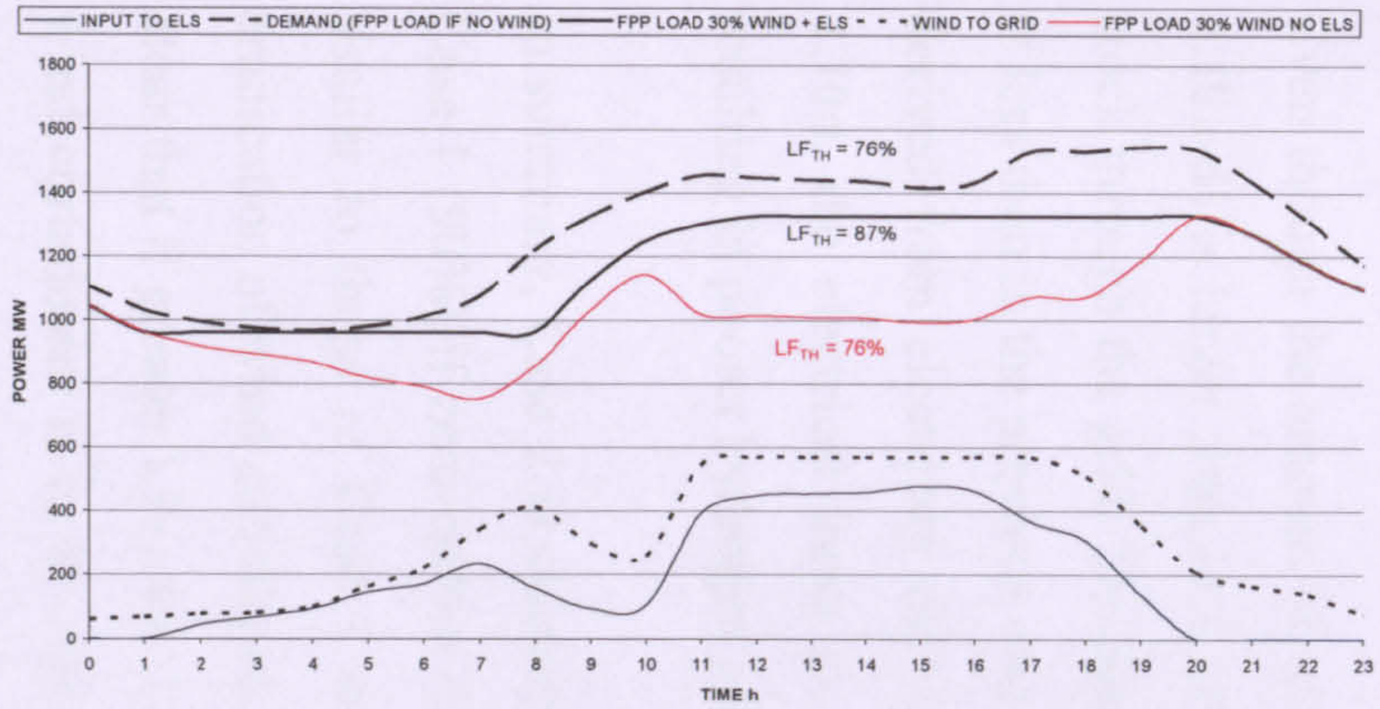

c)

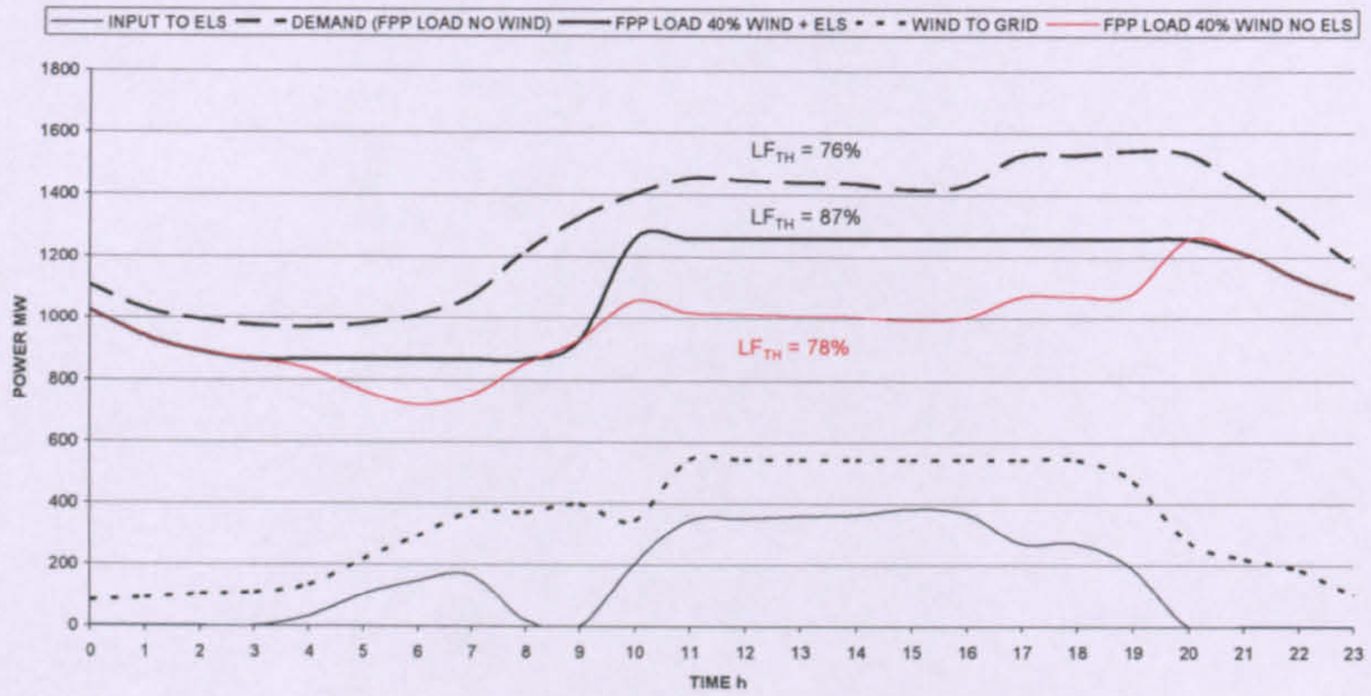

d)

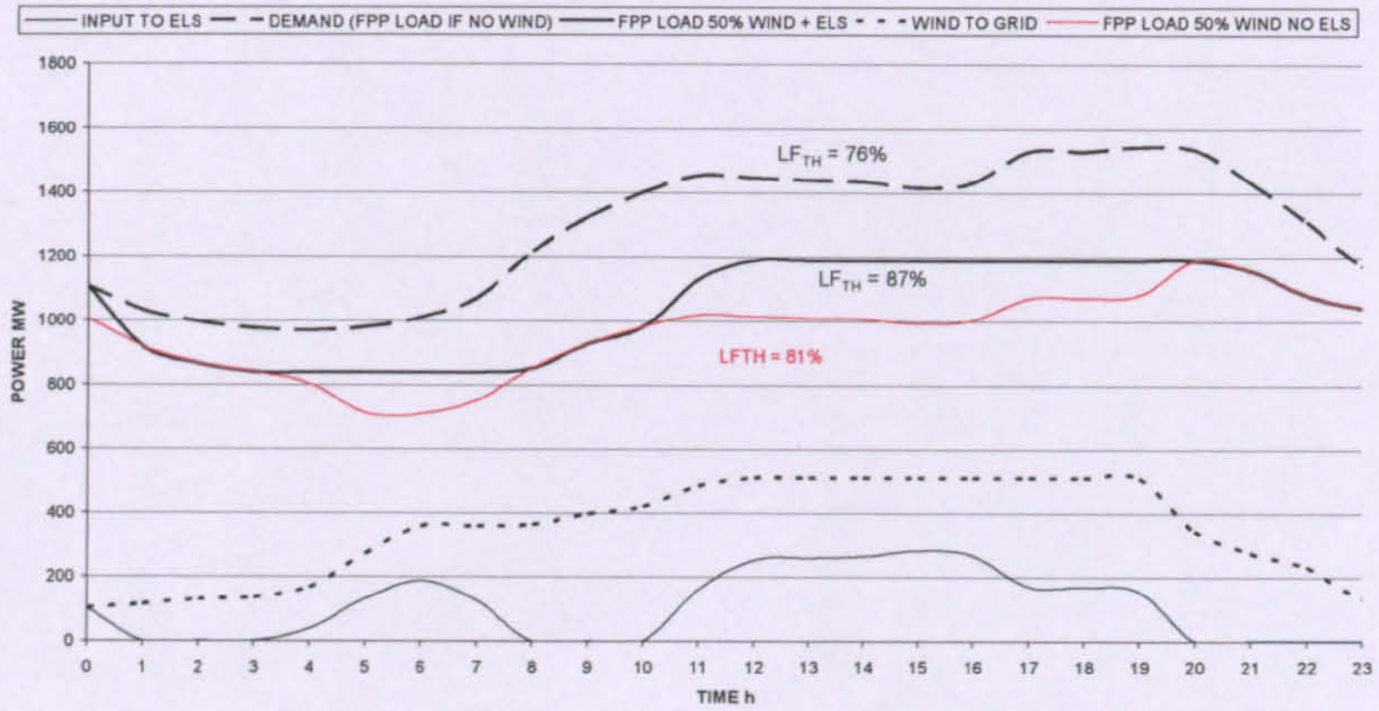

Figure 4.10. Results for CASE 2. Variable wind day. Effects of increasing penetrations of wind power upon the FPP load profile, the profile of wind power delivered to grid and the input profile to the electrolyser stock.

Even though the amount of wind power delivered to the grid (dotted curve in **Figures 4.10a-d**) is larger than in CASE 2, some of this, P_{WDE}, is now delivered to the DSE stock through the grid. The actual wind-derived electricity delivered to consumers P_{WC} is less than in the previous case, resulting in slightly higher values for carbon emissions derived from electricity delivered to consumers. As observed in **figures 4.10c and 4.10d**, the electrical input to ELS is much lower than in **Figures 4.7c and 4.7d**, resulting in poorer hydrogen yields.

In summary, Case 2 is characterized by a maximum achievable LF_{TH} equal to that of Case 1 (90%) if zero-carbon hydrogen is to be produced. The values of CI_e are fairly similar to those of Case 1 and thus greater than those of the Base Case; but the eradication of wind curtailment cannot be achieved by Case 2. From Cases 1 and 2 it is clear that if greater LF_{TH} and improved UF_E are to be achieved, while at the same time wind curtailment is to be eliminated, the carbon intensity of the generated hydrogen must be allowed to exceed zero. Thus combinations of the two approaches were analyzed in Case 3 where the carbon intensity of hydrogen was relaxed to 3 $kgCO_2$ / kg H_2.

4.3.4 CASE 3

By combining the former two systems, both DSE and SSE in conjunction with wind power plants are now implemented. Rather than producing zero-carbon hydrogen, an average carbon intensity of 3 kilograms of CO_2 emitted per kilogram of H_2 generated is permitted, so as to increase the utilization factor of the electrolyser stock while achieving high LF_{TH} values. Wind power generation is directed both to supply consumers' electrical demand P_C and to power ELS (embedded and supply-side). Main results for CASE 3 shown in **Tables 4.11 and 4.12** are for the maximum values of LF_{TH} achievable.

Φ_W %	20	30	40	50	70	100
IC_W (MW)	533	800	1,066	1,333	1,866	2,665
LF_{TH} (%)	87	92	95	99	100	100
CI_e ($kgCO_2/kWh$)	0.65	0.59	0.57	0.57	0.56	0.55
TC ($tCO_2 \times 10^3/d$)	30.9	28.1	27.1	27.1	26.7	26.2
P_{FPP} (GWh/d)	42.5	40.3	40.1	41.6	45.6	51.6
WC (%)	0	0	0	0	0	0
Y_H (t/d)	109	157	260	394	680	1,107
CI_H ($kgCO_2/kgH_2$)	3	3	3	3	3	3
IC_E (MW)	586	880	1,175	1,465	2,050	2,930
UF_E (%)	39	39	47	55	67	76

Table 4.11. Results for CASE 3. Steady Wind Scenario

Φ_W (%)	20	30	40	50	70	100
IC_W (MW)	533	800	1,066	1,333	1,866	2,665
LF_{TH} (%)	88	90	93	98	100	100
CI_c ($kgCO_2/kWh_e$)	0.69	0.65	0.61	0.57	0.56	0.56
TC ($tCO_2 \times 10^3/d$)	21.2	20.0	18.8	17.5	17.2	17.2
P_{FPP} (GWh/d)	29.4	28.8	28.2	28.1	29.9	32.4
WC (%)	0	0	0	0	0	0
Y_H (t/d)	84	121	162	213	356	565
CI_H ($kg\ CO_2/kg\ H_2$)	3	3	3	3	3	3
IC_E (MW)	565	865	1,130	1,465	1,980	2,798
UF_E (%)	30	29	29	30	38	42

Table 4.12. Results for CASE 3. Variable Wind Scenario

Using this more flexible approach, a greater LF_{TH} can be achieved for Case 3 than for Cases 1 and 2, especially at $\Phi_W > 40\%$. A virtually flat thermal load profile can be obtained, which would allow TPP to operate steadily across the day. LF_{TH} values of ~ 100% can be achieved for $\Phi_W > 40\%$ on both the steady and variable wind days, because CI_H is now allowed to be 3 $kgCO_2/kgH_2$. Much greater hydrogen yields and UF_E than in Case 2 are also obtained at high wind penetrations. For example, at Φ_W = 50%, Y_H = 394 t H_2 and UF_E = 55% on the steady wind day.

Aiming for higher load factors predictably implies that greater installed capacities of electrolysers will be required. This can be observed when comparing **Tables 4.11 and**

4.12 to **Tables 4.5 and 4.6**. Note that the methodology followed here was to use the AELM model to investigate the aggregate capacity of electrolysers required by the power system in order to optimize LF_{TH} and to minimize the curtailment of wind power. To maximise LF_{TH} for a given wind penetration, a maximum installed capacity of electrolysers needs to be identified, which (assuming curtailment is to be eradicated) corresponds to the day of highest wind capacity factor. In this study, on the steady wind day (capacity factor = 80%) the ratio of ELS capacity to wind capacity ranges between 1.06 and 1.10, if CI_H = 3 kg CO_2/kgH_2.

The relationships between UF_E and Φ_W for the steady and variable wind days can be observed in **Tables 4.11 and 4.12**. Clearly the higher the wind penetration the greater the amount of wind generation available and the higher the utilization of the electrolyser stock. Given that the average annual capacity factor of wind (24% in 2003 [17]) is much lower than the capacity factor on the steady wind day (80%), the annual average UF_E will be rather low. Several options can be considered in order to increase utilization. For example, DSE operation could be permitted on low wind days provided that an acceptable weekly/monthly/annual average CI_H is achieved. However, the increased adoption of zero-carbon thermal power sources (e.g. nuclear and CO_2-sequestered power plants) will yield a much greater utilisation during low wind periods without compromising CI_H. This is explored further in **Chapter 5**. Increased capacity utilization would have a profound effect on the ability to produce hydrogen economically.

By combining grid-embedded and supply-side electrolysers, wind curtailment is completely eliminated. On the downsides, carbon intensities and emissions derived from power generation become 10-30% higher when compared to CASE 1 and CASE 2 at $\Phi_W > 40\%$, since a larger proportion of wind-generated electricity is being delivered to the electrolyser stock.

Daily load profiles obtained from the combined "supply-side/embedded" implementation strategy for the variable wind scenario are shown in **Figure 4.11**.

a)

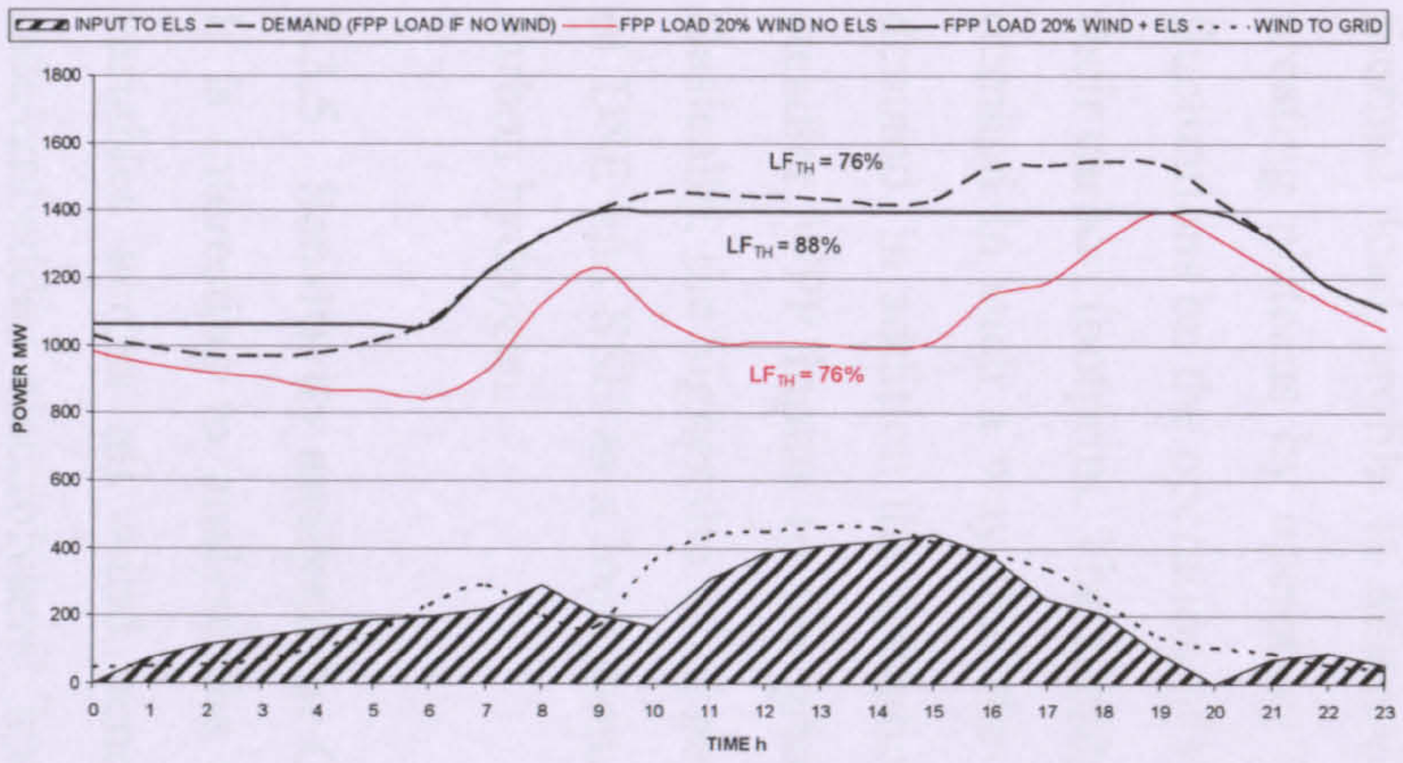

b)

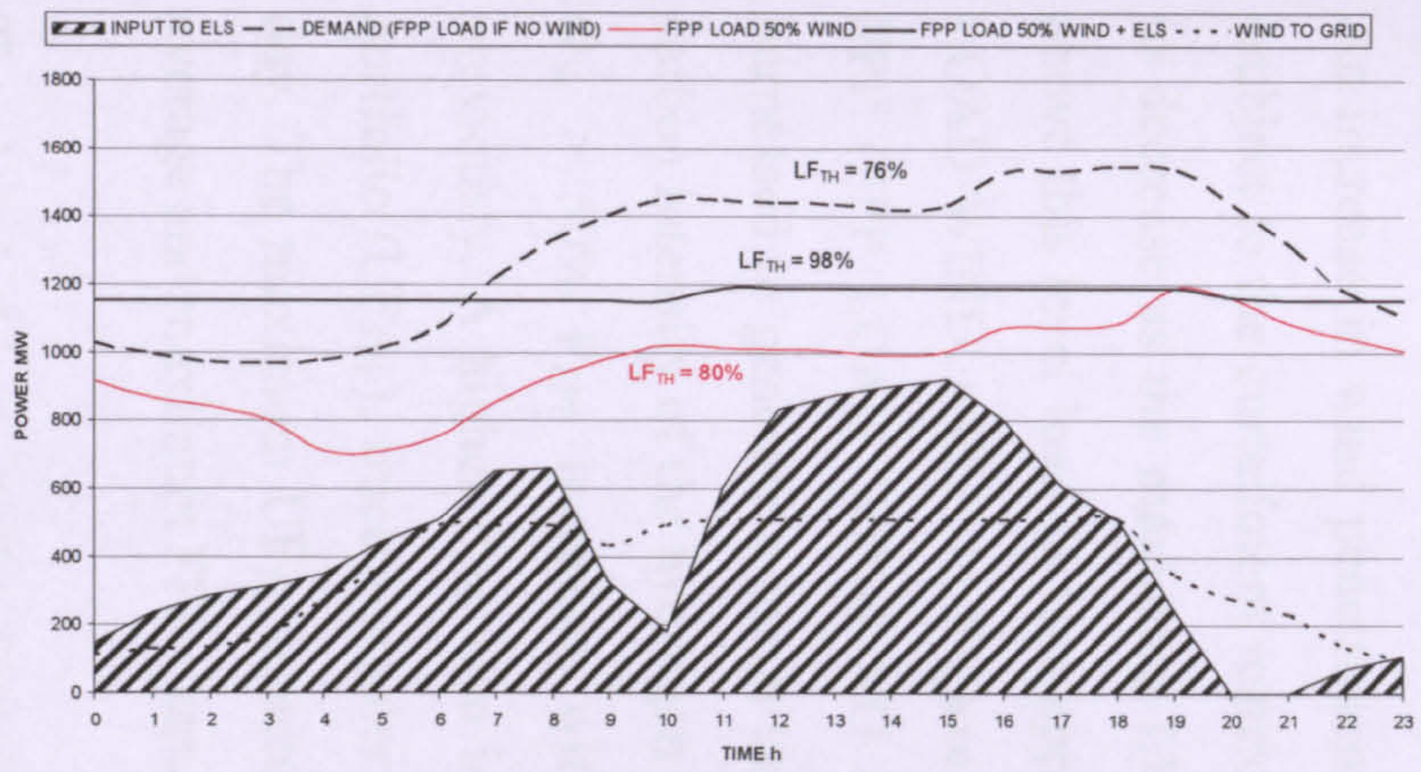

c)

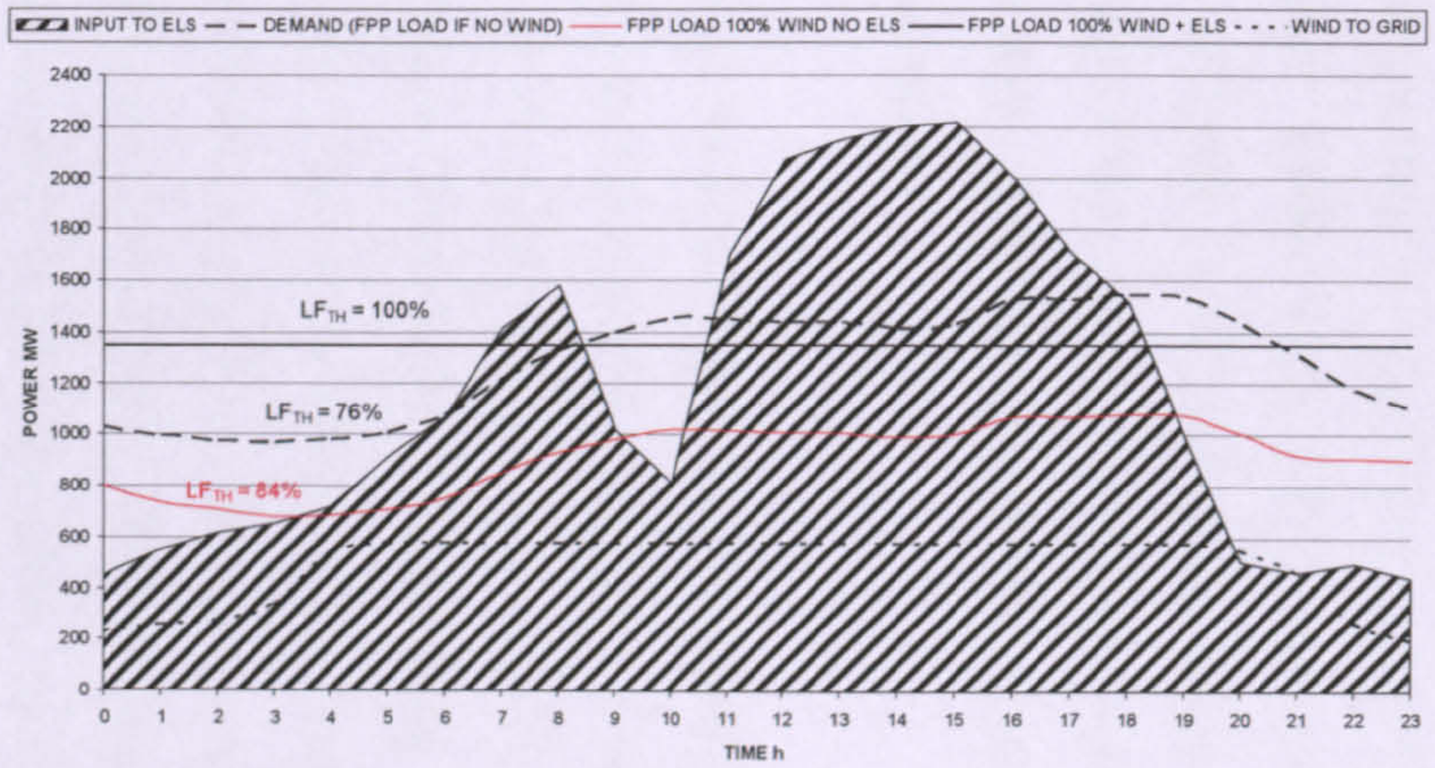

Figure 4.11. Results for CASE 3. Variable wind day. Effects of increasing penetrations of wind power from (a) 20% to (c) 100% upon the FPP load profile, the profile of wind power delivered to grid and the input profile to the electrolyser stock.

An increase in wind penetration means that more wind power is directed to the grid (subject to the curtailment restriction imposed by equation 4.14), and then causes P_{FPP} to decrease as the maximum LF_{TH} achievable increases; this is true for $\Phi_W \leq 40\%$; above this level load factors approach 100% and the new load imposed on FPP (FPP LOAD WIND + ELS in **Figure 4.11**) exceeds the peak load previously appointed to FPP (FPP LOAD WIND NO ELS), then creating a surplus of electricity that is harnessed to generate a much larger hydrogen output and higher UF_E but keeping the carbon intensity of the hydrogen produced constant at 3 kg CO_2 / kg H_2. This is why at $\Phi_W > 50\%$ P_{FPP} increases with Φ_W (see **Table 4.12**) rather than diminish like previously. A higher P_{FPP} also indicates a higher (daily) utilization factor of the FPP portfolio (UF_{FPP}), since a greater proportion of the installed capacity is used across the day. The maximum UF_{TH} is achieved on days when $LF_{TH} = 100\%$ in which case the average and maximum FPP outputs are the same.

The electrical input to the electrolysers stock becomes larger than in previous CASES 2 and 3, especially for high penetrations of wind power. By combining a SSE and DSE stock, a more stable operation of FPP can be obtained. For $\Phi_W > 50\%$, a quasi-flat thermal load profile is attained (see **Figures 4.11b and 4.11c**) filling valleys and creating plateaus by operating ELS as controllable additional loads, minimizing the fluctuations on the operation of FPP, hence maximizing their efficiency and minimizing their carbon footprint. The supply of electricity becomes effectively decoupled from the demand in such a way that the operation of FPP is less-dependent on the electricity demand. In addition the operational strategy for Case 3 is also effective for arranging steadier WPP inputs to the grid particularly at $\Phi > 40\%$ as shown in **Figure 4.11**. Basically, the higher the wind penetration, the greater the potential of a combined stock of DSE and SSE as a load management mechanism and the greater the yield of low-carbon hydrogen.

4.3.5 Sensitivity analysis for CASE 3

It is interesting to analyse the trade-off between the LF_{TH} targeted and the rest of variables across all wind penetrations. Within the context of combined supply-side/embedded electrolysers' implementations and following the operational strategy

described in **Chapter 2.2,** a sensitivity analysis has been carried out for the steady wind scenario in order to test to what extent a variation of the LF_{TH} targeted will affect the main inputs obtained from the model.

In **Figure 4.12** carbon intensities of hydrogen produced are plotted against the load factor of the FPP load profile.

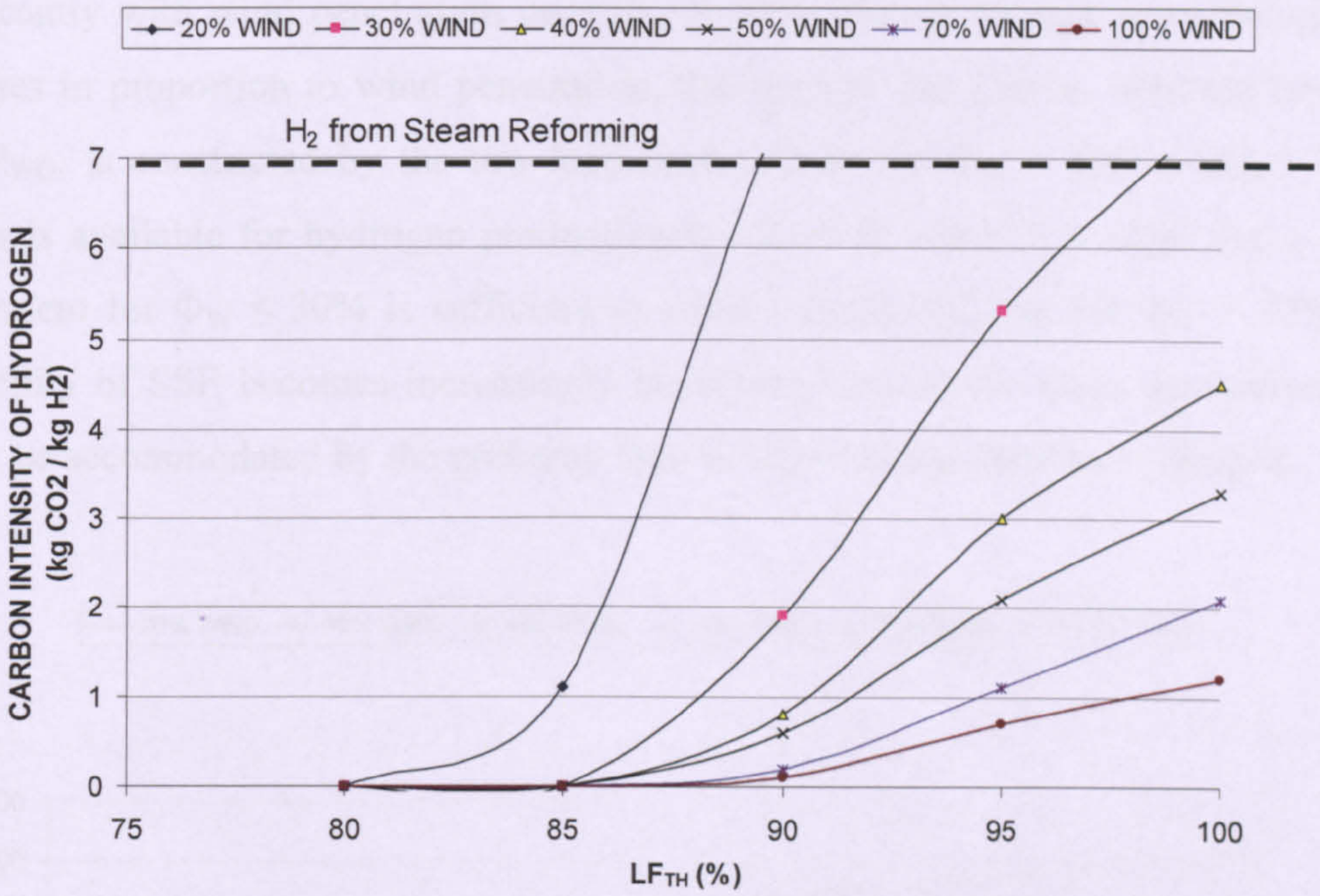

Figure 4.12. Case 3: for the steady wind day relationship between the carbon intensity of hydrogen and the load factor of the FPP load profile.

Overall, once CI_H is allowed to exceed zero, the higher the LF_{TH} sought the higher the carbon intensity of the hydrogen produced due to a larger share of FPP output being directed to the DSE stock:

$$\uparrow LF_{TH} \quad \rightarrow \quad \uparrow P_{FPDE} \quad \rightarrow \quad \uparrow CI_H$$

For any wind power penetration, the change observed in CI_H with LF_{TH} (**Figure 4.12)** is due to the relative increase in P_{FPDE} to power the DSE stock. For wind penetrations above 50%, it is possible to produce zero-carbon hydrogen up to a LF_{TH} of 88%. Higher

load factors can only be achieved if some electricity from fossil-fuelled power plant is delivered to the DSE stock, hence producing hydrogen of $CI_H > 0$.

Figure 4.13 and 4.14 show the net hydrogen production and the utilization factor of the ELS stock as a function of the load factor for the steady wind day. Predictably, the greater the load factor, the greater the hydrogen yield and the greater the electrolyser utilisation factor. For a given LF_{TH}, the hydrogen yield and utilization factor increase significantly with wind penetration once $\Phi_W > 30\%$. This is because even though P_W increases in proportion to wind penetration, the amount that can be admitted into the grid, P_{WG}, is constricted by the low-load limit and so for $\Phi_W > 30\%$ a larger wind surplus is available for hydrogen production via the SSE stock. It is clear that a DSE deployment for $\Phi_W \leq 30\%$ is sufficient to avoid curtailment, but for $\Phi_W > 30\%$ the availability of SSE becomes increasingly important because the wind generation that cannot be accommodated by the grid may then be harnessed to produce hydrogen.

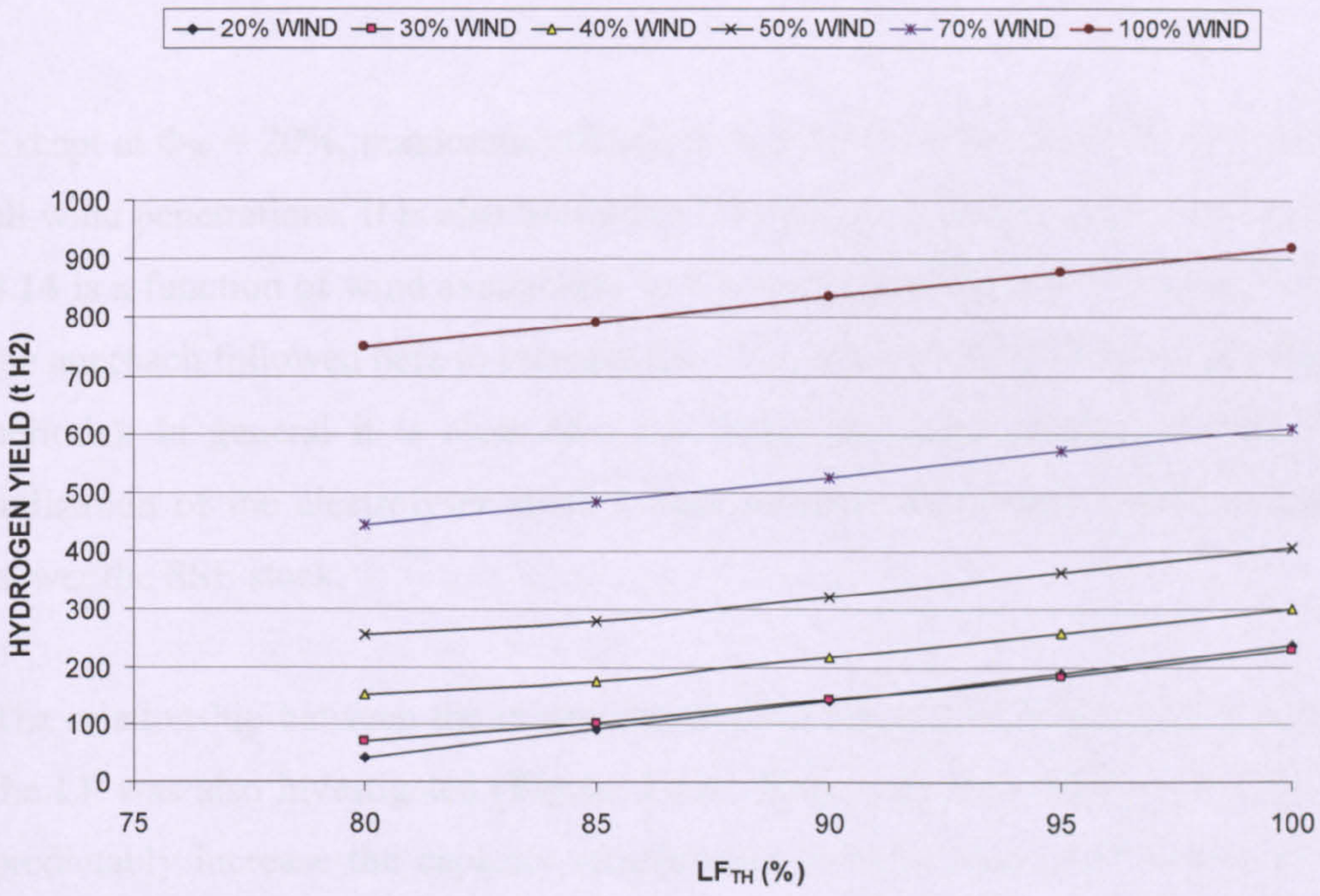

Figure 4.13. CASE 3: for the steady wind day relationship between the daily hydrogen yield and the load factor of the FPP load profile.

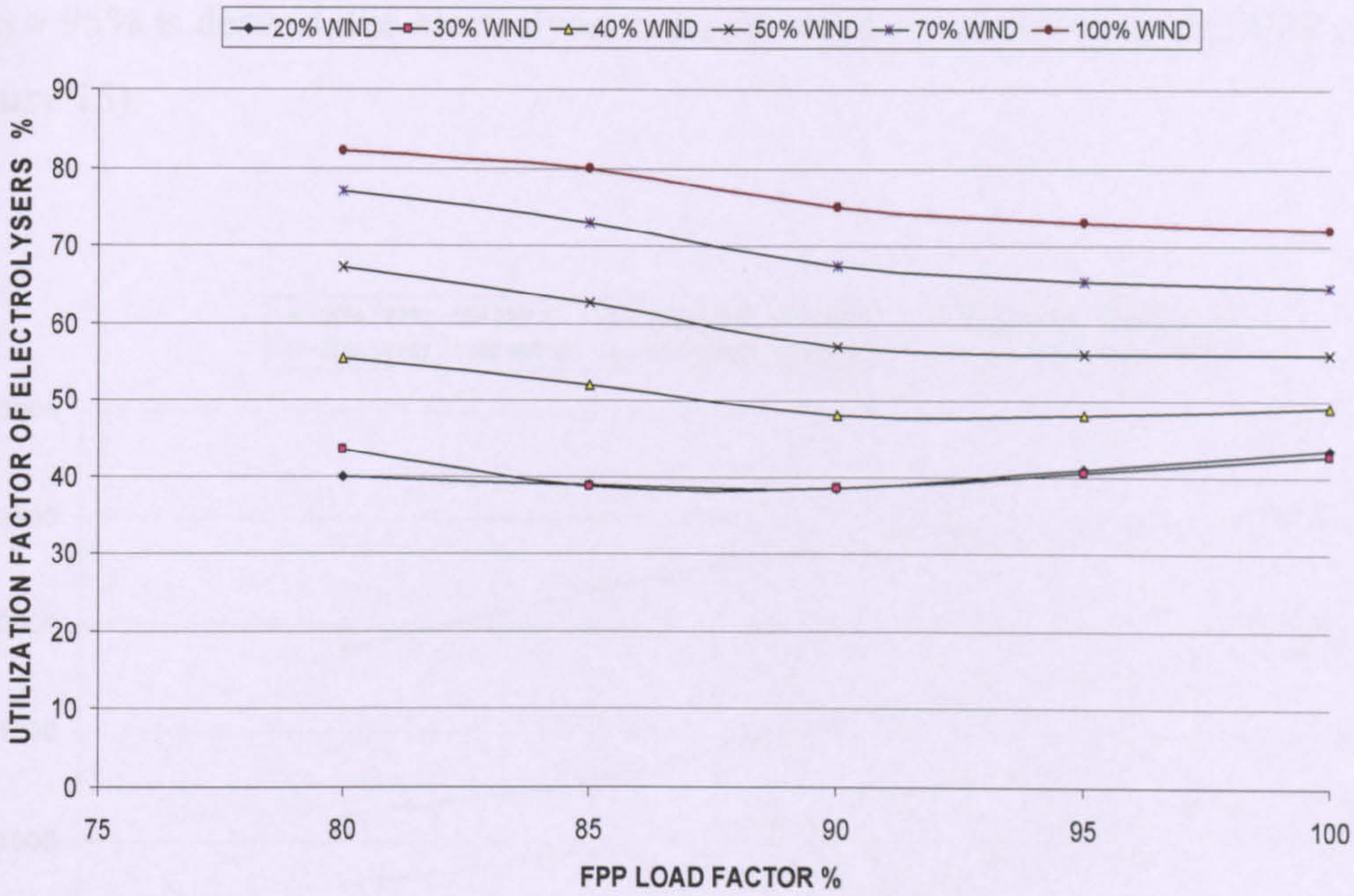

Figure 4.14. CASE 3: for the steady wind day relationship between the utilization factor of the electrolyser stock and the load factor of the FPP load profile.

Except at $\Phi_W = 20\%$, maximum utilization factors are achieved for $LF_{TH} = 80\%$ across all wind penetrations. It is also found that UF_E and so the shape of the curves in **Figure 4.14** is a function of wind availability in the morning and night-time period (remember the approach followed here to increase the LF_{TH} includes filling valleys precisely in this periods). In general it is clear how the higher the wind penetration the higher the utilization of the electrolyser stock[17], because more renewable output is available to power the SSE stock.

The relationship between the minimum installed capacity of electrolysers required and the LF was also investigated (**Figure 4.15)**. Aiming for very high values of LF_{TH} will predictably increase the capacity requirement, because more FPP output needs to be directed to the electrolyser stock. Therefore to maximise the load factor and minimise wind curtailment, an increase in LF_{TH} will require a very large electrolyser capacity. If

[17] Note this is the average utilization factor for the whole electrolyser stock as defined in Chapter 3.3.4, comprising supply-side and grid-embedded demand-side electrolysers.

LF_{TH} > 95% is desired, the electrolyser capacity must be greater than the WPP capacity (**Figure 15**).

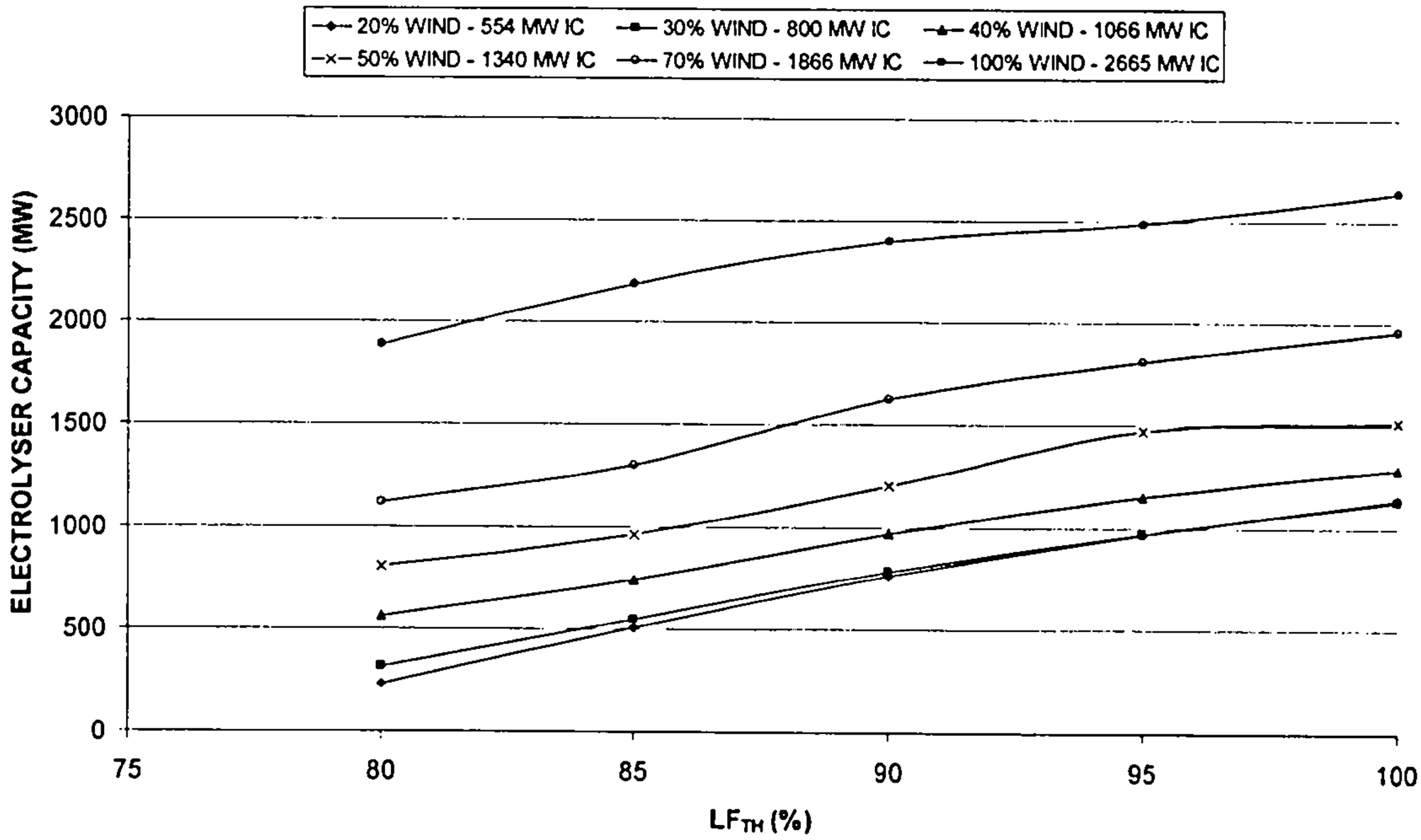

Figure 4.15. Case 3: relationship between installed capacity of electrolysers and the load factor of the FPP load profile.

The ratio between SSE and DSE capacity of the electrolyser stock is plotted in **Figure 4.16** for increasing wind penetrations. For Φ > 30% the required SSE-to-DSE ratio increases steadily with Φ_W, and the proportion of SSE relative to the total installed capacity of electrolysers increases from 0% at Φ = 30% (with LF_{TH} = 92%), to 72% at Φ_W = 100% (with LF_{TH} = 100%). This is a direct consequence of the low-load limit being 30%, which determines the amount of wind power that can be directed to the grid, P_{WG}, and by implication the optimum DSE capacity to be installed.

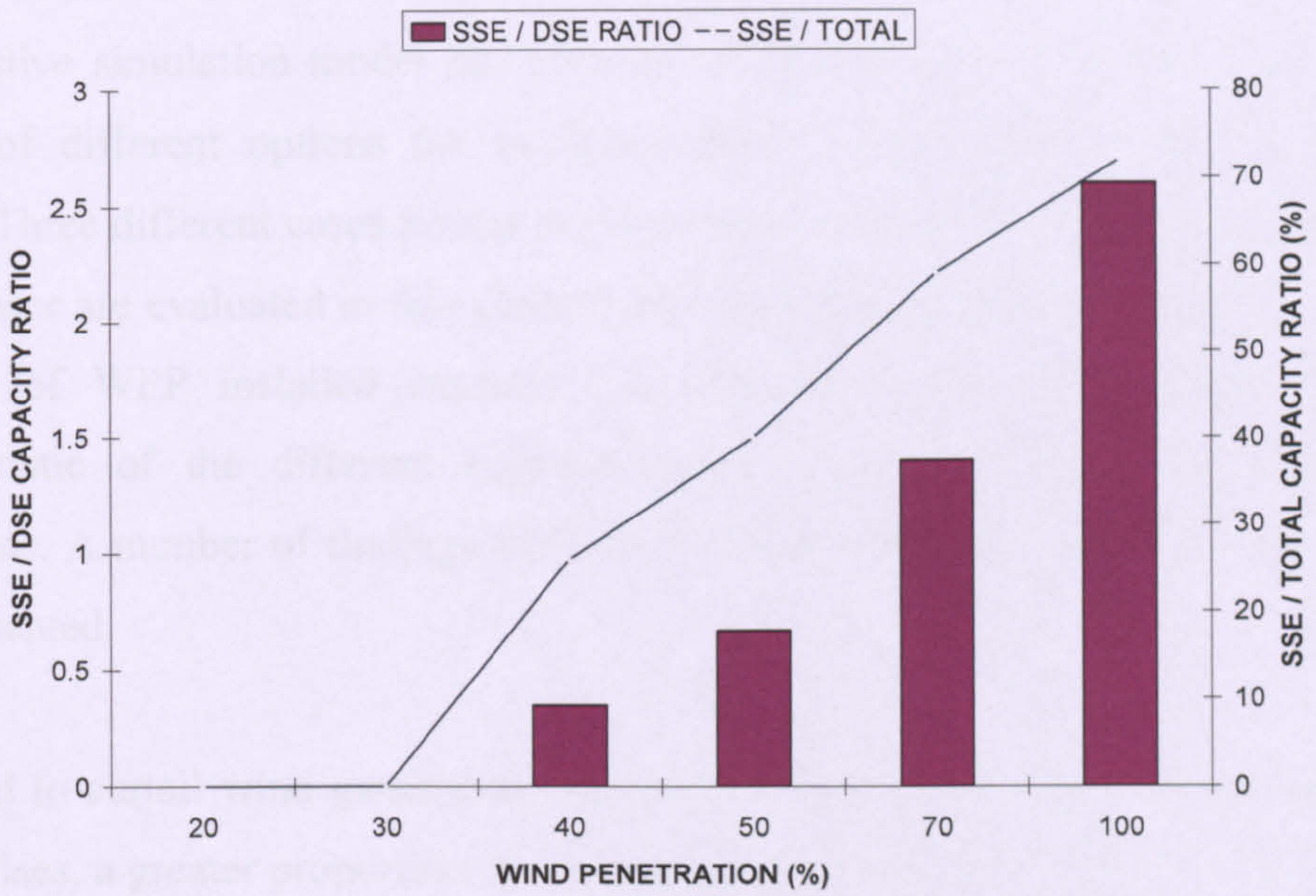

Figure 4.16. CASE 3: relative requirements for supply-side and demand-side electrolysers

The worthwhile objective of achieving high load factors and high wind penetrations, results in a substantial requirement for electrolysers, but these are then able to operate at greater UF_E and produce very high hydrogen yields on days of high wind availability (**Figures 4.13 and 4.14**). For example, as Φ_W increases from 20% to 100%, while maintaining LF_{TH} = 100%, the required installed capacity of electrolysers increases 2.3 fold from 1140 MW to 2640 MW, but the amount of hydrogen produced increases almost four times from 238 to 918 tonnes respectively (**Figure 4.13**) and the utilization factor of the electrolyser stock increases from 42% to 76% (**Figure 4.14**). Furthermore this 918 tonnes produced when Φ_W = 100% (at LF_{TH} = 100%) would have a carbon intensity of only 1.2 kg CO_2 / kg H_2, whereas at Φ_W = 20% and LF_{TH} = 100% the output of 238 tonnes would be produced at an unacceptably high carbon intensity of 13.9 $kgCO_2$ / kgH_2.

In summary, the benefits obtained from implementing of a combined stock of DSE and SSE in the power system increase significantly with wind penetration because high values of UF_E and Y_H can be achieved at CI_H = 3 $kgCO_2$ / kgH_2.

4.4 DISCUSSION

A predictive simulation model has been developed for time sequential operation and control of different options for implementation of electrolysers within the power system. Three different cases for the implementation of electrolysers in connection with wind power are evaluated in this chapter and preferred electrolyser capacity levels as a function of WPP installed capacity are identified. This section summarizes the characteristic of the different implementation cases and points out benefits and limitations. A number of findings that can be drawn from the analysis of the cases are also presented.

The need to curtail wind generation increases markedly with wind power penetration. As this rises, a greater proportion of the electricity demand than theoretically needed (if all the wind-generated electricity could be integrated into the grid) must be met by thermal power plant. Hence there are diminishing carbon-abatement benefits per new MW installed if wind power can only be directed to the grid. If high penetrations are to be achieved in future power systems, effective load management techniques are essential. Rather than simply increase the amount of wind power introduced to the grid and curtail it when necessary, it is suggested here that any wind power that cannot be accommodated can instead be directed to SSE for producing zero-carbon hydrogen, thus improving the justification for installing more wind power. On days of high or variable wind availability, this approach (Case 1) can smooth the load profile placed on thermal power plant and yield LF_{TH} values of up to 90%.

For all the implementation cases analysed, morning-time (say between 00:00 and 06:00 am) and night-time wind availability (between 20:00 and 24:00 pm) seems to be the decisive factor with a view to increase LF_{TH} and reduce wind curtailment. Therefore operation of electrolysers should always be strongly subject to wind power forecast especially during morning and night-time periods. For example, depending on wind forecast 2-3h ahead during the morning period, it would be beneficial in terms of maximizing the daily LF_{TH} to anticipate if possible the ramping-up of the FPP load predicted by the model, provided that there is enough wind power coming into the system.

If a combined supply-side and demand-side stock of electrolysers is implemented (Case 3), wind curtailment can also be eradicated, but a LF_{TH} of 100% can be achieved. This provides the greatest possible degree of freedom for achieving stable and efficient operation of thermal power plant, which will have a significant effect on CI_e. Besides this, Case 3 substantially improves electrolyser utilisation e.g. on the steady wind at Φ_W = 100% day from 53% in Case 2 up to 76% in Case 3.

When $LF_{TH} < 90\%$, Case 1 is as effective as Case 3 (for fixed values of LF_{TH} and Φ_W, the same values of CI_e, CI_H, Y_H, UF_E and IC_E are achieved). However, to achieve say an LF_{TH} of 90% at Φ_W = 50%, Case 3 permits 60% of the electrolysers to be located at the points of hydrogen demand so reducing hydrogen infrastructure requirements.

Unlike Cases 1 and 3, Case 2 cannot achieve the objective of eradicating wind curtailment. However where wind curtailment is not yet a major issue ($\Phi_W < 40\%$) and the main objective is to produce moderate amounts of low/zero carbon hydrogen for distributed applications at minimal infrastructural cost, Case 2 would be a recommended option relative to Case 3, as it offers similar results in terms of CI_e, CI_H, Y, UF_E and IC_E for given values of load factor and wind penetration while avoiding hydrogen distribution costs. For $\Phi \geq 40\%$, Case 2 can only achieve hydrogen yields of similar magnitude to those achieved by Case 3 at the expense of allowing CI_H to approach that associated with hydrocarbon reformation methods.

For Case 2 the power input to electrolysers is a function of the amount of wind power that can be integrated into the grid, subject to curtailment at periods of low demand and high wind availability. At $\Phi_W \geq 40\%$ the wind power directed to consumers increases (and hence CI_e decreases) at the expense of the wind power feed to the electrolyser stock due to the low-load limit restriction, which reduces the hydrogen yield. Thus although more wind power is produced at higher wind penetrations, it cannot be directed to the electrolyser stock through the grid and thus the hydrogen yield does not increase. Should a higher threshold apply for the low-load limit restriction (see **Appendix C**), this would only influence the value of wind penetration above which the

aforementioned effect appears, without modifying the trade-off between Y_H and CI_e. Under the assumptions imposed in this analysis, it is not possible to increase the carbon abatement potential of wind power for Case 2, while at the same time aiming for larger hydrogen yields.

Figure 4.17 shows the relationship between the carbon intensity of electricity and wind penetration for each Case, where the fuel mix selected corresponds to that of the steady wind day in **Figure 3.8 Chapter 3**. The dashed line 1 shows the CI_e that could theoretically be achieved if all wind power production could be integrated without curtailment.

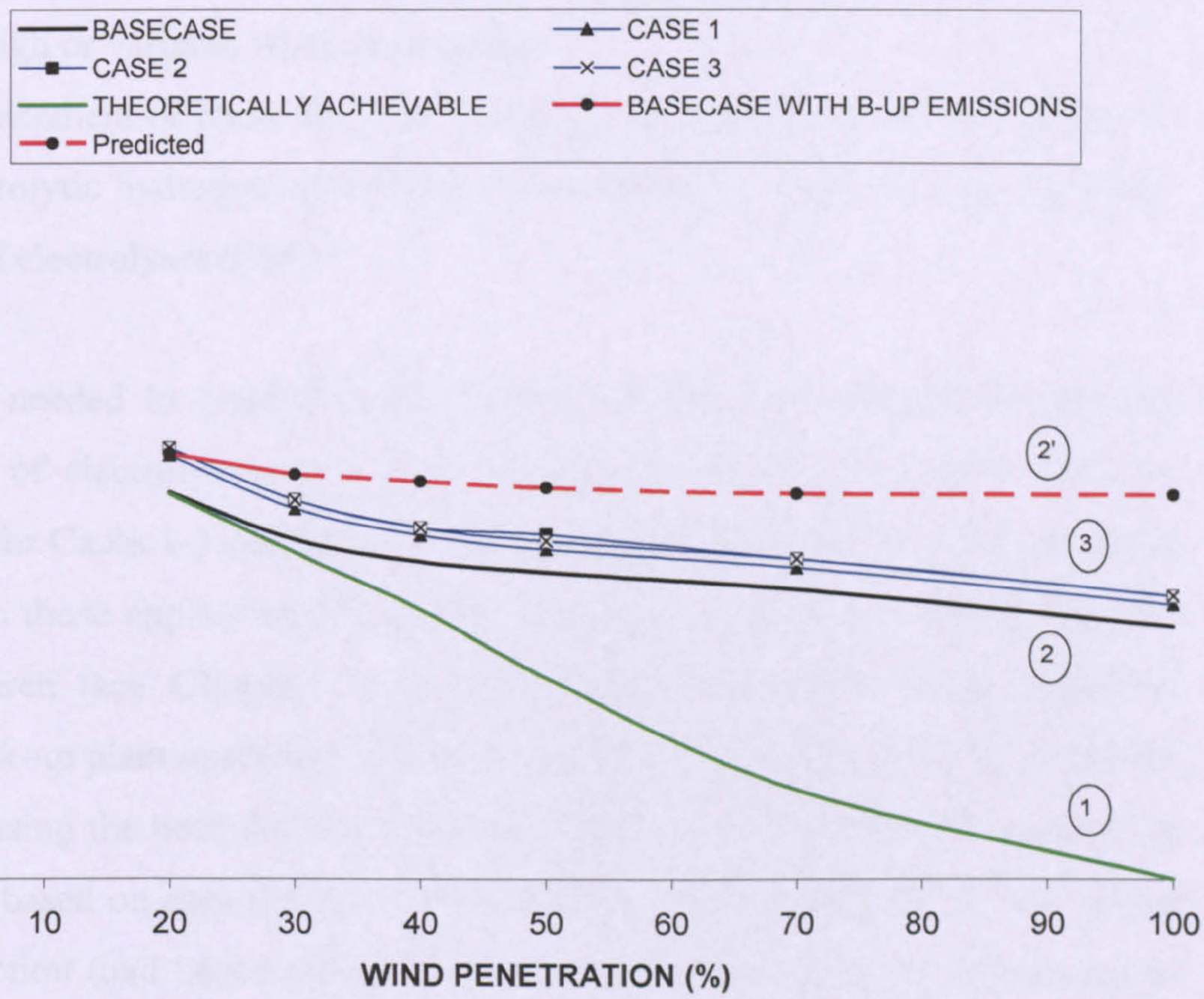

Figure 4.17. Relationship between thecarbon intensity of grid electricity and wind penetration for the steady wind day.

① :Theoretically achievable if no wind curtailment and neglecting back-up emissions;

② : Base Case, neglecting back-up emissions;

②': Base Case, projection from existing data allowing for back-up emissions;

③ : Cases 1-3

Greater values are exhibited for Cases 1, 2 and 3 (curve 3) relative to the Base Case (curve 2). This however is just a consequence of the decrease in the wind generation delivered to consumers (due to some electricity been delivered to electrolysers). Curve 3 in **Figure 4.17** overestimates the carbon intensities associated with Cases 1-3, because it has not been possible to quantify all of the associated carbon saving benefits. These include:

- A more stable and predictable operation of FPP due to the much greater LF_{TII} achieved in a power system with a large electrolyser stock.
- A reduced operational requirement for supply/demand matching with back-up FPP on days of high or variable wind availability.
- The displacement of fossil fuel use in applications across the energy system by low-carbon electrolytic hydrogen, (for which it is important to realise a high utilisation factor per MW of electrolyser stock).

Further work is needed to quantify these carbon benefits derived from widespread implementations of electrolysers as a load management mechanism before accurate estimates of CI_e for Cases 1-3 can be made. This could be attempted by using computer models similar to those applied by [1], [2] and is proposed here as an interesting area for further research (see **Chapter 7**). However, with respect to carbon emissions derived from back-up plant operation, optimisation of the load factor itself would lower the CI_e by decreasing the need for back-up plant operation. In **Figure 4.17**, curve 2' is an extrapolation based on data for $\Phi_W = 20$ and $\Phi_W = 30\%$ available from [2], where the fuel consumption (and hence carbon emissions) from back-up plant is assumed to increase with wind penetration [1], [2]. If CO_2 penalties due to back-up plant emissions are taken into account, Curve 2 becomes Curve 2' in **Figure 4.17.** This lies well above the curves 3 for Cases 1, 2, 3 and illustrates the likely reduction (not increase) in CI_e due to the implementation of electrolysers.

The carbon intensity of hydrogen is mainly determined by the LF_{TII} pursued. Large hydrogen yields can only be obtained at the expense of increasing CI_{II} (**Figures 4.12**

and **4.13**). For instance, for $\Phi_W = 40\%$, if low-carbon hydrogen of $CI_H = 4.5$ kgCO_2/kg H_2 is produced, Y_H doubles with respect to that obtained if only zero-carbon hydrogen were produced for the same size electrolyser stock. High hydrogen yields are attained at high LF_{TH} (**Figure 4.13**) also leading to higher CI_H (**Figure 4.12**). Only at $\Phi_W > 50\%$ can both large Y_H and $CI_H \leq 3$ kgCO_2/kg H_2 be obtained with $LF_{TH} > 95\%$.

Although the analysis presented in this chapter is based on daily outputs, an annual average estimate can be made for the main outputs assuming a day of 24% capacity factor[18] and multiplying by 365 days. For instance, for Case 3 at $\Phi_W = 50\%$, the average load factor of the FPP load profile across 1 year could reach 84% and the average carbon intensity would be 0.58 kg CO_2 / kWh. The total carbon emissions across the year would be around 8 Mt CO_2 and 36,135 tones of H_2 would be produced. The average annual utilization factor of the electrolyser stock would stand at 16%.

Because the electrolyser stock is sized to eliminate wind curtailment, this results in rather low utilization factors. For example, at $\Phi_W = 50\%$ it is found that around 980 MW of electrolysers are required to eradicate wind curtailment (Case 1), and yet the capacity actually in use on the variable wind day exceeds 600 MW ($UF_E > 60\%$) for only 5h of that day. Clearly UF_E increases with the wind capacity factor (CF). Therefore other locations with a higher annual average CF will yield higher UF_E. For instance, an annual CF of 35% would increase the average annual UF_E from 16% to 25%. Increased capacity utilisation would have a profound effect on the ability to produce hydrogen economically. Several additional measures can be proposed to increase UF_E:

- A decision can be made about what level of electrolyser capacity in relation to wind installed capacity should be installed in practice. For example, if the capacity of the electrolyser stock is reduced to 70% of wind installed capacity and the wind capacity factor is 35%, the annual UF_E approaches 30% for Case 3 at $\Phi_W = 50\%$.

[18] The average annual wind capacity factor for Eastern Denmark in 2003 was 24% [17].

- The model presented in this chapter is extended in **Chapter 5** to consider the deployment of other zero-carbon power sources (e.g. nuclear and CO_2-sequestered power plants) in order to increase UF_E. Annual utilization factors in excess of 50% can then be obtained by deploying a zero-carbon thermal capacity equaling 25% of system peak demand.

- Note the results presented are specific values based on the data employed from the Eastern Denmark power system. However the methodology devised is applicable to a generic power system and the approach is capable of generating the minimum electrolyser capacity required for any wind penetration.

4.5 CONCLUSIONS

When considering power systems with large penetrations of RE, active load management via electrolysers is found an attractive option with the view of optimizing the operation of the power system. The approach described in **Chapter 3** has been applied for implementing and controlling a large stock of electrolysers in conjunction with high penetrations of wind power. Several alternatives for implementation and operation of electrolysers can be suggested, including both demand-side and supply-side configurations. Preferred capacity levels and operational strategies are identified for the electrolyser stock, with the objectives of (i) maximising the efficiency of the electricity system by increasing the load factor of the aggregate FPP load profile; (ii) increase the capture of intermittent RE sources by reducing wind power curtailment; and (iii) create a supply of zero/low-carbon hydrogen to be used in other energy sectors.

For all the implementation cases considered here spreadsheet modelling was applied to high penetrations of wind power using wind generation and demand data available from the Eastern Denmark power system. Wind data was scaled up to produce wind penetrations of up to 100% of system maximum demand. First results obtained from a preliminary analysis suggest that it is certainly possible to increase the load factor of the aggregate FPP load profile by integrating electrolysers into the system. Operation of

electrolysers can be adapted (switching on and off as required) to increase demand at will, filling valleys and creating plateaus on the FPP load profile, allowing FPP a more stable and efficient operation, thus reducing their carbon footprint. Results indicate that introduction of electrolysers are capable of increasing the load factor up to 100% (a virtually flat FPP load profile) if a combined "supply-side/demand-side" electrolyser implementation strategy is introduced. This constitutes an unprecedented achievement for the power industry, which can be utilised to minimise the carbon intensity of electricity produced by fossil-fuelled power generators. For comparison, load factor of the aggregate FPP load profile in GB on a typical winter day (10/12/2002) was calculated from demand data available in [75], resulting a value of 77%.

The approach followed also intends to maximize the capture of wind resources through minimisation of wind curtailment. It is found that as wind power penetration increases the amount of wind power that must be curtailed rises dramatically, and a larger proportion of electricity than theoretically needed (if all wind-generated electricity could be integrated into the grid) must now be generated from FPP, reducing the carbon savings derived from WPP. Thus when all wind-generated electricity is directed to the grid, there are diminishing returns with respect to achieving the carbon abatement potential. Rather than simply increase uncontrollably the amount of wind power introduced in the electricity grid, leading to a large proportion of the renewable resource being wasted, it is suggested here that all the wind power resource that can not be accommodated within the electricity grid can instead be directed to a SSE stock for the production of low/zero-carbon hydrogen, allowing the absorption of higher penetrations of wind power.

There is a trade-off in terms of the carbon benefits derived from increasing LF_{TH}, the utilization of the electrolyser stock and the carbon penalties imposed. It is also observed that the more variable the system demand (significant differences between minimum and maximum daily demand, and hence low LF_{TH}), the more beneficial will be an increase of LF_{TH} to obtain high utilization factors for the electrolyser stock. Also results show that large hydrogen yields can only be obtained at the expense of the hydrogen's carbon intensity (see **Table 4.10**). Only at wind penetrations above 50% can both large

hydrogen yields and $CI_H \leq 3$ kgCO_2/kg H_2 be obtained with $LF_{TH} > 95\%$ (see **Figures 4.12 and 4.13**).

In a region of high renewable resource, the electrolyser capacity and the wind capacity needs to be coupled in a deployment strategy that aims to maximise wind penetration, minimise wind curtailment, maximise FPP load factor and maximise hydrogen production. Results show that for a combined stock of supply-side and demand-side electrolysers, the optimum ratio of electrolyser capacity to wind installed capacity is between 1.06 and 1.10 (i.e. it is greater than the required capacity of wind power plant – see **Table 4.11**). Thus it is imperative that low-cost electrolyser systems are developed. It is suggested here that the load factor target should increase as wind penetration increases, and very high load factors should only be sought at very high wind penetrations, at which stage the electrolyser installed capacity needs to at least equal the wind installed capacity.

For the data employed, and in the absence of significant amounts of distributed generation (DG) on the demand side, distributed electrolysers may be deployed alone (Case 2) for wind penetrations below 30%, but above this level the amount of large scale wind power that can be integrated into the grid becomes constricted, and a combined scheme including both supply and demand-side electrolysers is required to achieve high Φ_W and LF_{TH} values. The SSE capacity is required to absorb the wind power output that would otherwise need to be curtailed. However this conclusion will be different if a large deployment of dispersed generation is included. In that case more DSE could be deployed to exploit the output available from distributed renewable generation, not restricted by the amount of wind power that can be integrated in the electricity transmission system. Then DSE and DG could be controlled so as to increase LF, the hydrogen yield and decrease the carbon intensity of electricity beyond the levels presented here. Furthermore the combination of DSE and DG in the domestic sector could extend the benefits of the concept proposed here by further decarbonising other energy sectors through large scale production and usage of clean H_2 for example for domestic transport and heating purposes. The analysis of this option is beyond the scope of this paper, but it is a valuable topic for further analysis.

The results of this study are suggestive, not definitive, due to the broad scope of the analysis. In the long term, an enhanced power system may be developed with very large penetrations of zero-carbon power sources and electrolysers with capacities exceeding SMD as suggested in [67], [82] in order to increase Y_H, UF_E above the levels suggested here, as well as minimizing CI_e. If done so, an extension of the FPP and WPP capacity required to cover the system demand would be needed. This could be achieved by deploying large capacities of zero-carbon DG and/or other zero-carbon power sources in addition to WPP. A future expansion of this study including the deployment of other zero-carbon power sources (e.g. nuclear and CO_2-sequestered power plants) is presented in **Chapter 5**. Implications of this modification on the flexibility of the power system and its capability to absorb higher intermittent wind power inputs (reducing wind curtailment) are reviewed in the next chapter.

While annual electricity demand growth may be limited, the intermittent renewable input could grow rapidly to satisfy a growing zero-carbon hydrogen demand, using both the electricity system and hydrogen to meet an increasing fraction of the general requirements for end use energy. For future energy systems with a general hydrogen demand far in excess of consumer demand for electricity, an optimization based on other parameters (e.g. CI_H, Y_H, UF_E) rather than those investigated here (namely LF_{TH} and wind curtailment) may be more appropriate. This is discussed further in **Chapter 5.**

CHAPTER 5 - IMPLEMENTATION AND CONTROL OF ELECTROLYSERS IN CONJUNCTION WITH WIND POWER AND ZERO-CARBON THERMAL POWER PLANT

5.1. INTRODUCTION

A significant capacity of intermittent renewable power sources, and specifically wind power, is required to produce large amounts of "clean" hydrogen due to their inherent low annual capacity factor. Also, the intermittent nature of wind power implies that the electrolyser stock will need to absorb fluctuating inputs resulting in a low utilization factor (see **Chapter 4**). These are undesirable factors from an economic investment point of view. For a national energy system to achieve a substantial displacement of fossil fuels by electrolytic hydrogen, the required scale of production is so vast that the installed capacity of zero-carbon power sources need to far exceed SMD. Therefore other zero-carbon power sources of higher capacity factors[19] will be required in any electrolyser implementation strategy, in order to increase the scale of H_2 production and the utilization of electrolysers above the levels derived from renewable hydrogen production.

The deployment of zero-carbon thermal power plant (e.g. CO_2-sequestered, nuclear power plant) within the electricity system in conjunction with intermittent renewable sources opens enormous possibilities for large-scale generation of zero-carbon hydrogen. As an example, the capacity of an electrolyser fully dedicated to a nuclear power plant required to deliver a certain volume of H_2 would be around one third that of an electrolyser required for a wind power plant, simply because the ratio of their capacity factors is approximately 1:3 (a CF of 75-85% usually applies for a nuclear power plant[20]). Or conversely an electrolyser of a certain rating dedicated to a nuclear power plant will produce 3 times more hydrogen per annum that of an identical electrolyser coupled to a wind power plant. Furthermore the combination

---

[19] Average CF of wind generation in Denmark in 2003 was 24% [17]. Average CF of wind generation in Britain is estimated at about 30% [7].

[20] Capacity factor is used to measure how intensively each type of power plant is used with respect to their rated capacity. This is also sometimes expressed in the literature as plant load factor but the use of CF has been chosen here to avoid confusion with the load factor of the aggregate thermal load profile (statistical parameter, see nomenclature).

of both supply pathways, i.e. wind power plant (WPP) and zero-carbon thermal power plant (ZPP) would address the problem of wind intermittency, yielding a much greater utilization of the electrolyser stock and very high LF_{TH} values without compromising the carbon intensity of both electricity and hydrogen delivered to consumers..

This chapter extends the analysis presented in **Chapter 4** to consider a power system which includes a deployment of dispatchable zero-carbon thermal power plant (ZPP). The methodology is applied again to daily load profiles for studying the implementation and control of ELS in the power system, but in addition the AELM spreadsheet model is now applied over a timeframe of 1 week so as to identify likely variations in the principal parameters across periods longer than 24h. Both for the daily and weekly analyses the same three implementation cases for the electrolyser stock are considered, namely supply-side electrolysers (SSEs), demand-side electrolysers (DSEs) or a combination of both (SSEs + DSEs). The objectives now are to:

- increase the scale of hydrogen production (Y_H);
- increase the utilization factor of electrolyser stock (UF_E);
- minimize the carbon intensity of electricity (CI_e),

with respect to those values obtained previously with a large deployment of intermittent renewable power sources.

Regarding the deployment of ZPP, three penetration levels ranging from 10% to 35% are considered, $10\% \leq \Phi_{ZPP} \leq 35\%$. The upper limit corresponds to minimum summer demand in Eastern Denmark, which is normally considered as a threshold for the deployment of baseload generating capacity in islanded power systems with no significant interconnections.

Again by following a heuristic approach several operational strategies are evaluated for the utilization of electrolysers in conjunction with zero-carbon thermal power plant and wind power plant. The main objectives with respect to a wide

implementation of electrolysers in the power system remain the same: maximise the load factor of the aggregate fossil thermal load TH_G; minimize wind power curtailment; and generate zero/low carbon hydrogen for use in other sectors of the energy system. An assessment is also carried out of the potential of a wide deployment of electrolysers in conjunction with zero-carbon power sources for lowering CI_e drastically. At all times the electrolyser stock is operated in such way that the combined load represented by consumers' demand and electrolysers never exceeds the system maximum demand (SMD).

5.2. DESCRIPTION OF APPROACH

5.2.1 Description of the model and modifications included

A methodology is now developed for implementing and controlling a large stock of electrolysers with increasing penetrations of wind and zero-carbon thermal power sources in order to maximise LF_{TH} on days of different wind availability and system demand. Special attention is given in this chapter to low wind days in order to maximise both the average utilization factor of the electrolyser stock across the year and the hydrogen yield.

Preferred capacity levels and operational strategies for the electrolyser stock and power plant are considered, where three types of power plant are available: (i) equivalent wind power plant (WPP); (ii) equivalent zero-carbon thermal power plant, e.g. CO_2-sequestered or nuclear power plant (ZPP); and (iii) fossil-fuelled thermal power plant, namely coal, gas and oil fuelled plant (FPP). On the demand side, three independent loads are considered: equivalent electricity consumer load (P_C), an embedded "demand-side electrolyser stock" (DSE) and a "supply-side electrolyser stock (SSE)". No other energy storage technologies or load management mechanisms are considered. In summary, the generic power system considered here is the same as that depicted in **Chapter 4** plus a stock of ZPP. A schematic is shown in **Figure 5.1**.

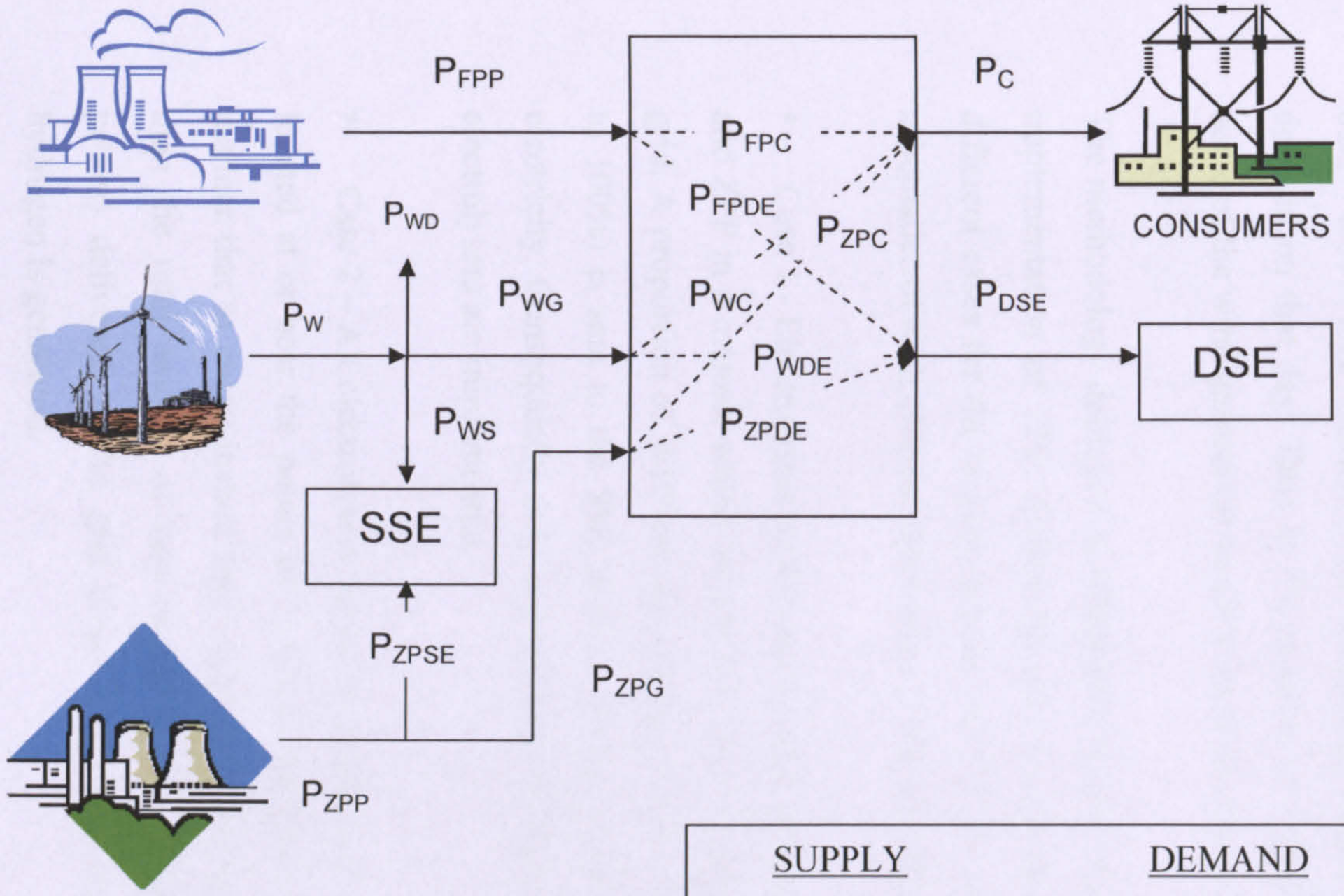

Figure 5.1. Schematic of the considered power system with a stock of demand-side and supply-side electrolysers

SUPPLY	DEMAND
$P_{FPP} = P_{FPC} + P_{FPDE}$	$P_C = P_{FPC} + P_{WC} + P_{ZPC}$
$P_w = P_{WG} + P_{WSE}$	$P_{SSE} = P_{WSE} + P_{ZPSE}$
$P_{ZPP} = P_{ZPSE} + P_{ZPG}$	$P_{DSE} = P_{FPDE} + P_{WDE} + P_{ZPDE}$

Following this scheme, WPP, ZPP and FPP feed electricity through the grid to consumers and to DSE located at or near the main points of hydrogen demand. Also an additional load consisting of a SSE stock is placed on the supply-side, at or near the primary WPP and ZPP, with the main purpose of absorbing all the wind power output that cannot be accommodated by the grid which is otherwise curtailed. For example, for an islanded power system with Φ_W = 100% (Φ_W = SMD) and Φ_{ZPP} = 35%, on a day of high wind availability when say 80% (SMD × 0.8) of the wind capacity and 90% of the ZPP output (SMD × 0.35 × 0.9) is available, the total zero-carbon electricity output would be (SMD × 0.8) + (SMD × 0.35 × 0.9) = 1.12 × SMD, which exceeds that required to cover the power system demand on that day. Thus in the absence of a SSE stock to absorb the surplus some of the wind generation would clearly need to be curtailed.

The methodology deployed in **Chapter 4** is now modified in order to include the implementation of ZPP. Following the scheme depicted in **Figure 5.1**, three different cases for the implementation of ELS are considered. **Figure 5.2** shows schematics of each of these three cases. They are referred to as:

- Case 1 - Electrolysers on the supply side, located at or near the primary WPP and ZPP in a manner which avoids having to transfer all of the generation to the grid. A proportion of WPP production P_{WSE} (0 to 100%) and ZPP output P_{ZPSE} (0 to 100%) is sent to the SSE stock, with no contribution whatsoever from grid electricity. Consequently only zero-carbon hydrogen is generated. No embedded electrolysers are implemented.

- Case 2 – All electrolysers on the demand-side, embedded within the grid and located at or near the points of hydrogen demand. They are operated in such a manner that at every instant their aggregate electrical input P_{DSE} is always less than the total amount of zero-carbon power (wind plus zero-carbon thermal power) delivered to the grid (P_{WG} + P_{ZPG}). Consequently only zero-carbon hydrogen is generated.

- Case 3 – A combination of Cases 1 and 2. Electrolysers deployed both on the supply side and demand side. The production of low-carbon hydrogen with an average carbon intensity of 3 kg CO_2 / kg H_2 (kilograms of CO_2 emitted per kilogram of H_2 generated) is now considered and analysed against the production of zero-carbon hydrogen.

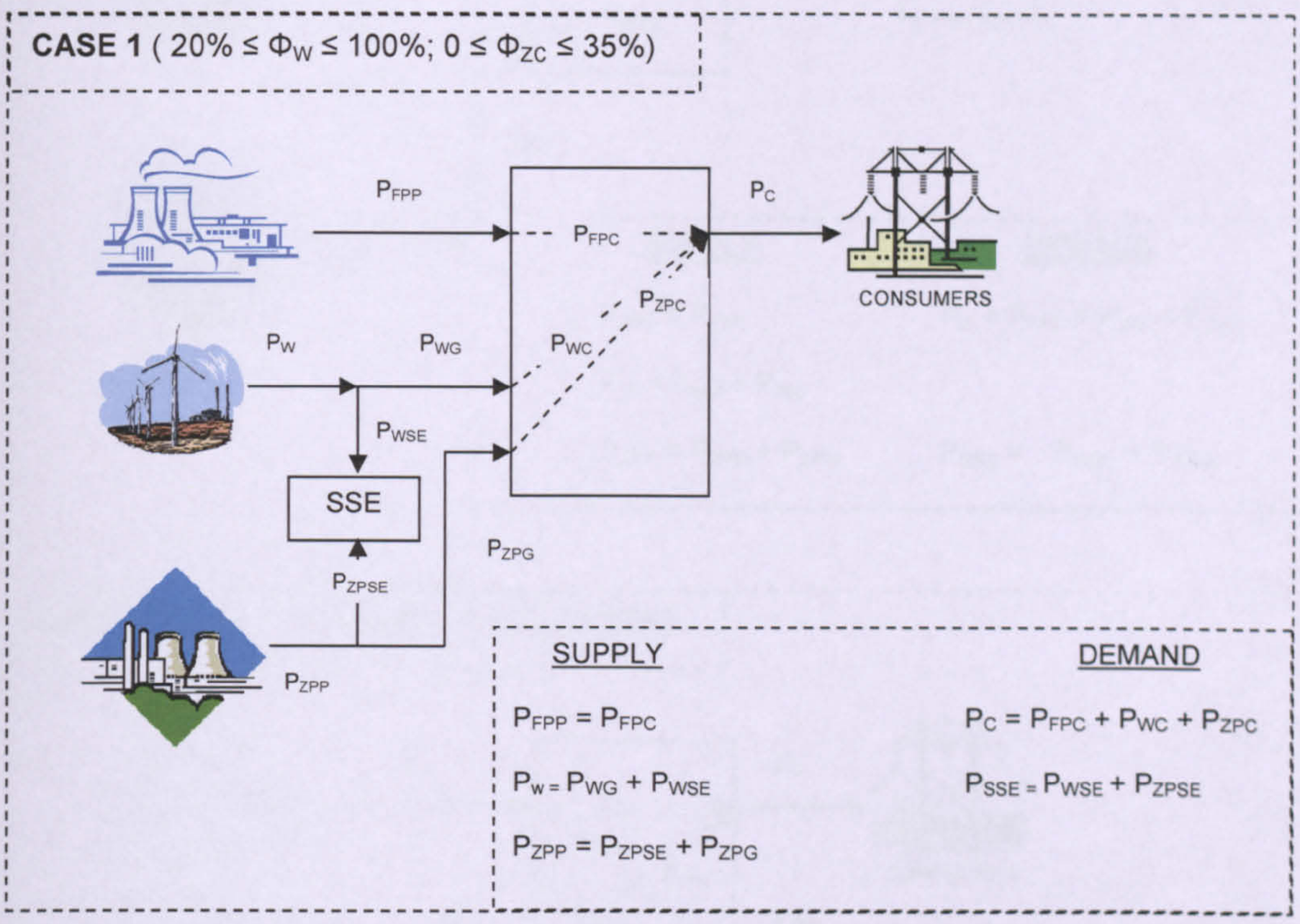

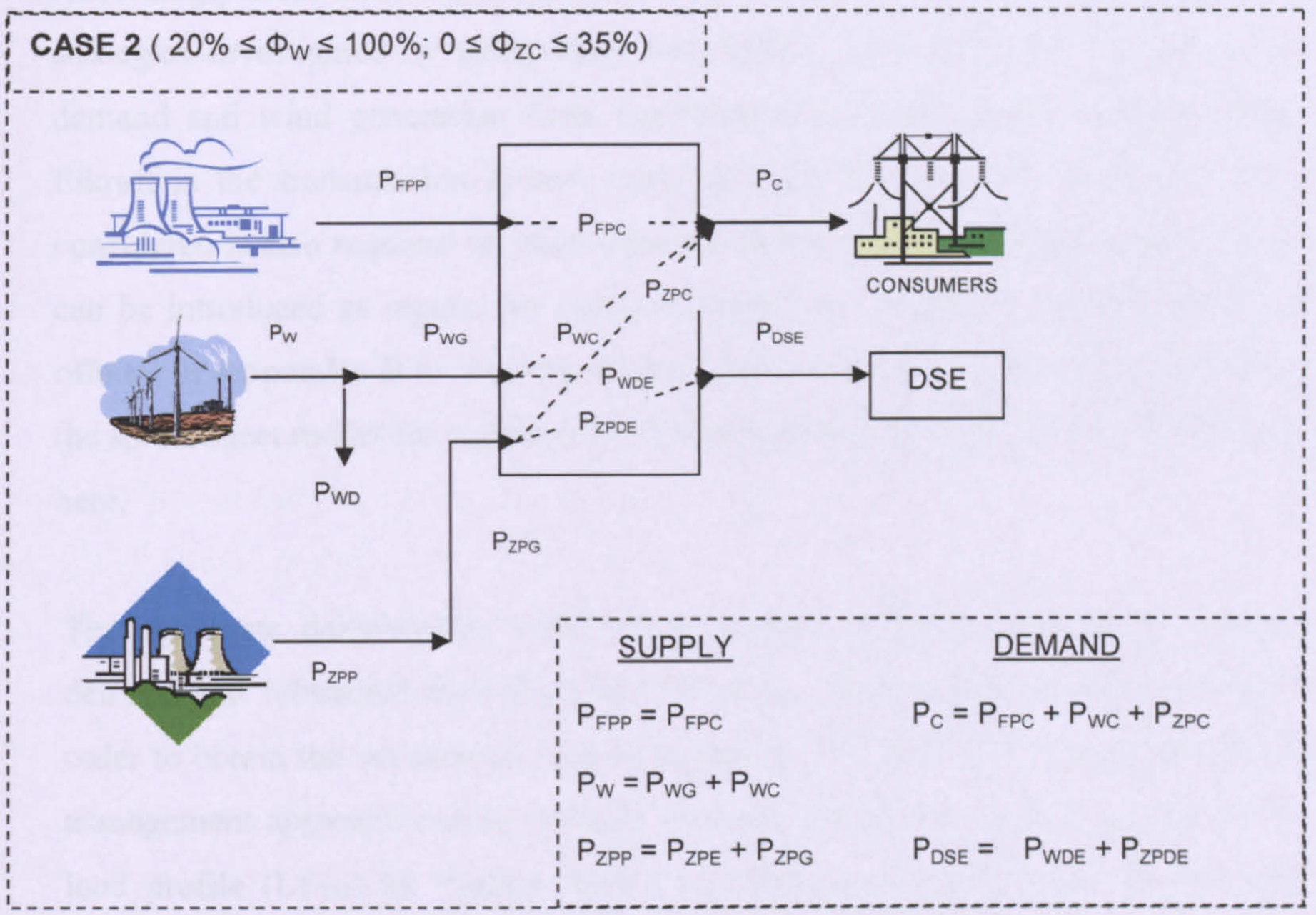

Figure 5.2. Cases considered for the implementation of electrolysers in conjunction with zero-carbon power plant and wind power plant

Accordingly these three implementation cases have been simulated and operational strategies investigated by using daily and weekly time series for the electricity demand and wind generation from the Eastern Denmark power system, where Elkraft is the transmission system operator [17]. The fuel mix for every case considered is also required as input data and different electricity generation mixes can be introduced as inputs. An analysis applied to a different demand profile is offered in **Appendix B** to investigate similarities and differences in the outputs of the spreadsheet model for regions with different demand profiles to those presented here.

The aggregate daily/weekly wind power output profile is taken as a negative demand and subtracted from the total consumers' daily/weekly demand profile in order to obtain the net thermal load to be met by FPP and ZPP. The adopted load management approach was to increase the daily load factor of the aggregate FPP load profile (LF_{TH}) by "valley filling" at morning and night-time periods and creating day-time plateaus that are much broader than the conventional peak (e.g. a daily plateau from 09:00 onwards). In addition the aggregate load placed in FPP is reduced during peak periods (increasing LF_{TH} but also minimizing CI_c) through operation of ZPP mainly at peak times. Electrolysers are then operated as additional controllable loads, so that the load placed on fossil-fuelled thermal power plant can be increased or decreased in time phase with the zero-carbon power inputs to the electrical grid (wind and zero-carbon thermal). An additional approach is explored for the analysis applied to a weekly period, where the daily plateaus created on the FPP profile are extended so as to maintain a steady operation of FPP for longer periods, evaluating the implications this has on the other parameters.

Results are presented for 24h and 168h periods on a time interval of one hour based on historical data from [17],[78]. The general outputs are then daily/weekly energy balances, load profiles, hydrogen yields and carbon intensities for electricity and hydrogen as well as average hourly power flows for the 24h and 168h periods studied. However the methodology is applicable to any appropriate time-base and for any period provided the required input data are available.

5.2.2 Description of control strategies devised

In order to evaluate and optimize the operation of ZPP, WPP and FPP in connection with the electrolyser stock three different operational strategies have been evaluated for each one of the implementation cases described above.

In principle some or all ZPP could be used for baseload or peak electricity generation. Identifying the preferred strategy for a particular power system depends on the type of plant available within the ZPP stock, and also requires detailed economic considerations which lie beyond the scope of this investigation. For instance, nuclear power plant are more suitable for steady base-load generation, whereas other ZPP like CCGT plant (Combined Cycle Gas Turbine) with CO_2 sequestration might be operated in a load-following mode to provide either base-load or peak electricity as required. Both options have been considered here in order to fully evaluate the implications of deploying and operating additional ZPP in the power system. In summary the strategies deployed here are as follows:

A. Using ZPP both for H_2 production and for baseload electricity generation. A constant proportion of the ZPP output is directed to the grid to satisfy consumer demand D_C while the remainder is sent to the electrolyser stock. Some wind generated electricity is also used to meet D_C subject to the LF_{TH} target.

B. ZPP output is primarily used to cover D_C subject to the LF_{TH} target, the remainder being directed to the electrolyser stock. No WPP are implemented in this case.

C. Using ZPP mainly to supply consumers at peak demand periods subject to the LF_{TH} target and the remaining is sent to the electrolyser stock. Some wind generated electricity is also used to meet D_C, while the remaining is directed to ELS.

For all the operational strategies each day at a specified time (e.g. 23:00 or t = -1), the operator of the system would access forecasts of consumer demand, wind power and ZPP availability for the time period appointed (24h or 168h in the analysis presented in this chapter) on a certain time-interval. Based on this information and taking into account the LF_{TH} targeted, a preferred daily scheduling operation of FPP, WPP, ZPP and electrolysers for each time-interval is devised. An improved FPP load profile of greater LF_{TH} can then be targeted by adding the electrolyser load P_E (i.e. filling valleys in the net fossil load profile) and also subtracting the zero-carbon thermal load P_{ZPP} when appropriate (i.e. peak shaving of the net FPP load profile). At the end of the 24h/168h period, load profiles can be plotted for the operation of FPP, WPP, ZPP and electrolysers; and daily/weekly energy parameters (such as WC, Y_H, UF_E, CI_c, TC, CI_H) obtained by integration of hourly average power values.

The main assumptions are those described in **Chapter 3**, including a 30% load limit (LLL) for the wind power output directed to the grid, as expressed in equation (5.1) below:

$$P_{WG} = P_{WC} + P_{WDE} \leq 0.3\ (P_C + P_{DSE}) \qquad (5.1)$$

An evaluation of this assumption is carried out in **Appendix C** to assess the implications of deploying increasing amounts of non-flexible power plant (e.g. nuclear power plant) on the ability of the power system to integrate large intermittent renewable inputs. Clearly the higher the proportion of inflexible plant in the system (e.g. nuclear power plant), the lower LLL would be. However, a large deployment of electrolysers would offset this trend by increasing the demand during morning and night-time valleys in the aggregate FPP load profile and therefore the amount of wind power that the system can effectively absorb at those times. The average daily and weekly capacity factor of ZPP is taken at 90%, allowing for forced and planned outage hours.

A detailed description of the operational strategies suggested is given below:

A1) STRATEGY A – CASE 1:

A proportion X% of the ZPP output P_{ZPG}[21] is directed to the grid and the remainder output P_{ZPSE} is directed to the SSE stock.

$$P_{ZPSE}(t) = P_{ZPP}(t) - P_{ZPG}(t) \quad (5.2)$$

Based on this information and taking into account the LF_{TH} desired, the FPP load profile P_{FPP} is obtained by filling the early morning and night-time valleys to create a late morning-afternoon plateau at the level of the maximum load appointed to FPP, but of much greater duration than applies for the conventional FPP profile.

Subject to the low load limit,

$$P_{WC}(t) \leq 0.3\ P_C(t) \quad (5.3)$$

The wind power output is directed to the grid and the SSE stock

$$P_{WC}(t) = P_C(t) - [P_{FPP}(t) + P_{ZPG}(t)] \quad (5.4)$$

$$P_{WSE}(t) = P_W(t) - P_{WC}(t) \quad (5.5)$$

Because zero-carbon hydrogen is required ($CI_H = 0$),

$$P_{FPSE}(t) = 0 \quad (5.6)$$

The operational strategy for the SSE stock, $P_{WSE}(t)$, can be defined:

$$P_{SSE}(t) = P_{ZPSE}(t) + P_{WSE}(t) + P_{FPSE}(t) \quad (5.7)$$

The net electrical energy exchanges are obtained across a specific time period. For example, in the case of the load placed on thermal power plant:

$$E_{FPP} = \sum P_{FPPi}(t) \times \Delta t \qquad i = 1,\ldots,n \quad (5.8)$$

Where $P_{FPPi}(t)$ = average power output at i

Once the energy flows have been obtained, the main output variables (such as UF_{FPP}, UF_{EL}, CI_e, CI_H) can be computed.

---

[21] In the results presented herein this parameter has been set-up at 50% but note this variable can be changed according to the optimization criteria selected (e.g. maximization of Y_H, UF_E, minimization of CI_e), clearly a function of the specific H_2 and electricity demand to be supplied.

A2) STRATEGY A – CASE 2:

A proportion X% of the ZPP output P_{ZPC}^2 is directed to the grid and the remainder output P_{ZPSE} is directed to the DSE stock.

$$P_{ZPDE}(t) = P_{ZPP}(t) - P_{ZPC}(t) \quad (5.9)$$

Based on this information and taking into account the LF_{TH} desired, the FPP load profile P_{FPP} is obtained as in Strategy A1.

Subject to the low-load limit,

$$P_{WC}(t) + P_{WDE}(t) \leq 0.3\,[P_C(t) + P_{DSE}(t)] \quad (5.10)$$

The wind power output is directed to the grid and the DSE stock:

$$P_{WC}(t) = P_C(t) - P_{FPP}(t) - P_{ZPC}(t) \quad (5.11)$$

$$P_{WDE}(t) = P_W(t) - P_{WC}(t) \quad (5.12)$$

Because zero-carbon hydrogen is required ($CI_H = 0$),

$$P_{FPDE}(t) = 0 \quad (5.13)$$

The operational strategy for the DSE stock, $P_{DSE}(t)$, is then defined subject to the restriction:

$$P_C(t) + P_{DSE}(t) \leq SMD \quad (5.14)$$

$$P_{DSE}(t) = P_{ZPDE}(t) + P_{WDE}(t) + P_{FPDE}(t) \quad (5.15)$$

The net electrical energy exchanges obtained for a specific time period.

Once the energy flows have been obtained, the main output variables can be computed.

A3) STRATEGY A – CASE 3:

A proportion X% of the ZPP output P_{ZPC}^2 is directed to the grid exclusively to cover consumer demand P_C and the remainder output P_{ZPSE} is directed to the SSE stock.

$$P_{ZPDE}(t) = 0 \quad (5.16)$$

P_{FPP} is obtained by filling valleys and creating a plateau greater than applies to the conventional FPP profile, taking into account the LF_{TH} desired and ZPP availability.

Subject to the carbon intensity of hydrogen appointed (e.g. $CI_H = 3$), the WPP output is directed to the grid, and the aggregate FPP load P_{FPP} is allowed to exceed the consumer demand ($P_C - P_{ZPC}$) by an amount P_{FPDE} which is directed to the DSE stock where:

$$\text{If } CI_H = 0 \quad \text{then} \quad P_{WC}(t) = [P_C(t) - P_{ZPC}(t)] - P_{FPP}(t) \tag{5.17}$$

$$\text{and} \qquad P_{FPDE}(t) = 0 \tag{5.18}$$

$$\text{If } CI_H > 0 \quad \text{then} \quad P_{WC}(t) = 0 \tag{5.19}$$

$$\text{and} \qquad P_{FPDE}(t) = P_{FPP}(t) - [P_C(t) - P_{ZPC}(t)] \tag{5.20}$$

Subject to the low load limit,

$$P_{WC}(t) + P_{WDE}(t) \leq 0.3\,[P_C(t) + P_{DSE}(t)] \tag{5.21}$$

The wind power output is directed to the grid, and the DSE stock

$$P_{WC}(t) = P_C(t) - P_{FPP}(t) \tag{5.22}$$

$$P_{WDE}(t) = P_W(t) - P_{WC}(t) \tag{5.23}$$

The operational strategy for the DSE stock, $P_{DSE}(t)$, is then defined subject to the restriction:

$$P_C(t) + P_{DSE}(t) \leq SMD \tag{5.24}$$

$$P_{DSE}(t) = P_{FPDE}(t) + P_{WDE}(t) \tag{5.25}$$

The remainder WPP output, if any, is directed to the SSE stock and the operational startegy for the SSE stock, $P_{SSE}(t)$, is defined :

$$P_{SSE}(t) = P_{ZPSE}(t) + [P_W(t) - P_{WC}(t) - P_{WDE}(t)] \tag{5.26}$$

The net electrical energy exchanges are obtained for a specific time period. Once the energy flows have been obtained, the main output variables can be computed.

A4) STRATEGY B – CASE 1:

Subject to the LF_{TH} desired and ZPP availability, P_{FPP} is obtained by filling valleys and creating a plateau at the level of the maximum load appointed to FPP, but of greater duration than applies to the conventional FPP profile.

The ZPP output is primarily directed to the grid and the remainder output P_{ZPSE} is directed to the SSE stock.

$$P_{ZPG}(t) = P_C(t) - P_{FPP}(t) \quad (5.27)$$

$$P_{ZPSE}(t) = P_{ZPP}(t) - P_{ZPG}(t) \quad (5.28)$$

Because zero-carbon hydrogen is required ($CI_H = 0$),

$$P_{FPSE}(t) = 0 \quad (5.29)$$

The operational strategy for the SSE stock, $P_{SSE}(t)$, can be defined:

$$P_{SSE}(t) = P_{ZPSE}(t) + P_{FPSE}(t) \quad (5.30)$$

Finally the net electrical energy exchanges are obtained across a specific time period. Once the energy flows have been obtained, the main output variables can be computed.

A5) STRATEGY B – CASE 2

As in A4, P_{TH} is obtained by filling valleys and creating a plateau greater than applies to the conventional FPP profile, taking into account the LF_{TH} desired and ZPP availability.

The ZPP output is primarily directed to the grid to supply consumer demand:

$$P_{ZPC}(t) = P_C(t) - P_{FPP}(t) \quad (5.31)$$

The remainder ZPP output, P_{ZPDE}, is directed to the DSE stock :

$$P_{ZPDE}(t) = P_{ZPP}(t) - P_{ZPC}(t) \quad (5.32)$$

Since $CI_H = 0$, then

$$P_{FPDE}(t) = 0 \quad (5.33)$$

The operational strategy for the DSE stock, $P_{DSE}(t)$, is then defined subject to the restriction:

$$P_C(t) + P_{DSE}(t) \leq SMD \quad (5.34)$$

$$P_{DSE}(t) = P_{ZPDE}(t) + P_{FPDE}(t) \quad (5.35)$$

The net electrical energy exchanges are obtained for a specific time period, and the main output variables can be computed.

A6) STRATEGY B – CASE 3

As previously, P_{TH} is obtained by filling valleys and creating a plateau greater than applies to the conventional FPP profile.

Subject to the carbon intensity of hydrogen appointed (e.g. $CI_H = 3$), the ZPP output is primarily directed to the grid, and the aggregate FPP load P_{FPP} is allowed to exceed the remainder consumer demand ($P_C - P_{ZPC}$) by an amount P_{FPDE} which is directed to the DSE stock where:

If $CI_H = 0$ then $P_{ZPC}(t) = P_C(t) - P_{FPP}(t)$ (5.36)

and $P_{FPDE}(t) = 0$ (5.37)

If $CI_H > 0$ then $P_{ZPC}(t) = 0$ (5.38)

and $P_{FPDE}(t) = P_{FPP}(t) - P_C(t)$ (5.39)

A proportion X % of the remainder ($P_{ZPP} - P_{ZPC}$) ZPP output, P_{ZPDE}, is directed to the DSE stock and the remainder of ($P_{ZPP} - P_{ZPC}$), P_{ZPSE}, is directed to the SSE stock.[22]

[22] In the results presented herein this variable has been set-up at 50%. However this can be modified e.g. to suit a desired ration of SSE to DSE capacity to be deployed.

$$P_{ZPDE}(t) = (X / 100) \cdot [P_{ZPP}(t) - P_{ZPC}(t)] \quad (5.40)$$

$$P_{ZPSE}(t) = [\,(100 - X) / 100\,] \cdot [P_{ZPP}(t) - P_{ZPC}(t)] \quad (5.41)$$

The operational strategies for the DSE stock, $P_{DSE}(t)$, and the SSE stock, $P_{SSE}(t)$, can be defined, subject to the restriction:

$$P_C(t) + P_{DSE}(t) \leq SMD \quad (5.42)$$

$$P_{DSE}(t) = P_{FPDE}(t) + P_{ZPDE}(t) \quad (5.43)$$

$$P_{SSE}(t) = P_{ZPSE}(t) \quad (5.44)$$

The net electrical energy exchanges are obtained for a specific time period, and the main output variables can be computed.

A7) STRATEGY C – CASE 1

The forecasted wind generation profile, P_W, is subtracted from the predicted consumer demand profile, P_C, to obtain the residual demand to be met by thermal power plant, $P_{FPP}(t) + P_{ZPG}(t)$.

Subject to the low load limit,

$$P_{WC}(t) \leq 0.3\ P_C(t) \quad (5.45)$$

The wind power output is directed to the grid and the SSE stock

$$P_{WC}(t) = P_C(t) - [P_{FPP}(t) + P_{ZPG}(t)] \quad (5.46)$$

$$P_{WSE}(t) = P_W(t) - P_{WC}(t) \quad (5.47)$$

Based on this information and subject to ZPP availability, the FPP load profile P_{FPP} is obtained by filling the early morning and night-time valleys to create a late morning-afternoon plateau at the level of the maximum load appointed to FPP, but of much greater duration than applies for the conventional FPP profile, taking into account the LF_{TH} desired.

The ZPP output is primarily directed to the grid, P_{ZPG}, to supply the remainder consumer demand:

$$P_{ZPG}(t) = P_c(t) - P_{WC}(t) - P_{FPP}(t) \quad (5.48)$$

The remainder ZPP output, P_{ZPSE}, is directed to the SSE stock:

$$P_{ZPSE}(t) = P_{ZPP}(t) - P_{ZPG}(t) \quad (5.49)$$

Because zero-carbon hydrogen is required ($CI_H = 0$),

$$P_{FPSE}(t) = 0 \quad (5.50)$$

The operational strategy for the SSE stock, $P_{SSE}(t)$, can be defined:

$$P_{SSE}(t) = P_{ZPSE}(t) + P_{FPSE}(t) \quad (5.51)$$

The net electrical energy exchanges are obtained across a specific time period. Once the energy flows have been obtained, the main output variables can be computed.

A8) STRATEGY C – CASE 2

The forecasted wind generation profile, P_W, is subtracted from the predicted consumer demand profile, P_C, to obtain the residual demand to be met by thermal power plant, $P_{FPP}(t) + P_{ZPG}(t)$.

Based on this information and subject to ZPP availability, the FPP load profile P_{FPP} is obtained by filling the early morning and night-time valleys to create a plateau at the level of the maximum load appointed to FPP, taking into account the LF_{TH} desired.

The ZPP output is primarily directed to the grid to supply consumer demand:

$$P_{ZPC}(t) = P_C(t) - P_{FPP}(t) \quad (5.52)$$

The remainder ZPP output, P_{ZPDE}, is directed to the DSE stock:

$$P_{ZPDE}(t) = P_{ZPP}(t) - P_{ZPC}(t) \quad (5.53)$$

Subject to the low load limit,

$$P_{WC}(t) + P_{WDE}(t) \leq 0.3\,[P_C(t) + P_{DSE}(t)] \quad (5.54)$$

The wind power output is directed to the grid, and the DSE stock

$$P_{WC}(t) = P_C(t) - P_{FPP}(t) \quad (5.55)$$

$$P_{WDE}(t) = P_W(t) - P_{WC}(t) \quad (5.56)$$

$$\text{Since } CI_H = 0, \text{ then } P_{FPDE}(t) = 0 \quad (5.57)$$

The operational strategy for the DSE stock, $P_{DSE}(t)$, is then defined subject to the restriction:

$$P_C(t) + P_{DSE}(t) \leq SMD \quad (5.58)$$

$$P_{DSE}(t) = P_{ZPDE}(t) + P_{FPDE}(t) \quad (5.59)$$

The net electrical energy exchanges are obtained for a specific time period, and the main output variables can be computed.

A9) STRATEGY C – CASE 3:

As in A8, the FPP load profile P_{FPP} is obtained by filling the early morning and night-time valleys, taking into account the LF_{TH} desired, ZPP and WPP availability.

Subject to the carbon intensity of hydrogen appointed (e.g. $CI_H = 3$), the ZPP output is primarily directed to the grid to supply consumer demand, and the aggregate FPP load P_{FPP} is allowed to exceed the remainder consumer demand ($P_C - P_{ZPC}$) by an amount P_{FPDE} which is directed to the DSE stock where:

$$\text{If } CI_H = 0 \quad \text{then} \quad P_{ZPC}(t) = P_C(t) - P_{FPP}(t) \quad (5.60)$$

$$\text{and} \quad P_{FPDE}(t) = 0 \quad (5.61)$$

$$\text{If } CI_H > 0 \quad \text{then} \quad P_{ZPC}(t) = 0 \quad (5.62)$$

$$\text{and} \quad P_{FPDE}(t) = P_{FPP}(t) - P_C(t) \quad (5.63)$$

A proportion X % of the remainder ($P_{ZPP} - P_{ZPC}$) ZPP output, P_{ZPDE}, is directed to the DSE stock and the remainder of ($P_{ZPP} - P_{ZPC}$), P_{ZPSE}, is directed to the SSE stock.[23]

$$P_{ZPDE}(t) = (X / 100) \cdot [P_{ZPP}(t) - P_{ZPC}(t)] \quad (5.64)$$

$$P_{ZPSE}(t) = [\,(100 - X) / 100\,] \cdot [P_{ZPP}(t) - P_{ZPC}(t)] \quad (5.65)$$

Subject to the LF_{TH} appointed and the low load limit,

$$P_{WC}(t) + P_{WDE}(t) \leq 0.3\,[P_C(t) + P_{DSE}(t)] \quad (5.66)$$

The wind power output is primarily directed to the grid to supply the remainder consumer demand, if any:

$$P_{WC}(t) = P_C(t) - P_{FPP}(t) - P_{ZPC}(t) \quad (5.67)$$

The remainder WPP output, P_{WDE}, is directed to the DSE stock :

$$P_{WDE}(t) = P_W(t) - P_{WC}(t) \quad (5.68)$$

The operational strategy for the DSE stock, $P_{DSE}(t)$, is then defined subject to the restriction:

$$P_C(t) + P_{DSE}(t) \leq SMD \quad (5.69)$$

$$P_{DSE}(t) = P_{FPDE}(t) + P_{ZPDE}(t) + P_{WDE}(t) \quad (5.70)$$

The remainder WPP output, if any, is directed to the SSE stock :

$$P_{WSE}(t) = P_W(t) - P_{WC}(t) - P_{WDE}(t) \quad (5.71)$$

The operational startegy for the SSE stock, $P_{SSE}(t)$, is defined :

$$P_{SSE}(t) = P_{ZPSE}(t) + P_{WSE}(t) \quad (5.72)$$

[23] In the results presented herein this variable has been set-up at 50%. However this can be modified e.g. to suit a desired ration of SSE to DSE capacity to be deployed.

5.3. RESULTS

5.3.1 Modelling set-up

Three different operational strategies have been analysed for each implementation case described in **Chapter 2.1.** Also results obtained previously in **Chapter 4** (i.e. with only WPP and FPP implemented on the supply side) are referred to here as the Base Case. The benefits of the implementation of additional ZPP in the power system are then discussed relative to the Base Case. Variables included in the analysis are:

- Load factor of the aggregate FPP profile, $\mathbf{LF_{TH}}$ **(%)**
- Total amount of H_2 produced, $\mathbf{Y_H}$ **(t / day)**
- Average daily utilization factor of ELS, $\mathbf{UF_E}$ **(%)**
- Average carbon intensity of electricity, $\mathbf{CI_e}$ **(kg $\mathbf{CO_2}$ / $\mathbf{kWh_e}$)**
- Total carbon emissions derived from electricity generation, **TC (t $\mathbf{CO_2}$ × $\mathbf{10^3}$/ d)**
- Wind generation curtailed, **WC (%)**
- Installed capacity of ELS required, $\mathbf{IC_E}$ **(MW)**
- Net system generating capacity, including WPP, ZPP, FPP and ELS, **NGC (MW)**
- Installed capacity of ELS required as a proportion of net system installed capacity, $\boldsymbol{\beta_E}$ **(%)**

Note LF_{TH} is calculated here only for the aggregate FPP load profile, and thus is comparable with those results obtained in **Chapter 4** when $\Phi_{ZPP} = 0\%$. The analysis in this chapter focuses on the variable and particularly the low wind day, in order to evaluate to what extent the objectives of increasing Y_H and UF_E can be achieved for $\Phi_{ZPP} \leq 35\%$ with respect to those values obtained in **Chapter 4**. An additional variable is introduced now, namely β_E, to analyse the capacity of the ELS stock required in relation to the total system generating capacity.

As in **Chapter 4** the capacity factors for wind generation on the high, variable and low wind days stand at 80%, 42% and 16% respectively. The installed capacity of

wind generation in Eastern Denmark in January 2003 of 573 MW is taken as the datum for calculations on steady and low wind scenarios, and 743 MW for the variable wind scenario. Wind penetration levels ranging from 20% to 100% are considered. A complete description of the baseline wind scenarios selected is offered in **Chapter 3.3.2**.

Total system demand for the steady, variable and low wind day selected previously is 47,603, 30,750 and 47,276 MWh respectively, and is held constant across all wind penetration levels. Both winter (steady and low wind day) and summer demand profiles (variable wind day) are investigated.

Wind penetration, Φ_W, and ZPP penetration, Φ_{ZPP}, are both referred herein as installed capacity relative to system maximum demand (SMD) in 2003, namely 2,665 MW. Total generating capacities in the islanded power system considered for incremental capacities of WPP and ZPP are shown in **Figure 5.3**. It is considered that 3 MW of installed WPP would displace 1 MW of effective FPP capacity, given that the ratio of their average capacity factor (CF, see **Glossary of Terms**) is approximately 1:3; and ZPP replaces FPP on a MW by MW basis thus assuming both have the same average CF. To account for the lower CF of WPP it is assumed that the plant margin[24] increases over a fixed SMD of 2,665 MW as wind penetration rises. These assumptions are based on the conclusions of recent studies [84], [60] concerning power system management and operation.

[24] Plant margin is usually defined as the amount by which the net generation capacity (i.e. directly connected and able to generate) exceeds that strictly required to cover SMD. This surplus is kept to cover for understated demand forecast, unexpected plant breakdown or unavailability due to maintenance and repair, since generating units are not available to generate 100% of the time. It is usually expressed as a percentage of SMD. Hence a system with a SMD of 2,665 MW and 3,834 MW of NGC will have a safety plant margin of (3,834 - 2,665) / 2,665 = 0.44 or 44%.

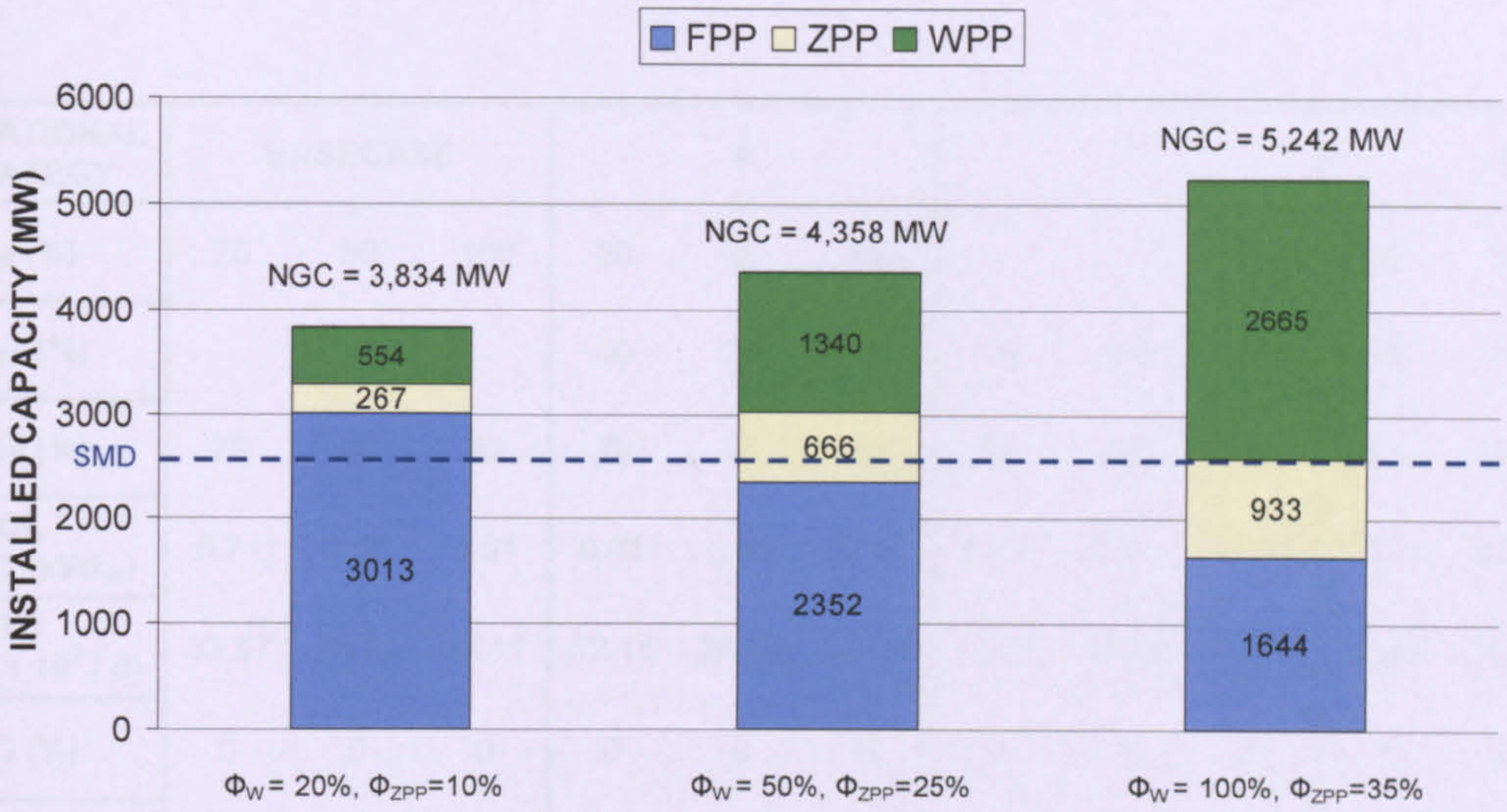

Figure 3. Generating capacities required to Cover SMD for the islanded power system considered without electrolysers deployed.

Clearly because of the low CF of WPP (typically 20-30%) compared to (60-80%) for ZPP and FPP, an increasing net generating capacity (NGC in **Figure 5.3**) is required to cover the same SMD as wind penetration increases. The criteria followed here has been to maintain an "effective plant margin" (do not confuse with plant margin) of 30% of SMD as Φ_W rises to account for periods of low wind availability. For example from **Figure 5.3**, at Φ_W =20%, Φ_{ZPP} = 10%, 554 MW of installed WPP capacity equals to (554 / 3) = 185 MW of "effective thermal (ZPP or FPP) generating capacity" since the ratio of their average CF is roughly 1:3. This 185 MW added to 267 MW of ZPP capacity and 3,013 MW of FPP capacity will make up to 3,465 MW of "effective thermal capacity", which gives (3,465 – 2,665) / 2,665 = 0.30 or 30% of "effective plant margin".

5.3.2 Results for CASE 1 (SSE only)

CASE 1 includes an electrolyser stock deployed at or near WPP and ZPP. Some zero-carbon fossil electricity from ZPP and wind-derived electricity is directed to the grid, the remaining being directed to the SSE stock. Electrolysers are powered solely by WPP and ZPP, and so zero-carbon hydrogen is produced. Results for the low and variable wind scenarios considered are shown in **Tables 5.1 and 5.2**.

OPERATIONAL STRATEGY	BASECASE			A			B			C		
Φ_W (%)	20	50	100	20	50	100	-	-	-	20	50	100
Φ_{ZPP} (%)	-	-	-	10	25	35	10	25	35	10	25	35
LF_{TH} (%)	79	80	82	79	81	85	86	92	95	87	94	100
CI_e (kg CO_2/kWh$_e$)	0.71	0.60	0.51	0.68	0.53	0.41	0.71	0.57	0.44	0.70	0.52	0.36
TC (t $CO_2 \times 10^3$ / d)	33.57	28.37	24.11	32.15	25.06	19.38	33.57	26.95	20.80	33.09	24.58	17.02
WC (%)	0	0	0	0	0	0	0	0	0	0	0	0
Y_H (t H_2 / d)	26	48	110	82	226	370	92	174	209	123	216	302
UF_E (%)	11	10	10	30	34	29	80	60	52	35	30	24
IC_E (MW)	455	1,105	2,240	575	1,405	2,660	240	600	840	695	1,515	2,650
NGC (MW)	4,289	5,463	7,482	4,409	5,763	7,902	3,705	4,065	4,305	4,529	6,063	7,892
β_E (%)	11	20	30	13	24	34	6	15	20	15	26	34

Table 5.1. Results for CASE 1. Low Wind Scenario

OPERATIONAL STRATEGY	BASECASE			A			B			C		
Φ_W (%)	20	50	100	20	50	100	-	-	-	20	50	100

Φ_{ZPP} (%)	-	-	-	10	25	35	10	25	35	10	25	35
LF_{TH} (%)	90	94	96	85	91	93	91	100	100	93	100	100
CI_e (kg CO_2/kWh$_e$)	0.68	0.55	0.47	0.62	0.41	0.24	0.68	0.46	0.29	0.62	0.29	0.07
TC (t $CO_2 \times 10^3$ / d)	20.9	16.9	14.5	19.4	12.6	7.4	20.9	14.2	8.9	19.1	11.4	6.5
WC (%)	0	0	0	0	0	0	-	-	-	0	0	0
Y_H (t H_2 / d)	88	165	415	131	335	622	71	126	126	121	222	435
UF_E (%)	52	39	33	47	50	49	62	44	31	37	31	34
IC_E (MW)	455	1,105	2,240	575	1,405	2,660	240	600	840	695	1,515	2,650
NGC (MW)	4,289	5,463	7,482	4,409	5,763	7,902	3,705	4,065	4,305	4,529	6,063	7,892
β_E (%)	11	20	30	13	24	34	6	15	20	15	26	34

Table 5.2. Results for CASE 1. Variable Wind Scenario

For Strategies A and C, both electricity from ZPP and wind-derived electricity are directed to the grid to cover a proportion of consumer demand, thus reducing the carbon intensity of delivered electricity and hence total carbon emissions derived from electricity generation for all wind penetrations with respect to the Base Case, where no ZPP are available in the power system. The relationship between the carbon intensity of electricity CI_e and wind power penetration Φ_W is plotted in **Figures 5.4 and 5.5**.

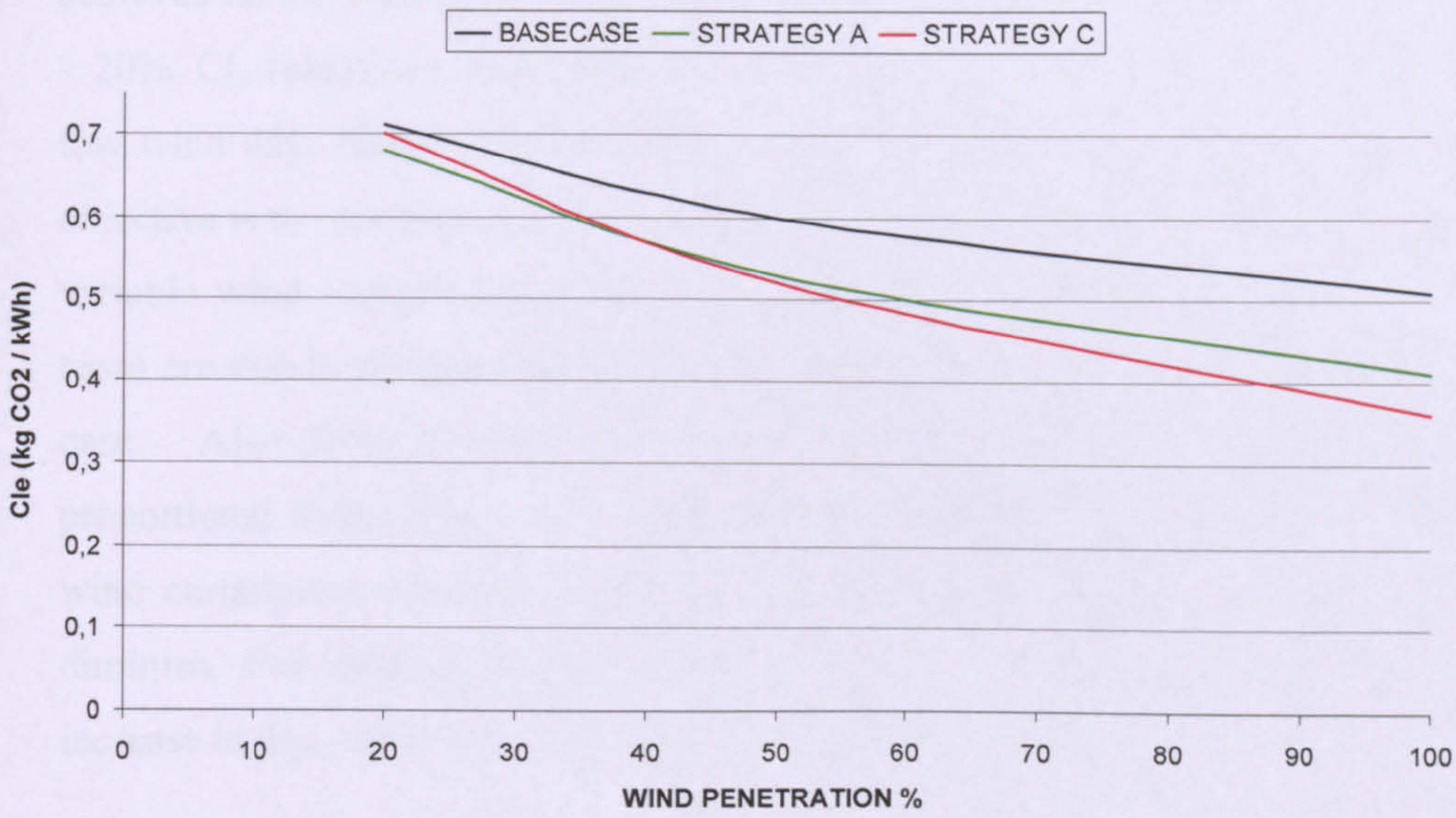

Figure 5.4. CASE 1. Average daily carbon intensity of electricity CI_e versus wind power penetration for low wind scenario.

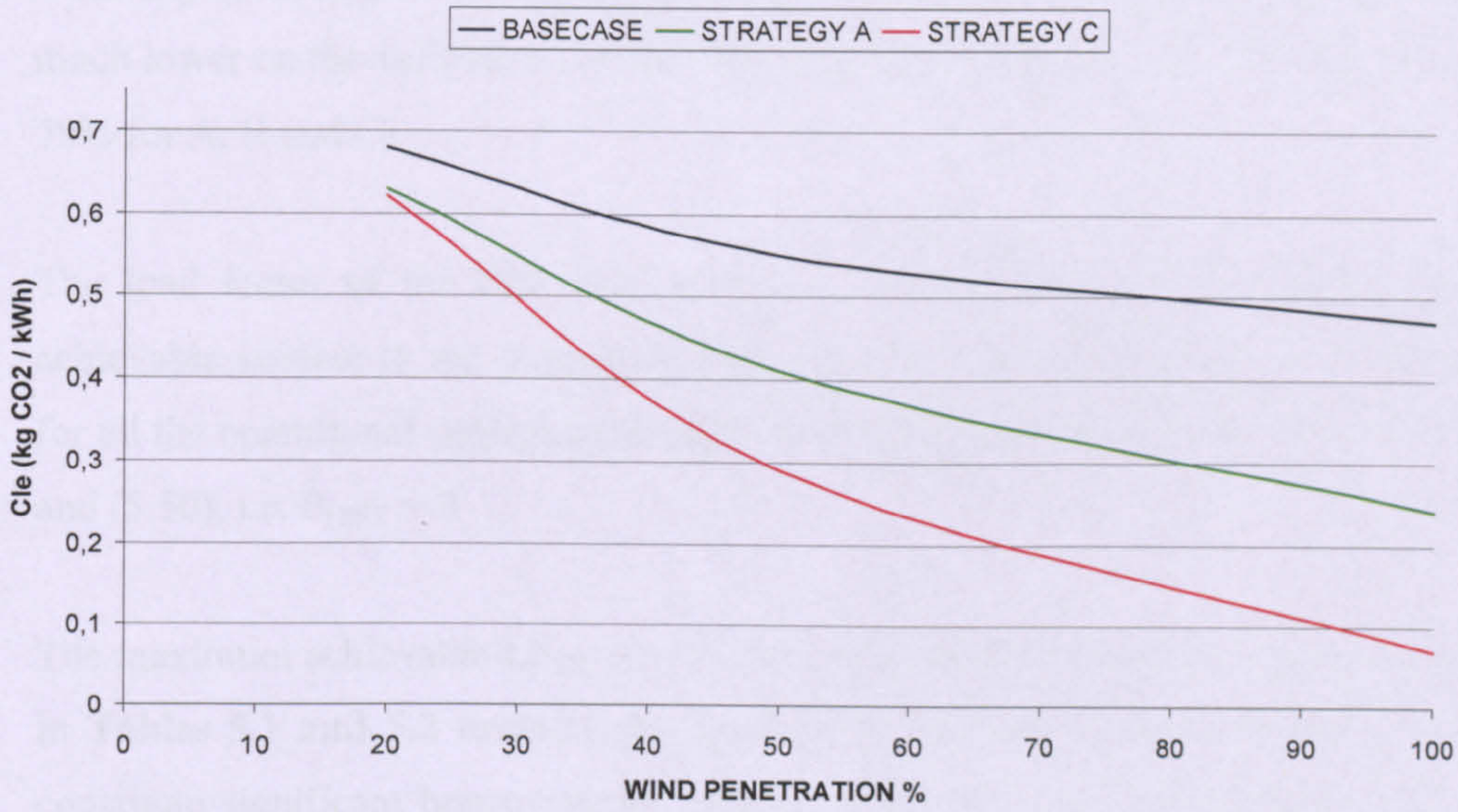

Figure 5.5. CASE 1. Average daily carbon intensity of electricity CI_e versus wind power penetration for variable wind scenario.

Looking at **Figure 5.5**, higher reductions in CI_e with respect to the Base Case are achieved on the variable wind day for Strategies A and C. For $\Phi_{ZPP} > 10\%$ and $\Phi_W > 20\%$ CI_e values are 13-85% less on the variable wind day and 5-29% less on the low wind day. Hence ZPP are clearly more effective than WPP when the main objective is to minimize CI_e. The differences in values of CI_e between the low and variable wind scenario for Strategy B (remember no WPP are deployed in this case) are due to different demand profiles applied as inputs to the model in each case. Also from **Figures 5.4 and 5.5**, the reduction of CI_e increases is proportional to the increase in wind penetration at $\Phi_W < 40\%$. Above this value wind curtailment becomes significant and the carbon benefits of increasing Φ_W diminish. For strategy B the reduction of CI_e is roughly proportional to the increase in Φ_{ZPP} since there are no wind curtailment issues.

Total carbon emissions from electricity generation, TC, achieve identical reductions to those of CI_e with respect to the Base Case. Note TC values are obtained multiplying CI_e values by the total system demand on the day selected. Total consumer demand on the variable wind day is 35% lower than on the low wind day (30.75 GWh vs 47.3 GWh respectively) and therefore TC values are much lower on the variable wind day (e.g. less than half at $\Phi_{ZPP} > 25\%$ and $\Phi_W > 50\%$ for A, B and C).

The load factor of the FPP load profile is calculated as the maximum value achievable subject to the restriction that only zero-carbon hydrogen is produced for all the operational strategies considered, as expressed in equations (5.6), (5.29) and (5.50), i.e. $P_{FPSE} = 0$

The maximum achievable LF_{TH} for the low and variable scenario are those shown in **Tables 5.1 and 5.2** respectively. Load Factors obtained when including ZPP constitute significant improvements relative to the Base case, approaching 100% (e.g. a flat FPP load profile) even for the low wind scenario for wind penetrations of 100%. Wind curtailment is completely eliminated for all strategies and wind scenarios. Note this is extremely important especially for high wind penetrations

above 30%, where a large part of the resource is wasted when no electrolysers are implemented (see **Chapter 4.3.1**).

The hydrogen yield Y_H increases significantly with respect to the Base Case, particularly on a low wind day. This is plotted in **Figure 5.6**. For strategy A, up to 5 fold for $\Phi_{ZPP} = 25\%$, $\Phi_W = 50\%$ and for strategy C, up to 5 fold for $\Phi_{ZPP} = 10\%$, $\Phi_W = 20\%$; and to a less extent for strategy B. Once $LF_{TH} = 100\%$ is achieved for B, two different optimization strategies could be followed as Φ_{ZPP} further increases:

1. To minimize CI_e (increasing P_{ZPG} to reduce P_{FPP} at the expense of maintaining P_{ZPSE} constant) and then keep Y_H constant.
2. To maximize Y_H (increasing P_{ZPSE} at the expense of maintaining P_{ZPG} and P_{FPP} constant) and then keep CI_e constant.

The first strategy was selected in this analysis to assess the potential of a deployment of ELS in combination with ZPP to reduce CI_e significantly from those values attained when only WPP are deployed in the power system. This is why Y_H remains constant in **Figure 5.6** even though Φ_{ZPP} increases; but then CI_e reduces as Φ_{ZPP} increases (**Table 5.2**). Clearly there is a trade-off between Y_H and CI_e. This is discussed further in this same chapter in sections 3.4 and 4.

a) Low wind day

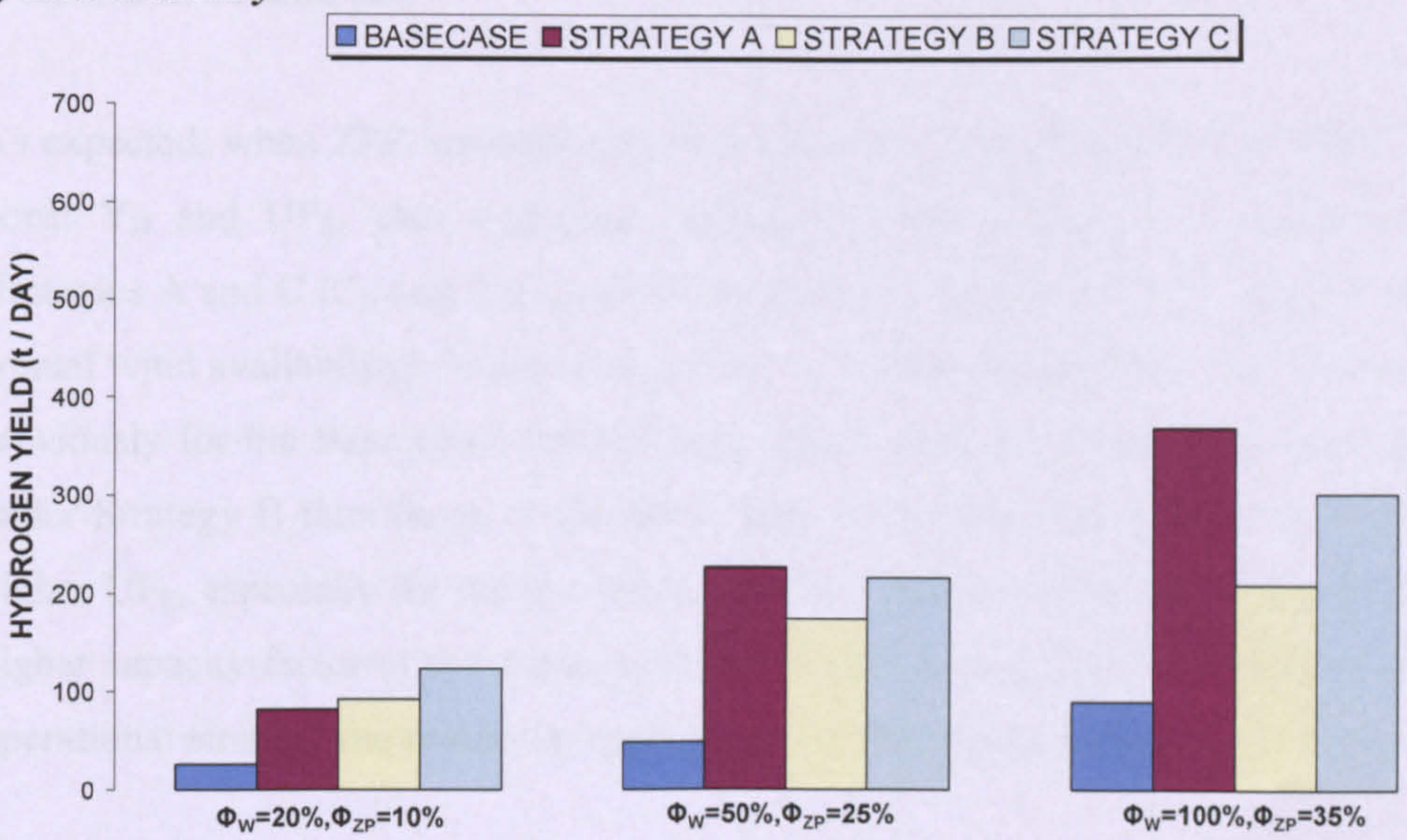

b) Variable wind day

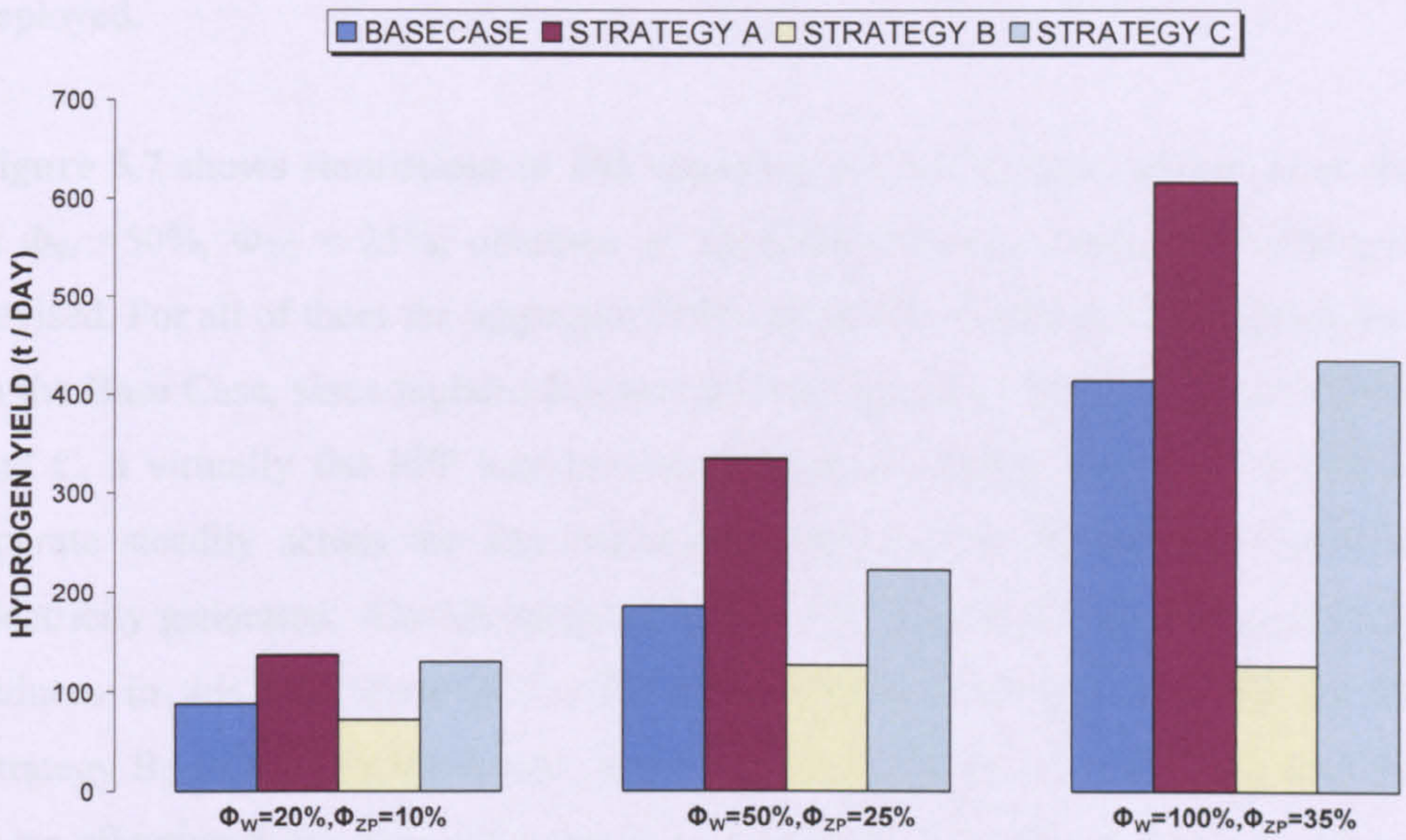

Figure 5.6. CASE 1. Daily hydrogen production versus wind power penetration for the (a) low and (b) variable wind scenario

The utilization factor of electrolysers also increases appreciably on the low wind day, especially for strategy B. For a low LF_{TH} target priority is given to the generation of zero-carbon H_2, whereas for high LF_{TH} target at high Φ_{ZC}, Φ_W an increasing amount of the ZPP output is directed to consumers instead so as to minimize CI_e, which causes UF_E to decrease. Further discussion on UF_E is presented in **Section 5.5.**

As expected, when ZPP are deployed in the power system in addition to WPP to boost Y_H and UF_E, also a greater capacity of electrolysers is required. For strategies A and C IC_E and thus β_E are dictated by the steady wind day (maximum annual wind availability), being between 1.2 – 1.4 times higher than that obtained previously for the Base Case. Interestingly, lower capacities of ELS are required under Strategy B than those of the Base case, at the same time achieving much higher UF_E, especially for the low wind scenario. This is simply due to the much higher capacity factor of the power source, i.e. ZPP, versus WPP. Note under this operational strategy the minimum capacity of the SSE stock required to achieve a

certain LF_{TH} is dictated by the capacity of ZPP available since no WPP are deployed.

Figure 5.7 shows simulations of 24h operation periods for the variable wind day at Φ_W =50%, Φ_{ZC} = 25%, obtained by applying the three operational strategies devised. For all of them the aggregate FPP load profile becomes more regular than in the Base Case, since higher LF_{TH} are achieved when implementing ZPP. For B and C, a virtually flat FPP load profile is achieved, which would allow FPP to operate steadily across the day minimizing their carbon footprint per kWh of electricity generated. Also the daily aggregate FPP output, which determines CI_e, reduces in this case from 26.7 GWh for the Base Case to 22.7 GWh for the Strategy B, 19.8 GWh for A and finally to 18.2 GWh for C, which becomes the more effective if the main objective is to minimize CI_e. The average load placed on fossil plant (average value of the dotted curves in **Figure 5.7**) falls by more than 30% from 1,111 MW for the Base Case down to 760 MW for C.

Finally **Figure 5.8** displays the electrical input to the SSE stock (variable wind day at Φ_W =50%, Φ_{ZC} = 25%) with the discrete contributions of WPP and ZPP for A and C. For A the output of ZPP directed to ELS remains constant across the 24h period, the remainder being used for baseload electricity generation; whereas for C the ZPP output to ELS is reduced during the afternoon period and then ZPP is used mainly for peak electricity generation in order to minimize CI_e. The proportions of ZPP output directed to ELS and to supply consumers' demand could be adapted to a specific energy system as well as changed across days depending on the preferred carbon abatement strategy and the hydrogen and electricity demands. Further discussion on this topic is offered below in **Section 5.5.**

Looking at **Figure 5.8c** for the strategy B the output from ZPP is controlled in such a manner that hydrogen is mainly produced during low demand periods (i.e. at morning and night time) whereas during the afternoon period when consumer demand is at its highest level, ZPP is directed primarily to satisfying this demand (see **Figure 5.7c**). While in the Base Case the SSE stock is exclusively supplied by

WPP and therefore subject to wind availability, the deployment of ZPP in addition to WPP for strategies A and C allows a more flexible operation since the ratio of electricity supplied to consumers and to SSE (P_{ZPG} / P_{ZPSE} in **Figure 5.2**) can be modified at will in order to (i) maximize the production of hydrogen during periods of low consumers' demand and (ii) improve LF_{TH} and by implication minimize the FPP carbon footprint. This flexibility is one of the advantages of deploying ZPP in a power system containing a large stock of electrolysers.

Note that the total aggregate ZPP output, which is the sum of the ZPP output delivered to the grid in **Figure 5.7** and the ZPP output delivered to the SSE in **Figure 5.8,** remains constant across the day at ZPP full rate, in this particular case 2,665 (SMD) × 0.25 (Φ_{ZPP} = 25%) × 0.9 (CF_{ZPP} = 90%) = 600 MW. This minimizes load changes on the operation of ZPP and therefore the wear and tear imposed on them.

a)

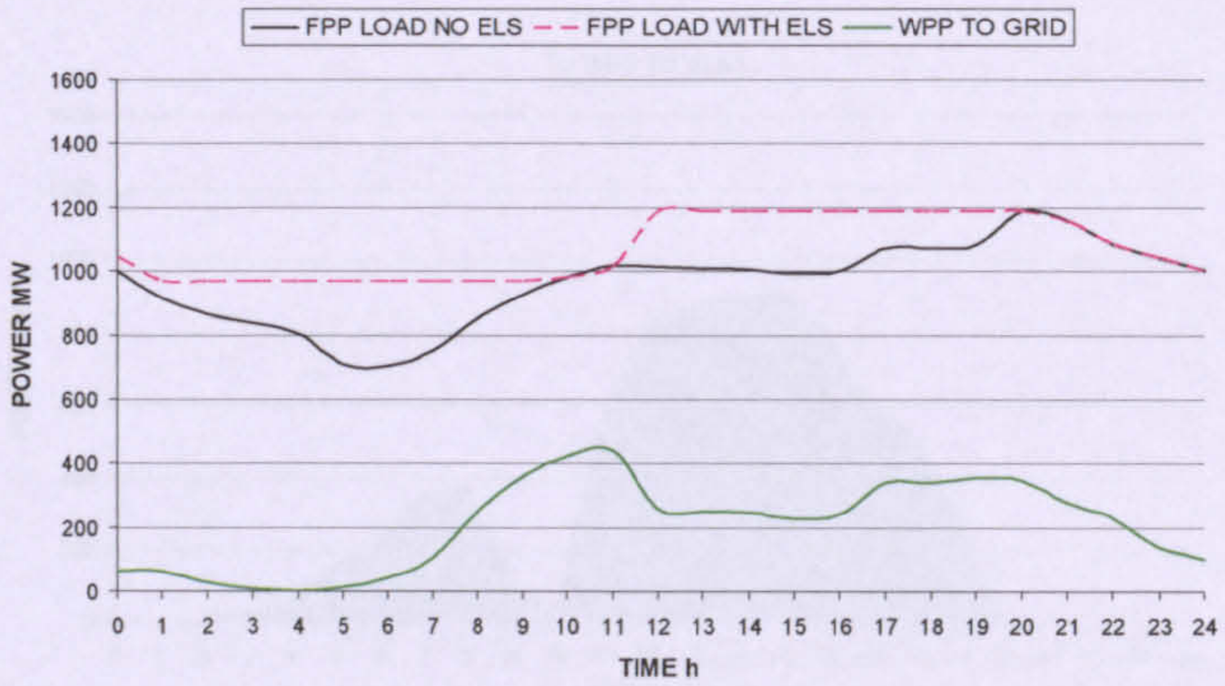

b)

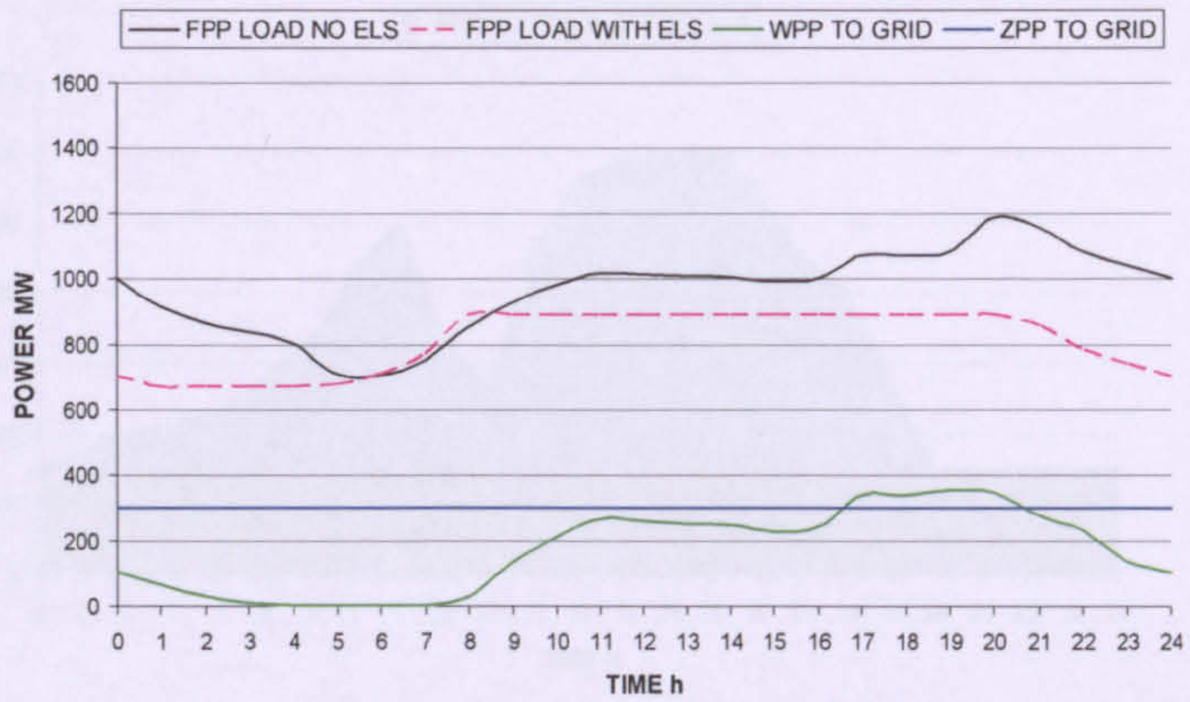

c)

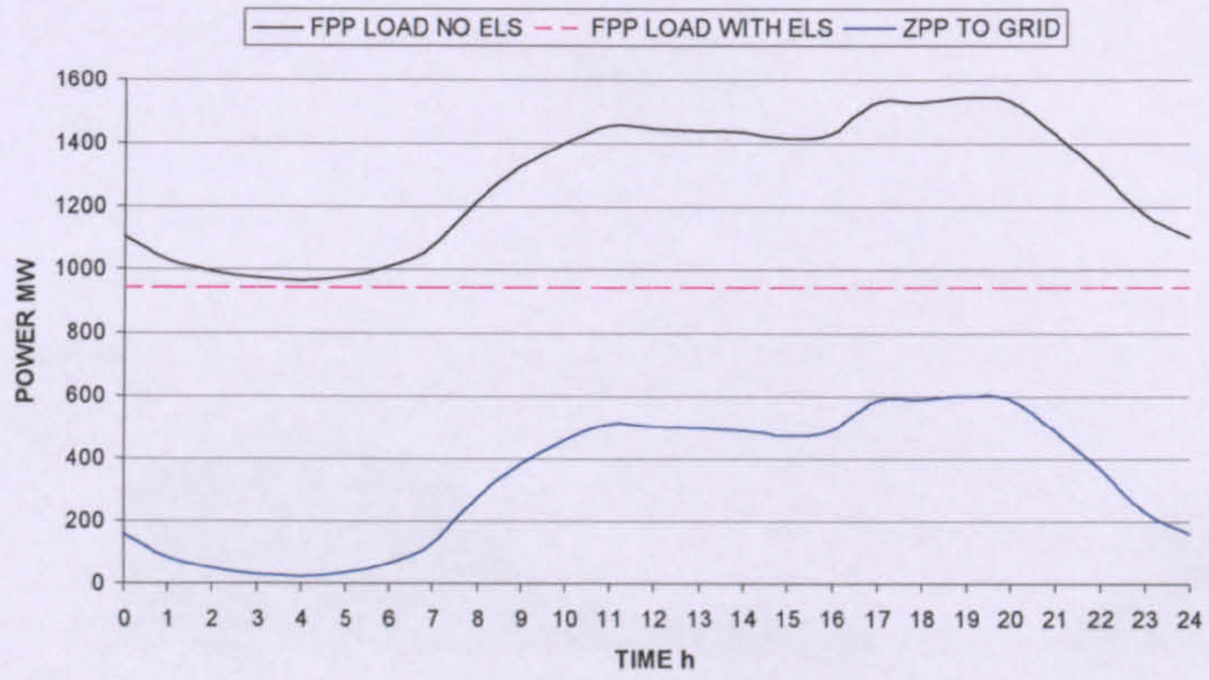

d)

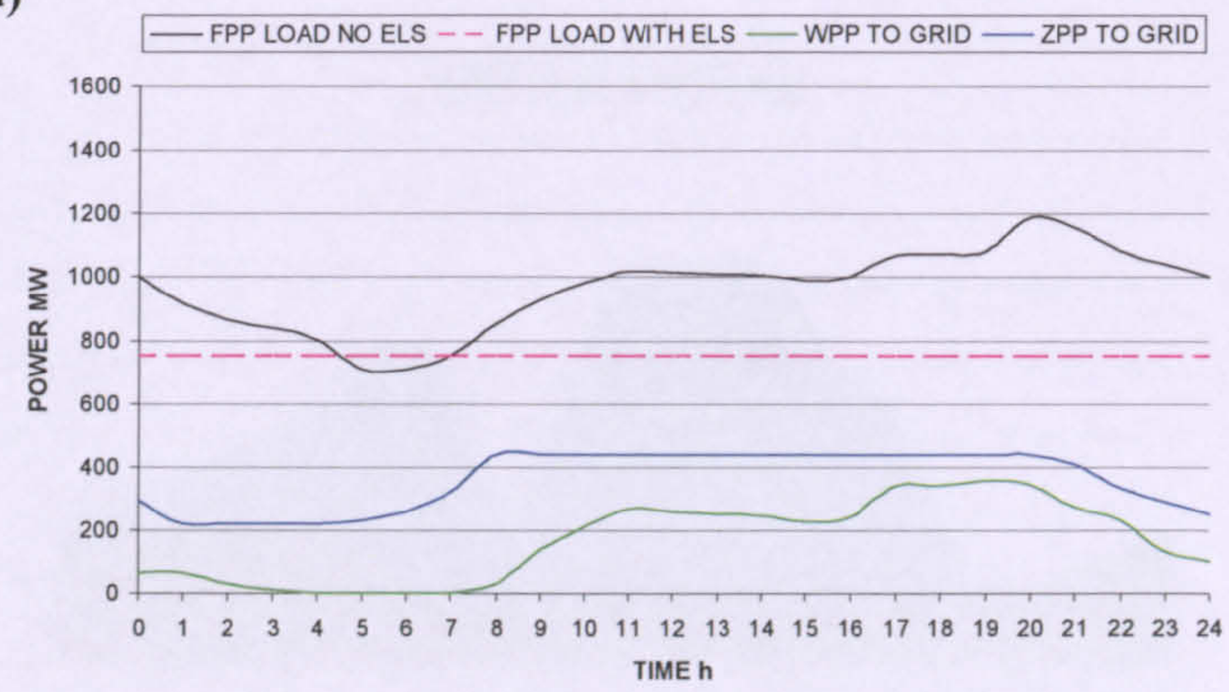

Figure 5.7. CASE 1. Variable wind day. Influence of the operation of SSE in the aggregate FPP load, WPP and ZPP output delivered to grid.

a) Base case
b) Strategy A
c) Strategy B
d) Strategy C

a)

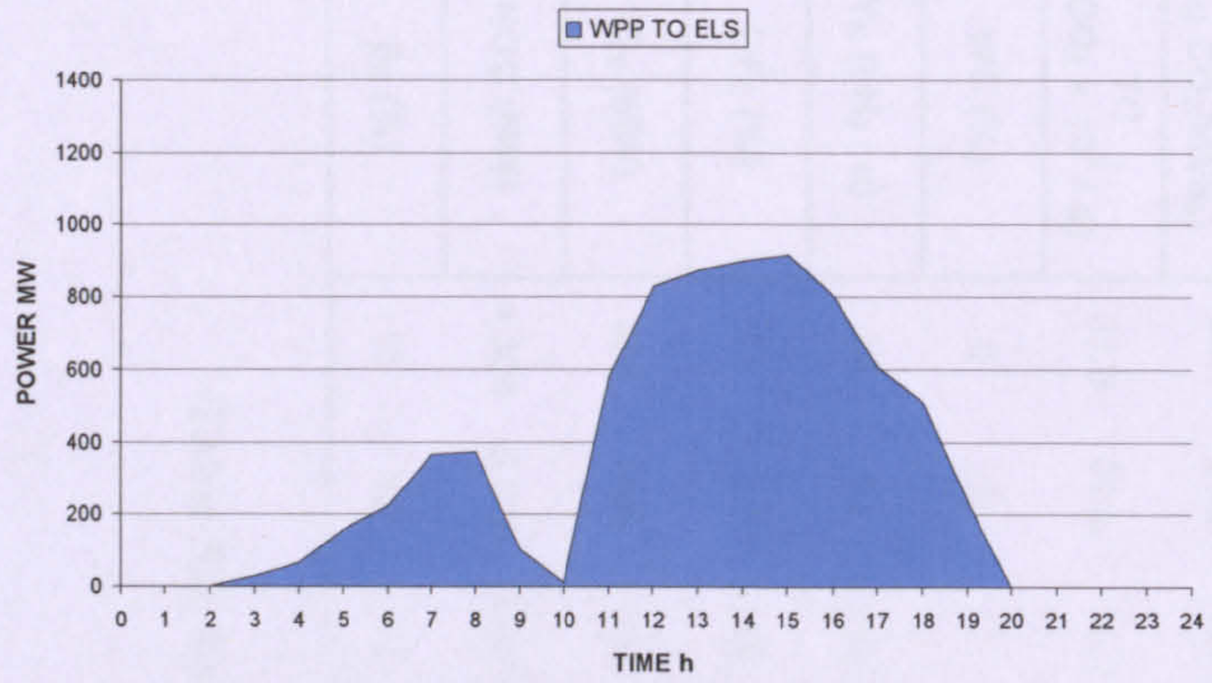

b)

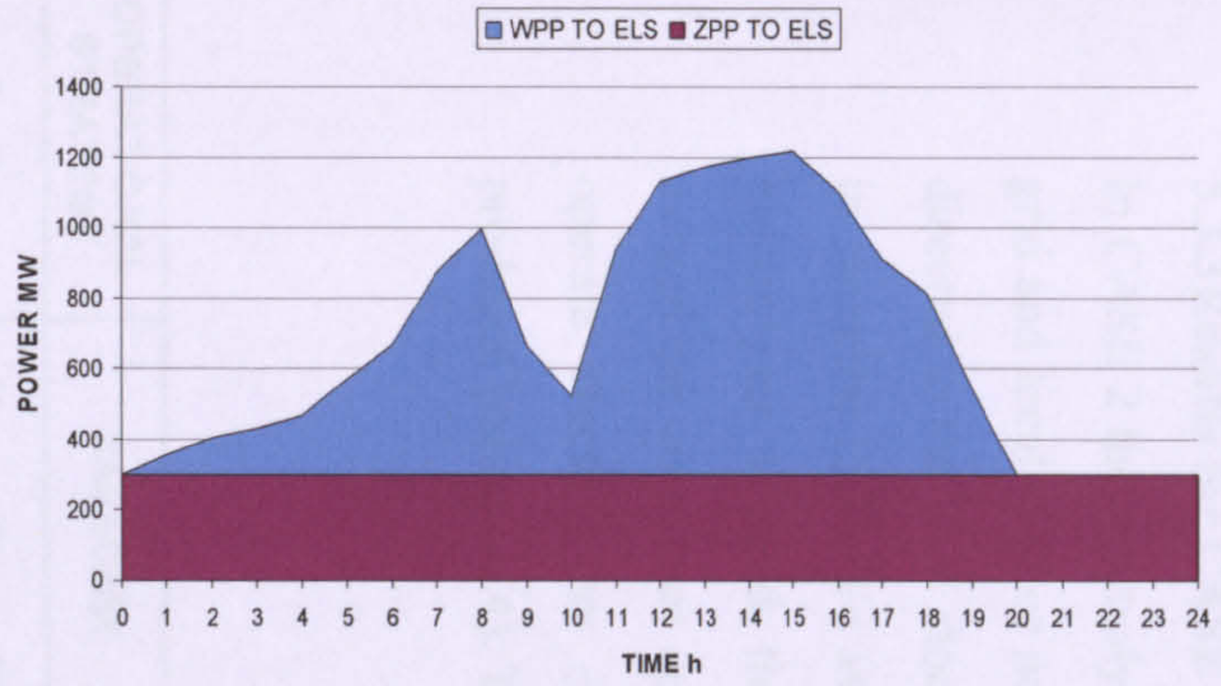

c)

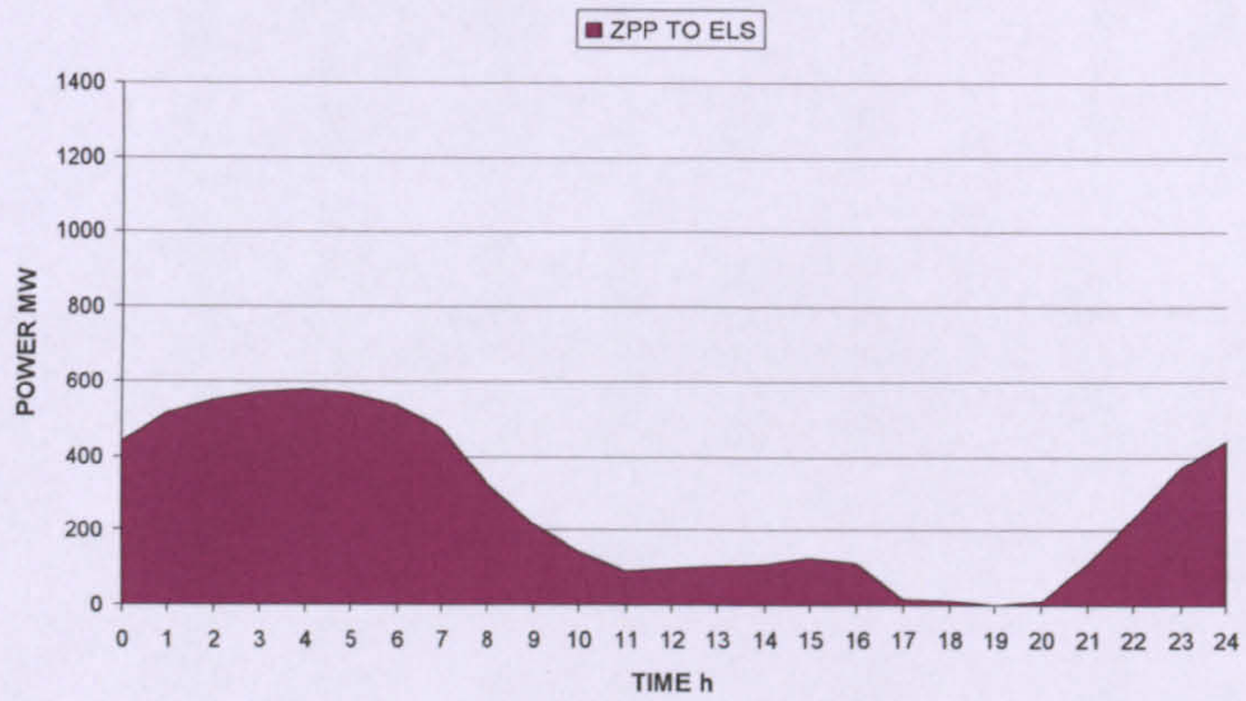

d)

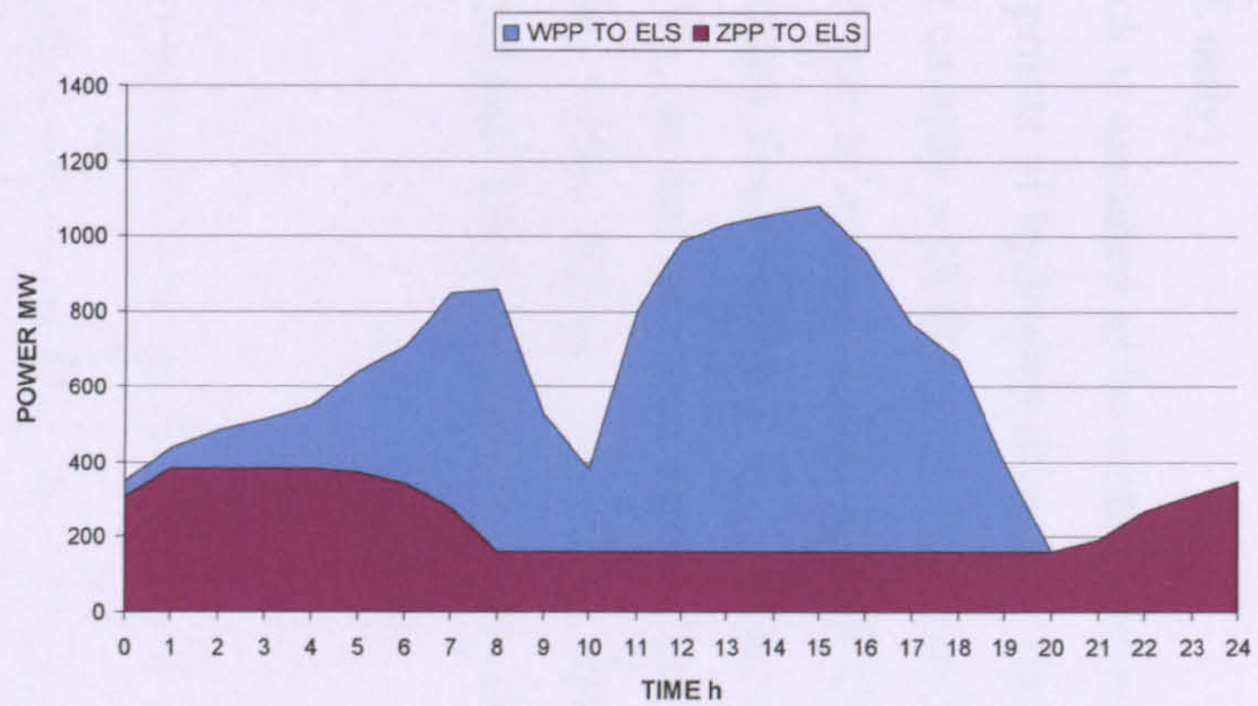

Figure 5.8. CASE 1. Variable wind day. Aggregate electrical input to the "supply-side electrolyser stock".

a) Base case
b) Strategy A
c) Strategy B
d) Strategy C

5.3.3Results for CASE 2 (DSE only)

In CASE 2 the electrolyser stock is assumed to be embedded within the electrical grid and located at or near the points of hydrogen demand. Total electrical power directed to the DSE stock must comply with the load limit condition as expressed in equation (5.1). To avoid the use of any fossil-derived electricity to cover the electrolyser demand, the aggregate fossil thermal load, P_{FPP}, is not allowed to exceed the consumer demand, P_C, so that no fossil-derived electricity is used to operate electrolysers (equation 5.13). Hence only zero-carbon hydrogen is produced (equation 4). **Tables 5.3 and 5.4** display main results for CASE 2.

OPERATIONAL STRATEGY	BASECASE			A			B			C		
Φ_W (%)	20	50	100	20	50	100	-	-	-	20	50	100
Φ_{ZPP} (%)	-	-	-	10	25	35	10	25	35	10	25	35
LF_{TH} (%)	79	80	82	79	81	85	86	92	95	87	94	100
CI_e (kg CO_2/kWh$_e$)	0.71	0.58	0.44	0.68	0.53	0.41	0.72	0.57	0.44	0.70	0.52	0.36
TC (t $CO_2 \times 10^3$ / d)	33.8	27.6	21.0	32.4	25.2	19.5	33.8	27.1	21.0	33.3	24.8	17.1
WC (%)	0	0	3	0	0	0	-	-	-	0	0	0
Y_H (t H_2 / d)	26	48	102	82	226	370	92	174	209	123	216	302
UF_E (%)	11	16	28	29	38	57	78	59	52	35	33	36
IC_E (MW)	455	645	745	575	1,170	1,340	240	600	840	695	1,415	1,760
NGC (MW)	4,304	5,338	7,482	4,409	5,528	6,582	3,705	4,065	4,305	4,529	5,773	7,002
β_E (%)	11	12	10	13	21	20	6	15	20	15	25	25

Table 5.3. Results for CASE 2. Low Wind Scenario

OPERATIONAL STRATEGY	BASECASE			A			B			C		
Φ_W (%)	20	50	100	20	50	100	-	-	-	20	50	100
Φ_{ZPP} (%)	-	-	-	10	25	35	10	25	35	10	25	35
LF_{TH} (%)	86	90	94	86	93	95	91	100	100	94	100	100
CI_e (kg CO_2/kWh$_e$)	0.68	0.55	0.47	0.63	0.41	0.25	0.68	0.46	0.29	0.62	0.29	0.07
TC (t $CO_2 \times 10^3$ / d)	20.9	16.9	14.5	19.4	12.6	7.7	20.9	14.1	8.9	19.1	11.4	6.5
WC (%)	0	37	63	0	24	51	-	-	-	0	25	51
Y_H (t H_2 / d)	71	93	78	136	270	345	71	126	126	129	230	293
UF_E (%)	35	30	22	49	48	54	62	44	31	41	41	52
IC_E (MW)	455	645	745	575	1,170	1,340	240	600	840	645	1,160	1,160
NGC (MW)	4,304	5,338	7,482	4,409	5,528	6,582	3,705	4,065	4,305	4,529	5,773	7,002
β_E (%)	11	12	10	13	21	20	6	15	20	15	20	17

Table 5.4. Results for CASE 2. Variable Wind Scenario

The maximum achievable LF_{TH} is a function of the restrictions imposed by equations (3) and (4), and therefore the same values as in Case 1 are obtained for the low and variable wind days. Values for the carbon intensity of electricity, CI_e, and total carbon emissions, TC, are equal to those obtained for Case 1 since these are directly determined by the LF_{TH} target.

As the electrolyser stock is embedded within the grid, the elimination of wind curtailment cannot be achieved because the low-load limit restriction does not allow all available WPP production to come into the grid (see **Chapter 4**). Still, the amount of WPP generation that must be discarded is reduced by 19-35% with respect to the Base Case.

For the low wind scenario, identical hydrogen production rates Y_H as in Case 1 are obtained because wind availability is low on this day and thus no wind curtailment occurs for $\Phi_W \leq 100\%$, although the utilization factor of ELS is now higher for strategies A and C. However for the variable wind day Y_H values are clearly lower than in Case 1 for $\Phi_W > 20\%$ (e.g. reducing from 584 t H_2/day to 293 t H_2/day for Strategy C at $\Phi_W = 100\%$, $\Phi_{ZC} = 35\%$). These are shown in **Figure 9**. The reduction of Y_H from Case 1 to Case 2 is related to the amount of wind curtailed WC. In Case 2 there is a limit to the wind generation than can be absorbed by the grid and directed to DSE and the rest has to be curtailed (WC in **Table 4**), whereas if SSE are deployed (Case 1), the wind power output otherwise curtailed can be used to produce more hydrogen and WC = 0. Note that for both SSE and DSE implementations it is implicit that ELS are able to handle intermittent wind input profiles (see main model assumptions in **Chapter 3**). This assumption is further discussed in **Chapter 6**.

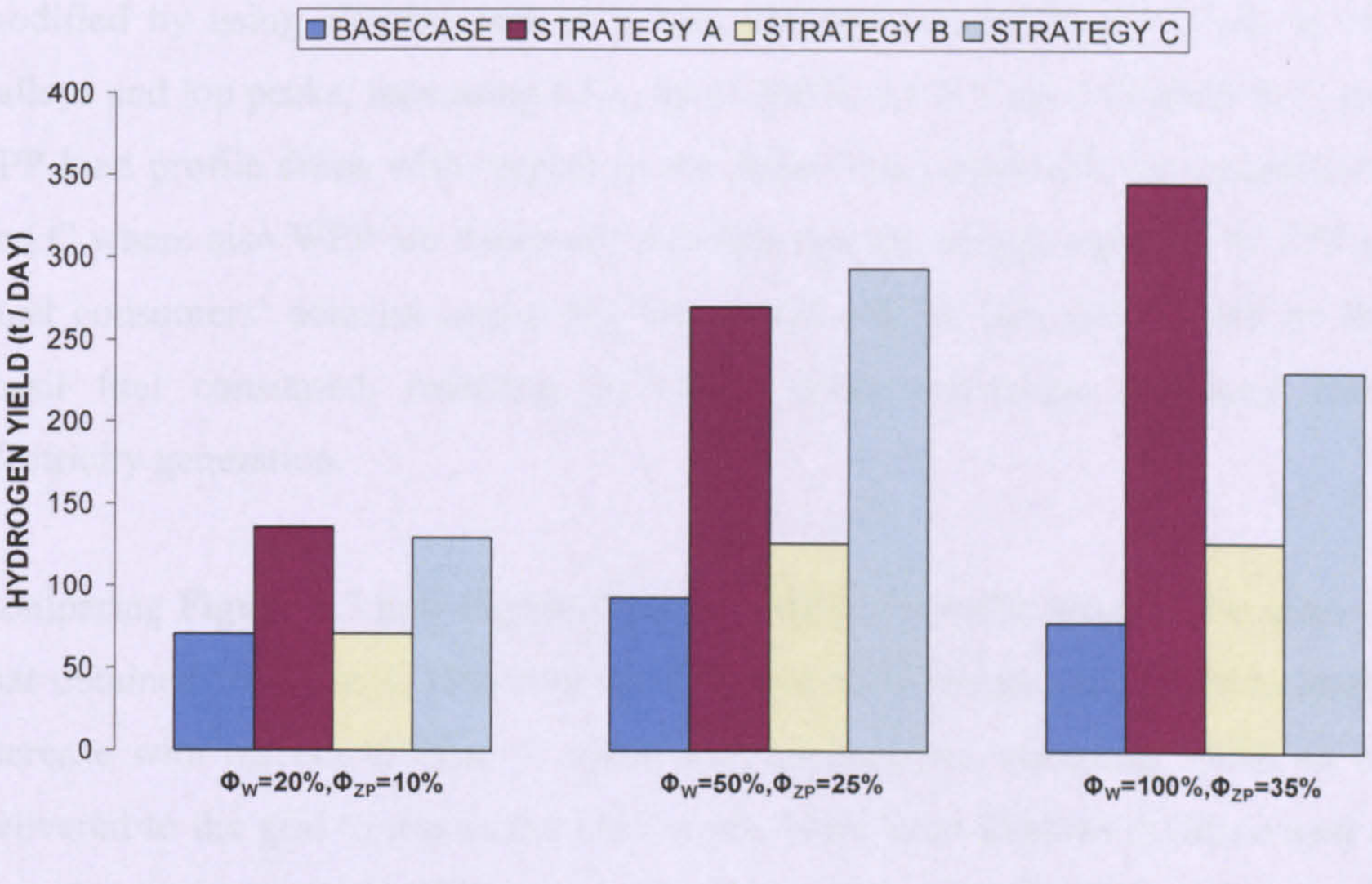

Figure 5.8. CASE 2. Daily hydrogen production versus wind power penetration for variable wind day

For Strategies A and C a lower capacity of ELS is required now when the electrolyser stock is deployed on the demand side, and higher UF_E are obtained, particularly for C. The same IC_E and β_E values are obtained for B as in Case 1. Remember IC_E and β_E are determined by the day of maximum wind availability across the year and therefore the same values stand for the low and variable wind day in **Tables 5.3 and 5.4**.

Figure 5.10 displays daily profiles for the variable wind scenario obtained by applying the three operational strategies. As in the Base Case, time-controlled operation of ELS along with ZPP and WPP allows fossil-fuelled power plants to operate more steadily and increase their utilization factor and efficiency, thus reducing carbon emissions emitted per kWh_e produced. When comparing results obtained when including ZPP **(Figure 5.10 b, c and d)** with respect to those of the Base Case (**Figure 5.10a**), it can be observed how B and C permit a virtually flat FPP load profile for $\Phi_{ZC} = 25\%$. The aggregate load to be covered by FPP can be modified by using electrolysers as a load management mechanism both to fill valleys and lop peaks, increasing LF_{TH} up to 100%. As in Case 1 (**Figure 5.7**), the FPP load profile drops with respect to the Base Case, especially for strategies A and C where also WPP are deployed, meaning that the energy supplied by FPP to meet consumers' demand across the 24h period will be less, and so will be the fossil fuel consumed, resulting in lower carbon emissions produced from electricity generation.

Comparing **Figure 5.7 and Figure 5.10**, the FPP load profile remains the same to that obtained for Case 1. However the ZPP and WPP outputs to the grid clearly increase with respect to Case 1, since more zero-carbon electricity needs to be delivered to the grid to power the DSE stock. Note from **Figures 5.10b, c and d** how the total aggregate ZPP output remains constant at 600 MW, only now all ZPP output is directed to the main grid since the DSE is embedded at the bottom the power system. Furthermore, by deploying and controlling a DSE the daily WPP output delivered to the grid becomes smoother, which has key benefits for the operation and management of the power system (see **Chapter 2**).

a)

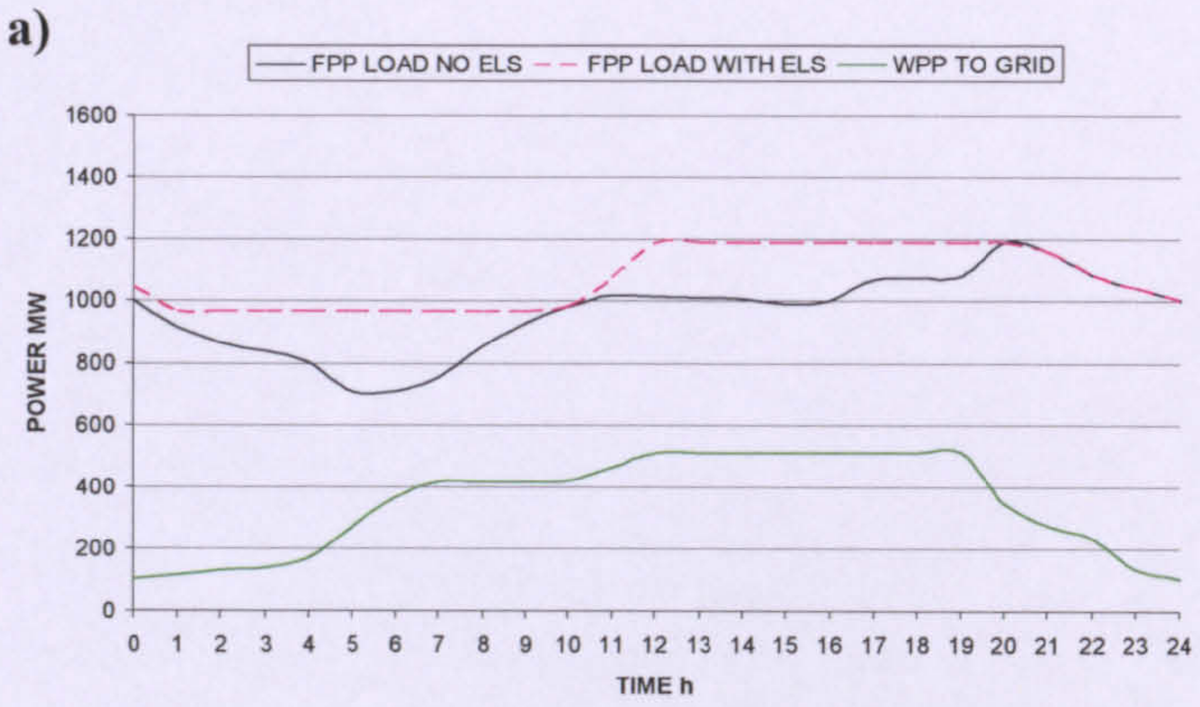

b)

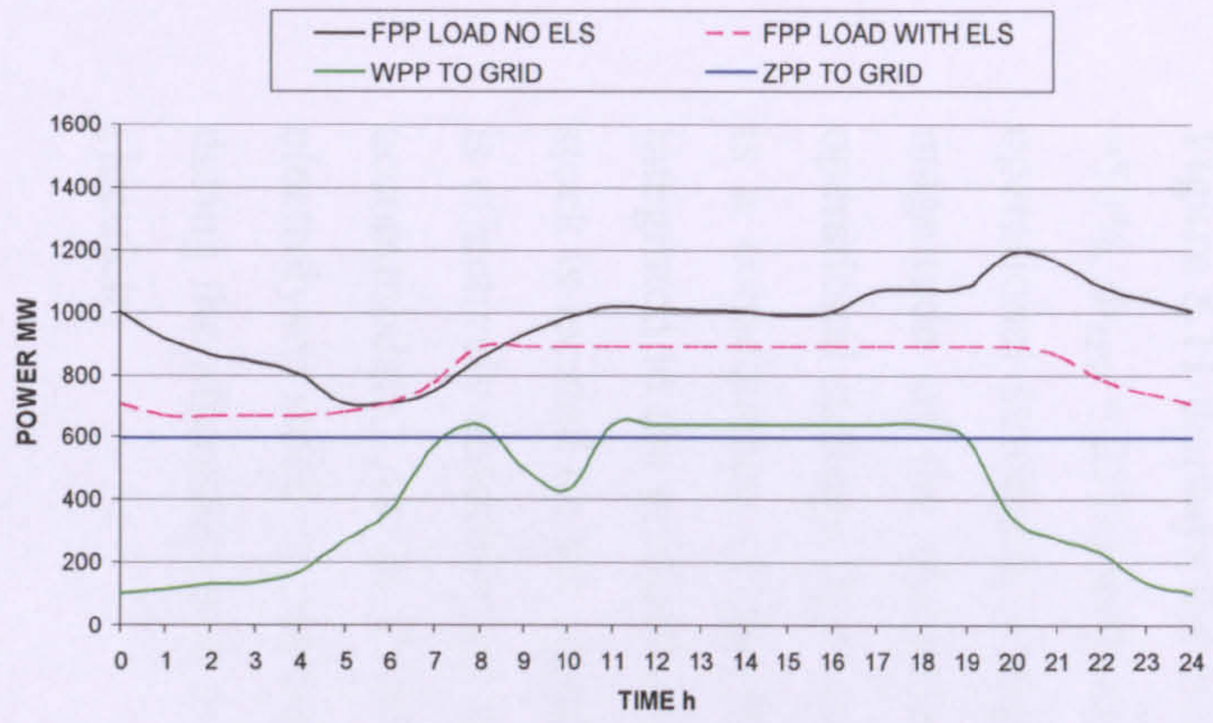

c)

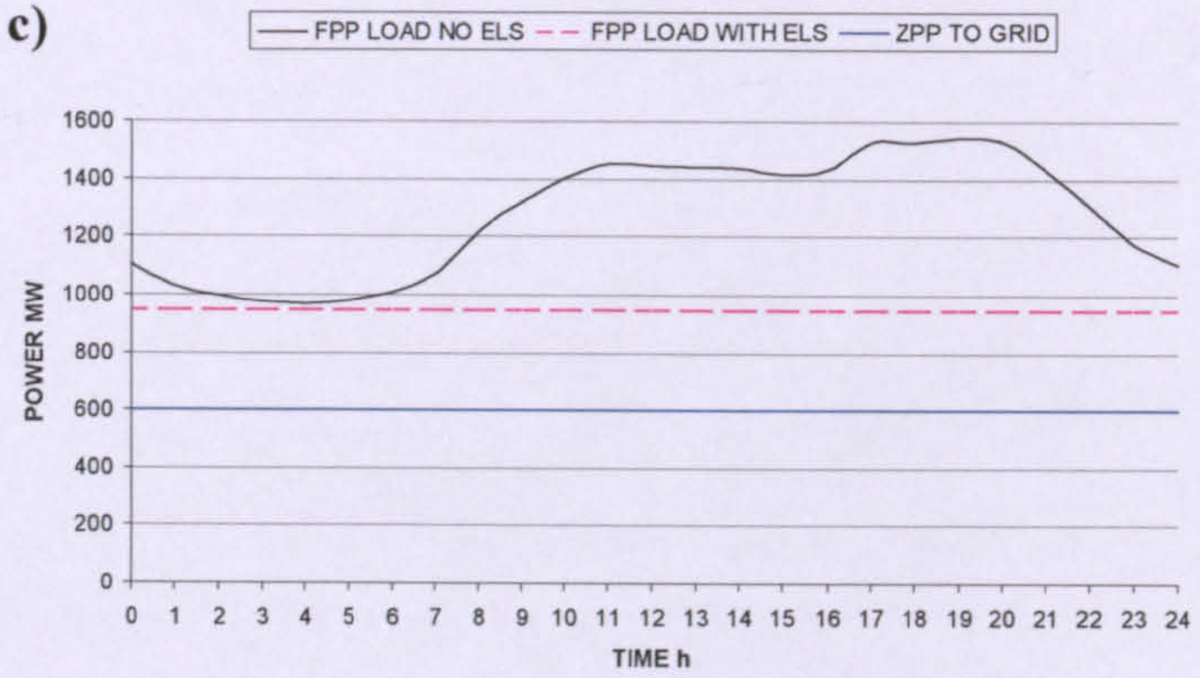

d)

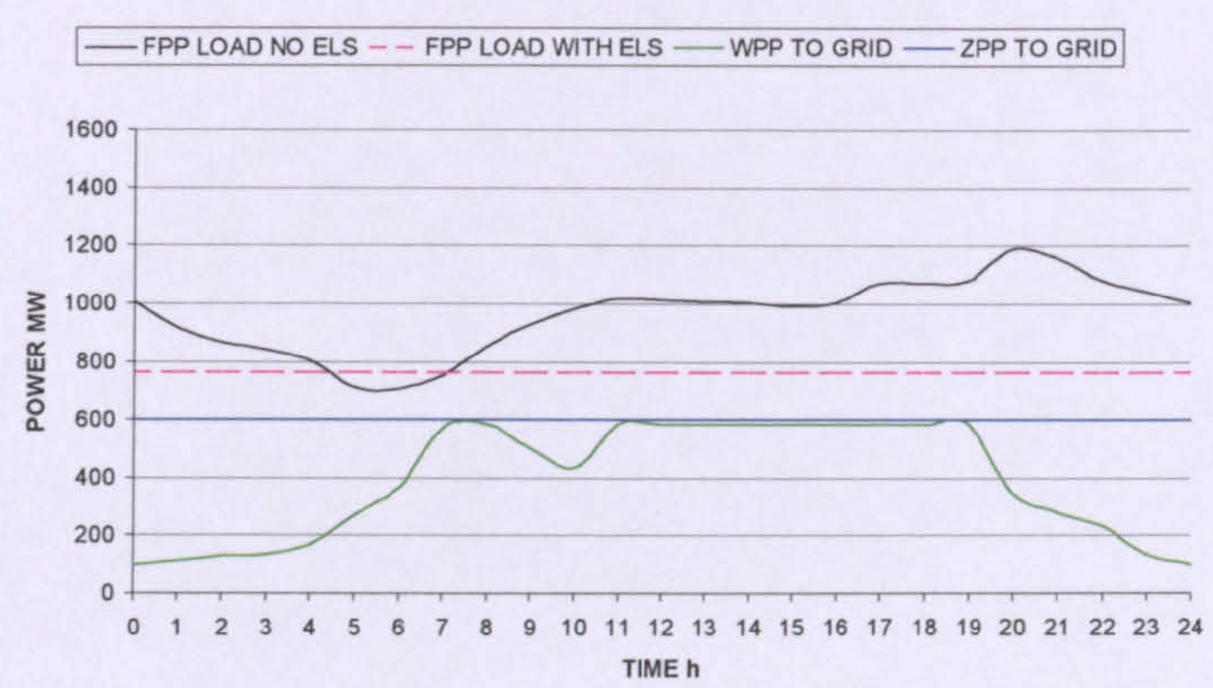

Figure 5.10. CASE 2. Variable wind day. Effects on aggregate fossil load, WPP and ZCPP output delivered to grid and input to electrolysers.

a) Base case
b) Strategy A
c) Strategy B
d) Strategy C

Figure 5.11 displays the electrical input to the DSE stock (variable wind day at Φ_W =50%, Φ_{ZPP} = 25%) with the contributions of both WPP and ZPP. In general for all operational strategies, compared to those obtained for CASE 1 (**Figure 5.8**), the magnitude of the electrical input to the DSE stock is lower (except for the operational strategy B) and therefore lower amounts of hydrogen are produced. This is a consequence of the limitation on the amount of wind power that can be integrated in the grid and directed to ELS. On the other hand when the electrolyser stock is located on the supply side such restriction does not exist and the SSE stock is effectively absorbing all the wind power output that the electricity system can not accommodate. As in CASE 1, for strategy A the ZPP output directed to the electrolyser stock is constant across the day, while for B and C this is reduced during the afternoon period and during that time ZPP is used mainly to meet peak electricity demand.

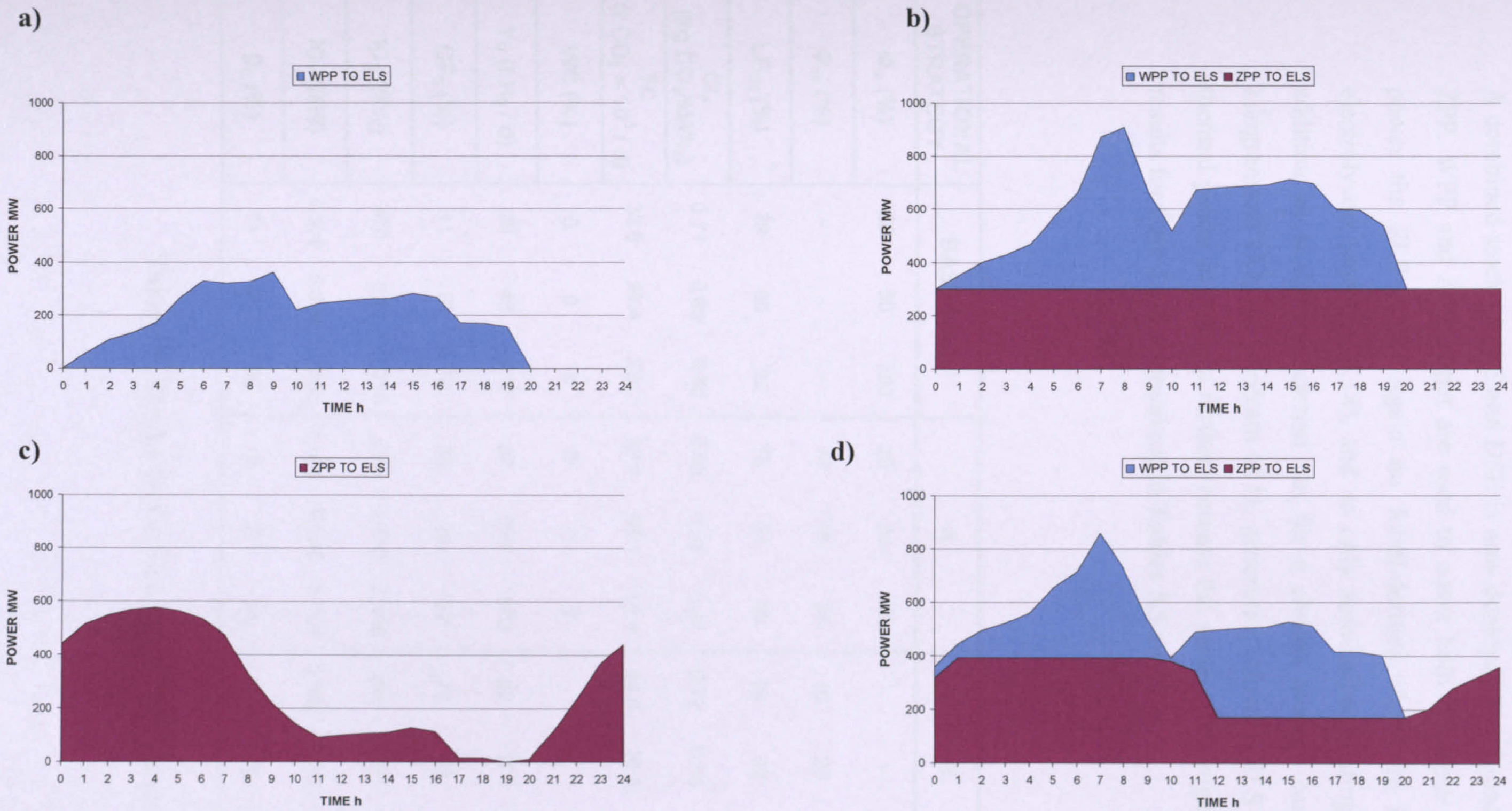

Figure 5.11. CASE 2. Variable wind day. Aggregate electrical input to the "demand-side electrolyser stock".

a) Base case
b) Strategy A
c) Strategy B
d) Strategy C

5.3.4 Results for CASE 3 (Combined stock of SSE and DSE)

A combined stock of SSE and DSE is now deployed in conjunction with WPP and ZPP. WPP and ZPP output are used to cover both consumer demand P_C and to power the ELS stock. Again no fossil-derived electricity is used to operate electrolysers (equation 5.18), and so only zero-carbon hydrogen is produced. In addition an analysis is carried out for a chosen average carbon intensity of 3 kilograms of CO_2 per kilogram of H_2 generated; allowing ELS to take some fossil thermal power in order to further increase the scale of hydrogen production. Main results for Case 3 are summarized in **Tables 5.5 and 5.6**.

OPERATIONAL STRATEGY	BASECASE			A			B			C		
Φ_w (%)	20	50	100	20	50	100	-	-	-	20	50	100
Φ_{zc} (%)	-	-	-	10	25	35	10	25	35	10	25	35
LF_{TH} (%)	79	80	82	79	81	85	86	92	95	87	94	100
CI_e (kg CO_2/kWh$_e$)	0.71	0.60	0.50	0.68	0.53	0.41	0.72	0.56	0.44	0.70	0.52	0.36
TC (t $CO_2 \times 10^3$ / d)	33.6	28.4	23.6	32.1	25.1	19.4	34.0	26.5	20.8	33.1	24.6	17.0
WC (%)	0	0	0	0	0	0	-	-	-	0	0	0
Y_H (t H_2 / d)	26	48	110	82	226	370	92	171	208	123	216	302
UF_E (%)	11	10	10	30	29	27	78	59	52	35	29	23
IC_E (MW)	470	920	2,240	575	1,610	2,895	240	600	840	695	1,580	2,745
IC_T (MW)	4,304	5,338	7,482	4,409	5,988	8,137	3,705	4,065	4,305	4,529	5,938	7,987
β_E (%)	11	21	30	13	27	36	6	15	20	15	27	34

Table 5.5. Results for CASE 3 Low Wind Scenario

OPERATIONAL STRATEGY	BASECASE			A			B			C		
Φ_w (%)	20	50	100	20	50	100	-	-	-	20	50	100
Φ_{zc} (%)	-	-	-	10	25	35	10	25	35	10	25	35
LF_{TH} (%)	90	94	96	86	91	93	91	100	100	94	100	100
CI_e (kg CO_2/kWh$_e$)	0.68	0.55	0.47	0.63	0.41	0.24	0.68	0.46	0.29	0.62	0.29	0.07
TC (t $CO_2 \times 10^3$ / d)	20.9	16.9	14.5	19.4	12.6	7.4	20.9	14.1	8.9	19.1	11.4	6.5
WC (%)	0	0	0	0	0	0	-	-	-	0	0	0
Y_H (t H_2 / d)	88	165	415	136	334	616	71	126	126	129	222	435
UF_E (%)	52	39	33	49	43	44	62	44	31	37	29	33
IC_E (MW)	470	920	2,240	575	1,610	2,895	240	600	840	695	1,580	2,745
IC_T (MW)	4,304	5,338	7,482	5,988	8,137	3,705	4,065	4,305	4,529	5,938	7,987	5,988
β_E (%)	11	21	30	27	36	6	15	20	15	27	34	27

Table 5.6. Results for CASE 3. Variable Wind Scenario

Values for the maximum LF_{TH} achievable are equal to those obtained for Cases 1 and 2, as imposed by equations 3 and 4. Values of CI_e also remain the same as directly subject to the LF_{TH} targeted. Eradication of wind curtailment is achieved across all wind penetrations and operational strategies for the three wind scenarios analysed.

Interestingly, for all operational strategies the hydrogen production rates, Y_H, are the same as those obtained in Case 1 and thus higher than those of Case 2. For strategy C the capacity of a combined stock of SSE and DSE required, expressed as the ratio β_E, is higher than the DSE stock installed in Case 2. This is because a SSE stock is deployed in Cases 1 and 3 to absorb the zero-carbon output of WPP, which

is otherwise curtailed if only DSE are deployed (see **Table 5.5**). The same values of Y_H and same ELS capacity as in Case 1 are obtained for B, and therefore same values of UF_E. However, for the Base Case and strategy A at $\Phi_W > 20\%$ a higher capacity of ELS is required if splitting the ELS stock between SSE and DSE (**Tables 5.5, 5.6**), but (for the same LF_{TH} targeted) the same amount of H_2 as in Case 1 is produced, thus resulting in lesser UF_E of the combined SSE + DSE stock as opposed to deploy simply a SSE stock (**Tables 5.1, 5.2**). Further discussion on the utilization of the ELS stock is offered below in **Section 3.5.2.**

When daily load profiles for CASE 3 are produced following the three operational strategies devised (**Figure 5.12**), the FPP load profiles are the same as those obtained for CASE 1, and so the same values of LF_{TH}, CI_e are obtained. But the WPP and ZPP output delivered to the grid varies because now a DSE is deployed and then more zero-carbon electricity needs to be directed to the main grid to supply both consumer's demand and DSE. Only when the carbon intensity of hydrogen is permitted to exceed zero and operation of ELS is no longer restricted by equations (3) and (4), results for CASE 3 become different to those of CASE 1. This is further discussed below. Interestingly, the aggregate inputs to the ELS stock (SSE + DSE) are identical to those shown in **Figure 5.7** and thus same Y_H are obtained. The only difference is the location of the electrolyser stock. For Case 3 the total ZPP output directed to ELS is halved between SSE and DSE, i.e. the ratio P_{ZPSE} / P_{ZPDE} is taken at 1 (see the description of operational strategies). However this ratio could be changed and adapted to any specific power system, as well as changed from day to day, week to week, and so on according to particular requirements just as specific hydrogen demand requirements, storage availability or delivery availability for the case of hydrogen produced at the supply side through SSE. These are topics related to end-use applications of hydrogen and are explored in more detailed in **Chapter 6**".

a)

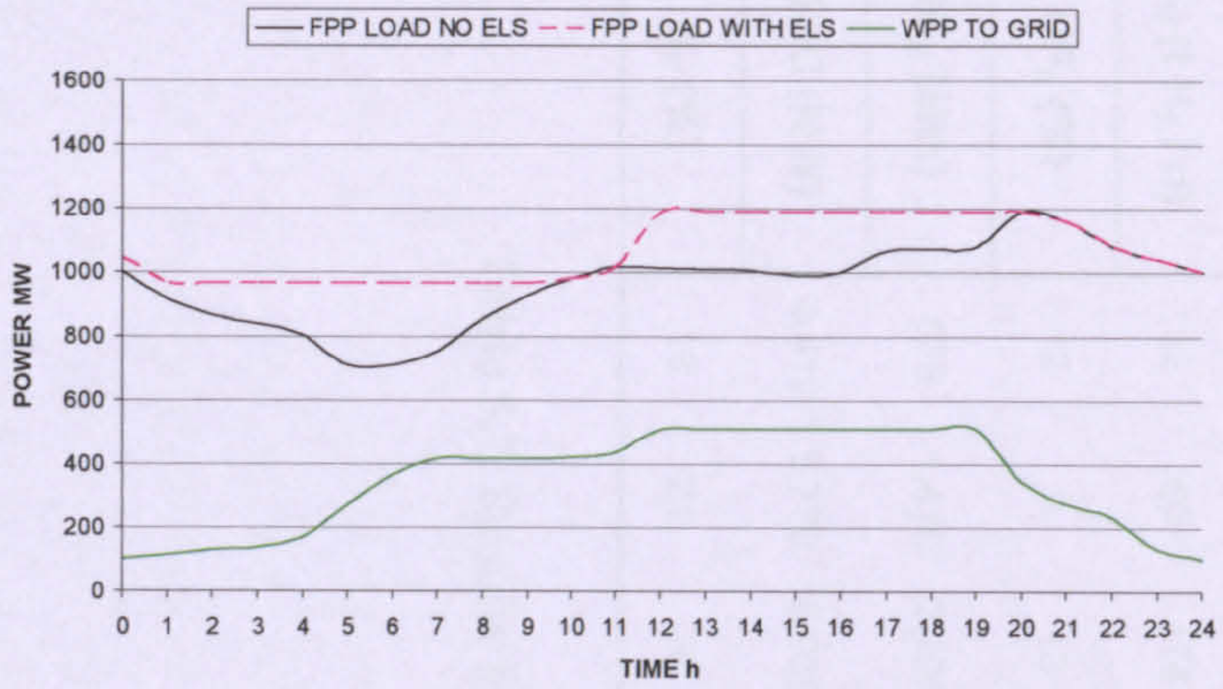

b)

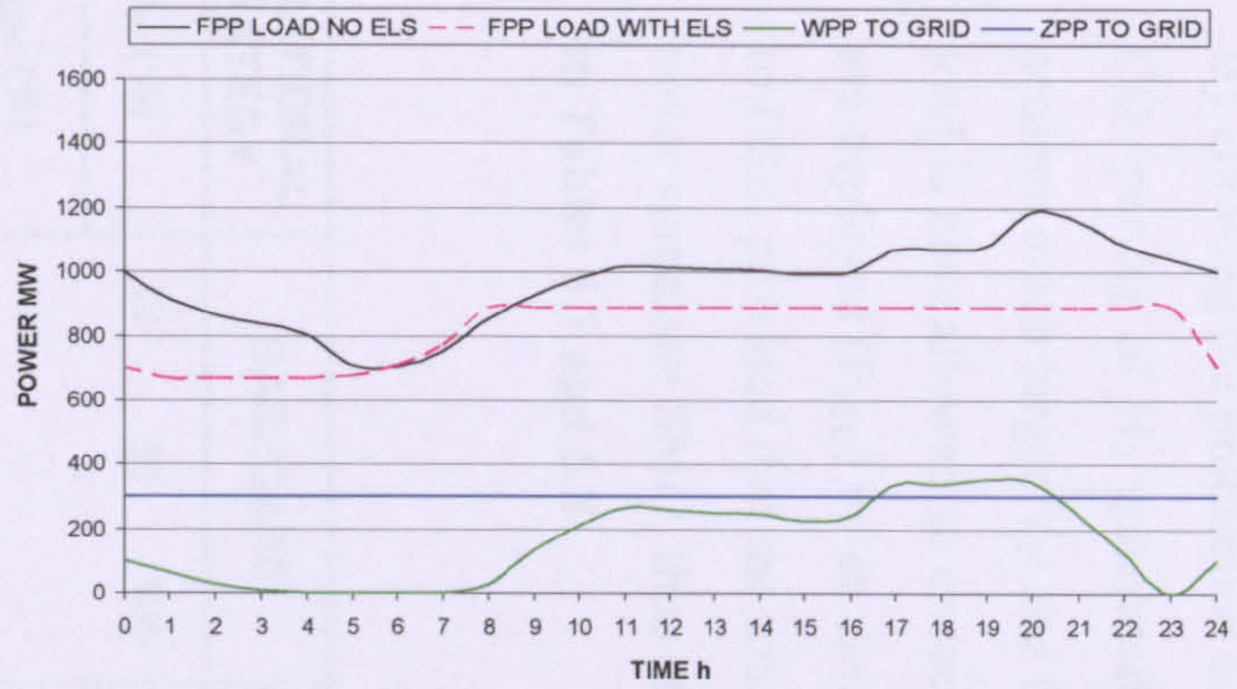

c)

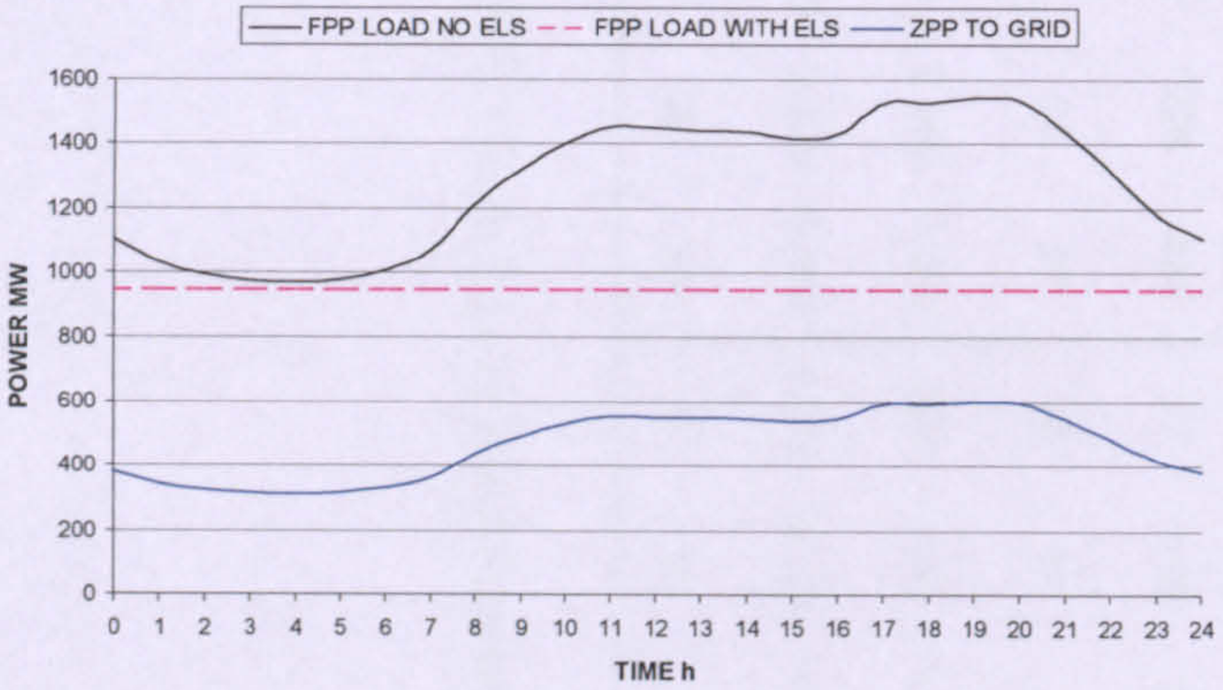

d)

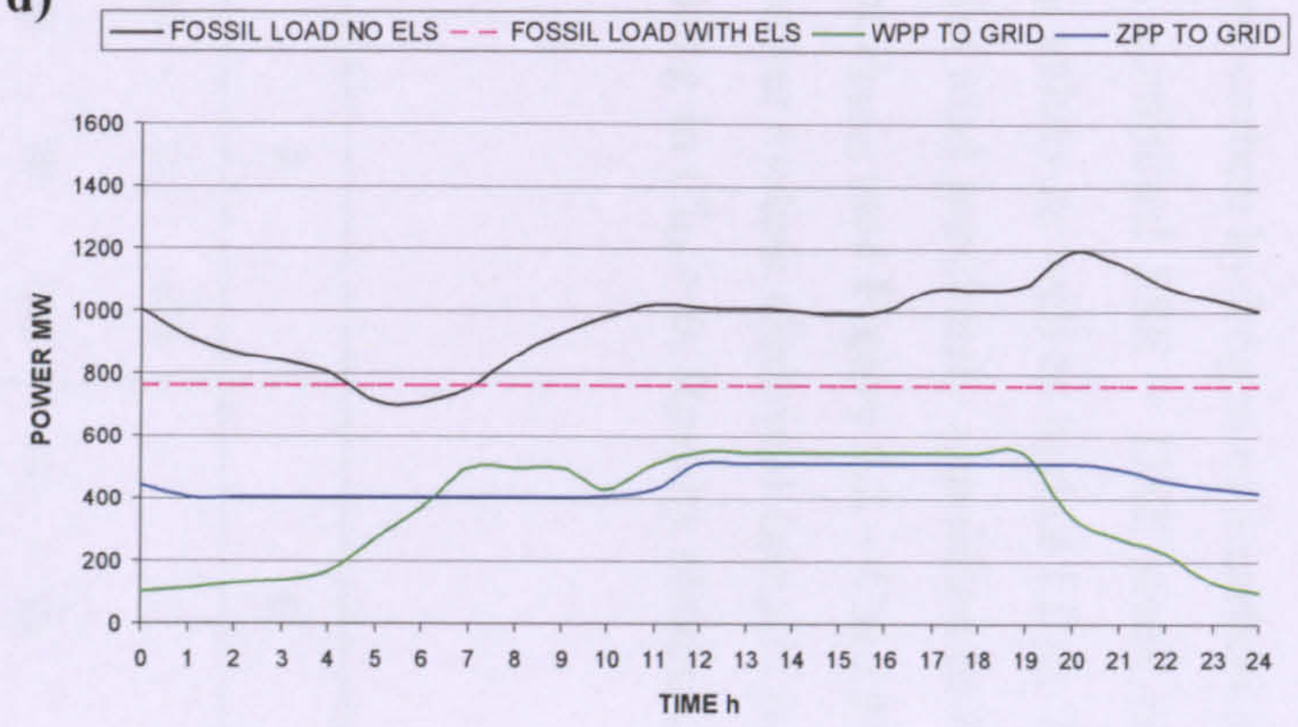

Figure 5.12. CASE 3. Variable wind day. Effects on aggregate fossil load, WPP and ZCPP output delivered to grid and input to electrolysers.

a) Base case
b) Strategy A
c) Strategy B
d) Strategy C

By allowing the production of low-carbon hydrogen of a carbon intensity of 3 kg of CO_2 per kg of H_2 generated, a combined SSE + DSE stock can be operated to achieve much larger Y_H and UF_E values as well as higher LF_{TH}. The aggregate FPP load is now allowed to exceed the load previously appointed to FPP when no ELS are deployed (P_{FPC}) by an amount P_{FPDE} (see **Figure 5.2 – Case 3**) which is directed to DSE, provided that the total power system electrical demand (consumers + DSE) never surpasses SMD, thus resulting in $CI_H > 0$. Results obtained are shown below in **Tables 5.7 and 5.8**.

OPERATIONAL STRATEGY	BASECASE			A			B			C		
Φ_W (%)	20	50	100	20	50	100	-	-	-	20	50	100
Φ_{ZPP} (%)	-	-	-	10	25	35	10	25	35	10	25	35
LF_{TH} (%)	80	81	88	80	81	93	84	92	100	87	98	100
CI_e (kg CO_2/kWh$_e$)	0.71	0.61	0.53	0.68	0.51	0.41	0.70	0.55	0.45	0.67	0.53	0.50
TC (t $CO_2 \times 10^3$ / d)	33.6	28.8	25.1	32.1	24.1	19.4	33.1	26.0	21.3	31.7	25.1	23.6
WC (%)	0	0	0	0	0	0	-	-	-	0	0	0
Y_H (t H_2 / d)	32	60	174	91	228	435	77	169	256	124	253	566
UF_E (%)	12	9	13	24	23	27	46	44	46	31	23	28
IC_E (MW)	575	1,410	2,795	795	2,060	3,360	350	800	1,160	840	2,310	4,145
NGC (MW)	4,410	5,770	8,035	4,630	6,420	8,600	3,815	4,265	4,825	4,675	6,670	9,395
β_E (%)	13	24	35	17	32	39	9	19	28	18	35	44

Table 5.7. Results for CASE 3, $CI_H = 3$, Low Wind Scenario

OPERATIONAL STRATEGY	BASECASE			A			B			C		
Φ_W (%)	20	50	100	20	50	100	-	-	-	20	50	100
Φ_{ZPP} (%)	-	-	-	10	25	35	10	25	35	10	25	35
LF_{TH} (%)	88	98	100	91	100	100	91	100	100	98	100	100
CI_e (kg CO_2/kWh$_e$)	0.69	0.56	0.55	0.64	0.45	0.37	0.68	0.58	0.53	0.63	0.57	0.45
TC (t $CO_2 \times 10^3$ / d)	21.2	17.2	16.9	19.7	13.8	11.4	20.9	18.1	16.3	19.4	17.5	13.8
WC (%)	0	0	0	0	0	0	-	-	-	0	0	0
Y_H (t H_2 / d)	84	214	504	167	439	874	71	234	405	152	621	1,115
UF_E (%)	30	32	38	44	44	54	42	61	73	38	56	56
IC_E (MW)	585	1,410	2,795	795	2,060	3,360	350	800	1,160	840	2,310	4,145
NGC (MW)	4,410	5,770	8,035	4,630	6,420	8,600	3,815	4,265	4,825	4,675	6,670	9,395
β_E (%)	13	24	35	17	32	39	9	19	28	18	35	44

Table 5.8. Results for CASE 3, $CI_H = 3$, Variable Wind Scenario

For the same Φ_W, Φ_{ZPP}, higher LF_{TH} can be obtained than when producing zero-carbon hydrogen. For instance, by operating ZPP in combination with the ELS stock, LF_{TH} can increase up to 100% (flat FPP load profile) for the operational strategies B and C at Φ_{ZPP}= 35% even on a low wind day, and a flat FPP load profile can be scheduled for all the operational strategies on a variable wind day at $\Phi_W \geq 50\%$, $\Phi_{ZPP} \geq 25\%$. In short higher load factors can be obtained at lower Φ_W, Φ_{ZPP} if $CI_H > 0$ is permitted.

As the main objective now is to increase Y_H and UF_E and no priority is given to decrease the carbon intensity of electricity, values for CI_e are higher than those obtained when only zero-carbon hydrogen is generated, and this is the reason why TC almost doubles when aiming for $LF_{TH} = 100\%$ at high Φ_W, Φ_{ZPP}. This is because for high LF_{TH} approaching 100%, priority is now given to the generation of low-carbon H_2 over the reduction of CI_e and then an increasing amount of the ZPP and WPP

output is directed to the electrolyser stock, reducing the proportion of the ZPP output directed to consumers which then penalizes CI_e.

A significant increase in Y_H values is obtained if permitting CI_H = 3 kg CO_2 / kg H_2, especially on the variable wind day, up to 1.4 fold for strategy A, up to 3 fold for strategy B and up to 2 fold for strategy C at Φ_{ZPP} = 35%. Note this is always at the expense of higher values of CI_e. As expected, in order to increase the scale of hydrogen production larger capacities of electrolysers are required, in particular for operational strategies B and C. Hence the utilization of the electrolyser stock only improves significantly by between 25%-100% on a variable wind day at $\Phi_W > 20\%$, $\Phi_{ZPP} > 10\%$, but can not be enhanced on the low wind day.

Given the trade-off existing between the amount of H_2 produced, Y_H, and its carbon intensity, CI_H, it is interesting to analyse the relationship between them. This is plotted in **Figure 5.13** for a fixed carbon intensity of electricity CI_e = 0.48 kg CO_2 / kWh_e, variable wind day at Φ_W =50%, Φ_{ZPP} = 25% and for $CI_H < 6$ kg CO_2 / kg H_2, which applies for the minimum value of the carbon intensity when hydrogen is produced from conventional hydrocarbon reformation methods.

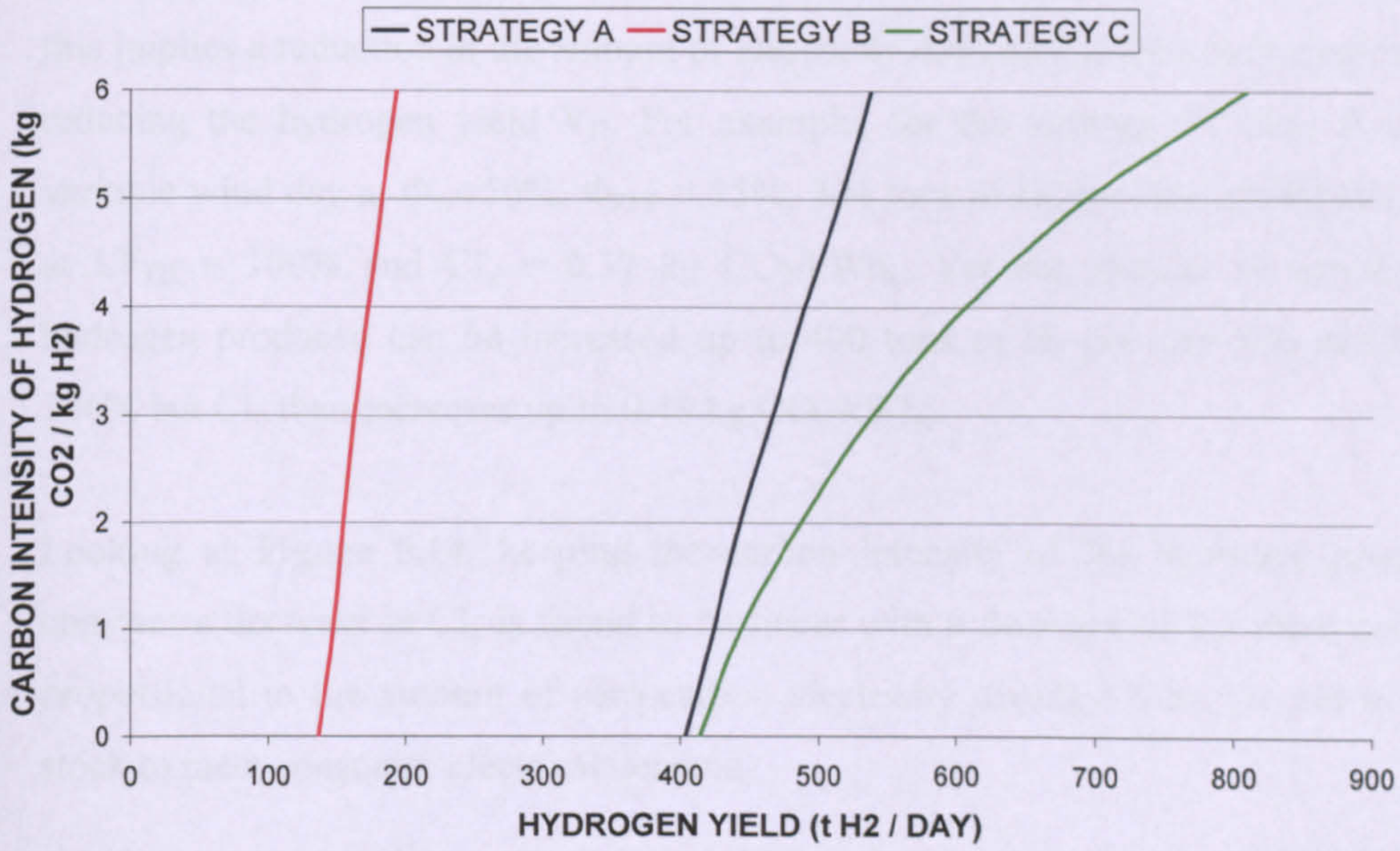

Figure 5.13. Case 3. Variable wind day. Φ_W = 50%, Φ_{ZPP} = 25%. Sensitivity of CI_H with Y_H at CI_e = 0.48 kg CO_2 / kWh_e

From **Figure 5.13**, for the operational strategies A and C it is possible to produce over 400 tonnes of zero-carbon H_2 per day when using both ZPP and WPP to operate the electrolyser stock, which is almost thrice the amount of zero-carbon H_2 produced when only ZPP are deployed in the power system (Strategy B). It is important to bear in mind though that the size of the ELS stock is significantly smaller for the strategy B (see **Tables 5.2, 5.4 and 5.6**).

When allowing $CI_H > 0$, the strategy C clearly affords the maximum benefits when compared to A and B. For instance, by permitting $CI_H = 3$ kg CO_2 / kg H_2 (well below that of hydrogen produced from hydrocarbons), Y_H increases by 30% from 414 to 538 tons H_2 / day. From **Figure 5.13**, under the operational strategy A such an increase is only possible by producing hydrogen at $CI_H = 6$ kg CO_2 / kg H_2, which approaches the carbon intensity of fossil-generated hydrogen.

There is also a strong trade-off between CI_e and Y_H. The carbon intensity of the electricity delivered to consumers can be minimized by decreasing the amount of fossil-derived electricity delivered and increasing the proportion of zero-carbon electricity (both from ZPP and WPP) directed to meet consumer demand. However this implies a reduction in the amount of electricity delivered to the electrolyser stock, reducing the hydrogen yield Y_H. For example, for the strategy C, Case 3 on the variable wind day at Φ_W=50%, Φ_{ZPP} = 25%, 304 tons of H_2 per day can be produced at LF_{TH} = 100% and CI_e = 0.37 kg CO_2/kWh$_e$. Yet the amount of zero-carbon hydrogen produced can be increased up to 400 tons of H_2 per day also at LF_{TH} = 100% but CI_e then increases up to 0.48 kg CO_2/kWh$_e$.

Looking at **Figure 5.14**, keeping the carbon intensity of the hydrogen produced constant a decrease in CI_e is found to be linear with a decrease of Y_H since both are proportional to the amount of zero-carbon electricity diverted from the electrolyser stock to meet consumer electrical demand.

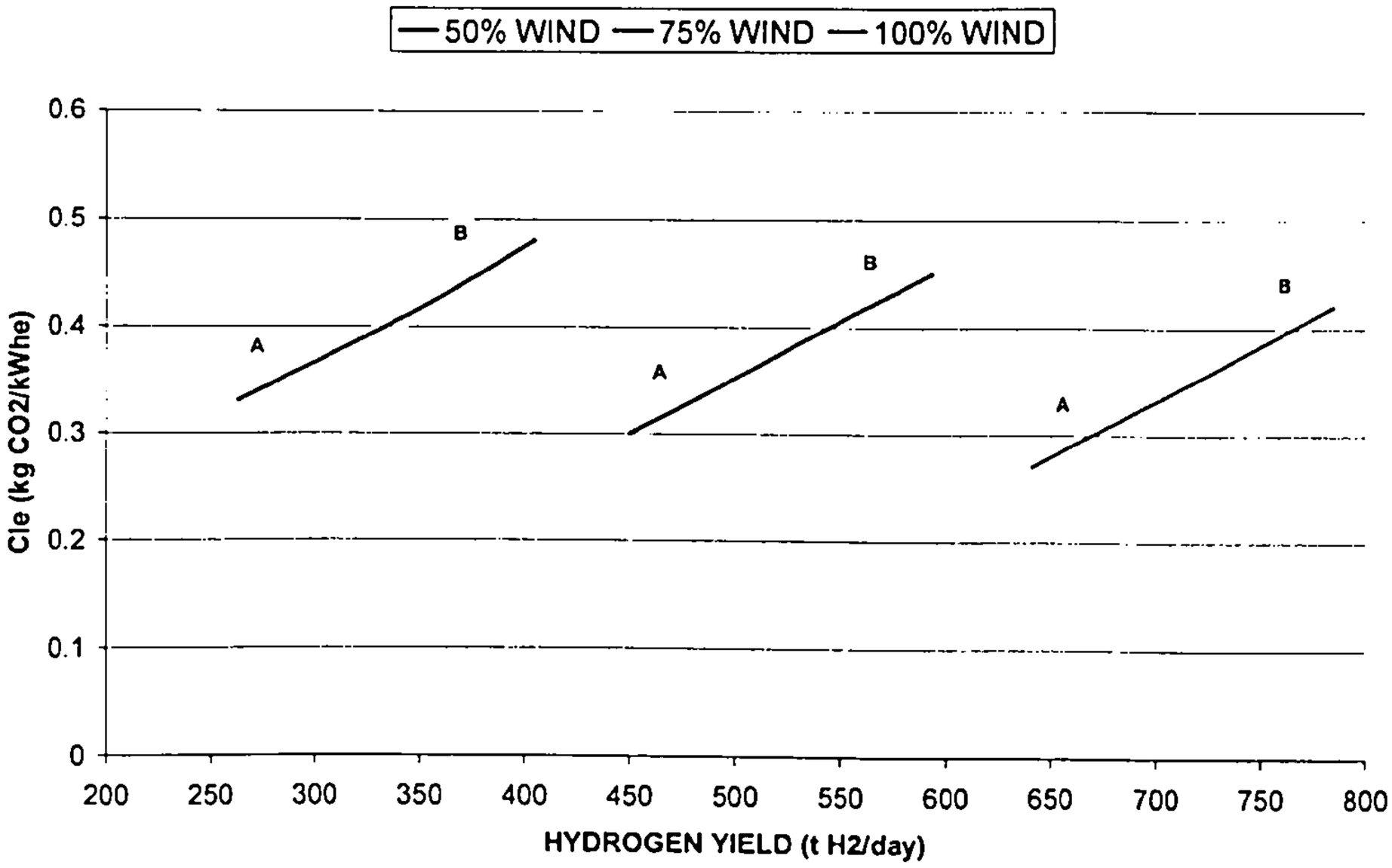

Figure 5.14. Case 3, Operational Strategy C. Relationship between the hydrogen production rate and the carbon intensity of electricity delivered to consumers at LF_{TH} = 100%, $CI_H = 0$.

The implementation of ZPP, in addition to WPP, gives greater flexibility in terms of the optimum pair of values (CI_e, Y_H) to be selected for a specific energy system and on a specific day depending on the preferred carbon abatement strategy and the hydrogen and electricity demands required. For instance, for an energy system with a large demand for zero carbon hydrogen (e.g. for transport purposes), it could be more beneficial to select values on the area B of the curves shown in **Figure 5.14**, at the expense of achieving less benefits in terms of reducing CI_e; whereas for an energy system with a dominant electricity demand, values on the area A of the curve could be more appropriate. Further discussion on the trade-off between Y_H, CI_e and CI_H is offered in below in **Chapters 3.5 and 4.**

Daily load profiles for CASE 3 when CI_H = 3 kg CO_2/kg H_2 are displayed in **Figure 5.15** for Φ_W = 50%, Φ_{ZPP} = 25%. Load inputs to the electrolyser stock are shown in **Figure 5.16**.

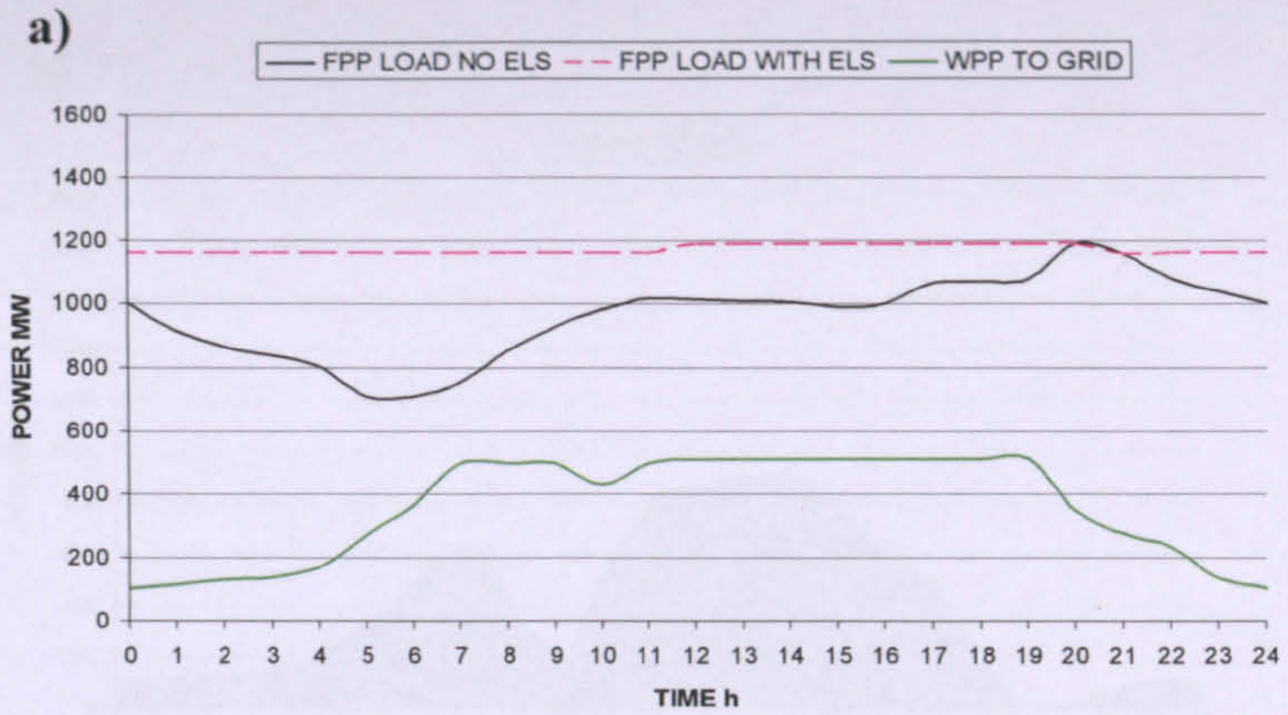

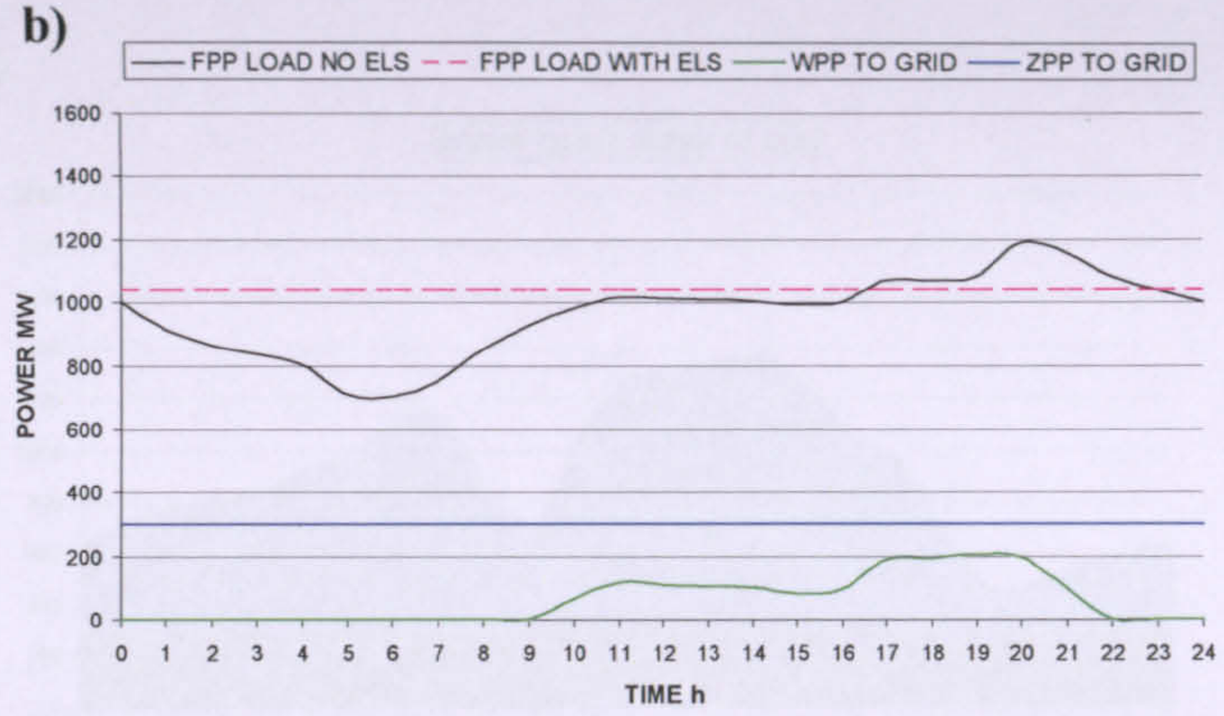

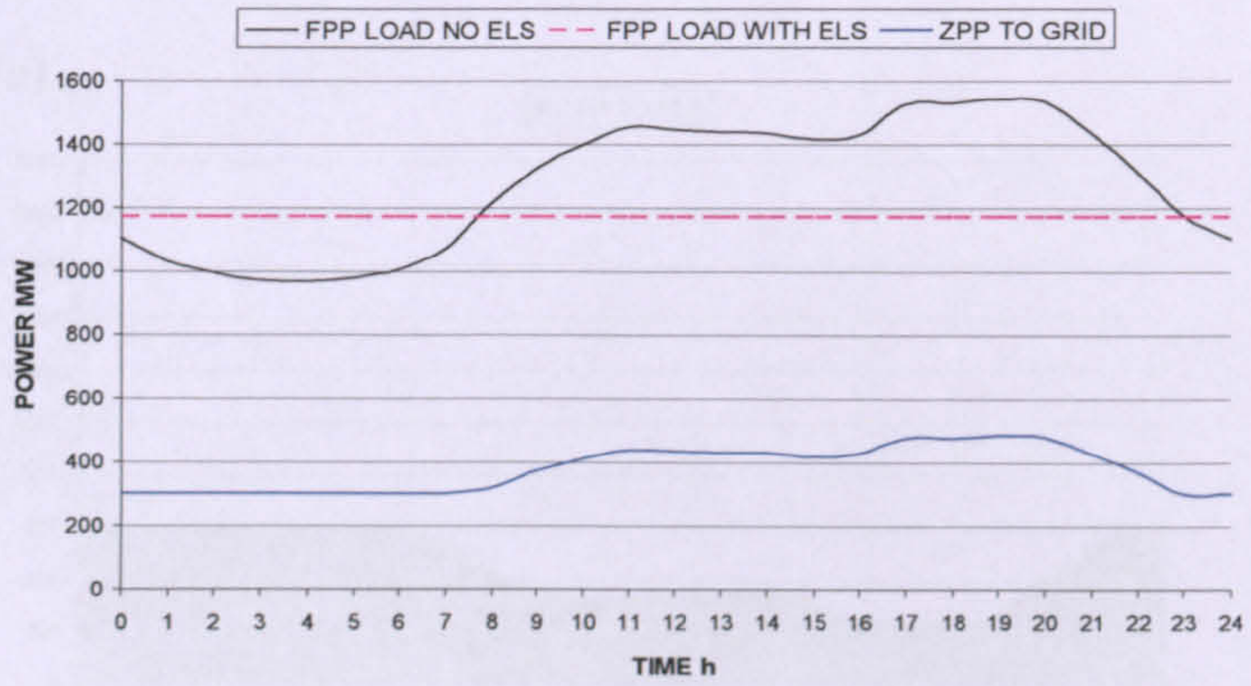

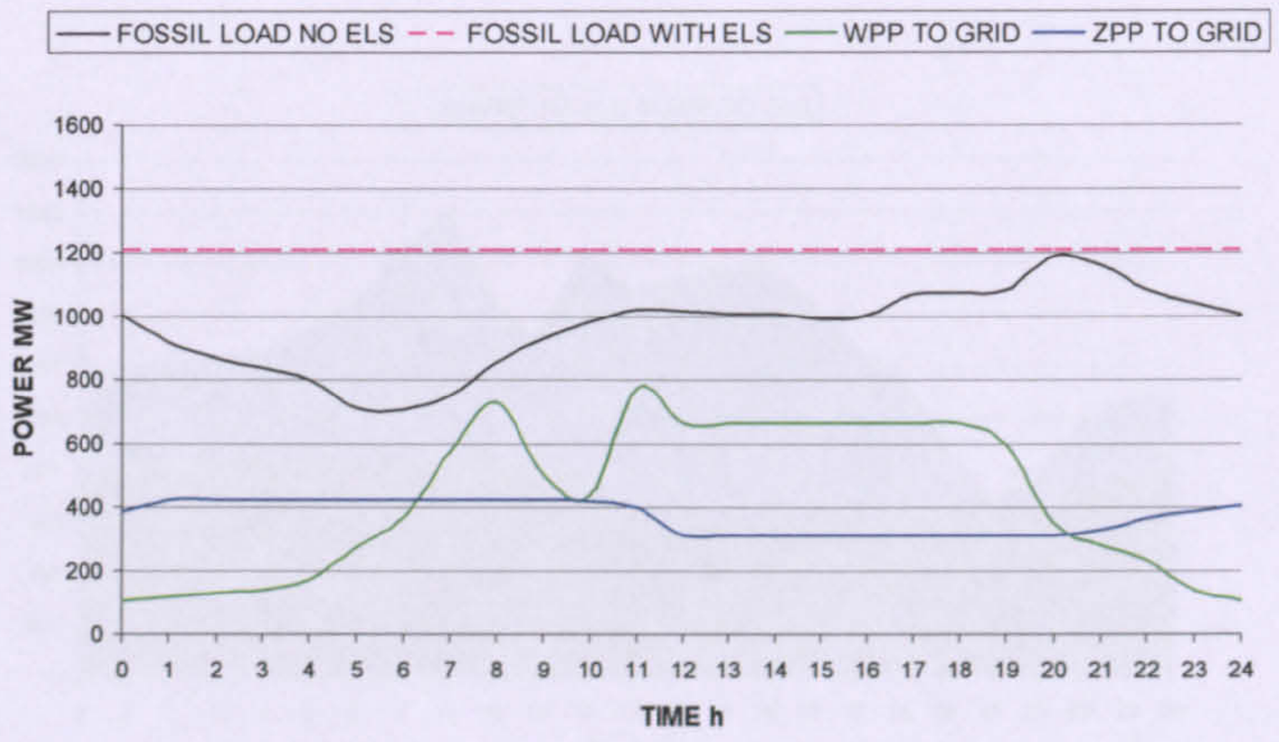

Figure 5.15. CASE 3, CI_H = 3 kg CO_2/kg H_2. Variable wind day. Effects on aggregate fossil load, WPP and ZCPP output delivered to grid and input to electrolysers.

a) Base case
b) Strategy A
c) Strategy B
d) Strategy C

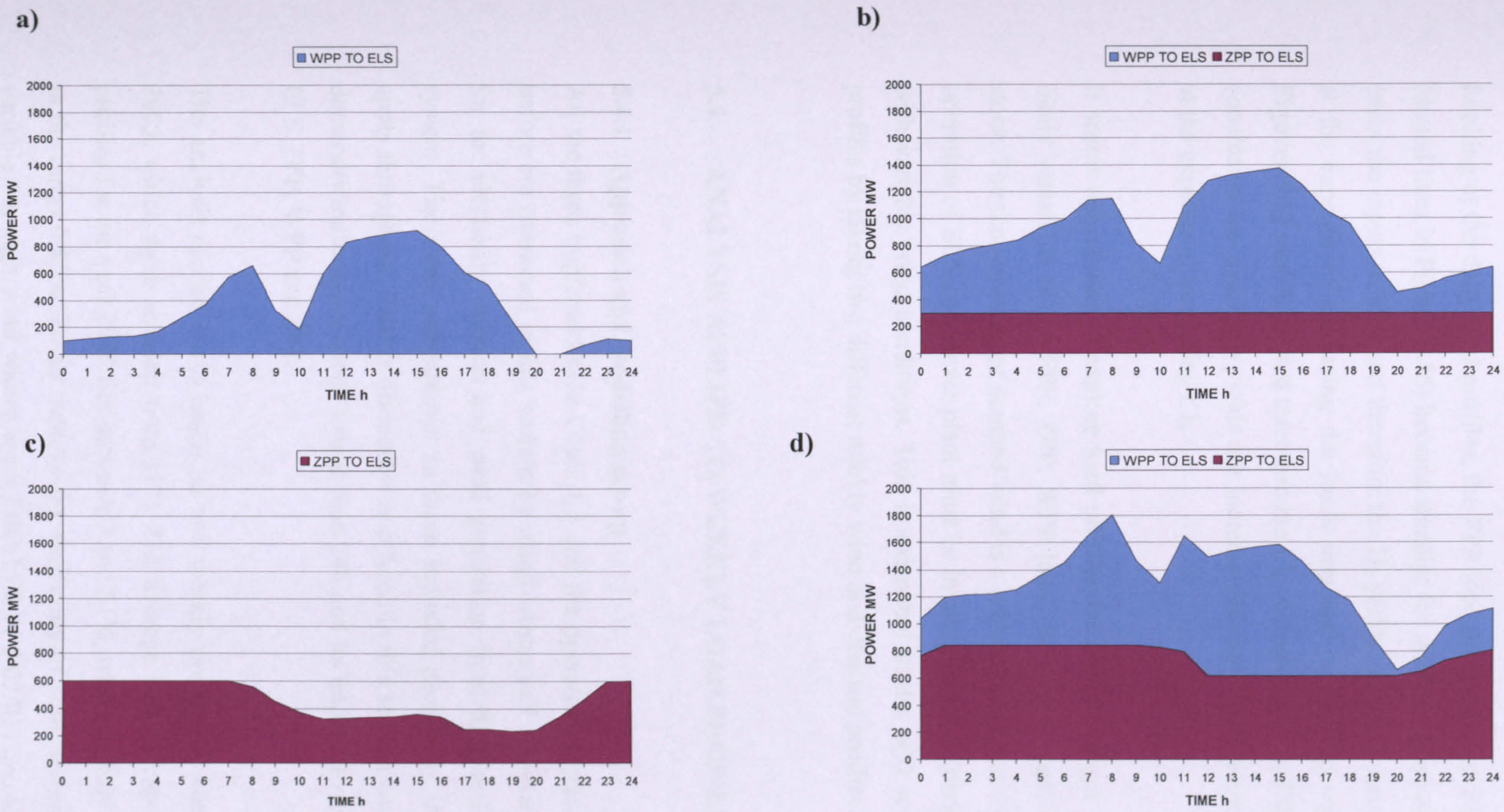

Figure 5.16. CASE 3, CI_H = 3 kg CO_2/kg H_2. Variable wind day. Aggregate electrical input to the "demand-side electrolyser stock".

a) Base case
b) Strategy A
c) Strategy B
d) Strategy C

Looking at the daily load profiles, the FPP load profiles when ELS are implemented (dotted lines in **Figure 5.15**) become steadier for the Base Case and Strategy A. In all cases the inputs to ELS and therefore the H_2 yields are much larger (see **Figure 5.16**) at the expense of increasing the loads imposed on FPP (compare dotted lines in **Figures 5.12 and 5.15**) and therefore the CI_e (compare CI_e in **Tables 5.6 and 5.8**). In conclusion the hydrogen yields are incremented significantly when relaxing CI_H but at the expense of increasing CI_e.

It seems appropriate to explore load profiles for periods longer that 24h to identify likely variations of the FPP, ZPP, WPP loads as well as inputs to the electrolyser stock. The time-phasing of demand/wind is a critical factor and its implications on the operation of ELS and power plant must be investigated over periods longer than 24h with variable wind conditions. This is examined in the next section for 168h load profiles by taking two different weekly wind and demand profiles.

5.4 ANALYSIS APPLIED TO WEEKLY LOAD PROFILES

5.4.1 Approach and modelling set-up

All the three implementation Cases 1-3 and the operational strategies A-C described before are examined in this section by using winter and summer weekly time series for the electricity demand and wind generation from the Eastern Denmark power system. The same assumptions as those included previously in the daily analysis apply throughout. Further discussion is offered in this section on the time-phasing of demand/wind across periods longer than 24h and its implications on the operation of ELS, FPP, WPP and ZPP.

The analysis carried out is based on two weekly profiles of wind power output for 2003, which were selected from [17]. The average weekly capacity factor of wind profiles for the year 2003 lies between 3 and 51%, whereas daily capacity factors are in the range 0-80%. To account for the variability of wind across the year, a relative variable but high wind winter week (28/01/03 to 3/02/03) and a high wind summer week (19/06/03 to 25/06/03) were selected. The capacity factor of the winter week is

36% and the capacity factor of the summer week is 44%. The winter week was selected to assess the variability of wind across a weekly period and its implications on the operation and management of a large ELS stock. The summer week was selected as the week of maximum capacity factor over the summer period in order to further evaluate the benefits of a wide deployment of ELS in terms of eliminating wind curtailment at periods of low demand and high wind availability. Hourly wind generation data from [17] was up-scaled in the same way as previously done for the daily profiles to produce specific wind penetration levels of 20%, 50% and 100%.

Two weekly profiles containing hourly demand data corresponding to both the winter and summer weeks previously selected were employed. Demand and wind generation profiles analysed were as described in **Chapter 3.3.2**.

The same methodology as described in **Section 5.2** was used to obtain an optimised weekly FPP load profile. There are several ways of raising valleys and creating plateaus in the FPP load profile by adding or subtracting the electrolyser load as required. It is suggested here that, once the WPP and ZPP outputs available have been subtracted from the demand for each hour, values for the residual load to be met by FPP can be obtained and these can be increased (subject to the CI_{II} appointed) or decreased by adding/subtracting the electrolyser load as required (in case of the operational strategies B and C, also by adding/subtracting the ZPP load when appropriate) to create plateaus on the FPP load profile, but of greater duration than applies to the conventional FPP load profile (without ELS). At the end of the weekly period, weekly load profiles are obtained for the operation of FPP, WPP, ZPP and the ELS stock, and weekly parameters are obtained from the integration of hourly average power values.

Regarding the length of the plateaus created in the weekly FPP load profile, several decisions can be made, and the operational strategy C allows the greatest flexibility in this way. For instance, a daily plateau can be aimed, or instead an alternative strategy can be followed by prolonging the daily plateau (subject to the restrictions imposed by equations **(5.2)-(5.4)** so that only zero-carbon H_2 is produced). In this case attention was not given to increasing the average weekly load factor of the aggregate FPP load profile, but instead the objective is to maximize the length of the daily

plateaus created so FPP can be operated at constant predictable rates for longer periods, minimizing their carbon footprint and the increased wear and tear imposed on them during the process of changing load levels (see **Chapter 2**). This will be discussed further below (see **Results for Case 3**).

Results are presented for the two weekly periods (168h) selected. The outputs are weekly energy balances, load profiles, hydrogen yields, average weekly utilization factors of the ELS stock, carbon intensities as well as average hourly power flows for the 168h period studied. The main objectives with respect to a large deployment of electrolysers in the power system remain the same, namely optimize the operation of FPP, minimize wind power curtailment and maximize hydrogen production.

5.4.2 Results and discussion

Results obtained for the three operational strategies A, B and C and for the implementation Cases 1 (SSE), 2 (DSE) and 3 (SSE +DSE) as well as the Base Case (only WPP and FPP implemented on the supply side) are offered here. Both results for the winter and the summer week are offered. The main variables included in the analysis remain the same.

Note the installed capacity of electrolysers required is determined as previously by the day of maximum capacity factor across the year (steady wind day, CF = 80%) and therefore this parameter is not be discussed any further here. This installed capacity is taken as the datum for the calculation of the average weekly utilization factor of the electrolyser stock, UF_E.

1) Results for Case 1

An electrolyser stock can be deployed at or near the main WPP and/or ZPP and only zero-carbon hydrogen is produced. Results for the winter and summer weeks are shown in **Tables 5.9 and 5.10.**

OPERATIONAL STRATEGY	BASECASE			A			B			C		
Φ_W (%)	20	50	100	20	50	100	-	-	-	20	50	100
Φ_{ZPP} (%)	-	-	-	10	25	35	10	25	35	10	25	35
CI_e (kg CO_2/kWh_e)	0.66	0.59	0.53	0.63	0.49	0.39	0.65	0.56	0.44	0.63	0.45	0.31
TC (t CO_2 × 10^3 / week)	215.7	192.8	173.2	205.9	160.2	127.5	212.4	183.0	143.8	205.9	147.1	101.3
WC (%)	0	0	0	0	0	0	-	-	-	0	0	0
Y_H (t H_2 / week)	372	1,083	2,403	869	2,089	3,817	408	1,244	1,488	904	1,701	3,070
UF_E (%)	24	29	32	45	44	43	51	62	53	39	33	34
IC_E (MW)	470	920	2,240	575	1,405	2,660	240	600	840	695	1,515	2,650
LF_{TH} (%)	75	72	72	75	69	66	74	88	91	79	74	70

Table 5.9. Results for CASE 1, Winter Week

OPERATIONAL STRATEGY	BASECASE			A			B			C		
Φ_W (%)	20	50	100	20	50	100	-	-	-	20	50	100
Φ_{ZPP} (%)	-	-	-	10	25	35	10	25	35	10	25	35
CI_e (kg CO_2/kWh_e)	0.66	0.57	0.52	0.61	0.43	0.33	0.65	0.51	0.37	0.59	0.34	0.20
TC (t CO_2 × 10^3 / d)	157.1	135.7	123.8	145.2	102.3	78.5	154.7	121.4	88.1	140.4	80.9	47.6
WC (%)	0	0	0	0	0	0	-	-	-	0	0	0
Y_H (t H_2 / week)	506	1,391	3,254	891	2,375	4,674	526	1,091	1,405	785	1,703	3,740
UF_E (%)	32	37	43	46	50	52	65	54	50	34	33	42
IC_E (MW)	470	920	2,240	575	1,405	2,660	240	600	840	695	1,515	2,650
LF_{TH} (%)	79	80	86	77	75	81	81	89	86	81	77	92

Table 5.10. Results for CASE 1, Summer Week

For the operational strategies A and C, CI_e and TC reduce when using ZPP and WPP to deliver electricity to consumers with respect to the Base Case. For the strategy B reductions are less significant since no WPP are deployed on the supply side. As expected the reduction in carbon emissions increases with Φ_W, especially across the summer week since wind availability is high. For example, for the strategy C at Φ_W = 100% on the summer week CI_e (and thus TC) reduces by over 70% with respect to the Base Case from 0.52 to 0.20 kg CO_2/kWh$_e$ whereas a 42% reduction (from 0.53 to 0.31 kg CO_2/kWh$_e$) is achieved during the winter week. Both weeks present at least one day of low wind availability (see **Figures 3.6 and 3.7 in Chapter 3**), so when comparing with the daily values of CI_e the average weekly CI_e figures are somewhat in between those obtained before for the low and variable wind day (see **Tables 1 and 2**).

The hydrogen production rates attained in the Base-Case are higher than those of the Strategy B but always lower than values achieved where both ZPP and WPP are deployed on the supply side under the strategies A and C. This is plotted in **Figure 5.16**. Also for A and C the hydrogen yield across the week is higher during the summer week due to a higher wind availability, reaching a maximum of 4,674 tonnes of H_2 at Φ_W = 100%, Φ_{ZPP} = 35% for the strategy A. To place this into context 4,674 t H_2 (or 155.6 GWh H_2 LHV) would be sufficient to cover 40% of the average weekly road transport energy demand in East Denmark[25].

[25] Due to the lack of statistical data available specifically for East Denmark, this has been calculated from the total yearly transport energy demand in Denmark in 2003 (East Denmark plus West Denmark) [79] averaging for 52 weeks and based on the assumption that the transport demand in Eastern Denmark is 46% of total transport energy demand in Denmark (population in Eastern Denmark accounts for 46% of total population in Denmark [84]).

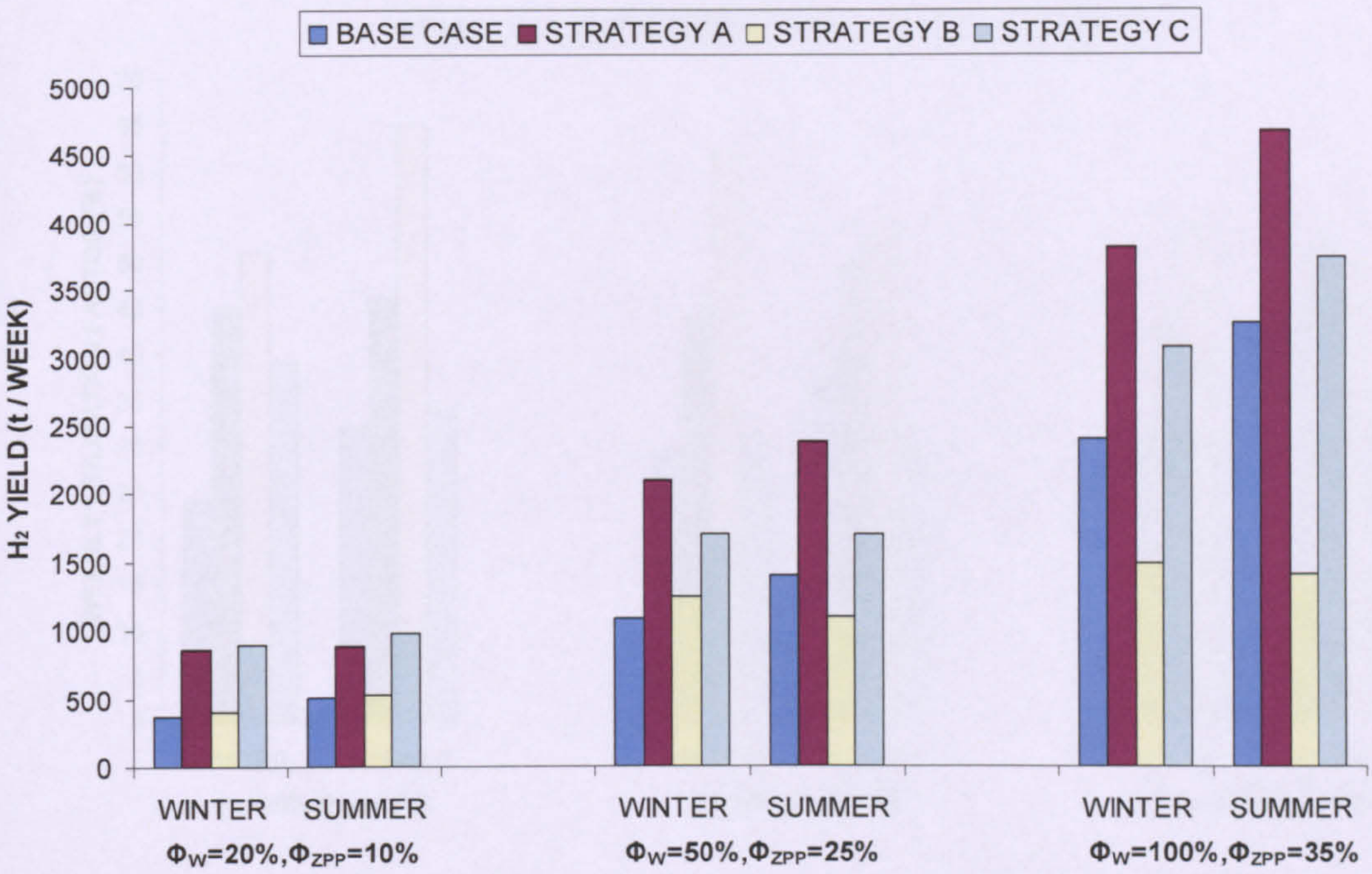

Figure 5.16. CASE 1, Weekly hydrogen production versus WPP and ZPP penetration for the weekly periods selected.

For the strategy B, the hydrogen yield does not increase significantly with Φ_{ZPP} for $\Phi_{ZPP} > 25\%$, since priority is given to minimizing CI_e instead of maximizing Y_H in this case. As a consequence, CI_e and TC are similar to those obtained for the operational strategy A but without deploying WPP, yet at the expense of obtaining hydrogen production rates less than half of those achieved under the strategy A.

Curtailment of wind resource is completely eliminated for all strategies and wind scenarios. This is because except for the operational strategy B the ELS stock is sized according to the day of maximum wind availability across the year (see modelling assumptions in **Chapter 3**) so as to eradicate wind curtailment. As a consequence the average weekly UF_E is not as high as expected, and they are similar to the values obtained before in the daily analysis presented in this same chapter. The weekly UF_E is plotted versus Φ_W and Φ_{ZP} in **Figure 5.17**.

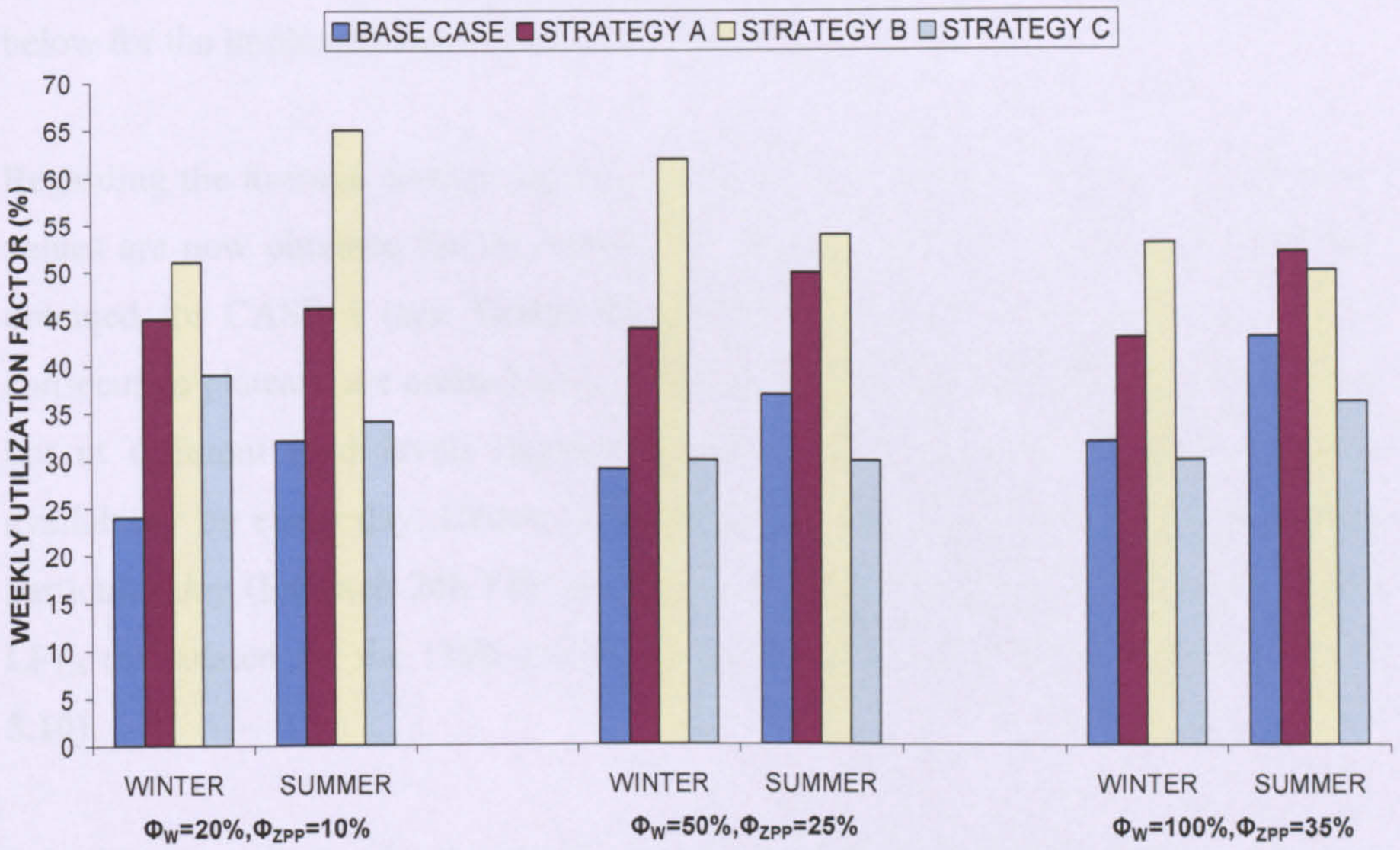

Figure 5.17. CASE 1. Average weekly utilization factor of SSE versus WPP and ZPP penetration for the two weekly scenarios.

Values range from 43 to 52% for the operational strategy A and 33% to 42% for C, with the highest range corresponding to the summer week when wind availability is high and more zero-carbon hydrogen can then be produced. The highest values of UF_E are obtained for the strategy B, always above 50%. Note in this case no WPP are deployed and thus the SSE is sized according to the ZPP installed capacity and is not subject to wind availability. In theory it would be possible to increase UF_E values by decreasing the size of the ELS stock, but at the expense of having some wind curtailment. This alternative does not lie within the analysis presented in this investigation and thus is not discussed here any further. Possible modifications and improvements of the AELM model are discussed in **Chapter** 7.

By implementing a SSE stock wind curtailment is completely eliminated both for the winter and summer week even at periods of high wind availability. This would have profound benefits on the capability of WPP to further mitigate carbon emissions by harnessing the surplus wind generation and producing both zero-carbon electricity

and hydrogen. It would also reduce the economic penalties for the WPP operators caused by wind curtailment (see **Chapter 2**). Further discussion on WC is offered below for the implementation CASE 2 (DSE stock only).

Regarding the average weekly load factor of the FPP load profile, LF_{TH}, the highest values are now obtained for the strategy B. Yet they always lie below daily values obtained for CASE 1 (see **Tables 5.1 and 5.2**). This is because a succession of consecutive plateaus are created now, each one corresponding to one day of the week but at different load levels depending on the daily demand and specific wind availability on every day. Hence even though the load factor calculated across any particular day (for each 24h FPP profile) can rise up to 100%, the average weekly LF_{TH} (calculated for the 168h profile) is always below 100% (see **Tables 5.9 and 5.10**).

It is then more illustrative to plot the daily LF_{TH} across the week. This is shown in **Figures 5.18 and 5.19** for $\Phi_W = 50\%$ and $\Phi_{ZPP} = 25\%$ along with wind and demand weekly profiles. When no ELS are deployed the daily LF_{TH} ranges from 71% to 89% depending on wind availability. By looking at these Figures the lowest values of daily LF_{TH} correspond to the days of lowest wind availability and vice versa. Also looking at **Figures 5.18 and 5.19** the most beneficial in terms of increasing daily LF_{TH}'s are operational strategies B with daily load factors between 92% and 100% and C with values in the range 95-100%.

a)

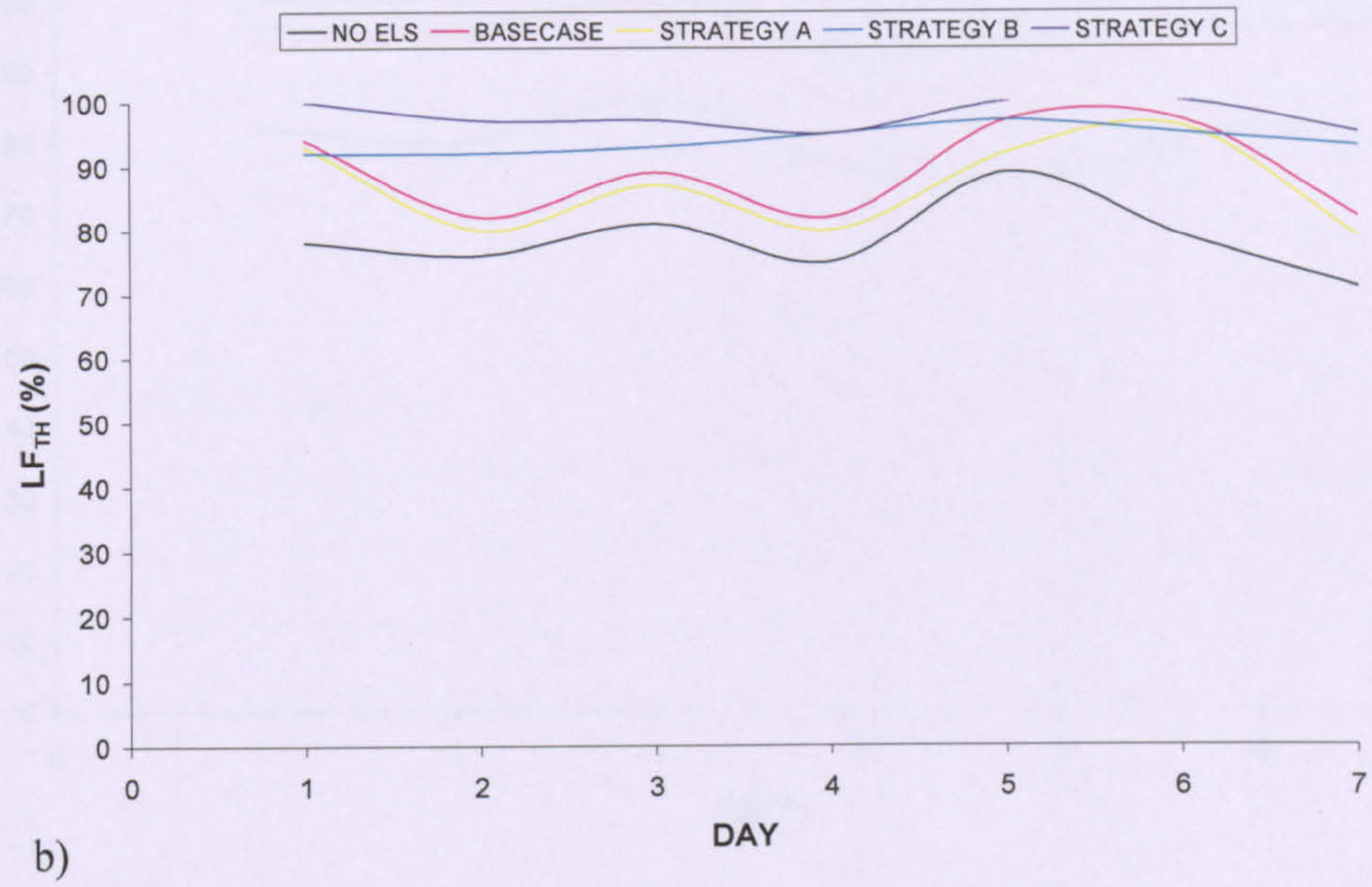

b)

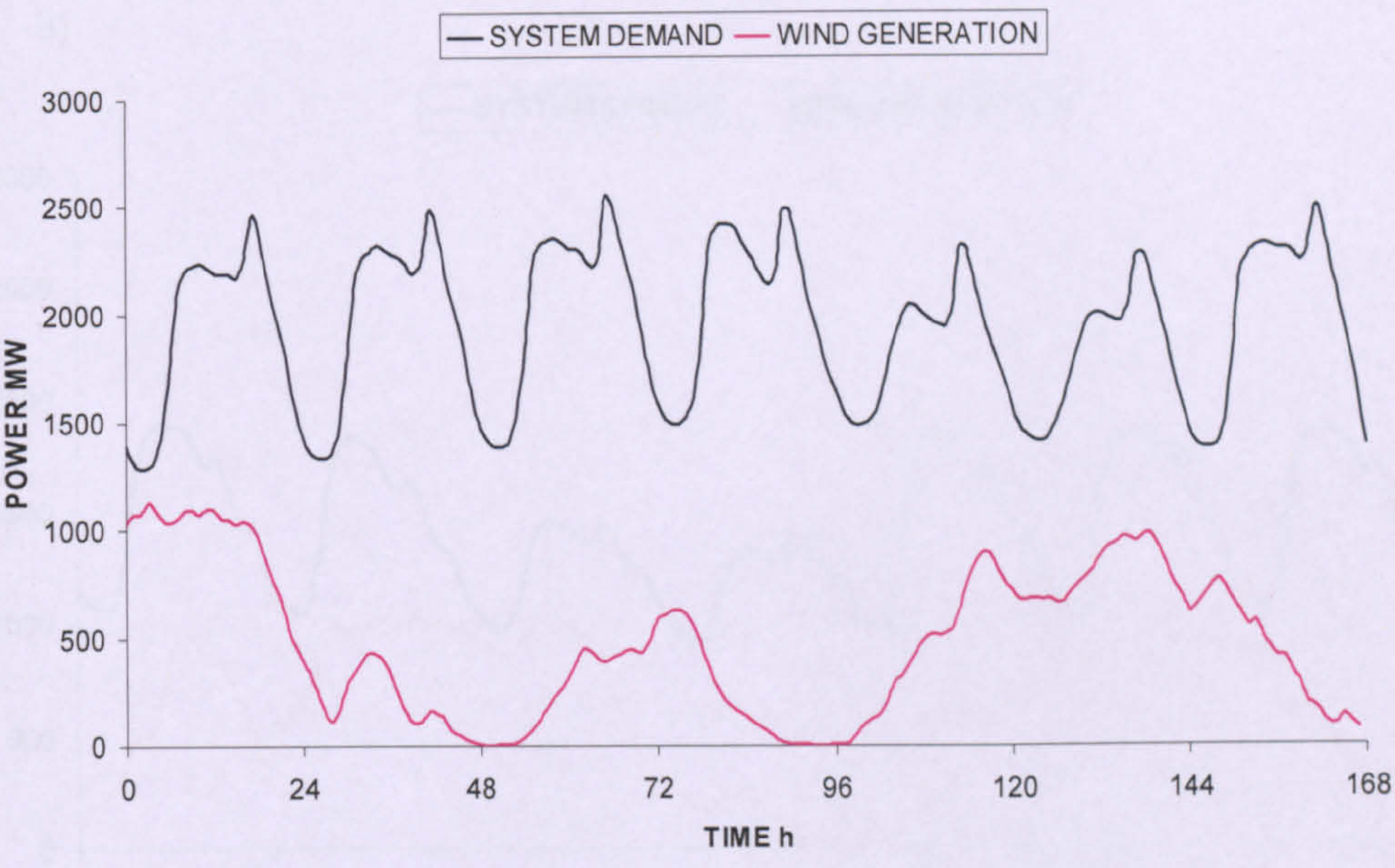

Figure 5.18. CASE 1, winter week, $\Phi_W = 50\%$ and $\Phi_{ZPP} = 25\%$

a) Daily load factor of the aggregate FPP load profile.

b) System demand and wind generation profiles.

a)

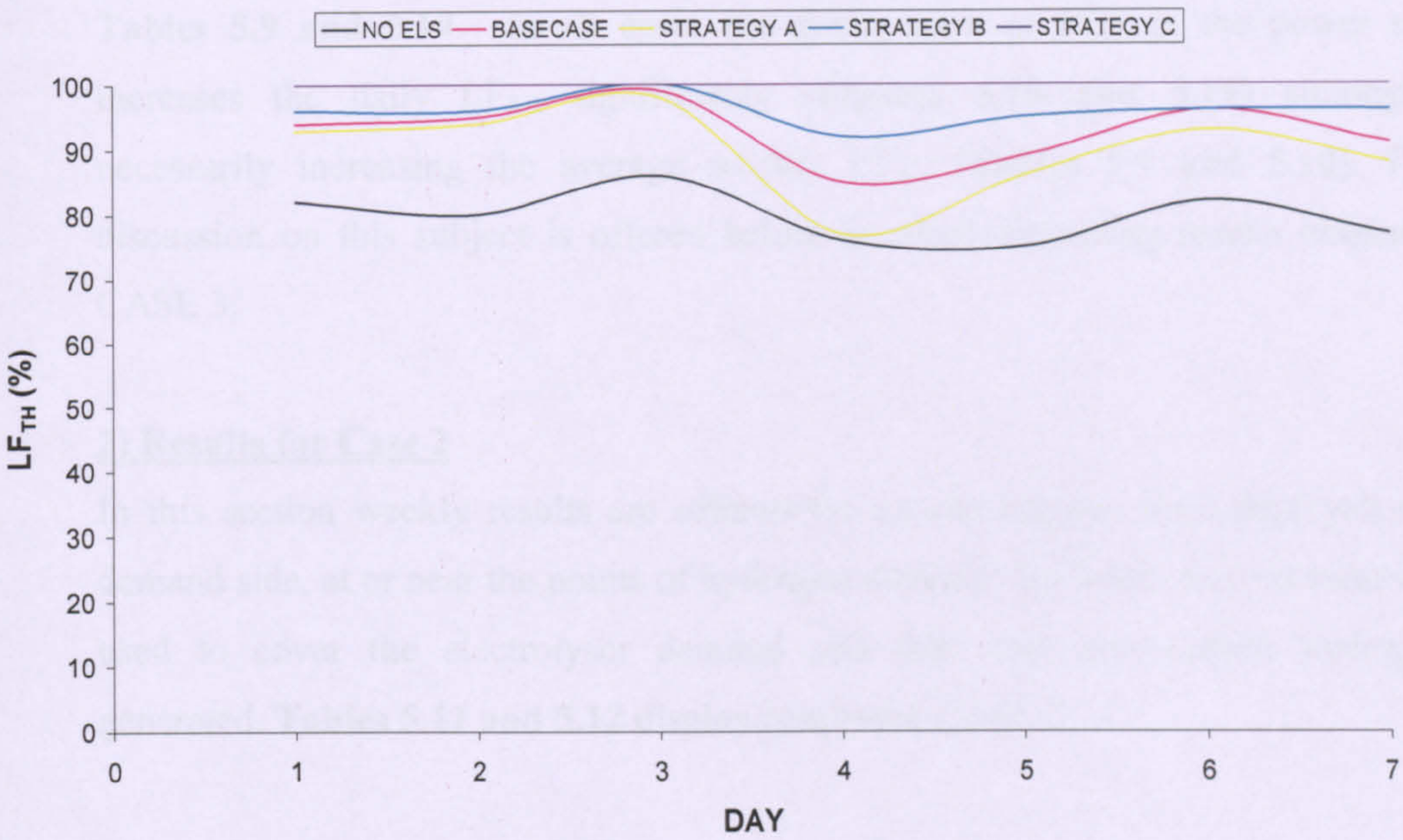

b)

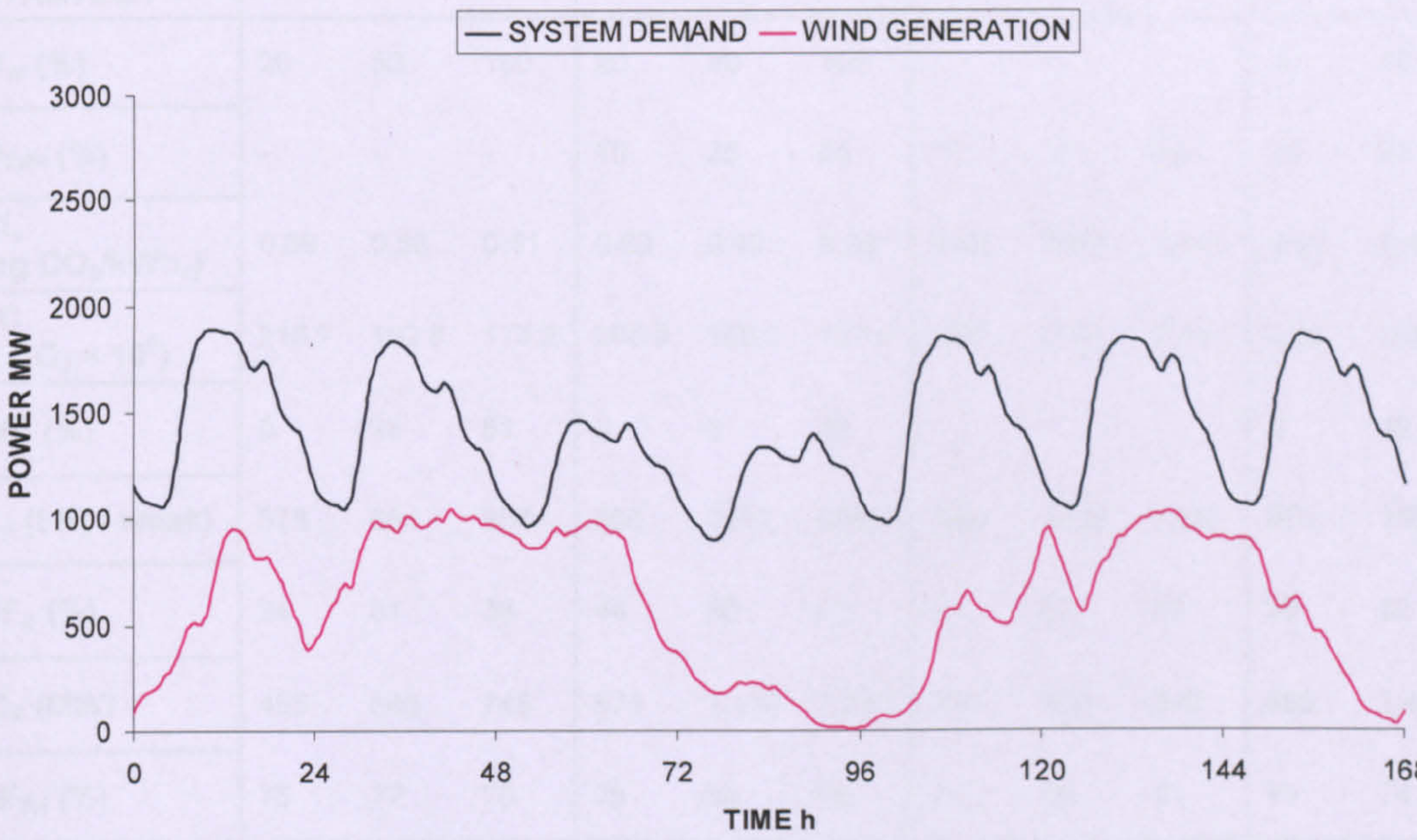

Figure 5.19. CASE 1, summer week, $\Phi_W = 50\%$ and $\Phi_{ZPP} = 25\%$

c) Daily load factor of the aggregate FPP load profile.

d) System demand and wind generation profiles.

It is now worth comparing the daily LF_{TH} with the average weekly values offered in **Tables 5.9 and 5.10**. In all cases the deployment of ELS in the power system increases the daily LF_{TH} significantly (**Figures 5.18 and 5.19**) although not necessarily increasing the average weekly LF_{TH} (**Tables 5.9 and 5.10**). Further discussion on this subject is offered below in when discussing results obtained for CASE 3.

2) Results for Case 2

In this section weekly results are offered for an electrolyser stock deployed on the demand side, at or near the points of hydrogen demand. No fossil-derived electricity is used to cover the electrolyser demand and thus only zero-carbon hydrogen is generated. **Tables 5.11 and 5.12** display results for CASE 2.

OPERATIONAL STRATEGY	BASECASE			A			B			C		
Φ_W (%)	20	50	100	20	50	100	-	-	-	20	50	100
Φ_{ZPP} (%)	-	-	-	10	25	35	10	25	35	10	25	35
CI_e (kg CO_2/kWh$_e$)	0.66	0.58	0.51	0.63	0.49	0.39	0.65	0.56	0.44	0.63	0.45	0.31
TC (t $CO_2 \times 10^3$)	215.7	192.8	173.2	205.9	160.2	127.5	0.65	0.56	0.44	0.63	0.45	0.31
WC (%)	0	25	51	0	8	32	-	-	-	0	12	38
Y_H (t H_2 / week)	373	684	957	856	1967	2854	398	1244	1488	903	1503	1948
UF_E (%)	24	31	38	44	50	63	49	62	53	39	32	33
IC_E (MW)	455	645	745	575	1,170	1,340	240	600	840	695	1,415	1,760
LF_{TH} (%)	75	72	70	75	69	66	74	88	91	79	74	70

Table 5.11. Results for CASE 2, winter week

OPERATIONAL STRATEGY	BASECASE			A			B			C		
Φ_W (%)	20	50	100	20	50	100	-	-	-	20	50	100
Φ_{ZPP} (%)	-	-	-	10	25	35	10	25	35	10	25	35
CI_e (kg CO_2/kWh$_e$)	0.66	0.57	0.52	0.61	0.43	0.33	0.65	0.51	0.37	0.59	0.33	0.17
TC (t $CO_2 \times 10^3$)	140.4	78.5	40.5	145.2	102.3	78.5	154.7	121.4	88.1	140.4	78.5	40.5
WC (%)	2	32	62	0	21	51	-	-	-	0	29	60
Y_H (t H_2 / week)	504	757	808	891	1955	2661	526	1091	1372	785	1066	1140
UF_E (%)	33	35	32	46	50	59	65	54	49	34	19	11
IC_E (MW)	455	645	745	575	1,170	1,340	240	600	840	695	1,415	1,760
LF_{TH} (%)	79	80	86	77	75	81	81	89	86	81	76	81

Table 5.12. Results for CASE 2, summer week

As discussed before the maximum achievable LF_{TH} is a function of the restrictions imposed by equations (3) and (4) and thus the same daily and weekly LF_{TH} apply for Case 1 and Case 2. Also values for CI_e and TC are equal to those obtained for Case 1, given that these are subject to the target LF_{TH}.

Values of Y_H from **Tables 5.11 and 5.12** are plotted in **Figure 5.20.**

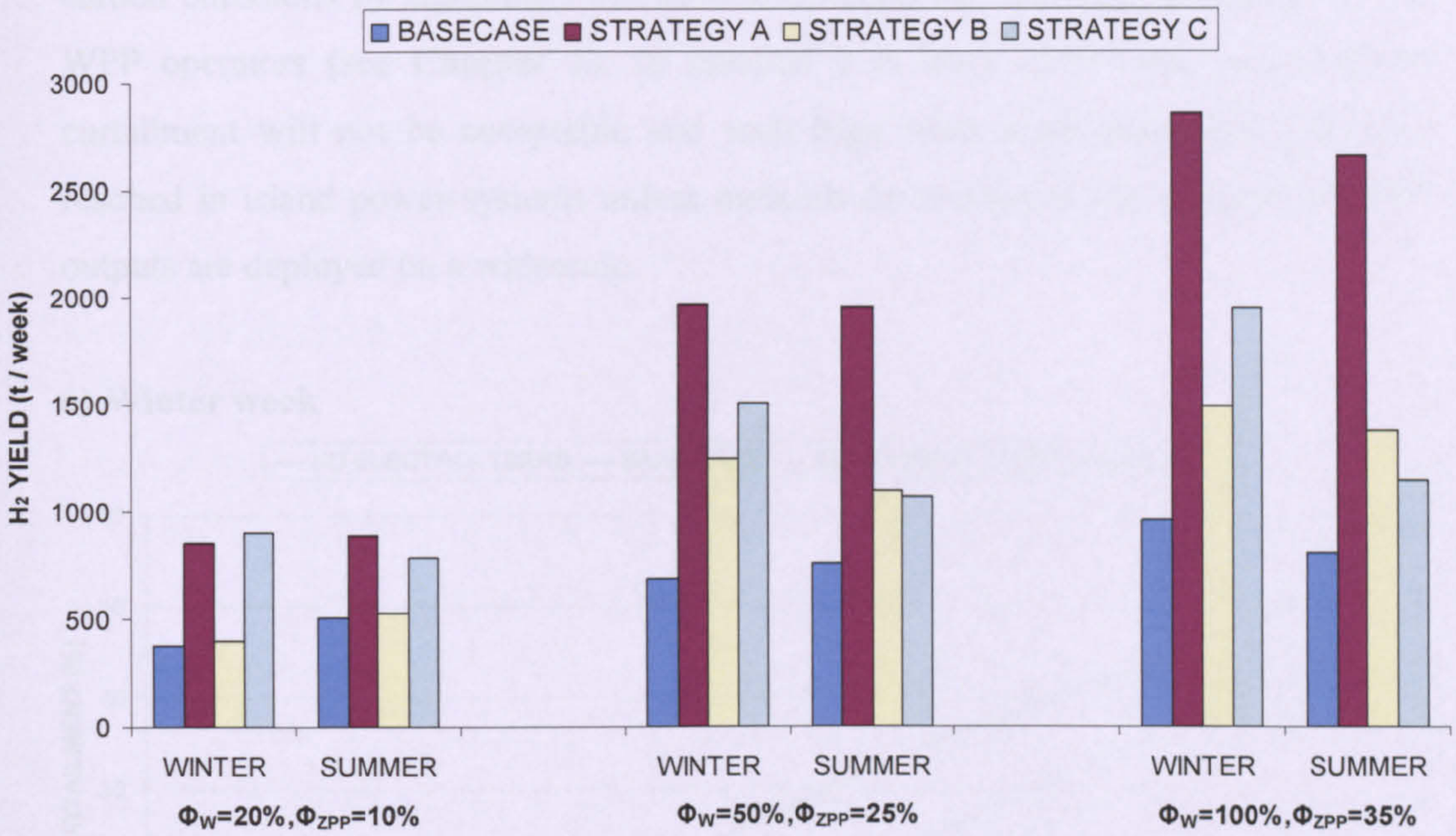

Figure 5.20. CASE 2, Weekly hydrogen production versus WPP and ZPP penetration for the weekly periods selected.

When comparing **Figure 5.20** with **Figure 5.16** the range of values of Y_H are clearly lower than those obtained for Case 1 for both the winter and summer week except for the operational strategy B. This is a mere consequence of wind curtailment and the limit imposed on the amount of intermittent wind generation that can be absorbed by the power system and directed to the DSE. No WPP are deployed for strategy B and therefore no wind curtailment exists, resulting in same values of Y_H whether the electrolyser stock is located on the supply side or on the demand side.

Wind curtailment is plotted in **Figure 5.21** for increasing wind penetrations. As observed previously in the daily analysis, the eradication of wind curtailment is not achievable when deploying a DSE, but the amount of wind generation discarded is reduced by 18% - 47% for strategy A and between 3% - 20% for C with respect to the Base Case, with the higher range corresponding to the winter week. It is found that, for the islanded power system considered in this analysis, if no DSE stock is implemented, around 40% of the wind resource available would be curtailed at Φ_W = 50% and nearly 70% of the aggregate WPP output at Φ_W = 100% during the summer week. This would have profound consequences on the capability of WPP to mitigate

carbon emissions by replacing FPP, as well as important economic penalties for the WPP operators (see **Chapter 2**). In practice it is more likely that such level of curtailment will not be acceptable and such high wind penetrations will never be reached in island power systems unless methods for managing the intermittent WPP outputs are deployed on a widescale.

a) Winter week

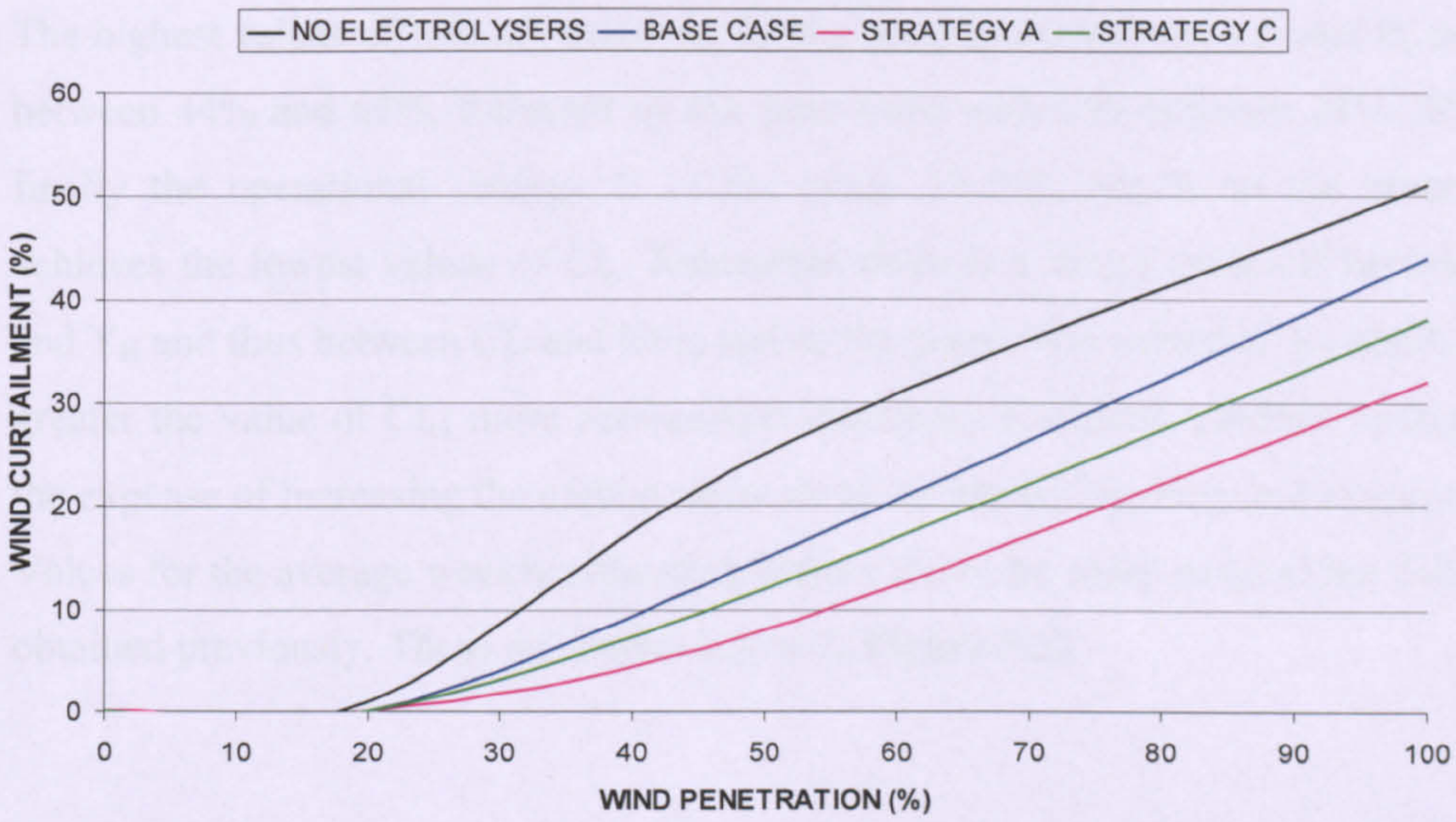

b) Summer week

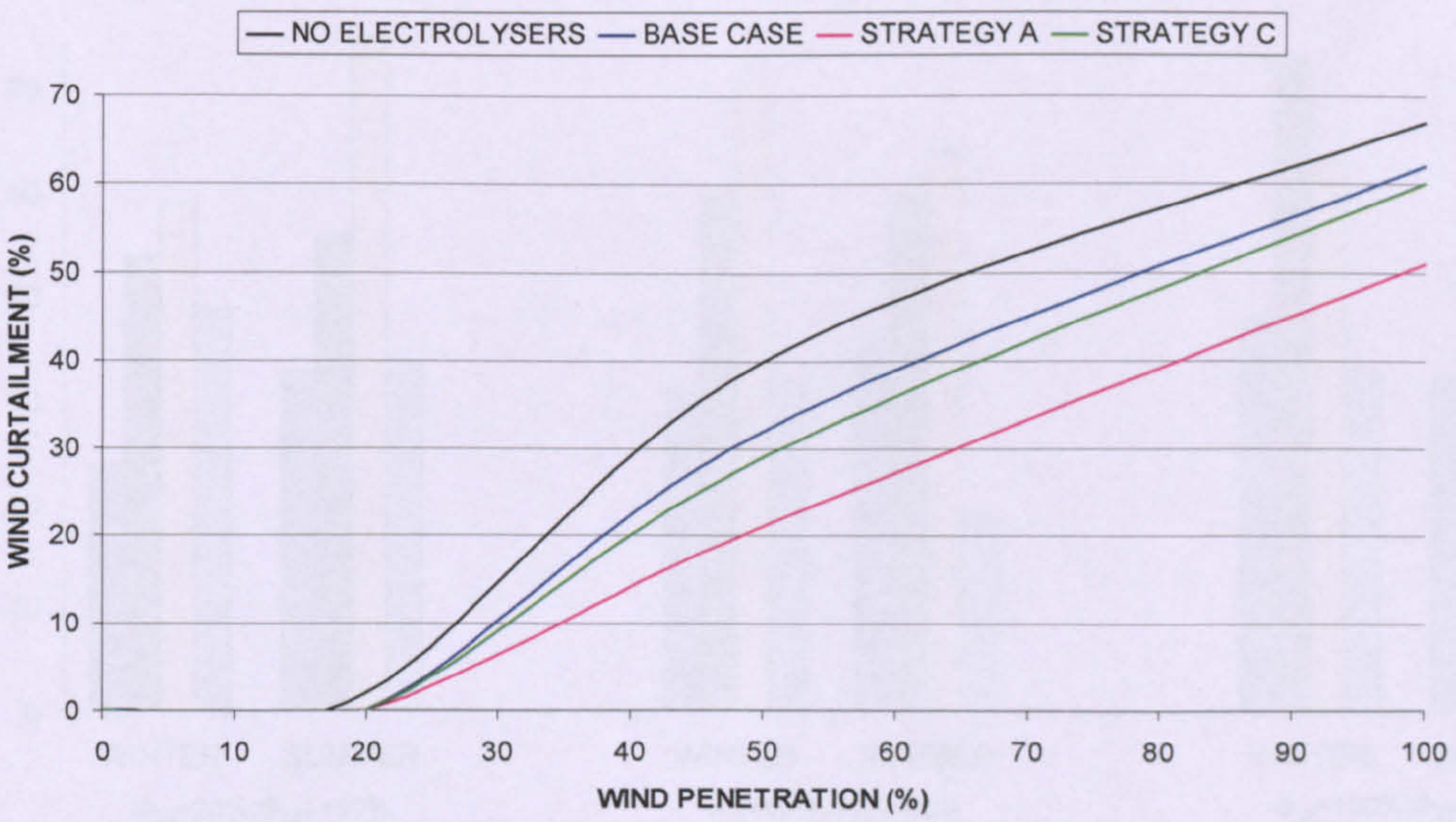

Figure 5.21. Wind curtailment for increasing wind power penetrations for several DSE implementation cases

Regarding the utilization factor of the DSE, when comparing with Case 1 higher values are attained for the winter week at $\Phi_W > 50\%$ because lower ELS capacities are deployed; and similar values to those of Case 1 for the summer week. In general lower values are obtained during the summer week at $\Phi_W > 20\%$ because a greater proportion of wind generation is then curtailed, reducing the amount of hydrogen produced and therefore UF_E.

The highest values of UF_E are achieved for the operational strategies A and B, ranging between 44% and 65%, followed by the Base Case with UF_E between 24%-38% and finally the operational strategy C in the range 19-39% which on the other hand achieves the lowest values of CI_e. Remember there is a strong trade-off between CI_e and Y_H and thus between CI_e and UF_E, and so the greater the values of Y_H and UF_E the greater the value of CI_e; more zero-carbon electricity is used to produce hydrogen at the expense of increasing the carbon intensity of the electricity delivered to consumers. Values for the average weekly utilization factors are in the same range to the daily UF_E obtained previously. These are shown below in **Figure 5.22**.

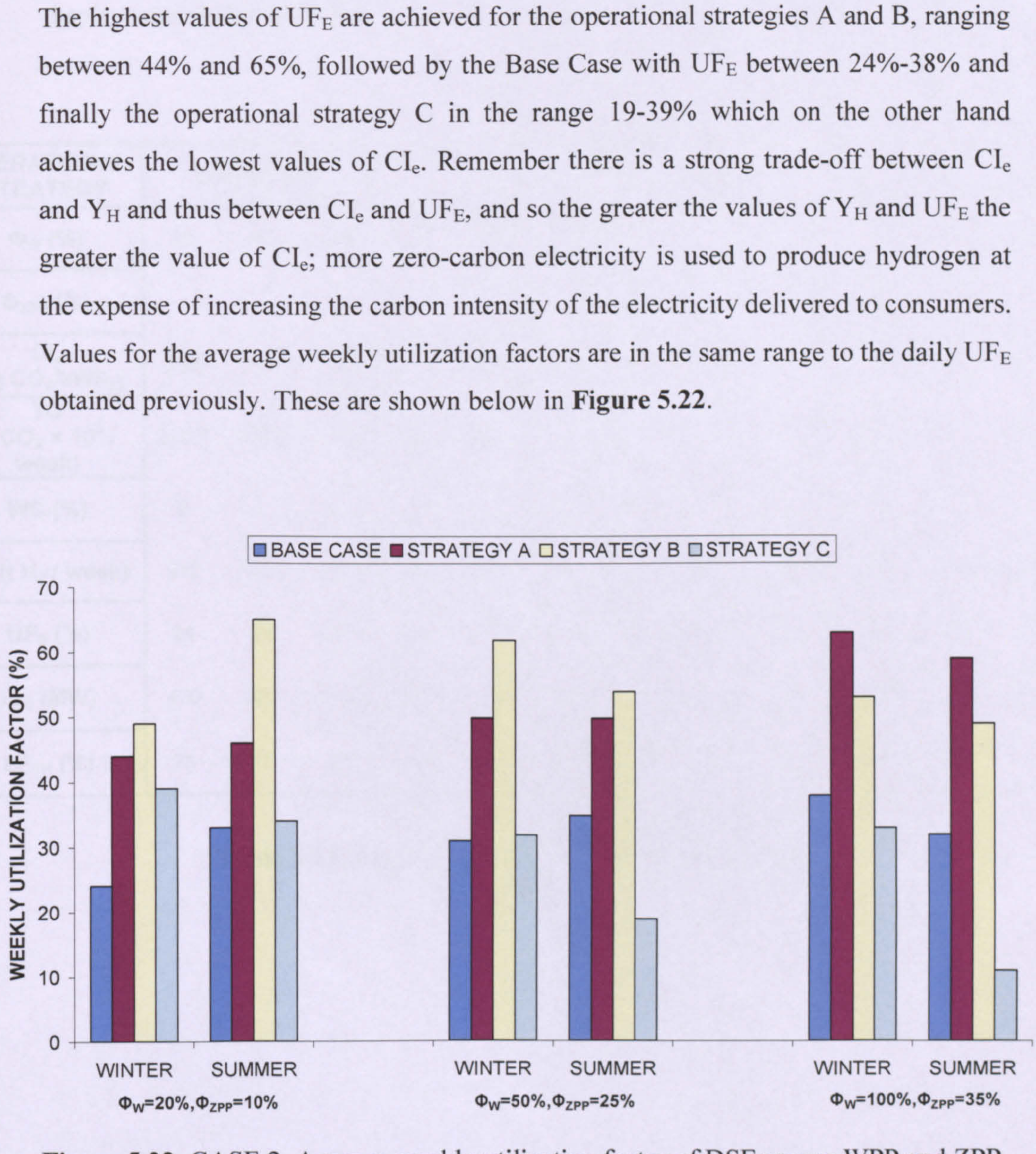

Figure 5.22. CASE 2. Average weekly utilization factor of DSE versus WPP and ZPP penetration for the two weekly scenarios.

3) Results for Case 3, zero-carbon hydrogen produced

Finally results are offered for a combined stock of SSE and DSE deployed in conjunction with WPP and/or ZPP. Firstly an analysis is presented considering the production of zero-carbon hydrogen. Then results are shown for a chosen CI_H = 3 kg CO_2 per kg of H_2 produced so as to increase Y_H and UF_E. **Tables 5.13 and 5.14** display results for CASE 3, $CI_H = 0$.

OPERATIONAL STRATEGY	BASECASE			A			B			C		
Φ_W (%)	20	50	100	20	50	100	-	-	-	20	50	100
Φ_{ZPP} (%)	-	-	-	10	25	35	10	25	35	10	25	35
CI_e (kg CO_2/kWh$_e$)	0.66	0.59	0.53	0.63	0.49	0.39	0.65	0.56	0.44	0.63	0.45	0.31
TC (t $CO_2 \times 10^3$ / week)	215.7	192.8	173.2	205.9	160.2	127.5	212.4	183.0	143.8	205.9	147.1	101.3
WC (%)	0	0	0	0	0	0	-	-	-	0	0	0
Y_H (t H_2 / week)	372	1,083	2,403	869	2,089	3,817	398	1,244	1,488	904	1,701	3,070
UF_E (%)	24	29	32	45	38	38	49	62	53	39	28	29
IC_E (MW)	470	920	2,240	575	1,630	2,965	240	600	840	695	1,770	3,175
LF_{TH} (%)	75	72	70	75	69	66	74	88	91	79	74	70

Table 5.13. Results for CASE 3, $CI_H = 0$, winter week

OPERATIONAL STRATEGY	BASECASE			A			B			C		
Φ_W (%)	20	50	100	20	50	100	-	-	-	20	50	100
Φ_{ZPP} (%)	-	-	-	10	25	35	10	25	35	10	25	35
CI_e (kg CO_2/kWh$_e$)	0.60	0.57	0.52	0.61	0.42	0.33	0.65	0.51	0.37	0.59	0.32	0.17
TC (t $CO_2 \times 10^3$ / d)	142.8	135.7	123.8	145.2	100.0	78.5	154.7	121.4	88.1	140.4	76.2	40.5
WC (%)	0	0	0	0	0	0	-	-	-	0	0	0
Y_H (t H_2 / week)	506	1,391	3,254	891	2,375	4,674	526	1,091	1,372	785	1,650	3,529
UF_E (%)	32	38	43	46	43	47	69	54	49	34	28	32
IC_E (MW)	470	920	2,240	575	1,630	2,965	240	600	840	695	1,770	3,175
LF_{TH} (%)	79	80	86	77	75	81	81	89	86	81	76	81

Table 5.14. Results for CASE 3, $CI_H = 0$, summer week

As in the daily analysis presented previously values obtained for LF_{TH}, CI_e and TC are the same as those obtained for Cases 1 and 2. Also Y_H values result the same as in Case 1 and higher than in Case 2. However since the ELS installed capacity is higher now than in Case 1 for the strategies A and C at $\Phi_W > 20\%$, the weekly average UF_E are to some extent lower when deploying a combined SSE + DSE stock. Wind curtailment is eliminated across all the operational strategies and also for the Base Case both during the winter and summer week. When comparing with the daily values obtained for UF_E in **Tables 5.5 and 5.6** the ranges obtained are quite similar, the weekly UF_E being somewhat higher. The highest utilization is achieved for the Strategy B when only ZPP are deployed, followed by A and finally C which in contrast yields the lowest values of CI_e (**Tables 5.13 and 5.14**). The ranges of values of UF_E obtained are very similar for the winter and summer week, as observed in **Figure 5.23.**

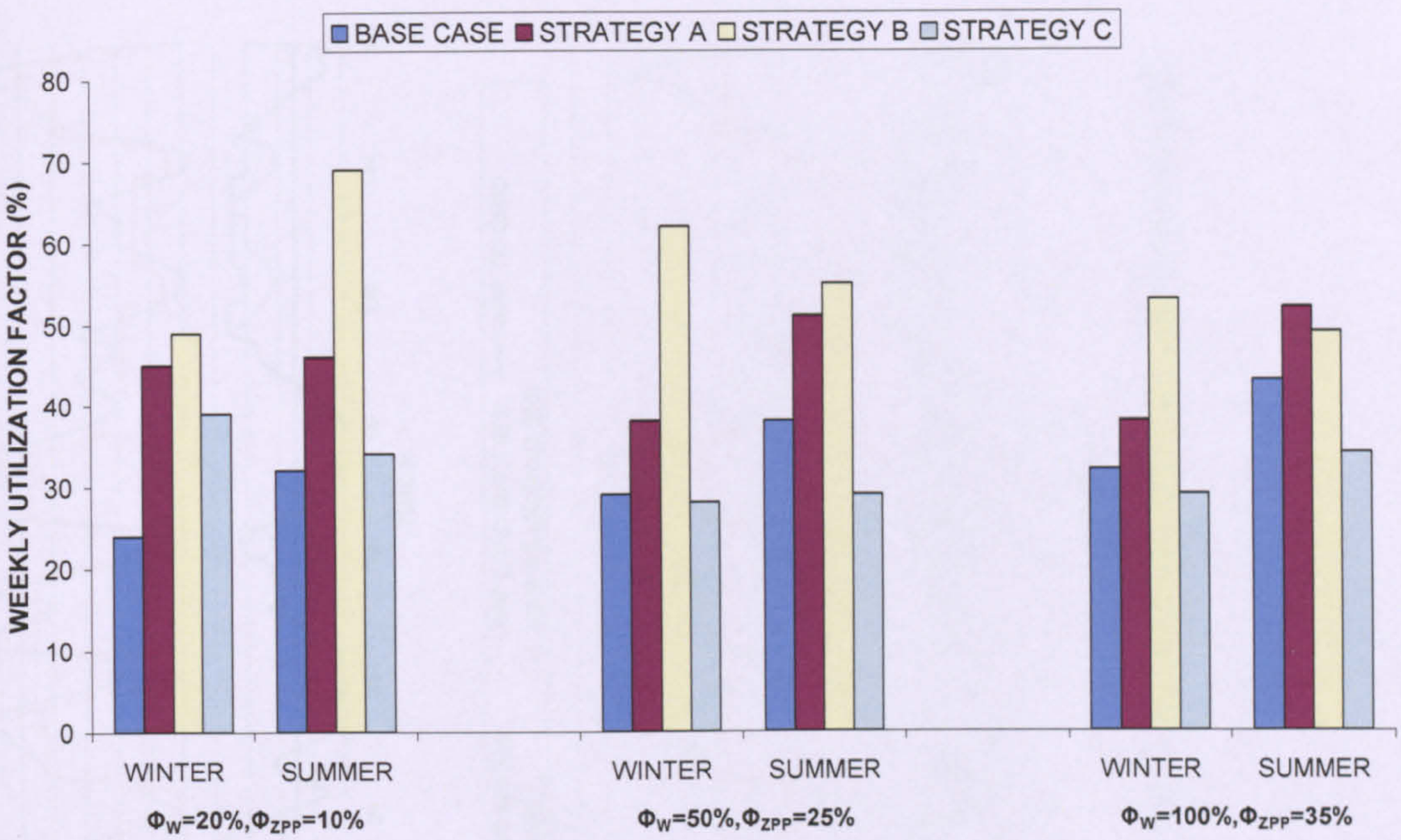

Figure 5.23. Case 3. Average weekly utilization factor of the SSE+DSE stock versus WPP and ZPP penetration for the two weekly scenarios.

Aggregate load profiles of FPP, ZPP and WPP across the weekly period were also investigated. **Figures 5.24 and 5.25** show simulations of weekly operation periods at $\Phi_W = 50\%$, $\Phi_{ZPP} = 25\%$ for the winter and summer week respectively.

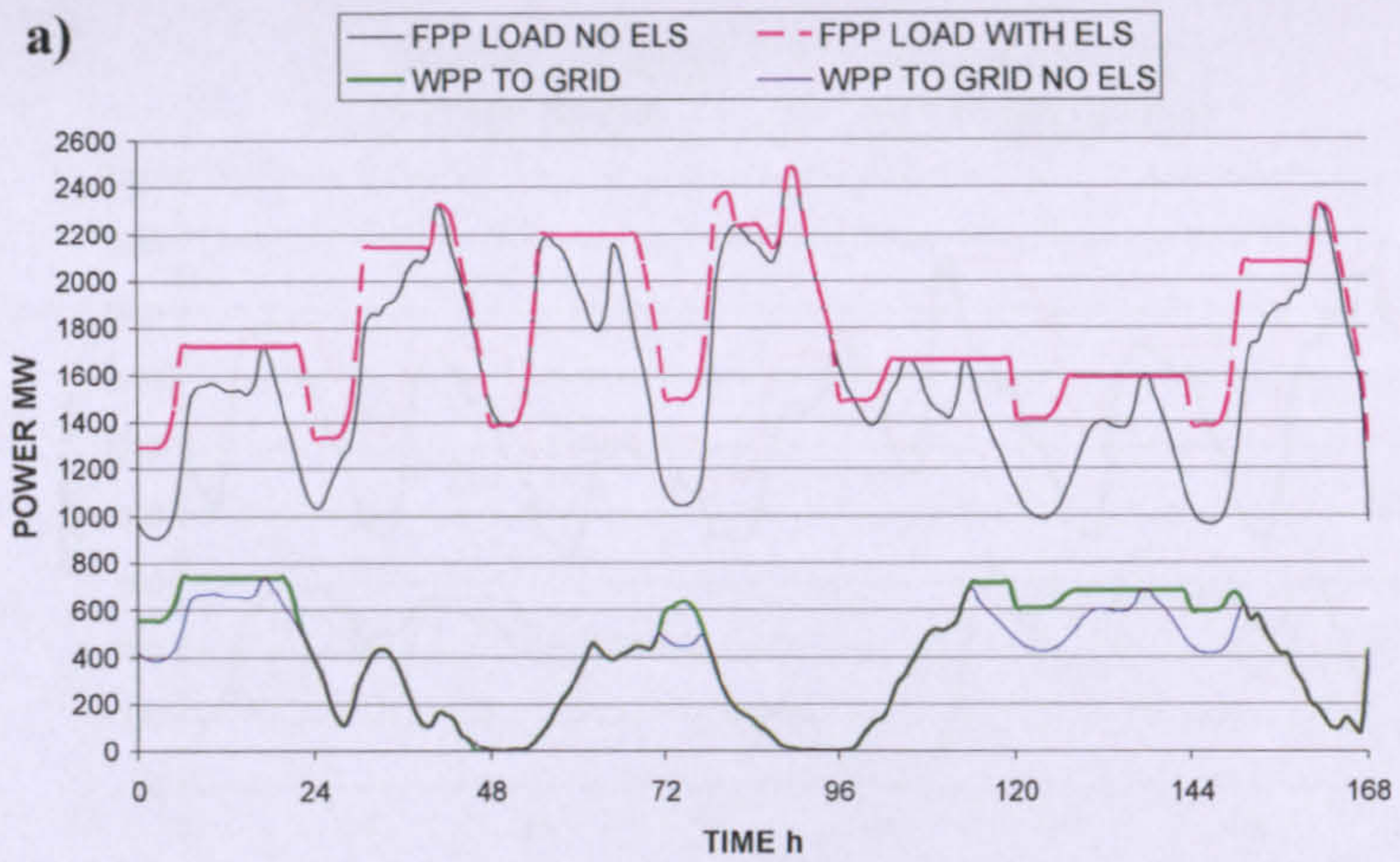

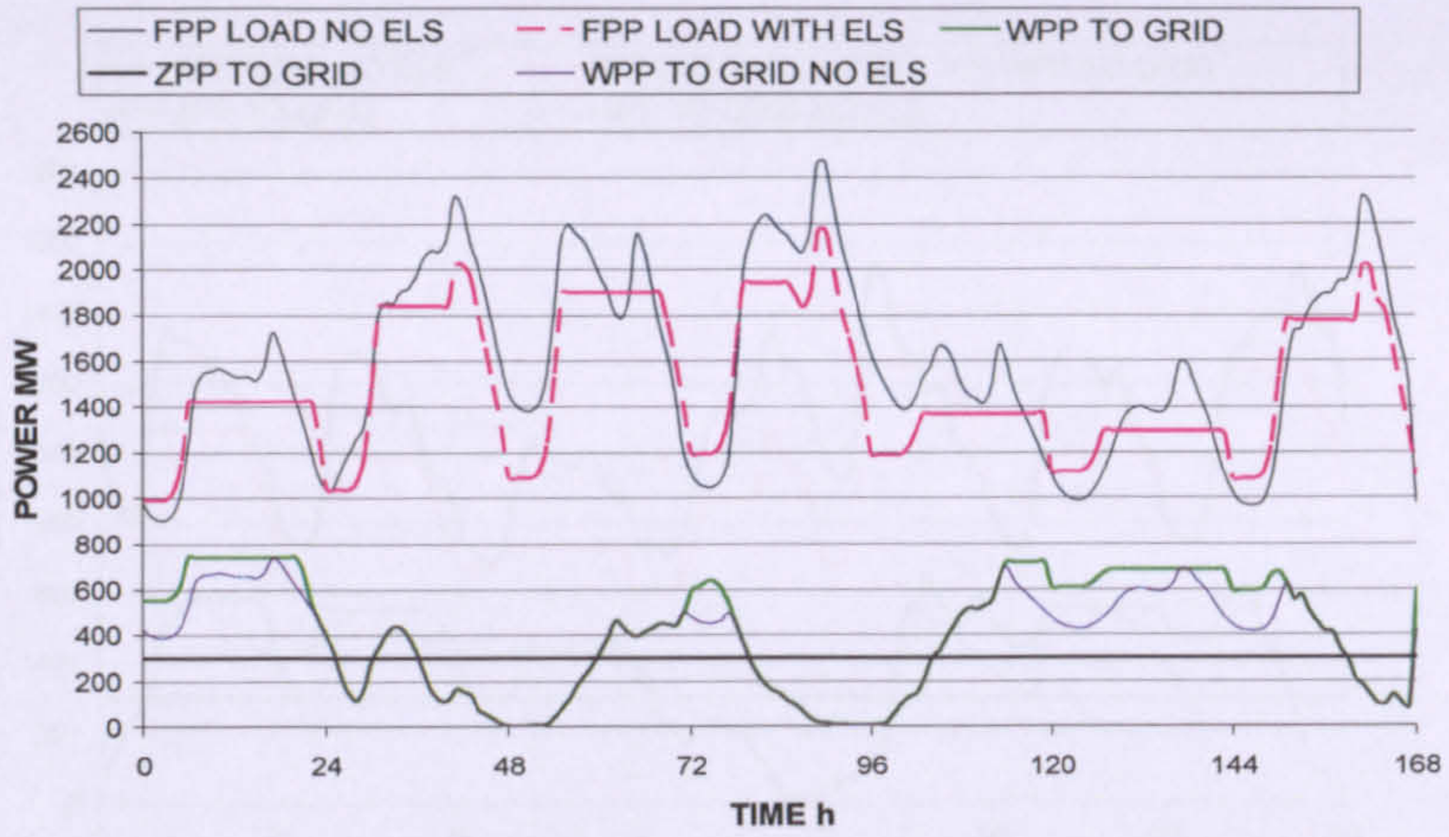

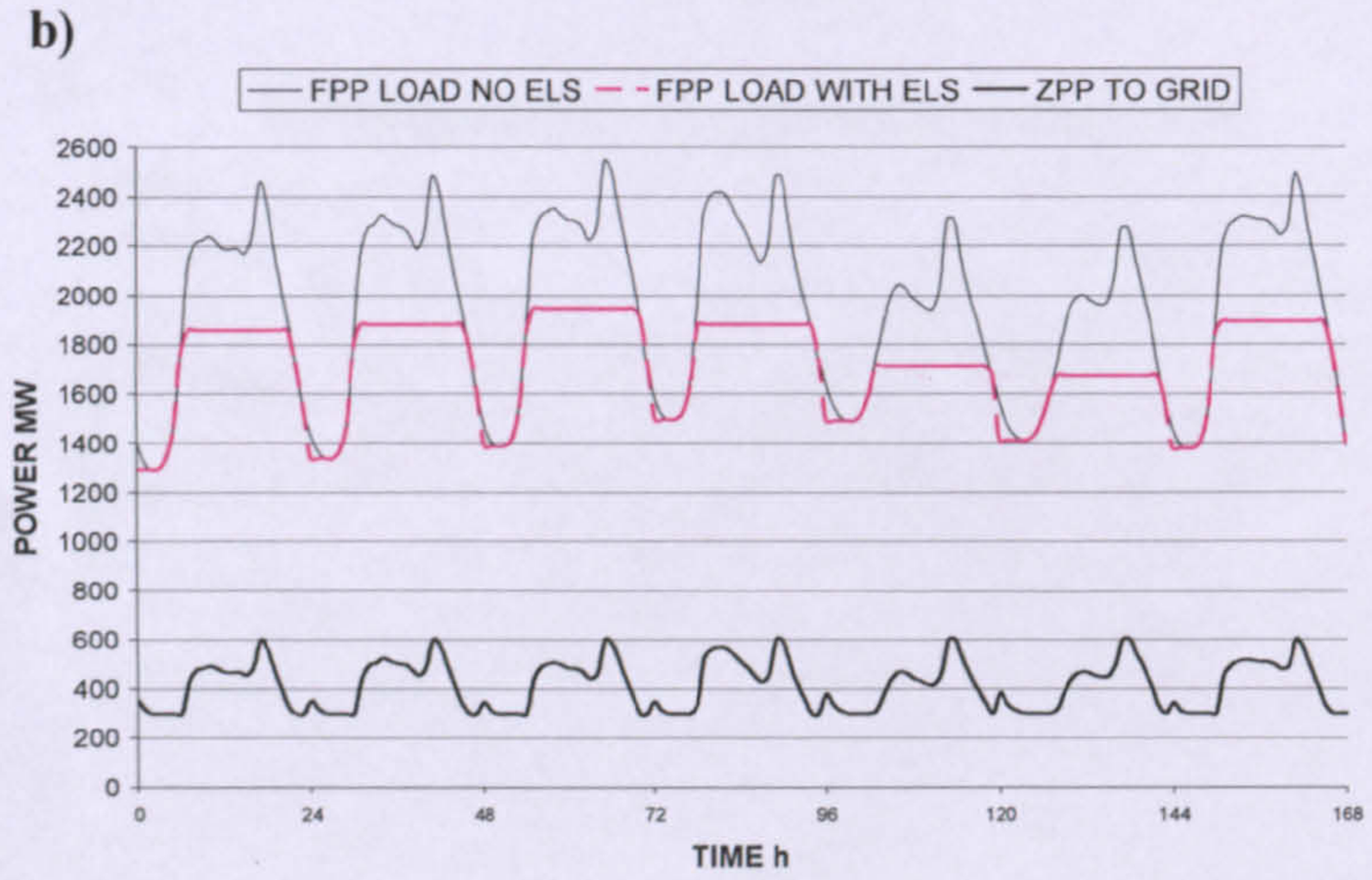

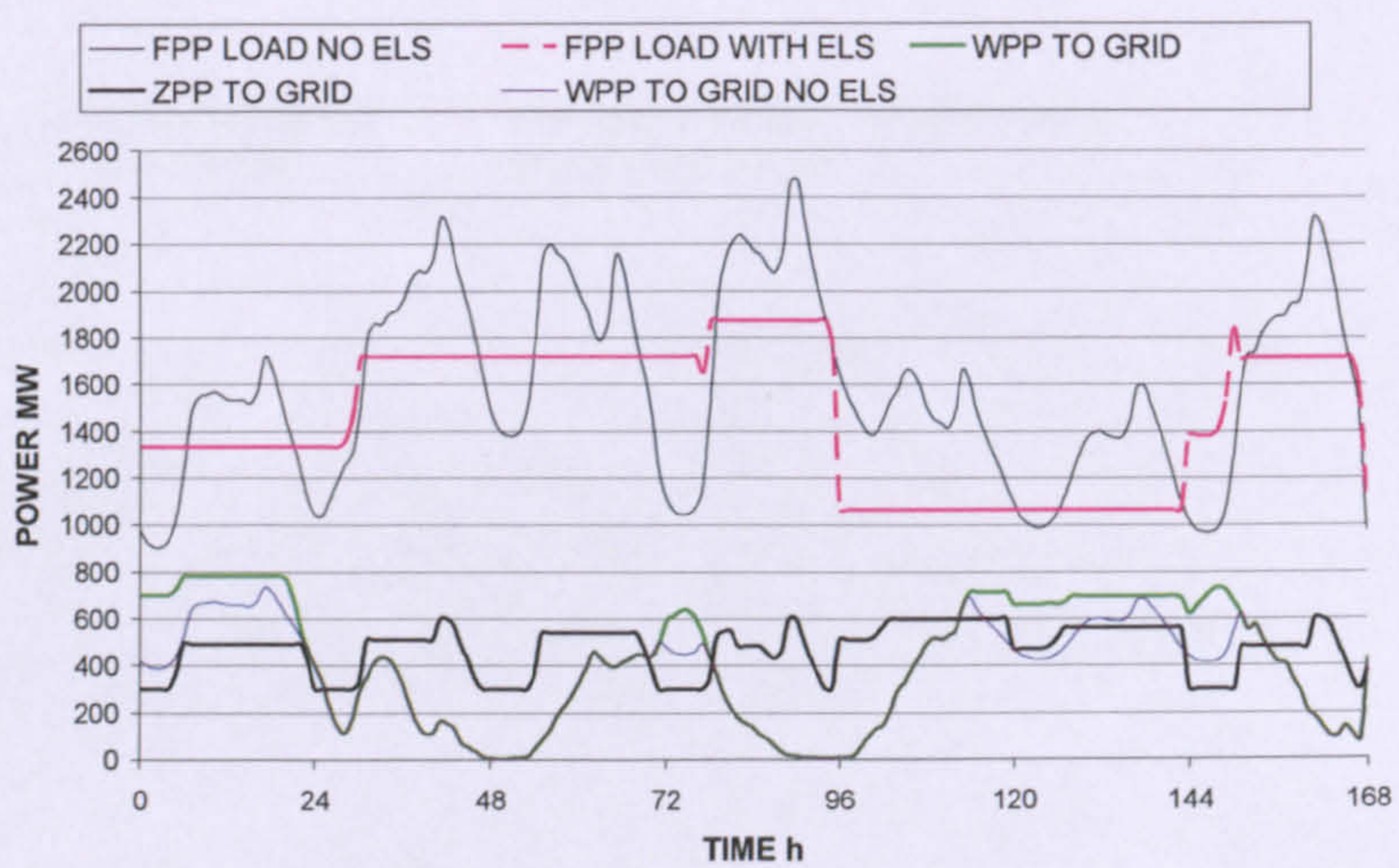

Figure 5.24. CASE 3. Winter week, Φ_W=50%, Φ_{ZPP}=25%. Effects on aggregate FPP load, WPP and ZPP output delivered to grid.

a) Base case
b) Strategy A
c) Strategy B
d) Strategy C

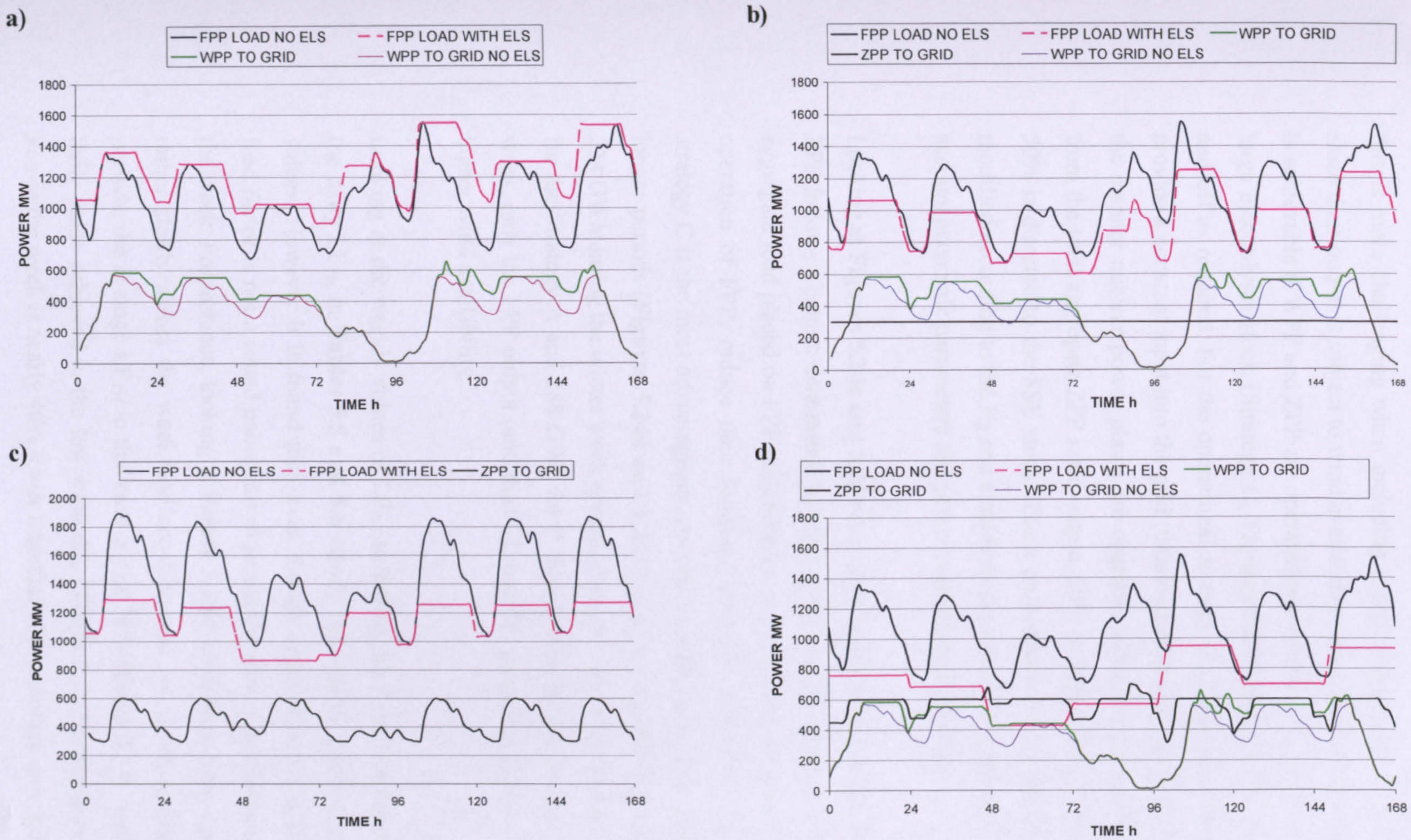

Figure 25. CASE 3, $CI_H = 0$. Summer week, Φ_W=50%, Φ_{ZPP}=25%. FPP, WPP and ZPP output delivered to grid

a) Base case
b) Strategy A
c) Strategy B
d) Strategy C

For all the strategies the aim was to create daily plateaus so as to maintain the operation of FPP as constant as possible to minimize their carbon footprint. Clearly this is more challenging when including a high penetration of WPP in the system since their output is subject to wind availability (see **Figures 5.24a and 5.25a**). Yet it is achievable if WPP and ZPP are operated in a transient mode in combination with a large electrolyser stock (Strategy C, **Figures 5.24d and 5.25d**), switching them on and off as required. For the operational strategy A (**Figures 5.24b and 5.25b**) ZPP provide a constant input into the grid (baseload electricity generation) for example in the manner nuclear power plants are operated today. In the simulation shown here from the total aggregate ZPP rated output, 50% is delivered to the grid and the other 50% is directed to the SSE stock. These proportions can be maintained constant or modified according to the H_2 and electricity demands to cover and/or also taking into account economic parameters and power market specifications.

Looking at **Figures 5.24c and 5.25c** it is clear how for the strategy B the operation of ZPP follows a pattern determined by the system demand which in this case equals the aggregate load placed on FPP with no ELS in the system. In terms of optimizing the operation of FPP, reduce their load and therefore minimize CI_e, the operational strategy C is the most advantageous. As well as achieving a flat operation of FPP for longer periods (**Figures 5.24d and 5.25d**), also the weekly aggregate FPP output is 234 GWh during the winter week compared to 301 GWh for the Base Case, 250 GWh for the Strategy A and 288 GWh for B. Similar results are obtained for the summer week, only the FPP output (and thus CI_e and TC values) is lower in all cases due to higher wind availability.

Looking at the weekly values of LF_{TH} in **Tables 5.13 and 5.14** and comparing with the daily LF_{TH} in **Tables 5.5 and 5.6** clearly the weekly figures lie below the daily values. However it is found that, even though appropriate for a daily analysis, the load factor is not a sound parameter to assess the carbon performance of FPP across the week. For instance, looking at **Figure 5.25d**, even though the operation of FPP is rather steady across the week and constant load levels are maintained for longer periods, the average LF_{TH} in this case is just 76% (**Table 5.14**), well below the 94% daily value achieved in the low wind day (**Table 5.5**). Furthermore the average CI_e across the week is nearly 40% lower than that of the average during the low wind day

(0.32 kg CO_2/kWh$_e$ versus 0.52 kg CO_2/kWh$_e$ respectively). Also comparing across operational strategies, the LF_{TH} on the summer week at Φ_W = 50% for the Base Case is 80% (**Table 5.14**), and 76% for the Strategy C, and yet the FPP output is lower and clearly less variable for C (**Figures 5.24 and 5.25**), and then CI_e is lower for the Strategy C (**Table 5.14**), because the aggregate load placed on FPP is much lower (118 GWh for C and 206 GWh for the Base Case).

For all the strategies, subject to wind availability a daily plateau can be pursued as shown in **Figure 5.25**, or instead an alternative strategy can be followed by prolonging the daily plateau as shown in **Figure 5.26**. However this is not possible for the winter week while maintaining $CI_H = 0$ because there is not enough wind availability and therefore this alternative is only discussed here for the summer week. The implications of relaxing CI_H on the ability to create longer plateaus on the FPP load profile is discussed below in this same chapter. For the sake of discussion this alternative strategy will be named Strategy C_L (summer week). When comparing Strategy C_L (**Figure 5.26**) and Strategy C (**Figure 5.25d**), the benefits of Strategy C_L on the operational performance of FPP are clear. A more optimized operation of FPP is achieved with fewer load changes, and also the weekly hydrogen yield increases by 16% from 1,650 (55 GWh H_2 LHV) to 1,911 tonnes of H_2 (64 GWh LHV). However by extending the duration of the plateau the aggregate weekly load imposed in FPP increases by 13% from 118 GWh to 134 GWh, and consequently CI_e and TC increase by 13% as well.

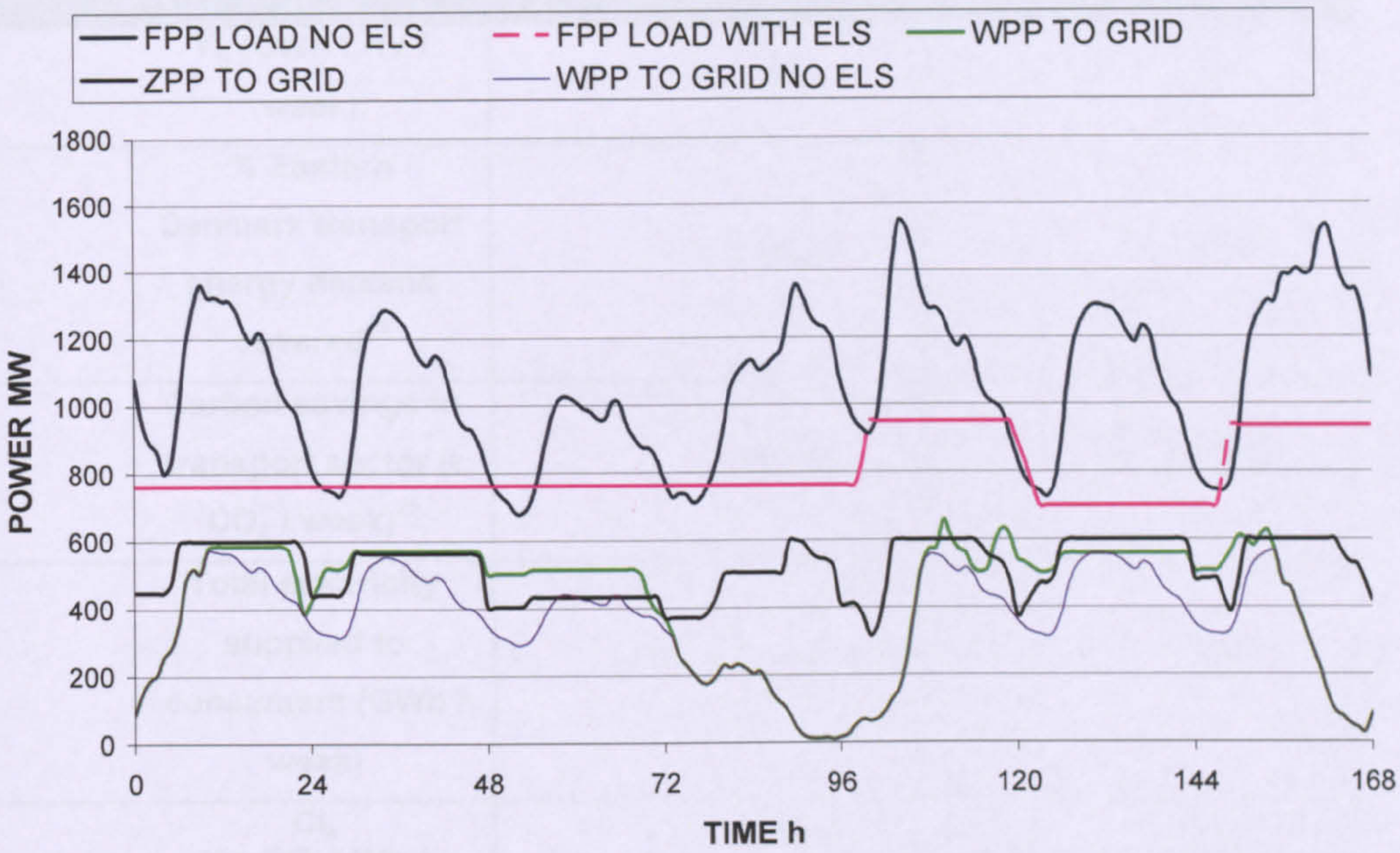

Figure 5.26. CASE 3, $CI_H = 0$. Summer week, Φ_W=50%, operational strategy C_L. Modified FPP load to increase the length of the daily plateaus

For the case of East Denmark, a comparison between Strategies C and C_L can be made. **Table 5.15** shows energy and carbon parameters corresponding to both strategies assuming that all the hydrogen produced is used in the transport sector and 1 kWh of H_2 displaces 1 kWh of transport fossil fuel.

	Strategy C	Strategy C_L
Y_H (GWh LHV / week)	55	64
% Eastern Denmark transport energy demand covered[26]	14.3	16.6
Carbon savings in transport sector (t CO_2 / week)[25]	18,596	21,590
Total electricity supplied to consumers (GWh / week)	238	238
CI_e (kg CO_2/kWh$_e$)	0.32	0.36
TC (t CO_2 / week)	76,160	85,680

Table 5.15. CASE 3, summer week, Φ_W=50%, Φ_{ZPP}=25%. Energy and carbon parameters derived from operational strategies C and C_L (see **Footnote 3**)

The increase in Y_H allows an increase in carbon savings from transport of 2,990 t CO_2 per week from strategy C to strategy C_L but in this particular case CI_e increases from 0.32 to 0.36 kg CO_2 per kWh$_e$ delivered to consumers and then TC increases by 8,920 t CO_2 per week. However a more careful analysis is be needed to fully assess all the carbon benefits associated with the optimization of the operation of FPP. These would include:

1. A more stable and predictable operation of FPP due to a more steady load profile attained when implementing the ELS stock

[26] Total average transport energy demand in East Denmark in 2003 was 385 GWh per week. Total average carbon emissions allocated to the transport sector in 2003 in East Denmark were 130,040 tonnes CO_2 per week [81].

2. A reduced operational requirement for supply/demand matching with back-up FPP on days of low or variable wind availability

Allowing for these carbon benefits it is expected that the increase in TC would be much lower than 8,920 t CO_2 due to the reductions achieved in carbon emissions from back-up plant operation when selecting the strategy C_L instead of the strategy C.

Instead of increasing the duration of the daily plateaus on the FPP profile, other short term objectives could be aimed for; for instance creating shorts plateaus in the aggregate FPP load lasting for say 2-3h, depending on a number of additional restrictions like wind availability, fossil fuel availability, power market conditions and economic objectives. Ultimately the optimal strategy to follow must be identified within the context of the specific energy system under consideration and the optimization parameters selected. Some of these practical implementation topics are discussed in **Chapter 6**.

It is also interesting to analyse the time-phasing operation of ELS referred to consumer demand and wind availability. A simulation of the time-sequential operation of the electrolyser stock for the same case shown in **Figure 5.26** is plotted in **Figure 5.27**.

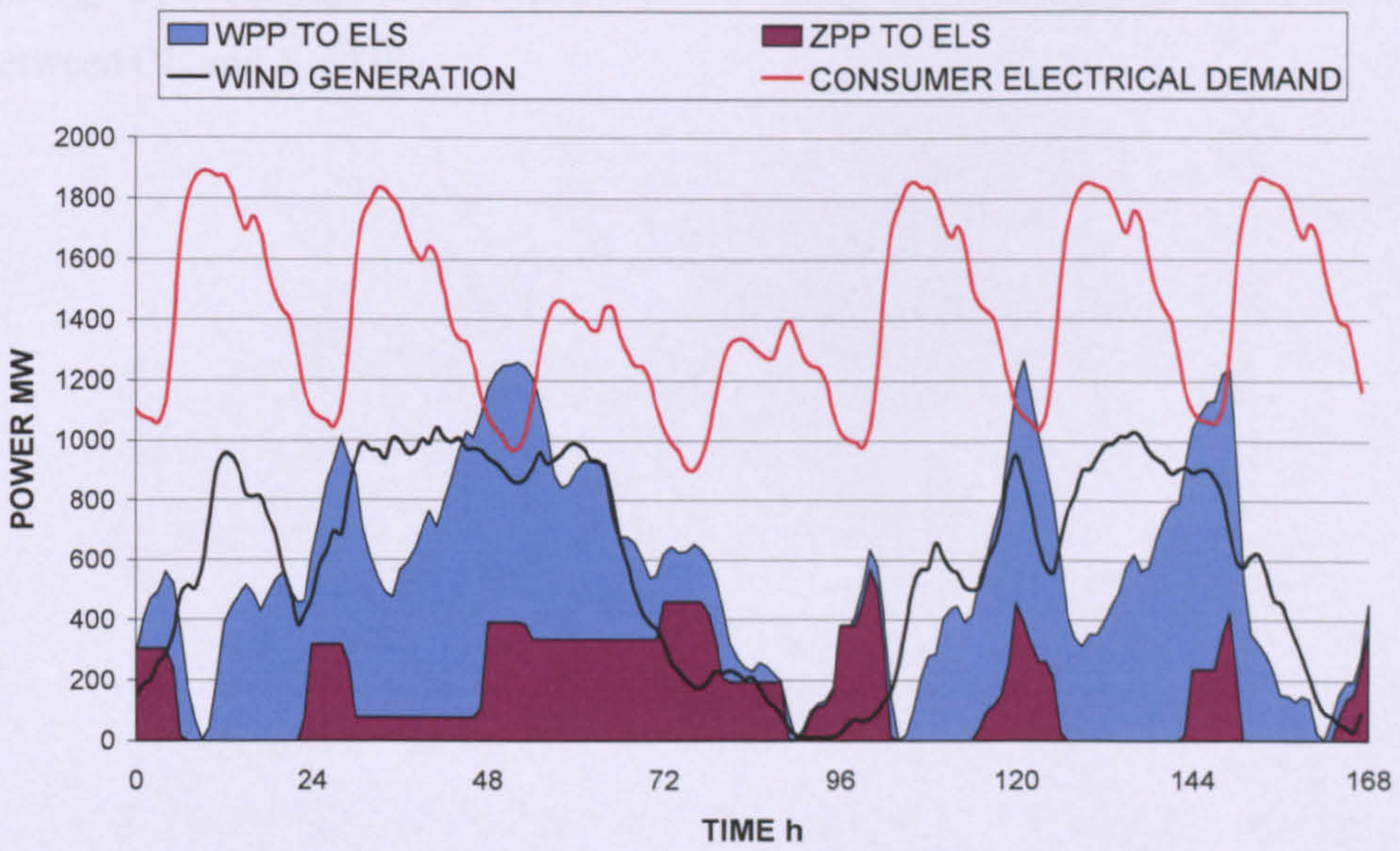

Figure 5.27. CASE 3, $CI_H = 0$. Summer week, Φ_W=50%. Aggregate electrical input to the SSE + DSE stock. Influence of consumer's electrical demand and wind availability

From **Figure 5.27**, every time there is a decrease in electrical consumer's demand (red curve), e.g. during the night time, the aggregate input to the ELS stock also is allowed to increase and vice-versa. Also when the WPP output drops the electrical input to ELS must decline but still some hydrogen can be produced using electricity supplied by ZPP, increasing the average utilization of the ELS stock.

Another interesting observation can be drawn from **Figures 5.26 and 5.27.** Even in days of low wind availability the aggregate FPP load does not need to ramp-up and can be maintained constant by both increasing the ZPP output directed to grid and decreasing the electrical input to ELS. When an appropriate optimized operational strategy is applied to the SSE + DSE stock, in combination with ZPP, then the operation of FPP is not affected by wind availability and the benefits of a large implementation of ELS in the power system can be fully exploited.

4) Results for CASE 3, $CI_H = 3$ kg CO_2 / kg H_2

Comparing **Figures 5.28 and 5.29** with **Figures 5.16 and 5.23** (note Y_H values are the same for CASES 1 and 3 when $CI_H = 0$), when the carbon intensity of hydrogen is allowed to exceed zero, higher Y_H and UF_E can indeed be achieved in particular for strategy C, but always at the expense of increasing CI_e, making clear again the trade-off between CI_e and Y_H, UF_E.

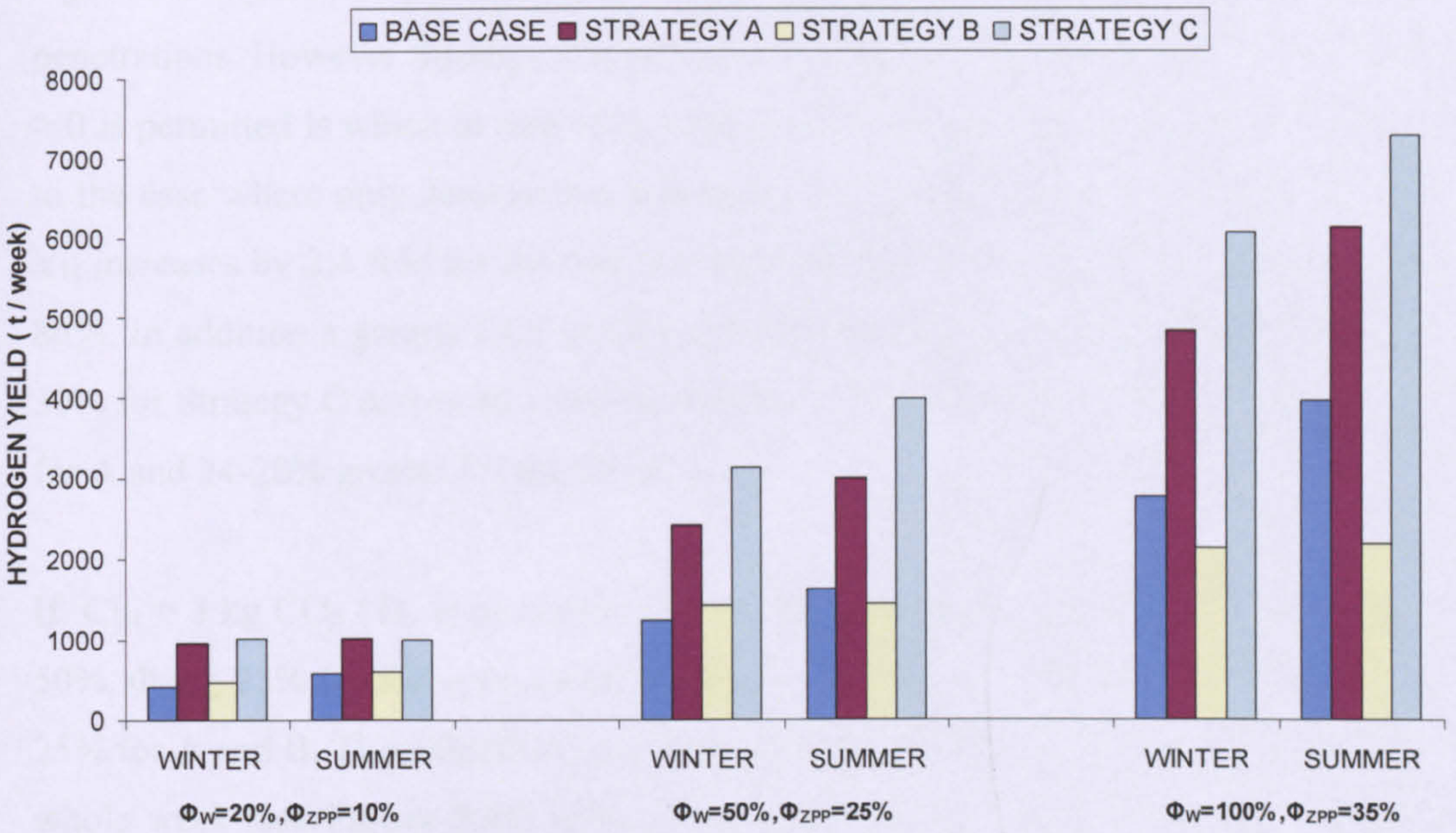

Figure 5.28. CASE 3, $CI_H = 3$ kg CO_2/kg H_2. Weekly hydrogen production versus WPP and ZPP penetration for the weekly periods selected.

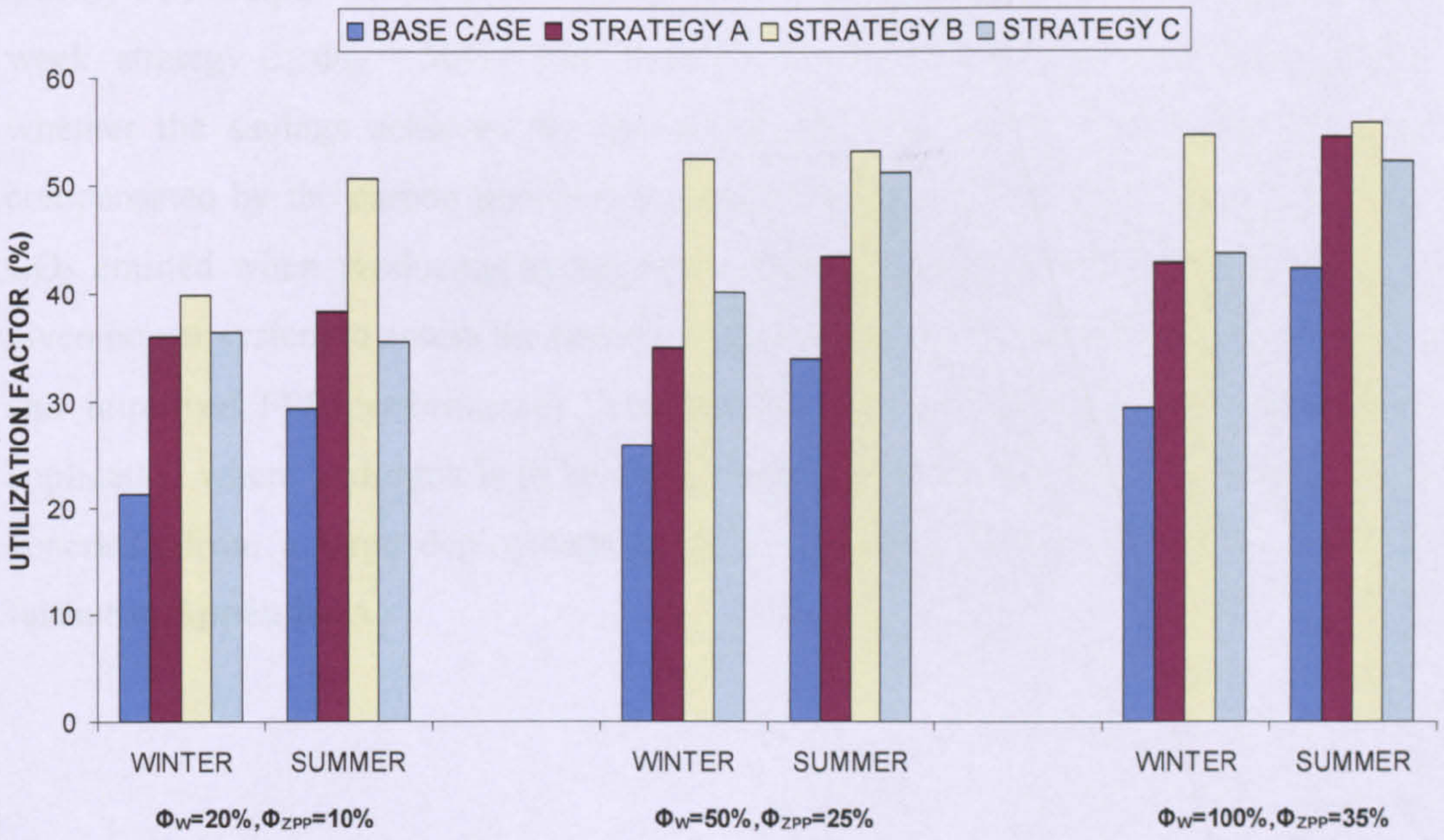

Figure 5.29. Case 3, $CI_H = 3$ kg CO_2/kg H_2. Average weekly utilization factor of the SSE+DSE stock versus WPP and ZPP penetration for the two weekly scenarios.

Again the highest UF_E values are attained for Strategy B across all WPP and ZPP penetrations. However Strategy C attains the highest increase in Y_H and UF_E when $CI_H > 0$ is permitted is which in turn incurs the highest increase in CI_c and TC with respect to the case where only zero-carbon hydrogen is produced. For instance, at $\Phi_W = 50\%$ Y_H increases by 2.4 fold for the summer week but then CI_c and TC increases by nearly 80%. In addition a greater ELS stock is required in order to increase Y_H, explicitly by 30% for Strategy C across all wind penetrations, 33-46% greater for B, 13-26% greater for A and 24-28% greater for the BaseCase.

If $CI_H = 3$ kg CO_2 / H_2 is permitted, the weekly average LF_{TH} achieves 100% at $\Phi_W \geq 50\%$, $\Phi_{ZP} \geq 25\%$ for the operational strategy C, and $LF_{TH} = 100\%$ at $\Phi_W > 50\%$, $\Phi_{ZP} > 25\%$ for A and B. This effectively means that FPP could be operated steadily across the whole week (see **Figure 5.30**) without any load changes, maximizing their utilization and minimizing their carbon footprint. From **Figure 5.30,** the WPP directed to the grid becomes more regular and predictable when deploying a large SSE+DSE stock with the consequent benefits for power system management. On the other hand, the aggregate weekly FPP output would double in this case from 118 GWh to 237 GWh (summer week, strategy C, $\Phi_W = 50\%$), increasing TC by nearly 80%. To accurately evaluate whether the savings achieved by increasing the scale of H_2 production would be compensated by the carbon penalties imposed when $CI_H > 0$ (i.e. increase in TC and CO_2 emitted when producing hydrogen), a specific analysis would be needed for a given power system to assess the benefits achieved when increasing CI_H (i.e. greater Y_H and improved FPP performance). Also results will vary depending on the end-use application where hydrogen is to be used. Potential end-use applications for hydrogen generated from a large deployment of ELS within the power system are explored further in **Appendix A.**

a)

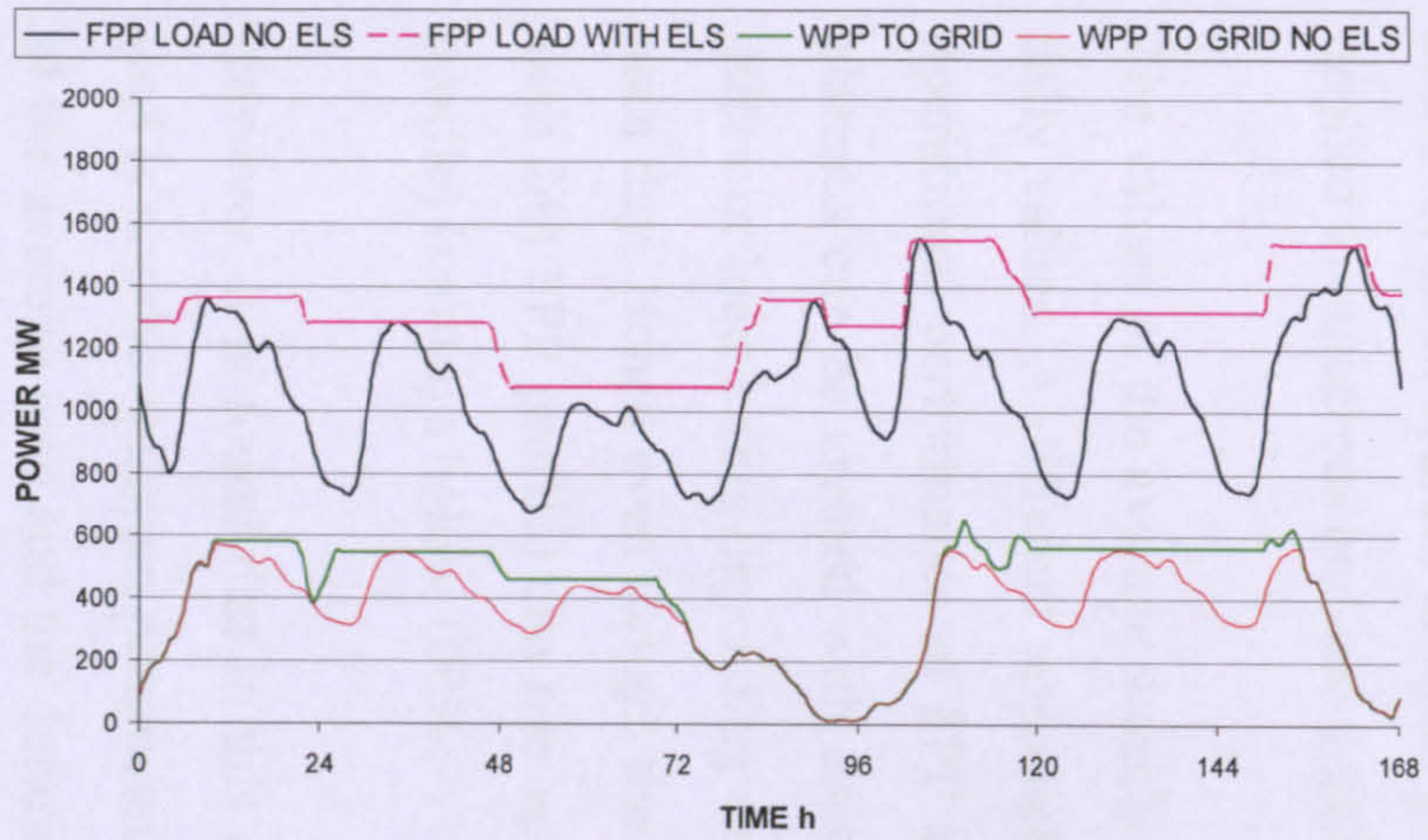

b)

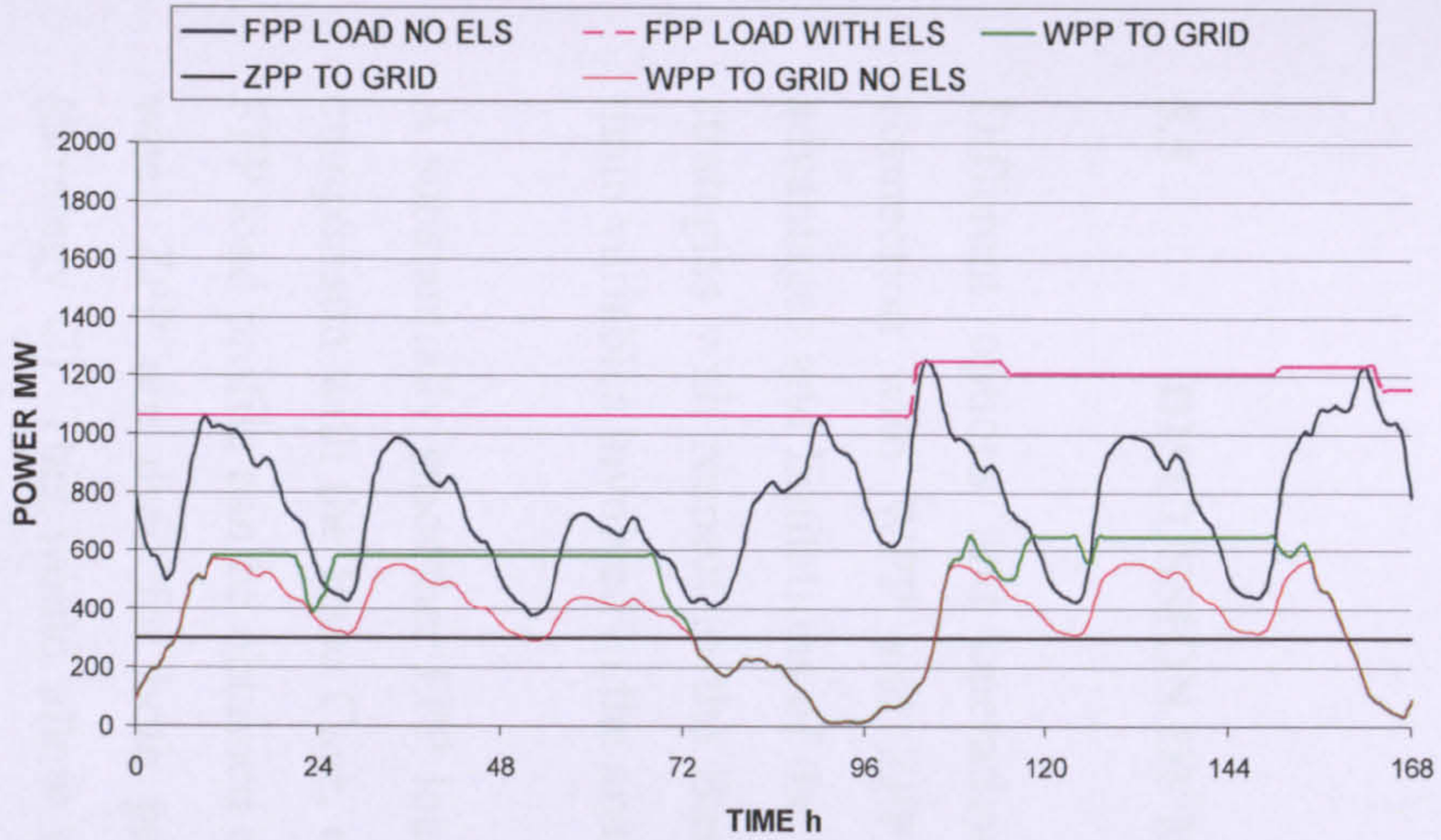

c)

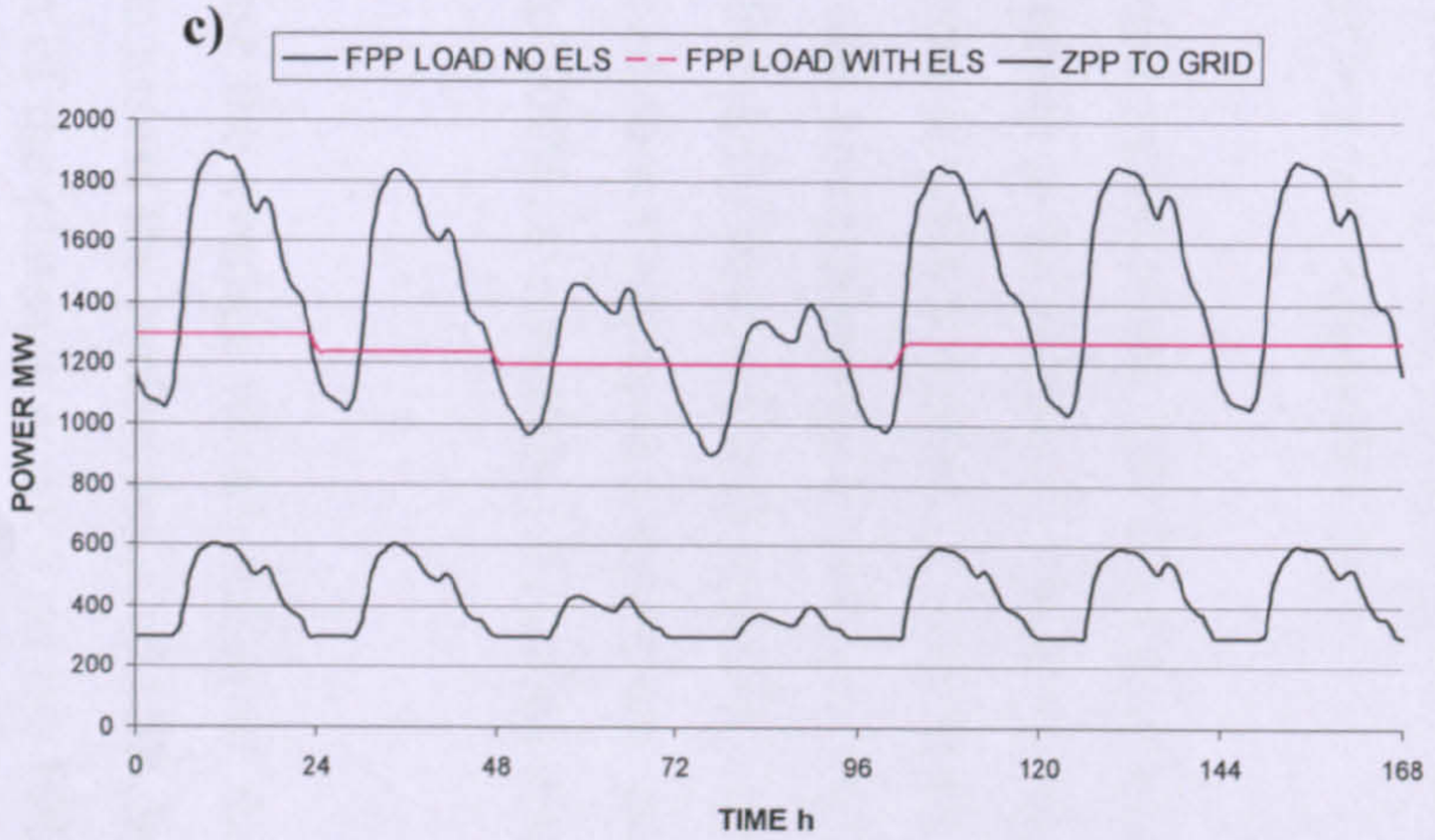

d)

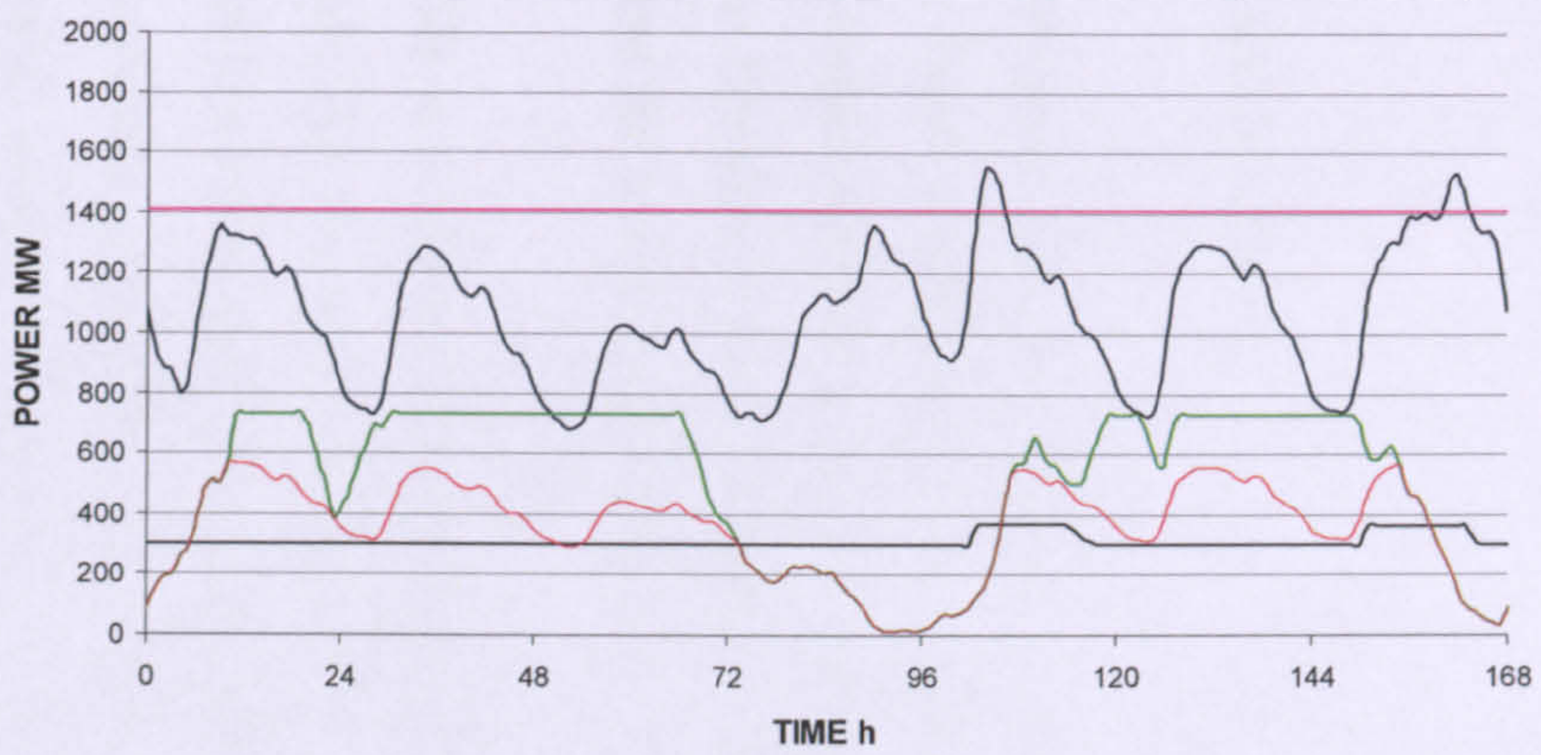

Figure 5.30. CASE 3, summer week, Φ_W = 100%, CI_H = 3 kg CO_2 / kg H_2. FPP, WPP and ZPP output delivered to grid

a) Base case
b) Strategy A
c) Strategy B
d) Strategy C

5.5 DISCUSSION OF MAIN RESULTS

Different options and operational strategies for the implementation of ELS in connection with WPP and ZPP have been evaluated. This section evaluates the advantages and limitations of the three implementation cases and proposed operational strategies with respect to the Base Case through a more detailed examination of the main variables involved in the analysis and the results presented in this chapter.

A substantially smoother FPP load profile is achieved for all implementation cases in comparison with the Base Case, especially for the strategies B and C. A virtually flat FPP load profile can be obtained even on low wind days (i.e. LF_{TH} approaching 100%) when ZPP are used for both peak electricity generation and hydrogen production (Strategy C). This would allow substantial carbon benefits in the power system, by increasing the penetration of zero-carbon power sources beyond those levels considered feasible today, as well as allowing FPP to operate more steadily across the day. In addition, clean sources of hydrogen (and by-product oxygen) are created which may be applied to numerous end-use applications (see **Appendix A**).

The values of the average weekly load factor of the FPP load profile always lie below daily values. A different approach needs to be followed when aiming to improve the operational performance of FPP across a weekly period. A succession of consecutive plateaus can be created with each one corresponding to one day of the week, but at different load levels depending on the daily demand and specific wind availability on each day. Hence even though the load factor calculated across any particular day (for each 24h FPP profile) can rise up to 100%, the weekly LF_{TH} (calculated for the 168h profile) is always below 100%.

However, it is found that in this case the average weekly LF_{TH} of the aggregate FPP load is not the optimum parameter to assess the performance of FPP. Instead, the value of the average load and the duration of the plateaus created on the FPP aggregate load

profile are far more significant measures of performance. The former will determine the carbon intensity of the electricity supplied CI_e and the latter indicates how long FPP are operating at a steady rate without load changes, thus maximizing their efficiency. Scarce date is available in the literature to estimate accurately the CO_2 emissions derived from the increased use of fossil back-up capacity for supply/demand balancing purposes as wind penetrations increases (see **Chapter 2**). Accurate modelling would be required to estimate these carbon implications and then the carbon benefits derived from a large electrolyser implementation as a load management mechanism. This is proposed here as an area for further research (see **Chapter 7**).

In general terms, CI_e (without accounting for back-up emissions) always decreases with respect to the Base Case when deploying ZPP and WPP in combination with a large electrolyser stock, because the load imposed on FPP falls. When the load factor is set up as an input to the model, this will determine the power and energy flows from FPP, ZPP and WPP directed to the grid, and therefore the carbon intensity of the electricity delivered. Thus if only zero-carbon hydrogen is to be produced, as imposed by the restrictions in equations (5.6), (5.29), (5.50), the three implementation cases will attain identical values of CI_e when the same target load factor is sought, independently of where the electrolyser stock is located.

A trade-off exists between the carbon intensity of electricity delivered to consumers, the average carbon intensity of the hydrogen generated and the total amount of H_2 produced. If CI_H is allowed to exceed zero and low-carbon hydrogen is produced, greater Y_H can be achieved. However the carbon savings achieved when increasing Y_H must be evaluated against the increase in carbon emissions released when producing hydrogen at $CI_H > 0$ along with the increase in TC due to a greater load placed on FPP. Depending on the specific hydrogen and electricity demands and provided that an average CI_H is not surpassed (i.e. a yearly average), some flexibility in terms of "relaxing" the carbon intensity of hydrogen (so as to further increase the scale of hydrogen production) may yield overall carbon benefits. This is to be analysed within

the context of the specific energy/power system under consideration and a definitive conclusion cannot be cannot be extracted from the analysis of a single power system.

Regarding wind curtailment, similar results to those shown in **Chapter 4** are observed. Case 2 cannot achieve the objective of eradicating wind curtailment (see **Figure 5.21**). Where wind curtailment is not yet a major issue ($\Phi_W < 40\%$) and the main objective is to produce moderate amounts of zero carbon hydrogen for distributed applications at minimal infrastructural cost, Case 2 is a reasonable option relative to Cases 1 and 3 which, for fixed values of LF_{TH} and Φ_W, Φ_{ZPP}, offers similar results in terms of CI_c, Y_H, UF_E and β_E. Because of the requirement to curtail wind generation, Case 2 can only achieve hydrogen yields of similar magnitude to those achieved by Cases 1 and 3 at the expense of allowing CI_H to approach that associated with hydrocarbon reformation methods.

For the operational strategies B and C the optimum installed capacity ratio of ELS is nearly the same for Cases 1 and 3 when the same LF_{TH} is targeted. The only difference is the location of the electrolyser stock. However for Strategy A results are different across the three implementation cases, with the higher β_E ratios corresponding to Case 3 and the lower values for case 2. Note that β_E is calculated for each implementation case as the maximum hourly electrical load required on the day of highest wind availability (high wind day). When the electrolyser stock is split between a SSE and a DSE stock (Case 3) this would be the sum of the maximum hourly load required for the SSE stock plus the maximum load required for the DSE stock, thus resulting in β_E values higher by 10-15% than those obtained for Case 1, even though same LF_{TH} and same Y_H are obtained on the low and variable wind day.

Comparing across the operational strategies greater β_E values are obtained for strategies A and C when compared with the Base Case in order to absorb the electrical output from both ZPP and WPP. Only when no WPP are deployed in the system (Strategy B) and the electrolyser stock is only fed by ZPP, are lower electrolyser capacities than the Base Case requires, when they are equal to the ZPP capacity available in the system for

the ZPP penetrations considered. For the operational strategy A, β_E values are of the order of the wind capacity installed in the system, whereas for C these are in excess of wind capacity, but then lower CI_c and higher LF_{TH} are obtained.

For fixed Φ_W and Φ_{ZPP}, the size of the electrolyser stock required to achieve the objectives of maximizing Y_H, UF_E, LF_{TH} and minimizing CI_c will be a function of: (i) the shape of the demand profile of the power system under consideration, in particular the magnitude (depth) of the morning and night-time valleys on a day of maximum system demand; (ii) the maximum wind availability expected across the year; and (iii) the LF_{TH} targeted.

Results displayed for LF_{TH} reflect the maximum values achievable subject to the restriction that only zero-carbon hydrogen is produced for all the operational strategies considered, as expressed in equations (5.6), (5.29) and (5.50). For the same implementation case considered values of IC_E will vary between strategies A and C depending on the maximum LF_{TH} achieved. Should the same LF_{TH} be desired for both operational strategies, then the same capacity of ELS would be required.

For all implementation cases considered, both Y_H and UF_E increase substantially with respect to the values obtained previously when no ZPP are deployed (Base Case). If a SSE stock is implemented Y_H and UF_E can be further improved, particularly on days of low wind availability, by increasing the amount of zero-carbon thermal power directed to the electrolyser stock, although at the expense of increasing the carbon intensity of the electricity delivered to consumers. For example, for Strategy A Case 3 at Φ_W=100%, Φ_{zc} = 35%, 370 tonnes of H_2 per day can be produced with UF_E = 26% and CI_e = 0.41 kg CO_2/kWh$_e$ when 50% of the aggregate ZPP output is directed to the SSE stock. Yet the amount of zero-carbon hydrogen produced can be increased by 27% up to 471 tonnes of H_2 per day with UF_E = 33%, but then CI_e increases to 0.48 kg CO_2/kWh$_e$. Again depending on the power and energy system under consideration and specifically on the hydrogen and electricity demands to be covered, optimum values for

Y_H, UF_E and CI_e could be found in order to maximize the net carbon benefits derived from a large implementation of electrolysers (see **Chapter 7**).

Hence additional deployment of ZPP in combination with ELS eliminates one of the drawbacks of implementing a large stock of electrolysers in conjunction with high penetrations of WPP (see **Chapter 4**), and makes the case for a large deployment of ELS economically more attractive.

5.6 CONCLUSIONS

This chapter presents an extension of the approach and the results presented in **Chapter 4** for the implementation of a large stock of electrolysers in the power system, consisting of the additional development of ZPP (e.g. CO_2 sequestered, nuclear) with the objectives of (i) increasing the scale of H_2 production; (ii) increasing the utilization factor of electrolysers; and (iii) minimizing the carbon intensity of electricity with respect to the values obtained previously when solely WPP are implemented in the system. Results presented are based on demand and wind generation data obtained from the Eastern Denmark power system. Wind penetrations of $20\% \leq \Phi_W \leq 100\%$ and $10\% \leq \Phi_{ZPP} \leq 35\%$ The main conclusions obtained from the analysis presented in this chapter are:

- The deployment of electrolysers in combination with both ZPP and WPP is a considerable benefit. In particular much greater hydrogen yields and electrolyser utilization factors can be obtained especially on days of low wind availability, thus solving the main drawbacks of a pure wind-hydrogen (or more generally renewables-hydrogen) implementation.

- As a consequence of implementing additional ZPP in the system additional carbon benefits can be obtained in terms of reducing the carbon intensity of the electricity delivered to consumers. For example at $\Phi_W = 100\%$, if an installed capacity

of ZPP totalling 35% of SMD is deployed in the system, on a variable wind day (CF = 42%) the carbon intensity of electricity can be reduced to less than half that obtained previously (i.e. for the Base Case) while achieving a virtually flat thermal load profile (i.e. LF_{TH} = 100%).

- Wind curtailment can be completely eliminated if a SSE stock is implemented. Electrolysers would absorb all the wind power resource that the power system cannot accommodate, producing zero-carbon hydrogen and enabling higher penetrations of wind power far beyond the limits considered feasible today.

- There is a strong trade-off between the carbon intensity of the electricity delivered and the amount of zero-carbon hydrogen produced by the electricity system. The hydrogen yield could be increased beyond the levels presented here, but at the expense of dedicating less zero-carbon electricity to cover consumer electrical demand thus increasing the carbon intensity of electricity. Depending on the energy system under consideration and specifically on the hydrogen and electricity demands to be covered, defined values for CI_e and Y_H can be sought and then the benefits obtained from the production of zero-carbon hydrogen and the optimization of the power system can be fully maximised.

- If the objectives pursued are maximizing Y_H, UF_E and minimizing CI_e the deployment of ZPP is more beneficial than just installing WPP, since lower ELS capacities are required to attain such goals. However maximum benefits are attained when implementing both ZPP and WPP particularly at high wind penetrations, using ZPP both for electricity generation and hydrogen production, but operating them in such manner that the output directed to cover consumer electrical demand increases (thus decreasing the output directed to ELS) at times of peak consumer demand (Strategy C). Furthermore the deployment of ZPP in addition to WPP allows a further decrease in the load imposed on FPP and hence reduces CI_e and TC.

- Large capacities of electrolysers in excess of the installed wind capacity, and far above the ZPP installed capacity, are required in order to attain the aforementioned objectives as well as smoothing the FPP load profile with respect to the values obtained without deploying ZPP in the power system.

- For a power system without a significant wind penetration and leaving aside economic factors, the choice of location of the electrolyser stock is not decisive and same benefits are obtained in terms of LF_{TH}, CI_c, Y_H and UF_E. However for wind penetrations above 30% when wind curtailment becomes significant a SSE stock at the main WPP is required to absorb the wind generation that cannot be accommodated within the power system. Furthermore for wind penetrations above 30% and ZPP above 10% it is found that a DSE stock is not required to achieve the objectives followed in this analysis. In fact lower installed capacities are required when the electrolyser stock is deployed entirely on the supply side at or near the main WPP and ZPP. Only when considering infrastructure costs the deployment of some electrolysers embedded within the grid at or near the points of hydrogen demand could be an attractive option. This would be the subject of an economic analysis and therefore it is beyond the scope of the investigation presented here.

In summary the deployment of electrolysers in combination with zero/low-carbon thermal power plant within the electricity system opens vast possibilities for:

1) Large-scale generation of zero-carbon hydrogen for a variety of end-use applications.

2) Optimization of the power system, in terms of increasing the penetration of intermittent renewable resources that the system can integrate and allowing a more efficient operation of fossil-fuelled power plant.

The synergy between these two carbon-abatement measures can be further exploited when deploying electrolysers in the power system in conjunction with both ZPP and

WPP. Then ZPP could be used to complement large-scale wind generation, providing power and hydrogen at the optimum rates required at any time. A wide-scale deployment of electrolysers has vast potential to facilitate high penetrations of zero-carbon power sources beyond those levels considered feasible today, while integrating them into other energy sector (e.g. heating and transport) using electrolytic hydrogen as energy vector.

Even though economic parameters have not been accounted for in this analysis, the increase in hydrogen production rates and utilization factor of the electrolyser stock obtained when ZPP are deployed can make the case for a large deployment of electrolysers economically more attractive for electric utilities, with additional benefits in terms of increased efficiency and environmental performance of their FPP portfolio.

CHAPTER 6 - ELECTROLYSERS FOR LOAD MANAGEMENT: IMPLEMENTATION CONSIDERATIONS

If large penetrations of zero-carbon power sources are to be achieved through a wide scale implementation of electrolysers, the configuration and operation of current electricity systems may need some modification. This chapter explores the regulatory, economic and technical implications arising from the implementation of a large electrolyser stock on the supply side, demand side or a combination of both.

The most significant practical implementation topics are reviewed here, along with some proposed measures to optimize the operation of ELS in combination with ZCPP and particularly WPP (in general RE) using current electrolyser technology. Clearly the technical, regulatory and economic implications that may arise when implementing and operating a large electrolyser stock as a load management mechanism will be distinct for SSE and DSE, and therefore are treated separately here.

6.1. BACKGROUND TO WATER ELECTROLYSER TECHNOLOGY

Electrolysis has been used for approximately 100 years for hydrogen production. The first large installation was by Norsk-Hydro in 1927 in Norway. Further plants were erected by Cominco in Trail, British Columbia, Canada in 1940 and, from 1945, some other plants with capacities up to 33,000 Nm^3 /h of hydrogen (MW_e input scale). The erection of large electrolysis plants nowadays depends strongly on the availability of cheap electricity mainly from hydropower stations. Moderate power costs are an additional incentive. A total of ca. 4-5 % of the world current hydrogen production is by means of electrolysis (mainly as a by-product of chlorine-alkali electrolysis). The rest is derived from hydrocarbon sources, mainly via steam methane reforming and partial oxidation of NG (over 80% of total H_2 production), followed by coal and naphtha, although this situation is likely to change in the near future due to both increasing cost and scarcity of NG and oil and environmental concerns [67], [85].

Electrolysis of water comprises the dissociation of water molecules into hydrogen and oxygen gas. If a potential is applied across an electrochemical cell with a suitable electrolyte, the following reaction occurs:

$$H_2O_{(l)} \rightarrow H_{2\,(g)} + \tfrac{1}{2}\, O_{2\,(g)} \qquad (6.1)$$

where (l) expresses liquid state and (g) gaseous state. Oxygen is formed during the electrolysis at the anode, hydrogen at the cathode.

The Gibbs free energy (ΔG) of this reaction can be written as:

$$\Delta G = \mu\,(H_2) + \tfrac{1}{2}\,\mu\,(O_2) - \mu\,(H_2O) = \Delta G^{\circ} + RT \ln\,(pH_2 \cdot pO_2^{1/2}) \qquad (6.2)$$

where μ (H2), μ (O2), and μ (H2O) are the chemical potentials of hydrogen, oxygen and water respectively, pH_2 and pO_2 are the partial pressures of hydrogen and oxygen respectively and ΔG° is the Gibbs free energy at standard conditions.

The reversible potential to electrochemically split water can be found using the Nernst equation:

$$\begin{aligned} E^{rev} &= -\,(\Delta G / \ nF) = -\,(\Delta G^{\circ} / \ nF) - (RT/nF) \ln\,(pH_2 \cdot pO_2^{1/2}) \\ &= E^{\circ} - (RT / nF) \ln\,(pH_2 \cdot pO_2^{1/2}) \end{aligned} \qquad (6.3)$$

where n is the number of electrons involved, R is the gas constant, T is temperature (K), F is the Faraday constant (96500 A·s/mol), and E° is the standard decomposition potential. Then at standard conditions (298 K, 1 atm) $E^{rcv} = E^{\circ} = 1.23$ V.

The actual potential required in an electrochemical cell is the sum of several voltages:

$$U = E^{rcv} + E_1 + E_2 + I \cdot R \qquad (6.4)$$

Where U is the overall cell voltage, E^{rev} the reversible potential, E_1 and E_2 the anode and cathode overvoltages respectively at the phase boundary electrolyte-electrode, I·R the voltage drop due to electrical resistance of the electrolyte system (also known as ohmic drop), all of them expressed in volts. E_1 and E_2 are influenced by the electrode material, surface conditions and electrolcatalyst deposition (typically parameters like catalyst type and loading, particle density and size); and I·R depends mainly on current density, conductivity of the electrolyte, permeability of the cell separator and the distance between electrodes. **Figure 6.1** shows the cell voltage as a function of current density with the contributions of E^{rev}, E_1, E_2 and I·R. Clearly the anode overpotential is the decisive factor and mainly responsible for the voltage supply required in the electrolysis cell and the choice of anode electrocatalyst is critical [86].

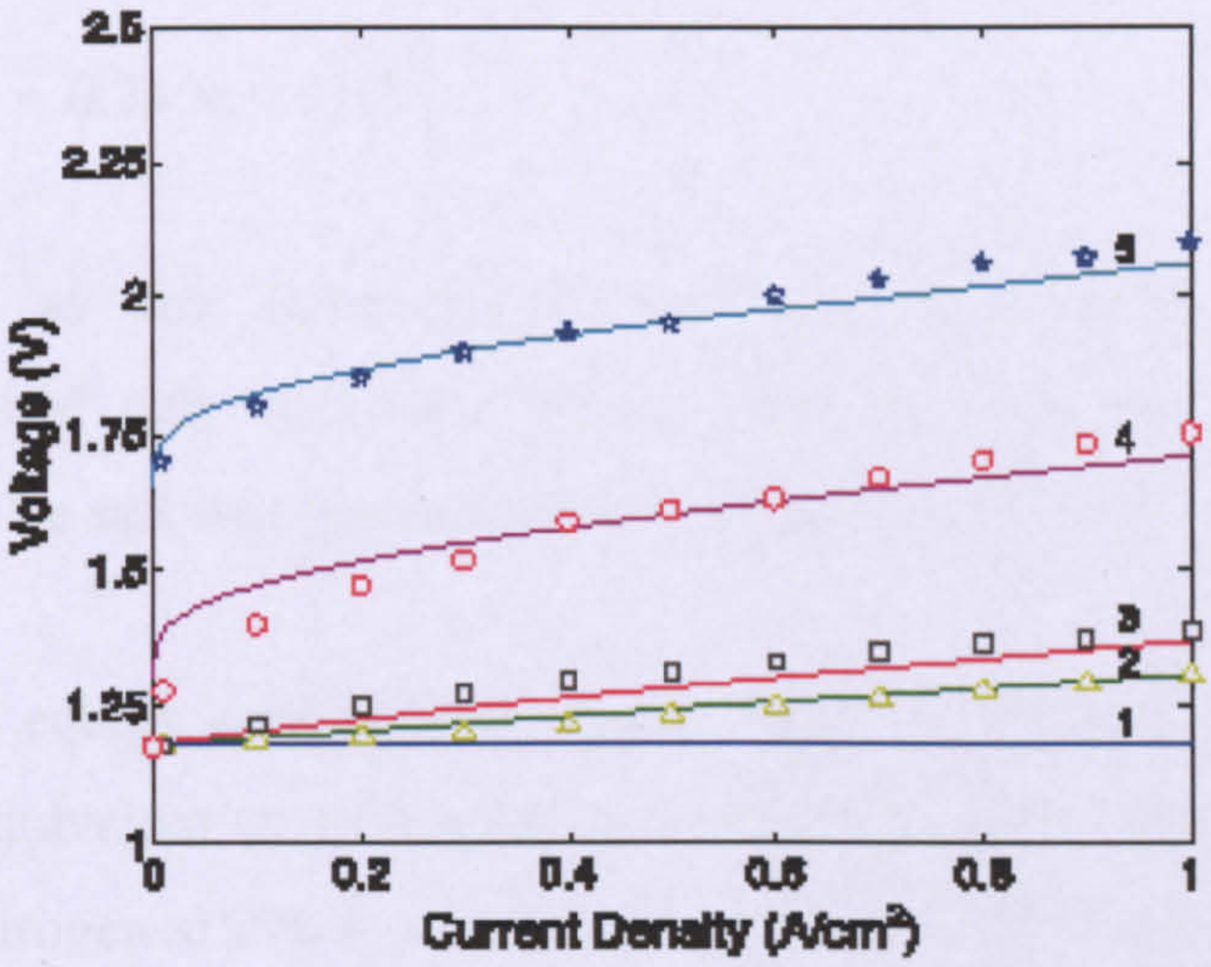

Figure 6.1. Actual potential of an electrochemical cell for two different anode catalysts). Contributions of (1) E^{rev}, (2) I·R, (3) cathode overpotential, (4) anode overpotential on Pt-Ir_2 and (5) anode overpotential on Pt [86].

From **Figure 6.1** E_1, E_2 and I·R all increase with current density. The anode overpotential increases sharply at low current density and slowly thereafter. Since the cathode reaction is relatively fast compared to the anode reaction, the overall cell

voltage increase with current density is mainly attributable to the kinetics of water dissociation at the anode [86].

The overall efficiency of an electrolysis cell related to the minimum voltage required is:

$$\eta = E^{rev} / U \tag{6.5}$$

Therefore under ideal reversible conditions $U = E^{rev}$ (at standard conditions). However this is not achievable because, in order for the reaction (6.1) to get started, it is necessary to overcome an additional energy barrier, namely the activation energy. As a result, an additional activation overpotential is always required to carry out the reaction. The activation overpotential increases with the current density applied and can be lowered by the choice of electrocatalyst. The value of

$$E_{th} = 1.23\ V + 0.25\ V = 1.48\ V \tag{6.6}$$

is denoted as the thermoneutral potential and defines the state where the electrochemical cell does not heat or cool and the cell would perform at 100% efficiency. The cell will produce heat at potentials above 1.48 V [87], [88], [89].

In terms of energy consumption (input energy / output hydrogen), 100% efficiency would be equivalent to 3.54 kWh of energy input per 1 Nm^3 of H_2 output, since the HHV of hydrogen at 298 K and 1 atm equals 3.54 kWh / Nm^3 H_2. Above 3.54 kWh all the energy supplied to the electrochemical cell will produce heat i.e. the lower the efficiency the higher the heat load produced.

Electrolysis differs from other methods of hydrogen production by its ability to produce H_2 with a carbon footprint that is a direct function of the carbon emission factor of the input electricity. Hence its significance for expanding the role of intermittent RE and other zero-carbon power sources (e.g. nuclear, CO_2-sequestered) across all sectors of the energy system. Electrolysers can be classified according to temperature of operation and type of electrolyte. To date the only commercially available technologies are

alkaline liquid electrolyte and solid polymer membrane electrolysers, although solid oxide electrolyser technology based on high temperature electrolysis has been the subject of increasing research over the past few years.

Alkaline electrolysers (AE) are based on alkaline liquid electrolytes, normally potassium hydroxide (KOH). Anode and cathode regions are separated by a diaphragm usually made of oxide ceramics or polysulfones, which allows the current to flow but is otherwise gas-tight. The cell is filled with the liquid electrolyte. **Figure 6.2** shows an schematic of an Alkaline Electrolysis cell.

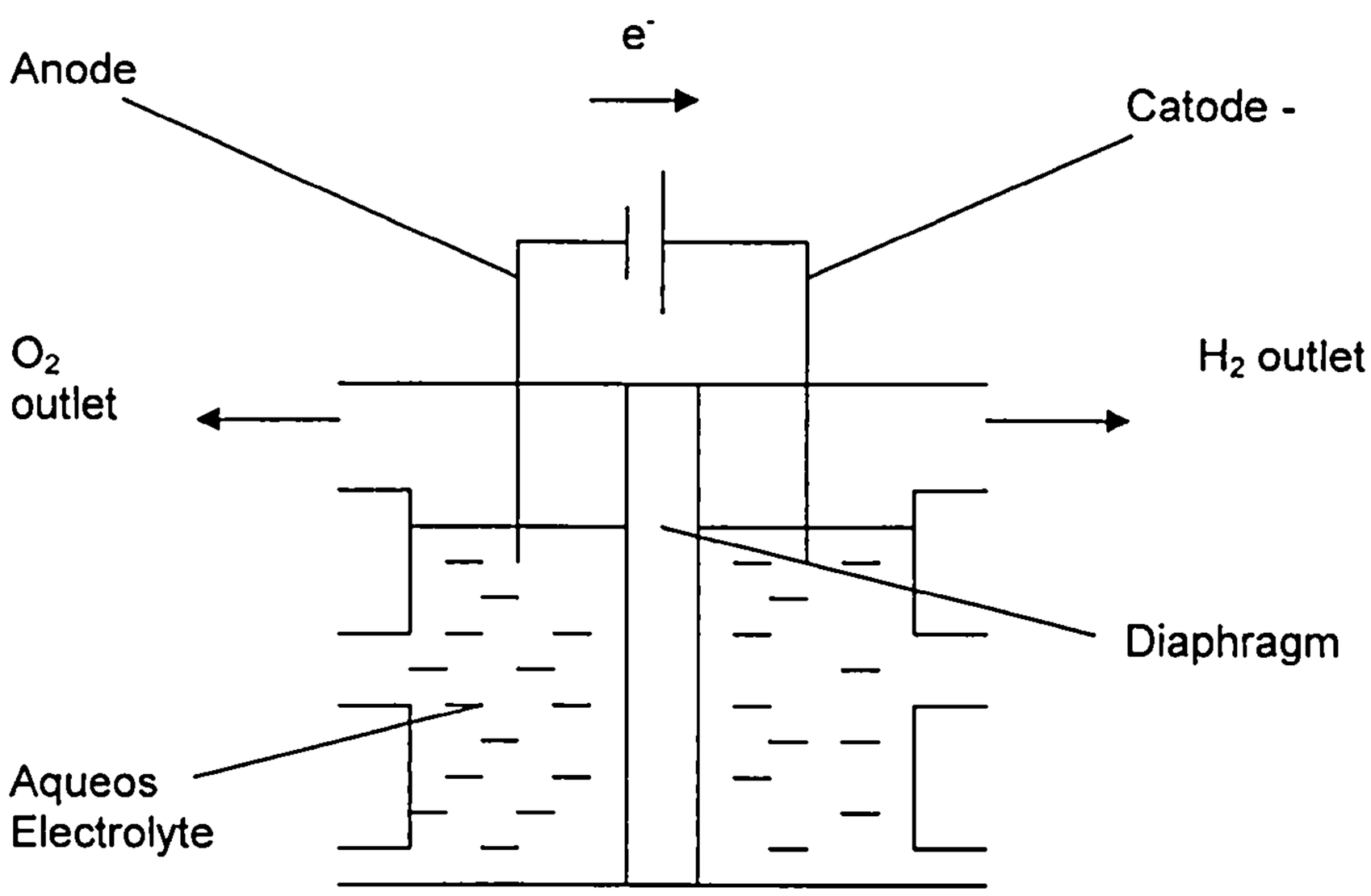

Figure 6.2. Schematic of an electrolyser or water electrolysis cell

The main reactions taking place in an AE are:

Cathode: $2\ H_2O + 2\ e^- \rightarrow H_2 + 2\ OH^-$ (6.7)

Anode: $2\ OH^- \rightarrow \frac{1}{2}\ O_2 + H_2O + 2\ e^-$ (6.8)

Overall Reaction: $H_2O_{(i)} \rightarrow H_{2(g)} + \frac{1}{2} O_{2(g)}$ (6.9)

To minimize the resistance losses of the electrolyte and due to the remarkable corrosion resistance of stainless steel in this concentration range usually 25 - 40 wt % potassium hydroxide solution is used [90]. Other electrolytes are aqueous sodium hydroxide or, for the chlor-alkali electrolysis, solutions of hydrochloric acid, sodium chloride, etc. Since the conductivity of conventional electrolytes increases with temperature, H_2 electrolytic units usually operate at 60 - 90 °C, just below the boiling point of the aqueous solution. [91].

The evolved gases are separated using an inert diaphragm which still allows the charge carrying ions to be transported between the electrodes. Traditionally this material was asbestos based, however this has been substituted (due to the health hazards involved in the use of asbestos) by woven polymers, inert ceramic such as titanates or a composite consisting of polymer and ceramic powder [87].

Physically an electrolyser consists of several electrolytic cells connected in parallel. Depending on the arrangement of the electrodes and the diaphragm, the cells may be designated as Unipolar or Bipolar cells. A characteristic of the Unipolar cell is that cathode and anode are either negative or positive and each have their own separate cell region. Bipolar cells are characterized by the fact that the electrodes are negative on one side and positive on the other, separated by an electrical insulator, usually a ceramic material. The arrangement of the bipolar electrodes is similar to the construction of a filter press, so that they are often named accordingly. A typical bipolar AE is shown in **Figure 6.3**.

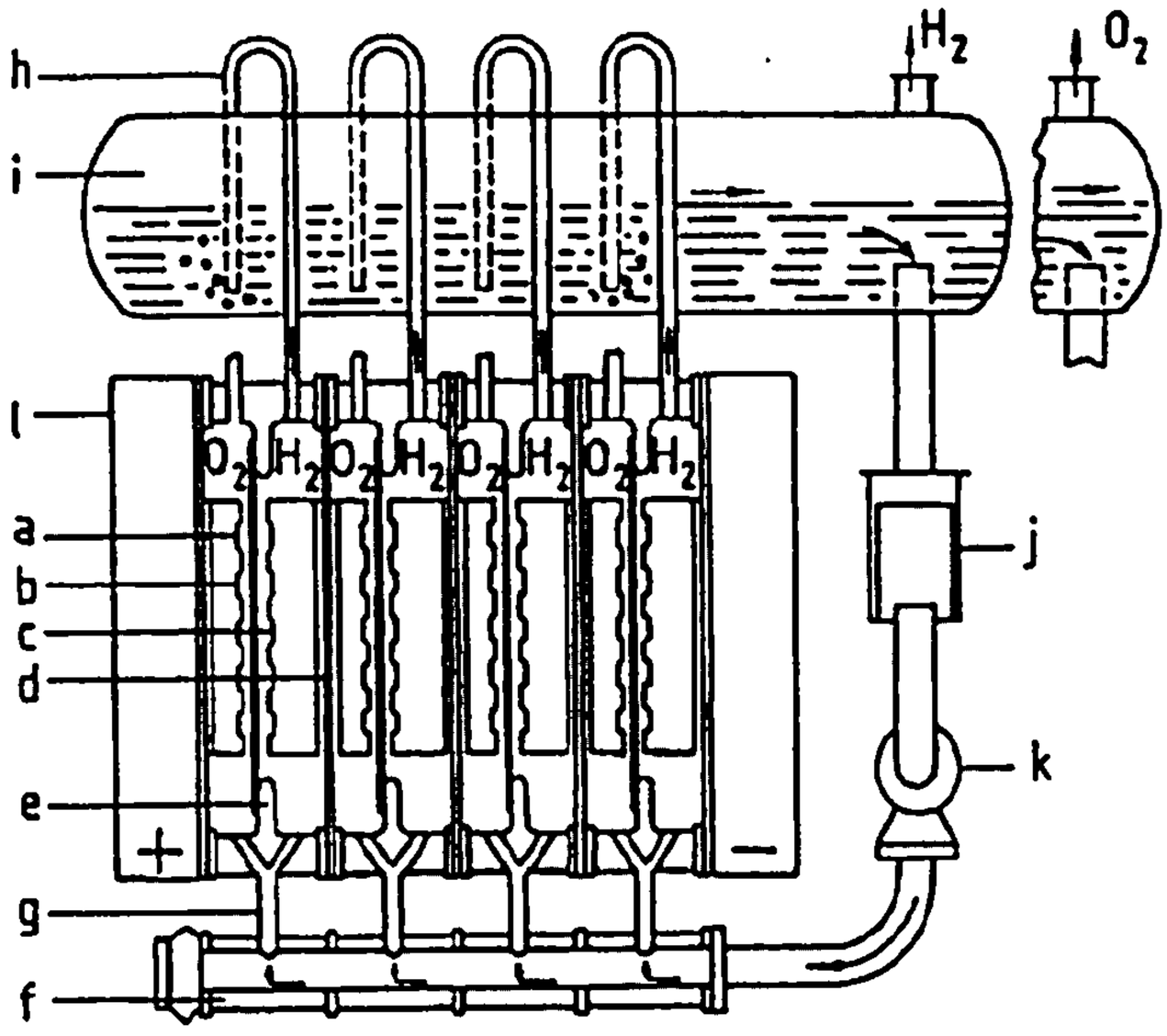

Figure 6.3. Cross section of a bipolar alkaline electrolyser unit [89]

Alkaline electrolysis is a well established technology with AE commercially available in the range of 0.5 – 100 Nm^3 H_2/h although units of $>10^3$ Nm^3/h are also built by ganging multiple units. They operate at temperatures of 70-90 °C with typical efficiencies quoted as 4-6 kWh_e / Nm^3 of hydrogen produced (corresponding to an efficiency range of 65-90% on a HHV basis) for steady-state operation at a current density of around 0.2-0.4 A/cm^2. Hydrogen gas purity usually exceeds 99.8%. Higher purities are possible with additional gas processing by means of catalytic conversion and/or adsorptive drying units (expensive units for high cost applications, e.g: space, electronics) [87], [89], [92].

To reduce the cell overvoltages the surface texture of the electrodes is usually activated and coated with various catalysts. One of the main advantages of AE technology is that the materials used are relatively cheap and commercial catalysts are free of noble metals. Next to platinum, which is not the optimum option for economic reasons, Ni-based materials have the lowest overvoltages. Thus the electrodes of bipolar cells are usually made of nickel or nickel-coated steel. Cobalt and iron anodes are also presently

being used. Advanced AE are usually built in the bipolar filter press configuration, and are operated at pressures ranging from 1 to 450 bar [92], [93].

Polymer electrolyte membrane electrolysers (PEME) represents a very promising technology for integration in RE-based systems. The electrolyte is a proton conducting membrane similar to the membrane applied in PEMFC. They usually operate at around 80°C, enabling faster start-up, shutdown and power fluctuation response compared to AE due to the absence of a liquid electrolyte. Typical commercial PEME have an electricity consumption of 4 – 7 kWh/Nm^3 (50-90% on a HHV basis) operating at current densities of between 1-3 A/cm^2 [67], [87], [94]. A schematic of a PEME is shown in **Figure 6.4**.

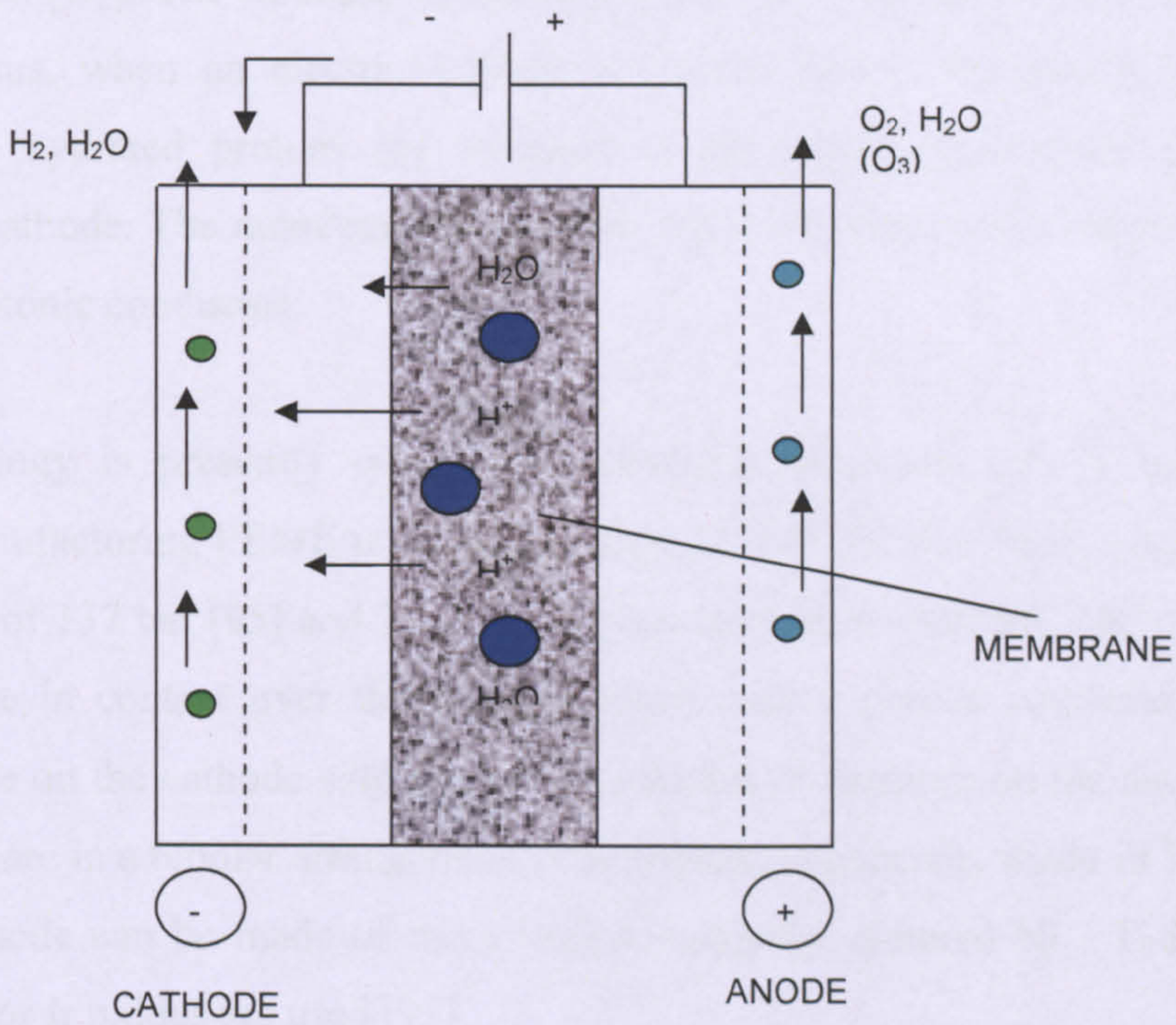

Figure 6.4. Schematic of a PEM Electrolyser

The electrode reactions are:

Cathode: $4\,H^+ + 4\,e^- \rightarrow 2\,H_2$ (6.10)

Anode : $2\,H_2O \rightarrow 4\,H^+ + 4\,e^- + O_2$ (6.11)

Overall reaction: $2\,H_2O_{(l)} \rightarrow 2\,H_{2\,(g)} + O_{2\,(g)}$ (6.12)

To achieve an appropriate performance the membrane must become saturated with the water supplied to the electrolyser so that these ionic or charged forms allow water to penetrate into the membrane structure but not the product gases, molecular hydrogen [H_2] and oxygen [O_2]. The resulting hydrated proton, H_3O^+, is free to move across the membrane. Thus, when an electric voltage is applied across the proton exchange membrane the hydrated protons are attracted to the negatively-charged electrode, known as the cathode. The membrane acts effectively as a conductor of electricity. It is said to be a protonic conductor.

PEME technology is presently commercial although there are only a handful of companies manufacturing PEME units in the range of 0.01-10 Nm^3 H_2/h. Operation at high pressures of 137 bar [95] and 206 bar [96] has been demonstrated. The electrodes in a PEME are in contact over the whole surface with a porous conductor; this is usually graphite on the cathode side and sintered nickel or titanium on the anodic side. The electrodes are in a bipolar arrangement. The cathode is normally made of Platinum; whereas the anode can be made of more varied materials: sintered Ni / Ti-Pd alloys coated with Pt or Ir oxides are used [97].

The standard membrane material used in PEME and PEMFC is Nafion®, manufactured by DuPont, a polyperfluorosulfonic acid polymer that is made into thin films ranging from 50 to 200μm, which has shown proven durability for over 30 years [98]. The critical disadvantage of Nafion is its price which remains at around \$500 / m^2 for a typical PEME system [99]. This factor, along with the necessity of using precious metal catalysts (based on platinum) and the limited volume of the market makes PEME a

relatively expensive technology. It is better suited to the market for small electrolysers, especially those applications where costs are not such an important factor (e.g. space and military applications). However PEME also offers the potential for low costs in mass production if inexpensive membranes and catalyst materials could be developed. Significant progress has recently been achieved in this area by the UK based company ITM Power. This British company has developed a new type of proton exchange membrane at a cost of around 1% that of Nafion that lends itself to highly automated manufacturing processes [100].

The main advantages of PEME over AE are the much higher current densities 1-3 A/cm^2 [87], which in turn imply a much smaller footprint; the obviation of systems to circulate the electrolyte and maintain its concentration; the wide range of power loadings, and very rapid power-up/power-down rates. The purity of the gases evolved from a PEME stack is typically 99.999% for H_2 and 99.9% for O_2, with some systems being designed to provide 99.99999% H_2. The need for purification steps beyond the electrolyser stack is less with PEME than AE due to the absence of the mixing effects of a liquid electrolyte. PEME technology also has the potential of being utilised as regenerative fuel cells since a PEM electrolyser basically operates in the reverse sequence of a PEM fuel cell. These have been used in a number of specialist space applications mainly in the US [101], [102], [87].

Apart from the electrolyser, an electrolytic H_2 generation plant consists of a number of different installations, such as power conditioning unit, water treatment and management, electrolyte circulation system (in case of AE based plants), gas compression (if we have a low pressure plant) and purification, and the instrumental and control system. **Figure 6.5** shows a typical flowsheet of an electrolytic H2 generation plant.

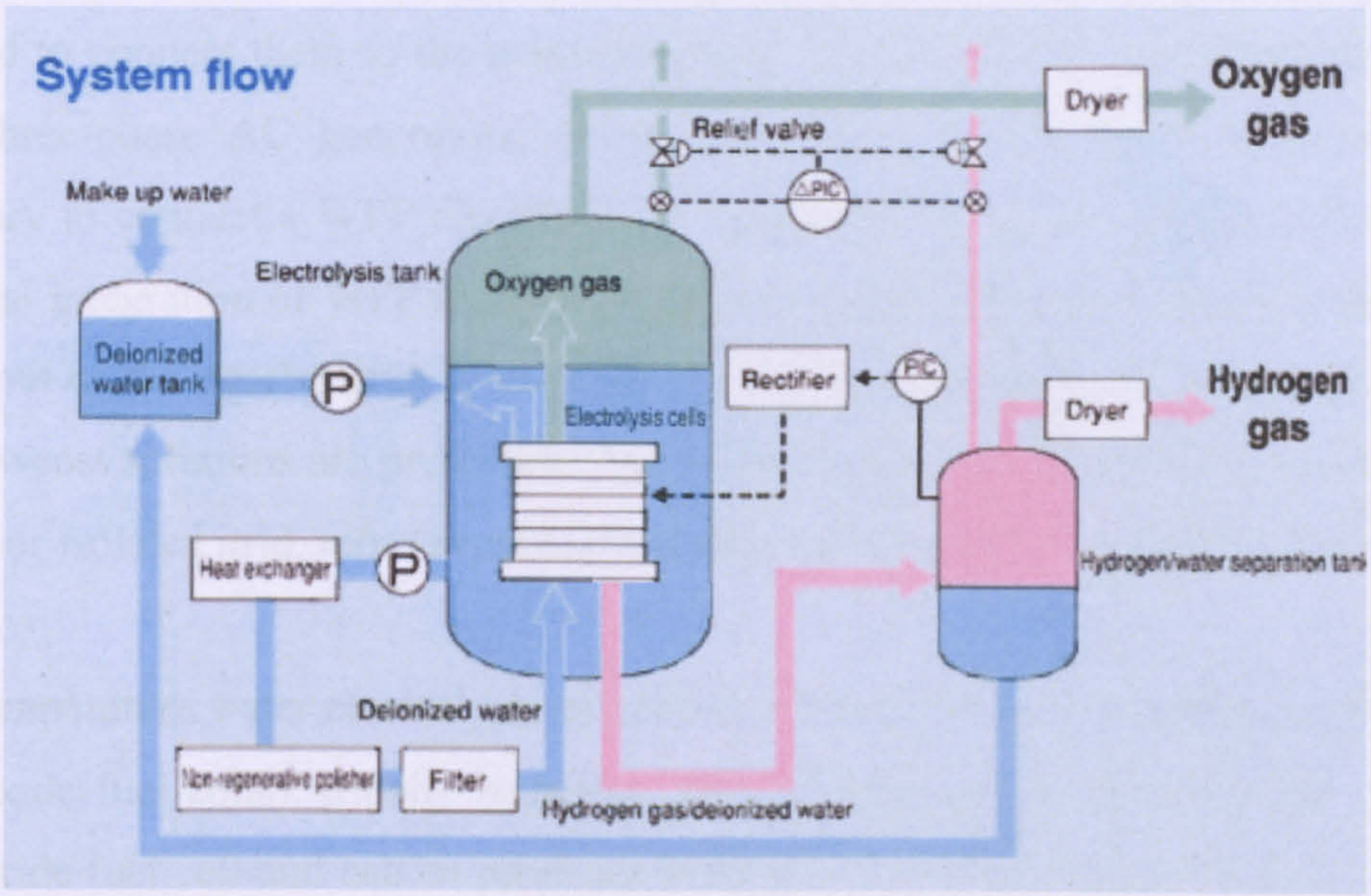

Figure 6.5. Flow diagram of typical PEM electrolysis plant [103]

The water consumed during electrolysis has to be continuously replaced; the consumption is around 1 liter per Nm^3 of H_2 produced [102], [104]. The conductivity of the water input to the electrolyser is proportional the content of impurities and will influence the content of impurities in the output gases. Hence minimum purity levels are required for the H_2O input to the electrolyser stack, about 1 μS/cm for PEME and 5 μs/cm for AE. Building-up of impurities also induces poisoning of the electrodes, promoting corrosion and causes quicker degradation of the polymeric electrolyte in PEME so is an important factor to take into account [92].

The power required, which in large plants is supplied in the form of three-phase current at a high voltage, must be transformed and rectified to the necessary DC voltage. In addition, power for the various auxiliary equipment, such as the electrolyte and water circulation pumps, compressors if needed and the instrumental and control system is also necessary.

Electrolysers require a DC current to operate and therefore an AC/DC rectification is required to connect them to the main electricity grid. Moreover, wind turbines usually drive three-phase AC generators, which means that an AC/DC conversion is also necessary to connect a WPP directly to an electrolysis plant. The optimal solution for electrical integration of WPP and electrolysers depends on geographical conditions and the layout of the nearby grid. If the system is to be connected to a strong grid, simple and low-cost solutions are preferable, but if the electrolysis plant must be connected to a weak or isolated grid, more sophisticated and costly solutions may be required.

High temperature water electrolysis systems are based on a solid oxide electrolyte (as in solid oxide fuel cells), usually based on zirconia. The cell is basically the same as a solid oxide fuel cell and can be arranged in tubular or planar "sandwich-type" systems. The operation of a solid oxide electrolyser (SOE) is based on the transferring of oxygen ions (O^{2-}) at temperatures of 800-1000°C [87]. The electrode reactions are as follows:

Cathode: $H_2O + 2e^- \rightarrow H_2 + O^{2-}$ (6.13)

Anode: $O^{2-} \rightarrow \frac{1}{2} O_2 + 2e^-$ (6.14)

Overall reaction: $H_2O_{(v)} \rightarrow H_{2(g)} + \frac{1}{2} O_{2(g)}$ (6.15)

The solid oxide electrolyser requires a source of high-temperature heat. By operating at elevated temperatures, the heat input meets some of the energetic requirement for electrolysis and so less electricity is required per unit of H_2 generated, compared with the other electrolyser technologies. Efficiency improvements of 30-40% over low-temperature electrolysis are considered achievable [87], [89]. To date, prototype SOE units have not achieved useful operational lives and substantial engineering problems still exist with respect to thermal cycling and gas sealing. High-temperature steam electrolysis through SOE technology is still the subject of laboratory research and may be viable in the long term.

Solid oxide electrolysis may be suitable for operation in conjunction with a high temperature nuclear plant, which could provide the electricity and high temperature

heat required and thereby facilitate large scale centralised production of hydrogen. However, when the objective is to maximize the capture of intermittent RE sources SOE technology is not appropriate and instead lends itself to steady-state operation [67]. Although the expansion of nuclear energy currently meets strong opposition in most countries, an increase in nuclear generation could be the easiest and quickest way of decreasing the carbon intensity of electricity production drastically (see **Chapter 5**) while producing large amounts of zero-carbon hydrogen. Should this happen SOE technology would have an important role to play.

6.2. TRANSIENT OPERATION OF ELECTROLYSERS

6.2.1. Transient operation and dynamic response

Fast power fluctuations like those produced when connecting AE with wind power sources can lead to incomplete separation of the gases from the electrolyte so that hydrogen and oxygen are mixed in the electrolyte [105]. The reason is that sudden changes in gas production affect the circulation balance of the electrolyte, and pressure differences between the electrodes may occur. Consequently, gas from one of the electrodes can diffuse through the gas separator to the opposite electrode. Hydrogen in oxygen is a safety risk regarding explosion, while oxygen in hydrogen lowers the purity and thus value of hydrogen. PEME technology on the other hand does not have a circulating electrolyte and presents less mixing problems. It is important to ensure as equal pressure levels as possible on the cathode side and the anode side to prevent gas impurities, although rapid fluctuations of the power input in PEME does not seem to affect the H_2 purity level significantly [106].

Another issue with AE systems coupled to intermittent power sources is how to operate the electrolyser during periods of low wind speed. Since the alkaline electrolyte is corrosive, the electrode will corrode if the production is stopped. The electrodes should be polarized as long as they are in contact with the electrolyte to prevent corrosion. A protective current must be provided from an external power source. For long idle periods with no hydrogen production, one option is to remove the electrolyte

completely from the system. However, such shutdown procedures increase the power consumption during start-up [76], [105].

PEME do not have a circulating liquid electrolyte but a solid electrolyte and therefore they are easier to operate and have faster start-up and load following capabilities when coupled with fluctuating power inputs (e.g. wind power), [107] and [87]. Conceptually, a PEME does not have a circulating liquid electrolyte, and suffers less inertia in heat and mass transfer processes, responding faster to input current fluctuations than an AE although this is still an R&D subject and little evidence has been found in the public domain of fluctuating transient operation of PEM electrolysers. An indication of the time response of a PEME when coupled with a wind generator is shown in **Figure 6.6**.

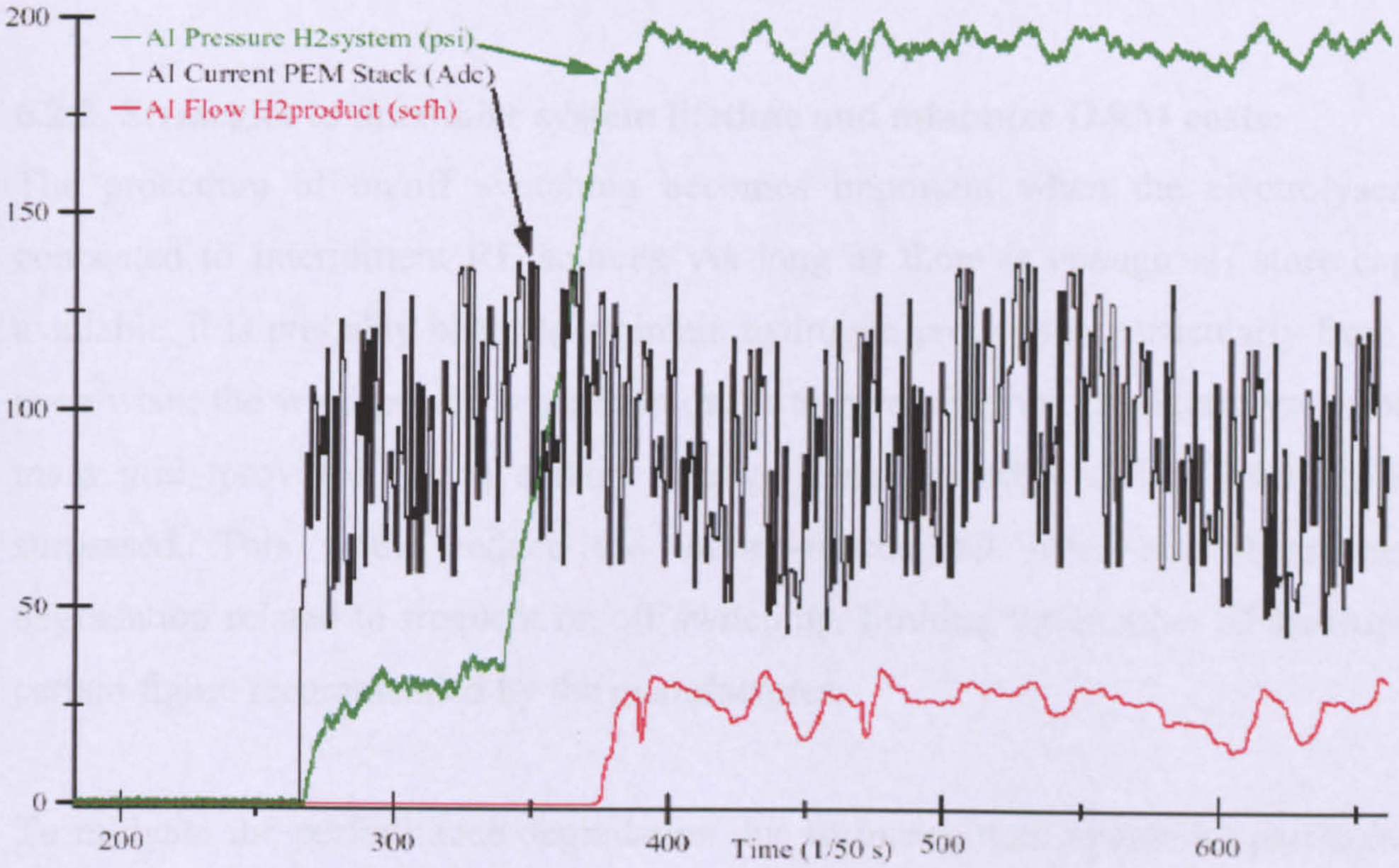

Figure 6.6. Transient response of a 5 kW PEM electrolyser with a simulated wind turbine input [108].

In addition, commercial AE have a minimum turndown point of between 15-25% of nominal power, limited by safety implications like the danger of 'stray electrolysis' due

to thermal gradients across the cell at low loads [76], [104]. PEME in contrast do not have a liquid electrolyte and present minimum turndown points of 0 – 5% of rated power [102] and [104], which makes them more suitable for intermittent operation and frequent on/off switching cycles. However long term durability and high efficiency under extreme fluctuating conditions are yet to be proven.

In practice some operating procedures are required when connecting electrolysers to RE input power sources, particularly for non-atmospheric systems during stop and start-up periods. The pressure balance must be maintained at all times during such periods and the electrolyser is normally purged with an inert gas (e.g. nitrogen) to remove oxygen from the hydrogen stream. Electrically operated (small scale systems) or more robust pneumatic operating on/off valves (large scale systems) are required for the purging sequence [107], [109].

6.2.2. Strategies to maximize system lifetime and minimize O&M costs:

The procedure of on/off switching becomes important when the electrolysers are connected to intermittent RE sources. As long as there is enough H_2 store capacity available, it is probably better to maintain hydrogen production particularly from AEs, even when the wind power generation drops to zero, feeding the electrolyser from the main grid, provided that a certain average annual/monthly carbon intensity is not surpassed. This would reduce the thermo-mechanical wear and electrochemical degradation related to frequent on/off switching, limiting the number of start-ups to a certain figure recommended by the manufacturer.

To mitigate the performance degradation due to intermittent operation, particularly in AE systems, batteries can be included in RE-H_2 systems to reduce the number of switching cycles of the electrolyser. The batteries can then feed the ELS during short periods of time when the RE output is not enough to maintain the electrolyser functioning within its operational limits [105], [110]. This can help to overcome the problems derived from the operation of ELS under numerous on/off cycles (purging issues, stack degradation, etc). The initial increase in the total capital investment of the RE-H_2 system may well be offset by the reduction in electrolyser O&M costs.

For large scale implementation scenarios of ELS like those proposed here PEME technology seems more suitable to be coupled with WPP and operated following more demanding load input profiles, whereas AE technology could be coupled with ZPP (e.g. nuclear power plant) and operated in a more stable manner with less load fluctuations. This approach is likely to maximize the overall efficiency of H_2 production (kWh of hydrogen) with respect to the input energy required (kWh of electricity). Once deployed and optimized, SOE technology could also contribute by using high temperature processes (e.g nuclear power plant) to further increase the scale of zero-carbon electricity and hydrogen production.

6.2.3 Efficiency considerations

- There is a number of ways that efficiency in integrated wind-hydrogen systems can be optimized. Firstly it is critical to design systems at the optimal size in combination with the RE source to which ELS are to be connected. Careful design can avoid decreasing the efficiency of capture of the RE resource (e.g. if ELS is undersized) or decreasing the utilization factor of the electrolyser (e.g. if the electrolyser is oversized), which increase the costs per unit of hydrogen produced.

- Protective current: high pressure AE (20-30 bar output) cannot be completely switched off during non operation and must maintain a protective current while on stand-by mode to protect the device against corrosion produced by the electrolyte. This stand by power loss can amount for up to 0.5 – 1% of rated power [105] which increases the overall energy consumption (kWh of electricity per Nm^3 of H_2 produced) especially in large-scale applications (MW size) if the ELS has to spend long periods in standby mode (low UF_E). Low pressure AE and PEM do not have that requirement (can be simply switched off) and may be more suitable for connection to RE where numerous on/off cycles are applied.

- For AE systems, the limited operational range of the electrolyser (around 20 – 100% of rated power) means that there will be times when the RE supply available is

beneath the range of the electrolyser and therefore it can not be used for H_2 production. Although switching the electrolyser off when the RE power input does not meet the minimum load requirement is always possible, other alternatives could be suggested. For example the troughs of RE power supply could be captured by appropriately sized batteries while reducing the ELS' switching cycles. Careful integrated design of the system comprising the RE source, battery and ELS is then required to optimize H_2 production and energy conversion efficiency. Another option would be feeding the electrolyser from the main grid at periods of low wind availability, provided that an appointed average CI_{II} (e.g. monthly or annually) is not exceeded. Both alternatives would also offer opportunities to increase the utilization of the electrolysers.

- The power interface between the wind generator and the electrolyser is one of the cornerstones of wind-ELS systems. This interface incurs efficiency penalties of between 5 and 10% and efficiencies fall even further at part load [107], [111]. Unfortunately wind-powered ELS will spend quite a lot of time operating at part load, so optimizing this interface would be one of the keys to improving the overall energy efficiency of coupled wind-electrolyser systems. For example by replacing the two separate power electronics interfaces with a single one that takes wild AC directly from the variable-speed wind turbine generator output and provides acceptable DC power to the electrolyser, efficiency improvements can be achieved while increasing the robustness of the wind turbine-electrolyser link. Furthermore, a single point of control could allow matching of the wind turbine and electrolyser electrical characteristics, thereby increasing the energy capture of the wind turbine.

- Careful electrolyser heat management would also improve efficiency by allowing it to reach optimum temperature quicker, reducing thermal cycling and capturing more of its by-product heat. Thermal management could even be used to integrate ELS with hydride storage systems and end-user low-grade heat demands (e.g. water heating). Furthermore heat loads generated by other components of the RE-ELS system (e.g. load controllers) can be used for keeping the electrolyser stack temperature within

nominal operating levels, thus minimizing start-up transients and increasing the efficiency of the overall system [112].

- When operating at part load, large electrolyser systems inevitably operate far from their efficiency design points. Efficiency of RE-electrolyser systems could be enhanced by modular design. Instead of a single large electrolyser with its auxiliary components (power conditioning, compressor, H_2 purification equipment, etc) rated at the appropriate capacity for the power source to which it is connected, it would be feasible to deploy several of these comprising a set of smaller systems able to operate in parallel. When the whole system is operating below rated capacity, only those modules required to meet the load would be operating, allowing operation close to system design efficiencies [113].

- When operated constantly under fluctuating conditions ELS' efficiency can decline over time as the number of switching cycles degrades the stack. Operational experience of AE under fluctuating conditions has shown efficiency losses of up to 8% after a significant number of on/off cycles is applied [114]. Public information on intermittent operation of PEME is scarce although one manufacturer has reported in excess of 11,000h of intermittent operation with no signs of membrane degradation or loss of performance [100]. Batteries could be integrated in the system to reduce the number of switching cycles of the electrolyser and therefore reduce efficiency penalties.

The examination of technical implementation issues published in the literature suggests that no unsolvable technical barriers exist to a large scale implementation of ELS, and their operation in combination with WPP and ZCPP is practically and technically feasible. Furthermore the approach proposed in this thesis is to be looked at within the context of future power and energy systems. By then the significant amount of current and foreseen investment in R&D for hydrogen technologies should deliver electrolysers and integrated zero carbon power-electrolyser systems more efficient and optimized (and at lower cost) than those available today.

6.3 PRACTICAL IMPLEMENTATION OF A LARGE ELECTROLYSER STOCK

Given an ELS stock size, a number of options can be selected in terms of size and number of electrolysers to be deployed. The optimum implementation strategy will depend upon a number of factors related to the characteristics of the power system and H_2 demand considerations. These topics are discussed below, along with the implications on the control strategies suggested in **Chapter 5**.

6.3.1 SSE Implementation:

A large SSE stock is likely to comprise medium and large scale electrolyser plants in the MW scale at a relatively small number of sites. The optimum implementation option will be based in practice in a number of factors, including:

The overall size and characteristics of the power system where the SSE stock is to be implemented (e.g. the individual size and loading flexibility of the generation plant mix available, geographic dispersion of RE generators within the system, etc). In particular power systems with a large proportion of large scale nuclear power plant (of 1 GW capacity or above) in their generation mix, may require a small number of large ELS plants (100-1,000 MW size) located at or near these nuclear power plants.

However when large SSEs are deployed in combination with ZPP other practical operational issues need to be considered. Looking at **Figure 5.8c in Chapter 5,** if the gradients of the curves become too steep, it might be technically difficult for large electrolyser plants to start-up, turn-up and down within short periods of time, whereas this may be more feasible for smaller electrolysers given that they require less time to switch on and reach operating temperature. For other power systems with ZPP and WPP of smaller capacity (e.g. 10-100 MW) the size of SSE would be smaller, possibly of similar capacity to the power plant to which they are connected.

Also depending on the Operational Strategy to be applied the preferred implementation option may be different. For instance for the Operational Strategy B in **Chapter 5** the

total size of the SSE stock would be smaller than that of the Base Case and Strategies A and C for a given Φ_W. In addition they will be connected to large ZPP (100-1,000 MW size). Thus it would make sense to deploy large SSE plants comprising 50 – 100 MW electrolysis units connected to a small number of ZPP. For the Basecase smaller ELS plants (e.g. 5 MW size) could be located at the WPP, matching the number of ELS to the size of the WPP. Strategies A and C would demand a combination of large scale SSE plants coupled to ZPP and smaller SSEs connected to WPP. Clearly every operational strategy will demand a different implementation approach.

To illustrate, for the **Basecase** presented in **Chapter 5** at Φ = 50% 1,105 MW of ELS capacity would be required (see **Table 5.1** in **Chapter 5**), coupled with 1,333 MW of wind capacity. Several options can be followed in terms of the number and size of electrolysers to be implemented, for example: 221 sites of 5 MW; 22 sites of 50 MW; or even 3 sites, 2 of them of 500 MW and another one of 105 MW of ELS capacity; all the above options totalling 1,105 MW of SSE. The preferred choice would depend on the size of the WPP available in the system. Provided that there are large WPP deployed within the power system, the latter option (2 sites of 500MW and 1 site of 105MW) would be feasible. Large offshore WPP (100-1,000MW) could be coupled to large SSE plants, e.g. 500MW size, comprising 5MW electrolysers connected to individual 5-10 MW wind turbines. This approach can maximize the flexibility of the SSE implementation case in order to achieve a practical operational profile as similar as possible to the ideal profile shown in **Figure 5.8a in Chapter 5.**

In cases where a local H_2 demand may exist near to the points where hydrogen is generated, the size of the SSE could be matched to such demand, assuming there is ample capacity to store all the H_2 produced (see **Assumptions & Description of approach in Chapter 3**). A "top-bottom" view has been taken here where the power inputs available for electrolysis (i.e. FPP availability subject to the targeted LF_{TH}, ZPP and WPP availability) determine the capacity of ELS to be installed and the rest of parameters analysed (CI_e, Y_H, UF_E, etc). It is then a supply-driven approach. Aiming for a practical implementation a specific demand-driven approach could be taken to match the supply-driven approach presented here. Such demand-driven analysis would

take into account the specific H_2 demands to be covered (size, time patterns, etc) which in turn will determine the size of the stores to be deployed.

For example consider a single hydrogen demand for H_2-powered local buses (via FCs or HICEs) nearby a WPP or ZPP. The size of the SSE to be deployed at this site would be a function of the maximum daily H_2 demand to cover (e.g. a 5 MW electrolysis plant operating at UF_E = 50% would suffice to refuel 70 FC buses daily[27]), whereas the time pattern, along with the expected WPP/ZPP availability, determines the size of the store required. Large industrial applications (e.g. ammonia production, glass production, methanol production, etc) will absorb larger H_2 demands, requiring SSE plants in excess of 50 MW size. On the other hand large industrial demands usually follow a continuous time-profile, minimizing the size of the store required.

Additionally the water requirement for large SSE plants is an element to be examined. An electrolysis plant requires about 11 litres of H_2O per kg of H_2 produced (1 litre per Nm^3 of H_2) [102], [104]. Therefore a 100 MW SSE plant operating at UF_E = 50% and efficiency of 70% (HHV basis), for instance, would consume around of 2,170 gallons of water per hour. Large SSE plants (50-100 MW size) located next to ZPP and/or large industrial applications are likely to have access to fairly constant water supplies which are required for cooling purposes. For instance a 500 MW thermal power plant employing a once-through cooling system consumes around 572,000 gallons of freshwater per hour [164]. Smaller SSE, e.g. 5 MW plants to supply local transport fuel demands, would require much smaller water supplies (e.g. around 108 gallons per hour for a 5MW SSE operating at UF_E = 50% and efficiency of 70%). These could be deployed in urban/rural areas where an appropriate water supply may be available. Clearly the availability of water is an aspect to be taken into account when designing a strategy for deploying a large SSE stock although water requirements of the electrolyser stock are rather low when compared to the inherent water requirements of the power system.

---

[27] **Assumptions:** electrolyser efficiency = 70% HHV (56 kWh_e required per kg of H_2 produced) including compression at 350 bar; daily mileage = 150 miles per bus; H_2 consumption taken at 10 miles per gallon of gasoline equivalent (mpgge) [115] – 1 US gallon of gasoline has approximately the same energy content as 1 kg of hydrogen.

The model presented in this thesis gives suggestions in terms of the overall SSE capacity required for a given WPP and ZCPP penetration in the power system and it seems likely that the SSE stock would comprise electrolyser plants in the MW scale. It is acknowledged that a practical implementation of a large SSE stock must take into account both demand and storage parameters like demand size and time pattern, storage size and possibly a time-variable indicating the state of charge of the H_2 store.

Storage facilities are required to ensure ability to meet a certain hydrogen demand regardless of WPP availability. Storage effectively provides the required match between H_2 supply and demand, ensuring hydrogen availability during periods of low wind availability, but also ensuring hydrogen can be produced at periods of high availability, regardless of the hydrogen demand usage rate. The storage size can be determined by making an assumption for the duration of a situation of virtually zero wind availability and taking into account an average daily H_2 demand. The former can be done through analysis of historical data for wind power production for a specific location.

These topics are site-specific and would be included in a specific demand-driven analysis. Although some indications are given herein this has been carried out by other authors [76], [116], [117] and is beyond the scope of the investigation presented here.

6.3.2 DSE Implementation:

A large DSE stock would consist of small scale ELS in the kW or low MW range, implying a large number of sites at or close to the points of H_2 demand. Taking the example presented in Chapter Wind +ZCPP at $\Phi = 50\%$ for the Basecase, 645 MW of ELS capacity are required (**Table 5.3 Chapter 5**). This DSE stock could comprise for instance: (i) 50 sites of 5 MW dedicated to H_2 production for local transport purposes (e.g. taxis and city buses); (ii) 3,225 sites of 200 kW located at selected non-domestic sites for heating and small vehicle fleets (a 200 kW electrolysis plant operating at UF_E

= 50% would suffice to refuel 25 LDVs daily[28]) ; (ii) 39,500 sites of 10 kW each for private transport refuelling and space/water heating purposes, or any combination thereof.

Unlike the SSE implementation, once the total size of the DSE stock applicable for a certain Φ_W, Φ_{ZC} is defined, the operational strategy selected (A, B or C) and the size and number of WPP, ZCPP would not affect the size and number of DSE sites, since they are not directly connected to the main power plant but to the low voltage grid (LV distribution network, $\leq$ 1 kV in the GB power system), although they are controlled in relation to WPP, ZCPP outputs and consumer electrical demand. Instead the size and number of DSE sites will be determined mainly by the local H_2 demand to be supplied (e.g. public city buses or domestic transport refuelling).

However in practice in the absence of significant amounts of dispersed generation a large scale DSE implementation needs to be achieved also taking into account the specific constraints of the LV distribution network. If they are deployed in excess in a certain area they may lead to congestion in some nodes of the low voltage network, requiring up-grading of LV transformers and network infrastructure. For instance taking the above example again (**Table 5.3 Chapter 5)** it is likely that options (ii) and (iii) (10 – 200 kW ELS) could be implemented at the LV level where the capacity of transformers would be enough to support such additional loads; whereas 200 kW – 5 MW ELS could be more suitable to be connected at the medium voltage level (1-36 kV in the GB power system) [119], [120]. The exact location and maximum size of electrolysers allowed at that site needs to be carefully planned possibly including some detailed network modelling at the distribution level to avoid congestion issues and maximize the benefits of this approach (see recommendations in **Chapter 7**).

[28] Assumptions: electrolyser efficiency = 70% HHV (56 kWh_e required per kg of H_2 produced) including compression at 350 bar; daily mileage = 50 miles per vehicle; H_2 consumption taken at 30 mpgge assuming HICE vehicles [118].

6.3.3 Combined SSE + DSE implementation:

Some combination of the above cases is chosen here and therefore both large and small scale ELS would be deployed in this case. Taking again the example presented in **Chapter 5** (Base Case, $\Phi_W = 50\%$) 1,170 MW of ELS capacity must be deployed, 590 MW of which are SSE and 580MW are deployed as DSE. They are operated in combination with 1,333 MW of WPP (**Table 5.5 Chapter 5).** The electrolyser stock is then a combination of MW size SSE located at or near appropriate WPP and kW size DSE embedded within the grid at the points of H_2 demand. For example, one option could be to deploy 118 × 5 = 590 MW of ELS at just one 590 MW offshore site; or select 118 different WPP each including one 5 MW ELS; or any number of WPP between 1 and 118 including ELS plants of between 5 and 590 MW. The distribution of the 580MW DSE stock would be a function of the local H_2 demand to be supplied and distribution network constraints. It could comprise for example 36 × 5 MW sites located at local buses depots and 40,000 dwellings including 10 kW ELS for domestic transport refuelling or heating demand.

The number of practical implementation options is vast and specific to the energy and power system under consideration. The ultimate choice will depend upon a number of factors like the number and size of WPP and ZPP available; the size and characteristics of the power system; the operational strategy to be deployed; the local constraints and configuration of the electricity network; and the size and location of a local demand for hydrogen (if any) near the location where the electrolysers are sited.

6.4 OPERATIONAL CONTROL OF A LARGE ELECTROLYSER STOCK:

The practical operation of a large electrolyser stock needs to be controlled in a way which is carbon efficient and also satisfies the needs of the relevant players, i.e. the electricity supply industry (TSO, electricity suppliers), the ELS' owners and the hydrogen end-users. The operation and regulation practices of current electricity systems may therefore need some modifications. All the control strategies proposed are based upon some form of operational control and without it a large-scale implementation of ELS would make no practical sense. This section explores the

regulatory and technical implications arising from the operation of a large electrolyser stock, and suggest some practical modes of operation of a SSE, a DSE stock or a combination of both.

6.4.1 Control of a large SSE stock:

When implementing ELS exclusively on the supply side the owners and operators of a SSE stock are likely to be the same owners/operators of WPP and ZCPP, i.e. the electric utilities. This implies that they would need to expand their current business mindset from producing and selling just one commodity, electricity, to be producers and suppliers of H_2 as well.

A widescale implementation of SSE could provide revenues to utilities not only by selling these two commodities (at minimum production cost when generated using surplus RE power) but also by providing grid management services. The latter could be done by following the TSO instructions in the same manner as power balancing services are traded today. Therefore even though the SSE stock is owned and operated by the electricity companies, in practice the TSO would regulate their operation in a similar manner as they regulate and schedule the operation of power plant today.

To illustrate this, let us take the example of a daily control strategy similar to that used to operate power systems today. Based on the demand expected, power plant declared availability and SSE availability for the following day, the TSO can schedule:

1) Aggregate load profiles for every "category" of power plant, namely FPP, ZCPP and WPP to assure that the consumer demand will be covered (see **Figure 5.7**).

2) A proposed load input profile to the aggregate SSE stock with the discrete contributions of WPP and/or ZPP depending on the operational strategy selected (see **Figure 5.8**).

Once the scheduled electricity generation profiles have been appointed, electricity can then be traded in the wholesale supply market in the same way that it is done today.

Those ZPP and WPP comprising SSE can use their surplus electricity available (if any) to produce zero-carbon hydrogen subject to the aggregate SSE load profile appointed by the TSO, acting effectively as a load management mechanism within the power system. Operation of SSE could be rewarded in the same way generators are paid for balancing services today to guarantee the availability of enough SSE capacity. This way the electric utilities can maximize the utilization of their generating portfolio and hence their revenues, eliminating wind curtailment issues arising for high penetrations of RE in the system. The operational strategies proposed here are designed in a manner that ZPP can achieve a **UF**[29] of 100% across the year (accounting for a **CF**[30] of 90% to allow for forced and planned outage periods) by co-producing electricity and hydrogen. This potentially eliminates cycling duties on ZPP completely, minimizing degradation and O&M costs derived.

If required, utilities could also use FPP to produce some H_2 provided that the average CI_H of their overall plant portfolio (FPP, ZPP and WPP) does not exceed a selected value, e.g. 3 kg CO_2 per kg of H_2 produced. The appointed CI_H could also come in the form of carbon allowances (e.g. on an annual basis) to the total amount of hydrogen produced for every electric utility, similar to the current carbon trading schemes already in place in Europe [121].

However, some issues may arise under this operational approach related to the willingness of the SSE operators (i.e. utilities) to effectively make their power plant available for electricity production should the production of hydrogen be more profitable for them. In practice, if a substantial hydrogen demand exist (e.g. for transport purposes):

- Would utilities choose to make more generating capacity available for hydrogen production instead of electricity because it proves to be more profitable for them?

---

[29] Ratio of the electrical output of a FPP over a designated period to the output that could have produced under continuous operation at **available** capacity during that period.

[30] Ratio of the electrical output of a FPP over a designated period to the output that could have produced under continuous operation at **rated** capacity during that period.

- How would this be regulated to guarantee supply of electrical consumer demand?

In answer to these questions, several options can be suggested. Taking the example of the UK power system, under current regulatory procedures generators must inform the TSO of the availability of their plant for each half hour of the next day so that the TSO can calculate the operating regime for all the power plant that will meet expected demand over the next day at lower cost [122]. Calculations take into account, amongst other things: demand forecast for the next day; transmission constraints (to avoid overloads); plant characteristics (e.g. start-up and cycling capabilities); and system stability (e.g. availability of reserve back-up plant). Power systems with higher wind penetrations (e.g. Denmark, Germany or Spain) follow similar procedures but also need to include in the calculations wind forecast and WPP availability for the next day [11] [123], [124].

When a large SSE stock is implemented, similar regulatory procedures can apply for ZPP and WPP for the co-production of electricity and hydrogen. For instance, regulatory measures can be implemented so that the generator must make a percentage X of its power output available for power generation. This would depend on the power plant and SSE installed capacity at a generating site, and could be a fixed figure across a certain period of time e.g. one year as regulated by the TSO. The rest, (100 – X) %, would be the maximum limit of generating capacity that can be used to produce zero-carbon H_2 if desired by the power plant operator. Under this scheme priority is then given to cover electrical consumer demand (mandatory) whereas the production of hydrogen is not compulsory.

On a daily basis, generators would need to inform the TSO of their total capacity available for electricity and H_2 generation (similar to current procedures applied to power systems), subject to the annual limits already in place. Based on this information and the demand expected for the following day the TSO can schedule the operational profiles for FPP, ZPP, WPP and the SSE stock. These would include operating regimes of generating units to meet expected consumer demand for the next day (in a similar way that it is done today), as well as recommended operational profiles for SSE. Since

a fixed limit has already been appointed on the generating capacity that can be used to produce hydrogen, power plant operators could not reduce electricity output in favour of producing more H_2. Furthermore, matching their generating capacity to the annual limits appointed by the TSO would in any case maximize their plant utilization and therefore revenues. Hence in the scheme proposed the operation of the SSE stock would be regulated but not fully controlled by the TSO.

Provided that there is a demand for zero/low carbon H_2, it is conceivable that this scheme could also incentivize the deployment of ZCPP and WPP versus FPP since they could maximize their revenues by producing two saleable products, hydrogen and electricity. In addition WPP operators would further maximize their income by avoiding wind curtailment. Undoubtedly this approach also implies that the TSO must expand its tasks to act as regulator of the electricity supply and H_2 supply in a way (by limiting the generating capacity available for electrolysis).

The implementation and control of SSE makes the role of the electricity supply industry (system operators, power utilities, etc) undoubtedly more complex and the potent load management tool made available in the form of a large SSE stock needs to be attractive enough to compensate for the additional regulating duties and capital investment. Interestingly some system regulators are already showing interest in deploying ELS as a load management mechanism to integrate large RE penetrations [125], [126].

6.4.2 Control of a large DSE stock:

Following this approach, small scale DSEs would probably be owned by the same end-use hydrogen consumer, e.g. domestic consumers, public transport companies and facilities requiring zero/low carbon H_2 e.g. for fleet vehicles, heating or back-up power purposes. However in terms of managing their operation a large DSE stock, unlike a SSE stock, would need to be fully controlled by the TSO on a real-time basis to guarantee (i) correct operation in relation to consumer electricity demand avoiding overloads in the low voltage network and (ii) production of zero-low-carbon hydrogen by operating electrolysers according to the WPP and ZPP outputs available in the system.

In terms of controlling and regulating the operation of a large DSE stock, it appears that the straightforward proposition of "buy the product (an electrolyser) and use it" which applies to virtually all commodities, could not apply to the approach proposed in this thesis, otherwise the objectives of minimizing wind curtailment, maximizing the production of zero/low carbon H_2 and optimizing the operation of FPP would not be achieved. The operation of a large electrolyser stock needs to be regulated from the start, particularly when they are embedded within the power system at the low voltage level; otherwise the carbon intensity of the H_2 produced could be worse than conventional fossil-generated hydrogen and there could be grid congestion issues.

There are a number of practical issues that need to be considered if a large DSE stock is to be deployed and operated as controllable loads in the power system:

- How would the DSE stock be operated in practice to guarantee both the correct operation of the electricity system and production of zero-carbon hydrogen?

- What would be the value propositions to potential DSE owners so as to deploy a large DSE stock?

A large DSE stock embedded within the grid needs to be operated in time-phase with consumer electrical demand, WPP and ZPP available outputs. However for the operational strategies A and C suggested (see **Chapter 5**) some ELS could be operated continuously, e.g. across 24h periods in time-phase with ZPP (purple area in **Figures 5.11b and 5.11d, Chapter 5**). The proportion of DSE stock allowed to operate in this way would depend mainly on the ZPP capacity available for H_2 production.

Other H_2 customers with less restrictive H_2 requirements could be incentivized to install and operate DSEs in a more flexible manner subject to the WPP outputs available and the consumer electrical demand at any time (blue area in **Figures 5.11a, b and d, Chapter 5**). By implication for those electrolysers operated in this manner enough H_2

storage capacity needs to be deployed to cover hydrogen demand (e.g. for domestic transport or heating purposes) during periods of low wind availability. The size of the H_2 storage is a site-specific issue beyond the context of this study and is not considered here any further.

If a daily operating strategy is required, based on the demand expected, power plant declared availability and DSE availability for the following day, the TSO could schedule a suggested input profile for the aggregate DSE stock with the discrete contributions of WPP and/or ZPP depending on the operational strategy selected (see **Figure 5.11 Chapter 5**). Based on this information the TSO would then control the operation of DSEs on a real-time basis, using updated information on wind generation (MW) and system demand (MW), in order to get as close as possible to the suggested load input profile previously scheduled (MW) for the DSE stock. The updated operation strategy would then govern the switching of the electrolyser stock following the scheduling plan.

Alternatively DSEs could be allowed to operate also at periods of low wind availability at the expense of relaxing the carbon intensity of the hydrogen produced. The TSO could then allow an increased utilization of the DSE stock provided that carbon emissions derived from H_2 generation do not exceed specific values appointed. Estimated carbon emissions could be estimated daily by the TSO once the aggregate electrical input to the DSE stock and the FPP, ZPP and WPP output profiles have been scheduled.

For the purpose of this investigation it was assumed that ample hydrogen storage capacity exists to absorb the DSE stock output at any given time. In practice a real control strategy would have to take into account the charge status of the H_2 stores adjacent to the electrolysers. In extreme if the associated store is full then the DSE must stop. A real-time strategy must then include a state-of-charge variable to account for the availability of storage capacity.

Some additional infrastructure would be required for the TSO to control the operation of a large number of small scale ELS embedded within the grid. This would basically need to comprise communications to switch the electrolyser on and off or change load as required, an interface with a load control point located at the electrolyser site and metering arrangements. In addition the electrolysers must be equipped with transceivers to carry out specific instructions as directed by the TSO control centre via Internet, GSM or radio frequency.

Due to the large number of small DSEs to manage it may not be practical for the system operator to instruct every electrolyser individually. Operation of a group of ELS could be carried out simultaneously in groups by aggregating inputs to achieve a certain level of controllable load. For example to manage a 1 MW controllable load a hundred 10 kW electrolysers located at individual dwellings within the same local area could be scheduled to operate simultaneously. Individual electrolysers would then carry out specific instructions as directed by an aggregator or local controller. Therefore a single instruction could be sent out by the TSO to the aggregator requiring a certain level of load change up to 1 MW. The local controller could then dispatch single instructions to individual electrolysers to switch on or off. Similar approaches have been suggested to control a large number of micro-CHP units embedded at the low voltage level of the power system [127], [128]. **Figure 6.7** shows a schematic of the proposed communication structure from the TSO to the electrolysers.

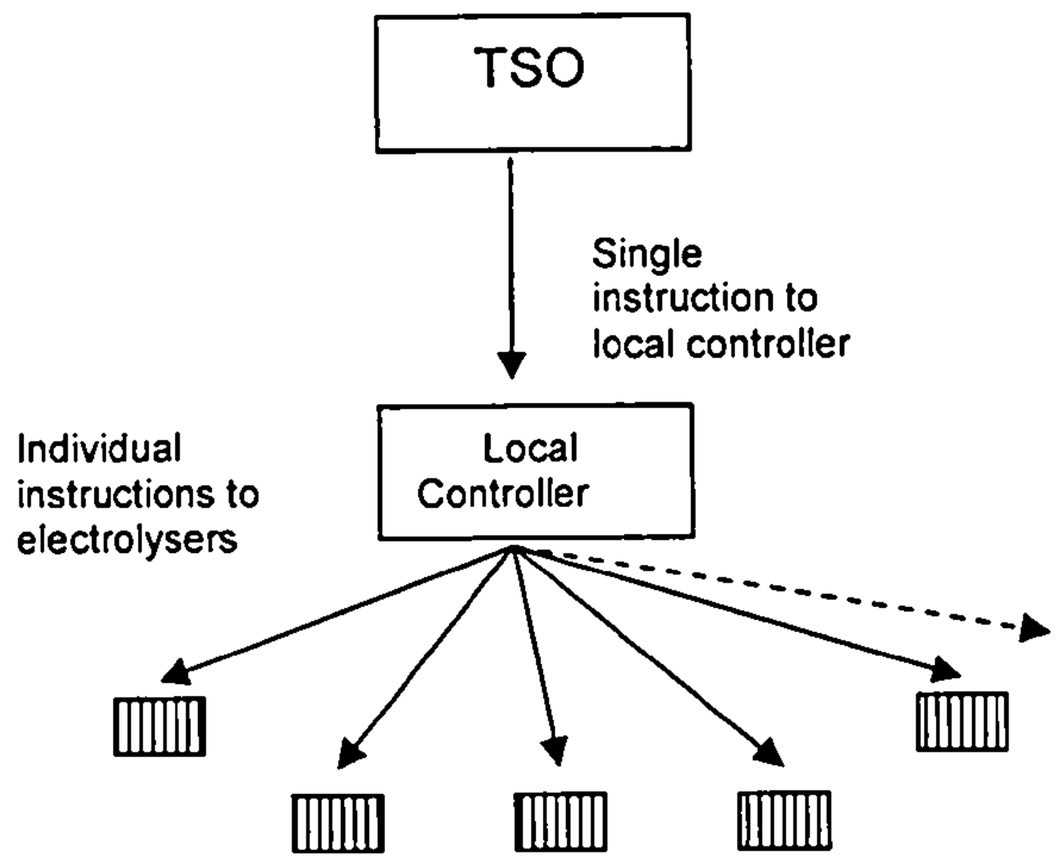

Figure 6.7 Suggested communication structure from the TSO to demand-side electrolysers via local controllers.

Under this configuration individual DSEs could operate following only on-off cycles. For instance let us assume that the aggregate electrical input to the DSE stock needs to be increased by 50 MW across a certain hourly period following an aggregate DSE input profile like that shown in **Figure 5.11a**. Fifty local controllers can then be appointed by the TSO to perform this action by switching on their 1MW loads in succession as shown in **Figure 6.7**. Note the response of 1MW DSE groups is assumed to be instantaneous according to the assumptions considered in **Chapter 3** as represented by vertical lines in **Figure 7**. In practice the lines representing 1MW increases would have a finite gradient accounting for the start-up period of the electrolysers, although for 10 kW ELS this would be in the order of a few seconds [108] and would barely affect the approach presented here.

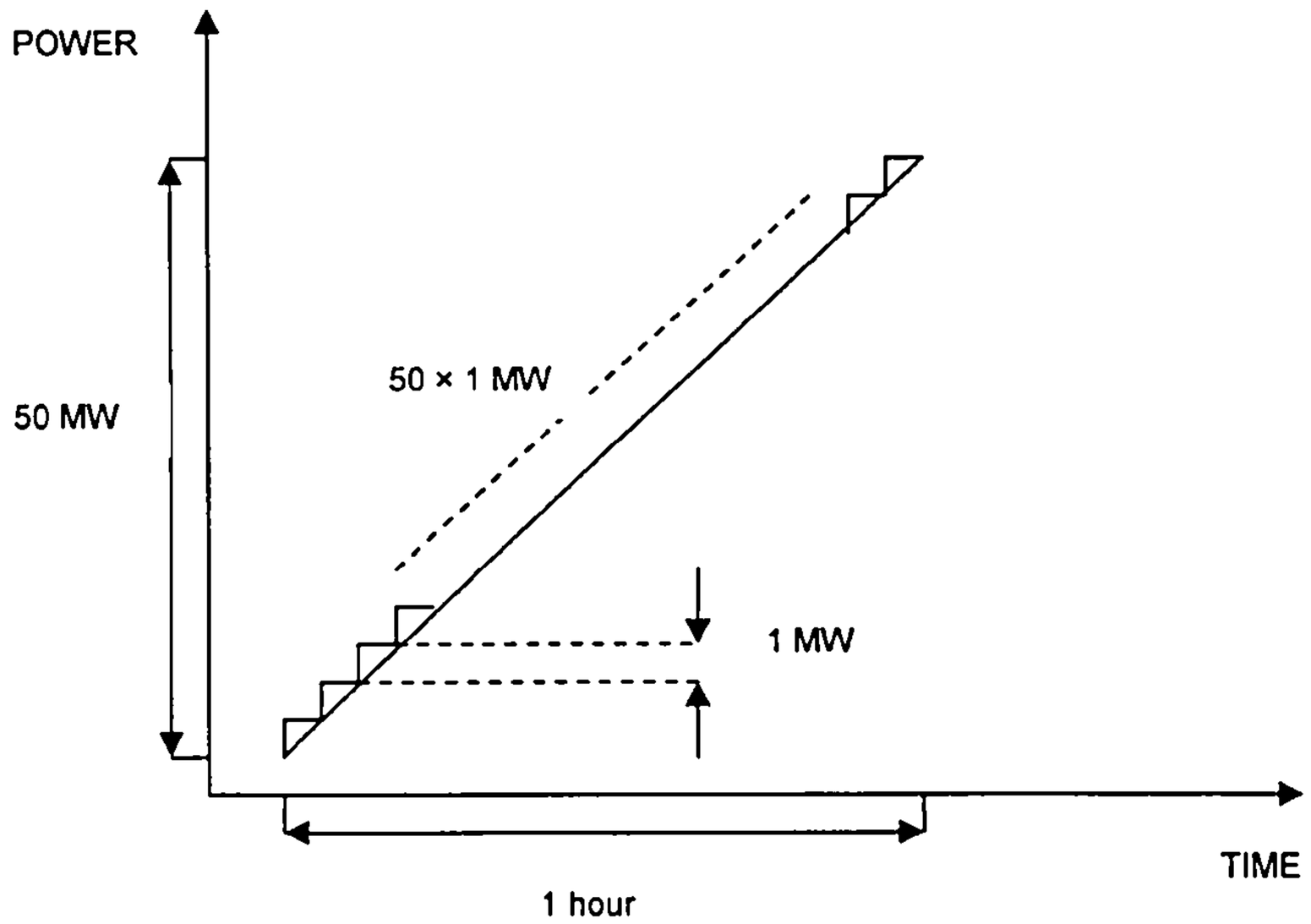

Figure 6.7. Aggregated response of groups of 1 MW DSE

Once the TSO has instructed the local controller to provide its available 1 MW load, one hundred 10 kW DSEs are then switched on by the local controller at the same time, and operated at rated capacity across the time-period appointed until an instruction is issued to switch them off. A merit order could be established so that the local 1MW DSE groups selected for operation by the TSO are those showing a longer record of idle periods. This way a more even distribution of utilization factors across the DSE stock would be achieved. The same procedure would apply for a downward load regulation. In this case the merit order would operate in the opposite way and the first DSE groups to be switched off would be those showing fewer records of idle operation. Additionally any practical control strategy should take into account the availability of the adjacent hydrogen stores and must include the state-of-charge of the H_2 stores as a primary control variable.

Another option for the local controller would be to operate more than one hundred 10 kW ELS at partial load distributing a 1MW load across them. Clearly controlling a larger number of DSEs makes this option more complex and possibly more costly. On

the other hand the response time to achieve a 1MW load increase would be lower. The simplest choice is probably optimal at the early stages of a large DSE implementation, and the control strategies can be progressively upgraded and optimized to become more sophisticated as more DSE are embedded in the power system.

It is conceivable that the costs of the communication infrastructure required could be shared between the DSE owners and the TSO provided that both have motivations to develop such infrastructure. For example the costs of the built-in equipment required to switch ELS on and off would be allocated to the DSE owner whereas the entire external communication infrastructure required would be paid for by the TSO. For the system operator these costs could be compensated by the accessibility to a large amount of controllable load in the form of electrolysers; and for electrolyser owners' an incentive would be the availability of an autonomous source of clean fuel for transport and heating purposes, independent from centralised H_2 supply depots.

However it is likely that stronger incentives have to be offered to potential adopters of DSE to achieve the implementation of a large electrolyser stock. These could come in the form of economic payments for the provision of load management services in the same way it is done today for demand side management and other ancillary services (see **Chapter II**). Basically the DSE owners would be rewarded for having their electrolysers available to be switched on or off as required. The main recipient of these load management services would be the system operator. Hence some form of commercial agreement would need to be established between the TSO and the DSE owners. One possibility would be to replicate and extend current arrangements for Demand Side Management services such that smaller providers (i.e. electrolyser owners') can participate. These arrangements could provide potential DSE owners with stronger economic incentives to install electrolysers at their premises.

CHAPTER 7 - CONCLUSIONS AND RECOMMENDATIONS

7.1 FINAL DISCUSSION AND CONCLUSIONS

This thesis has explored the synergistic benefits of applying zero-carbon power generation technologies (e.g. wind, nuclear or CO_2-sequestered power plant) and electrolysers. Electrolytic hydrogen produced from zero-carbon power sources can contribute to: maximization of RE penetrations, improved load management and stimulation of a zero-carbon hydrogen economy. In particular the operation of a large electrolyser stock as a load management mechanism in the power system has been explored, to enable the load placed on FPP to be increased or decreased in time phase with the availability of ZCPP inputs to the power system. Electrolysers are then used for hydrogen production both in the case of a fluctuating excess supply (e.g. during prolonged and rising wind generation) and during periods of low electricity demand. The supply of electricity becomes effectively decoupled from the demand in such a way that the operation of power plant becomes less dependent on consumer demand. In addition, this form of load management can lead to a higher average utilization rate for preferred zero-carbon thermal power plant.

A macro-system analysis has been carried out to assess the benefits and drawbacks of different electrolyser implementation strategies in the power system from an energy perspective, not an economic one. Optimum capacity levels for the electrolyser stock to be deployed in the system are identified, and parameters like hydrogen yield, carbon intensities and utilization factor of the electrolyser stock have also been investigated. A supply-side view has been followed, where no demand-side limitation exists to electrolyser operation and the size of the electrolyser stock is determined by the availability of ZCPP and FPP inputs. The investigation presented here, conducted on a generic basis, highlights the key factors and boundaries influencing a widescale implementation of electrolysers at national/regional level and can be used to make strategic decisions about the implementation of ELS as controllable loads in specific power systems.

For a given power/energy system and depending on the parameters to optimize (e.g. LF_{TH}, Y_H, CI_e, etc), preferred capacities for the DSE and SSE stocks can be identified and optimum operational strategies for FPP, ZCPP and the electrolyser stock can be selected so as to maximize the benefits of a wide implementation of ELS in the system. The system analysis offered here establishes the framework for a large deployment of ELS in the power system. Subsequent "demand-driven" analyses should be carried out to design the precise electrolyser systems to be deployed at selected sites (including ancillary components like H_2/O_2 stores and compressors). These analyses should take into account:

- The specific characteristics of the H_2 demand to which such sites are linked

- Local network restrictions like power and energy flows, voltage restrictions, and maximum connection capacity of the nodes existing within the area selected.

The specific demand-side analyses should be carried out within the boundaries established by the results of the system analysis. For example, the sum of ELS capacities obtained from all the demand analyses should never exceed the capacity of the ELS stock obtained from the system analysis, since the latter has been appointed to optimize the operation of the whole system.

A heuristic approach has been followed for implementing and controlling a large stock of electrolysers in conjunction with high penetrations of ZCPP for an island power system, so that very high load factors can be achieved on the FPP load profile during periods of different RE availability and consumer demand. The approach serves to identify macro capacity levels for the electrolyser stock required as a function of the penetration of zero-carbon power sources in the power system.

Following this approach a spreadsheet model (AELM model) based on power and energy flows has been developed. From power plant availability, demand and RE forecast profiles, which are the primary input data, the AELM model generates utilization strategies for the electrolyser stock, ZPP, WPP and FPP. Other general

outputs are energy balances, hydrogen yields and carbon intensities for electricity and hydrogen for the time period analyzed.

When considering power systems with high penetrations of ZCPP, active load management via electrolysers is found an attractive option with the view of optimizing the operation of the power system. The AELM model has been applied for implementing and controlling a large stock of electrolysers in conjunction with high penetrations of WPP and ZCPP with the main objectives of: (i) increasing the penetrations of RE in the power system (by reducing wind energy curtailment); (ii) maximizing the efficiency of utilization of FPP (by maximizing the load factor of the aggregate FPP load profile; and (iii) creating a source of zero/low-carbon hydrogen for existing and emerging hydrogen economy markets. Several alternatives for implementation and operation of electrolysers have been suggested, including both demand-side and supply-side configurations.

The main conclusions from the analysis presented in this thesis are summarized below:

1) Wind curtailment:

It is found that the need to curtail wind generation increases dramatically as wind power penetration rises. For example, for the wind and demand data analysed in **Chapter 4**, more than 30% of the resource is wasted for $\Phi_W = 50\%$, on a variable wind days of CF = 42%. As Φ_W rises, a greater proportion of the electricity demand than theoretically needed (if all the wind-generated electricity could be integrated into the grid) must be met by thermal power plant. Hence, along with the economic penalties imposed on wind farm operators there are also diminishing carbon-abatement benefits per new MW installed if wind power can only be directed to the grid. If high penetrations are to be achieved in future power systems, effective load management techniques are essential. Rather than simply increase the amount of wind power introduced to the grid and curtail it when necessary, it has been shown that the surplus wind power that cannot be accommodated can instead be directed to a electrolyser stock located at or near the main WPP for producing zero-carbon hydrogen, thus improving the justification

for installing more wind power. The AELM model has been designed to analyse the increased capture of RE resources by minimizing wind curtailment.

2) Increased load factor of the FPP load profile:

The load factor of the net FPP load profile acts as an indicator of the carbon performance of the FPP portfolio. The greater the load factor, the flatter the load profile faced by thermal power plant, the more efficient its operation and therefore the lower the average carbon intensity of the electricity generated. Results obtained suggest that it is indeed possible to substantially increase the load factor of the aggregate FPP load profile by integrating electrolysers into the system. Operation of electrolysers can be adapted (switching on and off as required) to increase demand at will, filling valleys and creating plateaus on the FPP load profile, to allow FPP a more stable and efficient operation, thus reducing their carbon footprint.

The deployment of electrolysers as controllable loads within the power system can effectively increase the daily LF_{TH} to maximum levels of 100% (a virtually flat FPP load profile) even on days of low wind availability (CF = 16%) at high wind penetrations of Φ_W = 100%, while producing zero-carbon hydrogen by operating ELS in time-phase with the ZCPP inputs to the system. For days of higher wind availability (CF $\geq$ 42%) LF_{TH} = 100% (daily value across a 24h period) can be achieved at $\Phi_W \geq 50\%$. This constitutes an unprecedented achievement for the power industry, which can be utilised to minimise the carbon intensity of fossil-fuelled power generators.

A different approach needs to be followed when aiming to improve the operational performance of FPP across periods longer than 24h. For instance for weekly periods a succession of consecutive plateaus can be created with each one corresponding to one day of the week, but at different load levels depending on the daily demand and specific wind availability on each day. Hence even though the load factor calculated across any particular day (for each 24h FPP profile) can rise up to 100%, the weekly LF_{TH} (calculated for the 168h profile) is always below

100%. However, it is found that in this case the average weekly LF_{TH} of the aggregate FPP load is not the optimum parameter to assess the performance of FPP. Instead, the value of the average load and the duration of the plateaus created on the FPP aggregate load profile are measures of performance far more significant. The former will determine the carbon intensity of the electricity supplied CI_e and the latter indicates how long FPP are operating at a steady rate without load changes, thus maximizing their efficiency.

3) Trade-offs between the main parameters analysed:

There is a trade-off in terms of the carbon benefits derived from increasing LF_{TH}, the utilization of the electrolyser stock and the carbon penalties imposed. It is further observed that the more variable the system demand (significant differences between minimum and maximum daily demand, and hence low LF_{TH}), the more beneficial will be an increase of LF_{TH} to obtain high utilization factors for the electrolyser stock and high hydrogen yields. However an increase in LF_{TH} implies an increase in the load imposed on FPP and therefore an increase in CI_e. Further analysis is required to evaluate the carbon benefits associated with a widespread implementation of electrolysers as a load management mechanism. These include:

- A more stable and predictable operation of existing FPP due to the much grcater LF_{TH} achieved in a power system with an electrolyser stock.
- A reduced operational requirement for supply/demand matching with additional back-up thermal power plant on days of high or variable wind availability.
- The displacement of fossil fuel use in applications across the energy system by zero/low-carbon electrolytic hydrogen, (for which it is important to realise a high utilisation factor per MW of electrolyser stock).

With respect to carbon emissions derived from back-up plant operation, optimisation of the load factor itself would lower the CI_e by decreasing the need for back-up plant operation. However very little data is available in the literature to estimate accurately the CO_2 emissions derived from the increased use of fossil back-up capacity for supply/demand balancing purposes as wind penetrations

increases. Therefore further research is needed to accurately quantify the carbon benefits obtained when implementing a large electrolyser stock as a load management mechanism. This is proposed below as an interesting area for further research.

There is a strong trade-off between the carbon intensity of the electricity delivered and the amount of zero-carbon hydrogen produced by the electricity system. The hydrogen yields could be increased (and hence the utilization of the electrolyser stock) beyond the levels presented here, but at the expense of dedicating less zero-carbon electricity to cover consumer electrical demand thus increasing the carbon intensity of electricity (see **Figure 5.14**). CI_e and Y_H correlate linearly since both are proportional to the amount of zero-carbon electricity diverted from the electrolyser stock to meet consumer electrical demand.

Depending on the energy system under consideration and specifically on the hydrogen and electricity demands to be covered, defined values for CI_e and Y_H can be sought and the benefits obtained from the production of zero-carbon hydrogen and the optimization of the power system can be fully maximised. Then the deployment of ZPP, in addition to WPP, gives greater flexibility in terms of the optimum pair of values (CI_e, Y_H) to be selected for a specific energy system and on a specific day depending on the preferred carbon abatement strategy and the hydrogen and electricity demands required. For instance, for an energy system with a large demand for zero carbon hydrogen (e.g. for transport purposes), it could be more beneficial to maximize Y_H at the expense of achieving a lower reduction in CI_e; whereas for an energy system with a dominant electricity demand, targeting minimum values of CI_e could be more appropriate. A specific analysis is needed for a given power system to obtain its optimum characteristic pair of values (CI_e, Y_H).

Much larger hydrogen yields can also be obtained at the expense of increasing CI_H. For instance, if low-carbon hydrogen of CI_H = 3 $kgCO_2/kg\ H_2$ is produced, Y_H can be increased by 2 fold with respect to the values obtained if only zero-carbon hydrogen were produced. Yet the benefits of increasing Y_H need to be evaluated against the carbon penalties imposed (see **Chapter 5**). It is possible that for other

power/energy systems, depending on the hydrogen and electricity demands and provided that an average CI_H is not surpassed (i.e. a yearly average, possibly in the range 0-3 kg CO_2/kg H_2), some flexibility in terms of "relaxing" the carbon intensity of hydrogen (so as to further increase the scale of hydrogen production) could yield overall carbon benefits.

4) Increased deployment of ZPP capacity:

The deployment of ZPP in addition to WPP is a considerable benefit. In particular much greater hydrogen yields and electrolyser utilization factors can be obtained especially on days of low wind availability, thus solving the main drawbacks of a pure wind-hydrogen (or more generally renewables-hydrogen) implementation. In addition, when implementing additional ZPP in the system added carbon benefits can be obtained in terms of reducing the carbon intensity of the electricity delivered to consumers. For example at Φ_W = 100%, if a ZPP penetration of 35% of SMD is deployed in the system, on a variable wind day (CF = 42%) the carbon intensity of electricity can be reduced by more than half that obtained previously (i.e. for the Base Case) while achieving a virtually flat thermal load profile (i.e. LF_{TH} = 100%).

Furthermore if the objectives pursued are maximizing Y_H, UF_E and minimizing CI_e the deployment of ZPP is more beneficial than just installing WPP, since lower ELS capacities are required to attain such goals. However maximum benefits are attained when implementing both ZPP and WPP particularly at high wind penetrations, using ZPP both for electricity generation and hydrogen production, but operating them in such manner that the output directed to cover consumer electrical demand increases (thus decreasing the output directed to ELS) at peak times (Operational Strategy C in **Chapter 5**).

5) Electrolyser capacities required and economic implications:

For all the implementation cases and operational strategies analysed, large electrolyser capacities (between 20% and 130% of the total ZCPP capacity deployed in the power system) are required to achieve the objectives of optimizing the utilization of FPP, maximizing the integration of RE and the production of hydrogen. This implies significant capital investment in deploying electrolysers

plus ancillary equipment (e.g. control systems, associated H_2, O_2 stores and compressors if required). However the economic justification for a large deployment of ELS improves as the unit cost of the electricity outputs from zero-carbon power plant decreases. An economic case may exist in the short/medium term for those power systems with large amounts of RE inputs and significant RE curtailment associated which translates into zero-carbon electrical inputs available for electrolysis at virtually zero cost. Moreover, the investment required in ELS must be placed into context and compared against the economic benefits delivered by a large ELS implementation:

- Reduction/elimination of network reinforcements entailed when integrating large penetrations of intermittent RE like wind power: the geographical availability of RE resources does not necessarily match the optimum locations for network integration. Often regions of high RE availability are located in areas of poor grid availability which implies grid reinforcements in order to exploit the RE resource. The implementation of ELS can attenuate these reinforcement costs by controlling and absorbing some of the RE inputs delivered to a specific grid node. There is a clear exploitable synergy between the expanding zero-carbon energy markets and emerging hydrogen energy markets.

- Reduction of impacts on balancing costs incurred in the system when integrating large RE penetrations: it has been found that the use of ELS as a load management mechanism can reduce the variability of RE inputs delivered to the grid and makes WPP more controllable (e.g. reducing peaks and smoothing wind input profiles directed to the network). This in itself would reduce the balancing costs resulting from: (i) capital costs of additional back-up reserve capacity required and (ii) operating costs from both the use of this additional reserve and increased cycling duties (thus reduced efficiency) of existing power plant, which incur both increased fuel and O&M costs (see **Chapter 2**).

- Associated reduction of emissions in other energy sectors (internalization of external environmental costs): avoided emissions from transport, domestic, industrial sectors. These benefits could come in the form of carbon tax rebates for

every kilogram of CO_2 displaced. For comparison, as of June 2007 the price of carbon allowances in the European Union Emission Trading Scheme was between 20-25 € per tonne of CO_2 [129].

- Revenues from hydrogen produced: in 2002, the market price of compressed gas hydrogen was between $7-11 per kg depending on consumed volume, consumer location and length of supply contract [130]. Looking at foreseen hydrogen applications, if replacing gasoline as a transport fuel at energy equivalent (assuming a pump price of $1.70 / litre of gasoline) a market value of $6.4 per kg of H_2 could be attributed.

To carry out an appropriate economic analysis it would be important to take into account that the economic benefits from a large implementation of ELS are borne at different economic levels including hydrogen and electricity producers, suppliers, network operators and end-users. A consistent basis needs to be defined for the aggregation of such cost benefits. Ultimately, all or most of the costs and benefits associated at different levels are likely to be passed on to hydrogen and electricity end-users.

6) Suggested path for a large implementation of electrolysers in the power system:

It is suggested here that for power systems with low penetrations of zero-carbon power sources, a large ELS stock could be deployed embedded within the grid, locating ELS next or close to the points where hydrogen (and ideally oxygen) is to be consumed, i.e. a DSE implementation. This would minimize infrastructure and distribution costs associated. However as ZPP and particularly RE penetrations increases, the amount of RE that can be integrated into the grid becomes constricted, and a combined scheme including both supply and demand-side electrolysers is required to achieve high Φ_W and LF_{TH} values. Some ELS can then be deployed on the supply side next to selected WPP and ZPP to satisfy an increasing zero/low carbon hydrogen demand and absorb the RE output that would otherwise need to be curtailed.

When large penetrations of ZCPP are achieved a combined SSE + DSE implementation combines the benefits of both implementation strategies in terms of: optimizing the operation of FPP, eliminating RE curtailment and maximizing the amounts of zero/low carbon hydrogen produced. In addition, distribution and Infrastructure requirements can be minimized since some ELS are deployed on the demand side. Furthermore a combined SSE + DSE implementation offers more flexibility in terms of controlling the WPP outputs and in fact allows smoothing the aggregate WPP input profile to the grid, maximizing the carbon benefits of a large deployment of ELS in the power system. The benefits of deploying a large ELS stock in the power system as a load management tool are maximized when the electrolyser stock is located both on the supply and demand side.

Ideally optimization of the operation of FPP should be carried out gradually, aiming for very high LF_{TH} approaching 100% (i.e. a virtually flat aggregate FPP load profile) only at very high WPP penetrations and moderate ZPP penetrations, at which stage the electrolyser installed capacity needs to: (i) approach the combined ZCPP capacity (WPP and ZPP) if only zero-carbon hydrogen is aimed; or (ii) exceed the overall ZCPP capacity if the production of low carbon hydrogen (e.g. of $CI_H \leq 3$ kg CO_2/ kg H_2) is to be permitted to further increase the utilization of the ELS stock and hydrogen yields.

In the long term, an enhanced power system may be developed with very large penetrations of zero-carbon power sources and electrolysers comprising both on and off-grid configurations with capacities exceeding the power system maximum demand. While annual electricity demand growth may be limited, the ZCPP inputs could grow rapidly to satisfy a growing zero-carbon hydrogen demand, using both the electricity system and hydrogen to meet an increasing fraction of the general requirements for end use energy. For future energy systems where very large ZCPP penetrations have displaced a large proportion of FPP capacity, and an established hydrogen demand exists far in excess of consumer demand for electricity, an optimization based on other parameters (e.g. CI_H, Y_H, UF_E) rather than those investigated here (namely LF_{TH} and wind curtailment) may be more appropriate.

The results of this study are suggestive, not definitive, due to the broad scope of the analysis. It is important to bear in mind that the key parameters of the analysis presented are very system-specific, and the outcomes for different energy/power systems will be different. However the intention is to establish a generic methodology and the boundary conditions for the deployment of a large electrolyser stock in any given power system. This is thought to be a valuable tool in the decision-making processes towards a more sustainable energy system and eventually towards the prospective hydrogen economy.

7.2 RECOMMENDATIONS FOR FURTHER WORK

The following recommendations are made for further investigation:

1) The approach followed intends to analyse the scope for increasing the capture of wind resources through minimisation of wind curtailment. The objective of complete elimination of wind curtailment requires rather large ELS capacities and entails low utilization factors since the wind power absorbed would rarely equal the rated capacity of the electrolyser stock. Both have undesirable economic implications. There is indeed a trade-off to be analysed between the sizing of the electrolyser stock and the capturing of the wind resource available. It might be worthwhile to relax the condition imposed referred to complete eradication of **wind curtailment**, i.e. WC = 0, and allow for several (low) levels of curtailment, for instance WC = 5%, 10% or 20%, in order to reduce the size of the electrolyser stock and increase the utilization factor.

2) Even though the approach presented in this thesis considers an island power system, a new variable could be included in the model accounting for the degree of interconnection of the power system expressed as the ratio of transfer capacity to the Maximum System demand in percentage. In this way a particular geographical area of any size of any power system could be taken as a singular entity, treated as a small power system in itself and modelled following the same approach presented here, provided that the degree of interconnection to neighbouring areas is known, as well as the rest of the parameters and inputs summarized in **Chapter 3**.

3) If distributed generation (e.g. micro-wind and building-integrated photovoltaics, DG) is widely deployed at the LV level of the power system then a much higher utilization of the DSE stock could be achieved while maintaining SMD at its current levels, hence obviating the need for network upgrading. Furthermore wide DG deployment could increase DSE capacity beyond the levels presented here not restricted by the amount of wind power that can be integrated in the electricity transmission system, provided transformers are not overloaded at the LV level. Operated in combination with DG, DSE can operate as a load management tool at the LV level, helping to smooth out domestic loads. The combination of DSE and DG could extend the benefits of the concept proposed here by further decarbonising other energy sectors through large scale production and usage of zero/low carbon H_2 e.g. for domestic transport and heating purposes. The addition of DG would imply adding an additional type of power plant in the generic power system depicted in **Figure 5.1**, and its full output, P_{DG}, could be directed to the DSE stock and to the grid in the proportions required where:

$$P_{DG} = P_{DGDE} + P_{DGC} \quad (7.1)$$

$$P_{DSE} = P_{WDE} + P_{ZPDE} + P_{FPDE} + P_{DGDE} \quad (7.2)$$

The rest of the features of the AELM would remain the same and the operational strategies could be modified to include different ratios of P_{DGC} to P_{DGDE}.

4) Modifications could be included in the approach suggested here to allow an expanded deployment of ZPP capacity beyond the levels considered here (say up to $\Phi_{ZPP} = 100\%$). This could be done by:

a. Allowing P_G to exceed the existing SMD (basically modifying the restriction imposed by equation 3.1) and increase the deployment of ZPP on the supply side and DSE on the demand side in an expanded electricity system. This would imply that the capacity of T&D system would need to be increased substantially, incurring large infrastructure decisions and capital investment.

b. Deploying ZPP in combination with SSE in off-grid configurations, for example at a small number of large sites. This option provides a different approach to that shown here that is essentially grid-independent. This would imply adding an additional type of power plant in the power system (see **Figure 5.1**), namely "equivalent off-grid ZPP", and its full output, P_{ZPPOG}, would be directed to the SSE stock where:

$$P_{ZPPOG} = P_{ZPOGSE} \quad \text{and} \quad P_{ZPOGG} = 0 \tag{7.3}$$

$$P_{SSE} = P_{WSE} + P_{ZPSE} + P_{ZPOGSE} \tag{7.4}$$

The rest of the features of the AELM and the operational strategies suggested would remain essentially the same.

Either option (or some combination of both) would increase Y_H, UF_E and reduced CI_e, TC far beyond the levels shown herein, using electrolytic hydrogen as the main means of reducing carbon emissions across all energy sectors, and allowing for a more radical shift towards future hydrogen-based energy systems. Additionally, the combination of different types of ZCPP (e.g. WPP, nuclear power plant and CO_2-sequestered power plant) in "micro-grids" could well be an attractive option to maximize the exploitation of local energy sources while maximizing the utilization of the electrolyser stock.

5) Economic analysis to estimate the costs of a wide implementation of ELS for systems with high penetrations of zero-carbon power plant, and evaluate them against the costs benefits derived from: (i) reduction of network upgrade requirements (if implementation of ELS is carried out below SMD levels); (ii) reduction of balancing costs or wind integration costs: avoided capital costs from new back-up generation requirements and operating costs (fuel and O & M costs imposed in FPP); (iii) avoided emissions across other energy sectors (internalisation of environmental benefits); (iv) market revenues from hydrogen (and oxygen) produced.

6) Estimate the **carbon benefits** derived from a more stable operation of FPP (increased LF_{TH}) and the potential **reduction of back-up generation**

requirements when implementing ELS as a load management mechanism on a wide scale in the power system. Detailed modelling of the operation and performance of several types of FPP like those included in [1], [2] would be required. Such modelling could be based in a number of parameters like: (i) start-up time and fuel consumption during start-up periods; (ii) relative increase of start-ups across a certain time period (e.g. a year) for different levels of RE penetration; and (iii) increase in fuel consumption per kWh_e generated when operating FPP at part load. This could be attempted by using computer models similar to those applied by the power industry today to optimize system performance and costs (e.g. PROMOD, CREEP software).

REFERENCES

[1] Future Application of Energy Storage in the UK. Strbac G, Black M. DTI Energy Storage Workshop, 2004.

[2] Impact of Wind Power Generation in Ireland on the Operation of Conventional Plant, ESB National Grid 2004.

[3] The Impacts of Increased Levels of Wind Penetration on the Electricity Systems of the Republic of Ireland and Northern Ireland. Gardner P, Snodin H, Higgins A, McGoldrick S. Garrad Hassan and Partners Ltd, 2003.

[4] Power limitations and energy yield evaluation for wind farms operating in island systems. Papathanassiou S, Boulaxis N. Renewable Energy, Volume 31, Issue 4, April 2006, pp 457-479

[5] Energy Storage, enabling a future for renewables? Baxter R, Renewable Energy World, July-August 2002.

[6] Electrolyser-based energy management: a means for optimizing the exploitation of variable renewable-energy resources in stand-alone applications. Crockett R.G.M, Newborough M, Highgate D.J. Solar Energy (1997) Vol. 61-5, p. 293-302.

[7] BWEA Briefing Sheet, Wind Turbine Technology, www.bwea.com

[8] GWEC, Greenpeace. Wind Force 12: A blueprint to achieve 12% of the world's electricity from wind power by 2020, June 2005.

[9] Eolica 2007 Anuario del Sector: Analisis y Datos, aee June 2007-06-23

[10] The impact of large scale wind power production on the Nordic electricity system. Holtinnen H, Helsinki University of Technology, Department of Engineering Physics and Mathematics, PhD thesis, 2004

[11] www.ree.es

[12] Wind report 2004, EON Netz GmbH, 2004

[13] Quantifying the System Costs of Additional Renewables in 2020. G.Strbac; ILEX Energy Consulting, Report to the DTI, October 2002

[14] Renewables and the UK Electricity Grid Supply Infrastructure. Laughton M.A, Power in Europe issue 383, September 2002

[15] The Carbon Trust and DTI Renewables Network Impacts Study, Annex 4. Milborrow D, Gonzalez S; November 2003

[16] Grid Impacts of Wind Power: A Summary of Recent Studies in the US. Parsons. B, Milligan M, NREL US, 2003

[17] www.eng.elkraft-system.dk

[18] UCTE System Adequacy Forecast, 2004-2010. Union for the Coordination of Transmission of Electricity, December 2003

[19] Operation of Power Systems with Significant Wind Power Import: The Blowing Network, Fox B, Flynn B, Persaud S, The Queen's University of Belfast, September 2000

[20] Frequency Response, M. Arthur, Presentation to Operations Forum of National Grid Transco, November 2002

[21] Power Quality Application Guide, Voltage Disturbances Standard EN 50160-Voltage Disturbances in Public Distribution Systems, H. Markiewicz, A. Klajn, July 2004

[22] Ancillary Service Provision from Distributed Generation, ILEX Energy Consulting for the DTI Technology Programme, 2004

[23] Provision of Power Reserve from Pumped Storage Hydro Plant. Lumb D, Hawkins N.T, IEE Colloquium on Economic Provision Of A Frequency Responsive Power Reserve Service, February 1998

[24] NYISO's Demand Response Programs, Reduce Energy and Get Paid 2005. Breidenbaugh A, March 2005

[25] www.DemandSideManagement.com

[26] IEA DSM Program, Task VIII - Demand-side Bidding in a Competitive Electricity Market, 2003

[27] IEA DSM Program, Task XIII – Demand Response Resources, January 2006

[28] Grid Impacts of Wind Power: A summary of Recent Studies in the US, B. Parsons, D. Brooks, B.Kirby, K.Dragoon, European Wind Energy Conference, Madrid, June 2003

[29] Comparative analysis on the part load performance of CCGT plants considering design performance and power control strategy, T S Kim, Energy 29 (2004) 71-85

[30] CO_2 Reduction targets call for applying bat; a new 800 MW CCGT plant South of Graz, J Tauschitz, M Hochfellner, Verbund-Austrian Thermal Power GmbH &b Co KG, October 2004

[31] Reduction in Carbon Dioxide Emissions: Estimating the Potential Contribution From Wind Power, D. White, Renewable Energy Foundation December 2004

[32] 9F Class Gas Turbine & Combined Cycle Upgrades for Operational Flexibility, A. Martin, J. McGuiness, GE Energy, Power-Gen Europe, Madrid, June 2007

[33] Flexible Load Operation and Frequency Support for Steam Turbine Power Plants, A. Wichtman, Siemens Power Generation, Power-Gen Europe, Madrid, June 2007

[34] The Application of Batteries as a back-up of Large Wind Farms, E. Spahic, G. Balzer, International Workshop on Large-Scale Integration of Wind Power and Transmission Networks for Offshore Wind Farms, Delft, October 2006

[35] Adiabatic Compressed Air Energy Storage for the Grid Integration of Wind Power, S. Zunft, C. Jakiel, M. Moller, C. Bullough, International Workshop on Large-Scale Integration of Wind Power and Transmission Networks for Offshore Wind Farms, Delft, October 2006

[36] Evaluation of Gas Turbine Startup emissions for New Source Permitting, Paper 546 Session No.EI-2a, Mostardy Platt Environmental, J. Macak III

[37] www.**nationalgrid**.com/UK

[38] Quantifying the System Costs of Additional Renewables in the UK'; G.Strbac; IEA Workshop on Wind Integration; May 2004

[39] The practicalities of Developing Renewable Energy; D.Milborrow; Submission to the House of Lords Science and Technology Committee Enquiry; October 2003

[40] Planning of the Grid Integration of Wind Energy in Germany Onshore and Offshore up to the Year 2020, DENA 2004 Wind Report, February 2005

[41] Design and Operation of Power Systems with Large Amounts of Wind Power, first results of IEA collaboration, H. Holtinnen, P. Meibom, A. Orths, F.

Van Hulle, C. Ensslin, L. Hofmann, A. Estanqueiro, G. Strbac, B. Parsons, B. Lemstrom; VTT 2006

[42] www.ewea.org

[43] Ancillary Service Provision from Distributed Generation, ILEX Energy Consulting for the DTI Technology Programme, 2004

[44] US Climate Change Technology Program – Technology Options for the Near and Long Term, November 2003, www.climatetechnology.gov/

[45] Balancing Fluctuating Wind Energy with Fossil Power Stations – Where are the Limits, W. Leonhard, K. Muller, ELECTRA, October 2002

[46] Coal-fired Power Generation: The Need to be Nimble, Blankinship S, Power Engineering International, June 2003

[47] Upgrades and enhancements for competitive coal-fired boiler systems, Kitto J. B, Bryk S A, Piepho J M, *1996 international joint power generation conference*, Houston Oct 1996

[48] Review of Energy Sources for Power Stations, Merz and McLellan, Consultation Document for the DTI, 1998

[49] NO_X emission control in gas turbines for combined cycle gas turbine plant, Moore M.J. Journal of Power and Energy (1997) 211-1: 43-52

[50] State of the Art of CCGT plant South of Graz, Tauschitz J, Hochfellner M, Energy Efficiency Conference, Vienna October 2004

[51] Reliability and Durability from Large Heat Recovery Steam Generators, Pearson M, Anderson R. W, proceedings IMechE Vol 213 Part A, February 1999

[52] Operation of Hybrid Wind-Pumped Storage Systems in Isolated Island Grids, Protopapas K, *Papathanassiou* S, Conference Proceedings MedPower 2004,Lemessos November 2004

[53] Why UK Wind Power should not exceed 10 GW, Sharman H, Proceedings of ICE-158 pp 161-169, November 2005

[54] European Wind Integration Experience, Ackerman T, Energynautics GmbH 2006

[55] Why Wind Power Works for Denmark, Sharman H, Proceedings of ICE 158 pp 66-72, May 2005

[56] Europe's PV sunrise, NATTA, Renew on Line 36, March-April 2002

[57] http://www.earth-policy.org/Indicators/Wind/2006_data.htm#table3

[58] Integration of Advanced Gas Turbine and Combined Cycle Technologies for High Efficiency with Operational Flexibility, McManus M, Baumgartner R, PowerGEN 2003, Las Vegas December 2003

[59] Integracion de la generacion Eolica en el sistema electrico, Alonso J F, Curso Energias Renoivables Universidad de Cantabria, Red Electrica February 2005

[60] Wind power variability and forecast accuracy in New Zealand, McQueen D, Wong Too P, White G, Garrad Hassan March 2007

[61] Technical Factors Affecting Wind Penetration in Large Electricity Systems, Paul Gardner, Garran Hassan & Partners Ltd, 2003

[62] Income loss due to wind energy rejected by the Crete island electrical network – the present situation, J K Kaldellis, K A Kavadias, A E Filios, Applied Energy 79 (2004) pp 127-144

[63] Giebel G, On the Benefits of distributed Generation of Wind Energy in Europe, PhD dissertation, University of Oldenburgh September 2000

[64] Analysis of Thermal Stress Evolution in the Steam Drum during Start-up of a Heat Recovery Steam Generator, Kim T. S, Lee D. K, Applied Thermal Engineering (2000) 20-11 pp 977-992

[65] The effect of wind power on CO_2 abatement in the Nordic countries. Energy Policy, (2004) 32/14. pp 1639-1652.

[66] www.ewea.org/documents/EWEA-2004Map-v2.pdf, 12th June 2005

[67] Low-cost polymer electrolysers and electrolyser implementation scenarios for carbon abatement, Smith A.F.G, Newborough M. Report to the Carbon Trust and ITM Power, 2004.

[68] Renewable energy sources – can they fill our future energy needs?, Leonhard W, Technical University Braunschweig, 2005.

[69] Control Analysis of Renewable Energy System with Hydrogen Storage for Residential Applications, A. Bilodeau, K. Agbossou, Journal of Power Sources (2006) vol 162-2, November 2006

[70] Electric round-trip efficiency of hydrogen and oxygen-based energy storage, E. Bernier, J. Hamelin, K. Agbossou and T. K. Bose International Journal of Hydrogen Energy (2005) Vol 30-2

[71] Use of water electrolysers in low carbon energy systems, A G Smith, PhD thesis, Heriot Watt University, Energy Academy, Engineering & Physical Sciences 2006

[72] Statistical Wind Power Forecasting Models: Results for US Wind Farms, M. Milligan, M. Schwartz, Windpower 2003, Austin, Texas, May 2003

[73] http://www.garradhassan.com/services/ghforecaster/accuracy.php

[74] European electricity supply industry: demand and generation prospects to 2020, Papageorgi A, Tribuzi G, Rossodivita A. Synopsis of the EURPROG Report 2002, EURELECTRIC, 2003.

[75] National Grid, 2005 GB Seven Year Statement, 2005

[76] Distributed energy systems with wind power and energy storage, M Korpas, PhD Thesis, Norwegian University of Science and Technology, Department of Electrical Power Engineering, 2004

[77] Large scale Wind hydrogen Systems, E. Liu, GE Global Research, September 2003

[78] www.ens.dk/sw11492.asp Annual Energy Statistics 2004

[79] Combined heat and power generation and district heating in Denmark: history, goals and technology, Manczyk H, Leach M. District Energy Publications, 2003.

[80] Renewable electricity factsheets EU countries. Energy Research Centre of the Netherlands, 2004.

[81] Energy Statistics 2005, Danish Energy Authority, December 2006

[82] Electric power required in the world by 2050 with hydrogen fuel production, P. Kruger, International Journal of Hydrogen Energy 30 (2005) pp. 1515-1522.

[83] Integrating Renewables into the Electricity System – A Historical Overview, M Laughton, Centre for Energy Policy & Technology, Imperial Colledge, January 2006

[84] www.dst.dk/yearbook

[85] Hydrogen markets 2006: existing and emerging applications, Visant Strategies Inc, April 2006

[86] A simple model for solid polymer electrolyte water electrolysis, P Choi, D Bessaravov, R. dtta, Solid State Ionics 175 (2004) 535-539

[87] Hydrogen production by water electrolysis: a review of technology and current research, A Marshall, Norwegian University of Science and Technology, August 2003

[88] The Electrolysis of Water: An Actuation principle for MEMS with a Big Opportunity, C Neagu, H Jansen, H Gardeniers, M Elwenspoek, Mechatronics: 571 – 581, 2000

[89] Electrolysis for hydrogen production, S Sunde, Haldor Topsoe Catalysis Forum, Hornbaek August 2006

[90] Design, operation and control of Solar-Hydrogen Energy Systems', Ulleberg Oystein, Ph.D. dissertation for the Department of Thermal Energy and Hydropower, Norwegian Univ. of Science and Technology, December 1999

[91] Kirk-Othmer Encyclopedia of Chemical Technology 2002, updated July 2007-08-12

[92] Hydrogen production from renewables, N Lymberopoulus, Centre for Renewable Energy Sources - Greece, September 2005

[93] 6500 psi Electrolysers for transport applications, Avalence LLC, NHA Annual Hydrogen Conference, Long Beach March 2006

[94] Pure Hydrogen Production by PEM electrolysis for Hydrogen Energy, S.A Grigoriev, V.I Porembsky, V.N Fateev, International Journal Of H2 Energy 2006 31 (2) 171-175

[95] The Potential of Electrolysers in Renewable Based SAPS, F Barbir, EHEC H-SAPS Workshop, Grenoble September 2003

[96] http://www.ginerinc.com/ogp.htm

[97] Performance of a PEM water electrolysis cell using $Ir_xRu_yTa_zO_2$ electrocatalysts for the oxygen evolution electrode, A Marshall, S Sunde, M Tsypkin, R Tunold, International Journal of Hydrogen Energy (2007), http://dx.doi.org/10.1016/j.ijhydene.2007.02.013

[98] Pure Hydrogen Porduction by PEM electrolysis for Hydrogen Energy, S.A Grigoriev, V.I Porembsky, V.N Fateev, International Journal Of H2 Energy (2006) 31 (2) 171-175

[99] Composite electrolyte for fuel cells, K Milton, M Robert, United States Patent 6630265, July 2003

[100]www.itm-power.com

[101]Regenerative Fuel Cell Test Rig Completed and Operational at Glenn Research Center, http://www.grc.nasa.gov/WWW/RT/2003/5000/5490bents.html

[102]http://www.distributed-energy.com/hydrogen_generation/onsite.html

[103]courtesy of H3 Energy Ltd

[104]www.hydro.com/electrolysers/

[105]Comparison of electrical energy efficiency of atmospheric and high pressure electrolysers, A Roy, S Watson, D Infield, International Journal of Hydrogen Energy (2006) 31-14 pp 1964-1979

[106]Renewable Electrolysis Integrated Systems Development and Testing, International Workshop on Pollution Prevention and Sustainable Development, K Harrison, November 2006

[107]Hydrogen Production Through Electrolysis, R J Friedland, a J Speranza, Proceedings of the 2002 US DOE Hydrogen Porgram Review, June 2002

[108]Renewable Electrolysis Integrated System Development and Testing, B. Kroposki, DOE Hydrogen, Fuel Cells & Infrastructure technologies Programme Review, May 2005

[109]Grimstad Renewable Energy Park, T Valand, W Bartholdsen, M Ottestad, M Vage, Agder University College Norway 2002

[110]Electric Round-trip Efficiency of hydrogen and Oxygen-based Energy Storage, E Bernier, J Hamelin, K Agbossou, International Journal of hydrogen Energy 30 (2005) 105-111

[111]Load control of a Wind Hydrogen Stand-Alone Power System, H. Miland, R. Glockner, P.Tayleor, International Journal of Hydrogen Energy (2006) 31-9 pp 1215-1235

[112]Market Potential Analysis for Introduction of Hydrogen Energy Technology in SAPS, Altener Programme, contract No. 4.1030/Z/01-101/200, IFE 2005

[113]The Management of Electricity via Storage of Hydrogen, R M Crocket, PhD dissertation, Cranfield University, September 1994

[114]Hydrogen and Renewables Integration (HARI), R Gammon, A Roy, J Barton, M Little, Centre for Renewable Energy Systems Technology, Loughborough University, March 2006

[115]ZEV and Near-ZEV Heavy Duty Hydrogen Hybrid Electrics, D Mazaika, P Scott, ISE Research, June 2003

[116]A techno-economic analysis of decentralised electrolytic hydrogen production for fuel cell vehicles, S Price-Richard, MSc Thesis, Department of Mechanical Engineering University of Victoria, 2004

[117]Renewable Hydrogen for Transportation, L S Krom, Final Report for the Wisconsin Energy Bureau, January 1998

[118]www.h2cars.de/

[119] Technical Guide to the Connection of Generation to the Distribution Network, K Jarrett, J Hedgecock, R Gregory, DTI Ner and Renewable Energy Programme, February 2004

[120]The Carbon Trust & DTI Renewables Network Impact Study, Annex 3: Distribution Network Topography Analysis, Mott MacDonald, November 2003

[121]An Operator's Guide to the EU Emissions Trading Scheme, Defra May 2006

[122]Restructuring of the Electricity Supply Industry in England and Wales, LCG Consulting, 2004

[123]CHP and District Heating in Denmark: History, Goals and Technology, H. Manczyk, M. Leach, 2003

[124]Background Study-Balancing System of Germany, Green Net Project WP4, D.J.Swider, September 2004

[125]Elsam Annual Report 2005, Elsam's Communications Department, April 2006

[126]Regular Meeting of the Power Authority of the State of New York, NYPA September 2006

[127]Acillary Service Provision from Distributed Generation, Ilex Energy Consulting, DTI October 2004

[128]Controlling micro-CHP systems to modulate electrical load profiles, Energy (2006) 32-7 pp 1093-1103

[129]www.carbonpositive.net/viewarticle.aspx?articleID=98

[130]TIG Chemical Market Reporter, Schnell Publishing Company, February 2003

[131] The Feasibility, Costs and Markets for Hydrogen Production, AEA Technology, September 2002

[132] H_2 in transport, Past, Present and Future, R. Wurster, L-B-Systemtechnik GmbH, May 2003

[133] Hydrogen fuelled gas turbine powered high-speed container ship: A technical and economic investigation, Veldhuis, I.J.S., Richardson, R.N. and Stone, H.B.J. International Conference on Fast Sea Transportation, St-Ptersburg, June, 2005

[134] Design of Hydrogen-Fuelled Aero Gas Turbines for Low Environmental Impact, F Haglind, R Singh, Proceedings of 17th International Symposium on Air Breathing Engines, Munich 2005

[135] Modelling the Feasibility of Using Fuel Cells and Hydrogen Internal Combustion Engines in Remote Renewable Energy Systems, J Cotrell, W Pratt, Windpower 2003, Austin, Texas May 2003

[136] Hydrogen Power Park Business Opportunities Cocept Project, R Hobbs, Arizona Public Service, April 2004

[137] Configuration and Technology Implications of Potential Nuclear Hydrogen System Applications, Argonne National Laboratory, July 2005

[138]Configuration and Technology Implications of Potential Nuclear Hydrogen System Applications, Nuclear Engineering Division Argonne National Laboratory for the US DOE, July 2005

[139] Business Plan ISO/TC 197, Hydrogen Technologies Executive Summary, September 2004

[140] Hydrogen supply for SPFC Vehicles, ETSU F/02/00176/REP, Imperial Colledge, 2000

[141] Industrial Inorganic Chemicals: Production and Uses, R. Thompson, The Royal Society of Chemistry 1995

[142] European Industrial Gases Sector remains stable despite Economic Climate', 2002, Eve Greb, Nicholas Baudouin, article for Standard & Poor's

[143] Fuel Cell Today Market Survey: Small Stationary Applications 2006, K. Adamson, December 2006

[144] Fuel Cells Canada, Bugyra, W.J., HFC 2004 conference, Toronto, Sept 2004

[145] Stationary FC Market Opportunities, Strategies and Forecasts, 2006 to 2012, WinterGreen Research, Sept 2006

[146] www.hydrogenenginecenter.com

[147] Survey of the Economics of hydrogen Technologies, C.E.G. Padro, V Putsche, NREL September 1999

[148] http://www.enaa.or.jp/WE-NET/index.html

[149] Fuel Cell Today Market Survey: Large Stationary Applications, K. Adamson, October 2006

[150] Matsushita Battery Develops micro FC Technology for Portable Electronic Devices, www.panasonic.com, January 4 2006

[151] Fuel Cell Today Market Survey: Portable Applications, G. Crawley, December 2006

[152] Defra e-Digest Statistics about the Global Atmosphere, www.defra.gov.uk/environment/statistics

[153] www.ace.mmu.ac.uk/Resources

[154] Annual European Community GHG Inventory 1990-2004 and Inventory Report 2006, EEA June 2006

[155] Fuel Cell Today 2006 Worldwide Survey, K. Adamson, G. Crawley, January 2007-09-24

[156] www.fuelcellpartnership.org

[157] Fuel Cell Today Market Survey: Automotive Hydrogen Infrastructure, G. Crawley, July 2006

[158] Hydrogen in the Energy Sector, W. Zittel, R.Wurster, Ludwig-Bölkow-Systemtechnik GmbH, June 1996

[159] Quantum h2 storage Systems, Andris R. Abele, ARB ZEV Technology Symposium Sacramento, September 2006

[160] H2 Storage, Gaps and Priorities, T. Riis, G. Sandrock, HIA HCG Storage Paper, IEA January 2006

[161] Energy Efficiency and Load Curve Impacts of Commercial Developments in Competitive Markets, EU/SAVE 132/01 EFF LOCOM Phase 1, November 2003

[162] www.caiso.com

[163] http://www.tepco.co.jp/en/index-e.html

[164] Power Stations Water Demand, A. Jones, London Climate Change Agency, August 2007

APPENDIX A: HYDROGEN APPLICATIONS

A.1 INTRODUCTION

This appendix aims to provide an overview of existing and prospective end-use applications of electrolytic hydrogen. It is not intended here to carry out a comprehensive literature review since numerous publications are available in the literature regarding existing and potential hydrogen applications (see for example [85] [131]. Instead, a summary of potential end-uses for electrolytic H_2 is offered. They are divided into three segments: stationary (small and large) power generation, portable power and transport applications. In addition, a description of current and prospective possibilities for hydrogen storage is included.

Today, hydrogen is still used primarily as a chemical in the petrochemical, electronics and food industries, but hydrogen has also the potential to be a clean fuel for every end-use energy need, including transportation, power generation, industrial heaters and portable power systems. Hydrogen has already been used as a fuel. Town gas, which was widely distributed during the first half of the 20th century before being replaced with natural gas, was 50% hydrogen. Hydrogen has also powered space exploration for several decades, and vehicles fuelled by hydrogen were already demonstrated in the US in the early 1970s [132].

When considering the environmental advantages of hydrogen, it is important to consider the complete fuel cycle, from extraction of the primary energy source to manufacture the hydrogen, its distribution and end-use. Only when hydrogen is produced and transported to the end-user via zero-carbon energy resources (like nuclear or RE-electrolysis) a strictly zero-carbon fuel can be obtained. Hydrogen, if produced in a sustainable manner, can be the basis of a low carbon economy, with the potential to deliver a drastic reduction in emissions of greenhouse gases and other atmospheric pollutants, the associated benefit of security of energy supply and the possibility of an infrastructure based on distributed generation.

Hydrogen usage offers a number of prospective benefits:

• A significant potential to contribute to diversity and security of fuel supply by reducing the global reliance on fossil fuels, given that all countries possess some form of sustainable primary energy source from which H_2 can be manufactured.

• Cleaner energy for a wide variety of end-use applications (stationary and mobile).

• Zero local greenhouse emissions at point of use.

• Absolute zero CO_2 life-cycle emissions when derived from nuclear or renewable energy sources and transported to the end-user via zero-carbon energy resources.

• A means of stimulating the development of renewable energy sources by providing an effective method of storing and distributing intermittent energy resources.

• A means of matching the time of energy demand with the availability of intermittent renewable energy sources such as solar power, wave, tidal and wind.

• An opportunity to broaden the role of renewable and nuclear power sources to supply clean fuels for transportation, heating and industrial purposes.

• An effective sustainable energy system where a conventional energy infrastructure either does not already exist (e.g. Third World countries) or could not otherwise exist (e.g. remote and island locations).

• An opportunity to upgrade lower-quality solid and liquid fossil fuels such as coal and heavy oils, thereby reducing emissions and extending their range of applicability.

But hydrogen also presents important disadvantages and barriers to its widespread use not solved yet:

- Lack of an appropriate supporting infrastructure for supplying a future high hydrogen demand. On the contrary, global fuel distribution infrastructures, based on oil and natural gas are well established, of low cost and of limited use for transporting gaseous hydrogen.

- On a volumetric basis, the energy density of H_2 is much poorer than that of traditional fuels like natural gas or gasoline. As a consequence, higher storage volumes are needed per unit energy. In fact, the lack of suitable low cost hydrogen storage options is the main technical barrier to its use as a transportation fuel.

- The lack of availability of commercially available low cost reliable end-use hydrogen technologies like FCs, HICEs and hydrogen turbines for transport, power and heat generation applications.

- The costs of manufacture, distribution, storage and use make hydrogen is currently much more expensive than traditional fossil fuels.

- Hydrogen raises concerns about safety because of its flammability, low density and non-visible flame. A safe and reliable hydrogen infrastructure still needs to be established and demonstrated.

Most of these issues arise from the infancy of the hydrogen industry for energy supply. While hydrogen has been used for many years as an industrial feedstock in the production of a range of products, from glass to plastics and semiconductors to pharmaceuticals, it is only recently that hydrogen has become a potentially viable alternative to oil as a transport fuel, and coal and gas as a fuel for heat and power generation.

H_2 can be used in fuel cells (FCs) to power a variety of applications, mobile and stationary, small and large scale. Fuel Cells have the potential to provide clean energy for transportation and stationary or portable power generation. They can provide heat and electricity for single dwellings or entire commercial building

facilities, to provide a small amount of electricity to a community grid, or a large amount of electricity to a large grid network. Yet extended durability and unit cost reductions need to be addressed before widespread commercialization can be achieved.

Hydrogen can also be used to generate electricity through the use of gas turbines and microturbines (small gas turbines). Conventional gas turbines can be modified to run efficiently on H_2 or H_2/NG blends and microturbines can provide high-efficiency reliable power for smaller-scale applications [133], [134].

Internal Combustion Engines (ICEs) can represent a transition technology for hydrogen in both stationary and mobile applications. As with gas turbines, conventional combustion engines can be modified to run efficiently on H_2, H_2/NG, H_2/diesel and H_2/gasoline mixtures. However ICEs have lower fuel-electricity efficiencies than fuel cells, which could limit their potential in stationary applications, were long term storage of energy as hydrogen is needed [135], [136]. On the other hand ICEs running on H_2 or bi-fuel mixtures might prove to be a more appropriate short-term option which is less disruptive for current vehicle manufacturers and consumers.

A.2 H_2 APPLICATIONS

A.2.1 Existing hydrogen uses and applications

Global H_2 consumption in 2003 was estimated to be 556×10^9 Nm^3 (50 million tonnes), (including intentionally produced H_2 as well as hydrogen that is produced as a by-product in the petrochemical industry and consumed on-site) with a growth rate of around 10% per year. **Figure A1** shows global H_2 consumption of intentionally produced hydrogen (41.1 million tonnes) by sector in 2003. As of 2005, the economic value of all hydrogen produced globally is estimated at $135 billion per year [137]. At present H_2 is consumed in a number of industrial applications, with today's largest consumers worldwide being ammonia production facilities, oil refineries, and methanol production plants. The rest of the hydrogen demand is for small-volume consumers like electronics, metallurgical industry,

glass making and food hydrogenation industries.

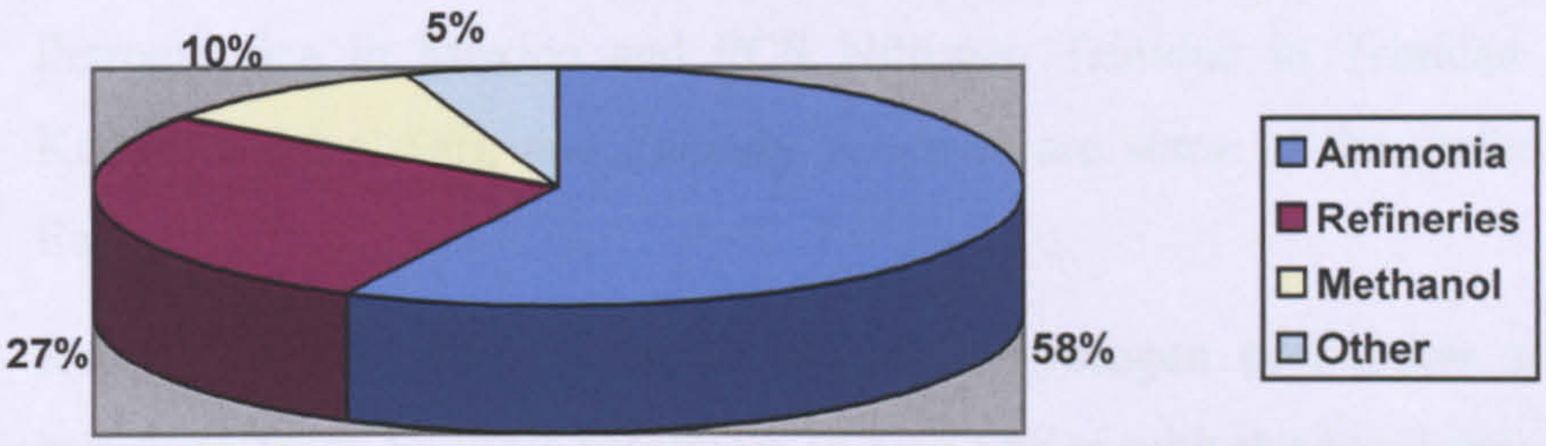

Figure A1. 2003 Global Consumption of Intentionally Produced Hydrogen [138]

About 95% of the world H_2 consumption is produced by the consumer at the site where it will be used (captive production) [138]. The remainder is produced and sold as merchant hydrogen. This includes gaseous product delivered by pipelines and liquid and gaseous H_2 delivered in cylinders and tank containers (liquid H_2 accounts for 20% of total merchant H_2 [139].

The hydrogen demand around the world varies by region. The US is by far the major user (19%), followed by Europe (13%) and Japan (4%), although the Middle East and South America have the potential for producing large quantities of H_2 from hydroelectricity and refineries. In Europe, the largest consumer is Germany (37%), followed by the UK (19%), France (11%), Italy (9%) and Spain (4%) [139].

Hydrogen feedstock for the ammonia market is essentially always generated on-site from NG reforming by the ammonia manufacturer and used to produce NH_3 via the Haber process, which is then used directly or indirectly as fertilizer, as compared to say petroleum refineries where third party suppliers of hydrogen are becoming more prevalent. Global ammonia production in 2003, at around 132 million tonnes, consumed an estimated 11.7 million tonnes of hydrogen [138]. Although global production of H_2 for NH_3 generation is projected to remain stable, the ammonia industry is quite sensitive to NG prices (the gas accounts for 70-79% of NH_3 production costs), particularly in the US and Europe. Consequently the US and Europe show a drop in ammonia-related hydrogen consumption (10% drop in the US and 18% in Europe between 1996 and 2003 [140], [138]) and a shift to

imported ammonia due to the increase in domestic NG prices. Some larger producers of ammonia and consequently of hydrogen include Farmland Industries, PCS Nitrogen Fertilizer, Terra and CF Industries in the U.S: Agrium in Canada, Petroquimica in Mexico and PCS Nitrogen Trinidad in Trinidad and Tobago. Kemira, Hydro Agri, and Zaklady Azotowe are some of the major producers in Europe.

Refineries' two major sources of on-site hydrogen production are by-product hydrogen from catalytic reformers (which varies with the requirement to produce high octane gasoline) and on-purpose production from hydrocarbons (the majority is based on steam methane or naphtha reforming). Oil refineries worldwide consumed about 9.5 million tonnes of H_2 in 2003. This is used to convert heavy crude to lighter fractions via hydrocracking more suitable for use as fuels and to remove organic sulphur compounds from crude oil via hydrodesulphurisation. While the trend is towards processing lower cost heavier crude oils and environmental regulations become tighter (e.g. low sulphur requirements), the demand for hydrogen from refineries grows steadily. Expected annual growth rates range from 4% to 5.5% for captive production and up to 10-15% for merchant hydrogen [138]. The top six on-purpose hydrogen producers among the world's petroleum refiners include Shell, Exxon, Mobil, Chevron, Texaco and Indemitsu, with a total hydrogen capacity ranging from 757 to 1260 tonnes per day) [91].

The manufacture of methanol represents the third largest use of hydrogen, after ammonia manufacture and hydrogen consumption in petroleum refineries. Similar to ammonia, the hydrogen for this market is typically generated on-site by the manufacturer from Steam Methane Reforming and not purchased from a third party. The hydrogen is produced as part of a carbon monoxide and hydrogen mixture called syngas and used mainly to produce formaldehyde, which finds extensive use in the construction industry; MTBE, used as an oxygenate in reformulated gasoline; acetic acid, formaldehyde and methyl methacrylate which are used to produce plastics and other synthetic materials. Global methanol production in 2001, at around 30 million tonnes, consumed an estimated 5.65 million tonnes of hydrogen coming mainly from NG reforming [138]. Although global methanol demand is expected to rise at 3 - 4% per year over the next years,

in the US and Europe the trends are to import methanol (almost two-thirds of domestic methanol consumption in t. e US) in reaction to rising NG prices. Methanex and SABIC are the two largest methanol producers in the world accounting for over 20% and 5% of global production, respectively [91]. In the US, large producers of methanol include Celanese, Beaumont Methanol Limited Partnership, Borden Chemicals and Plastics and Lyondell Methanol Company in the U.S. and Methanex Corporation. Methanor VoF in the Netherlands, Statoil in Norway and the Mitteldeutsche Erdoel refinery in Germany are some of the major methanol producers in Europe. Saudi Arabia, Indonesia and Malaysia are some of the countries in the rest of the world with significant methanol production.

Following this, the main hydrogen applications worldwide apart from the three mentioned above are as follows [141]:

- Food industry: to hydrogenate liquid oils (such as fish, cottonseed and corn), converting them to semisolid materials such as shortenings, margarine and peanut butter.

- Chemical processing: primarily to manufacture ammonia and methanol. Also to hydrogenate non-edible oils for soaps, insulation's, plastics, etc.

- Metal Production: as a protective atmosphere in high temperature operations such as stainless steel manufacturing; commonly mixed with Ar for welding Austenitic Stainless. Also used to support plasma welding and cutting operations.

- Pharmaceutical industry: to produce Sorbitol used in cosmetics, adhesives, surfactants and vitamins A and C.

- Electronics: to create special atmospheres in the production of semiconductor circuits.

- Aerospace: fuel spacecraft. Also to power life support systems and computers,

yielding drinkable water as a by-product.

- Power generation: hydrogen is used as a heat transfer medium for alternator cooling to improve the efficiency in thermal power plant.

- Laboratory applications: hydrogen is used both as a carrier and fuel gas in gas chromatography.

- Float glass production: to produce an inert, non-oxidising atmosphere over molten tin upon which glass lies.

- Meteorological applications: to fill weather balloons that carry radiosondes used to collect meteorological data.

High purity hydrogen is required for food, electronics, metallurgy and pharmaceuticals applications (> 99.95% (v)), and specially top high purity is required for electronics and laboratory applications (> 99.999% (v)).

Figure A2 shows the merchant H_2 consumption in the UK by sector (1996). Merchant H_2 is usually the primary source of hydrogen to industries mentioned above such as electronics, chemicals and very specific applications e.g., rocket fuels. The total merchant hydrogen supply in the UK in 1996 was about 210 million Nm^3, of which 44% was produced on the consumer's site, 33% was supplied by pipeline and 23% by road trailer [131]. The gas accounts for 3-4% of the total U.K industrial gases market and about 5% of the worldwide industrial gases market, and a 10% growth is forecast in the value of the H2 worldwide market between 2002-2006 [142].

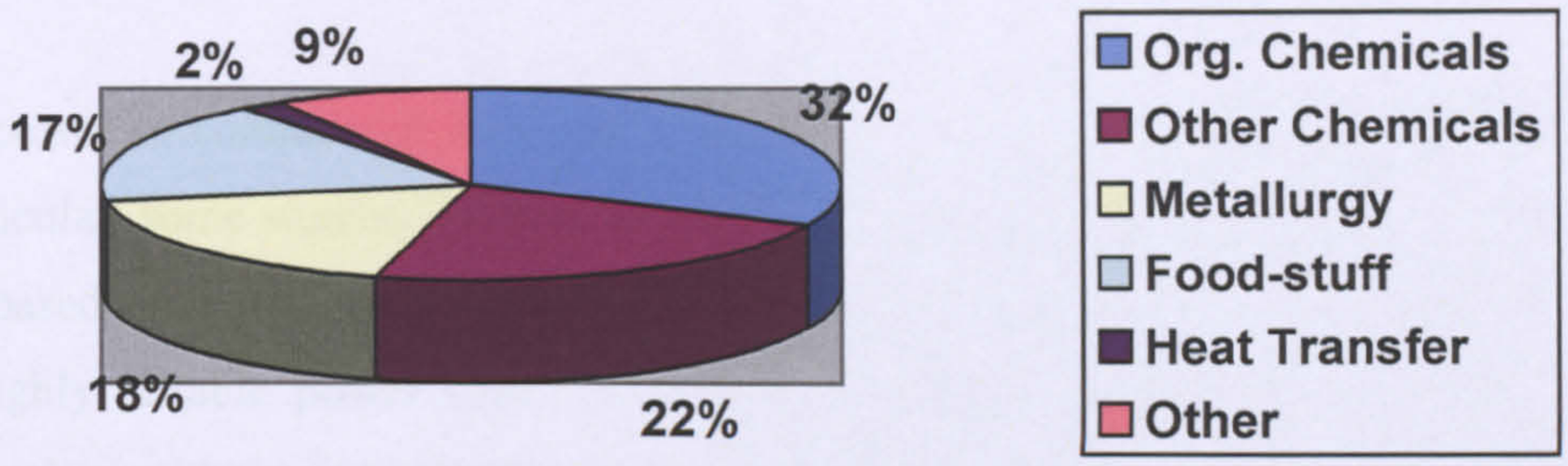

Figure A2. 1996 Merchant H2 consumption in the UK by sector [131].

Most of the marketed hydrogen is used nowadays where small volumes of high purity are required, particularly in cases where self-generation would be uneconomic. These applications tend to make use of hydrogen's strong reducing capability or its ability to saturate unsaturated hydrocarbons. Recently, environmental pressures on the petroleum refiners to meet more and more strict specifications for fuels, and rising oil prices that encourage oil companies to extract poorer source material (like tar sands and oil shale), have led to an increase in the demand of hydrogen for hydrodesulphurization and hydrocracking processes. Consequently, current demand for merchant H_2 is strongly influenced by the end use demand from sectors such as petroleum refining and ammonia production [142]. Finally, to put the industrial gas market for H_2 in perspective, present US use of H_2 for hydrocraking is roughly 4 million tonnes per year.

A.2.2Stationary power generation

Small Stationary:

Though dwarfed by the automotive market this area is seen with a high potential for widespread use of hydrogen in the near future. Development and deployment of small stationary applications for hydrogen, defined here as those with an electrical output of less than 10 kW, is at a high level.

Typically perceived as one of the entry markets for FCs, these are designed for a number of markets, ranging from uninterruptible power supplies (UPS) and back-

up power in commercial and remote locations to domestic CHP applications. In particular, some studies [143] suggest that back-up power could pave the way for H_2-based small stationary applications. Backup power and UPS are required when a highly reliable power source is critical to keep a business or equipment in operation without interruption even if grid power is lost. The use of direct hydrogen to power FCs and hydrogen-powered ICEs in these applications could allow energy autonomy (if locally produced), rapid response and silent use (in the case of FC). Compactness and longer life of FC systems, if achieved, could replace battery systems and diesel gensets to provide clean primary or backup power for long periods as long as the source of zero-carbon H_2 fuel is available.

Hydrogen also offers many possibilities for domestic heat and power uses: H_2 can be combusted to produce heat for cooking or space heating with no greenhouse emissions. However it is worth remembering that from a life cycle point of view the hydrogen can be considered a zero-carbon fuel only if it has been generated via a free-carbon process. For example if generated at home via electrolysis from distributed RE sources (e.g. micro-wind or domestic-PV), hydrogen gives home power producers the potential for eliminating fossil fuels completely for all domestic energy uses. Fuel Cells can also be used for the residential market; in fact this sector is recognized as one of the largest potential market for FCs. Japan is clearly leading the way in this sector, with nearly 80% of all domestic FC installation in 2006, fuelled by strong government incentives [143].

Hydrogen can also be added directly into an existing natural gas supply. Mixtures of below 20% of H_2 by volume are commonly known as hythane, with very similar properties to NG, thus requiring minimal modifications to the associated fuel-handling infrastructure and end-use combustion equipment. A number of places around the world already have a H_2 within their NG supplies of up to 8% by volume [144]. The concept of injecting zero/low-carbon H_2 into the existing NG infrastructure represents another opportunity to reduce carbon emissions with minimal impacts upon end-users. A number of transport applications for hythane are also in operation e.g. in Montreal and California [67].

It is estimated that nearly 5,000 small stationary fuel cell systems are operating worldwide, with more than 1,500 systems installed in 2006. Key companies involved are Avista (US), Ballard (Canada), Ceramic Fuel Cells (Australia), Hydrogenics (Canada), Idatech (US) Nippon Oil (Japan), Plug Power (US), ReliOn (US), Sanyo Electric (Japan), Sulzer Hexis (Switzerland), Toshiba International Fuel Cells (TIFC, Japan), and Vaillant (Germany). Most of them have focused on PEM fuel cell systems, but SOFC systems are also a possibility [143]. Other fuel cell types are less suited to these applications because of their limited ability for load following and their higher operating temperatures which imply longer start-up periods. As far as domestic applications are concerned, most of the aforementioned companies presently recognize that they can not support the fuel cell systems they can produce today, not only as prices will be too high, but also because the lifetime of systems is still too short. As a result, with the exception of Japan, growing number of developers are repositioning themselves from residential towards backup, uninterruptible and remote power [143].

Other potential applications for hydrogen in this sector have also been identified: horticultural industry, to provide greenhouses with light and heat; recreation industry, to provide sports and fitness clubs with heat and power; health and care industry, e.g. for hospitals and nursing homes to provide electricity, heat and oxygen; fuel cell-powered forklifts.

To date costs of small stationary fuel cells are the main barrier to wide scale commercialization. In contrast with a cost target of $400 / kW (US DOE, 2010 cost target including Balance of Plant), current modules available are at least ten times higher, in the range of $4,000 - $8,000 / kW [143]. Costs below $1,500 / kW are thought competitive in this sector [145], but reliability and durability are yet to be proven.

Large stationary:

This category refers to heat and power generation from hydrogen with an electrical output ranging from 10 kW to the megawatt level and above.

Large power generation typically includes those applications that incorporate multiple buildings (e.g. universities and colleges, hospitals, industrial, government or military premises). In these facilities, the ability to generate electricity and heat onsite using fuel cells or hydrogen gensets has multiple benefits including air heating, laundry facilities, cafeteria facilities, preheating water for onsite boilers. The main advantage of using both electric power and heat is the very high overall efficiency achieved in these systems. A few existing H_2 power generators based on ICEs or FCs are presently able to power emergency lights, elevators, safety and fire management systems as well as other systems. One example is the Stuart Energy H2 Energy Station at a building in Hong Kong, capable of providing full power at over 6 hours at up to 240 kW. The North American company Hydrogen Engine Center (HEC) currently commercializes hydrogen gensets for stationary applications in the range of 17 kW to 250 kW [146].

The feasibility of H_2 usage in turbines has been verified by several turbine manufacturers, notably GEC Ahlstom. Although still at the research level, it has been reported [147] that turbines using hydrogen will likely be more efficient than those using NG because of the potential for higher inlet gas temperatures. The government of Japan, under its World Energy Network (WE-NET) program is currently working with several turbine manufacturers (Westinghouse, Mitsubishi Heavy Industries, and Toshiba) to develop hydrogen-based power systems that include combustion turbines. The overall goal of this 28-year program is the demonstration of a hydrogen-power system with 70.9% efficiency or greater by 2020 [148].

So far large stationary power is probably the most mature application possibility for fuel cells, having received considerable attention and investment for over 30 years. As of October 2006, it is estimated that more than 800 large stationary fuel cell systems have been built and operate worldwide, with a cumulative installed capacity above 100 MW [149].

The largest stationary fuel cell yet built was a 11 MW Phosphoric Acid Fuel Cell (PAFC) manufactured by Toshiba and UTC Fuel Cells (at that time known as International Fuel Cells), operating in Japan from 1991. Although PAFC

technology has traditionally been dominating in this sector, this dominance is now changing. Coinciding with this, PAFC is beginning to be superseded by three other fuel cell types: Molten Carbonate Fuel Cell (MCFC), Proton Exchange Membrane Fuel Cell (PEMFC) and Solid Oxide Fuel Cell (SOFC). MCFC and SOFC are both high temperature fuel cells and can operate at very high efficiencies, especially if the output heat is used and/or the fuel cell is integrated with a gas turbine, an option that has received attention for several years. PEMFC is also gaining a high share of large stationary power markets where lower power is required, around 250 kW and below [149]. In this range, the commercialisation of PEMFC, still far from realised, could benefit from investment in the technology for transportation and small stationary application. Large stationary fuel cell development is concentrated in the hands of a small number of manufacturers, namely Ansaldo Fuel Cells (Italy), Fuji Electric (Japan), Fuel Cell Energy (US), Mitsubishi (Japan), MTU (Germany), Siemens Power Generation (US, part of the Siemens group) and UTC Power (US).

A.2.3Portable applications

Demands for portable power have escalated with the introduction of advanced electronic devices, and traditional power sources have failed to keep up with new requirements. Portable power is considered one of the largest target areas of commercial adoption for fuel cells, due to its unique potential to effectively close the gap between portable power demands and performance.

State-of-the-art lithium batteries are already reaching their limit of energy density. This is becoming a limiting factor for producers of electronics while consumers are demanding greater processor capacity and battery life. Hydrogen-powered fuel cells represent a reasonable alternative power source for portable applications. They are lighter than batteries when comparing the amount of stored energy per kg, with longer lifetimes and higher efficiencies. Fuel cells can be used to power a variety of electronic appliances, from handheld electronics, such as mobile phones, personal digital assistants (PDAs) and MP3 players to larger equipment such as portable electric generators, laptop computers and handheld video cameras. Virtually any application that has traditionally used batteries can be powered by

FCs, with the potential to last more than four times as long as batteries before need for refuelling [150]. The market potential is quite vast and lends itself to mass production, but again long term durability and significant cost reductions of FC have yet to be achieved.

The two primary technologies for portable applications are polymer electrolyte membrane (PEM) and direct methanol fuel cell (DMFC) designs. It is estimated that about 10,000 portable fuel cell systems have been developed and operated worldwide, ranging from 1 watt to 1.5 kilowatts in power [151]. There has been a dramatic surge in the number of systems built in the last three years. Such growth is partially due to the number of companies who are beginning to turn their attention to this market. Companies involved in the development and commercialisation of portable fuel cells are Angstrom Power (US), Casio (Japan), DMFCC (US), Giner Electrochemical Systems (US), Hitachi (Japan), Jadoo Power (US), Neah Power Systems (US), NEC (Japan), Nokia (Finland), Samsung (Korea), SFC Smart Fuel Cell (Germany), Sony and Toshiba (Japan), Voller Energy (UK). In markets where power requirements are low, perhaps less than 100W, DMFC is expected to take a large share, and where more power is required PEMFC is likely to dominate [151].

Portable power could potentially be one of the early entry markets for fuel cell technology, and in the coming months and years it is expected to see more players entering this area, unveiling prototypes and commercial products.

A.2.4Transportation

The environmental and social benefits of using H_2-powered systems are especially profound in transportation, where present vehicles produce significant carbon dioxide emissions and are totally dependent on largely foreign produced oil. In terms of size, environmental impact and financial value, the transportation sector represents the biggest potential end-use for hydrogen. The almost full dependence of transport on fossil fuels all over the world, and its high share of responsibility in

many environmental problems urge the adoption of a clean, sustainable fuel. The following emissions UK & EU statistics illustrate this:

- Carbon dioxide emissions from road transport in the UK in 2004 were 33 million tonnes. Road transport makes up around 21% of total CO_2 emissions in the UK [152].

- Between 1990 and 2004, CO_2 emissions from the transport sector rose by 10% in the UK due to en increase in road transport, mainly freight [152].

- 32.9 million motor vehicles licensed in the UK [154] contribute to 69% of total carbon monoxide, 44% of nitrogen oxides, 27% of VOC and 23% of carbon dioxide released into the atmosphere [153].

- CO_2 emissions from road transportation in Europe rose by 26% between 1990 and 2004, accounting for 19% of total GHG emissions in 2004, and are set to rise by 30% by 2010. Road traffic and aviation are the fastest growing sources of carbon dioxide in Europe [154].

Alternatively, the usage of hydrogen as a transport fuel offers a number of potential **benefits**:

- Zero life-cycle emissions when derived from nuclear or renewable energy sources.

- Improved public health and safety from reduced exposure to fuel and emission dangers. Reduced vehicle urban noise levels and associated stress.

- Increased in national energy security, given that imported oil mainly derives from countries with low political stability.

- Support and acceleration of the long-term trend toward a clean hydrogen (and electricity clean) based economy.

For all these reasons, it is likely that the transportation sector will eventually become the largest market for hydrogen. This is evidenced by the development of increasing transport-related hydrogen R&D activities worldwide, including investments by major automobile manufacturers in FC vehicles and hydrogen ICE vehicles, although some of them are reluctant to appoint specific dates for widespread commercialization until major technological challenges like long-term FC durability and on-board H_2 storage are solved. Daimler-Chrysler (Germany), Ford (US), GM (US) and Toyota (Japan) cite 2015 as the breakthrough year for H_2-powered vehicles with full scale commercialization by 2020 but these dates are to be treated with caution. Overall and given the long term scarcity and instability of oil resources, there seems to be broad consensus amongst motor manufacturers and transport analysts that H2 vehicles could replace a large proportion of oil-based transport by 2050.

The development of a hydrogen infrastructure remains a critical part of the commercialization of H_2-powered vehicles. At the beginning of 2007, over 140 H_2 refuelling stations were operating worldwide as a result of diverse funding incentives and an increasing trend for companies to work together in joint development programmes and knowledge sharing schemes [155]. Several major companies are working together on solutions to storage, production and distribution and production issues to encourage the wide implementation of a H2-based transport system.

The US has the highest share of H_2 fuelling stations (nearly 60% of total depots worldwide). Particularly California has featured heavily during the past few years for the initial deployment of a hydrogen-based transport, and by the end of 2006 there were 39 H_2 stations and 156 FC vehicles in California [156]. The California H_2 Highway Scheme aims to build a network of 100 H_2 fuelling stations in Sacramento, Los Angeles, San Diego and San Francisco within 5 years. By 2010, the objective is to introduce 2,000 H_2 cars in these cities [157].

The Clean Urban Transport for Europe (CUTE) programme was a large scale field trial of FC buses and hydrogen infrastructure. CUTE began in November 2001 and

operated 27 FC buses in 9 European cities, and a further 6 buses in Iceland and Australia within associated programmes. One of the main goals of the CUTE project was to increase public knowledge and acceptance of hydrogen technologies and build the foundations for regulation and certification of H_2 technologies. The project has been successful in demonstrating FC technology as a solution to mass public transport requirements [157]. In the UK in particular, as part of the London H2 Transport Programme, the city has announced plans to introduce 70 hydrogen vehicles by 2010. By February 2006, the procurement of 10 H_2-fuelled buses had already begun. In Germany, Berlin's mass transport company BVG plans to order 250 H_2-powered buses so as to become the first city with a significant proportion of zero-emission vehicles.

Japan's FC Bus Demonstration Programme has been introduced from 2002 and will continue until 2010. The main objectives are to investigate the energy savings and environmental impact of FC and H2ICE vehicles and raise public awareness regarding hydrogen technologies. In South America, Brazil has announced a development and testing programme for 5 public FC buses during 2007 in Sao Paulo and neighbouring cities. The four year programme, if successful, will lead to extend the bus fleet to 100 vehicles. The project is supported by the United Nations Development Program [155].

In addition, niche transport applications seem to be a promising entry markets for fuel cells. Hydrogen-powered forklifts have seen a significant boost in activity within the last two years [155]. Forklifts appear to be particularly close to market commercialization, and the market for FCs as Auxiliary Power Units (APU) in caravans and camper vans has experienced rapid growth in 2006.

Hydrogen vehicles and associated infrastructure must still overcome important cost and technological hurdles if they are to become a viable alternative to the conventional gasoline or diesel vehicles, and therefore additional efforts at both the public and private levels are necessary to ensure that the benefits of hydrogen fuel are reached. However the recent trend for auto-manufacturers and infrastructure developers to work hand in hand on development projects may finally break through the barrier of what should come first, widespread commercialization of

H_2-powered vehicles or the development of an infrastructure to provide hydrogen to power them.

A.3 HYDROGEN STORAGE

Hydrogen can be presently stored as compressed gas, as cryogenic liquid, in solids (metal hydrides, carbon materials) and in liquid hydrogen carriers like methanol or ammonia. The preferred option for each application depends on a number of factors like the quantity of hydrogen to be stored, volume and weight restrictions amongst others.

Focusing on stationary storage systems suitable for electrolytically produced H_2, compressed gas storage is currently the simplest, lest costly and therefore preferred option. The size of pressure vessels will depend on the storage requirements and pressure. In the industrial sector there is a standardization of type of tanks available. As a result, cylindrical tanks with operating pressures of up to 440 bar and H2 capacities up to 4,500 Nm^3 are commercially available [112]. Small scale storage is carried out in the form of compressed gas cylinders for total volumes below 2,000 – 3,000 Nm^3. Stainless steel cylinders are available in capacities ranging from 0.35 - 8.9 Nm^3 and weights of 5.3 - 68 kg with operating pressures of up to 250 bar [158]. As a rule both large tanks and cylinders are available from manufacturers of technical gases (e.g. Air Products, BOC, Praxair, etc).

Because of the weight advantage, the last few years have seen the replacement of steel tanks with composite tanks (full-composite, alu-composite) particularly in transport applications. These tanks have sizes ranging from 0.05 Nm^3 to 0.4 Nm^3. The lowest storage density, at 0.5 kWh / kg, is achieved with steel tanks and 20 MPa pressure [158]. The highest storage density is that obtained with lightweight full-composite bottles which have rated operating pressures of up to 700 bar [159]. In the last few years the development has concentrated on weight reduction via the use of modern composite materials and at the same time increasing capacity through higher pressure levels. It is also expected that this development will continue for some time. The present costs are dictated by the very low production

quantities which mean that considerable cost reductions would be possible if the demand rises accordingly.

When storage requirements are in excess of 2,000 Nm^3 H_2 or hydrogen must be delivered to a site far away, liquefied hydrogen can be a suitable option. In some cases the increased storage density of liquid hydrogen can outweigh the benefit of reduced material costs associated with compressed gas storage. The storage technology for liquid hydrogen is presently state of the art thanks to extensive application in space travel. This form of storage is usually carried out with storage tanks having vacuum insulation. Common stationary tanks have capacities ranging from 2,000 Nm^3 up to 60,000 Nm^3 [158]. Liquid hydrogen tanks are available from suppliers of industrial gasses (Linde, Air Products, Air Liquide, Messer-Griesheim). Because of the high cost of insulation, liquid hydrogen storage is expensive. In addition, liquefying H_2 is an extremely energy-demanding process, consuming up to 30% of the energy content of the H_2 (LHV basis) [112]. Furthermore, storage of liquefied hydrogen gives losses of hydrogen due to boil-off effects. Boil-off losses can account for about 0.1% / day of the hydrogen content in medium- to large-scale cryogenic tanks [112]. These are small values, but for systems designed to cover seasonal energy storage needs (e.g. RE storage in islands and remote locations), the accumulated boil-off losses reduce the overall energy efficiency and increase the hydrogen production and storage capacity demand even further.

Underground storage is a special case of compressed gas storage that can prove cost-effective for very large storage requirements (millions of Nm^3, i.e. over 10^5 kg H_2) provided that the geological conditions in the area are appropriate, like abandoned mines or gas wells. In principle, the storage techniques used for natural gas are also applicable for the compressed storage of hydrogen. For large seasonal storage applications, underground porous storages, aquifers, salt caverns or rock caverns can be used because it offers the most inexpensive solution. The UK and France both have long term experience in the field of underground hydrogen storage. The British chemical concern ICI stores hydrogen in three brine compensated salt caverns in Teeside, England. Hydrogen is stored at pressures up to 50 bar in these up to 366 m deep caverns [112]. From 1957 until 1974, GAZ DE

FRANCE stored towngas with 50% hydrogen content without problem in 330 millions m^3 aquifer storage [112]. This underground hydrogen storage method is about two orders of magnitude cheaper than tank storage and can be highly appropriate for long-term seasonal energy storage. It is, however, only relevant for volumes of several million Nm^3.

Metal hydride (MH) storage is another commercial hydrogen storage method, particularly because of its high specific energy. Low temperature hydrides are currently available on a semi-commercial basis although storage capacity is limited to some tens of Nm^3 of hydrogen. These are low-temperature MH such as AB5 (A – rare earth metal, B – Ni as a basis, Co, Al, Mn, etc. as an alloying additive), AB2 (A – Ti, Zr, B – Mn, Fe, Cr), AB (eg. TiFe), etc [112]. The specific mass of some metal hydrides at ambient-temperature is approximately 0.018–0.025 kg H_2/kg MH so that the high weight of metal hydride storage devices is the main disadvantage, particularly for mobile applications. Because of the chemical properties, the loading of a metal hydride storage device is accompanied by generation of heat. And then, in order to release the stored hydrogen, heat must be applied. Depending on individual applications, the desired pressure and temperature levels can be specified by the choice of an appropriate alloy. The further development of metal hydride storage is concentrated on increasing the storage capacity, with the intended goal being a doubling of capacity. Reduction of costs is also being targeted. Should these goals be achieved, then metal hydride storage could represent an attractive option in the near future.

Several other possibilities for hydrogen storage are presently under development, particularly in the US and Japan. For instance, hydrogen can also be adsorbed (as molecules in the gaseous state) in certain materials such as active carbon. Another, interesting adsorption technique involves the storage of hydrogen in carbon graphite nanostructures. Currently, there are no commercial applications of carbon-based hydrogen storage. However, researchers are continuing to look into increasing the gravimetric capacity of these systems and to improve the overall system engineering, and work is continuing strongly in the US. Also being investigated is the high pressure storage in so-called "micro spheres", small glass spheres with diameters less than 100 microns that can withstand pressures up to

1000 MPa. This would then allow high storage densities to be achieved in such a storage device. Other storage options being investigated in the US and Japan are: non-conventional metal hydrides; alkali metal doped nanotubes; and H_2 storage in fullerenes [160].

APPENDIX B: ANALYSIS APPLIED TO A DIFFERENT DEMAND PROFILE

B.1 INTRODUCTION

In the electricity sector, a demand load profile shows the amount of electricity that consumers use over a certain period of time. Consumer electrical demand patterns display considerable variability with time of day, day of the week and season of the year, and also depend on other factors like the weather and country specific characteristics. The TSO uses the information provided by the aggregate demand profiles to schedule the operation of power plant in the system at any time. **Figure B.1** shows daily load profiles for winter working days in six different European countries. The daily load curves are shown as per unit profiles (normalisation by the average load of the day) so that it is possible to see differences in the profile between the countries.

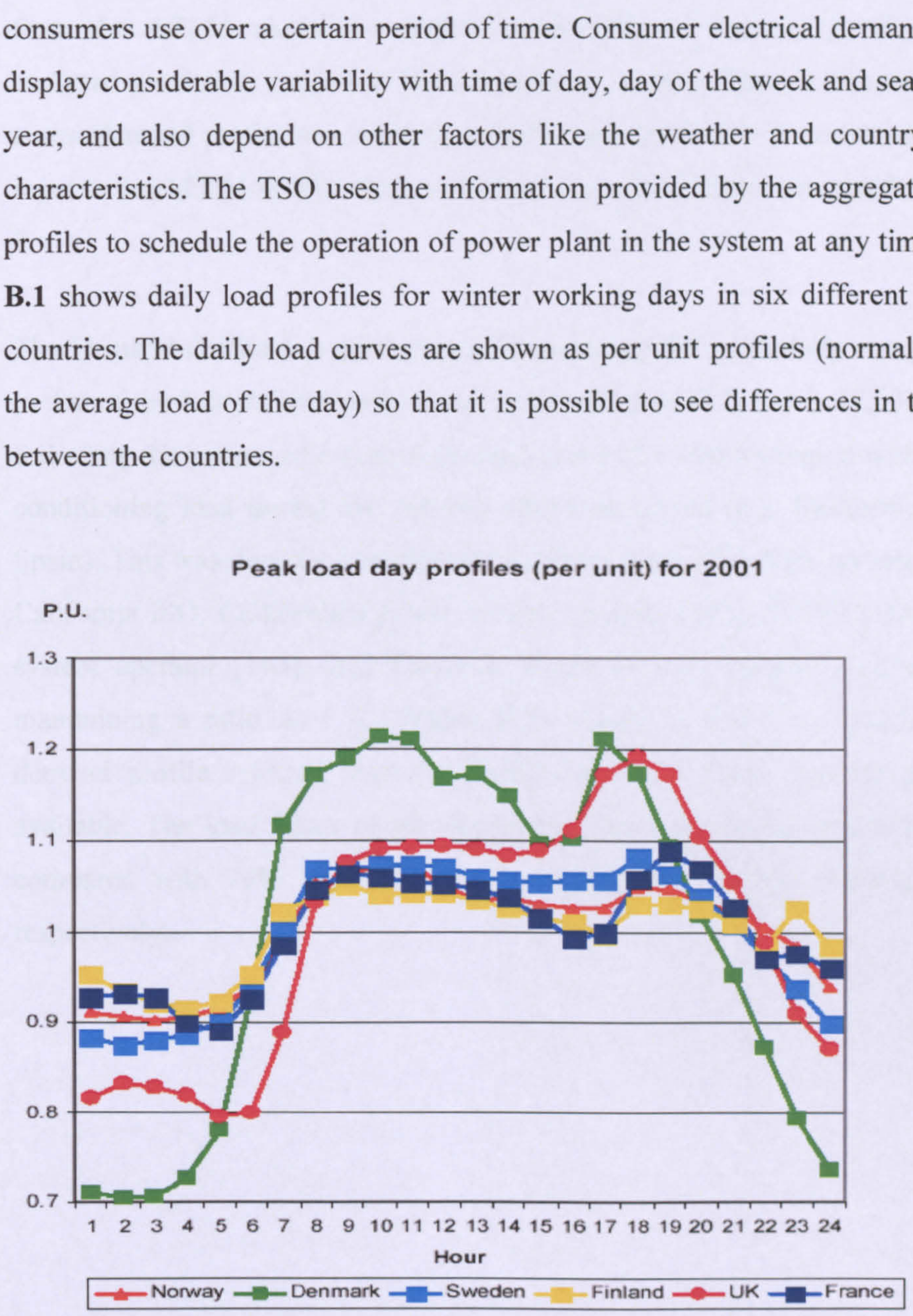

Figure B.1 Typical winter daily load profiles (as per unit curves) for six European countries [161]

Looking at **Figure B.1** all countries show lower consumer demand during night hours. However the size and shape of the demand profile varies across countries. Clearly different demand profiles will affect the scheduled operation of power generating plant (FPP, ZCPP and WPP) and the operation of the electrolyser stock. It seems appropriate to investigate the similarities and differences in the outcomes from the AELM model for regions with different demand profiles to those analysed previously (a typical North-European country, Eastern Denmark). Hence a new demand profile was created, namely Demand Profile 3, an introduced as an input to the AELM model, along with the same wind profiles described in **Chapter 3.**

The Demand Profile 3 is produced by maintaining the same daily energy demand to that of the Eastern Denmark winter profile (**Figure B.2**) that is 47,603 MWh but following the pattern of a system demand curve of a country/region with a high air conditioning load during the summer afternoon period (e.g. California, Japan or Spain). This was done by investigating different demand profiles corresponding to: California ISO, California's power system operator [162]; TEPCO, Tokyo's area system operator [163]; Red Electrica, Spain system operator [11]; and finally maintaining a ratio A_1 / A_2 (**Table B.1**) similar to that of a Spanish summer demand profile selected from [11] where historical daily demand profiles are available. The load factor of the demand profile 3 shown in **Figure B.2** is 67% compared with 79% and 83% for the winter and summer Denmark profiles respectively.

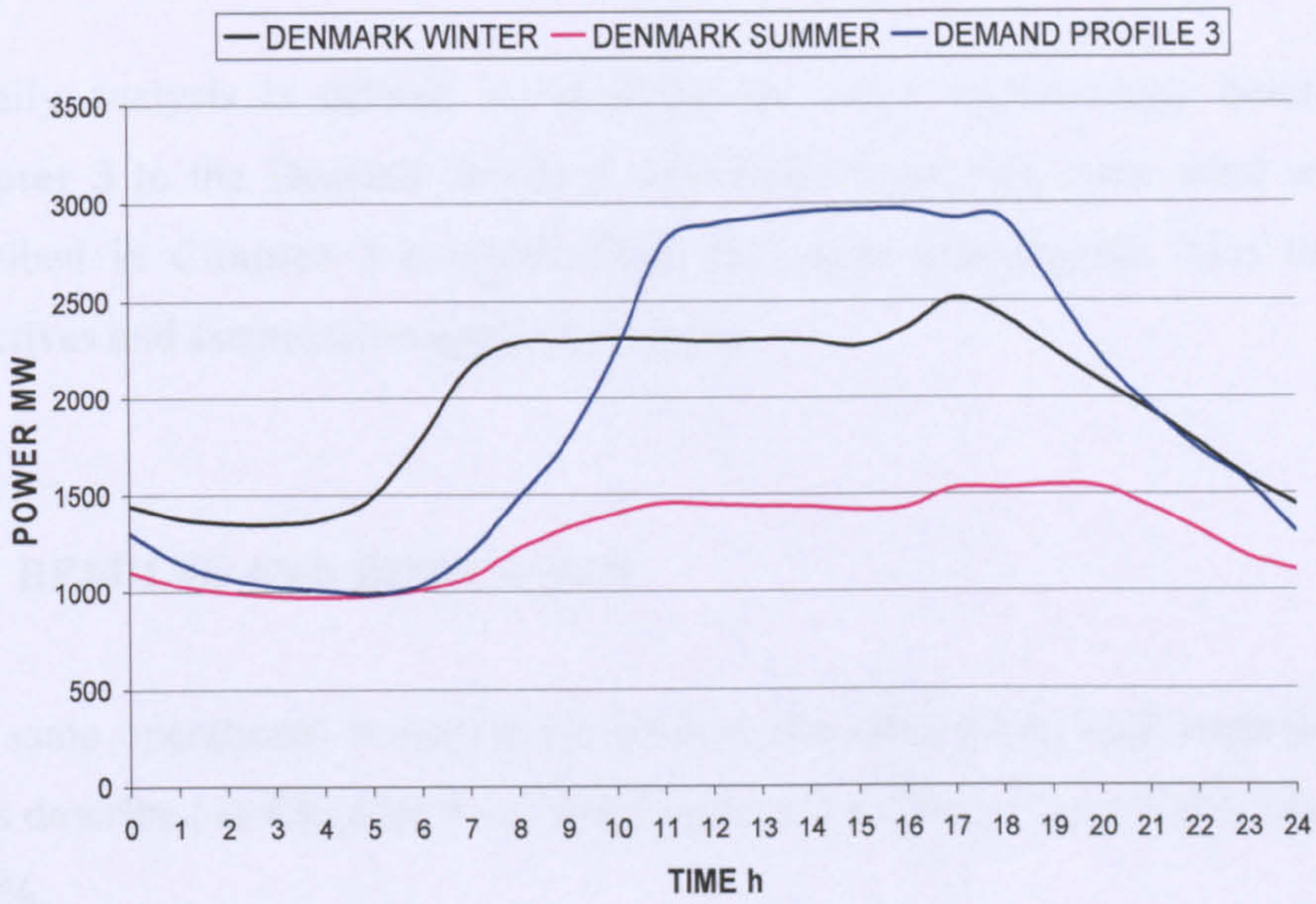

Figure B.2 Demand profiles analysed

DEMAND PROFILE	LF (%)	$A_1 \equiv$ MAX-MIN (GW)	A_2[31] $\equiv$ MAX GRADIENT (GW)	A_1 / A_2
Eastern Denmark summer	79	0.58	0.25	2.3
Eastern Denmark winter	83	1.16	0.67	1.7
Demand Profile 3	67	1.98	0.58	3.4
Spain summer	85	12.00	3.4	3.5

Table B.1. Statistical description of demand profiles

[31] For all the demand profiles analysed, including those from [11], [162] and [163], the maximum gradients in the aggregate system demand profile usually occur between 7:00 and 9:00h, except for Eastern Denmark winter profiles where demand occurs normally between 5:00 and 7:00h.

A daily analysis is offered by applying the same methodology described in **Chapter 3** to the Demand Profile 3 described above. The same wind scenarios described in **Chapter 3** available from [17] were investigated. Also the same objectives and assumptions apply throughout.

B.2 RESULTS AND DISCUSSION

The same operational strategies (as well as the Base Case) and implementation cases described in **Chapter 5** are analysed here for $20\% \leq \Phi_W \leq 100\%$, $0\% \leq \Phi_{ZPP} \leq 35\%$.

Wind penetration, Φ_W, and ZPP penetration, Φ_{ZPP}, are both referred to as installed capacity relative to maximum value of the Demand Profile 3, namely 2,965 MW. Total installed capacities in the islanded power system considered for incremental capacities of WPP and ZPP are shown in **Figure B.3** Assumptions for the overall effective capacity and plant margin are the same to those considered in **Chapter 5.3.1.**

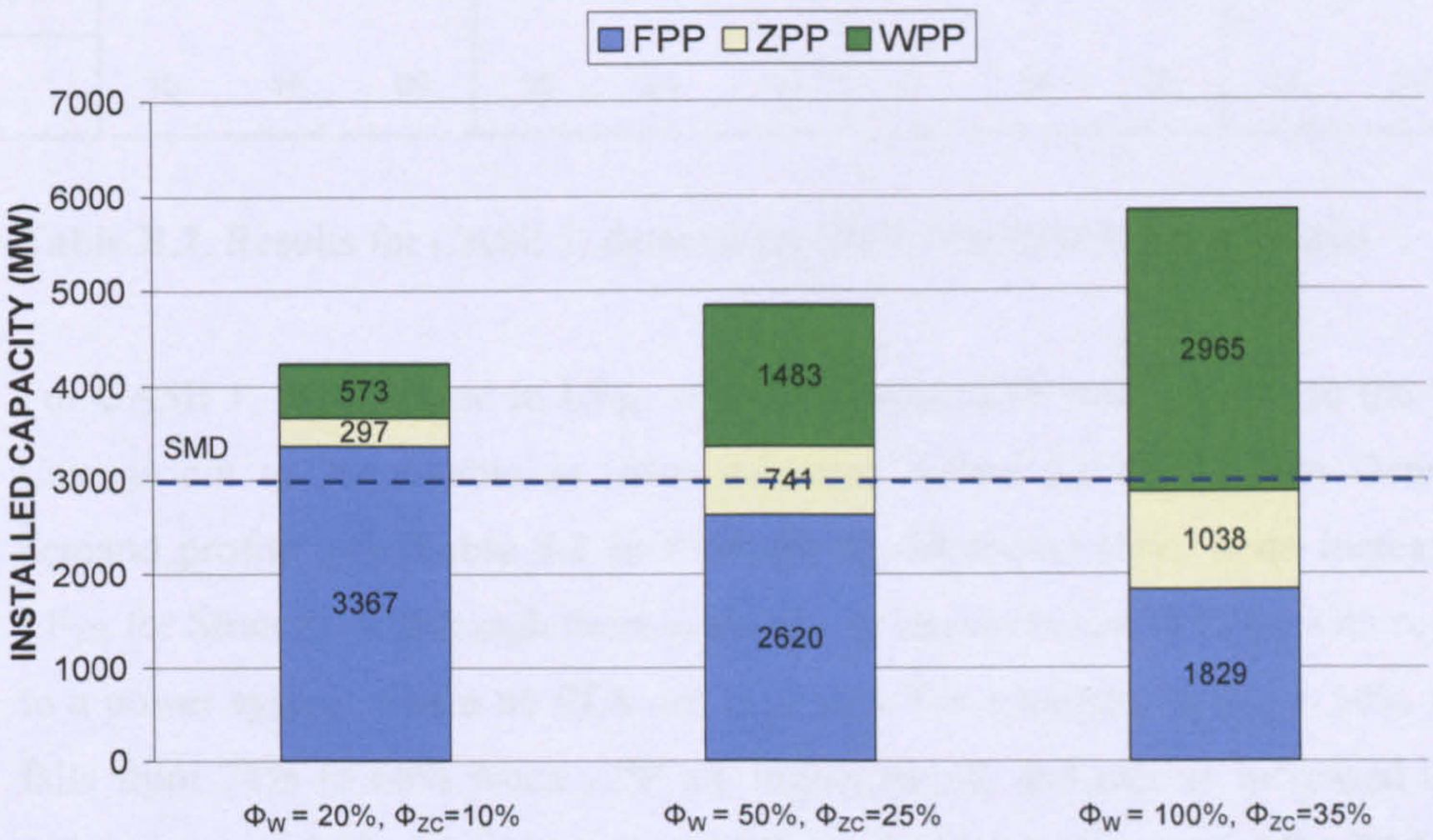

Figure B.3 Generating capacities for the islanded power system considered.

Results for the variable wind scenario are shown in Tables 2, 3 and 4 for CASES 1, 2 and 3 respectively.

OPERATIONAL STRATEGY	BASECASE			A			B			C		
Φ_W (%)	20	50	100	20	50	100	-	-	-	20	50	100
Φ_{ZPP} (%)	-	-	-	10	25	35	10	25	35	10	25	35
LF_{TH} (%)	70	74	72	68	69	63	67	66	70	70	88	90
CI_e (kg CO_2/kWh$_e$)	0.66	0.49	0.42	0.62	0.39	0.26	0.66	0.48	0.39	0.60	0.39	0.27
TC (t $CO_2 \times 10^3$ / d)	31.4	23.3	20.0	29.5	18.6	12.4	31.4	22.8	18.6	28.6	18.6	12.9
WC (%)	0	0	0	0	0	0	-	-	-	0	0	0
Y_H (t H_2 / d)	17	82	352	84	244	574	38	99	175	54	260	584
UF_E (%)	8	15	31	30	34	42	29	31	39	16	30	37
IC_E (MW)	450	1155	2365	585	1490	2830	270	670	935	715	1820	3300
IC_T (MW)	4687	6000	8197	4822	6334	8662	4125	4525	4790	4952	6664	9132
β_E (%)	10	19	29	12	24	33	7	15	20	14	27	36

Table B.2. Results for CASE 1, demand profile 3. Variable Wind Scenario

For CASE 1, the increase in LF_{TH} when deploying ZPP with respect to the Base Case is not as remarkable as those achieved before for the Eastern Denmark demand profile (see **Table 5.2 in Chapter 5**). Moreover there is no increase in LF_{TH} for Strategy A although there is always an improvement in LF_{TH} with respect to a power system where no ELS are deployed. For example, at Φ_W = 50% LF_{TH} falls from 74% to 66% when ZPP are implemented, and can be increased up to 69% on the variable wind day when SSE are deployed. However a flat FPP load

profile is not achievable now even for high Φ_W and Φ_{ZPP}. The maximum achievable LF_{TH} value is 90% for Strategy C at Φ_W = 100% and Φ_{ZPP} = 35%.

When comparing H_2 yields with those of **Table 5.2 in Chapter 5**, Y_H are lower across all operational strategies: 15-60% lower for the Base Case, 8-38% lower for Strategy A, 21-46% for B and between 0 and 58% lower for C. The lower range corresponds to Φ_W = 100%, so the reduction in Y_H is less significant when Φ_W increases. Note figures for Y_H represent maximum hydrogen production rates at $CI_H = 0$.

Increases in IC_E with respect to the Base Case are very similar to those obtained previously in **Table 5.2 (Chapter 5)**. Remember that for the Base Case and Strategies A and C the ELS stock is sized with the objective of eliminating wind curtailment completely across the year and thus according to the day of maximum wind availability (see main assumptions in **Chapter 3**). For the operational Strategy B the capacity of the electrolyser stock to be installed is equal to the capacity of ZPP installed. Interestingly, β_E values are almost identical to those shown in **Table 5.2**. This is because the electrolyser capacity matches the ZPP capacity for Strategy B and the assumptions regarding the overall effective capacity and plant margin remain the same to those of **Chapter 5**.

Figure B.4 displays the electrical input to the SSE stock (variable wind day at Φ_W =50%, Φ_{ZPP} = 25%) with the discrete contributions of WPP and ZPP. From **Figures B.4c and B.4d**, for Strategies B and C hydrogen is produced mainly during low demand periods, and in this case ZPP are used exclusively to meet consumer's demand at peak times.

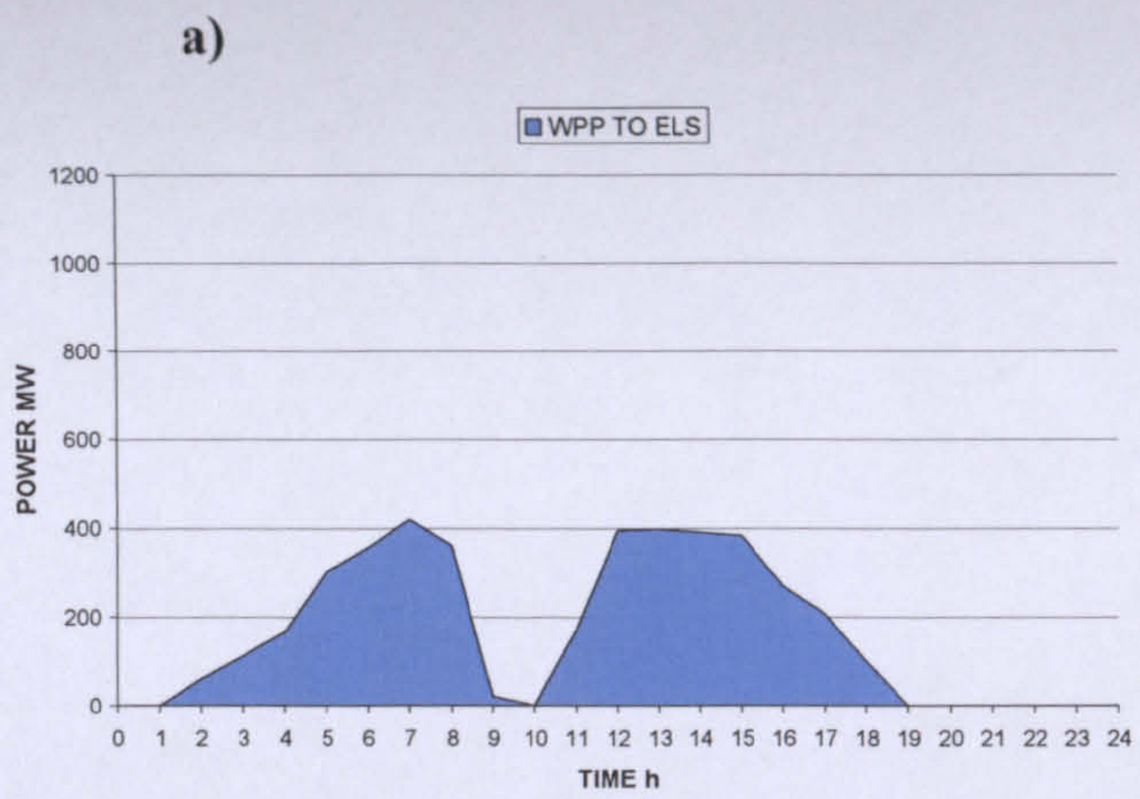

Figure B.4 CASE 1, Demand profile 3. Variable wind day. Aggregate electrical input to the "supply-side electrolyser stock".

a) Base Case
b) Strategy A
c) Strategy B
d) Strategy C

OPERATIONAL STRATEGY	BASECASE			A			B			C		
Φ_W (%)	20	50	100	20	50	100	-	-	-	20	50	100
Φ_{ZPP} (%)	-	-	-	10	25	35	10	25	35	10	25	35
LF_{TH} (%)	70	74	72	68	69	63	67	66	70	70	88	90
CI_e (kg CO_2/kWh$_e$)	0.66	0.49	0.42	0.62	0.39	0.26	0.66	0.48	0.39	0.60	0.39	0.27
TC (t $CO_2 \times 10^3$ / d)	31.4	23.3	20.0	29.5	18.6	12.4	31.4	22.8	18.6	28.6	18.6	12.9
WC (%)	0	18	52	0	9	42	-	-	-	0	15	45
Y_H (t H_2 / d)	17	28	46	86	216	329	38	99	175	54	217	316
UF_E (%)	8	14	23	31	50	63	29	31	39	16	33	37
IC_E (MW)	420	420	420	580	900	1090	270	670	935	715	1375	1760
IC_T (MW)	4657	5265	6252	4817	5744	6922	4125	4535	4790	4952	6219	7592
β_E (%)	9	8	7	12	16	16	7	15	20	14	22	23

Table B.3 Results for CASE 2, demand profile 3. Variable Wind Scenario

From Table B.3, eradication of wind curtailment can not be achieved when the ELS stock is located on the demand side. Reductions of WC with respect to the Base Case for Strategies A and C are similar to those obtained before for the Denmark demand profile (see **Table 5.4 in Chapter 5**).

Hydrogen production rates are lower than those of **Table 5.4,** across all operational strategies. Reductions arte within the same range to those of Case 1. Values for β_E are 2 – 4% lower than those obtained previously (**Table 5.4**). The utilization factors of the DSE are similar to those observed for Case 1 (**Table B.3**) for all operational strategies except for the Strategy A where lower IC_E lead to higher UF_E even though hydrogen production rates decrease by between 11 – 42% with respect to Case 1. When comparing UF_E values with those shown in **Table 5.4,** they are lower for $\Phi_W \leq 50\%$ but higher for $\Phi_W > 50\%$. **Figure B.5** displays simulations of load profiles for the variable wind day at Φ_W =50%, Φ_{ZPP} = 25%.

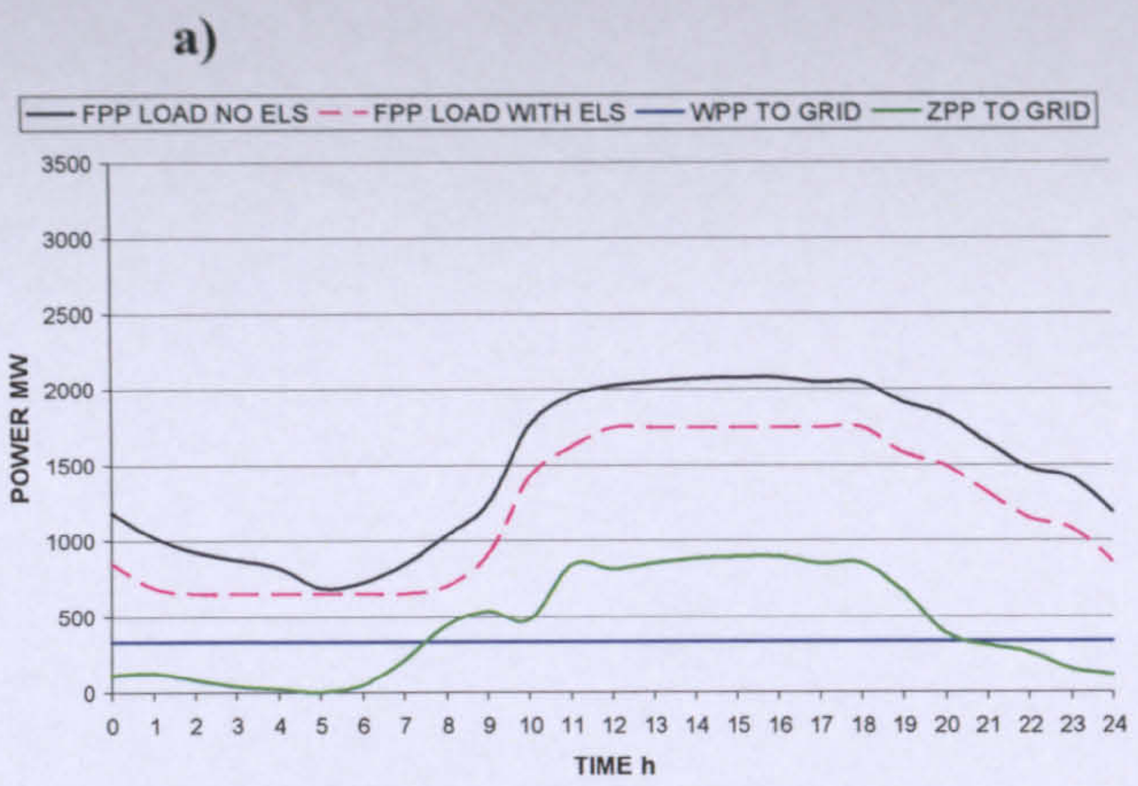

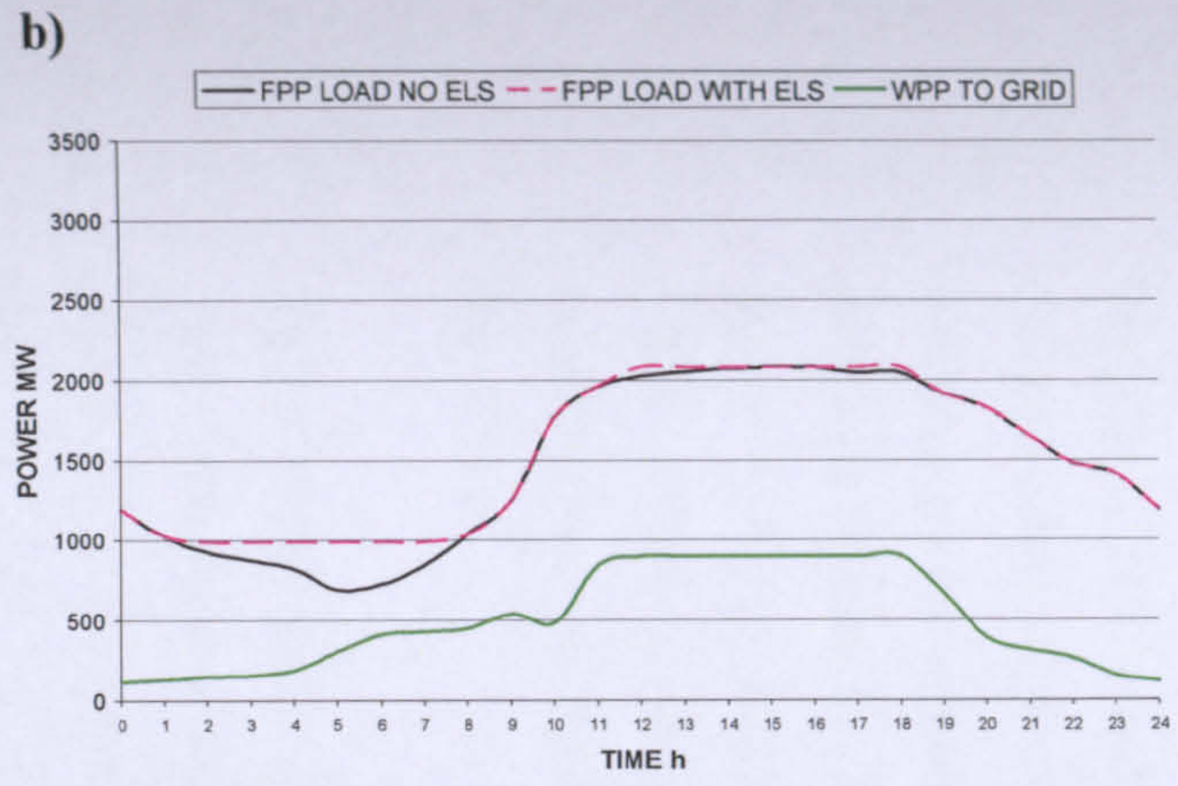

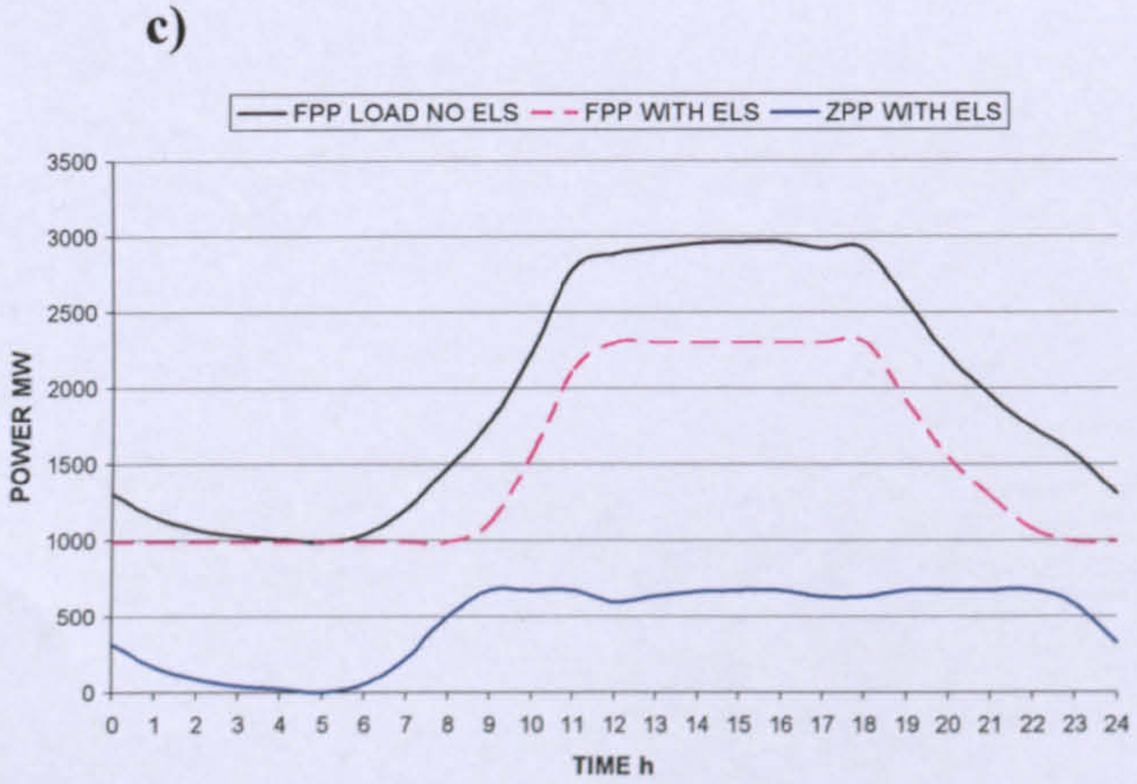

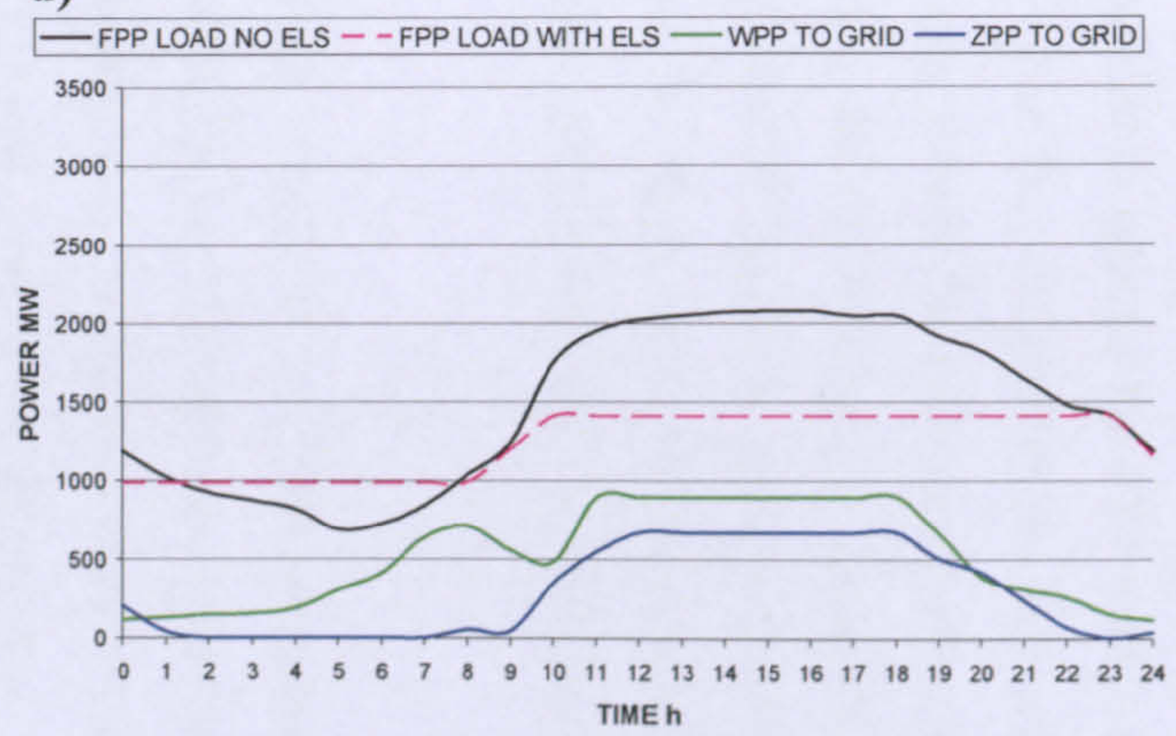

Figure B.5 CASE 2, Demand profile 3. Variable wind day. Effects on aggregate fossil load, WPP and ZCPP output delivered to grid and input to electrolysers.

a) Base case
b) Strategy A
c) Strategy B
d) Strategy C

From **Figure B.5,** it is not possible to achieve a flat FPP load profile for Demand Profile 3 is with any of the operational strategies. This is because the ratio between maximum system demand and minimum system demand (i.e. the height of the morning-time valley in **Figure B.2**) is higher for Demand Profile 3 and thus a higher capacity of ZPP would be needed to attain a flat FPP profile (LF_{TH} = 100%) at Φ_W = 50%. In other words for the same Φ_W, the greater the ratio of maximum to minimum in the aggregate system demand profile the greater the Φ_{ZPP} required to achieve a flat FPP load profile. For instance, for the Strategy C, Demand Profile 3 at Φ_W = 50% Φ_{ZPP} = 41% (i.e. 1,215 MW of ZPP installed capacity) is required to attain LF_{TH} = 100%, which is well above the Φ_{ZPP} value of 25% (666 MW of ZPP installed capacity) required for a power system with the Eastern Denmark winter profile and Φ_W = 50%.

Input profiles of the DSE at Φ_W =50%, Φ_{ZPP} = 25% are shown in **Figure B.6** In this case, from **Figure B.6d**, virtually no hydrogen is produced during the afternoon period when consumer demand is at its highest. During that period both ZPP and available WPP are used for peak electricity generation. When comparing with **Figure B.4** it is clear that H_2 production rates are much lower in this case because of the limitation on the WPP output that can be integrated in the grid and directed to DSE.

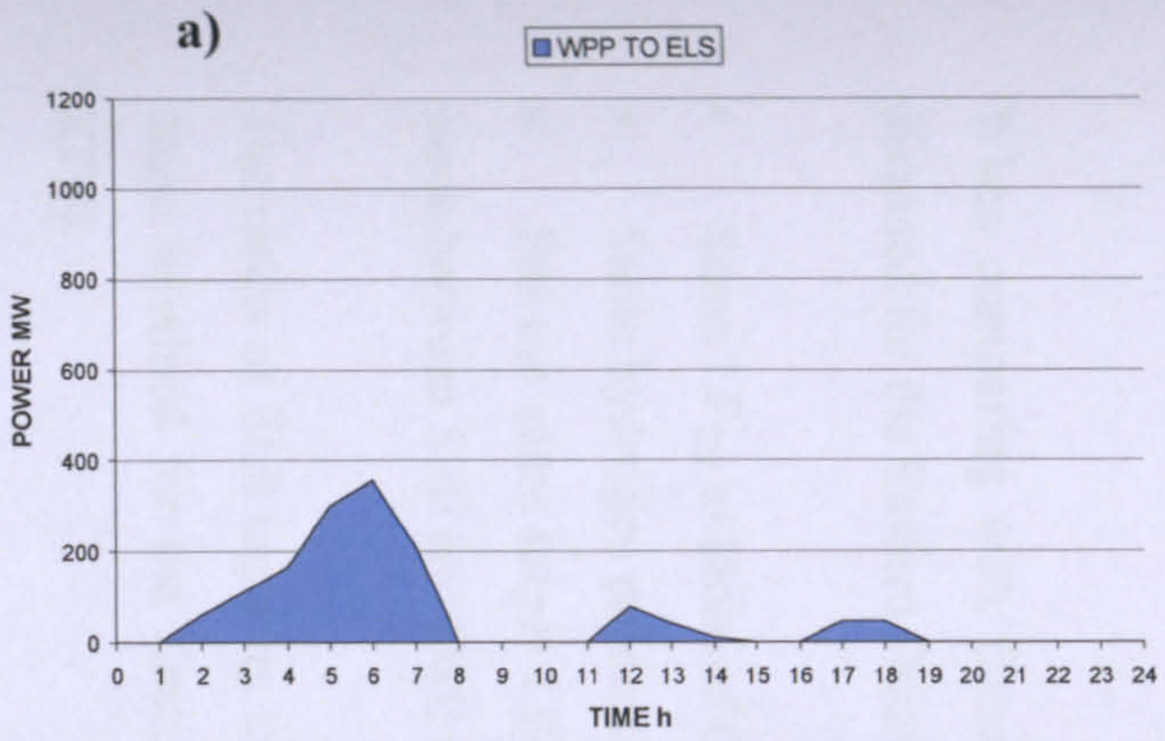

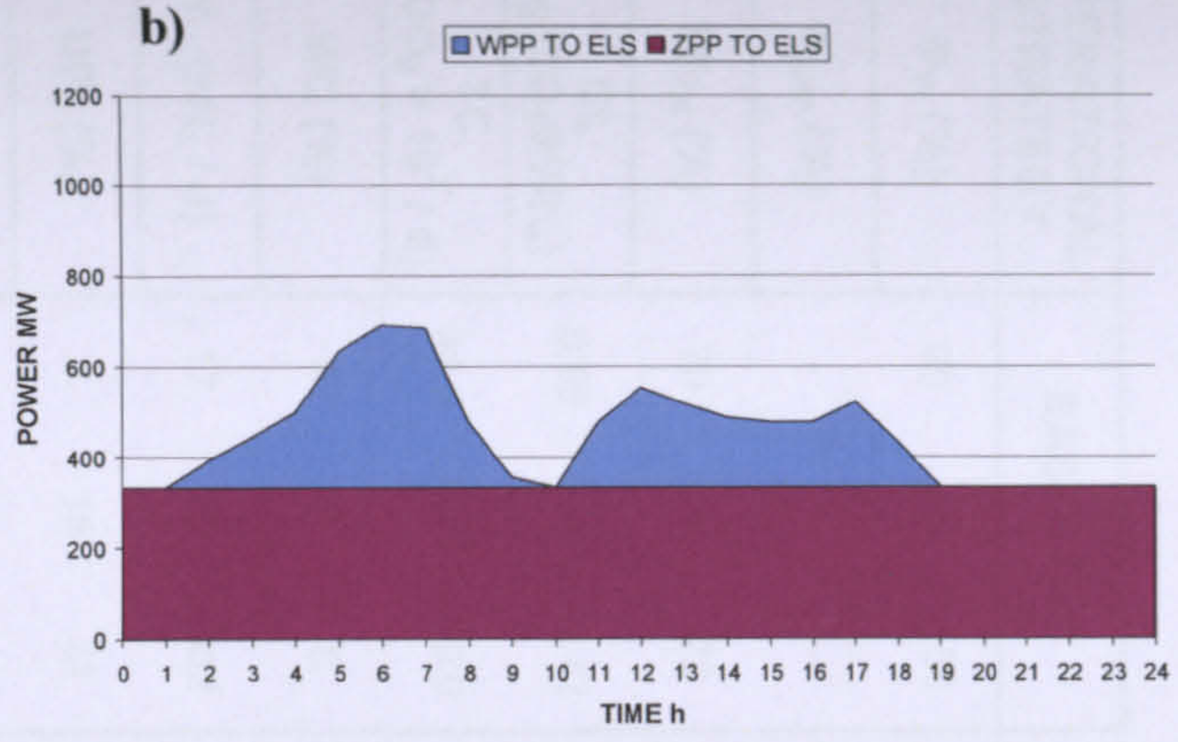

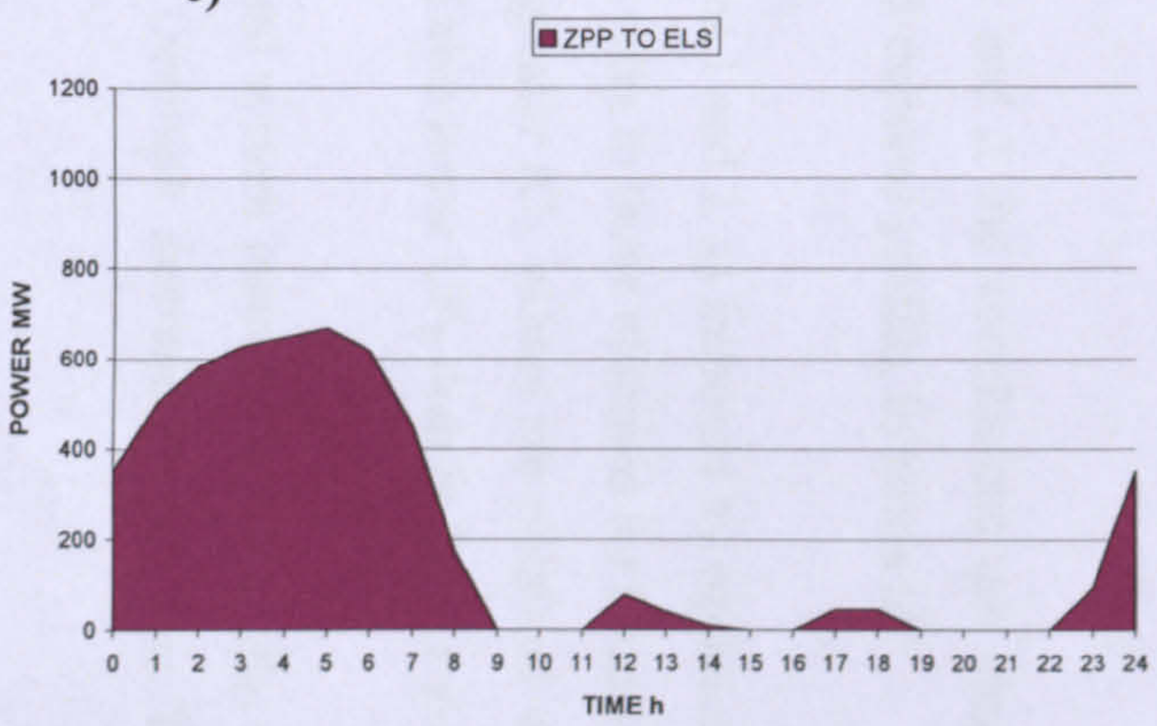

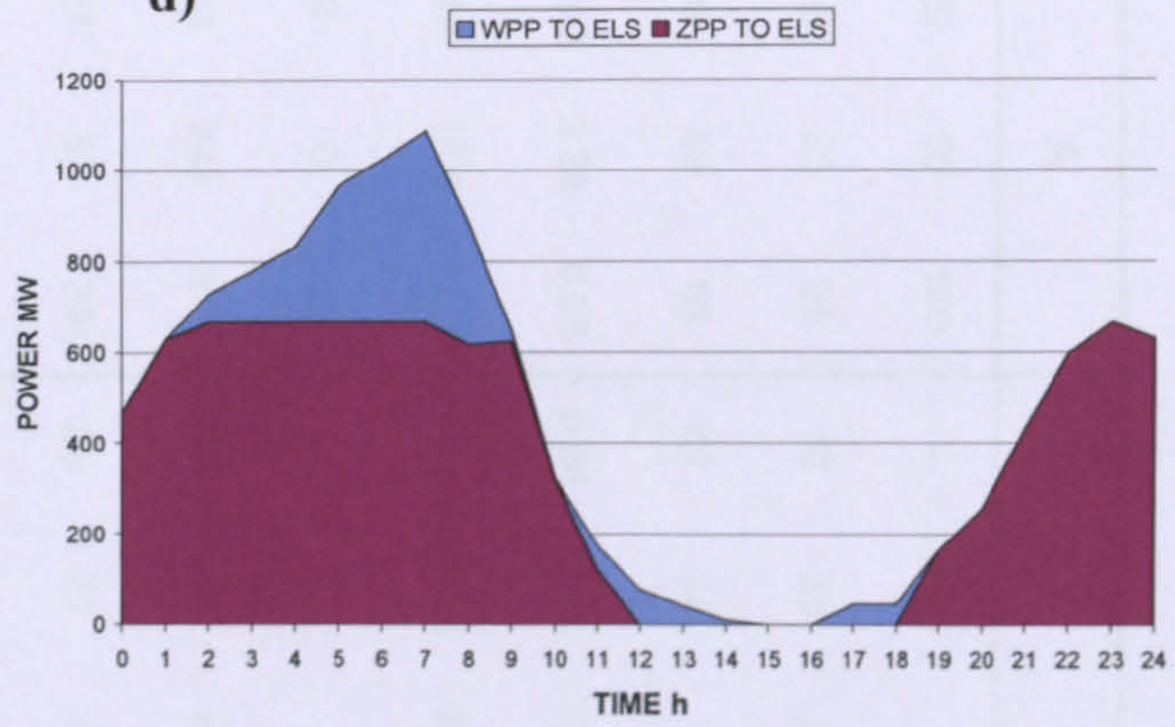

Figure B.6 CASE 2, Demand profile 3. Variable wind day. Aggregate electrical input to the "supply-side electrolyser stock".

a) Base case
b) Strategy A
c) Strategy B
d) Strategy C

OPERATIONAL STRATEGY	BASECASE			A			B			C		
Φ_W (%)	20	50	100	20	50	100	-	-	-	20	50	100
Φ_{ZPP} (%)	-	-	-	10	25	35	10	25	35	10	25	35
LF_{TH} (%)	70	74	72	68	69	63	67	66	70	70	88	90
CI_e (kg CO_2/kWh$_e$)	0.66	0.49	0.42	0.62	0.39	0.26	0.66	0.48	0.39	0.60	0.39	0.27
TC (t $CO_2 \times 10^3$ / d)	31.4	23.3	20.0	29.5	18.6	12.4	31.4	22.8	18.6	28.6	18.6	12.9
WC (%)	0	0	0	0	0	0	-	-	-	0	0	0
Y_H (t H_2 / d)	17	82	352	84	244	574	38	99	175	54	260	584
UF_E (%)	8	15	31	27	31	39	29	31	39	15	28	34
IC_E (MW)	450	1155	2365	655	1630	3065	270	670	935	755	1965	3530
IC_T (MW)	4687	6000	8197	4892	6474	8897	4125	4525	4790	4992	6809	9362
β_E (%)	10	19	29	13	25	34	7	15	20	15	29	38

Table B.4. Results for CASE 3, demand profile 3. Variable Wind Scenario

When comparing with Cases 1 and 2 the conclusions are almost identical to those obtained for the Eastern Denmark demand profile, in terms of:

- Same LF_{TH} to those of Cases 1 and 2, as imposed by equations (3) and (4).
- Same hydrogen production rates to those obtained for Case 1.
- For the same target LF_{TH} greater IC_E values are obtained when splitting the ELS stock between SSE and DSE and also lower UF_E than in Case 1 are achieved.

The ratios of ELS capacity to total system installed capacity, β_E, are almost identical to those obtained for the Eastern Denmark demand profile (see **Table 5.6 in Chapter ZPP**).

If CI_H is allowed to exceed zero to increase Y_H, UF_E, values of CI_e also increase, making clear the strong trade-off between Y_H and CI_e. For CI_H = 3 kg of CO_2 per kg of H_2, the increase in Y_H across all operational strategies was 28-43%, which is less marked than the increase obtained for the Eastern Denmark demand profile (see **Table 5.8 in Chapter ZPP**), while UF_E hardly increases. On the other hand, the increase in CI_e is much lower, between 3 and 8% compare to increases of up to 2 fold shown in **Table 5.8.** If higher Y_H are sought maintaining CI_H = 3, the increase in CI_e approaches those obtained formerly for the Eastern Denmark demand profile. For example, for the operational strategy C, variable wind day at Φ_W = 50%, if Y_H is boosted by 2 fold with respect to that obtained at CI_H = 0 (same increase to that observed from **Tables 5.6 and 5.8, Chapter 5**) then CI_e increases by 39%, once again making clear the strong trade-off between Y_H and CI_e.

B.3 MAIN CONCLUSIONS

In summary, when applying a demand profile with a higher ratio of maximum system demand to minimum system demand (see **Figure B.2**) the main conclusions obtained in **Chapter 5** apply but it is also interesting to note the following points:

- For the same wind penetration, the greater the ratio of maximum load to minimum load in the system demand profile, the greater the required IC_E and ZPP capacities to achieve a flat FPP load profile (LF_{TH} = 100%) while producing zero-carbon hydrogen. For Demand Profile 3, a flat FPP profile cannot be obtained even at Φ_W = 100% if CI_H is not allowed to exceed zero. However a more regular FPP profile can always be attained when deploying ZPP for both electricity peak generation and hydrogen production (Strategy C), allowing FPP to operate with less load changes across the day thus decreasing the carbon footprint.

- Even though the size of the ELS stock increases slightly when the ratio of maximum to minimum load increases, the same ratio of ELS capacity to total

system installed capacity, β_E, is required regardless of the shape of the demand profile analysed when the same wind power profiles are introduced as inputs to the model. This is a consequence of sizing the ELS stock for the day of highest wind availability (steady wind day of CF = 80% in this analysis) with the objective of eliminating wind curtailment across the year (See model description and assumptions in **Chapter 3**).

- For the same β_E, Φ_W and Φ_{ZPP} the rates of hydrogen production become lower and thereby lower utilization factors of the ELS stock are achieved. Or conversely a higher ratio of maximum system demand to minimum system demand implies higher Φ_W and Φ_{ZPP} to maintain the values of Y_H and UF_E.

- For all the operational strategies investigated, in order to achieve the objectives of minimizing wind curtailment, maximizing LF_{TH}, maximizing Y_H and minimizing CI_e while leaving aside economic parameters (e.g. power market conditions), the benefits of a widespread deployment of ELS are maximized when electrolysers are operated mainly at periods of low consumer demand and ZPP output is delivered to the ELS stock exclusively during such periods.

APPENDIX C: SENSITIVITY ANALYSIS OF THE LOW LOAD LIMIT RESTRICTION

C.1 INTRODUCTION

Besides the minimum loading levels inherent to thermal power plant, to counter for the possibility of a sudden large drop in wind generation (this can be produced by a sudden loss in wind resource or by a network fault that exceeds the ride-through capability of the wind generators), a dynamic penetration limit is also enforced in power systems with a significant wind power installed capacity, which effectively limits the amount of wind power that can be directed to the electrical grid [4]. These constraints result in an overall low load limit (LLL) characteristic for a specific power system which ultimately depends on: (i) the size and interconnections of the power system; (ii) type and size of conventional units in operation; (iii) dispersion of the wind generators within the system; and (iv) power market regulation and practice. Typical values are around 30% [4, 13] and therefore a low-load limit of 30% was assumed through this thesis, meaning that at any time wind power will be discarded if the equivalent aggregate wind power output exceeds 30% of the system demand as expressed in **equation 3.2 (Chapter 3).**

Therefore for every power system there is a limit to the amount of intermittent wind power that can be integrated. When wind power production exceeds the amount that can be safely absorbed by the electricity system while still maintaining adequate reserves and dynamic control of the system, some of the available wind power must be curtailed. The curtailment of wind generation during periods of high availability but low demand inhibits the production of low carbon electricity despite the availability of sufficient wind power plant within the power system and presents an economic penalty for wind farm operators. According to an investigation carried out concerning the economic penalties imposed by wind power curtailment in the Greek islands [62] the corresponding income loss for wind power plant in recent years has been continuously increasing with wind penetration, reaching values of approximately 25,000 € per MW of installed wind power, representing more than 5% of the capital invested by the WPP operator. Clearly this situation diminishes the financial capacity of existing WPP and also discourages new investors intending to enter the sector.

Clearly the higher the proportion of inflexible plant in the system (e.g. nuclear power plant), the lower LLL would be. However, a large deployment of electrolysers would offset this trend by increasing the demand during morning and night-time valleys in the aggregate FPP load profile and therefore the amount of wind power that the system can effectively absorb at these times.

An investigation of the LLL restriction has been carried out to evaluate its implications on the ability of the power system to integrate large intermittent renewable inputs and large electrolyser capacities. For the three implementation Cases 1, 2 and 3 and the operational strategies A and C considered in **Chapter 5**, a sensitivity analysis was undertaken for the variable wind day to reveal how the main parameters, namely LF, CI_e, WC, Y, UF_E and IC_E are influenced by the LLL. Note the operational strategy B did not consider any intermittent RE plant deployed in the system and therefore it is included in the analysis. Although typical values for LLL in island power systems are around 30%, conservative operating policies in large island systems often dictate values as low as 15%. On the other hand, limits in excess of 40% have also been applied in small islands [4]. Therefore two additional values have been considered: (i) reducing the LLL down to 15% (e.g. for a power system with a high proportion of flexible diesel and oil-fired units); and (ii) increasing the LLL up to 45% (e.g. for a power system with a high proportion of inflexible nuclear power plant).

The same objectives and assumptions as those of **Chapter 5** are followed here. Daily energy parameters obtained for the variable wind day (CF = 42%) are presented, along with the electrolyser capacities required (obtained from the steady wind day).

C.2 RESULTS FOR CASE 1

The SSE stock is powered solely by WPP and ZPP, and so zero-carbon hydrogen is produced. Results for the variable wind day and operational strategies A and C are shown in **Tables C.1 and C.2**

Φ_W (%)	20			50			100		
Φ_{ZPP} (%)	10			25			35		
LLL (%)	15	30	45	15	30	45	15	30	45
LF_{TH} (%)	86	86	87	86	91	91	85	93	100
CI_e (kg CO_2/kWh_e)	0.63	0.63	0.63	0.43	0.40	0.40	0.31	0.24	0.18
WC (%)	0	0	0	0	0	0	0	0	0
Y_H (t H_2 / d)	136	136	136	361	335	335	682	622	553
UF_E (%)	47	47	47	53	50	50	53	49	43
IC_E (MW)	575	575	575	1405	1405	1405	2660	2660	2660

Table C.1 Case 1, variable wind day, operational strategy A. Sensitivity of main variables to the LLL

From **Table C.1**, the installed capacity of electrolysers required, IC_E, remains constant with the LLL for all wind penetrations. However the hydrogen yield, Y_H decreases when the LLL increases for wind penetrations above 20%, and therefore the utilization factor of the electrolyser stock, UF_E, decreases. This effect is more accentuated for high wind penetrations above 50%. The carbon intensity of the electricity delivered to consumers, CI_e, decreases when the LLL increases since more wind-generated electricity is then allowed to come into the grid. For Φ_W = 20%, Φ_{ZPP} = 10%, the maximum LF_{TH} achievable remains practically constant when LLL increases, but LF_{TH} increases appreciably with LLL for $\Phi_W > 20\%$, especially for wind penetrations approaching 100% of system maximum demand.

Φ_W (%)	20			50			100		
Φ_{ZPP} (%)	10			25			35		
LLL (%)	15	30	45	15	30	45	15	30	45
LF_{TH} (%)	92	94	94	100	100	100	100	100	100
CI_e (kg CO_2/kWh$_e$)	0.61	0.62	0.62	0.36	0.29	0.29	0.17	0.07	0.02
WC (%)	0	0	0	0	0	0	0	0	0
Y_H (t H_2 / d)	123	121	121	282	222	222	547	435	372
UF_E (%)	36	37	37	34	31	41	34	32	34
IC_E (MW)	695	695	695	1705	1515	1140	3020	2650	2270

Table C.2 Case 1, variable wind day, operational strategy C. Sensitivity of main variables to the LLL

Looking at **Table C.2**, the installed capacity of electrolysers required, IC_E, decreases when the LLL increases for wind penetrations above 20%. The hydrogen yield, Y_H decreases when the LLL increases for wind penetrations above 20%, but the utilization factor of the electrolyser stock, UF_E, does not decrease steadily as in the operational strategy A (see **Table C.1**), and in fact increases for LLL > 30% at Φ_W > 20%. Interestingly, the LLL does not affect Y_H and CI_e at $\Phi \leq 50\%$ (**Table C.2**). This is because the FPP load profile (function of the LF_{TH} appointed) does not get affected by the LLL at $\Phi_W \leq 50\%$ and the proportion of WPP output directed to consumers (which determines CI_e), and to the SSE stock (which determines Y_H) remains the same when LLL increases. However for high wind penetrations above 50%, the WPP output is much greater and then the LLL restriction has a significant influence over the FPP profile, and the carbon intensity of the electricity delivered to consumers, CI_e, decreases notably when LLL increases (more wind-generated electricity is available to cover consumer demand), but at the expense of producing less hydrogen. Lower CI_e values are obtained for Strategy C (**Table 2**) when comparing with Strategy A (**Table 1**), with CI_e approaching zero for LLL = 45% at Φ_W = 100%, Φ_{ZPP} = 35% but at the expense of

producing less H_2. The maximum LF_{TH} achievable remains fairly constant when LLL increases and higher values than those of Strategy A are obtained.

C.3 RESULTS FOR CASE 2

The DSE stock is powered solely by WPP and ZPP, and zero-carbon hydrogen is produced. Results for the variable wind day and operational strategies A and C are summarized in **Tables C.3 and C.4.**

Φ_W (%)	20			50			100		
Φ_{ZPP} (%)	10			25			35		
LLL (%)	15	30	45	15	30	45	15	30	45
LF_{TH} (%)	86	86	87	86	91	91	85	93	100
CI_e (kg CO_2/kWh$_e$)	0.63	0.63	0.63	0.43	0.40	0.40	0.31	0.24	0.18
WC (%)	26	0	0	58	24	0	75	51	31
Y_H (t H_2 / d)	116	136	144	192	270	330	269	345	388
UF_E (%)	60	52	53	67	48	49	76	54	43
IC_E (MW)	405	575	575	595	1170	1405	735	1340	1865

Table C.3. Case 2, variable wind day, operational strategy A. Sensitivity of main variables to the LLL.

From **Table C.3**, IC_E now increases when the LLL increases, since a greater WPP output is allowed to enter the grid to supply both consumer demand and DSEs. As opposed to Case 1, Y_H increases when LLL increases for wind penetrations above 20%, but the utilization factor of the electrolyser stock, UF_E, follows a downward trend especially at $\Phi_W > 50\%$. The maximum load factor achievable and carbon intensity of electricity remain the same as in Case 1 since they are dictated by the LLL and CI_{ll} appointed (equations 5.1 and 5.6 in **Chapter 5**). In summary, the strategy A for Case 2

finds large benefits for power systems with high LLL, in terms of increasing Y_H, LF_{TH} and at the same time decreasing CI_e.

Φ_W (%)	20			50			100		
Φ_{ZPP} (%)	10			25			35		
LLL (%)	15	30	45	15	30	45	15	30	45
LF_{TH} (%)	92	94	94	100	100	100	100	100	100
CI_e (kg CO_2/kWh$_e$)	0.61	0.62	0.62	0.36	0.29	0.29	0.17	0.07	0.02
WC (%)	29	0	0	63	25	5	79	51	35
Y_H (t H_2 / d)	83	129	130	114	230	257	125	293	301
UF_E (%)	33	41	41	25	41	46	22	53	54
IC_E (MW)	520	645	645	945	1160	1160	1160	1160	1160

Table C.4. Case 2, variable wind day, operational strategy C. Sensitivity of main variables to the LLL.

Looking at **Table C.4**, the installed capacity of electrolysers required, IC_E, does not increase for LLL > 30%. This is because on the steady wind day the maximum power input (WPP and ZPP) to DSE remains constant when LLL increases. On the variable wind day however the hydrogen yield increases when the LLL increases for wind penetrations below 50%, and UF_E follows the same trend. As previously, CI_e decreases when the LLL increases since more wind-generated electricity is allowed to come into the grid. The maximum LF_{TH} achievable remains constant when LLL increases. The same LF_{TH} values as in Case 1 are obtained, since they are a function of the restrictions imposed by equations 5.1 and 5.6 **(Chapter 5)**.

C.4 RESULTS FOR CASE 3

A combined stock of SSE and DSE is deployed. WPP and ZPP output are used to cover both consumer demand P_C and to power the ELS stock. Only the production of zero-carbon hydrogen is considered.

Φ_W (%)	20			50			100		
Φ_{ZPP} (%)	10			25			35		
LLL (%)	15	30	45	15	30	45	15	30	45
LF_{TH} (%)	86	86	87	86	91	91	85	93	100
CI_e (kg CO_2/kWh$_e$)	0.63	0.63	0.63	0.43	0.40	0.40	0.31	0.24	0.18
WC (%)	0	0	0	0	0	0	0	0	0
Y_H (t H_2 / d)	133	136	131	348	334	329	669	616	553
UF_E (%)	48	49	47	45	43	46	48	44	41
IC_E (MW)	575	575	575	1610	1610	1465	2835	2895	2780

Table C.5. Case 3, variable wind day, operational strategy A. Sensitivity of main variables to the LLL

On the steady wind day, when LLL increases above 30% more WPP output is allowed to enter the grid and a greater proportion of it is directed to cover consumer demand. Hence the maximum power input to the ELS stock diminishes, resulting in lower IC_E values (**Table C.5**). For this same reason, Y_H reduces for LLL > 30%. UF_E remains fairly constant with LLL for $\Phi_W \leq 50\%$, and diminishes when LLL increases for wind penetrations above this limit. Values for the maximum LF_{TH} achievable are equal to those obtained for Cases 1 and 2, as imposed by equations 5.1 and 5.6. Values of CI_e also remain the same as they are subject to the LF_{TH} targeted.

Φ_W (%)	20			50			100		
Φ_{ZPP} (%)	10			25			35		
LLL (%)	15	30	45	15	30	45	15	30	45
LF_{TH} (%)	92	94	94	100	100	100	100	100	100
CI_e (kg CO_2/kWh$_e$)	0.61	0.62	0.62	0.36	0.29	0.29	0.17	0.07	0.02
WC (%)	0	0	0	0	0	0	0	0	0
Y_H (t H_2 / d)	120	129	129	282	222	222	543	435	368
UF_E (%)	36	37	39	33	29	39	36	33	32
IC_E (MW)	695	695	695	1770	1580	1185	3120	2745	2365

Table C.6. Case 3, variable wind day, operational strategy C. Sensitivity of main variables to the LLL

As in the operational strategy A (**Table C.5**) IC_E decreases when LLL increases for Φ_W > 20%, Φ_{ZPP} > 10%. LF_{TH} and CI_e values are the same to those of Cases 1 (**Table C.2**) and 2 (**Table C.4**), as imposed by the LLL and the CI_H. Values of Y_H are the same as those obtained in Case 1 and thus higher than those of Case 2. The capacity of the electrolyser stock, IC_E, is also similar to those values obtained in Case 1 (**Table C.2**), and thus very similar UF_E values are attained for Case 3 (**Table C.6**). In summary, for Strategy C very similar results are obtained for Cases 1 and 3 with respect to changes in the LLL, only the location of the electrolyser stock is different.

To summarize, for all implementation cases as LLL increases there is more WPP output entering the grid and therefore CI_e decreases as expected. On the other hand the hydrogen yield decreases for Cases 1 and 3 since less WPP output is available for the SSE stock as the capacity of the system to absorb wind generation (i.e. the LLL) increases. The load factor does not show significant changes when LLL increases except for very high wind penetrations approaching 100% of system demand. If the objective is

to maximize Y_H, using ZPP for baseload electricity production (Strategy A) is the optimum strategy, whereas using ZPP mainly for peak electricity production (Strategy C) allows minimization of CI_e, reaching unprecedented values of 0.02 kg CO_2/kWh$_e$ when LLL = 45% at Φ_W = 100% and Φ_{ZPP} = 35%. However this comes at the expense of attaining lower hydrogen production rates. Again the trade-off between CI_e and Y_H is clear and becomes more accentuated as LLL increases.